To the Graduate Council:

I am submitting herewith a dissertation written by D. Mark Steinhauff entitled "Sequence Stratigraphy and Comparative Diagenesis of Middle Ordovician Shelf to Shelf-Edge Limestones, The Copper Creek Allochthon, East Tennessee." I have examined the final copy of this dissertation for form and content and recommend that it be accepted in partial fulfillment of the requirements for the Doctor of Philosophy Degree, with a major in Geology.

Kenneth R. Walker, Major Professor

We have read this dissertation
and recommend its acceptance:

Accepted for the Council:

Associate Vice Chancellor
and Dean of the Graduate School

# SEQUENCE STRATIGRAPHY AND COMPARATIVE DIAGENESIS OF MIDDLE ORDOVICIAN SHELF TO SHELF-EDGE LIMESTONES, THE COPPER CREEK ALLOCHTHON, EAST TENNESSEE

A Dissertation

Presented for the

Doctor of Philosophy

Degree

The University of Tennessee, Knoxville

D. Mark Steinhauff

August, 1993

VOLUME 1

Frederick Paul Steinhauff
Sept. 9, 1928 - June 4, 1992

# ACKNOWLEDGMENT

I wish to express my appreciation to Ken Walker for his support as my advisor; Drs. S.G. Driese, M.L. McKinney and E.L. Wehry for serving on my committee and for their helpful comments and suggestions; Drs. T.W. Broadhead, K.C. Lohmann, and L.A. Taylor, and Messrs. M. Doty and A. Patchen for their help, suggestions, and advise; and Dr. C.I. Mora for sticking up for me. Past and current graduate students L.J. Foreman, F.C. Furman, B. Glumac, D.G. Jernigan, R.E. Johnson, M. Kozar, E.C. Rankey, K.E. Roberson, K. Srinivasan, K. Tobin, W.K. Waggoner, and L.J. Weber are thanked for their help. Dr. Paula Lawson is thanked for being patient. Finally, special thanks go to my parents.

Ruppel (1979) developed the initial stratigraphic framework used for this work and provided slightly less than 1/5 of the total thin-sections used to develop all the water-depth curves. Unpublished point-count data were provided by Ruppel (1979), Breland (1980) and Jernigan (1987), and unpublished biostratigraphic data were provided by Keith Roberson, University of Tennessee and Anita Harris, U.S. Geological Survey. Roberson also provided valuable help in the field and a small suite of thin-sections from the lowermost parts of the Old Thorn Hill and Idol Mine sections. Ruppel (1979), Johnson (1988), and Jernigan (1987) provided 21, 47, and 50 thin-sections, respectively, from the Red House Branch section. Additional samples from Red House Branch were provided by Jernigan from which Steinhauff cut additional thin-sections. A modest grant to Steinhauff from the Southeastern Section of the Geological Society of America helped defray some field expenses. Some of the preparation costs for this dissertation were provided by NSF grant EAR-9103491 to K.R. Walker. Other aspects of this work were supported from the Carden Fund, the Mobil Carbonate Fund and the Discretionary Funds of the Department of Geological Sciences, University of Tennessee. Figures in chapters 2 and 3 were drafted by Dennis Felts. Analysis of $^{87}Sr/^{86}Sr$ ratios was performed by Steve Goldberg at the University of North Carolina; all stable isotope ratio and electron microprobe analyses were performed by the author.

# ABSTRACT

Surfaces of subaerial exposure in Middle Ordovician strata are correlated among seven stratigraphic sections, four on the shelf (+ 400 m thk) and three at or near the shelf-edge (300 m thk) near Thorn Hill, TN. These exposure surfaces define stratigraphic sequences within an apparently non-cyclic, largely subtidal, carbonate succession. Facies geometry is based on outcrop observation, analysis of thin-sections (+1,000) and consideration of water-depth curves based on multiple lines of evidence. In platform succession, most sequences are bounded by exposure surfaces, but in more continuously subtidal areas, periods of shallowing and drowning did not always occur. Apparently-non-cyclic carbonate strata have fourth-order subsequences that are grouped into third-order sequences based on the occurrence of pronounced and less pronounced exposure surfaces. Fifth-order parasequences occur within third- and fourth-order sequences. Parasequences are not correlative across the shelf nor from the shelf to the shelf-edge, and many are probably the result of lateral environmental migration. Surfaces of subaerial exposure are correlated from shelf to shelf-edge positions, showing that some sequences or "beats" are missing. Beats are missed in three ways: 1) sea-level remains below the shelf-edge even though sea-level is oscillating, 2) tectonic uplift exposes the shelf until subsidence allows submergence, and 3) during drowning.

Sequence stratigraphy provide a framework within which it is possible to interpret later diagenetic events. Cross-cutting relationships observed in polished slabs and thin-sections using conventional and cathodoluminescent petrography provide the basis for deciphering relative timing of different phases and for interpreting diagenetic origin. Isotopic ($\delta^{18}O$, $\delta^{13}C$, $^{87}Sr/^{86}Sr$) and trace element (Mg, Mn, Fe, Sr) analyses of individual carbonate phases provides supporting evidence.

Cavities and vugs are developed below many third- and fourth-order sequence boundaries. Early diagenetic phases filling these cavities represent a "second-cycle" or (?) "third-cycle" of early diagenesis. Fibrous calcite ($\delta^{18}O$ = -6.0 to -4.1‰, PDB; N=89) is interpreted as marine. Bladed and clear blocky calcite are more depleted in $\delta^{18}O$ than -6.0‰ and are interpreted as meteoric. Bladed and blocky clear calcite do not show the large $\delta^{13}C$ depletions reported for meteoric phases in younger rocks. Lack of $\delta^{13}C$ depletion may be related to absence of land plants which might have provided $^{12}C$ to the groundwater.

Intermediate through late burial phases at the shelf-edge have more depleted $\delta^{18}O$ values, higher Fe and Mn contents, and are more enriched in $^{87}Sr$ than their counterparts on the shelf. If the source of fluids precipitating late burial phases was the Sevier basin to the southeast, then fluids at the shelf-edge would have encountered less carbonate rock than fluids traveling to shelf positions.

Analysis of temperatures assumed from burial curves, an assumed range of likely brine compositions, and known $\delta^{18}O$ values for late burial calcite and dolomite suggest that the Sevier basin is the most likely source of burial fluid that precipitated late burial phases. This analysis further suggests that burial fluids could have been generated in the Sevier basin before the end of the Middle Ordovician (ca. 450 Ma).

"It was known that the bed rock of this valley is predominantly limestone of the Chickamauga group; and in the absence of definite information to the contrary it would be quite possible for this limestone to be traversed by solution channels, which could be independent of the surface drainage, and might run for miles underground, even conceivably passing beneath the Clinch River to emerge in springs which might be used by people for drinking purposes."

Paris B. Stockdale (1951) in reference to Bethel Valley.

# TABLE OF CONTENTS


| Chapter | | Page |
|---|---|---|
| 1. | Introduction | 1 |
| | Background | 1 |
| | Objectives and content | 3 |
| | Chapter 2: relative sea-level changes | 3 |
| | Chapter 3: shelf to shelf-edge | 5 |
| | Chapter 4: diagenesis | 6 |
| | Chapter 5: diagenetic trend in third-order sequences | 6 |
| | Study area and general stratigraphy | 7 |
| | Study area | 7 |
| | General stratigraphy | 8 |
| | Methods | 11 |
| | Significance of study | 13 |
| | General significance | 13 |
| | Regional significance | 14 |
| 2. | Sequence stratigraphy of an apparently non-cyclic carbonate succession: recognizing subaerial exposure in largely subtidal stratigraphic sequences Middle Ordovician, East Tennessee | 17 |
| | Abstract | 17 |
| | Introduction | 19 |
| | Objectives | 20 |
| | Study area | 20 |
| | Paleobathymetric data | 22 |
| | Bathymetric indicators | 22 |
| | Evidence for subaerial exposure | 23 |
| | Methods | 26 |
| | Degrees of exposure | 31 |
| | Lithologies | 32 |
| | Description | 32 |
| | Mud-rich lithologies | 32 |
| | Peloidal and associated lithologies | 42 |
| | Echinoderm grainstone | 42 |
| | Coated-grain lithologies | 43 |
| | Other lithologies | 43 |
| | Fossil content | 43 |

Chapter Page


Lithologic interpretation . . . . . 44
Correlation across the shelf . . . . . 44
Biostratigraphic and lithostratigraphic correlation . . . . . 44
Exposure surfaces . . . . . 47
Correlation of deepening events . . . . . 49
Defining stratigraphic sequences with paleobathymetric indicators . . 49
Water-depths . . . . . 49
Types of stratigraphic sequences . . . . . 50
Discussion of stratigraphic sequences . . . . . 62
Third-order Sequence 1 . . . . . 63
Third-order Sequence 2 . . . . . 63
Third-order Sequence 3 . . . . . 66
Third-order Sequence 4 . . . . . 67
Third-order Sequence 5 . . . . . 68
Discussion: Fischer plots "cycles," and sea-level change . . . . . 69
Using Fischer plots to recognize changes in relative sea-level 69
Limitations of Fischer plots . . . . . 71
Conclusions . . . . . 72

3. Recognizing exposure, drowning, and "missed beats": shelf to shelf-edge sequence stratigraphy of Middle Ordovician non-cyclic carbonates, East Tennessee . . . . . 75

Abstract . . . . . 75
Introduction . . . . . 77
Objectives . . . . . 78
Study area . . . . . 79
Previous work . . . . . 82
Bathymetric indicators using multiple lines of evidence . . . . 82
Evidence of post-depositional water-depth changes . . . . . 87
Methods . . . . . 88
Lithologies . . . . . 97
Description of on-shelf lithologies . . . . . 97
Description of shelf-edge lithologies . . . . . 97
Fossil content . . . . . 98
On-shelf and shelf-edge water-depths . . . . . 99
Correlation of exposure surfaces . . . . . 100
Correlation of deepening events . . . . . 103
Types of stratigraphic sequences . . . . . 108

Chapter Page


Third-order sequences . . . . . 108
Fourth-order subsequences . . . . . 109
Parasequences: possible "fifth-order" packages . . . . . 110
Discussion of stratigraphic sequences . . . . . 110
Third-order Sequence 1 . . . . . 110
Third-order Sequence 2 . . . . . 112
Third-order Sequence 3 . . . . . 116
Third-order Sequence 4 . . . . . 118
Third-order Sequences 5, 6, and 7 . . . . . 120
Discussion: exposure, drowning, and missed beats . . . . . 122
Exposure . . . . . 123
Evidence for drowning . . . . . 123
Missed beats . . . . . 126
Conclusions . . . . . 128

4. Comparative diagenesis of Middle Ordovician shelf to shelf-edge limestones, the Copper Creek allochthon, East Tennessee . . . . . 130

Abstract . . . . . 130
Introduction . . . . . 131
Objectives . . . . . 133
Study area . . . . . 134
Previous work . . . . . 138
Methods . . . . . 142
Thin-sections and slabs . . . . . 142
Cathodoluminescence . . . . . 143
Stable isotopes of carbon and oxygen . . . . . 143
Electron microprobe analysis . . . . . 145
$^{87}Sr/^{86}Sr$ analysis . . . . . 146
Description of diagenetic phases . . . . . 147
Early diagenetic non-ferroan phases . . . . . 147
Intermediate to early burial phases . . . . . 157
Late burial phases . . . . . 164
Interpretation of paragenetic sequence . . . . . 171
Early diagenetic non-ferroan phases . . . . . 171
Early to intermediate burial phases . . . . . 180
Late burial phases . . . . . 181

Chapter Page

Discussion of calcite filled cavities and vugs . . . . . 182
Interpretation: shelf-edge diagenetic example . . . . . 183
Interpretation: on-shelf diagenetic example . . . . . 186
Conclusions . . . . . 190

5. Preliminary analysis of diagenetic trends in third-order stratigraphic sequences, Middle Ordovician, East Tennessee . . . . . 194

Introduction . . . . . 194
Objectives . . . . . 194
Background . . . . . 196
Study area . . . . . 197
Methods . . . . . 197
Diagenetic trends . . . . . 198
On-shelf and shelf-edge fibrous and bladed calcite . . . . . 198
On-shelf blocky calcite and ferroan calcite veins . . . . . 199
Progressive shelf-edge to on-shelf enrichment of $\delta^{18}O$ in late to middle burial phases . . . . . 207
Whole-rock trace element values in third-order stratigraphic sequences . . . . . 211
Conclusions . . . . . 217

6. Conclusion . . . . . 220

Summary . . . . . 220
Future work . . . . . 226
Is present day groundwater flow influenced by depositional and diagenetic features? . . . . . 226
Sequence stratigraphic correlation . . . . . 229
Relationship to Mississippi Valley-type deposits? . . . . . 230
Paleoecology . . . . . 230

Chapter Page

References . . . . . 232

Appendices . . . . . 251

Appendix A. Measurement conventions and description of stratigraphic sections . . . . . 252
Measurement conventions and definitions . . . . . 253
Description of stratigraphic sections . . . . . 255
Thorn Hill section . . . . . 255
Old Thorn Hill section . . . . . 279
Idol Mine section . . . . . 301
Cedar Springs section . . . . . 318
Poor Valley Creek section . . . . . 327
Red House Branch section . . . . . 331
Cuba section . . . . . 342

Appendix B. Petrographic constituent analyses . . . . . 346
Explanation . . . . . 347

Appendix C. Interpreted water-depths . . . . . 363
Explanation . . . . . 364

Appendix D. Stable isotope ratio analyses of carbon and oxygen . . 394
Explanation . . . . . 395
Standards and reference gases . . . . . 395
"Known" or accepted values for standards . . . . . 395
Data quality . . . . . 396
Rejected and qualified data . . . . . 396
Key to abbreviations . . . . . 397

Appendix E. Electron microprobe analyses of trace elements . . 416
Explanation . . . . . 417

Appendix F. Radiogenic strontium analyses (87Sr/86Sr with $\delta^{13}C$ and $\delta^{18}O$) . . . . . 453
Procedures for Sr isotopic analysis of carbonate . . . . . 454

Appendix G. Atomic absorption analyses (whole-rock) . . . . . 456
Explanation . . . . . 457

Vita . . . . . 460

# ILLUSTRATIONS


| Figure | | Page |
|---|---|---|
| 1.1 | Location map showing general location of on-shelf and shelf-edge localities in relation to East Tennessee. | 9 |
| 1.2 | General stratigraphic and temporal relationships the Tippecanoe Sequence Sloss (1963) in the study area | 10 |
| 2.1 | Location map | 21 |
| 2.2 | Water-depth criteria substantially modified after Benedict and Walker (1978) | 24 |
| 2.3 | Middle Ordovician algal depth indicators of Moore (1978) | 25 |
| 2.4 | Composite columnar section, Thorn Hill area | 27 |
| 2.5 | Subaerial exposure indicators | 29 |
| 2.6 | Limestone lithologies in thin-section | 36 |
| 2.7 | Additional mud-rich and coated-grain lithologies | 38 |
| 2.8 | Ternary diagrams show limestone lithologies for Middle Ordovician on-shelf environments in East Tennessee | 40 |
| 2.9 | Ternary diagrams show fossils in limestone lithologies for Middle Ordovician on-shelf environments in East Tennessee | 41 |
| 2.10 | Key to stratigraphic location of sequence diagrams of figures 2.11 - 18 | 51 |
| 2.11 | Key to facies for stratigraphic sequence diagrams of figures 2.12-2.18. | 52 |
| 2.12 | Stratigraphic subsequences 1A, 1B, 1C, 2B, 2C, and 2D | 53 |
| 2.13 | Stratigraphic subsequences 2E and lower 2G | 54 |
| 2.14 | Stratigraphic subsequences 2E, 2G, 2H, 2I, and 2J | 55 |
| 2.15 | Stratigraphic subsequences upper 2I, and 2J, 2K, 3A, 3B, 3C lower 3D | 56 |
| 2.16 | Stratigraphic subsequences 3D, 4A, 4B, 4C, and lower 4D | 57 |
| 2.17 | Stratigraphic subsequences 4C, 4D, 4E, and lower 4F | 58 |
| 2.18 | Stratigraphic subsequences 4F, and lower Sequence 5 | 59 |
| 2.19 | Fischer plot for composite Middle Ordovician on-shelf section (i.e., Figure 2.4) | 60 |
| 3.1 | Location map for the study area within the Copper Creek allochthon | 80 |
| 3.2 | Stratigraphic sequences 1-5, Thorn Hill area | 81 |
| 3.3 | Indicators of subaerial exposure | 83 |
| 3.4 | Shelf-edge Lithologies | 85 |
| 3.5 | Ternary diagrams compare Middle Ordovician limestone lithologies from on-shelf environments to similar environments at or near the shelf-edge in East Tennessee | 90 |

Figure Page


3.6 Ternary diagrams compare fossil content of Middle Ordovician limestone lithologies from on-shelf environments to similar environments at or near the shelf-edge in East Tennessee. . . . . 91
3.7 Key to facies for stratigraphic sequence diagrams and columnar sections of figures 3.8, 3.9, 3.10, 3.11, 3.12, and 3.12 . . . . . 92
3.8 Stratigraphic subsequences 1A, 1B, 1C, 2B, 2C, and 2D on the shelf in the Thorn Hill area . . . 93
3.9 Stratigraphic subsequences 1B, 1C, 2B, 2C, and 2D at the shelf-edge in the Red House Branch area . . . . . 94
3.10 Lithostratigraphic and biostratigraphic comparison of shelf-edge or near shelf-edge sections; Red House Branch (left) is compared to the reference section at Cuba (right) . . 95
3.11 Lithostratigraphic and biostratigraphic comparison of shelf-edge or near shelf-edge sections; Poor Valley Creek (left) is compared to the reference section at Cuba (right) . . . . . 96
3.12 Composite columnar sections comparing the Thorn Hill area at the shelf (left) to the Red House Branch area at or near the shelf-edge (right) . . . . . 101
3.13 Stratigraphic subsequences 1A-4D . . . . . 105
3.14 Subsequences 1A-4D, restored across depositional strike . . . . . 106
3.15 Modified Fischer plots comparing fourth-order subsequences from the composite Middle Ordovician on-shelf section for the Red House Branch area to the composite shelf-edge of near shelf-edge section for the Red House Branch area. . . . . 125
4.1 Location map for East Tennessee . . . . . 135
4.2 Subsequences 1A-4D restored across strike . . . . . 136
4.3 Perspective view of three burial curves for central East Tennessee . . 139
4.4 Photomicrographs of diagenetic features . . . . . 140
4.5 $\delta^{18}O$ versus $\delta^{13}C$ for early diagenetic non-ferroan phases . . . . . 149
4.6 Electron microprobe analyses of weight percent manganese versus mole percent $MgCO_3$ of shelf-edge and on-shelf fibrous calcite . . . . . 153
4.7 Comparison of $\delta^{18}O$ versus $^{87}Sr/^{86}Sr$ values for on-shelf and shelf-edge phases . . . . . 154
4.8 $\delta^{18}$ versus $\delta^{13}C$ for intermediate to early burial phases . . . . . 158

Figure Page


4.9 $\delta^{18}$ versus $\delta^{13}C$ for late burial phases . . . . . 161
4.10 Electron microprobe analysis of weight percent iron versus mole % $MgCO_3$ of shelf-edge and on-shelf ferroan, blocky white calcite . . . . . 162
4.11 Electron microprobe analysis of weight percent manganese versus mole % $MgCO_3$ of shelf-edge and on-shelf ferroan, blocky white calcite . . . . . 163
4.12 Electron microprobe analysis of weight percent iron versus mole percent $MgCO_3$ for late burial ferroan calcite . . . 165
4.13 Electron microprobe analysis of weight percent manganese versus mole percent $MgCO_3$ for late burial ferroan calcite . . . . . 166
4.14 Photo-negative shows calcite filled vug developed during subaerial exposure and / or freshwater diagenesis . . 169
4.15 Shelf-edge paragenetic sequence . . . . . 172
4.16 On-shelf paragenetic sequence . . . . . 173
4.17 Different possible burial temperatures and burial fluid compositions are compared for dolomite and calcite at the shelf-edge. . . . . 176
4.18 Different possible burial temperatures and fluid compositions are compared for dolomite and calcite on-shelf . . . . . 178
4.19 Electron microprobe traverse (right) along calcite filled cavity (photo-negative image- left) shelf-edge locality at Poor Valley creek, Subsequence 2C (approximately 12 to about 17 meters above the Knox unconformity) . 184
4.20 Electron microprobe traverse (right) along calcite filled cavity (photo-negative image - left) from on-shelf locality at Idol Mine section, Subsequence 3D (234.7 meters above the Knox unconformity) . . . . . 187
5.1 Values of $\delta^{18}O$ for fibrous calcite versus stratigraphic position above the Knox unconformity . . . . . 200
5.2 Simple linear regressions (method of least squares), for third-order sequences 2, 3, and 4 on the shelf . . . . . 201
5.3 Multiple regression with interaction using stratigraphic sequence 2 and 3 . . . . . 203
5.4 Multiple regression with interaction using stratigraphic sequences 3 and 4 . . . . . 204
5.5 On-shelf vein calcite $\delta^{18}O$ values against stratigraphic position (N=12) . . . . . 206
5.6 On-shelf vein calcite $\delta^{18}O$ values against vein width . . . . . 206
5.7 $\delta^{18}O$ values for different types of burial calcite are plotted against stratigraphic position . . . . . 208
5.8 Whole-rock trace element values relative to third-order stratigraphic sequences at on-shelf and shelf-edge positions . . . . . 214

# TABLES


| Table | | Page |
|---|---|---|
| 2.1 | Facies criteria | 33 |
| 2.2 | Facies interpretations | 45 |
| 2.3 | "Guiding principles" involved in correlation along strike (on the shelf) | 48 |
| 3.1 | "Guiding Principles" involved in correlation across strike (on-shelf to shelf-edge) | 104 |
| 4.1 | Summary of geochemical data for shelf-edge phases | 151 |
| 4.2 | Summary of geochemical data for on-shelf phases | 152 |
| 6.1 | Stratigraphic nomenclature for the Chickamauga Group in the White Oak Mountain thrust sheet and probable 3rd-Order stratigraphic sequences | 228 |

# CHAPTER 1

## INTRODUCTION

### BACKGROUND

Patterns of cementation observed by Jernigan (1987) in Middle Ordovician carbonate strata near Thorn Hill, Tennessee represent the starting point for this dissertation. Jernigan noted that near shelf-edge reef, skeletal sand-bank/sand-flat grainstones and packstones of the coeval Holston and Rockdell Formations contain abundant carbonate cements that he interpreted to have formed in the marine, freshwater, and burial diagenetic environments. Working within the lithostratigraphic framework developed by Ruppel (1979) and Ruppel and Walker (1982, 1984), Jernigan was able to recognize different proportions of cement types in successive stratigraphic layers. This lead to a cementation history that was discussed, expanded upon, and further interpreted by Steinhauff and Walker (1987) and Walker et al. (1987a,b,c). Supporting carbon and oxygen isotope and trace element geochemistry was presented by Steinhauff et al. (1988, 1989a,b,) and Steinhauff (1989) to help corroborate fabric relationships.

Jernigan made his most important observation using a cement priority point-counting method. Standard grain-priority point-counting would count the interior of a snail as "snail", although the interior space might be filled with cement. However, using "cement-priority" the same area would be counted as cement. This point-

counting showed that some horizons are dominated by 1) fibrous marine calcite and micritic marine cement, 2) by equant freshwater cement, and 3) pore central, ferroan calcite cement and ferroan baroque dolomite cement. These differing horizons were interpreted as marine dominated, freshwater-dominated, and burial-dominated, respectively. The cement horizons commonly occur in triplets with a lower-marine cemented horizon (10-20 m), followed by a thick freshwater cemented horizon (40-60 m), capped by a thin horizon with unusually abundant burial cement. Near the shelf-edge at Red House Branch several triplet horizons are vertically stacked.

Further on the shelf in coeval skeletal grainstones, freshwater cement usually dominates, and marine and burial cement is much less common. Steinhauff (1987) suggested that one marked burial horizon can be traced from shelf-margin into correlative rocks at several on-shelf localities. Correlation of other cement horizons was less clear. However, because burial cement is the latest deposited material, the correlative horizon may have retained porosity longer than sediments above and below. Thus, Steinhauff et al. (1989a,b,) hypothesized that this burial cement horizon might delineate the pathway of later fluid flowing shelfward from thick basinal shales to the southeast. Thus, they envisioned two possible mechanisms to account for these stacked triplet horizons. First, the stacked triplet-horizons may represent areas of reduced porosity developed through preferential marine cementation and residual enhanced porosity. Alternatively, the stacked triplet-horizons may represent fine-scale, relative sea-level oscillations.

It became clear that other questions, such as those regarding changes in sea-level and possible exposure, needed to be addressed first before the significance of these stacked triplet-horizons could be further assessed. Thus, the present investigation concentrates on the possible occurrence of surfaces of subaerial exposure, possible changes in relative sea-level, and the resulting diagenesis.

## OBJECTIVES AND CONTENT

This dissertation considers the sequence stratigraphy and diagenesis of Middle Ordovician carbonate strata near Thorn Hill and Red House Branch, Tennessee. The dissertation consists of three substantive chapters (chapters 2, 3, and 4) each of which are presented as "stand alone" papers. Chapter 5 presents substantive results of a preliminary investigation. Conclusions are summarized in Chapter 6. Hypotheses entertained by each substantive chapter are stated below in italics.

### Chapter 2: Relative Sea-Level Changes and Correlative Surfaces of Subaerial Exposure

Chapter 2 considers four apparently non-cyclic, on-shelf carbonate stratigraphic sections deposited along depositional strike. Chapter 2 addresses three hypotheses formulated from previous work (i.e., Jernigan, 1987). First, *just as with cyclic carbonates, evidence for changes in relative sea-level occurs within each stratigraphic section.* Second, *this evidence will help reveal surfaces of subaerial exposure that have been previously overlooked because of the apparently non-cyclic*

*nature of this succession.* Third, *these surfaces of subaerial exposure occur within, and are correlative between each of these four stratigraphic sections.*

Water-depth curves and, despite the flaws of the technique, Fischer plots were used to help assess changes in relative sea-level. Water-depth of deposition was established using multiple lines of evidence to determine a range of possible water-depths. Inflection points in water-depth curves indicated stratigraphic intervals that, on further detailed analysis, were found to also contain subtle indicators of subaerial exposure. This evidence for subaerial exposure was used to define packages of rock, bounded above and below by surfaces of subaerial exposure. These packages comprise third- and fourth-order stratigraphic sequences which are correlative between all four stratigraphic sections. The term subsequence is used for fourth-order sequences. Fifth-order sequences or "parasequences" are only partially bounded by surfaces of subaerial exposure (i.e., the surfaces cannot be correlated across the shelf at all four stratigraphic sections).

Because these stratigraphic sequences, subsequences and parasequences represent shallowing-upward packages similar to cycles, it was possible to construct Fischer plots, substituting sequences, subsequences, and parasequences for cycles. One of the ways in which one might interpret a Fischer plot is in terms of relative sea-level rise and fall (an over-simplification to be sure, and one that is considered in Chapter 2). Thus, a relative sea-level rise would be expressed as a positive departure from the horizontal and a relative sea-level fall as a negative departure from the horizontal (e.g., Read and Goldhammer, 1988).

## Chapter 3: Shelf to Shelf-Edge

Chapter 3 shows how the sequence stratigraphy worked out for the Middle Ordovician shelf is related to shelf-edge and near shelf-edge strata. Chapter 3 addresses three hypotheses formulated from the results of Chapter 2. First, *evidence for changes in relative sea-level can be found in strata deposited in deeper water at or near the shelf-edge.* Second, *some, but not all, of the surfaces of subaerial exposure and accompanying stratigraphic sequences found on the shelf can be correlated to the shelf-edge.* Third, *some stratigraphic sequences represented at either on-shelf or shelf-edge positions will lack corresponding shelf-edge or on-shelf counter parts due to "missed beats."*

Water-depth curves and Fischer plots were again used to assess changes in relative sea-level at the shelf-edge. Many inflection points on water-depth curves indicate stratigraphic intervals were also found to contain subtle indicators of subaerial exposure and/or drowning. However, some inflection points mark times of substantial shallowing but not subaerial exposure. This evidence was used to define packages of rock bounded above and below by surfaces of subaerial exposure, or by pronounced shallowing without exposure. These packages or sequences defined at the shelf-edge were correlated to the shelf within an existing biostratigraphic framework (Bergstrom 1971, 1973, 1977; Carnes, 1975; Bergstrom and Carnes, 1976; and Anita Harris - personal communication to Keith Roberson, 1990) and lithostratigraphic framework (Ruppel, 1979; Ruppel and Walker, 1982, 1984).

## Chapter 4: Diagenesis

Chapter 4 relates diagenetic products filling pore space within the Middle Ordovician stratigraphic sequences, considered in chapters 2 and 3, to possible changes in relative sea-level and later development of marine, freshwater, and burial diagenetic environments. Moreover, Chapter 4 shows how the relative timing of pore filling phases is related to stratigraphic sequence development. Chapter 4 addresses three hypotheses. First, *early diagenetic pathways for sediments on the shelf were different than those for sediments at the shelf-edge.* Second, *meteoric phases will not show the large depletions in* $\delta^{13}C$ *that other workers have observed in younger rocks (e.g., Saller and Moore, 1991). Large depletions in* $\delta^{13}C$ *will be absent because these Middle Ordovician strata are slightly older than the first major radiation of land plants (Gray, 1984, 1985).* Third, *the Sevier basin is the most likely source for burial fluids that precipitated late ferroan phases at on-shelf and shelf-edge positions.*

Petrographic and geochemical evidence are used to support all three hypotheses. Additionally, burial curves for the Middle Ordovician of East Tennessee (Walker et al., 1992) are used to help constrain the possible timing and pathway of late diagenesis.

## Chapter 5: Diagenetic Trends in Third-Order Sequences

Chapter 5 presents light stable isotopic and trace element data with preliminary interpretations regarding the evolution of third-order stratigraphic sequences. Two hypotheses are investigated. First, *early and late diagenetic processes were different*

*among third-order stratigraphic sequences.* Second, *early and late diagenetic processes were different on the shelf as compared to those at the shelf-edge during the time that third-order Sequence 2 was deposited, but later, by the time third-order sequences 3 and 4 were deposited, shelf and shelf-edge processes had become similar.* Chapter 5 discusses the shelf-edge succession of sequences 3 and 4. By the time Sequence 4 was deposited, platform interior sediments had prograded to the shelf-edge. Thus, Chapter 5 speculates that early diagenetic processes affecting Sequence 3 on the shelf were similar to those at the former shelf-edge. Chapter 5 further speculates that because these early diagenetic processes had become similar, later diagenesis on the shelf and at the former shelf-edge was similar as well in these upper sequences.

## STUDY AREA AND GENERAL STRATIGRAPHY

### Study Area

The study area consists of four on-shelf localities and three shelf-edge or near shelf-edge localities (Fig. 1.1). A regional environmental/stratigraphic framework, based on these and other sections, was developed by Walker (1977, 1980, 1985), Ruppel (1979), and Ruppel and Walker (1982, 1984).

Four on-shelf localities are exposed along the northwest limb of the Copper Creek allochthon and are shown in Figure 2.1 of Chapter 2. A more than 540 meter thick succession of Middle Ordovician strata ranging from the upper Knox Group through the Five Oaks, Lincolnshire, Rockdell, Benbolt, Wardell, Witten and

Moccasin formations is exposed along-strike, near Thorn Hill Tennessee. From southwest to northeast these localities include the Thorn Hill (TH), Old Thorn Hill (OTH), Idol Mine (IS), and Cedar Springs (CS) sections. Each section is separated from the other by approximately 2 km.

Strata at three shelf-edge localities are overturned and exposed on the southwest limb of the Copper Creek allochthon (Fig. 1.1). An approximately 300 meter thick succession of Middle Ordovician strata ranging from the upper Knox Group through the Five Oaks, Lenoir, Holston and Rockdell formations is exposed along strike. These sections do not contain exposures of the upper Middle or Upper Ordovician. From southwest to northeast, these localities include the Poor Valley Creek (PVC), Red House Branch (RHB), and Cuba (CU) sections. These localities are separated from each other by about 3 km and 6 km, respectively and are shown in Figure 3.1 of Chapter 3. On-shelf localities are palinspastically separated from the shelf-edge by about 20 km.

## General Stratigraphy

Stratigraphic names applied to the Middle Ordovician succession in this work are those used by Ruppel and Walker (1984) (Fig. 1.2). These names were first introduced by Cooper and Prouty (1943) and by Cooper (1945). Walker (1985) and Byerly et al. (1986) recognized three second-order stratigraphic sequences in the Paleozoic section exposed at Thorn Hill, Tennessee. This work considers the lower third of their Sequence II. Sequence II is recognized elsewhere as the Tippecanoe

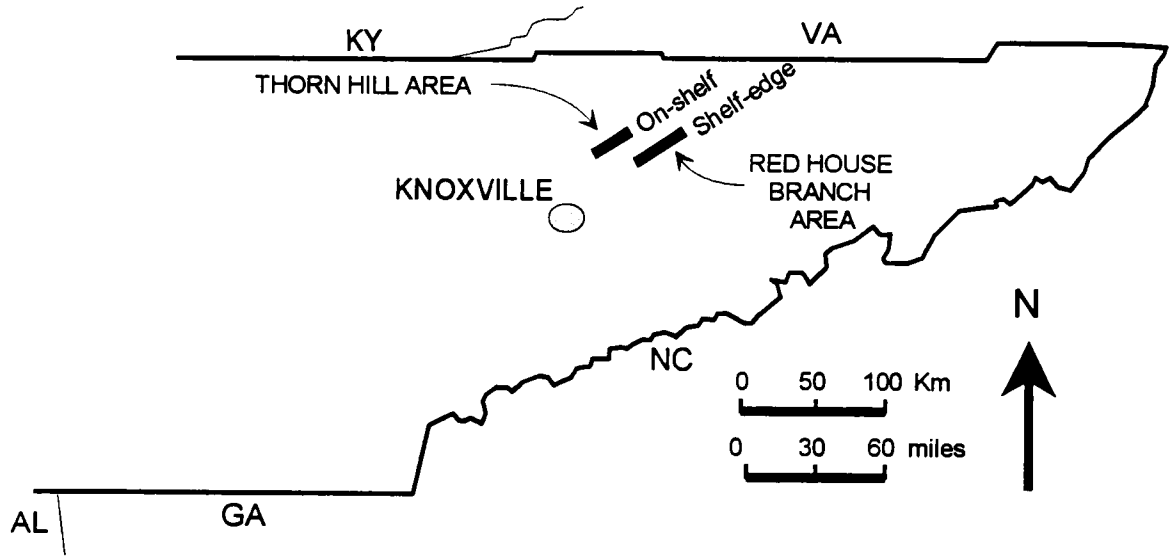



Figure 1.1 Location map showing general location of on-shelf and shelf-edge localities in relation to East Tennessee. The Thorn Hill study area includes four measured sections: Thorn Hill (TH), Old Thorn Hill (OTH), Idol Mine section (IS), and Cedar Springs (CS). The location map for Chapter 2 (Fig. 2.1) shows these locations in more detail. The Red House Branch area consists of three measured sections: Poor Valley Creek (PVC), Red House Branch (RHB), and Cuba (CU). The location map for Chapter 3 (Fig. 3.1) shows these locations in more detail.

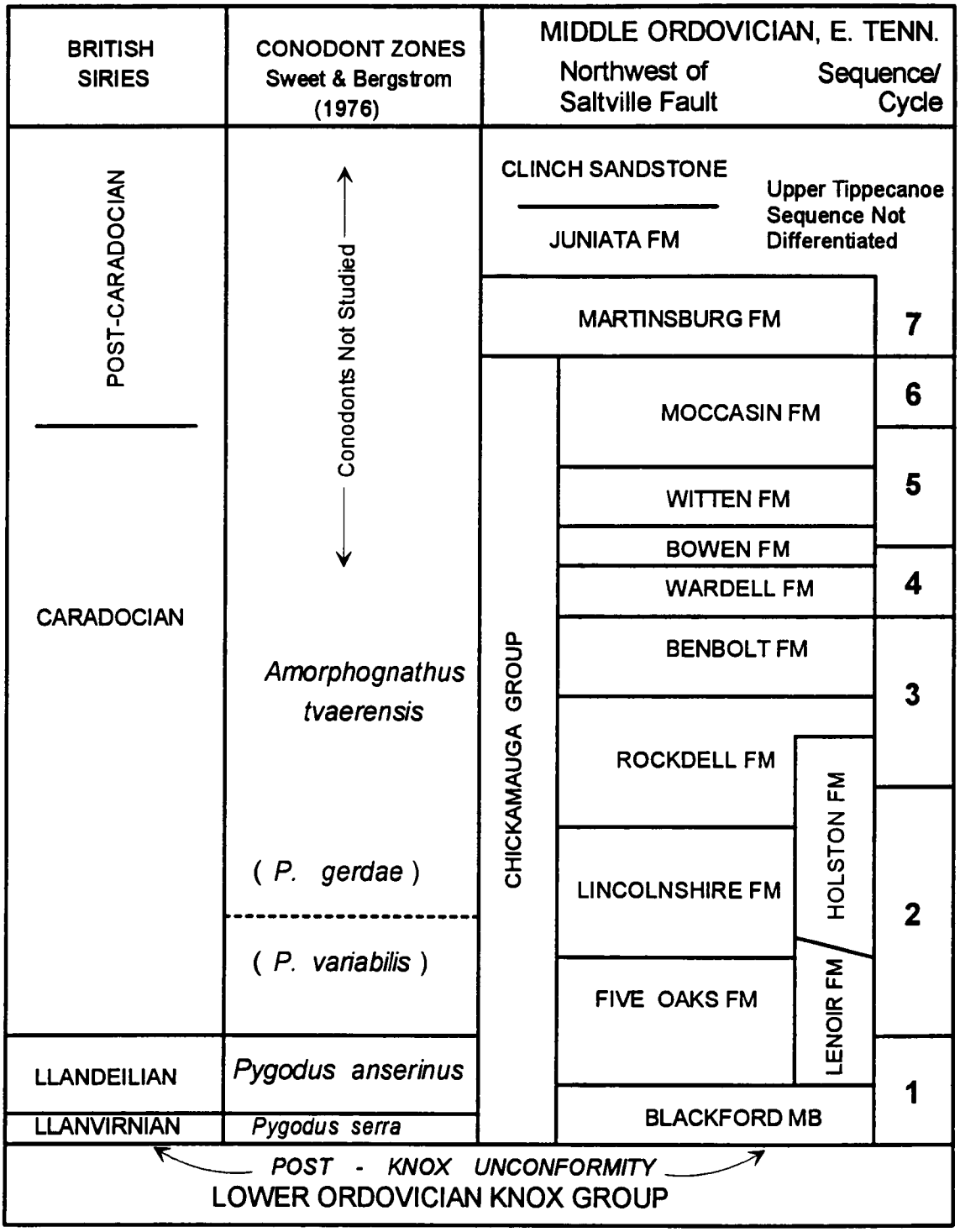



Figure 1.2 General stratigraphic and temporal relationships the Tippecanoe Sequence (Sloss, 1963) in the study area. The present study comprises third-order sequences 1, 2, 3, and 4 of the Middle Ordovician succession of the Copper Creek allochthon in East Tennessee.

sequence (Sloss, 1963); and the Second-Order O-S (Ordovician-Silurian) Supercycle (Vail,et al., 1977).

## METHODS

A suite of 1041, 45 X 75 mm thin-sections from 784 stratigraphic intervals were used to look for the presence or absence of selected Middle Ordovician water-depth criteria. About 700 of these thin-sections were prepared by Steinhauff using a Microtech automated thin-section machine. Ruppel (1979) provided slightly less than 1/5 of the total thin-sections used and Johnson (1988), and Jernigan (1987) provided 47, and 50 thin-sections, respectively, from the Red House Branch section. Additional samples from Red House Branch were provided by Jernigan from which Steinhauff cut additional thin-sections. A small number of thin-sections from the Old Thorn Hill and Idol Mine sections were provided by Keith Roberson. Approximately one-half of each thin-section was stained with a combined stain of potassium ferricyanide and alizarin red-S after Dickson (1965, 1966) to help identify dolomite and phases containing ferrous iron. Polished slabs from more than 325 of these stratigraphic intervals were prepared to look for features that occur at a scale inappropriate for thin-section observation. Slabs ranged in size from about 50 X 100 mm to 200 X 250 mm. Thin-sections prepared using the Microtech, along with their corresponding billets, provided the materials for additional isotopic and trace elemental work. Comparative and supporting lithologic observations were made using 171 thin-sections provided by Breland (1980) from the Knoxville area (Chapters 2 and 3, Appendix B).

Thin-sections containing abundant calcite cements (about 300) were examined under cathodoluminescence to observe stratigraphic and cross-cutting relationships not otherwise observable with conventional petrography. Cathodoluminescence was also used to help screen samples to ensure that only a single phase was sampled for stable carbon and oxygen isotopes, radiogenic strontium, and trace elements.

Phases analyzed for isotopes (258 samples) and trace elements (more than 1,020 points were probed) were cut with a water-cooled saw and polished to help identify different cement phases for sampling. Microsamples were obtained with a microscope-mounted microdrill capable of drilling constituents to about 0.3 mm in diameter. The microdrill and common acid extraction line used to extract stable isotopes of carbon and oxygen was built by Lincoln Foreman, with assistance from K.R. Walker. All geochemical analyses, with the exception of radiogenic strontium, were preformed using the facilities of the Department of Geological Sciences at the University of Tennessee. Additional details concerning stable isotopic, electron microprobe, and radiogenic strontium analyses are presented in Chapter 4 and the results are presented in appendices D, E, and G, respectively. Details concerning whole-rock atomic absorption analyses are considered in Chapter 5, and the results are presented in Appendix F.

# SIGNIFICANCE OF STUDY

## General Significance

**1) Non-Cyclic Carbonates.** This work is perhaps the first to seriously address the phenomenon of non-cyclic carbonates. A major difference between non-cyclic and cyclic carbonates is that evidence for exposure or shoaling in non-cyclic carbonates is generally subtle and only observable at a microscopic scale. Indeed, chapters 2 and 3 provide a method, albeit a tedious one, and a model that future workers might use to further investigate non-cyclic carbonates.

**2) Sequence Stratigraphy and Diagenesis.** Recent studies of carbonate successions tend to emphasize either sequence stratigraphy or diagenesis, but not both. Chapter 4 attempts to interpret observed diagenetic patterns within a sequence stratigraphic framework. For example, relative changes in sea-level established using lithologic criteria (i.e., water-depth curves and Fischer plots) are supported and corroborated with geochemical evidence (chapters 2 - 5).

**3) Paleoecology.** This work provides a wealth of material (more than 1,000 thin-sections) suitable for a Middle Ordovician paleoecologic study within a sequence stratigraphic framework.

## Regional Significance of Study

**1) Sequence Stratigraphic Correlation.** Water-depth curves, Fischer plots, and the sequence stratigraphic framework developed in chapters 2 and 3 provide a new means for correlation of Middle Ordovician strata. The potential for correlation is greatest within East Tennessee and the Southern Appalachians. However, it may some day be possible to correlate some of the sequences or changes in relative sea-level to other parts of the world.

**2) Depositional Model.** This work also provides a depositional model and a detailed three dimensional interpretation of six Middle Ordovician formations (Lenoir, Five Oaks, Lincolnshire, Rockdell, Holston, and Benbolt) that have wide spread distribution throughout East Tennessee and southeast Virginia. The cross-sections of Figures 2.12 - 2.18 and Figures 3.9, 3.13, and 3.14 provide an important resource for comparative study of these formations at other localities.

**3) Late Burial Diagenesis: Possible Relation to Mississippi Valley-Type Deposits.** This study provides evidence for the timing of late burial diagenesis and the introduction of hot metal-bearing brines from the Sevier basin to the shelf-edge and into the Middle Ordovician carbonate platform. Oxygen isotope data for late phases and an assumed range of possible burial fluid $\delta^{18}O$ composition indicates a range of possible temperatures needed to produced these Middle Ordovician burial phases. These temperatures are compared with burial curves for East Tennessee. This

analysis suggests that burial fluids hot enough to have produced late burial phases in the Middle Ordovician succession could have been produced in the Sevier basin before the end of the Middle Ordovician (about 450 Ma).

Importantly, this work examines a succession that lies geographically and stratigraphically between the Mississippi Valley-type deposits in the Lower Ordovician Knox Group of the Copper Ridge district (Churnet et al., 1982) and the Sevier basin (Shanmugam and Walker, 1980). The Sevier basin has been considered a possible source for Mississippi Valley-type brines by a number of workers (e.g., Kesler et al., 1988; Walker and Foreman, 1990). Most economic studies are limited to the ore body and to those rocks closely associated with it (e.g., Ebers and Kopp, 1979; Kesler et al., 1988) or to the shales of the basin thought to have been responsible for fluids producing the mineralization (e.g., Cathles and Smith, 1983; Furman, 1990). In contrast, this study examines a succession that lies temporally and geographically between the proposed starting point (the Sevier basin) and at least one end point (the Idol Mine) of zinc mineralization. Successions such as this one have been largely ignored by economic geologists, yet they may contain valuable evidence regarding the source, evolution, and timing of Mississippi Valley-type deposits.

Different basins thought to be responsible for Mississippi Valley-type deposits have been evaluated by Cathles and Smith (1983). They suggest that basins such as the Sevier, which likely reached 3 to 5 km depths before the end of the Ordovician, could have produced episodic pulses of geopressured brines responsible for Mississippi Valley-type mineralization. If the burial fluids that precipitated the latest

phases in this Middle Ordovician succession are the same ones that lead to the Mississippi Valley-type deposits in the Copper Ridge district, then the possible timing of zinc mineralization may be much earlier than most workers have previously suggested (e.g., Elliot and Aronson, 1987; Misra and Fulweiler, 1992). For example, Kesler et al., (1988) suggested that zinc mineralization occurred between about 405 and 320 Ma in the Copper Ridge district. Interestingly, Hill and Wedow (1971) proposed an early Middle Ordovician timing of collapse breccias associated with the zinc deposits in East Tennessee. If fluids expelled from the Sevier basin were responsible for zinc mineralization, then the present study suggests that these fluids could have been coeval with, or have closely followed the collapse breccias associated with the zinc deposits in the Copper Ridge district. This Middle Ordovician succession also may also contain evidence of post-ore mineralization (i.e., Bachtadse et. al., 1987; Lu and Craig, 1992).

# CHAPTER 2

## SEQUENCE STRATIGRAPHY OF AN APPARENTLY NON-CYCLIC CARBONATE SUCCESSION: RECOGNIZING SUBAERIAL EXPOSURE IN LARGELY SUBTIDAL STRATIGRAPHIC SEQUENCES, MIDDLE ORDOVICIAN, EAST TENNESSEE


### ABSTRACT

Non-cyclic carbonates are those where shallowing-upward features are sparse and not easily recognizable in outcrop, and where few subsequences and parasequences are capped by peritidal lithologies. A 400 meter thick succession of Middle Ordovician non-cyclic carbonates occurs at four on-shelf localities exposed along a 6 km transect on the northwest limb of the Copper Creek allochthon of East Tennessee. By using paleobathymetric analysis it is possible to unravel the sequencing of stratigraphic units in this succession.

Water-depth of deposition is established using multiple lines of evidence to determine a range of possible water-depths. Inflection points in water-depth curves indicate stratigraphic intervals that, on further detailed analysis, also contain subtle indicators of subaerial exposure. Such indicators help deduce changes in water-depth after deposition. These indicators include erosional truncation, mudcracks, crystal or vadose silt, calcite filled vugs lined by reddish crusts, and pendant cements (observed under cathodoluminescence).

Seven surfaces of subaerial exposure or drowning define seven "third-order" sequences in the entire Middle and Upper Ordovician. The present study analyzes the lower four and the lower part of the fifth (Middle Ordovician) "third-order" sequences (100 ± m thick) and their contained 22 "fourth-order" (10-20 m thick) subsequences (Five Oaks Fm through Witten Fm) that appear to be correlative across the shelf. These third- and fourth-order sequences contain "fifth-order" or "meter-scale" packages. These are comparable in scale to the parasequences of other authors. Meter-scale packages are not correlative from place to place and many of these are probably the result of lateral environmental migration. Sequence and subsequence lithologies differ vertically and horizontally and cannot be generalized.

Stratigraphic sequences, subsequences, and parasequences represent shallowing-upward packages similar to cycles. However, these sequences, subsequences, and parasequences differ from the usual cycles in that they mostly lack peritidal caps, and evidence for exposure and shoaling is subtle and usually revealed only through microscopic examination. They differ from most previously described subtidal cycles in that they are capped by exposure surfaces.

A Fischer plot, substituting subsequences and parasequences for cycles, supports interpretations previously made for this succession based on other lines of evidence (e.g., Ruppel, 1979; Ruppel and Walker, 1982, 1984) and helps clarify new observations revealed through water-depth analysis.

# INTRODUCTION

Because carbonate shelves are nearly horizontal and mostly form in very shallow water, they provide one of the most accurate gauges for investigating changes in sea-level. Sediment type, geometry, and diagenesis on carbonate shelves and platforms record information about sea-level changes. Additionally, because of early cementation, carbonate shelf sediments are often less compacted than sediments on siliciclastic shelves. Thus, carbonate shelves may be more sensitive to sea-level changes than siliciclastic shelves.

Shallowing-upward, meter-scale carbonate packages, termed "cycles," have been increasingly recognized throughout the geologic record (e.g., Fischer, 1964; Read et al., 1986; Read, 1989; Koerschner and Read, 1989; Goldhammer et al., 1987, 1990). These shallowing-upward packages are readily identified in outcrop and appear to be systematically arranged within larger-scale successions. Many of these researchers have envisioned eustatic oscillation of sea-level as the primary mechanism leading to the occurrence of these shallowing-upward, meter-scale packages and their systematically arranged larger-scale counterparts. Other workers (e.g., Kozar, et al., 1990; Hardie et al., 1991) have, however, noted that autocyclic causes of relative sea-level change may have also been a driving force.

Non-cyclic sections are those where shallowing-upward features, such as capping cryptalgal laminites or capping fenestral mudstones, are sparse or not recognized in outcrop. Examples of non-cyclic carbonate sections include the Middle Cambrian of the Llano uplift, Texas; the Johns Wash Member of the Orr Formation,

House Range, Utah (Osleger, 1990); and those parts of the Upper Cambrian Conasauga Group in East Tennessee that were deposited in deeper water (e.g., Weber, 1988; Kozar et al., 1990).

## Objectives

Although the results of cyclic carbonate sequence studies have been somewhat controversial (e.g., Kozar et al., 1990; Hardie et al., 1991) no one doubts that sea-level has varied throughout geologic time. However, non-cyclic carbonate sequences are also common in the record, and the response to sea-level variation in such sequences is less well known. Relative sea-level change is elucidated in just such a non-cyclic carbonate succession by documenting changes in water-depth (i.e., the sum of subsidence, eustacy and sedimentation) and the occurrence of surfaces of subaerial exposure in an approximately 6 km long transect of a more than 400 meter thick Middle Ordovician shelf succession. Water-depth analysis provides valuable supporting evidence for the occurrence of surfaces of subaerial exposure. Knowledge of carbonate facies geometry is based on outcrop and thin section observation and is constrained by surfaces of subaerial exposure.

## Study Area

The studied localities include (from southwest to northeast) the Thorn Hill (TH), Old Thorn Hill (OTH), Idol Mine (IS), and Cedar Springs (CS) sections. Each section is separated from the other by approximately 2 km (Fig. 2.1). A regional stratigraphic framework, based on these and other sections, was

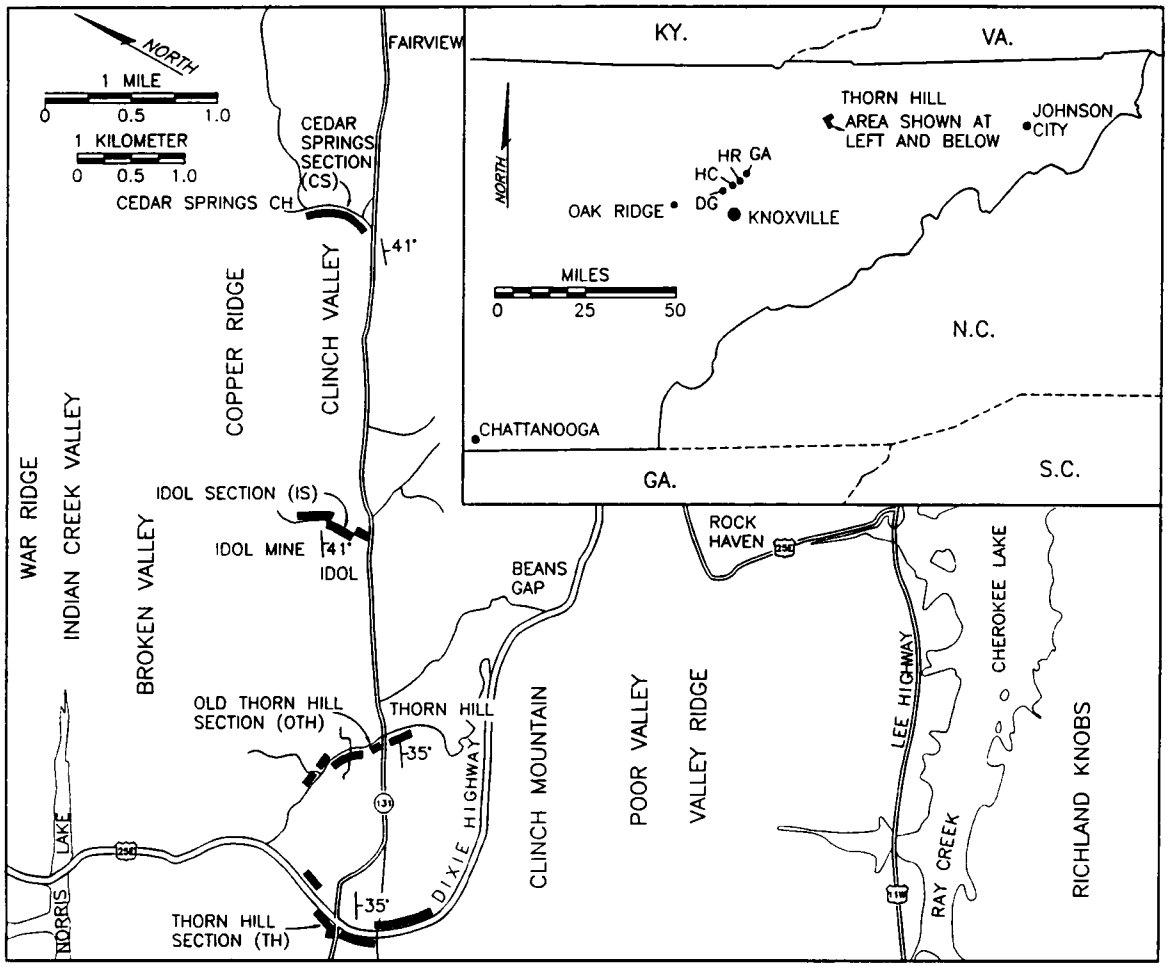



Figure 2.1. Location map. Inset, upper right, shows Thorn Hill study area (solid "L" ) in relationship to East Tennessee. Surrounding map indicates sampled sections (heavy black) at Thorn Hill (TH), Old Thorn Hill (OTH), Idol Mine section (IS), and Cedar Springs (CS). Lithologic comparison is made with samples provided by Breland (1980) from the same strike belt in the Knoxville area at Dry Gap (DG), Halls Cross Roads (HC), Harbison (HR), and Graveston (GA).

developed by Walker (1977, 1980, 1985), Ruppel (1979), and Ruppel and Walker (1982, 1984). A more than 540 meter thick succession of Middle Ordovician strata ranging from the upper Knox Group through the Five Oaks, Lincolnshire, Rockdell, Benbolt, Wardell, Bowen, Witten, and Moccasin formations is exposed in this area.

Supporting lithologic point-count data are considered from a similar on-shelf Middle Ordovician succession in the same fault block, approximately 50 km to the southwest, near Knoxville (Fig. 2.1). Samples from these localities were collected and described by Breland (1980). They include, from southwest to northeast, the Dry Gap (DG), Halls Cross Roads (HC), Harbison (HR), and Graveston (GA) sections (Fig. 2.1).

## PALEOBATHYMETRIC DATA

Paleobathymetric inferences are commonly based on data that only indirectly correlate with depth (e.g., Wilson, 1975; Elrick and Read, 1991; Osleger and Read, 1991). Establishment of relative depth relationships is feasible if multiple lines of evidence are used. Suites of indicators are used so that a range of possible water-depths is determined using as many indicators as possible (e.g., Elias, 1937; Benedict and Walker, 1978). The indicators used here are revised, and the number is enlarged from Benedict and Walker (1978).

### Bathymetric Indicators

Bathymetric indicators are of four types: 1) chemical, 2) sedimentologic, 3) biologic, and 4) stratigraphic. Each category contains criteria observable at different

scales, ranging from microscopic (in thin-section) to patterns of regional scope. All the indicators we have listed are not applicable in every situation. Indeed, some indicators (e.g., those for very deep water) were not used at all. Rather, emphasis is on those indicators that are most useful in the study of on-shelf and shelf-edge Middle Ordovician sequences (Figs. 2.2 and 2.3).

## Evidence for Subaerial Exposure

As chemical, physical, biological, and stratigraphic indicators are analyzed, each category of information can be reexamined within the context of the entire framework. Taken together, these indicators reveal water depths at the time of sediment deposition. Following deposition, however, subsequent changes in water-depth can occur. Subaerial exposure is one such post-depositional change that commonly occurs in shallow-water carbonates. When sea-level drops well below the platform margin and sediments are exposed for long periods, evidence for exposure is generally easy to recognize (e.g., Esteban and Klappa, 1983). However, if sea-level remains at or near the platform margin and sediments experience only a short period of exposure, then evidence for that exposure becomes subtle. Inflection points in water-depth curves that record water-depth at the time of deposition help point out stratigraphic intervals that may only contain subtle indicators of subaerial exposure. Such additional indicators are here termed "subaerial exposure indicators."

Subaerial exposure indicators include erosional truncation, mudcracks, crystal or vadose silt, calcite filled vugs (lined with reddish crusts), penecontemporaneous

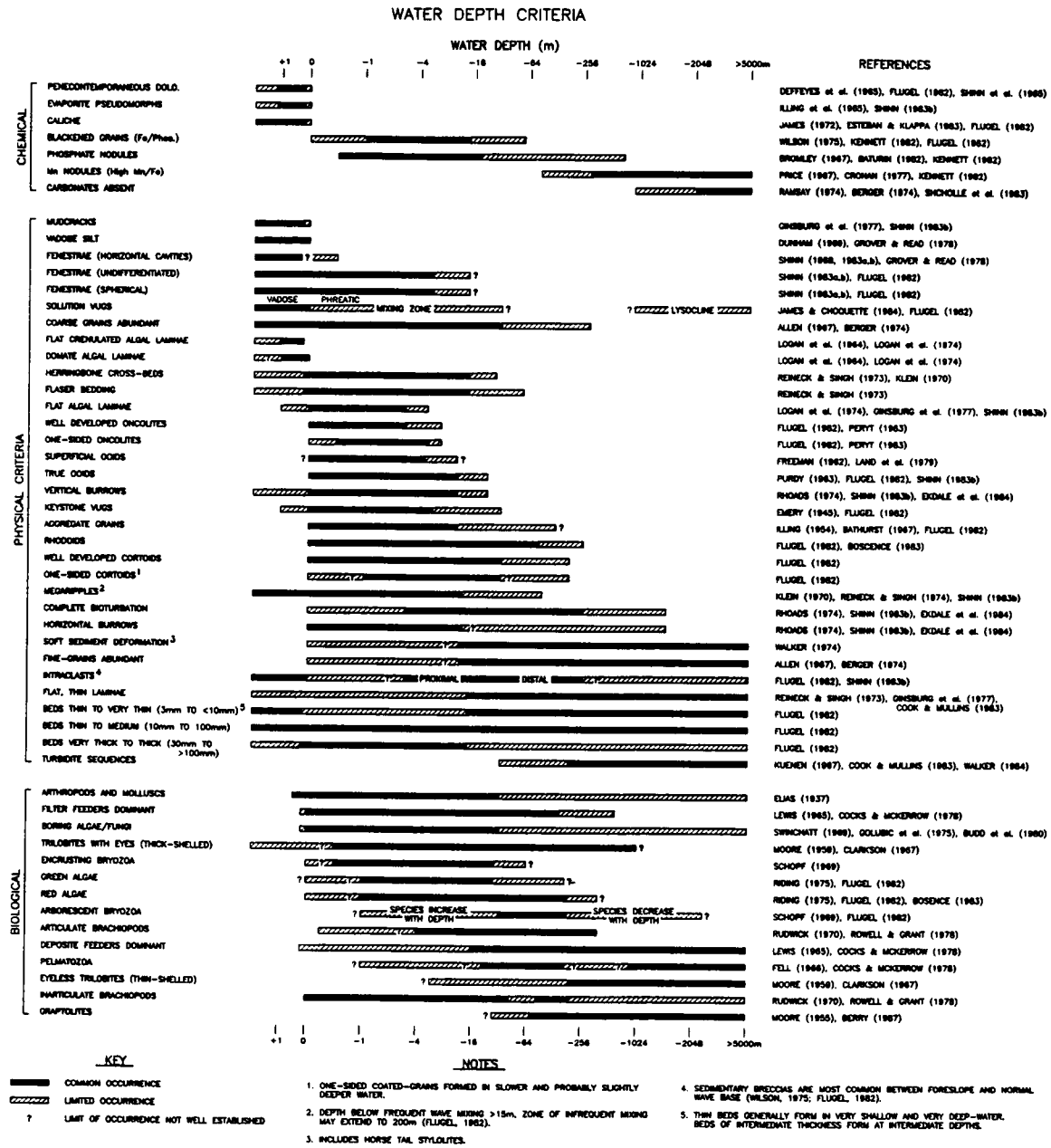



Figure 2.2. Water-depth criteria substantially modified after Benedict and Walker (1978).

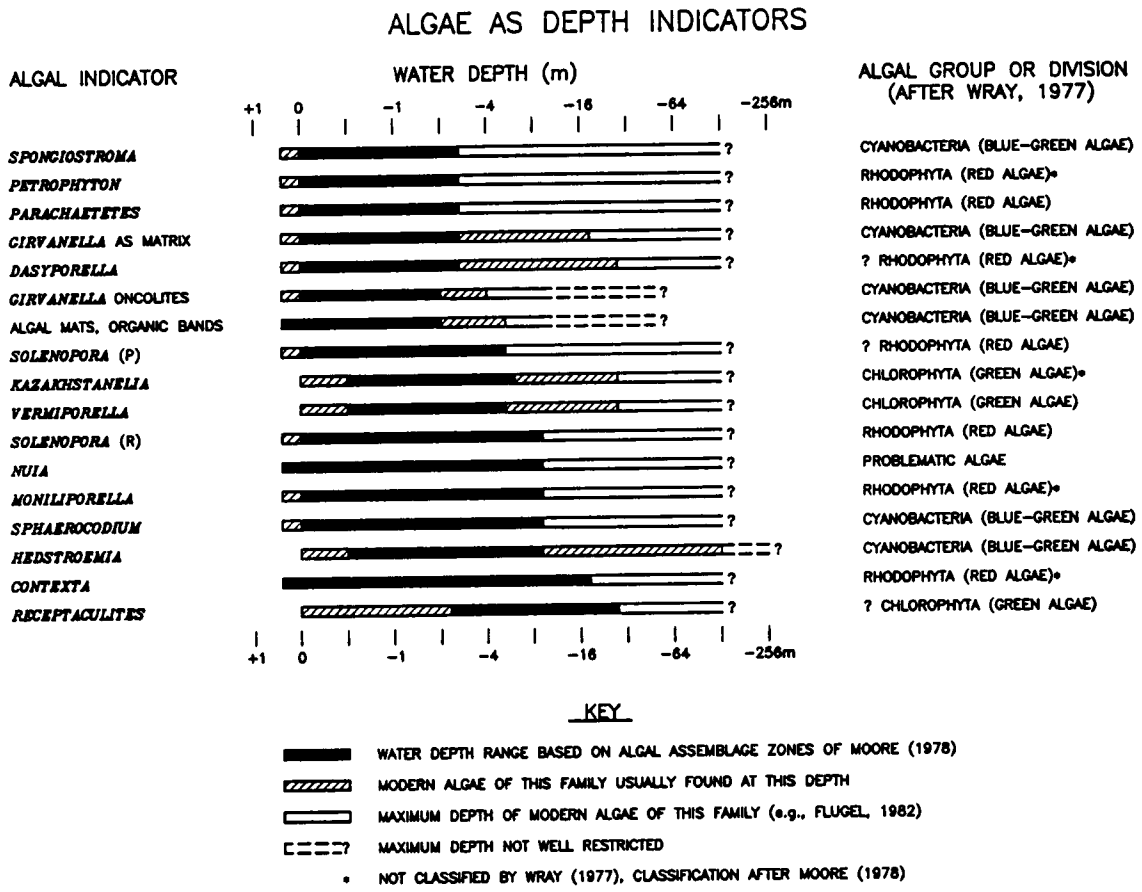



Figure 2.3. Middle Ordovician algal depth indicators of Moore (1978).

dolomite, and pendant cements (observed under cathodoluminescence). Trace element and stable carbon and oxygen isotopic data support these observations (Steinhauff et al., 1989a,b). Crystal or vadose silt, pendant cements and solution vugs also occur within many of these truncated fenestral mudstones (Figs. 2.5 and 2.5). Additional and related examples are described and / or illustrated by Steinhauff (1989), Steinhauff et al. (1989a,b), and Srinivasan et al. (1989).

## Methods

Each successive, lithologically homogeneous stratigraphic interval, represented by at least one 50 X 75 mm thin-section, was scored for the presence or absence of selected Middle Ordovician water-depth criteria (Figs. 2.2 and 2.3). Some criteria, such as thickness of bedding and presence of megaripples, are best observed in the field. A total of 789 thin-sections from 680 different stratigraphic intervals from the Thorn Hill area were used. Additionally, polished slabs from more than 250 of these stratigraphic intervals were prepared to examine for criteria such as burrows, flat algal laminae, and different categories of fenestrae. These features can be difficult to discern in the field and are commonly at a scale inappropriate for thin-section observation. Thus, when slabs were observed, serially cut sections (generally two or more) were prepared for each stratigraphic interval examined. These slabs ranged in size from about 50 X 100 mm to 200 X 250 mm. Comparative and supporting lithologic observations were also made using 162 thin-sections prepared by Breland (1980) from coeval rocks cropping out in the Knoxville area (Fig. 2.1).

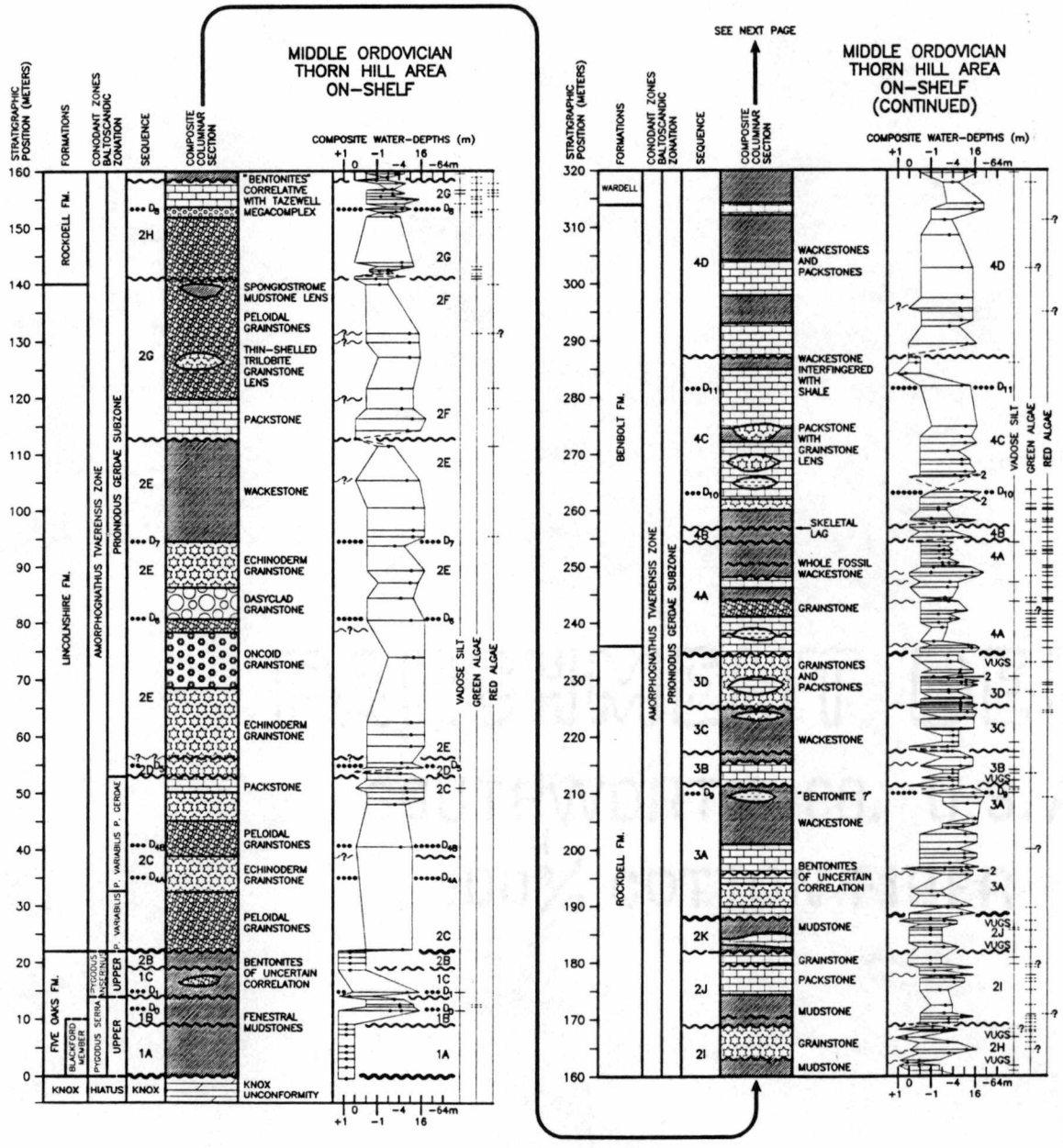



Figure 2.4. Composite columnar section, Thorn Hill area. A. Water-depth curves are based on Thorn Hill and Old Thorn Hill sections. More detailed key to lithologies is given in Figure 2.11. Conodont zonation is based on Carnes (1975) and later work by Anita Harris (Keith Roberson, personal communication). Because recognized formation boundaries (i.e., Ruppel and Walker, 1992, 1984) are gradational facies transitions, the base of the Rockdell Formation and Benbolt Formation are indicated here to coincide with the surfaces of subaerial exposure separating subsequences 2G and 2H and sequences 3 and 4, respectively. Previous workers (e.g., Ruppel , 1979) have placed the base of Rockdell as much as 20 meters both above and below the position indicated here and the have placed the base of the Benbolt as much as 10 meters both above and below the position indicated here.

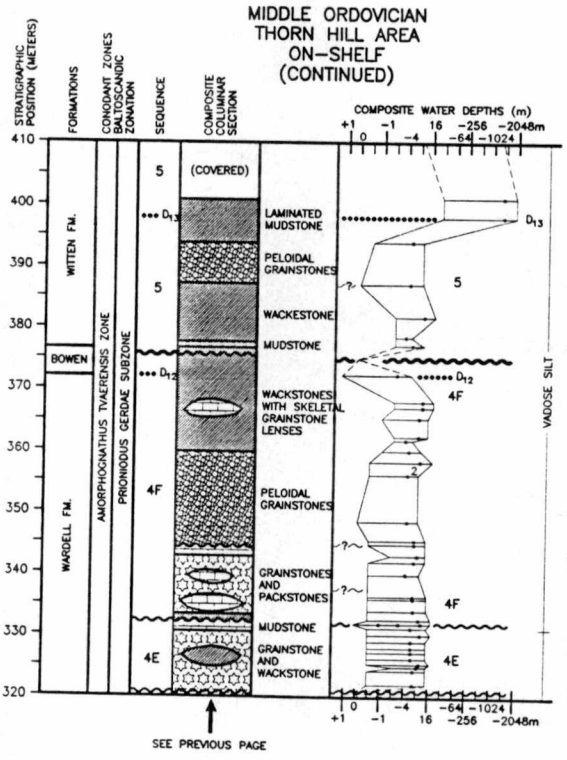
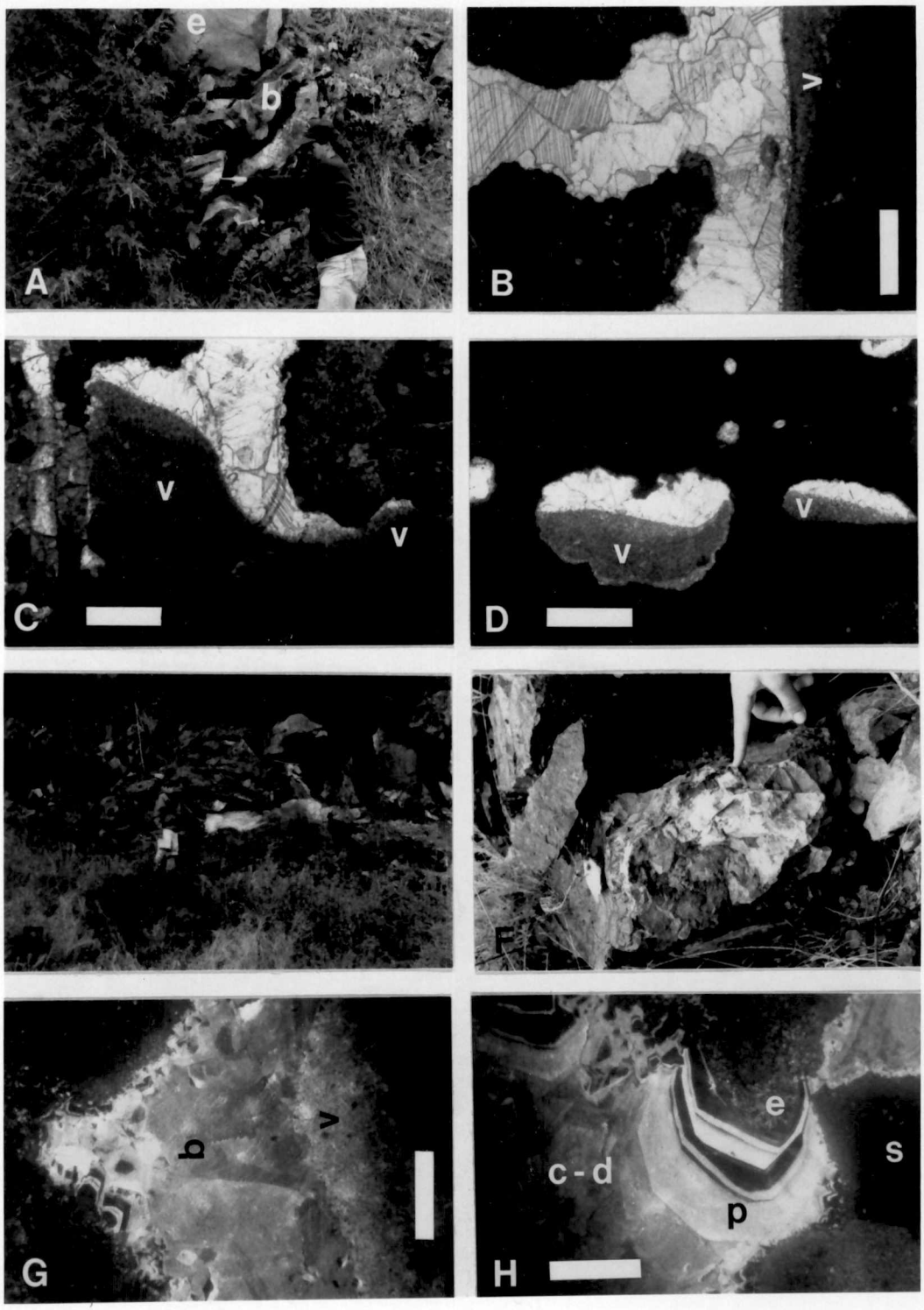



Figure 2.4. Composite columnar section, Thorn Hill area. B. Figure is continued. Note that the Witten Formation is approximately 73.1 meters thick and is overlain by the Moccasin Formation of nearly 200 meters thickness.

Figure 2.5. Subaerial exposure indicators. Scale bars at bottom of field, represent 1 mm. **A.** Exposure surface at Idol Mine section (IS) separating third-order sequences 3 and 4, between 235 to 250 m above Knox unconformity. Strata dip about 40° southeast, "up" to left margin of page. Wackestone / mudstone (facies L) below indicated irregular exposure surface is truncated by mud-rich peloidal grainstones (transitional facies) which grade vertically and laterally with bioclastic wackestone / packstone (b) (facies B) and are overlain by transitional echinoderm grainstone (e). **B.** Geopetal vadose silt (v) along bottom of blocky clear calcite (Ave. $\delta^{13}C$ = -0.8 ‰, $\delta^{18}O$ = -7.4 ‰ PDB, N = 2) filled cavity hosted in bioclastic wackestone / packstone (facies B) and whole fossil wackestone (facies A), 213.5 m above Knox, Thorn Hill section; "up" to left margin of page, plane polarized light (PPL). **C.** Vadose silt (v) is perched with stratigraphic layering in blocky clear calcite ($\delta^{13}C$ = -2.0 ‰, $\delta^{18}O$ = -7.8 ‰ PDB, N = 5) filled cavity hosted in bioclastic wackestone / packstone (facies B) and mudstone (facies L), 210.2 m above Knox, Thorn Hill section; PPL. **D.** Additional vadose silt (v). Area surrounding pore is lighter than surrounding micritic matrix suggesting leaching of iron-oxide and other trace metals from matrix during exposure. Same stratigraphic interval as C., PPL. **E.** Calcite filled vugs, indicated and arrowed, are lined by reddish crusts followed by early fibrous calcite ($\delta^{13}C$ = 0.6 ‰, $d^{18}O$ = -4.8 ‰ PDB, N = 4) truncated by ferroan coarse sparry calcite ($\delta^{13}C$ = 0.5 ‰, $d^{18}O$ = -8.3 ‰ PDB, N = 3). Vugs are hosted in mudstone (facies L) 185 m above Knox, Thorn Hill section. **F.** Calcite filled vugs and fenestrae are lined by reddish crusts followed by early fibrous calcite, not shown, ($\delta^{13}C$ = 0.6 ‰, $\delta^{18}O$ = -4.9 ‰, PDB, N = 15) which in some cases is truncated by ferroan coarse sparry calcite ($\delta^{13}C$ = 1.0 ‰, $d^{18}O$ = -6.6 ‰, PDB, N = 2). Note cleavage of coarse sparry calcite. Vugs are hosted in bioclastic wackestone / packstone (facies B) and (mudstone facies L) admixed with peloidal grainstone, 230 to 236 m above the Knox, Idol Mine section, PPL. **G.** Pendent cements under cathodoluminescence (CL) within blocky calcite filled cavity (b) underlain by vadose silt (v), same interval figured in C and D. "Up" to left margin of photo. **H.** Zoned pendent cement (p) observed under CL grew as overgrowth in optical continuity with echinoderm ossicle (e). Ferroan coarse sparry calcite (c-d) ($\delta^{13}C$ = 0.3 ‰, $\delta^{18}O$ = -7.4 ‰, PDB, N =1) is dully luminescent and sediment (s) is non-luminescent, 214.1 m above Knox, Thorn Hill section.


e
b
A
v
B
v
v
C
v
v
D
F
p
v
G
e
c-d
p
s
H

Resolution of water-depth decreases as water-depth increases (Benedict and Walker, 1978). That is to say, indicators of shallow water-depths discriminate a narrower range of possible water-depths than do those indicating deeper water-depths (Fig. 2.2.). Thus, a geometric scale was selected to plot a range of possible water-depths at the time of deposition (e.g., Figs. 2.2, 2.3, and 2.4). These ranges are based on chemical, physical, biological, and stratigraphic indicators. A midpoint for each range is also plotted. At some stratigraphic intervals, more than one thin-section was observed. When these thin-sections come from slightly different lithologies (e.g., skeletal grainstone versus skeletal packstone), slightly different water-depth ranges may be indicated for each lithology. For these intervals, the combined range is plotted and two "midpoints" are indicated (e.g., Fig. 2.4).

"First iteration" water-depth curves were plotted and compared with detailed, bed-for-bed, lithologic descriptions at a scale of 1 inch to 1 meter. Stratigraphic intervals having inflection points indicating possible exposure or shoaling were reexamined for the presence of post-depositional indicators of subaerial exposure. Evidence of exposure comes from outcrop and thin-section examination. The "first iteration" water-depth curves were then replotted to reflect the fact that some stratigraphic intervals have experienced subaerial exposure (dashed lines on water-depth curves, e.g., Fig. 2.4).

## Degrees of Exposure

Pronounced surfaces of exposure (shown by heavy wavy lines in Figs. 2.4, 2.12 - 2.18) are indicated where fenestral mudstones are truncated by cross-bedded grainstones and packstones. Truncated fenestral mudstones contain most, if not all, of the post-depositional indicators of exposure. Less pronounced surfaces of exposure are indicated by crystal or vadose silt and one or more subaerial exposure indicators (Fig. 2.5).

# LITHOLOGIES

## Description

Seventeen limestone facies are recognized within this approximately 400 meter thick Middle Ordovician, on-shelf succession. These facies are assigned the letters A through O and are also numbered. The numbers generally correspond to the standard microfacies numbers recognized by Wilson (1975) and Flugel (1978, 1982). Not all of the standard microfacies are represented. Indeed, some limestone facies numbers are modified to account for criteria characteristic of Middle Ordovician limestones, but not generally recognized in younger rocks (Table 2.1). A detailed account of facies criteria is presented in Appendix A. Facies criteria include: 1) the type of matrix, 2) occurrence of allochems such as peloids, aggregate-grains, and coated-grains, 3) sedimentary structures, 4) flora and fauna, and 5) lateral and vertical facies relationships (Figs. 2.5, 2.6, and 2.7).

Facies P though S are "unnumbered" and do not fit the standard microfacies scheme. These include two carbonate facies mixed with siliciclastic detritus: facies Q, a siltstone / carbonate siltstone and shale; and facies R, a shale / shaly carbonate. Also included are facies P, a dolomitic limestone; and facies S, thin-bedded bentonite (Table 2.1; see also, Fig. 2.11, and Appendix A).

The seventeen limestone facies of the succession have widespread distribution throughout the Middle Ordovician shelf sequence in East Tennessee. For example, Figures 2.8 and 2.9 show ternary fields for these facies based on point-count data of Ruppel (1979) and Jernigan (1987) from the Thorn Hill area combined with point-count data of Breland (1980) from a similar on-shelf succession in the same fault block approximately 50 km to the southwest, near Knoxville (Fig. 2.1; Appendix B).

## Mud-Rich Lithologies

Mud-rich lithologies are ubiquitous and account for the largest proportion, more than 40%, of this Middle Ordovician succession (Figs. 2.6, 2.7, and 2.8). Mud-rich lithologies generally occur as nodular beds less than 0.25 meters thick and may be interbedded with a wide variety of grainstones. Echinoderm / bryozoan

Table 2.1: Facies Criteria

| | Carbonate Lithologic Criteria | | | | | | Biotic Criteria | | | | | | Other Criteria | |
|---|---|---|---|---|---|---|---|---|---|---|---|---|---|---|
| Lithology/ Microfacies* | Rock Name Dunham (1962) | Matrix | Peloids | Aggregate-Grains | Coated-Grains | Sedimentary Structures | Organisms: Primary | Organisms: Accessory | Biota: Diversity | Biota: Abundance | Flora | Whole Fossils vs. Fragments | Lateral and Vertical Facies Relations | Comments |
| A / 8 | Wackestone | Mud | Rare | Rare | Rare | Fenestrae; horizontal cavities; keystone vugs, rare | Pelmatozoa, arborescent bryozoa | Rare | Low | Low to moderate | Green algae, rare | Whole fossils | Gradational with facies 9, 10g, 12p, 12g (rarely), 16, 17, and 19. | Preserved infauna and epifauna and vertical burrows. |
| B / 9 | Bioclastic Wackestone/ Packstone | Mud | Rare | Rare | Rare | Bioturbated sediment; Domate algal laminae, rare | Pelmatozoa, bryozoans | Thick-shelled trilobites, sponge spicules | Moderate | Moderate to low | Green algae rare, red algae less common | Whole bryozoans, other fossils as fragments | Gradational with facies 8, 10g, 12p, 12g, 16, 17, 19, 22, shale and siltstone. | Occurs as beds 0.5 to 2 m thick with thin, interfingering grainstone beds, < 0.5 m thick. |
| C / 10g | Grainstone/ Cortoid Grainstone | Spar with small amounts of mud | Rare | Rare | Very abundant to abundant, most are partially coated | ?Megaripples | Pelmatozoa | Gastropods, thick-shelled trilobites, articulate brachiopods | Moderate to high | Moderate to high, Girvanella Oncolites Common | Green algae abundant to rare, red algae rare | Fragments rounded and worn | Gradational with facies 8, 9, 11, 12g, 12p, 13, 16 and 22. | Generally thick bedded, + 1 m thick. Grains more worn, fewer coated-grains than facies 11 |
| D / 11 | Grainstone/ Cortoid Grainstone | Spar with small amounts of mud | Rare | Abundant oncoids common | Very abundant to abundant, most are partially coated | Not observed | Pelmatozoa, encrusting bryozoa | Gastropods, thick-shelled trilobites, articulate brachiopods | High | Moderate to high | Green algae rare, red algae less common | Fragments | Gradational with facies 10g, 12g and 16. | No worm-grains. Coated-grains well-developed, oncoids common. |
| E / 12g | Echinoderm Grainstone | Spar | Rare | Rare | Rare | Megaripples | Pelmatozoa, bryozoa | Thick-shelled trilobites | Moderate | High | Green algae abundant to sometimes absent. Red algae less common | Fragments | Gradational with facies 9, 10g, 11, 12p, 13, 17, 18 and 19 (rarely). | Generally occurs as amalgamated beds, 1 to 2 m thick. |
| F / 12p | Echinoderm/ Bryozoan Packstone | Mud and lesser amounts of spar | Rare | Rare | Rare | ?Flaser bedding; keystone vugs; flat algal laminae, rare | Pelmatozoa, bryozoa | Thick-shelled trilobites | Moderate | High | Green algae abundant to sometimes absent. Red algae less common | Fragments very abundant, some fossils whole | Gradational with facies 8, 9, 10g, 12g, 13, 16, 17, 19 and 22. | Generally thick bedded, one or more meters thick. |
| G / 13 | Oncoid Grainstone | Spar, mud is rare | Rare | Rare to present | Very abundant to abundant, oncoids well-developed | ?Megaripples; organic bands; flat algal laminae, rare | Thick-shelled trilobites, gastropods | Pelmatozoa, articulate brachiopods | High | Low to moderate | Green algae abundant to rare, red algae rare | Fragments | Gradational with facies 10g, 11, 12g, 12p, 16, 17, 19, and 22. | No worm-grains, oncoids better developed than facies 10 and 11. |

| Lithology | Carbonate Lithologic Criteria | | | | | | Biotic Criteria | | | | | | Other Criteria | |
|---|---|---|---|---|---|---|---|---|---|---|---|---|---|---|
| H / 14 | Grainstone, Conglomeratic lag | Spar | Rare | Rare | Partially coated-grains | Not observed | Pelmatozoa, bryozoa, thick-shelled trilobites | Rare | Low | Low | Green algae abundant, red algae present | Fragments reworked | Gradational with facies 9, 10g, 21, and 22. | Very rare lithology, few thin beds, < 1 m thick. Blackened and phosphate coated-grains abundant. |
| I / 16 | Peloidal Grainstone | Spar, small amounts of mud | Very abundant | Rare to abundant | Rare to common, generally partially coated | Rare ?megaripples, ?flaser bedding | Ostracodes | Rare, sometimes with gastropods | Low | Low to moderate | Green algae rare to common, red algae less common | Whole ostracodes, other fossils as fragments | Gradational with facies 9, 10g, 11, 12g, 12p, 17, 18, 19, 19i, 19f shale, and siltstone. | Occurs as amalgamated beds, 0.5 to 2 m thick. Superficial ooids present. |
| J / 17 | Grainstone/ Peloidal Grainstone | Spar, mud is rare | Very abundant to common | Very abundant | Rare to common, generally partially coated | Rare | Ostracodes, sometimes with gastropods | Pelmatozoa, articulated brachiopods, thick-shelled trilobites | Low | High to moderate | Green algae rare to common, red algae less common | Whole ostracodes, other fossils as fragments | Gradational with facies 8, 9, 10g, 11, 12g, 12p, 19, and 22. | Superficial ooids present, problematic algae Nuia common to abundant. |
| K / 18 | Dasycladacean Grainstone | Spar | Rare | Present | Abundant to present, generally one-sided | ?Megaripples, intraclasts present in some beds | Dominated by green algae | Pelmatozoa, thick-shelled trilobites | Low | Low organism abundance | Green algae very abundant. Red algae abundant to present. | Whole fossil algae, other fossils as fragments. | Gradational with facies 11, 12g, 12p and 16. | Rare lithology, only a few beds, about 1 m thick. |
| L / 19 | Wackestone/ Mudstone | Mud | Very abundant to common | Rare to common | Present | Fenestrae present, but not abundant, organic bands present | Ostracodes gastropods, encrusting bryozoans | Rare or absent | Low | Low | Green algae rare, red algae absent | Whole ostracodes, other fossils as fragments | Gradational with facies 8, 9, 11, 12p, 16, 17, 19i, 19f and 22. | Generally occurs as massive, discontinuous beds, < 0.5m thick. |
| L / 19i | Laminated Wackestone/ Mudstone | Mud | Abundant to common | Rare | Rare | Flat algal laminae, fenestrae present, but not abundant | Ostracodes gastropods | Rare or absent | Low | Low | Green algae rare, red algae absent | Whole ostracodes, other fossils as fragments | Gradational with facies 19, 19f, 16 and 17. | Laminated beds < 0.5m thick. |
| L / 19F | Fenestral Wackestone/ Mudstone | Mud | Abundant to common | Rare to present | Present | Fenestrae, horizontal cavities, flat algal laminae | Ostracodes | Rare or absent | Low | Low | Green algae rare, red algae present | Whole ostracodes, other fossils as fragments | Gradational with facies 19, 19i, 16 and 17. | Bedded as facies 19 (above). |
| M / 21 | Spongiostrome Mudstone | Mud | Abundant | Common | Partial algal oncoids | Flat algal laminae | Encrusting bryozoans, pelmatozoans | ?Ostracodes | Low | Low | Spongiostroma | Bryozoans whole, pelmatozoans as fragments | Gradational with facies 14, 16, 17. | Very rare lithology, one 0.5m bed, observed base Rockdell Fm. OTH section. |

| Lithology | Carbonate Lithologic Criteria | | | | | | Biotic Criteria | | | | | | Other Criteria | |
|---|---|---|---|---|---|---|---|---|---|---|---|---|---|---|
| N / 22 | Wackestone/ Packstone-Oncoid Wackestone Packstone | Mud | Abundant to common | Common to abundant | Very abundant to abundant, generally one-sided | ?Flaser bedding | Thick-shelled trilobites | Gastropods | Low | Low | Girvanella oncoids common, green algae abundant, red algae less common | Fragments | Gradational with facies 9, 10g, 11, 16, and 17. | Girvanella oncolites common. Problematic algae Nuia abundant. |
| O / 24 | Lithoclastic Grainstone/ Packstone | Spar and mud | Abundant | Abundant to common | Not observed | Not observed, but intraclasts abundant in some beds | ?Ostracodes | Not observed | Low | Low | Not observed | Fragments | Gradational with facies 16, 19, and dolomitic limestone. | Rare lithology, only one, 1m thick bed near Knox unconformity |
| P Not Numbered | Dolostone/ Dolomitic Limestone | Fine-grained dolomite and mud | Rare | Not observed | Not observed | Laminae | Rare fragments only | Not observed | Low | Low | ?Stromatolites | Fragments | Gradational with facies 16, 17, 19 and 24. | Rare lithology. |
| Q Not Numbered | Siltstone/ Carbonate Siltstone | N/A | Not observed | Not observed | Not observed | Vertical burrows | Brachiopods occur in carbonate-rich intervals | Not observed | Low | Low | Not observed | Brachiopods occur as whole fossils | Gradational with facies 9, 16, 17, 12p and 19. | Rare lithology (Benbolt and Bowen Fms. only). |
| R Not Numbered | Shale/Shaly Carbonate | N/A | Not observed | Not observed | Not observed | ?Bioturbated sediment | Not observed | | Low | Low | Not observed | Not observed | Gradational with facies 9, 12p, 16 and 17. | Occurs in upper Benbolt and overlying formations. |
| S Not Numbered | Bentonite | Green clay | Not observed | Not observed | Not observed | ?Bioturbated sediment | Not observed | Not observed | N/A | N/A | Not observed | N/A | Gradational with facies 9, 16, 17, 12p, and 12g. | Thin beds throughout Middle Ordovician. |

Key

Very Abundant - Constituent comprises more than 50% of the allochems.
Abundant - More than three counts per thin-section observed in all thin-sections representative of facies.
Common - At least 1 to 3 counts per thin-section observed in all thin-sections representative of facies.
rare - One to three counts per thin-section observed in many, but not all thin-sections representative of facies.
present - Seen in about 1/4 to 1/2 of thin-sections representative of facies.

| Diversity | |
|---|---|
| High | > > 3 classes of organisms |
| Moderate | 2 to 3 Classes |
| Low | < 3 Classes |

| Abundance | |
|---|---|
| High | > 30% Allochems<br>> 30% Fossils |
| Moderate | > 30% Allochems<br>< 30% Fossils |
| Low | < 30% Allochems<br>or<br>< 20% Fossils |

*Microfacies numbers generally correspond to standard microfacies of Wilson (1975); however, some microfacies are modified (i.e., 10g, 12g, 12p, 19l and 19f) to account for criteria characteristic of Middle Ordovician limestones, but not generally observed in younger rocks.

Figure 2.6. Limestone lithologies in thin-section. Scale bars bottom of field, represent 1 mm. **A.** Echinoderm / bryozoan packstone (facies F), 178.5 m above Knox unconformity, Thorn Hill section; plane polarized light (PPL). **B.** Additional echinoderm / bryozoan packstone, same stratigraphic interval as A. **C.** Wackestone / mudstone (facies L), 7.3 m above Knox, Cedar Springs section; PPL. **D.** Peloidal grainstone (facies I), 22 m above Knox, Cedar Springs section, PPL. **E.** Grainstone with aggregated grains (facies J), 35 m above Knox, Cedar Springs section; PPL. **F.** Echinoderm grainstone (facies E), 328.6 m above Knox, Old Thorn Hill section; PPL. **G.** Grainstone with coated- and worn- bioclasts (facies C), 80.4 m above Knox, Cedar Springs section, PPL. **H.** Grainstone with coated-bioclasts and lumps (aggregated grains - facies D), 39.5 m above Knox, Cedar Springs section; PPL.

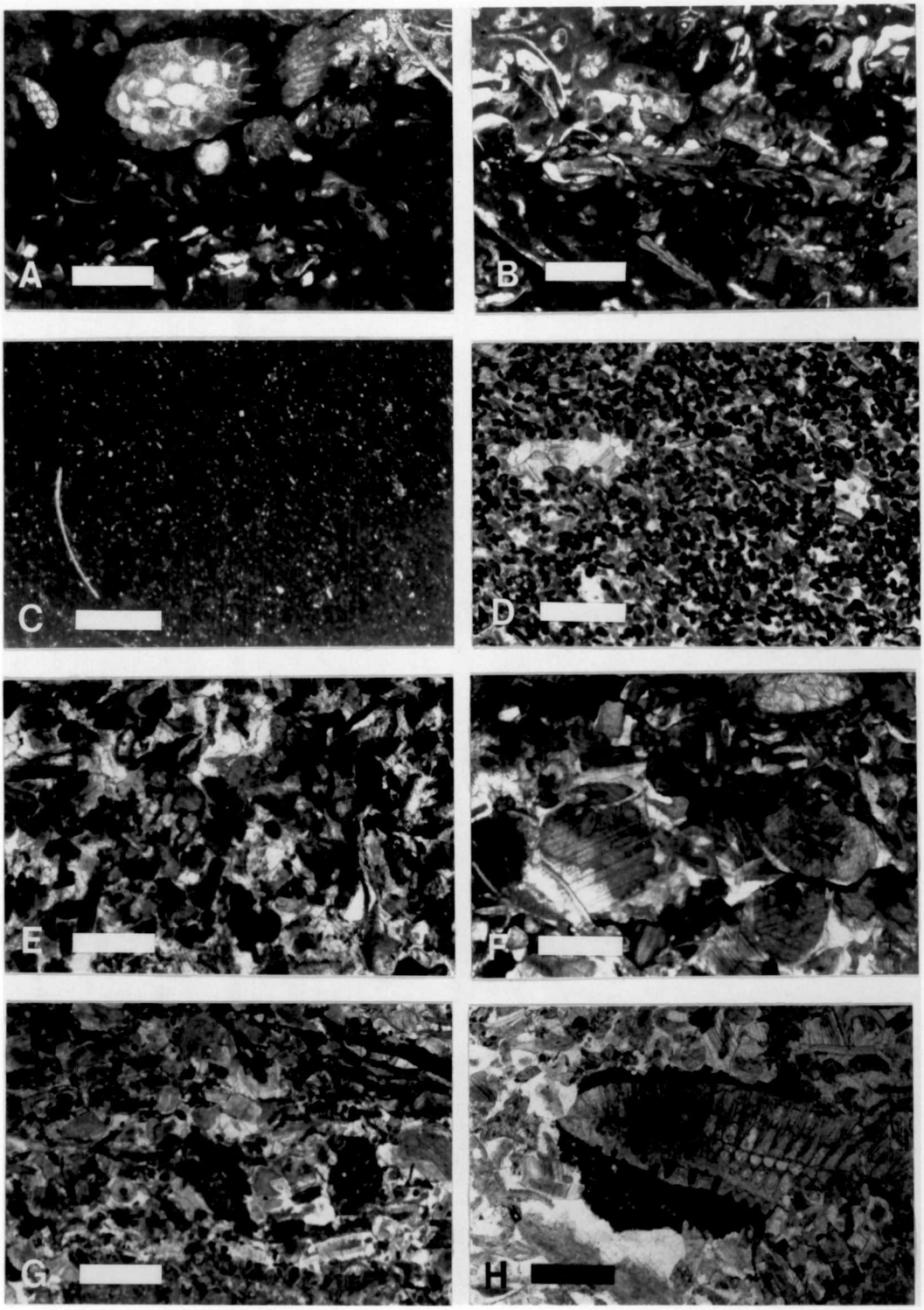
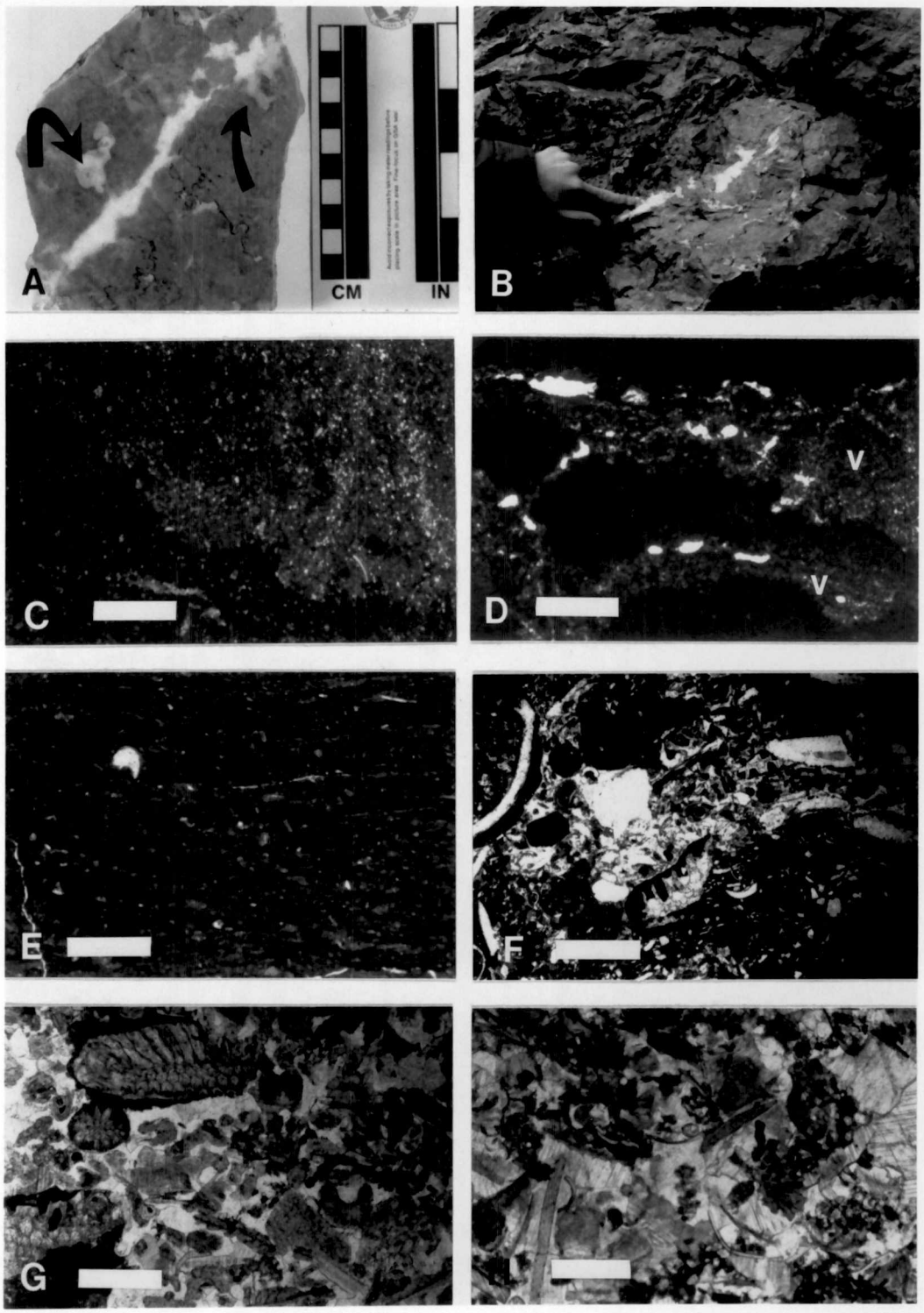

A
B
C
D
E
F
G
H

Figure 2.7. Additional mud-rich and coated-grain lithologies. Scale bars at bottom of field, represent 1 mm. **A.** Transitional wackestone / mudstone (facies L) 168.8 m above Knox unconformity, Thorn Hill section, polished slab. Vugs (arrowed) are filled with ferroan blocky white calcite (Ave. $\delta^{13}C$ = 0.6‰, $\delta^{18}O$ = -8.1‰ PDB, N = 2) **B.** Field relationship of calcite filled vugs and (?) calcite filled fractures to wackestone / mudstone host lithology, same stratigraphic interval as A. **C.** Wackestone / mudstone (facies L), 7.3 m above Knox, Cedar Springs section; plane polarized light (PPL). **D.** Laminated to fenestral wackestone / mudstone (facies L), 500.8 m above Knox, Old Thorn Hill section; PPL. Horizontal fenestrae contain vadose silt (v). **E.** Laminated wackestone / mudstone (facies L), 401.5 m above Knox, Old Thorn Hill section; PPL. **F.** Wackestone / packstone with oncoids and coated-grains (facies N), 119.6 m above Knox, Thorn Hill section; PPL. **G.** Grainstone with coated-bioclasts and lumps (aggregated grains - facies D), 40.5 m above Knox, Cedar Springs, PPL. **H.** Grainstone with coated- and worn-bioclasts (facies C), 80.4 m above Knox, Cedar Springs, PPL.


A
CM
IN
B
C
D
V
V
E
F
G

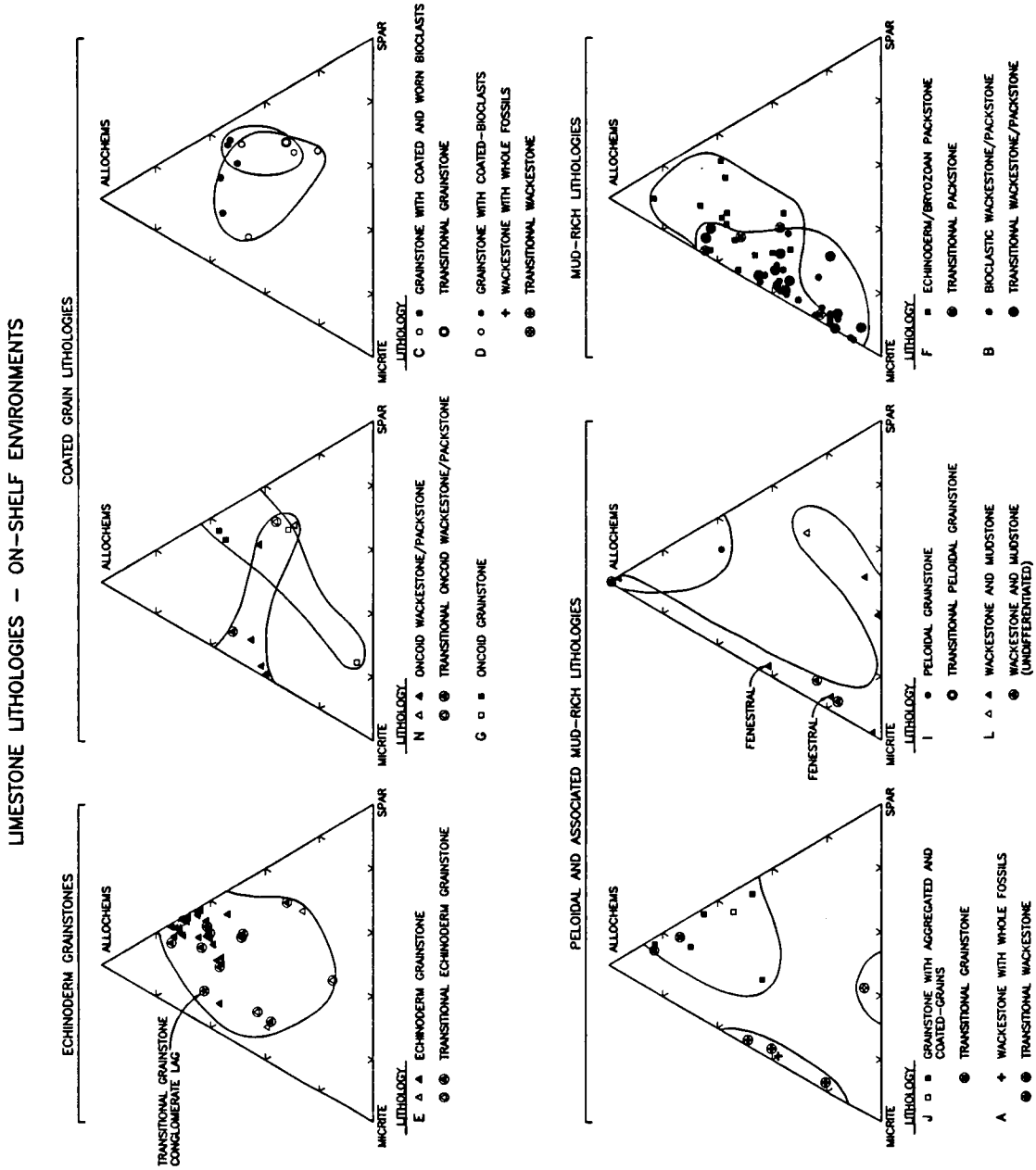



Figure 2.8. Ternary diagrams show limestone lithologies for Middle Ordovician on-shelf environments in East Tennessee. Selected point-count data from Ruppel (1979), Breland (1980), and Jernigan (1987). Open symbols indicate cement priority point-counting (i.e., Jernigan, 1987) and solid symbols indicate standard grain-priority technique. Standard grain-priority point-counting would count the interior of a snail as "snail", though the interior space might be filled with cement. Using "cement-priority" the area would be counted as cement. Symbols enclosed by a ring indicate transitional facies.

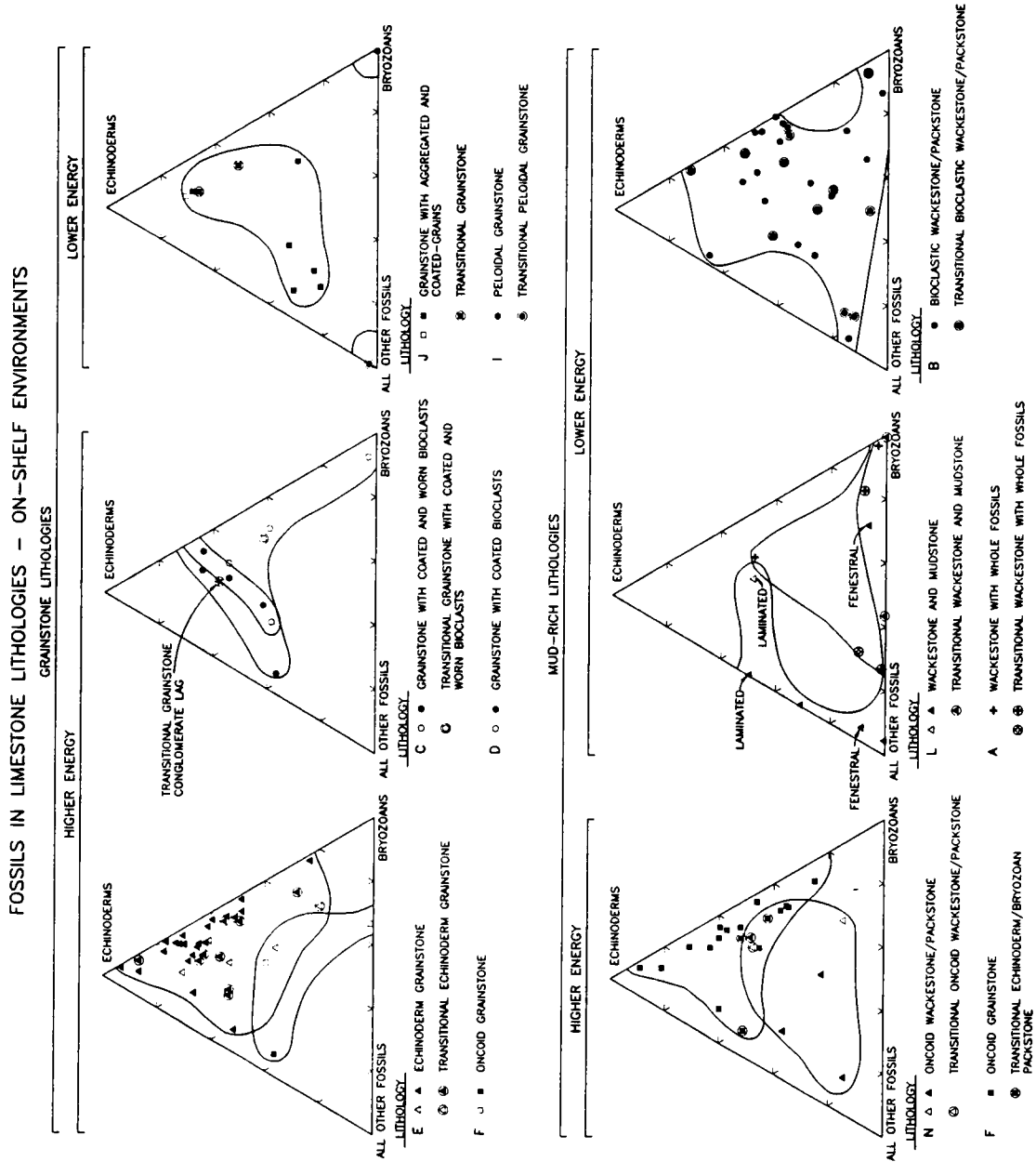



Figure 2.9. Ternary diagrams show fossils in limestone lithologies for Middle Ordovician on-shelf environments in East Tennessee. Selected point-count data from Ruppel (1979), Breland (1980), and Jernigan (1987), see caption Figure 2.8 for details.

packstone (facies F; Figs. 2.6A and 2.6B) and bioclastic wackestone / packstone (facies B; Figs. 2.5A-2.5D) are the most common and abundant mud-rich lithologies. Other mud-rich lithologies include whole fossil wackestone (facies A), wackestone / mudstone (facies L; Figs. 2.6C, 2.7A-2.7D), spongiostrome mudstone (facies M), and oncoid wackestone (facies N; Fig. 2.7F).

### Peloidal and Associated Mud-Rich Lithologies

Peloidal grainstones and their associated mud-rich lithologies account for slightly less than 30% of the total stratigraphic thickness, particularly within the Lincolnshire Formation (e.g., Figs. 2.4, 2.6, 2.7, and 2.8). Peloidal grainstones include facies I and J (Figs. 2.6D and 2.6E). Mud-rich wackestone / mudstone (facies L) occurs with massive, laminated, and fenestral fabrics (Figs. 2.7C-2.7E), all of which grade laterally and vertically into peloidal grainstones or other mudstones. Peloidal grainstones are also gradational with whole fossil wackestone (facies A) and bioclastic wackestone / packstone (facies B; Table 2.1, Appendix A).

### Echinoderm Grainstone

Echinoderm grainstones (facies E; Figs. 2.6F and 2.8) make up about 20 % of the total thickness of this succession. These grainstones commonly occur as amalgamated cross-bed sets up to several meters thick, interbedded with coated-grain or mud-rich lithologies (Fig. 2.4, Table 2.1). Where echinoderm grainstones occur as thin-bedded lenses within mud rich-lithologies, they generally contain a higher

proportion of bryozoans than thicker bedded echinoderm grainstones (Fig. 2.6F, 2.8, and 2.9).

### Coated-Grain Lithologies

Coated-grain lithologies are not particularly abundant, are generally thin-bedded (less than 0.5 meters thick), and account for only about 3% of the total stratigraphic thickness Fig. 2.4). Well developed oncoids occur in oncoid grainstone (facies G) and other lithologies, but are generally rare. Coated-grain lithologies include grainstones (facies C, D, and G; Figs. 6G, 6H, 7G, and 7H) and wackestone / packstone (facies N, Fig. 2.7F).

### Other Lithologies

Other lithologies make up about 5% of the total stratigraphic thickness. These lithologies include conglomeratic lag (facies H), dasycladacean algal grainstone (facies K), trilobite grainstone (lumped with facies E), dolostone and dolomitic limestone (facies P), and non-carbonate lithologies (facies O through S). (Table 1.2 and Appendix A).

### Fossil Content

Limestone facies can also be characterized by fossil content. Echinoderms and bryozoans are the most common and abundant fossils and generally occur as fragments (Figs. 2.6, 2.7, and 2.9). Where other fossils occur, two faunal associations are generally recognized: 1) an arthropod - mollusk association (i.e., thick-shelled trilobites and/or ostracods with gastropods) and 2) a brachiopod -

bryozoan association. Only in rare instances do other fossils account for any significant portion of the total rock. For example, several thin-shelled trilobite grainstone beds, less than 0.1 meter thick, crop out in the uppermost Lincolnshire Formation at the Thorn Hill section (Fig. 2.4). Sponges and sponge debris occur as cavity linings and fillings within mud-rich lithologies in the upper Rockdell and lower Benbolt formations.

### Lithologic Interpretation

These on-shelf lithologies represent a continuous suite of shallow water environments. Three lithologies may have been deposited at or slightly above mean sea-level (i.e., facies L, Q, and possibly facies M). Some lithologies were deposited in waters ranging from only a few centimeters to less than 6 meters in depth (i.e., facies D, G, and H). Other lithologies represent deposition in water generally ranging from about 0.5 to less than about 15 meters (i.e., facies E, F, I, K, N and O) and still others represent similar or slightly deeper water up to about 30 meters deep (i.e., facies C and Q). Shale and shaly carbonate (facies R) represent the deepest water deposition, possibly as deep as 150 meters. More detailed interpretations, including energy of environment and environment of deposition, are given in Table 2.2.

## CORRELATION ACROSS THE SHELF

### Biostratigraphic and Lithostratigraphic Correlation

Biostratigraphic investigations by Bergstrom (1971, 1973, 1977), Carnes (1975), Bergstrom and Carnes (1976), and Anita Harris (personal communication to

Table 2.2 Facies Interpretations

| Lithology/ Microfacies* | Rock Name after Dunham (1962) | Probable Water-Depth Range | Energy of Environ-ment | Environment of Deposition |
|---|---|---|---|---|
| A / 8 | Wackestone | >0 to 15m | Low- | Subtidal open platform or shelf lagoon below normal wave base. |
| B / 9 | Bioclastic Wackestone/Pack-stone | 0 to 12m | Low | Shallow shelf or lagoon with open circulation at or just below normal wave base. |
| C / 10g | Grainstone/Cortoid Grainstone | 0.5 to 30m | Very high to high | Very shallow, inter-tidal shelf or lagoon, shoals or tidal bars. |
| D / 11 | Grainstone/Cortoid Grainstone | 0.5 to 4m | Moderate | Very shallow, inter-tidal, shelf or lagoon, shoals or tidal bars in zone of winnowing. |
| E / 12g | Echinoderm Grainstone | 0.5 to 30m, generally less than 15 m | High to moderate | Shelf to shelf-edge subtidal environment above or near normal wave base. |
| F / 12p | Echinoderm/Bryo-zoan Packstone | 0.5 to 15m, generally less than about 12m deep | Moderate to low | Shelf to shelf-edge subtidal environment below or near normal wave base. |
| G / 13 | Oncoid Grainstone | < 0.5 to < 2m | High to moderate | Very shallow inter-tidal, shelf or lagoon, shoals or tidal bars in zone of winnowing. |
| H / 14 | Grainstone, Conglomeratic Lag | < 0.5 to 6m | Generally high | Represents slow ac-cumulation of coarse material in zone of winnowing, subtidal, agitated environment. |
| I / 16 | Peloidal Grainstone | < 0.5 to < 15m | Moderate to low | Very shallow, intra-tidal to subtidal, shelf or lagoon with mo-derate water circu-lation. |
| J / 17 | Grainstone/Peloidal Grainstone | > 0 to 8m | Moderate to low | Shallow, intertidal, shelf or lagoon with restricted circulation. |

| | | | | |
|---|---|---|---|---|
| K / 18 | Dasycladacean Grainstone | < 0.5 to 12m | High to moderate | Concentration of algal grains in tidal bars and channels. |
| L / 19 | Wackestone/Mudstone | exposed to < 2m deep | Low | Tidal flat, supratidal to intratidal. |
| L / 19l | Laminated wackestone/mudstone | Very deep 30 to > 1,000m | Very low | Deep open shelf or lagoon with restricted circulation. |
| L / 19F | Fenestral Wackestone/Mudstone | exposed to < 2m | Low | Tidal flat, supratidal to intratidal. |
| M / 21 | Spongiostrome Mudstone | 0 to 2m | Very low | Tidal flat, intertidal ponds. |
| N / 22 | Wackestone/Packstone - Oncoid Wackestone/Packstone | < 0.5 to 8m | Moderate to low | Shallow shelf or lagoon (? along margins of tidal ponds) with restricted circulation. |
| O / 24 | Lithoclastic Grainstone/Packstone | 0 to 10m | Generally low with brief periods of high energy | Represents filled channels and potholes developed on tidal flat. Clasts derived from lime mud on levees and algal mats. |
| P Not Numbered | Dolostone/Dolomitic Limestone | Very shallow, exposed to < 0.m | Low | Exposed tidal flat. |
| Q Not Numbered | Siltstone/ Carbonate Siltstone | 0.5 to 30m | Low | Deep lagoon receiving influx of siliciclastic material. |
| R Not Numbered | Shale/Shaly Carbonate | 0 to > 150m | Very low | Deep lagoon receiving influx of siliciclastic material. |
| S Not Numbered | Bentonite | Bedded bentonites are best preserved in low energy, shallow water environments, 0.5 to less than 15m deep. | Generally low, some bentonites may have been reworked in higher energy environments. | Ash fall preserved within shallow, low energy, subtidal and peritidal environments. |

*Microfacies numbers generally correspond to standard microfacies of Wilson (1975); however, some microfacies are modified (i.e., 10g, 12g, 12p, 19l, 19F) to account for criteria characteristic of Middle Ordovician limestones, but not generally observed in younger rocks.

Keith Roberson, 1990) and lithologic correlations by Ruppel (1979) and Ruppel and Walker (1982, 1984) provide the framework (see Fig. 2.4) for more detailed correlations.

On-shelf sections are spaced about 2 km apart (Fig. 2.1). Some beds at on-shelf positions can be traced laterally, away from the outcrop for 200 to 400 meters. Bentonite beds provide additional stratigraphic control. Prominent bentonite beds in the upper Moccasin Formation provide a time line (Time Line 5 of Ruppel and Walker, 1982; Walker, et al., 1983) for correlation of the on-shelf section at Cedar Springs with the shelf-edge section at Red House Branch. Green, clay-rich beds in the upper Rockdell Formation at Thorn Hill are probably bentonite (c.f., Fetzer, 1973) and appear to be correlative with reworked green, clay-rich beds at the Old Thorn Hill section.

## Exposure Surfaces

A number of assumptions or "guiding principles" (Table 3) constrain correlation of exposure surfaces. Most of these are based on application of standard stratigraphic principles (e.g., Krumbein and Sloss, 1951); others are derived from previous work combined with an understanding of carbonate depositional systems, and others are just common sense. Correlation of exposure surfaces from the shelf to the shelf-edge provide an additional framework in which to interpret these on-shelf sections (Steinhauff and Walker, in prep. a).

**Table 3**

**"Guiding Principles" involved in Correlation Along Strike (On the Shelf)**

1) The Knox surface is an appropriate stratigraphic datum.

2) Correlations within on-shelf, along strike sections (Thorn Hill, Old Thorn Hill, Idol Mine, and Cedar Springs sections) are simple and straightforward (Fig. 2.1). Thus, exposure surfaces are generally horizontal and do not "climb" in the section. Those that do "climb" in the section (generally less than 5 meters) probably reflect local differences in relief on the Knox surface rather than differential rates of accumulation and compaction across the shelf.

3) Pronounced exposure surfaces occurring at on-shelf positions correlate with other pronounced exposure surfaces at on-shelf positions. It is possible that these surfaces represent changes in water-depth that are regional or interregional in scope (i.e., represent uplift of a substantial area or eustatic drops in sea level).

4) Less-pronounced exposure surfaces generally correlate in an along strike direction with other less pronounced surfaces or with water-depth curve inflection points indicating shoaling. It is possible that these surfaces may also represent regional changes in water-depth, such as minor eustatic drops in sea level. However, it is also possible that these represent changes in water-depth that are local in scope (i.e., represent differential subsidence and / or compaction, migration of facies).

5) Inflection points recording water-depth increases will correlate across the shelf, and along depositional strike.

6) Correlation of inflection points of water deepening is constrained between exposure surfaces. That is to say, a deepening event can not be correlated across an exposure surface.

### Correlation of Deepening Events

Based on paleobathymetric analysis, a number of water deepening events occur within this Middle Ordovician succession. These water deepening events are relatively easy to correlate across the shelf because water-depth indicators are most sensitive to depth changes in shallow water (e.g., Figs. 2.2 and 2.4). These deepening events may be a result of eustatic sea-level rises or to decreases in deposition rate coupled with continued subsidence.

## DEFINING STRATIGRAPHIC SEQUENCES WITH PALEOBATHYMETRIC INDICATORS

### Water-Depths

The data indicate that maximum water-depths on the shelf never exceeded 20 meters within the Five Oaks, Lincolnshire, and Rockdell formations. Within the middle to upper Benbolt Formation and the lower Wardell Formation, maximum depths may have been slightly greater. Most on-shelf deposition likely occurred in only a few meters of water. Very conservative estimates are used for water-depth criteria (Figs. 2.2, 2.3, and Appendix C).

Many stratigraphic intervals, particularly those characterized by an abundance of oncoids and other coated-grains were probably deposited in very shallow water ($<$ 0.5 m) and may have been periodically exposed. Stratigraphic intervals containing abundant subaerial exposure criteria (pronounced surfaces) probably experienced exposure for longer periods. Those intervals containing fewer subaerial exposure

criteria (less pronounced surfaces) were probably exposed for somewhat shorter periods of time.

## Types of Stratigraphic Sequences

**Third-Order Sequences.** Starting with and including the basal Knox unconformity, seven pronounced surfaces of subaerial exposure are recognized in an approximately 600 meter thick succession of Middle and Upper Ordovician strata at on-shelf localities near Thorn Hill. These seven pronounced surfaces define seven stratigraphic sequences, numbered 1 through 7 (see Fig 1.2 of chapter 1; Figs. 2.4, and 2.10 - 2.19). The sixth surface occurs within the Moccasin Formation and has been well documented by Ruppel and Walker (1982, 1984) and Simonson (1985). The seventh surface, followed by a pronounced deepening, is at the top of the Moccasin and separates that formation from the overlying Martinsburg Formation (Simonson, 1985; Walker, 1985, 1992). The lower five surfaces are considered in this study (the lower 400 meters of the succession).

All of Middle Ordovician deposition took place over a period of approximately 20 to 25 million years. This is based on the biostratigraphic work of Bergstrom and Carnes (1976) and absolute ages assigned to series boundaries as summarized by Bond et al. (1988). The interval reported on here represents about 3/4 of the whole Middle Ordovician, and thus had a duration of 15 to 17 million years. The estimated time for deposition of each third order sequence is 2.5 to a little more than 3 million years. Thus, these sequences appear to be of similar temporal duration as those commonly referred to as the products of "third-order" eustatic cycles (e.g., Vail et al., 1977).

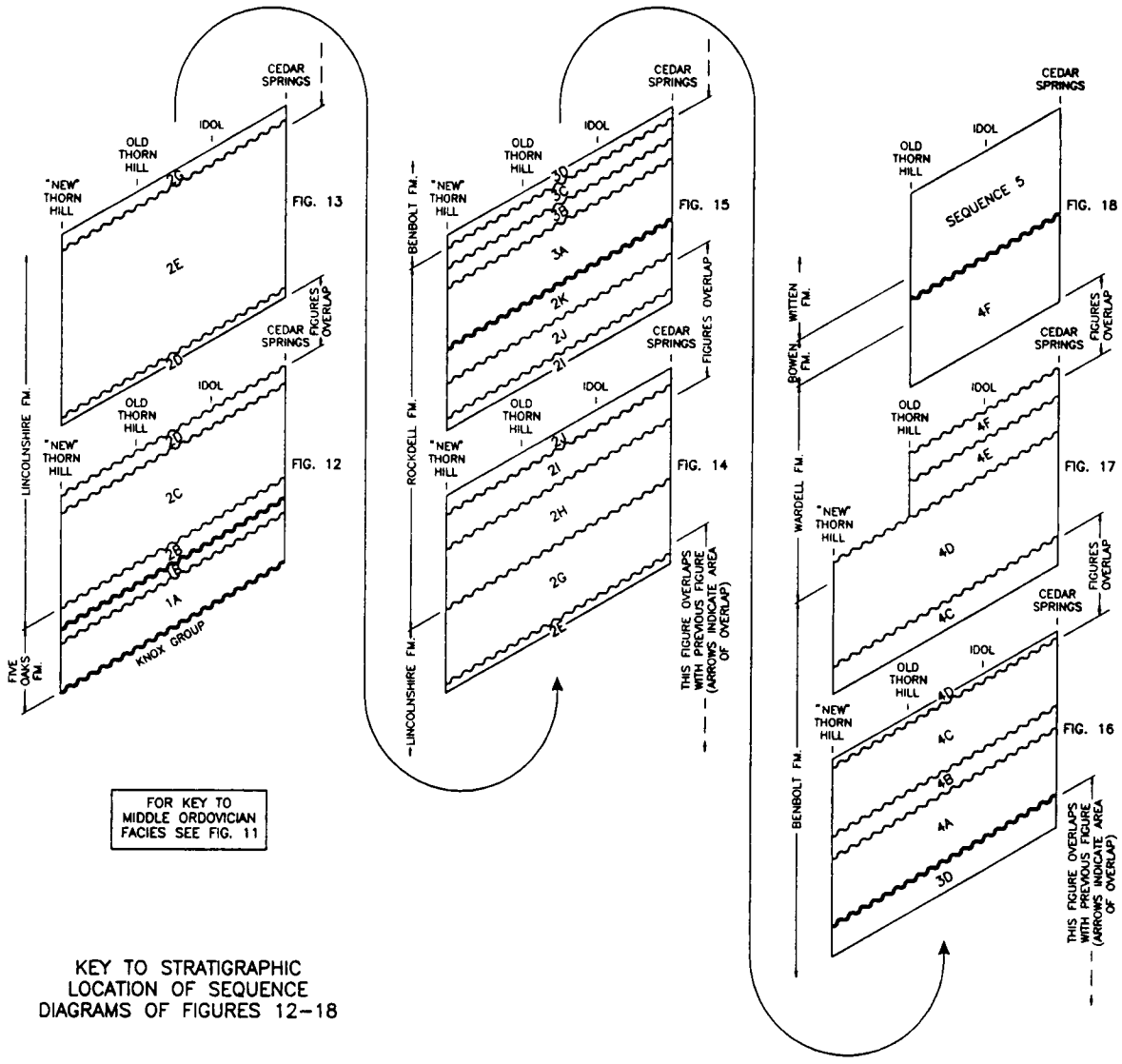



Figure 2.10. Key to stratigraphic location of sequence diagrams of figures 2.11 - 2. 18. Note that figures 2.12 - 2.18 slightly overlap each other in order to show development above and below all exposure surfaces. Note that many formational contacts in the study area have never been well defined (i.e., Ruppel, 1979). Hence, formational contacts indicated here and on figures 12-18 are based on the composite columnar section (Fig. 2.4).

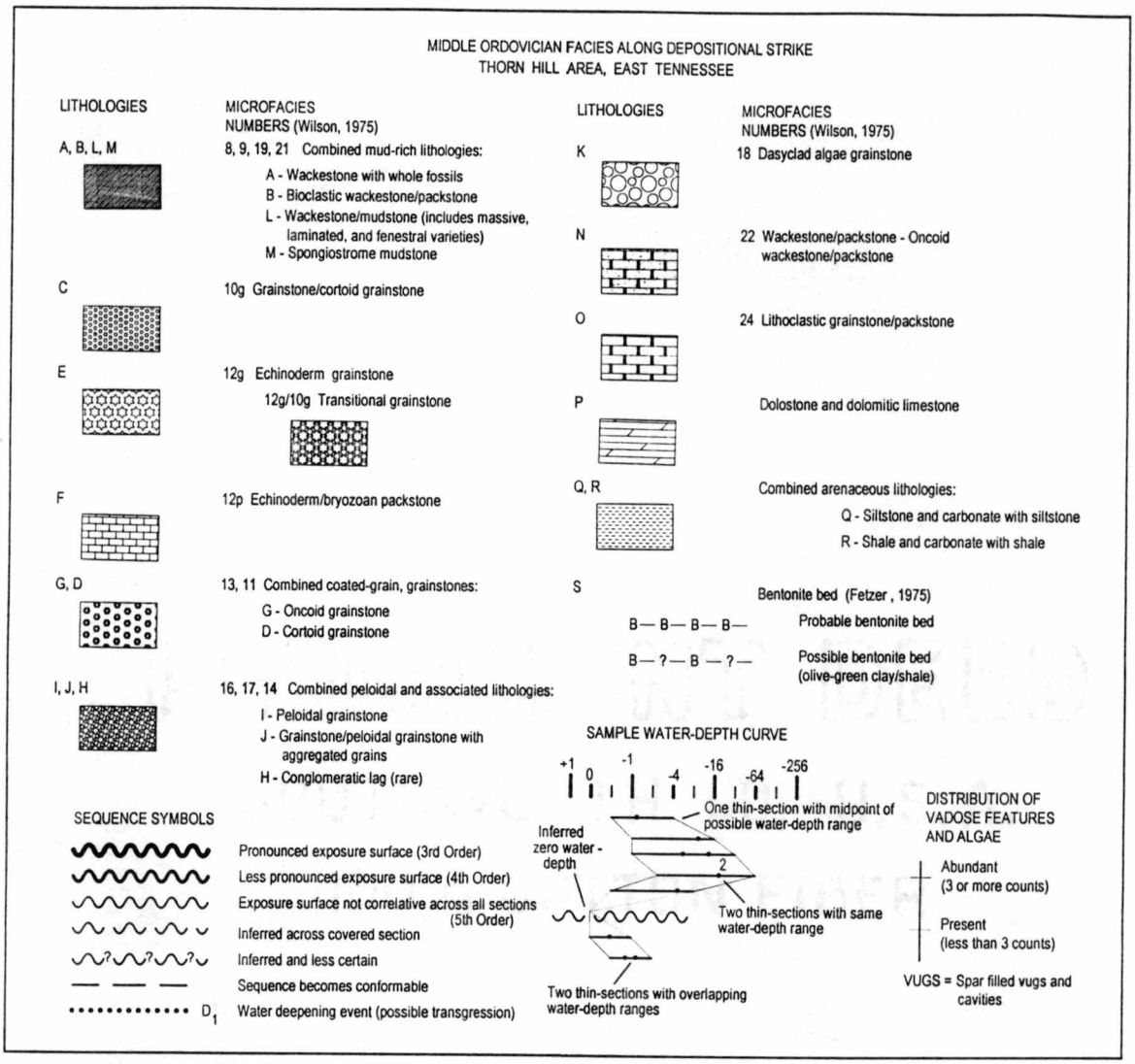



Figure 2.11. Key to Facies for stratigraphic sequence diagrams of figures 2.12 - 2.18. Note that mud-rich lithologies A, B, L, and M are combined. The actual amount of fenestral mudstone developed below many of the exposure surfaces is quite small (generally a lenses less than 0.5 meters thick).

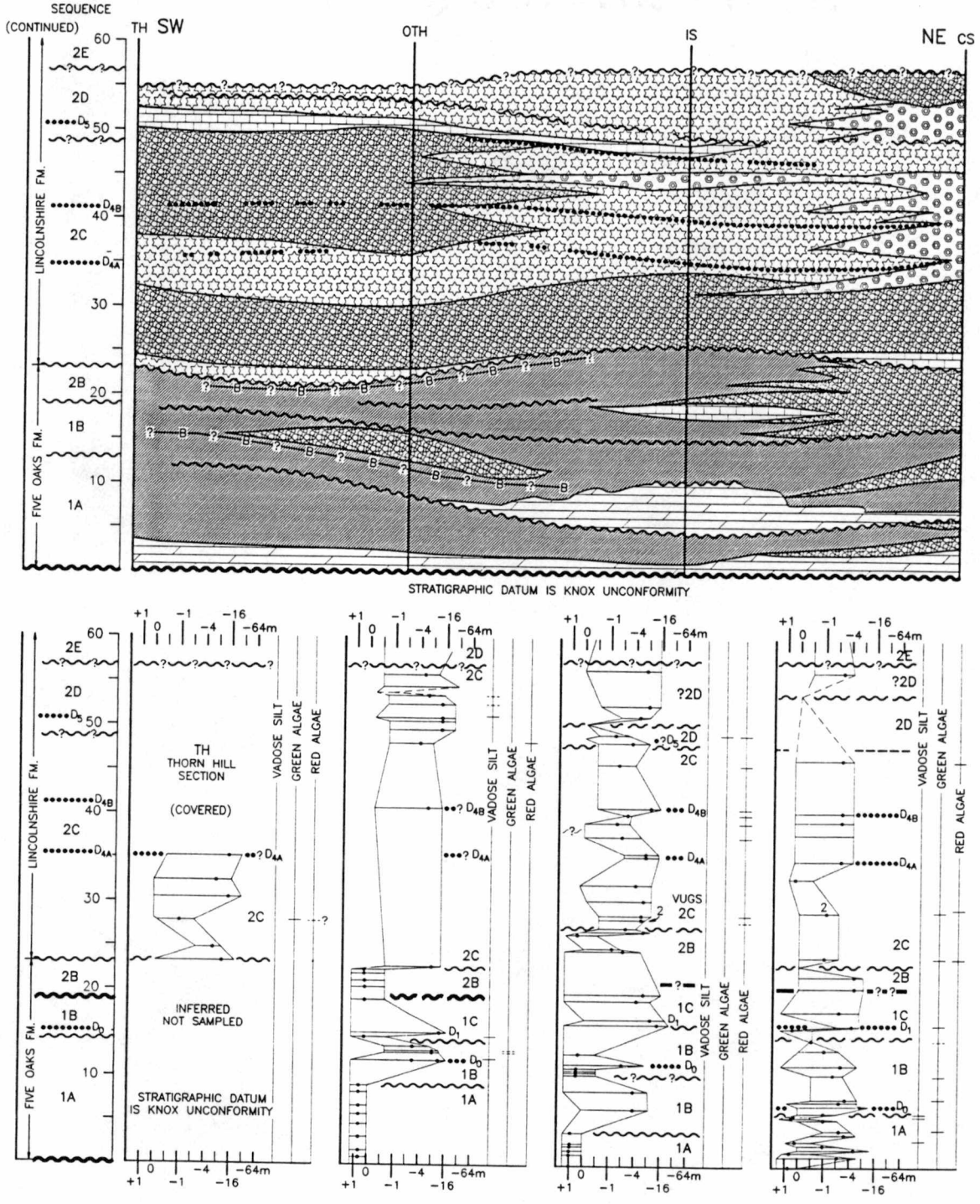



Figure 2.12. Stratigraphic subsequences 1A, 1B, 1C, 2B, 2C, and 2D. Bottom panel shows water-depth curves for stratigraphic sections (from southwest to northeast) at Thorn Hill (TH), Old Thorn Hill (OTH), Idol Mine (IS), and Cedar Springs (CS). Top panel shows corresponding restored cross-section. For key to stratigraphic location of sequence diagrams see Figure 2.10. For key to facies see Figure 2.11.

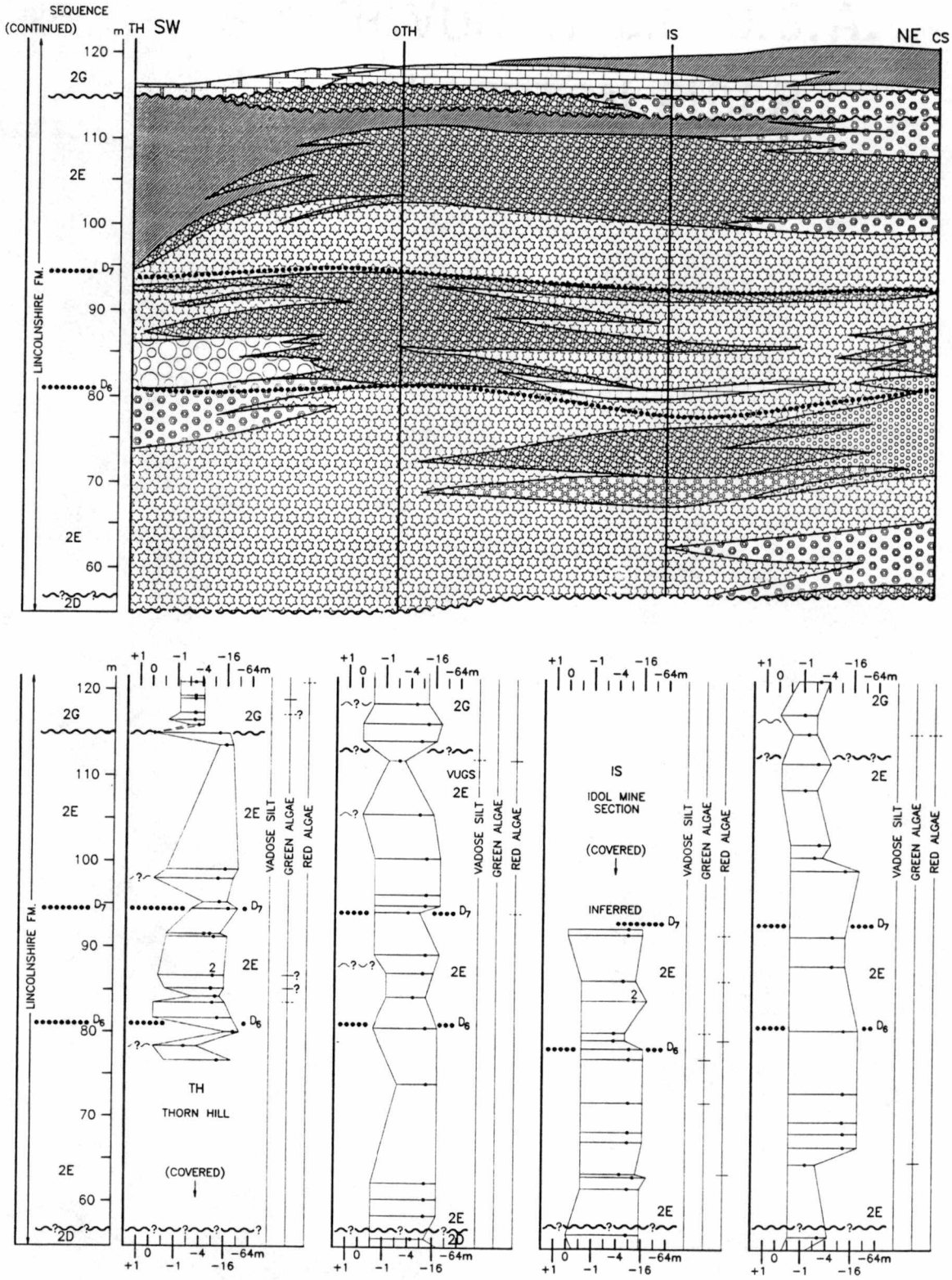



Figure 2.13. Stratigraphic subsequences 2E and lower 2G. Bottom panel shows water-depth curves, top panel shows corresponding restored cross-section. Stratigraphic sections are continued from Figure 2.12. For keys see figures 2.10 and 2.11.

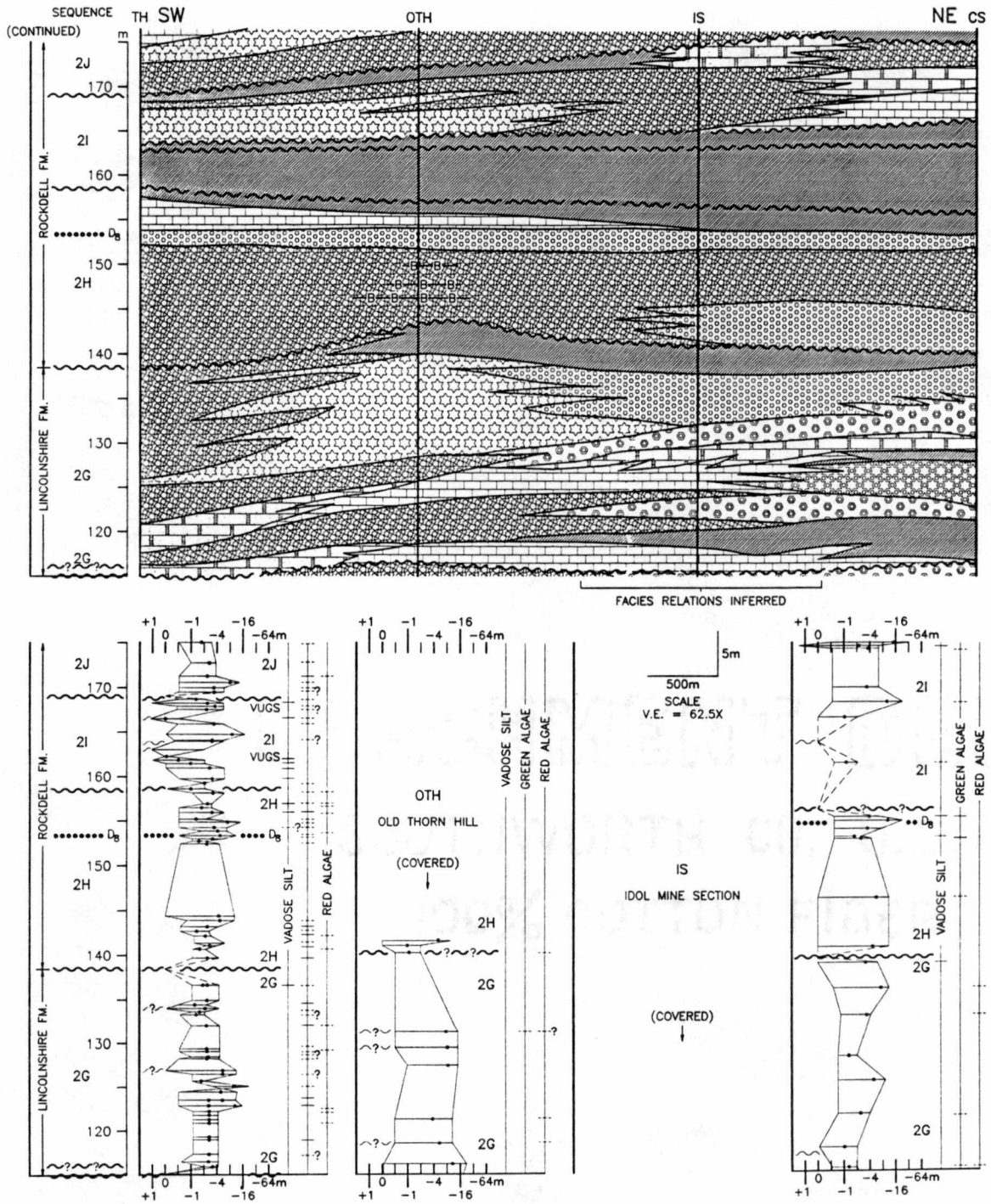



Figure 2.14. Stratigraphic subsequences upper 2E, and 2G, H, 2I and 2J. Bottom panel shows water-depth curves, top panel shows corresponding restored cross-section. Stratigraphic sections are continued from Figure 2.13. For keys see figures 2.10 and 2.11. Note that seven stratigraphic intervals at the Thorn Hill section are represented by two thin-sections with the same water-depth range. Lack of space does not permit these intervals to be indicated on the figure.

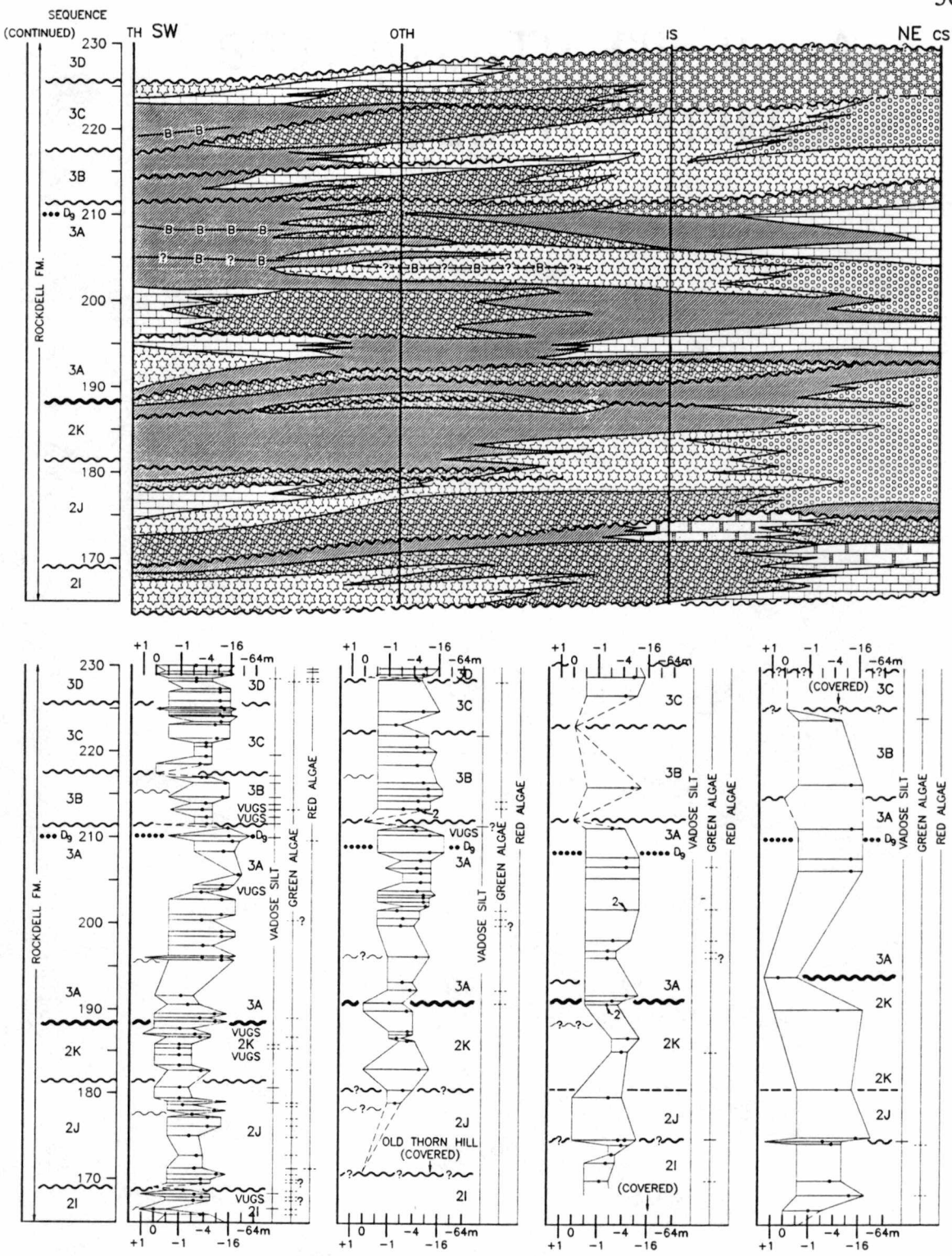



Figure 2.15. Stratigraphic subsequences upper 2I, and 2J, 2K, 3A, 3B, 3C and lower 3D. Bottom panel shows water-depth curves, top panel shows corresponding restored cross-section. Stratigraphic sections are continued from Figure 2.14. For keys see figures 2.10 and 2.11. Note that 16 stratigraphic intervals at the Thorn Hill section are represented by two thin-sections with the same water-depth range. Lack of space does not permit these intervals to be indicated on the figure.

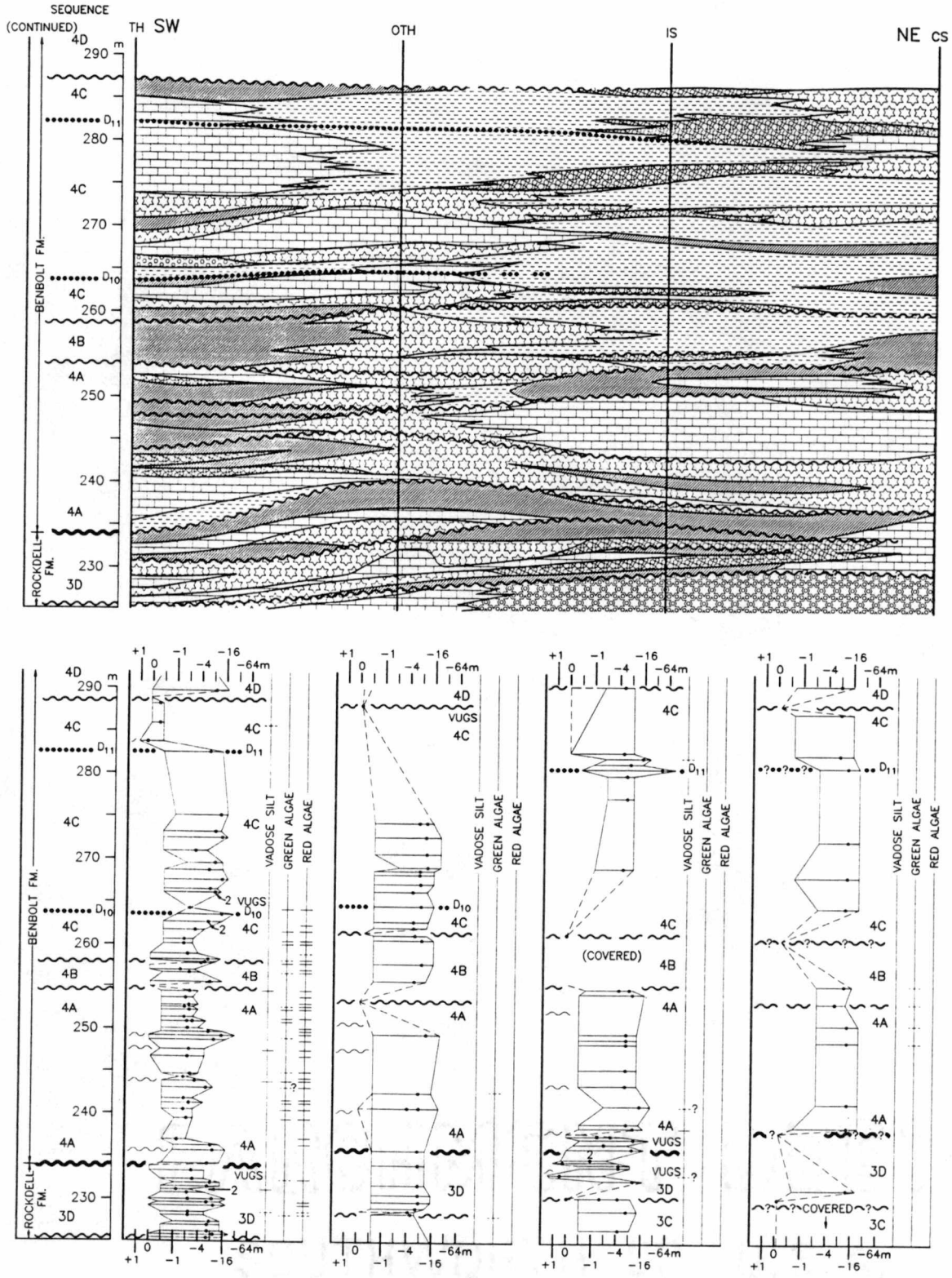



Figure. 2.16. Stratigraphic subsequences 3D, 4A, 4B, 4C, and lower 4D. Bottom panel shows water-depth curves, top panel shows corresponding restored cross-section. Stratigraphic sections are continued from Figure 2.15. For keys see figures 2.10 and 2.11.

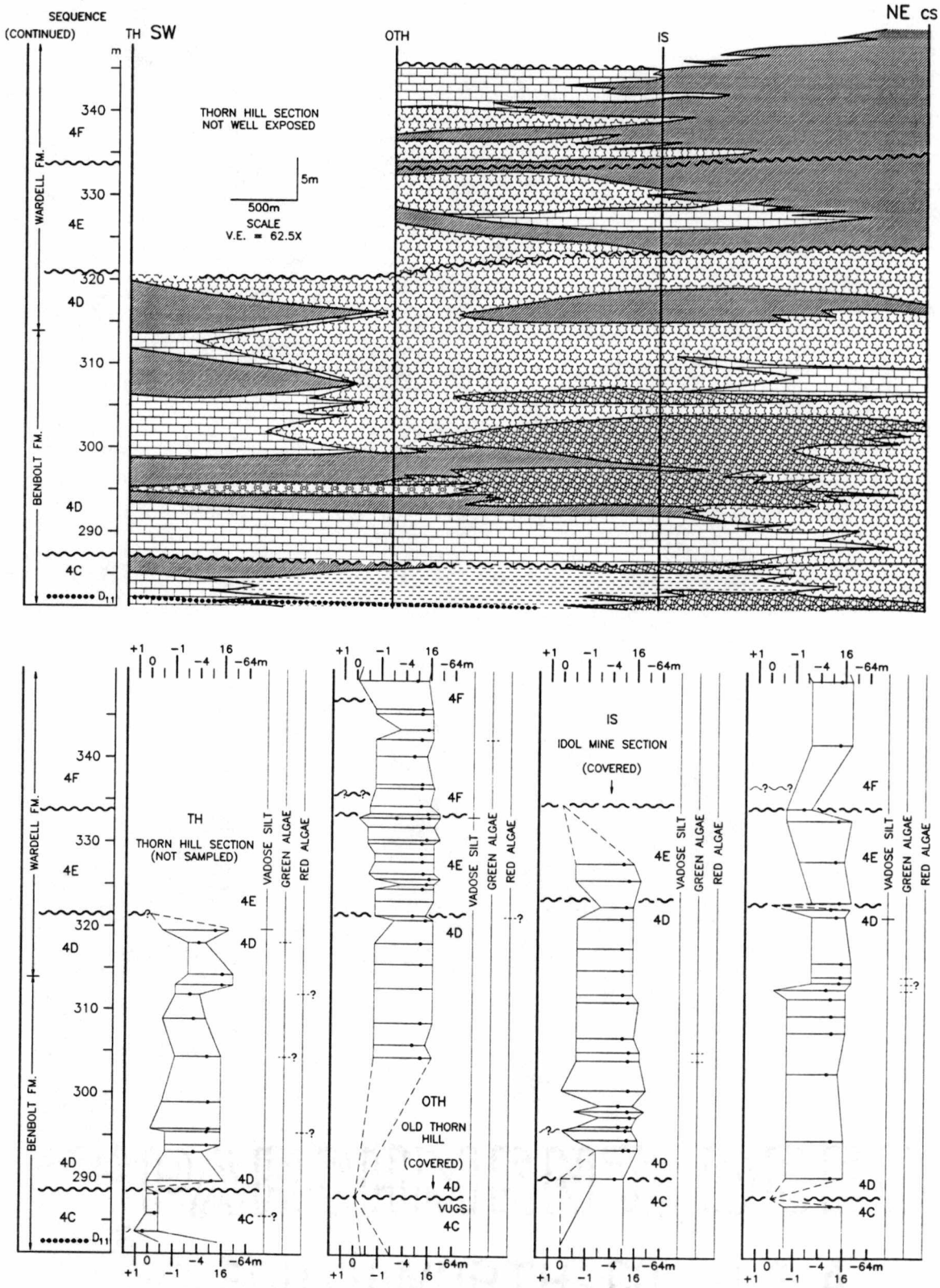



Figure 2.17. Stratigraphic subsequences upper 4C, 4D, 4E, and lower 4F. Bottom panel shows water-depth curves, top panel shows corresponding restored cross-section. Stratigraphic sections are continued from Figure 2.16. For keys see figures 2.10 and 2.11.

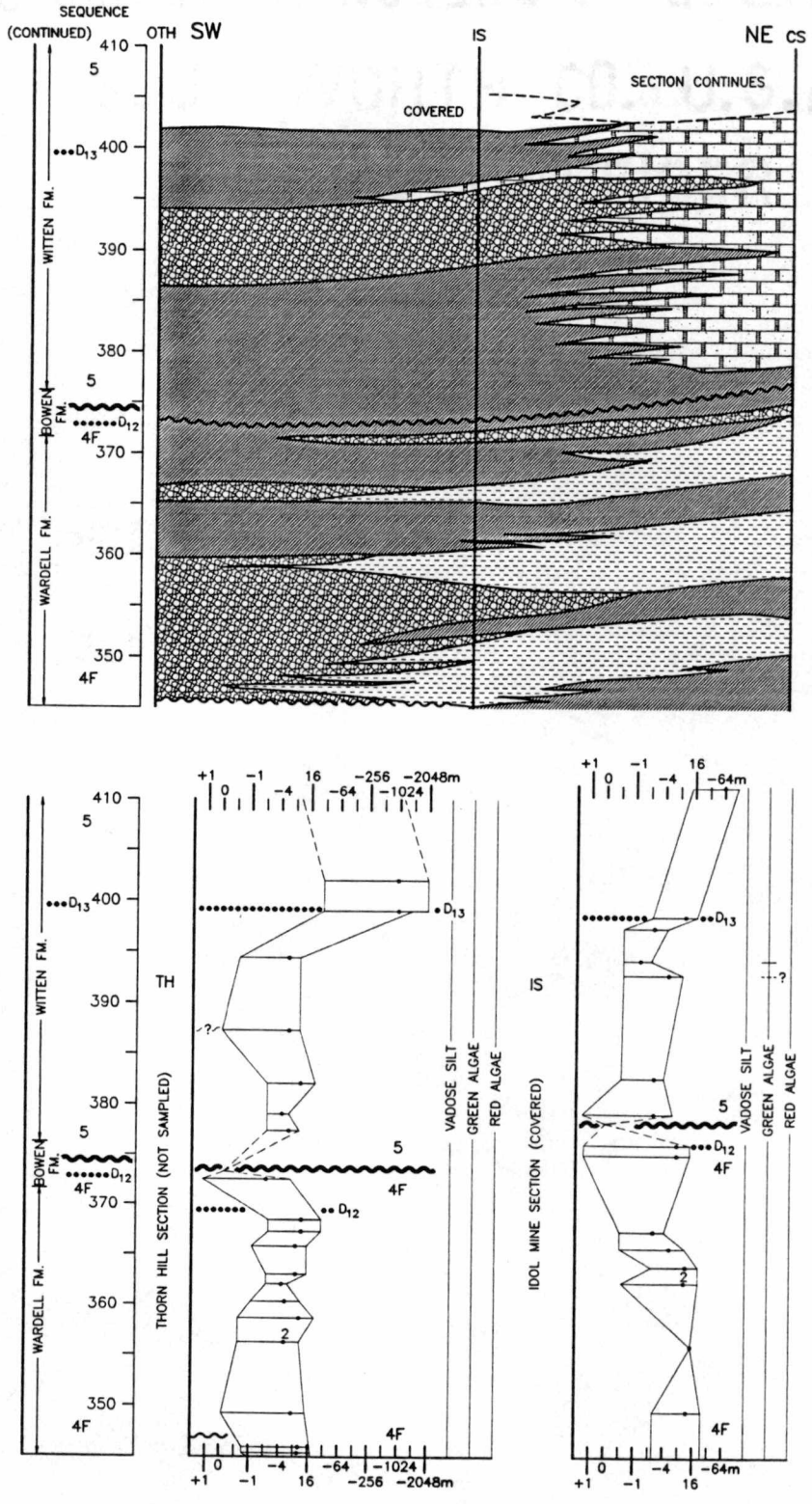



Figure 2.18 Stratigraphic subsequence of upper 4F, and lowermost Sequence 5. Bottom panel shows water-depth curves for stratigraphic sections (from southwest to northeast) at Old Thorn Hill and Cedar Springs (CS). Top panel shows corresponding restored cross-section. Stratigraphic sections are continued from Figure 2.17. For keys see figures 2.10 and 2.11.

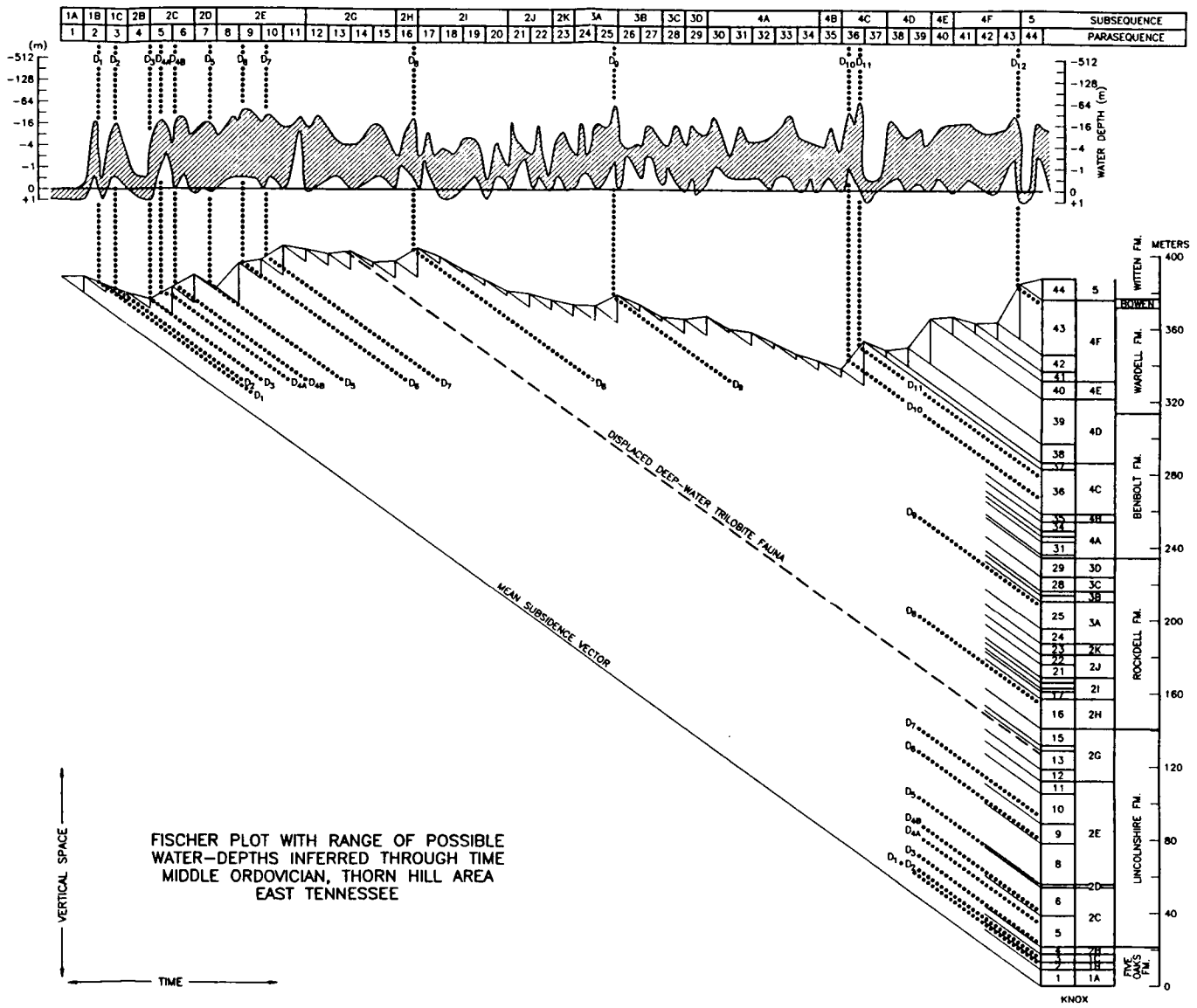



Figure 2.19. Fischer plot for composite Middle Ordovician on-shelf section (i.e., Figure 2.4). Dotted lines numbered D1 - D12 indicate deepening events and are projected from the vertical stratigraphic column at right, through the plotted subsequences, to the horizontal time axis. A range of possible water-depths is inferred for the shelf through time, shaded curve, top. This inferred curve is based on water-depth curves (figures 2.12 - 2.18) and assumes stratigraphic thickness is proportional to time (at best, only a first approximation). Note that the "positive" part of the possible water-depth scale extends to 1 meter above mean sea-level to indicate that some water-depth criteria (such as penecontemporaneous dolomite and certain categories of algae, see Figure 2.2) have documented occurrences that extend to about 1 meter or less above mean sea-level (e.g., Hardie, 1977).

**Fourth-order Subsequences.** Sequences bounded by pronounced exposure surfaces are subdivided by less pronounced exposure surfaces. These less pronounced exposure surfaces are correlated on the shelf, parallel to depositional strike (Figs. 2.10 - 2.18). Starting above the Knox unconformity, nineteen less pronounced exposure surfaces are recognized in the lower 400 meters (in sequences 1 - 4) of Middle Ordovician strata at on-shelf positions near Thorn Hill (Figs. 2.9 - 2.18). If these nineteen less pronounced surfaces are combined with the five pronounced surfaces, a total of 23 surfaces are recognized in approximately 400 meters.

This leads to a number of additional subsequences recognized within the previously defined and numbered third-order sequences. These subsequences bounded by less pronounced surfaces are designated alphabetically within the numbered third-order sequence in which they occur (e.g., 2A, 2B, 2C, etc.; Figs. 2.4, and 2.10 - 2.19). There are a total of 22 of these fourth-order subsequences. These subsequences appear to be of similar temporal duration (hundreds of thousands of years) and thickness as intervals referred to as the products of "fourth-order" sea-level cycles or "high-frequency" sea-level fluctuations. (e.g., Kendall and Schlager, 1981, Read, 1989).

**Parasequences: Possible "Fifth-Order" or "Meter-Scale" Packages.** Multiple shoaling events or possible exposure surfaces are indicated within many fourth-order subsequences. Evidence for shoaling comes from inflection points noted on water-depth curves and from lithologic changes (Figs. 2.4, and 2.10 - 2.19). Evidence for

these subtle lithologic changes is generally only apparent in thin-section or polished slabs.

Water-depth curve inflection points and subtle lithologic changes are not correlative across the entire 6 km on-shelf transect. For this reason, these partially correlative surfaces defined by water-depth curve inflections and subtle lithologic changes are here termed "parasequences" (Fig. 2.19). Quotation marks are used because the term "parasequence" has been used to describe beds or bed sets bounded by marine-flooding surfaces in siliciclastic shelves (e.g., Mitchum et al., 1991).

## DISCUSSION OF STRATIGRAPHIC SEQUENCES

### Third-Order Sequence 1

**Description.** Fenestral mudstones, dolomitic limestones, and very thin peloidal grainstones of the lower Five Oaks Formation occur above the Knox unconformity. At least two exposure surfaces can be traced along the shelf within Sequence 1 near Thorn Hill. These surfaces define fourth-order subsequences 1A, 1B, and 1C (Fig. 2.12).

Exposure surfaces within Sequence 1 are characterized by sharp lithologic contacts and single diagnostic exposure indicators, such as the presence of well-developed fenestral mudstones or the occurrence of dolomitic limestone. Because these surfaces generally lack multiple exposure indicators, they might best be described as intermediate between "pronounced" surfaces and less pronounced surfaces.

**Interpretation.** This lowermost Middle Ordovician sequence is presently being studied by Roberson (in prep.). Roberson has concluded that at least two exposure surfaces within Sequence 1 are regionally diachronous and the result of facies migration. Roberson suggests that the Five Oaks Formation within Sequence 1 represents infilling of the Knox surface with tidal flat deposits during initial Middle Ordovician transgression. He interprets exposure surfaces in the Five Oaks to represent migration of beach ridges through a tidal flat complex (Roberson, 1987; Roberson and Foreman 1989; Roberson and Walker, 1990; Roberson, in prep). Thus, the exposure surface at the top of Sequence 1 (top of the Five Oaks) is not a synchronous surface, but instead marks the migration of an erosional environment through space and time (Roberson and Walker, 1990).

Roberson believes that Sequence 1 sediments filled accommodation space made available by a migrating foreland basin/peripheral bulge combination. As the pair moved toward the craton, transgression and shallow water sedimentation occurred in the forward basin, followed by regression and subaerial exposure as the trailing bulge migrated progressively northwestward (i.e., indicated at the subsequence 1C / 2B boundary; Fig. 2.12).

### Third-Order Sequence 2

**Description.** Sequence 2, comprising the uppermost Five Oaks, Lincolnshire and lowermost Rockdell formations contains eight less pronounced exposure surfaces defining nine fourth-order subsequences (2B through 2K, Figs. 2.4, 2.10, and 2.12 - 2.15). Fourth-order subsequences 2A and 2F do not occur on the shelf but do occur

at the shelf-edge (see chapter 3). Sequence 2 consists primarily of peloidal grainstones, commonly mixed with coated-grains.

Thin beds (< 2 meters thick) of mud-rich packstones, wackestones, and fenestral mudstones occur immediately below many fourth-order exposure surfaces within Sequence 2 (i.e., surfaces separating subsequences 2C / 2D, 2E / 2G, H / 2I, 2I / 2J, and 2J / 2K) (Figs. 2.12 - 2.15). Relative development of exposure surfaces varies along strike. For example, below the lower surface bounding fourth-order Subsequence 2D, packstones of Subsequence 2C contain features indicating subaerial exposure at Old Thorn Hill. Possible or partial exposure is indicated below this surface at the Idol Mine section and very shallow water, probably without exposure at Cedar Springs (Fig. 2.12).

**Interpretation.** During deposition of Subsequence 2A, the shelf was exposed and sea-level was at or below the shelf-edge (Steinhauff and Walker, in prep. a). As relative sea-level rose, mudstones of Subsequence 2B were deposited and as relative sea-level rose well above the shelf-edge, Subsequence 2C grainstones were deposited on the shelf. The upper and lower bounding surfaces of Subsequence 2D indicate that relative sea-level twice dropped below the shelf-edge. Subsequence 2D represents an interval of time when sea-level rose but produced only a small amount of accommodation space.

A style of deposition similar to that of Subsequence 2C continued with subsequences 2E and 2G. Subsequence 2F was deposited only at the shelf-edge

(Chapter 3). A displaced deep-water, thin-shelled trilobite fauna occurs within shallow-water deposits of middle Subsequence 2G (Figs. 2.2 and 2.4). These thin-shelled, eyeless trilobites (e.g., *Lonchodomas* sp.) are generally restricted to deep-water environments (Maitland, 1979; Walker et al., 1980). This displaced fauna suggests that relative sea-level rose during deposition of Subsequence 2F (deposited at the shelf-edge) and may have slowed, reached high-stand, and possibly still-stand, during deposition of middle Subsequence 2G on the shelf.

The boundary between subsequences 2G and H marks the approximate transition from the Lincolnshire into the Rockdell Formation at on-shelf positions. This transition indicates a change from homogeneous, relatively open-shelf conditions, as suggested by generally mud-free peloid grainstones of the Lincolnshire Formation, to a wider spectrum of high-energy tidal environments as indicated by stacked skeletal grainstones and fenestral mudstones beds of the Rockdell Formation (i.e., subsequences 2I, 2J, and 2K). During deposition of subsequences 2I, 2J and 2K the shelf-edge "reef" tract of the Holston Formation prograded basinward (southeastward; Ruppel, 1979). This may have occurred in response to a long term, but slow, fall in relative sea-level. Subsidence of the shelf-edge may have kept pace with or barely out-paced relative sea-level fall during deposition of subsequences 2I through 2K. Intervening surfaces of subaerial exposure, bounding subsequences 2I through 2K, indicate that relative sea-level fell and periodically out-paced subsidence.

## Third-Order Sequence 3

**Description.** Subsequence 3A consists of grainstones and packstones of the uppermost Rockdell Formation. Uppermost Subsequence 3A consists of well-developed Rockdell lithologies (Fig. 2.15, see caption, Fig. 2.4). The increase in water-depth near the top of Subsequence 3A coincides with a similar increase at the top of the Holston Formation at the shelf-edge (Steinhauff and Walker, in prep. a; see also Benedict and Walker, 1978, and Walker et al., 1980). Subsequences 3B, 3C and 3D include nodular bedded packstones and fenestral mudstones of the Rockdell Formation (Figs. 2.15 and 2.16). Their lateral equivalents at the shelf-edge are skeletal grainstones of the Rockdell Formation (Ruppel, 1979). Spar filled vugs with solution features and smaller cavities floored with crystal or vadose silt are abundant within mud-rich subsequence 3A and 3C lithologies at Thorn Hill and Old Thorn Hill.

**Interpretation.** Profound paleoenvironmental changes accompanied deposition of Sequence 3. A substantial water-depth increase near the top of Subsequence 3A coincides with culmination of Holston deposition (Steinhauff and Walker, in prep. a). This stratigraphic level corresponds to a marine flooding surface coated with phosphate and manganese-rich nodules near Knoxville, 60 km south of our study area (Tobin and Walker, in prep.). Immediately upward, a drop in relative sea-level is indicated by the exposure surface separating subsequences 3A and 3B and by additional exposure criteria within Subsequence 3B. This may represent a type of drowning unconformity, followed by exposure or at least substantial shollowing.

The same sequence of events are indicated near Knoxville (Tobin and Walker, in prep.).

### Third-Order Sequence 4

**Description.** The Benbolt, Wardell, and lowermost Bowen formations comprise Sequence 4. Subsequences 4A through 4C of the lower Benbolt Formation consist of an array of coated-grain bearing grainstones and packstones characteristic of very shallow-water deposition (Figs. 2.4A and 2.16). Mud-rich lithologies of Sequence 4 are generally red to maroon in color due to iron-manganese oxides within the micritic matrix (Johnson, 1988). Shale, siltstone and skeletal wackestone and packstone beds are particularly abundant in Subsequence 4C. The Wardell Formation includes uppermost Subsequence 4D and subsequences 4E and 4F consisting of bryozoan-echinoderm wackestones and grainstone-packstones (Fig. 2.17). Subsequences 4D and 4F are similar in their content of grainstone and packstone beds, but 4D contains no mudstone or shale beds, whereas 4F has well-developed mudstone and shale beds up to several meters thick (Figs. 2.17 and 2.18). Deepening event $D_{12}$ occurs within the uppermost part of Subsequence 4F at the base the Benbolt Formation within peloidal and aggregate-grain grainstones (Fig. 2.18). These grainstones grade upward into thin-bedded silty mudstones containing mudcracks.

**Interpretation.** Shoaling sand banks of the Rockdell gave way to the deeper subtidal "lagoonal" deposits of the Benbolt. Lagoonal deposits of the Benbolt spread eastward over the former shelf-edge (Ruppel, 1979). Deepening event $D_{12}$ represents either a

minor change in water-depth or the migration of peloidal and aggregate-grains across mud-rich sediments on the shelf. Deepening event $D_{12}$ is followed by exposure indicated by mudcracks in the middle to upper part of the Bowen Formation.

### Third-Order Sequence 5

**Description.** Sequence 5 includes the uppermost Bowen, Witten (Figs. 2.4B and 2.18), and the lowermost part of the Moccasin (not shown) formations. Terrigenous siltstone, calcilutites, calcarenites and shales occur in various proportions throughout Sequence 5. The Bowen consists of calcareous siltstone and red calcareous claystone with mudcracks (Wedekind, 1986). The Witten is similar to the underlying Wardell. The Moccasin consists of distinctive gray limestone and red to yellow weathering shale. Ripple marks and mudcracks occur throughout the Moccasin (Simonson, 1985).

**Interpretation.** Sequence 4 marked the beginning of a reversal of paleobathymetry (Ruppel, 1979). This reversal continued with deposition of deeper water shelf deposits of the Wardell Formation in an epeiric sea to the west. These deeper water deposits of the Wardell prograded over lagoonal deposits of the Benbolt. On the shelf, this progradation occurred earliest at Cedar Springs and slightly later at Thorn Hill (Fig. 2.16). Eventually, the former basin to the east was completely filled and over topped by the tidal flat (and continental?) deposits of the Bays Formation (not shown). This tidal flat deposition progressed westward, transporting terrigenous silt

and clay to the west. The result was deposition of the tidal flat complex of the Moccasin Formation with the bathymetric slope reversed in geographic position (Ruppel and Walker, 1982, 1984; Simonson, 1985).

## DISCUSSION: FISCHER PLOTS, "CYCLES," AND SEA-LEVEL CHANGE

Sedimentation rate, type of sedimentation, local crustal movements, and eustatic sea-level control facies anatomy on carbonate shelves upon which deposition fills available accommodation space (e.g., Kendall and Schlager, 1981). In this study, as in other studies, it is difficult to separate the relative importance of these different primary controls. However, our detailed stratigraphic framework combined with water-depth curves has helped narrow the possible controls. A Fischer plot, substituting our subsequences and parasequences for cycles, is presented here as an alternative way to display the data (Fig. 2.19).

### Using Fischer Plots to Recognize Changes in Relative Sea-level

**The Fischer Plot.** Fischer (1964) used cumulative cycle thickness of peritidal carbonates corrected for linear subsidence plotted against average cycle period to infer changes in relative sea-level. Time was expressed as average cycle period. The considerable limitations associated with this technique are discussed below. On the Fischer plot, a relative sea-level rise is expressed as a positive departure from the

horizontal. This indicates the level to which the platform would fill if sedimentation were equal to linear subsidence and relative sea-level was static. Conversely, a relative sea-level drop is expressed as a negative departure from the horizontal (e.g., Read and Goldhammer, 1988).

**Carbonate Cycles.** Prevailing thought holds that peritidal cycle thickness is controlled by the total amount of accommodation space provided by subsidence and eustacy. Hence, stacks of thicker cycles are formed during a relative sea-level rise that produces accommodation space in excess of that developed by subsidence. In contrast, stacks of thinner cycles are formed during relative sea-level fall when accommodation space is reduced (e.g., Read and Goldhammer, 1988). Similarly, Osleger (1991, p. 919) proposed that "Subtidal cycles on passive margins appear to be a product of eustacy acting in concert with intrinsic processes such as storm and wave reworking and redistribution that act to maintain submergence below the zone on optimal carbonate productivity."

**Eustatic sea-level Change.** The Fischer plot may actually reflect true relative rise and fall in sea-level. However, shallowing-upward trends, be they based on lithofacies observable in the field or based on subtle criteria observable only in thin-section, do not necessarily record relative sea-level events. Rather, Osleger (1990) suggests that thickness of the stacks may actually record a long-term increases or

decrease in accommodation space generated by relative changes in sea-level. This may involve causes other than eustacy.

## Limitations of Fischer Plots

Fischer (1964) recognized three components or "dictators" to his plot: 1) relative changes in sea-level related to "accretion of sediments" and subsidence, 2) tectonic changes, and 3) eustatic changes. Because these different components are not easily resolved, there are limits on how the Fischer plot can be interpreted.

Aside from this, four other points merit attention. First, it is assumed that each cycle is of the same duration. This is almost certainly not true (e.g., Kozar et al., 1990; Hardie et al., 1991). Second, apparent long term rise and fall in sea-level may be generated by water-depth dependent sedimentation rates rather than changes in accommodation space controlled by changes in sea-level (e.g., Osleger, 1990). Because cycle thickness is a function of accommodation space, cycle thickness can be expected to increase with increasing space below base level. However, as water-depths increase beyond the limit of the photic zone, sedimentation rates in carbonates are depressed. Accordingly, one might expect a position on the outer shelf to record more inundations or more cycles, but that these cycles will be relatively thin (e.g., Koerschner and Read, 1990). Third, if a negative departure from the horizontal actually reflects relative sea-level drop, then once the sediments are exposed, this departure tells us nothing about the magnitude of the drop. Finally, the assumption of a linear rate of background subsidence is probably incorrect in many cases because

subsidence rate versus time is usually best expressed by some geometric "decay" curve. Moreover, subsidence may actually be "jerky."

## CONCLUSIONS

1) Stratigraphic sequences, subsequences, and parasequences represent shoaling-upward sediment packages similar to cycles. However, these sequences, subsequences, and parasequences differ from cycles in that evidence for exposure and shoaling is subtle and generally revealed only through detailed microscopic examination of numerous thin-sections and polished slabs. In fact, if sampling had been restricted to measurement and "bed-by-bed" logging (e.g., Osleger and Read, 1991), evidence for exposure or shoaling would not have been observed, nor would even some of the surfaces have been discerned that are indicated (i.e., Figs. 2.12 - 2.18).

2) The apparently non-cyclic, largely subtidal sequences of the present study are different from the subtidal cyclic successions described by Osleger (1991) and Osleger and Read (1991). The subtidal cycles of Osleger (1991, p. 917) " ... are distinguished by an upward increase in grain size, bed thickness, and cross-bedding and other high-energy sedimentary structures. Subtidal cycles are not capped by intertidal lithologies, nor do any of the subtidal cycles exhibit exposure features such as microkarst or vadose dissolution or cementation." Many similar features are illustrated in the present study. However, the distinguishing features described by Osleger (1991) and Osleger and Read (1991) do not appear to be systematically

arranged in the subtidal rocks of the present study. Furthermore, there is evidence for subaerial exposure within most the sequences described and illustrated in the present study (Figs. 2.12 - 2.18).

3) Sequence, subsequence, and parasequence lithologies differ both vertically and horizontally. They comprise a facies mosaic and cannot be generalized. Thus, a representation of the entire succession is presented in figures 2.12 through 2.18, rather than an idealized sequence.

4) Non-cyclic carbonates are amenable to the use of Fischer plots. If one applies a standard interpretation (i.e., Read and Goldhammer, 1988) to the Fischer plot (Fig. 2.19), the plot supports the broad interpretations previously made for this succession based on other lines of evidence (i.e., Ruppel, 1979; Ruppel and Walker, 1982, 1984). Thus, relative sea-level rises appear as positive departures from the horizontal and relative sea-level falls appear as negative departures from the horizontal. Indeed, the Fischer plot also helps clarify new observations revealed through water-depth analysis, such as deepening events (e.g., Fig. 2.4). However, these relative changes in sea level cannot be confidently interpreted as eustatic in nature.

5) Previously defined formations represent lithologic arrays dominated by several lithologies or facies. Similar lithologic arrays were established at different positions and at different times on the shelf. Such similar lithologic arrays (i.e., formations) are not necessarily correlative.

This paper attempts to answer "how" this particular non-cyclic carbonate

succession is different from and similar to cyclic successions. It also tries to explain how this non-cyclic succession responded to relative sea-level variation. Determining "why" this apparently non-cyclic succession differs so profoundly from clearly cyclic ones will require careful comparative study.

# CHAPTER 3

## RECOGNIZING EXPOSURE, DROWNING, AND "MISSED BEATS": SHELF TO SHELF-EDGE SEQUENCE STRATIGRAPHY OF MIDDLE ORDOVICIAN NON-CYCLIC CARBONATES, EAST TENNESSEE


### ABSTRACT

Stratigraphic sequences in a Middle Ordovician platform-interior carbonate succession (Steinhauff and Walker, in press) are correlated to the shelf-edge. Surfaces of subaerial exposure are correlated among seven stratigraphic sections, four at on-shelf positions and three at or near the shelf-edge near Thorn Hill, Tennessee. Surfaces of subaerial exposure define stratigraphic sequences within an apparently non-cyclic carbonate succession. Carbonate facies geometry is based on outcrop observation, analysis of thin-sections, and consideration of water-depth curves. In platform successions most sequences are bounded by exposure surfaces, but in more continuously subtidal areas periods of shallowing and drowning are discerned in bathymetric curves based on multiple lines of evidence and exposure did not always occur. Evidence for drowning is preserved in subtidal sediments and is indicated from water-depth curves based on multiple lines of evidence. Evidence for drowning unconformity is provided by cephalopod-rich limestone beds which overlie subtidal limestone and by black, iron-manganese oxide-rich sediment within these cephalopod-rich beds.

Apparently non-cyclic carbonate strata have fourth-order subsequences that are grouped into third-order sequences based on the occurrence of pronounced and less pronounced exposure surfaces. For example, seven pronounced surfaces of subaerial exposure define six third-order sequences at on-shelf positions at Thorn Hill, Tennessee. Detailed analysis within the shelf to shelf-edge succession reveals 20 less pronounced surfaces (separating fourth-order subsequences) and 3 pronounced surfaces (separating third-order sequences) with a total of 23 surfaces recognized in approximately 370 meters of section. Less pronounced surfaces define fourth-order subsequences that are correlative across the shelf. Many, but not all, of these fourth-order subsequences can be correlated to the shelf edge. Similarly, some fourth-order subsequences occur only at the shelf-edge. Within these third- and fourth-order sequences, fifth-order, "meter-scale" packages, or parasequences, occur. Parasequences are not correlative across the shelf or from the shelf to the shelf-edge, and many are probably the result of lateral environmental migration.

Stratigraphic sequences define shallowing-upward packages, similar to cycles, and are used to construct Fischer plots, substituting sequences for cycles, for both the on-shelf and shelf-edge stratigraphic successions. Surfaces of subaerial exposure are correlated from on-shelf to shelf-edge positions, showing that some sequences or "beats" are missing. Beats are missed in three ways: 1) Sea-level remains near or below the shelf-edge even though sea-level is oscillating causing deposition to be restricted to shelf-edge areas, 2) tectonic uplift exposes the shelf but not shelf-edge areas until subsidence allows resubmergence of the shelf, and 3) during drowning

which carries shelf margin areas to depths precluding carbonate deposition there though sediment does accumulate on the shelf.

## INTRODUCTION

Carbonate shelves provide one of the most accurate gauges for investigating changes in sea-level. Because the surface of these shelves is nearly horizontal, even small changes in sea-level expose or drown large areas. Sediment type, geometry, and diagenesis of carbonate shelves and platforms record information about sea-level changes. Previous work of this sort has concentrated on the shallower, peritidal parts of platforms. Although evidence may be subtle and much less plentiful, similar information concerning ancient changes in sea-level is also recorded at or near the shelf-edge in more continuously subtidal sediments.

Fischer plots have been used to help explain sea-level changes on ancient carbonate shelves (e.g., Fischer, 1964; Read et al., 1986; Read, 1989; Koerschner and Read, 1989; Goldhammer et al., 1987, 1990). Although interpretation of Fischer plots is controversial, they provide valuable clues for understanding deposition on carbonate shelves. Many workers have envisioned eustatic changes in sea-level as the primary mechanism leading to the occurrence of shallowing-upward, meter-scale packages termed "cycles" and their systematically arranged larger-scale counterparts (i.e., Read et al., 1986; Read, 1989; Koerschner and Read, 1989; Goldhammer et al., 1987, 1990). Other workers, however, note that autocyclic causes of relative sea-level change may have also played an important role (i.e., Kozar et al., 1990; Hardie,

et al., 1991). Fischer (1964) recognized three components or "dictators" to his plot: 1) relative changes in sea-level related to "accretion of sediments" and subsidence, 2) tectonic changes, and 3) eustatic changes. Because these different components are not easily resolved, there are limits on how the Fischer plot can be interpreted (e.g., Steinhauff and Walker, in press). The most serious limitation is the implicit assumption that each cycle is of the same duration. This is almost certainly not true (Kozar et al., 1990; Hardie et al., 1991). Indeed, it is likely that some cycles represented by sediment elsewhere will not be represented within any given stratigraphic succession. These absent cycles or "beats" may be missed when sedimentation rates are depressed or during periods of subaerial exposure (e.g., Hardie et al., 1986; Goldhammer, et al., 1990).

## Objectives

In chapter 2, I have documented relative changes in water-depth (i.e., the sum of subsidence, eustacy and sedimentation) and the occurrence of surfaces of subaerial exposure along an approximately 6 km transect of a more than 400 meter thick Middle Ordovician on-shelf succession near Thorn Hill, Tennessee. These surfaces of subaerial exposure define stratigraphic sequences within an apparently non-cyclic carbonate succession. These sequences define shallowing-upward packages, similar to cycles, that can be used to construct Fischer plots.

The present chapter shows how stratigraphic sequences of the Middle Ordovician carbonate platform interior documented in chapter 2 correlate to the shelf-

edge. Surfaces of subaerial exposure are correlated between seven closely spaced stratigraphic sections, four at on-shelf positions and three at or near the shelf-edge. Carbonate facies geometry is based on outcrop observation and is constrained by surfaces of subaerial exposure. Facies geometry is also inferred from stratigraphic and sedimentologic analysis of thin-sections and from analysis of water-depth curves. Because surfaces of subaerial exposure can be correlated from on-shelf to shelf-edge positions, it is also possible to show how each accompanying sequence occurring at an on-shelf position correlates or fails to correlate with its shelf-edge counterpart. That is, it is possible to show how some "beats" are missed at both on-shelf and shelf-edge localities. Missed beats are caused by distinctly different processes in the two areas.

## Study Area

The study area consists of four on-shelf localities and three shelf-edge or near shelf-edge localities. A regional environmental/stratigraphic framework, based on these and other sections, was developed by Walker (1977, 1980, 1985), Ruppel (1979), and Ruppel and Walker (1982, 1984). The four on-shelf localities are exposed along the northwest limb of the Copper Creek allochthon and are documented by Steinhauff and Walker (in press). A more than 540 meter thick succession of Middle Ordovician strata ranging from the upper Knox Group through the Five Oaks, Lincolnshire, Rockdell, Benbolt, Wardell, Witten and Moccasin formations is exposed along-strike. From southwest to northeast these localities include the Thorn Hill (TH), Old Thorn Hill (OTH), Idol Mine (IS), and Cedar Springs (CS) sections. Each

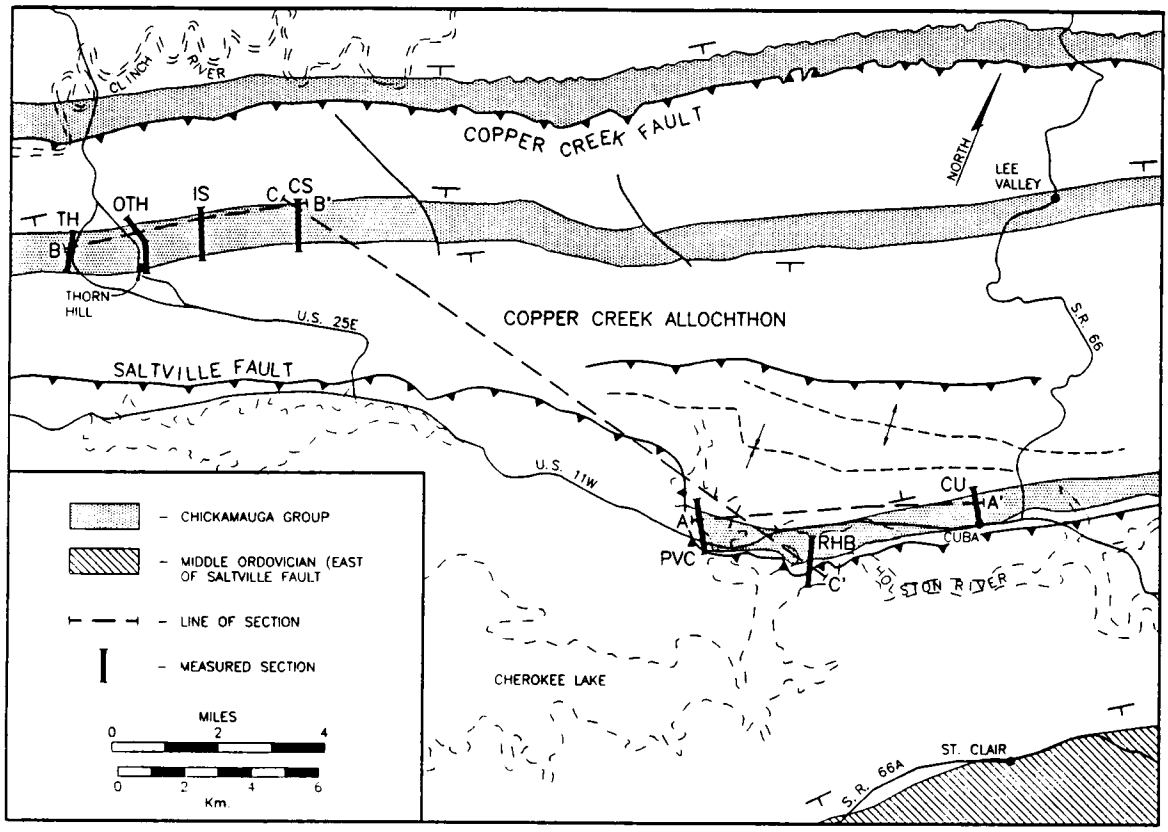



Figure 3.1. Location map for study area within the Copper Creek allochthon, modified from Ruppel (1979). Letters refer to sections considered in this study (solid section symbol). On-shelf sections are: Thorn Hill (TH), Old Thorn Hill (OTH), Idol Mine section (IS), and Cedar Springs (CS). Shelf-edge or near shelf-edge sections include: Poor Valley Creek (PVC), Red House Branch (RHB), and Cuba (CU). Additional sections provide supporting stratigraphic framework (i.e., Ruppel, 1979; Ruppel and Walker, 1982, 1984) for the present study.

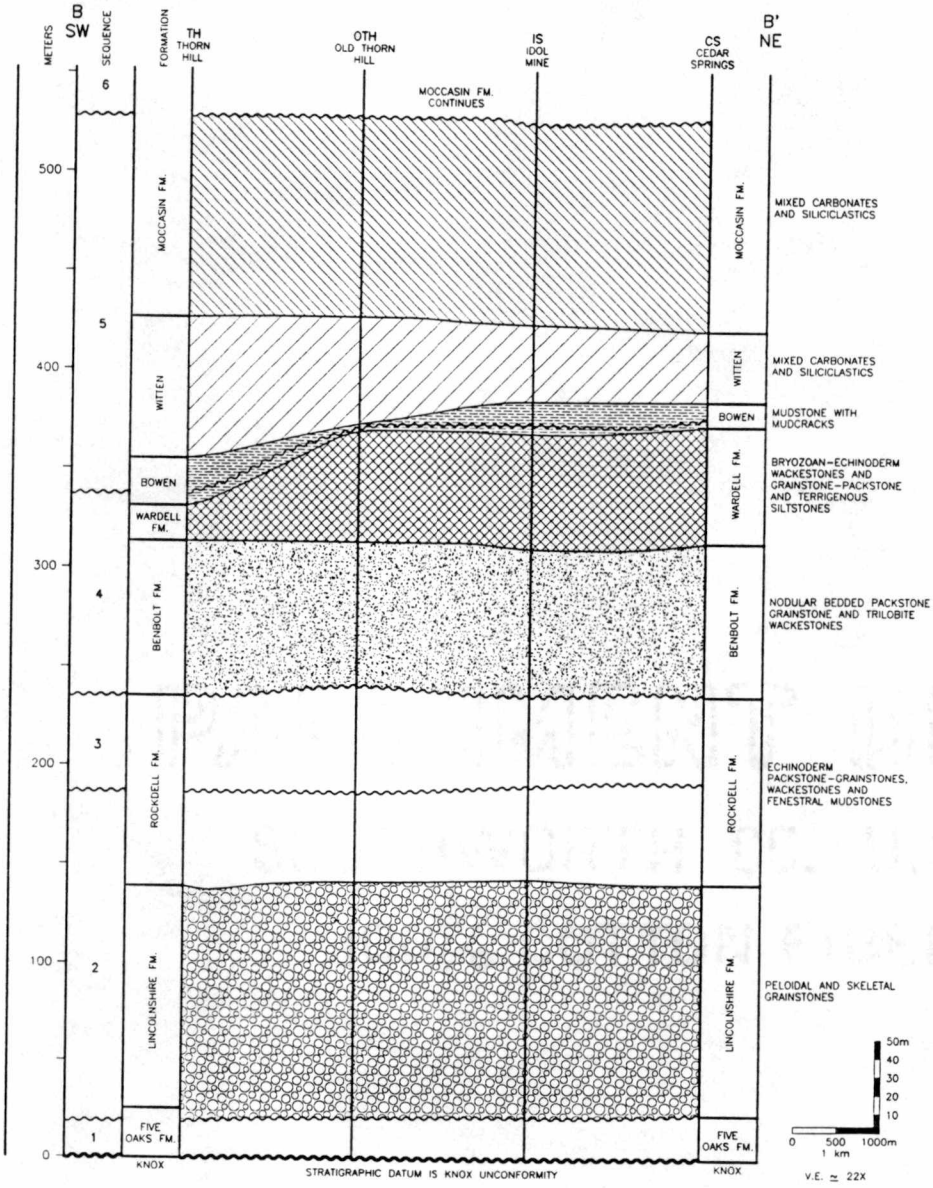



Figure 3.2. Stratigraphic sequences 1-5, Thorn Hill area. This on-shelf succession is restored along depositional strike (see chapter 2, and Steinhauff and Walker, in press). From southwest to northeast, sections occur at Thorn Hill (TH), Old Thorn Hill (OTH), Idol Mine section (IS), and Cedar Springs (CS).

section is separated from the other by approximately 2 km (Figs. 3.1 and 3.2). Strata at the three shelf-edge sections are overturned and exposed on the southwest limb of the Copper Creek allochthon. An approximately 300 meter thick succession of Middle Ordovician strata ranging from the upper Knox Group through the Five Oaks, Lenoir, Holston and Rockdell formations is exposed along strike. From southwest to northeast, these localities include the Poor Valley Creek (PVC), Red House Branch (RHB), and Cuba (CU) sections (Fig. 3.1).

## PREVIOUS WORK

Water-depth of deposition was established in chapter 2 using multiple lines of evidence to determine a range of possible water-depths (e.g., Elias , 1937; Benedict and Walker, 1978; Steinhauff and Walker, in press). Inflection points in water-depth curves indicate stratigraphic intervals that also contain subtle indicators of subaerial exposure. Such indicators help deduce changes in water-depth after initial deposition. These subaerial exposure indicators include erosional truncation, mudcracks, crystal or vadose silt, calcite filled vugs lined by reddish crusts, and pendant cements observed under cathodoluminesence (C.L.; Figs. 3.3 and 3.4).

### Bathymetric Indicators Using Multiple Lines of Evidence

Benedict and Walker (1978) and Steinhauff and Walker (in press) recognize four types of bathymetric indicators: 1) chemical, 2) sedimentologic, 3) biologic, and 4) stratigraphic. Each category contains criteria observable at different scales,

Figure 3.3 Indicators of subaerial exposure. Scale bars at bottom of field represent 1 mm. **A.** Typical exposure of mud-rich beds, on-shelf Thorn Hill section, about 220 meters above Knox unconformity. **B.** Geopetal vadose silt (v) along bottom of blocky clear calcite (Ave. $\delta^{13}C$ = -0.8‰, $\delta^{18}O$ = -7.4‰, N = 2) filled cavity. Host rock is bioclastic wackestone / packstone (facies B) and whole fossil wackestone (facies A), 213.5 m above Knox, Thorn Hill section; plane polarized light (PPL). **C.** Additional vadose silt (v) followed by blocky clear calcite, 213.5 m above Knox, Thorn Hill section; PPL. **D.** Fibrous calcite (f) ($\delta^{13}C$ = 0.8‰, $\delta^{18}O$ = -5.1‰ PDB, N = 6) grew along bottom of cavity followed by bladed calcite (not shown) ($\delta^{13}C$ = -0.3‰, $\delta^{18}O$ = -6.5‰ PDB, N = 5). Vadose silt (v) and ferroan coarse to blocky white calcite (c-b) occupy intermediate pore-filling positions followed by a final ferroan coarse blocky white calcite (c) ($\delta^{13}C$ = 0.7‰, $\delta^{18}O$ = -7.3‰ PDB, N = 1), 20.6 m above Knox, Poor Valley Creek section; PPL. **E.** Cavity filled with fibrous calcite (f) ($\delta^{13}C$ = 0.7‰, $\delta^{18}O$ = -4.9‰ PDB, N=2) followed by blocky clear calcite (b), and coarse to blocky clear calcite (c) ($\delta^{13}C$ = 0.7‰, $\delta^{18}O$ = -6.6‰ PDB, N = 1), 24.6 m above Knox, Poor Valley Creek section, PPL. **F.** Same cavity under cathodoluminescence (CL) shows that some blocky cements have pendant like shapes. **G.** More typical cavity, same stratigraphic interval as E and F, fibrous calcite (f) is truncated by ferroan coarse pink sparry calcite (c), Poor Valley Creek section; PPL. **H.** Pendant cement under CL, non-luminescent fibrous calcite (f) ($\delta^{13}C$ = 0.4‰, $\delta^{18}O$ = -6.7‰ PDB, N = 3) is followed by brightly luminescent, coarse, blocky calcite (c-b); and dully luminescent ferroan coarse sparry calcite (c-d) ($\delta^{13}C$ = 0.8‰, $d^{18}O$ = -10.2‰ PDB, N = 2); 41.5 m above Knox, Red House Branch section.

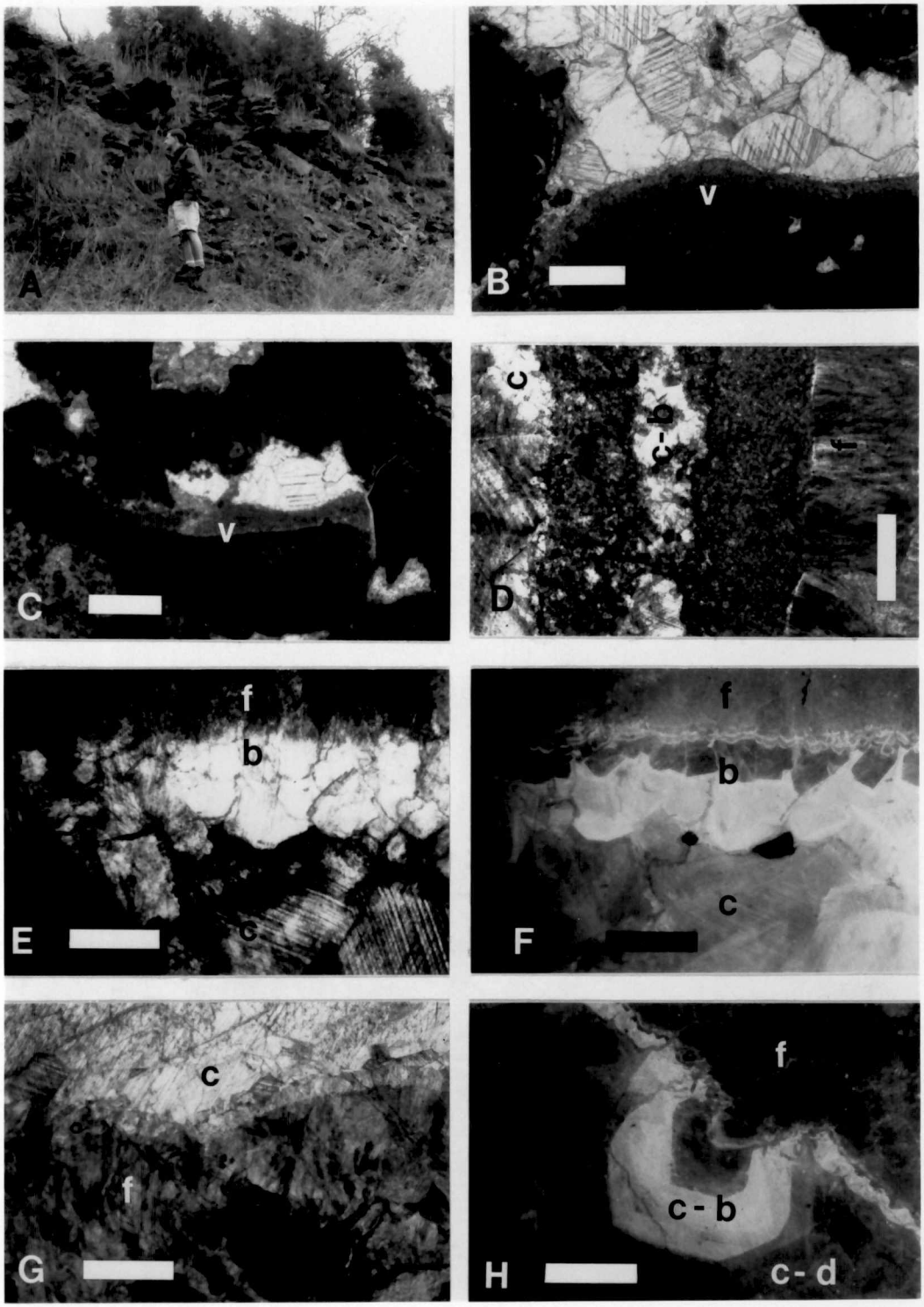
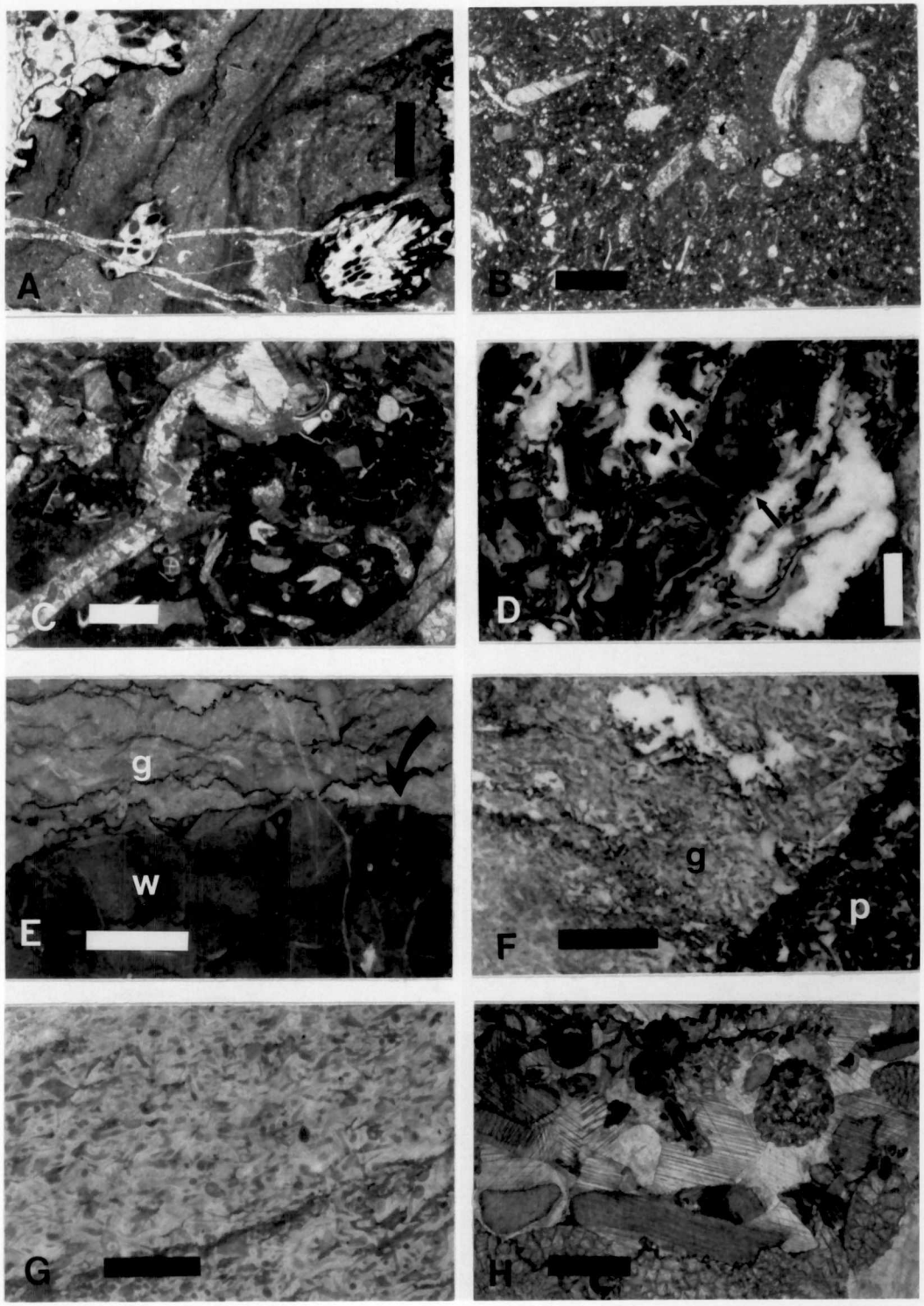

A
B
v
C
v
D
c
c-c
E
f
b
c
F
f
b
c
G
c
f
H
f
c - b
c - d

Figure 3.4. Shelf-edge lithologies: **A.** Bioclastic wackestone / packstone (facies B), 42.5 m above Knox, Red House Branch section; plane polarized light (PPL), scale bar = 1 mm. **B.** Additional bioclastic wackestone / packstone, same stratigraphic interval as A; PPL, scale bar = 1 mm. **C.** Echinoderm / bryozoan packstone (facies F), 57 m above Knox, Red House Branch section; PPL, scale bar = 1 mm. **D.** Echinoderm / bryozoan packstone (facies F). Black areas (arrowed) between spar filled cavities are iron-manganese oxide rich sediment, 20.6 m above Knox, Poor Valley Creek section; polished slab, "up" to left margin of page, scale bar = 2 cm. **E.** Wackestone (w) (facies A with facies L, poorly developed) is overlain by echinoderm grainstone (g) (facies E). Boring (arrowed) suggests wackestone was lithified and possibly exposed before grainstone was deposited, 41.5 m above Knox, Red House Branch section; polished slab, scale bar = 3 cm. **F.** Typical contact between echinoderm grainstone (g) (facies E) and echinoderm / bryozoan packstone (p) (facies F), 42 m above Knox, Red House Branch section; polished slab, scale bar = 3 cm. **G.** Echinoderm grainstone (facies E), 13.8 m above Knox, Poor Valley Creek section; polished slab, scale bar = 3 cm. **H.** Echinoderm grainstone (facies E) with bryozoan fragments, 50.5 m above Knox, Red House Branch section; PPL, scale bar = 1 mm.


A
B
C
D
g
W
E
g
p
F
G
H

ranging from microscopic (in thin-section) to patterns of regional scope. All the indicators are not applicable in every situation. Indeed, some indicators (i.e., those for very deep-water) were not used at all. Rather, emphasis is on those Middle Ordovician indicators that are most useful in the study of on-shelf and shelf-edge sequences (Fig. 3.3).

## Evidence of Post-Depositional Water-Depth Changes

As chemical, physical, biological, and stratigraphic indicators are analyzed, each category of information can be reexamined within the context of the entire framework. Taken together, these indicators reveal water-depths at the time of sediment deposition. Following deposition, however, changes in water-depth can occur. Subaerial exposure is one such post-depositional change that commonly occurs in shallow-water carbonates. When sea-level drops well below the platform margin and sediments are exposed for long periods, evidence for exposure is generally easy to recognize (e.g., Esteban and Klappa, 1983). However, if sea-level remains at or near the platform margin and sediments experience only a short period of exposure, then evidence for exposure becomes subtle.

Inflection points in water-depth curves that record water-depth at the time of deposition help point out stratigraphic intervals that may only contain subtle indicators of subaerial exposure. Subaerial exposure indicators include erosional truncation, mudcracks, crystal or vadose silt, calcite filled vugs, and pendant cements (observed under C.L.; Fig. 3.3). Additional and related examples are described and / or

illustrated by Steinhauff (1989), Steinhauff et al., (1989a,b), and Srinivasan et al. (1989).

In chapter 2, seven pronounced surfaces of subaerial exposure were described that define seven third-order sequences at on-shelf positions at Thorn Hill, Tennessee (see also, Fig. 1.2 of chapter 1). Detailed analysis within the shelf to shelf-edge succession reveals 20 less pronounced surfaces (separating fourth-order subsequences) and 3 pronounced surfaces (separating third-order sequences) with a total of 23 surfaces recognized in approximately 370 meters of section. Less pronounced surfaces define fourth-order subsequences that appear to be correlative across the shelf. These third- and fourth-order sequences contain "fifth-order" or "meter-scale" packages. These are comparable in scale to the parasequences of other authors. Parasequences are not correlative across the shelf and many of these are probably the result of lateral environmental migration. Pronounced surfaces of exposure (Fig. 3.2) are indicated at on-shelf positions where fenestral mudstones are truncated by cross-bedded grainstones and packstones. Truncated fenestral mudstones contain most, if not all, of the subaerial exposure indicators. Less pronounced surfaces of exposure are indicated by vadose silt and one or more other subaerial exposure indicators within the underlying rocks (see chapter 2).

## METHODS

Each successive, lithologically homogeneous interval, represented by at least one 50 X 75 mm thin-section, was scored for the presence or absence of selected

Middle Ordovician water-depth criteria (chapter 2; Steinhauff and Walker, in press). Some criteria, such as thickness of bedding and presence of megaripples, are best observed in the field. A total of 1041 thin-sections from 784 stratigraphic intervals were used. Additionally, polished slabs from more than 325 of these stratigraphic intervals were prepared to look for criteria such as burrows, flat algal laminae, and different categories of fenestrae. These features can be difficult to discern in the field and typically occur at a scale inappropriate for thin-section observation. Thus, when slabs were observed, serially cut sections (generally two or more) were prepared for each stratigraphic interval examined. These slabs ranged in size from about 50 X 100 mm to about 200 X 250 mm. Comparative and supporting lithologic observations were also made using 162 thin-sections provided by Breland (1980) from the Knoxville area (Figs. 3.5 and 3.6, see also chapter 2).

Resolution of water-depth decreases as water-depth increases (Benedict and Walker, 1978). That is to say, indicators of shallow water-depths discriminate a narrower range of possible water-depths than do those indicating deeper water-depths. Thus, a geometric scale was selected to plot a range of possible water-depths at the time of deposition (e.g., Figs. 3.7 - 3.11). A midpoint for each range is also plotted. At some stratigraphic intervals, more than one thin-section was observed. When these thin-sections come from slightly different lithologies (e.g., skeletal grainstone versus skeletal packstone), slightly different water-depth ranges may be indicated for each lithology. For these intervals, the combined range is plotted and two "midpoints" are indicated (e.g., Figs. 3.7 and 3.8).

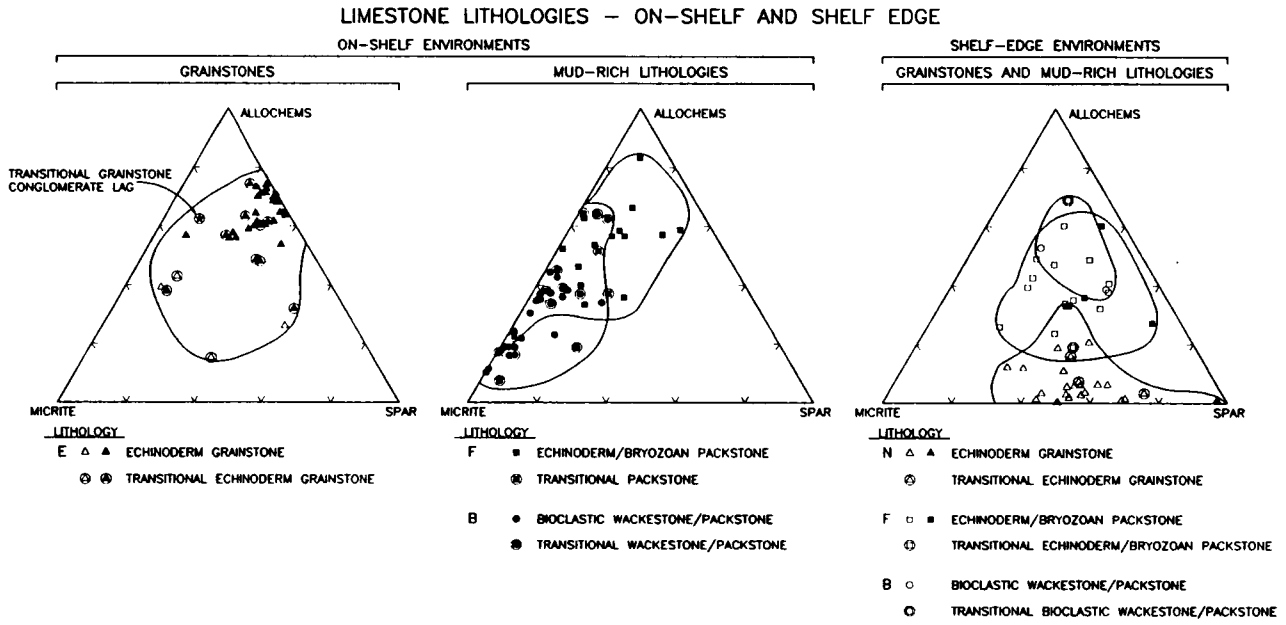



Figure 3.5. Ternary diagrams compare of Middle Ordovician limestone lithologies from on-shelf environments to similar environments at or near the shelf-edge in East Tennessee. Selected point-count data from Ruppel (1979), Breland (1980), and Jernigan (1987). Open symbols indicate cement priority point-counting (i.e., Jernigan, 1987) and solid symbols indicate standard grain-priority technique. Standard grain-priority point-counting would count the interior of a snail as "snail", though the interior space might be filled with cement. Using "cement-priority" the area would be counted as cement. Symbols enclosed by a ring indicate transitional facies where an estimated 1/2 to 2/3 of the plotted lithology is recognized.

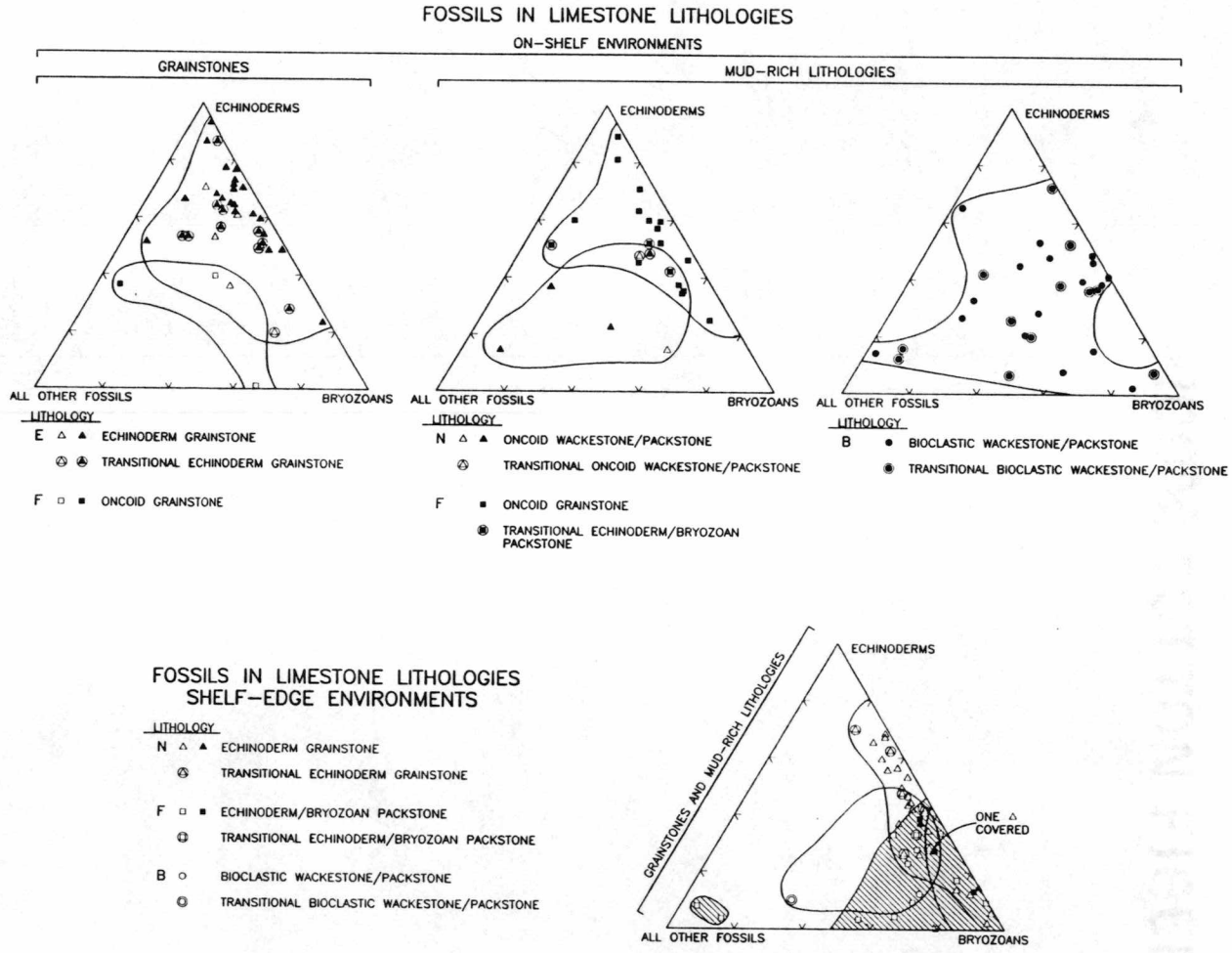



Figure 3.6. Ternary diagrams compare fossil content of Middle Ordovician limestone lithologies from on-shelf environments with the content in similar environments at or near the shelf-edge in East Tennessee. Selected point-count data from Ruppel (1979), Breland (1980), and Jernigan (1987), see caption Figure 3.5 for details.

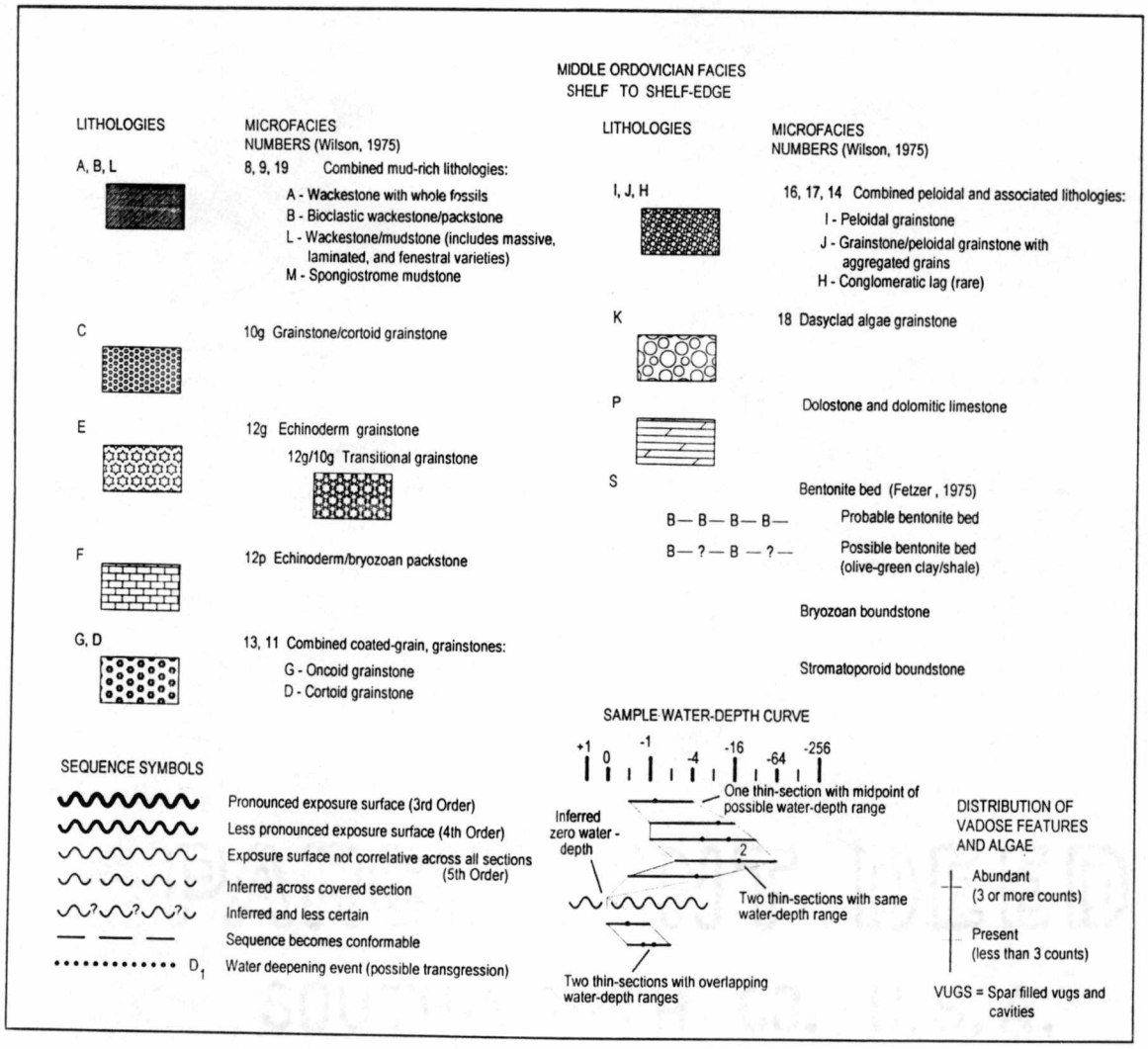



Figure 3.7. Key to facies for stratigraphic sequence diagrams and columnar sections of figures 3.8, 3.9, 3.10, 3.11, and 3.12.

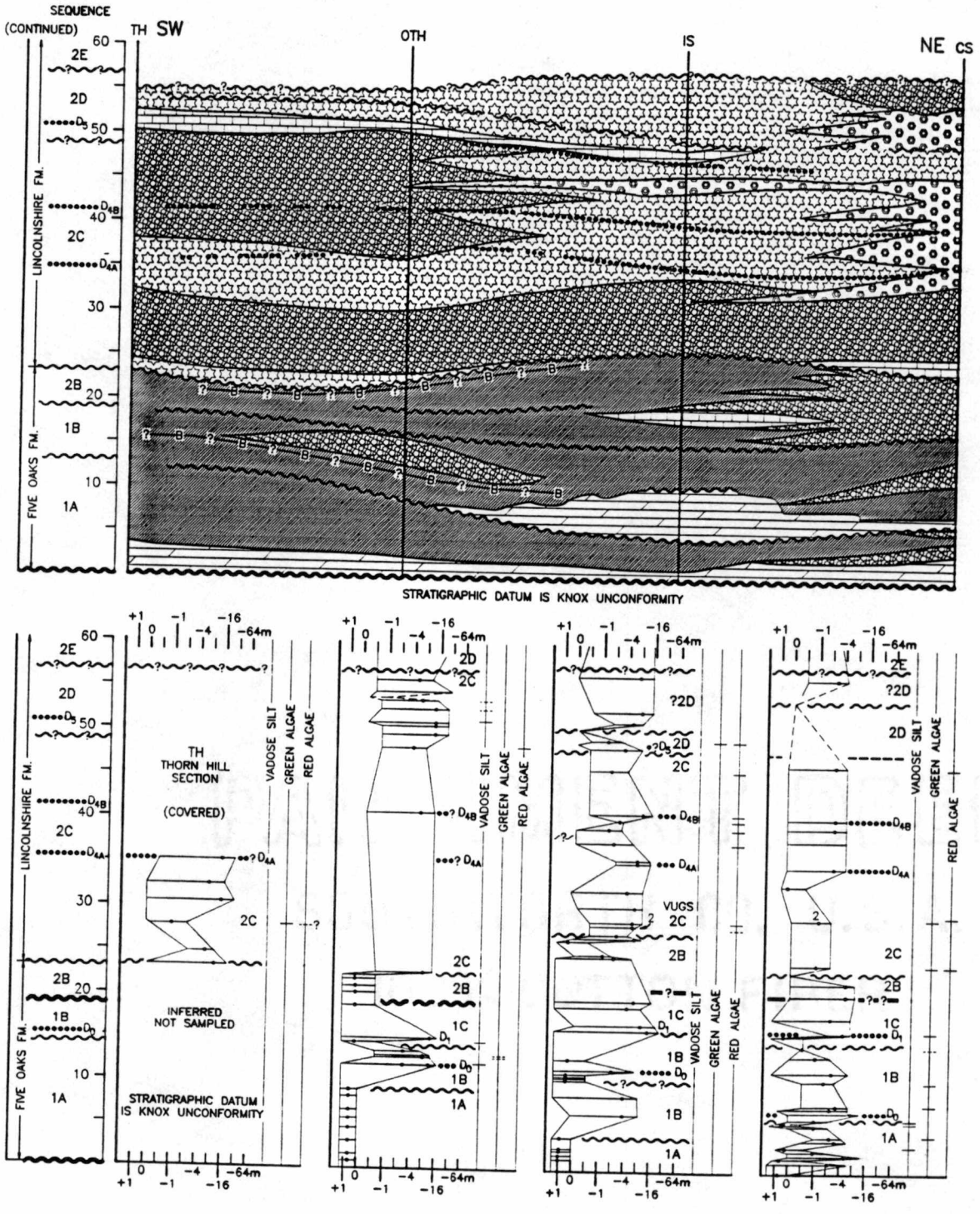



Figure 3.8. Stratigraphic subsequences 1A, 1B, 1C, 2B, 2C , and 2D on the shelf in the Thorn Hill area. Bottom panel shows water-depth curves for stratigraphic sections (from southwest to northeast) at Thorn Hill (TH), Old Thorn Hill (OTH), Idol Mine (IS), and Cedar Springs CS). Top panel shows corresponding restored cross-section. For key to facies see Figure 3.5.

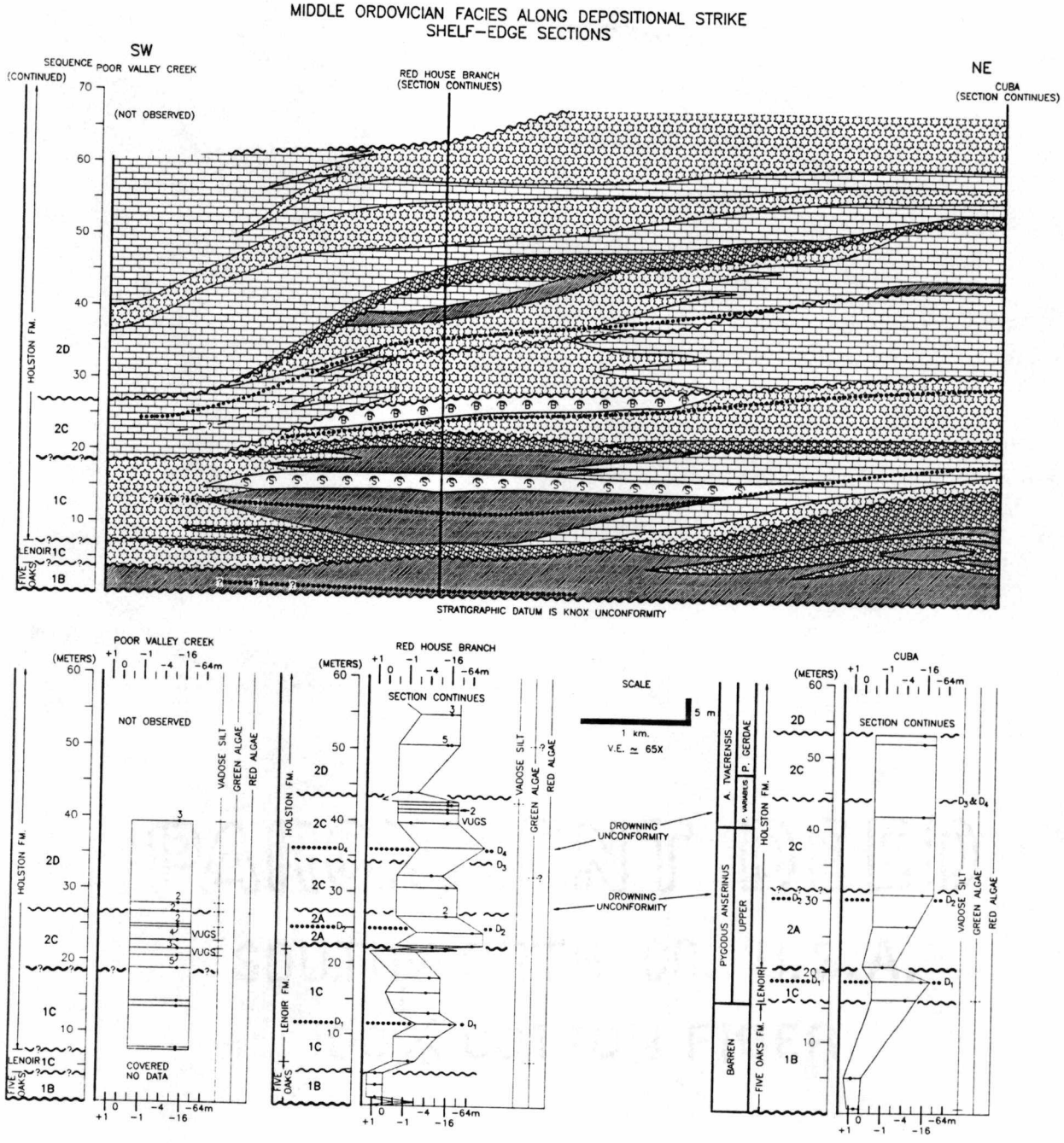



Figure 3.9. Stratigraphic subsequences 1B, 1C, 2B, 2C , and 2D at or near the shelf-edge in the Red House Branch area. Bottom panel shows water-depth curves for stratigraphic sections (from southwest to northeast) at Poor Valley Creek (PVC), Red House Branch (RHB), and Cuba (CU). Top panel shows corresponding restored cross-section. For key to facies see Figure 3.5.

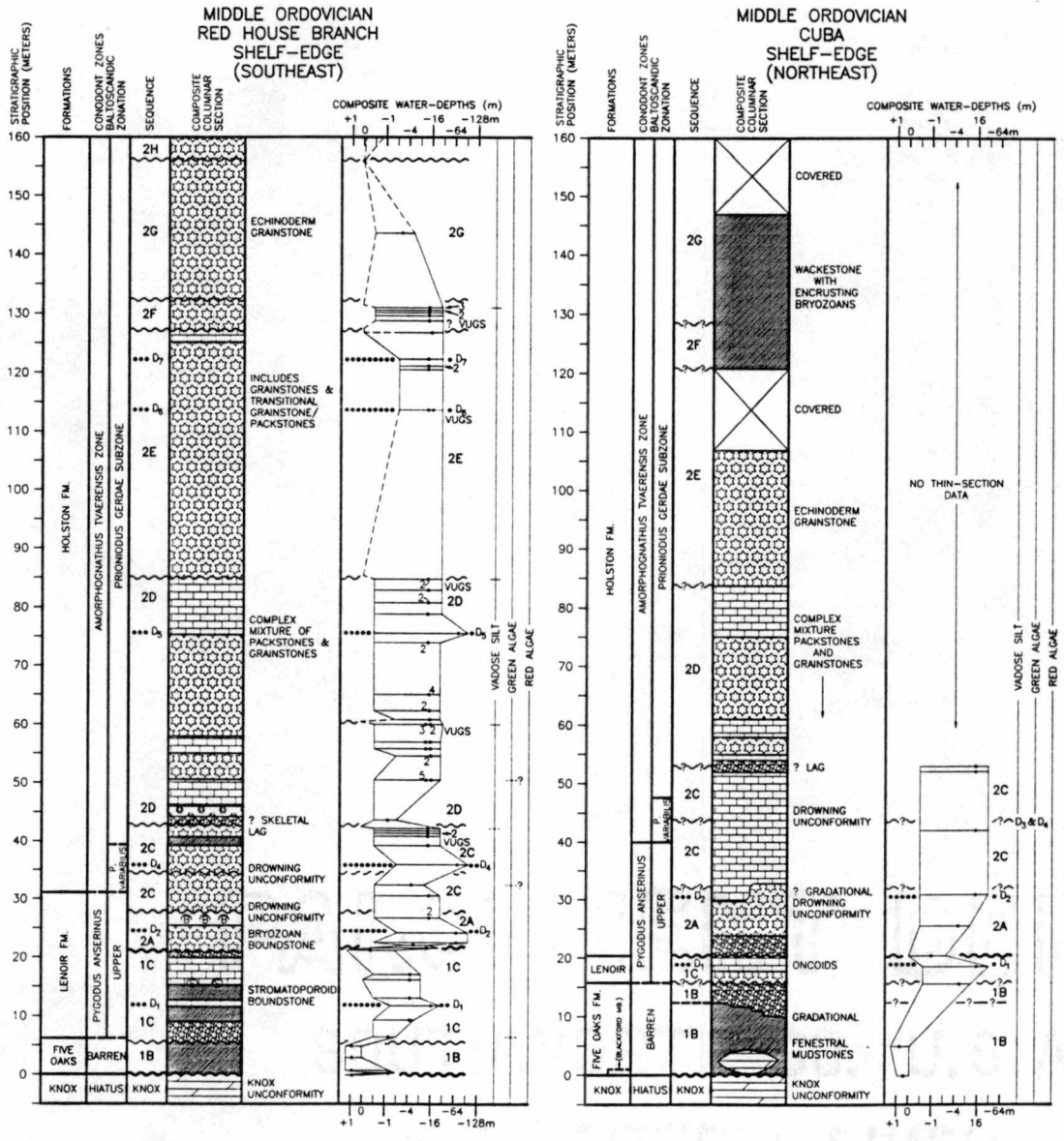



Figure 3.10. Lithostratigraphic and biostratigraphic comparison of shelf-edge or near shelf-edge sections; Red House Branch (left) is compared to the reference section at Cuba (right). Conodont zonation at Cuba (i.e., Carnes, 1975; Bergstrom and Carnes, 1976) is projected along depositional strike, into the sequence stratigraphic framework at Red House Branch, approximately 6 km to the southwest.

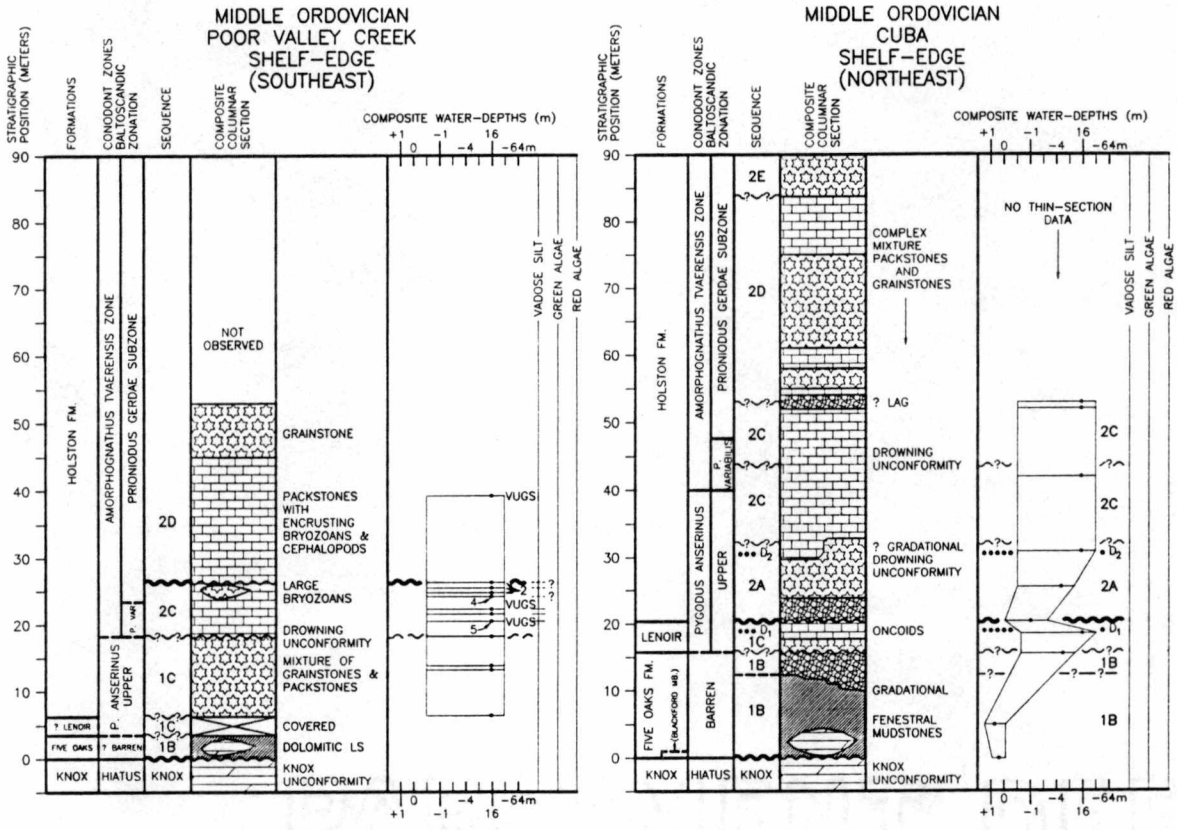



Figure 3.11. Lithostratigraphic and biostratigraphic comparison of shelf-edge or near shelf-edge sections; Poor Valley Creek (left) is compared to the reference section at Cuba (right). Conodont zonation at Cuba (i.e., Carnes, 1975; Bergstrom and Carnes, 1976) is projected along depositional strike, into the sequence stratigraphic framework at Poor Valley Creek, approximately 9 km to the southwest.

"First iteration" water-depth curves were plotted and compared with detailed, bed-for-bed, lithologic descriptions at a scale of 1 inch to 1 meter. Some stratigraphic intervals have water-depth ranges indicating possible subaerial exposure. Stratigraphic intervals having inflection points indicating possible exposure or shoaling were reexamined for the presence of post-depositional indicators of subaerial exposure. Evidence of exposure comes from outcrop and thin-section examination. "First iteration" water-depth curves were then replotted to reflect the fact that some stratigraphic intervals have experienced subaerial exposure (dashed lines on water-depth curves, e.g., Figs. 3.7 and 3.8).

## LITHOLOGIES

### Description of On-Shelf Lithologies

Seventeen on-shelf lithologies are documented in chapter 2, and Steinhauff and Walker (1992; in press). Here these lithologies are contrasted with shelf-marginal rock types.

### Description of Shelf-Edge Lithologies

A much smaller number of lithologies (9) occur at or near the shelf-edge when compared to those which occur on the shelf (17). Indeed, just three lithologies account for about 85% of the total thickness and occur throughout this shelf-edge succession. In order of relative abundance these are: echinoderm / bryozoan packstone (facies F), echinoderm grainstone (facies E), and bioclastic wackestone /

packstone (facies B) (Figs 3.4 and 3.5). All three lithologies are laterally and, less so, vertically gradational with each other. Six, more rare, lithologies account for the remaining stratigraphic thickness at the shelf-edge. These rarer lithologies generally occur only above and below unconformable surfaces (Fig. 3.9). Subaerial exposure is indicated at many, but not all of these surfaces.

Peloidal and associated mud-rich lithologies are restricted to the Five Oaks, Lenoir, and lowermost Holston formations at the shelf-edge (Fig. 3.9). At the shelf-edge, wackestone / mudstone (facies L) is well developed only within the Five Oaks Formation and is gradational with peloidal grainstone (facies I). Bioclastic wackestone (facies B) accounts for about 10% of the total stratigraphic thickness at the shelf-edge.

## Fossil Content

Limestone facies can also be characterized by fossil content. Echinoderms and bryozoans are the most common and abundant fossils and generally occur as fragments (Fig. 3.6). However, stromatoporoid and bryozoan boundstones occur at or near the shelf-edge (Figs. 3.9 and 3.10). Cephalopod-rich packstones occur along drowning unconformities at the sequence 1C / 2C and 2A / 2C surfaces at Poor Valley Creek and Red House Branch, respectively (Figs. 3.9, 3.10, 3.11). On the shelf, where other fossils occur, two faunal associations are generally recognized: 1) an arthropod - mollusk association (i.e., thick-shelled trilobites and / or ostracods with gastropods) and 2) a brachiopod - bryozoan association (Fig. 3.6).

## ON-SHELF AND SHELF-EDGE WATER-DEPTHS

Maximum water-depths on the shelf never exceeded 20 meters within the Five Oaks, Lincolnshire, and Rockdell formations. Within the middle to upper Benbolt Formation and the lower Wardell Formation, maximum water-depths may have been slightly deeper. Most deposition on the shelf likely took place in water that was only a few meters deep (chapter 2; Steinhauff and Walker, in press). Very conservative water-depth estimates were used for water-depth criteria. Many stratigraphic intervals, particularly those characterized by an abundance of oncoids and other coated-grains were probably deposited in very shallow water (less than one or two meters) and may have been periodically exposed. Stratigraphic intervals containing abundant subaerial exposure criteria (pronounced surfaces) probably experienced exposure for some considerable, but unknown length of time and those intervals containing fewer exposure criteria (less pronounced surfaces) were probably exposed for a shorter period.

Maximum water-depths at shelf-edge positions were on the order of 30 meters (Figs. 3.9 - 3.12). Estimates for minimum water-depths, on the other hand, are less easily determined because water-depth indicators become increasingly less sensitive in deeper water. That is to say, water-depth indicators do not discriminate very well between water-depth differences at depths of 20 to 100's of meters, whereas the indicators discriminate water-depth differences at depths of 0.5 to 20 meters rather well.

## CORRELATION OF EXPOSURE SURFACES

Biostratigraphic investigations by Bergstrom (Bergstrom, 1971, 1973, 1977; Bergstrom and Carnes 1976) and Anita Harris (personal communication to Keith Roberson, 1990), and lithologic correlations by Ruppel (1979) and Ruppel and Walker (1982, 1984) provide the framework for more detailed sequence stratigraphic correlations. Bentonite beds provide additional stratigraphic control. Prominent bentonite beds in the upper Moccasin Formation provide a time line (Time Line 5 of Walker, 1980; and Ruppel and Walker, 1982) for correlation of the on-shelf.

Biostratigraphic, lithostratigraphic, and sequence stratigraphic correlation along- strike on the shelf is relatively easy because on-shelf sections are separated from each other by only about 2 km. For example, some individual beds at on-shelf positions can be traced laterally for about 400 meters. Correlation along-strike on the shelf is described and illustrated in chapter 2 and Steinhauff and Walker (in press). Similar correlation along-strike, at the shelf-edge is illustrated by Figures 3.9, 3.10, and 3.11.

Correlation from the shelf to the shelf-edge is more difficult. Although the two areas are within the same fault block, in restored position shelf localities are separated from shelf-edge localities by about 20 km. For example, conodont biostratigraphy is used to help correlate sequences 1A through 2D and their constituent lithologies from the shelf to the shelf-edge. However, starting above about 50 meters from the base of the Knox unconformity, only the *Prionidous gerdae* Subzone of the *Amorphognathus tvaerensis* Zone is recognized at both on-shelf and

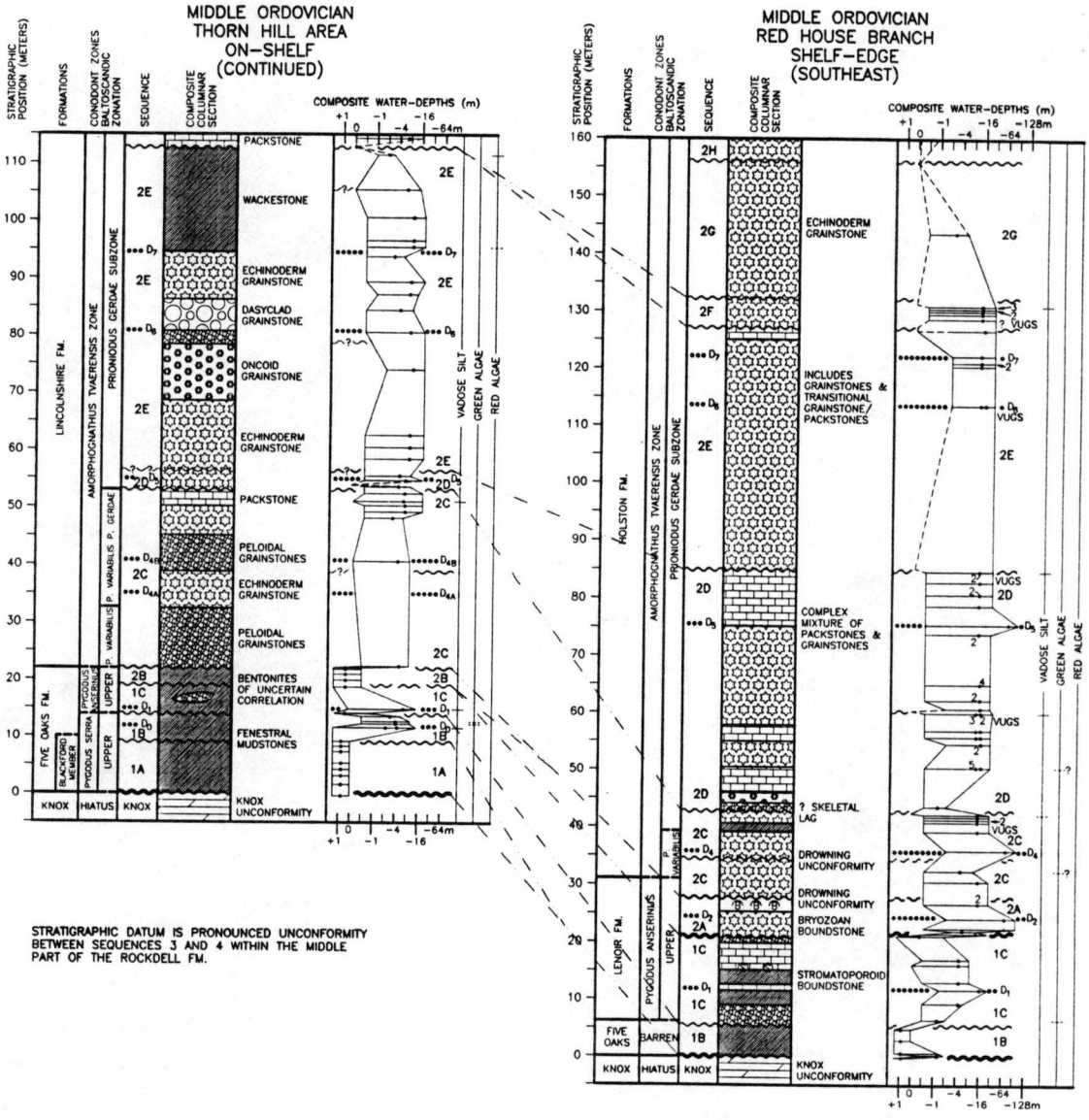



Figure 3.12. Composite columnar sections comparing the Thorn Hill area at the shelf (left) to the Red House Branch area at or near the shelf edge (right). A. Water-depth curves for the shelf are based on individual curves for the Thorn Hill and Old Thorn Hill sections (i.e., chapter 2; Steinhauff and Walker, in press). A more detailed key to lithologies is given in Figure 3.7. Conodont zonation is based on Carnes (1975) and later work by Anita Harris (Keith Roberson, personal communication).

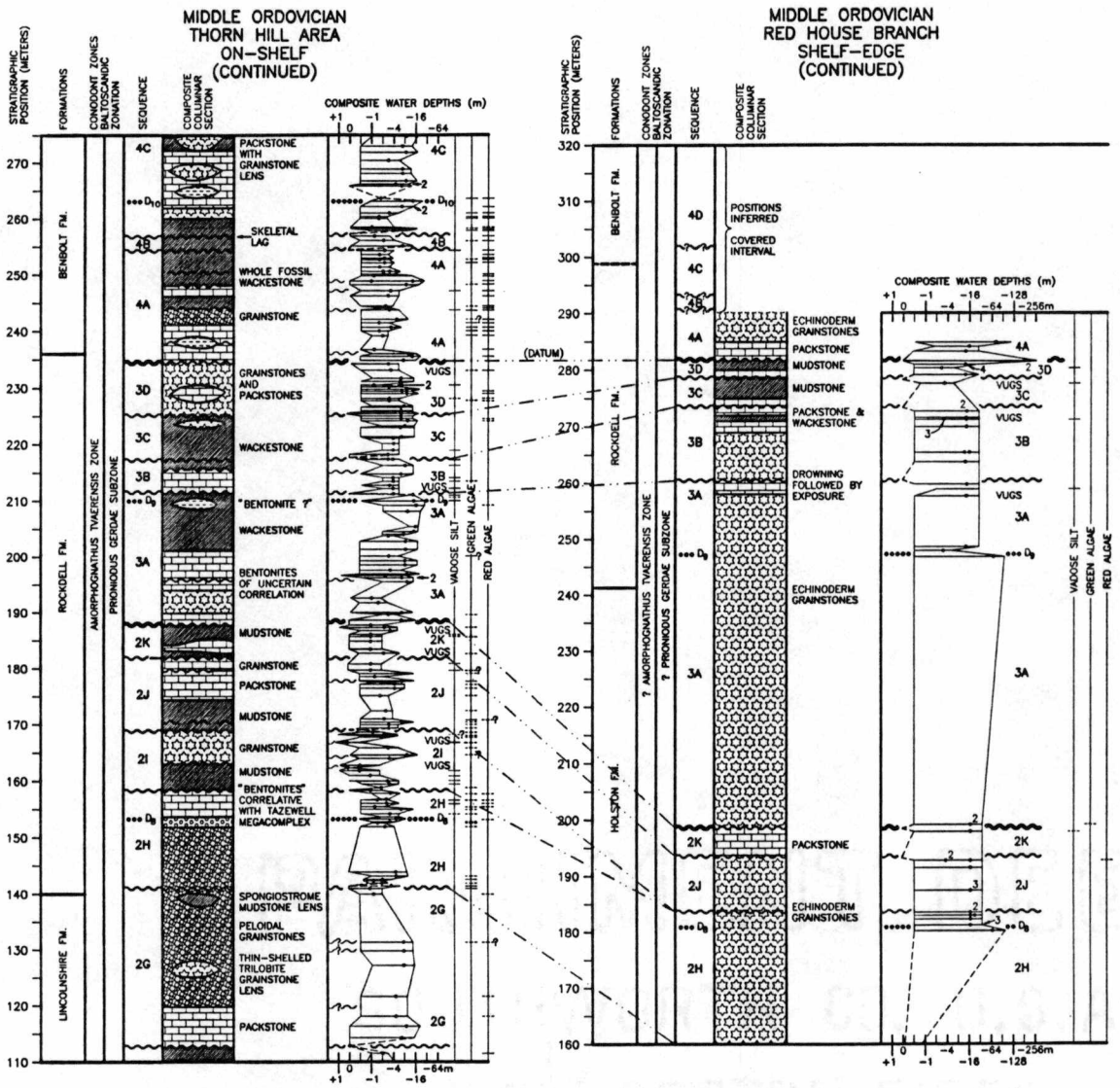



Fig. 3.12. Composite columnar sections comparing the Thorn Hill area at the shelf (left) to the Red House Branch area at or near the shelf edge (right). B. Figure is continued. Note that stratigraphic datum is the sequence 3D / 4A boundary.

shelf-edge positions. Thus, many unconformable surfaces of subaerial exposure and / / or drowning are correlated from the shelf to the shelf-edge based on relative stratigraphic position, occurrence of deepening events, and on lithologic patterns.

A number of assumptions or "guiding principles" constrain correlation (Table 3.1). Most of these guiding principles are based on application of standard stratigraphic principles (e.g., Krumbein and Sloss, 1951), others are derived from previous work combined with an understanding of carbonate depositional systems, and still others are based on simple common sense. "Guiding principles" for correlation along-strike on the shelf are described and illustrated in chapter 2. This chapter documents additional correlation along strike at or near the shelf-edge (Figs. 3.9, 3.10, and 3.11).

## CORRELATION OF DEEPENING EVENTS

A number of water-deepening events occur within this Middle Ordovician succession. These events are relatively easy to correlate across the shelf-along strike because water-depth indicators are most sensitive to depth changes in shallow water (Fig. 3.13). These deepening events may be a result of eustatic sea-level rises or to slow downs in deposition rate coupled with continued subsidence.

On the other hand, correlation of deepening events along depositional strike at the shelf-edge and from the shelf to the shelf-edge is more problematic (Figs. 3.12, 3.13, 3.14). For example, water-depth increases within sequences 2A and 2B at Red House Branch correlate with "deep" water at Poor Valley Creek. However, water-

## Table 3.1

### "Guiding Principles" Involved in Correlation Across Strike (on-shelf to shelf-edge)

1) The Knox surface is an appropriate stratigraphic datum.

2) During the initial Middle Ordovician transgression, a thicker succession accumulated at the shelf-edge that on the shelf (i.e., Ruppel and Walker, 1982, 1984; Bergstrom and Carnes, 1976). Thus, correlations made from the shelf-edge Holston formation to the on-shelf Lincolnshire and lower Rockdell formations should appear to "climb" in the section.

3) In general, water depths were shallower at on-shelf positions and deeper at shelf-edge positions. It follows, that more surfaces of exposure should occur at on-shelf positions and that not all of these surfaces will correlate to shelf-edge positions. For example most of the subsequence boundaries occurring on the shelf (i.e., Steinhauff and Walker, in prep.) do not correlate to the shelf-edge.

4) The lower Rockdell Formation was established as a shallow water facies equivalent of the shelf-edge Holston Formation. Later, the upper Rockdell prograded to a more shelf-edge position (e.g., Ruppel and Walker, 1981). In other words, about 2/3 of the Rockdell was deposited before its temporal equivalent appeared at the more shelf-edge position at Red House Branch. This means that exposure surfaces from about the upper most 1/3 of the Rockdell at on-shelf positions will correlate with exposure surfaces near the Holston / Rockdell contact at the shelf-edge. Furthermore, above the Holston/ Rockdell contact at Red House Branch, these exposure surfaces will no longer appear to "climb" in the section from on-shelf to shelf-edge.

5) With the lowermost 200 m of Middle Ordovician rocks, exceptions to #3 and 4 (above) can occur under the following conditions:

   a) If down-to-basin normal faulting occurred along or near the shelf-edge.

   b) Sea level remained at or near the shelf-edge for some period of time and little or no deposition occurred on the shelf.

6) Pronounced exposure surfaces occurring at on-shelf positions correlate with other pronounced exposure surfaces at shelf-edge positions or with less pronounced exposure surfaces at shelf-edge positions.

7) Inflection points recording water-depth increases on the shelf may correlate with inflection points recording water increases at the shelf-edge, even though these inflection points transgress time.

8) Correlation of inflection points of water depth increases is necessarily constrained between exposure surfaces. That is to say, a deepening event can not be correlated across an exposure surface.

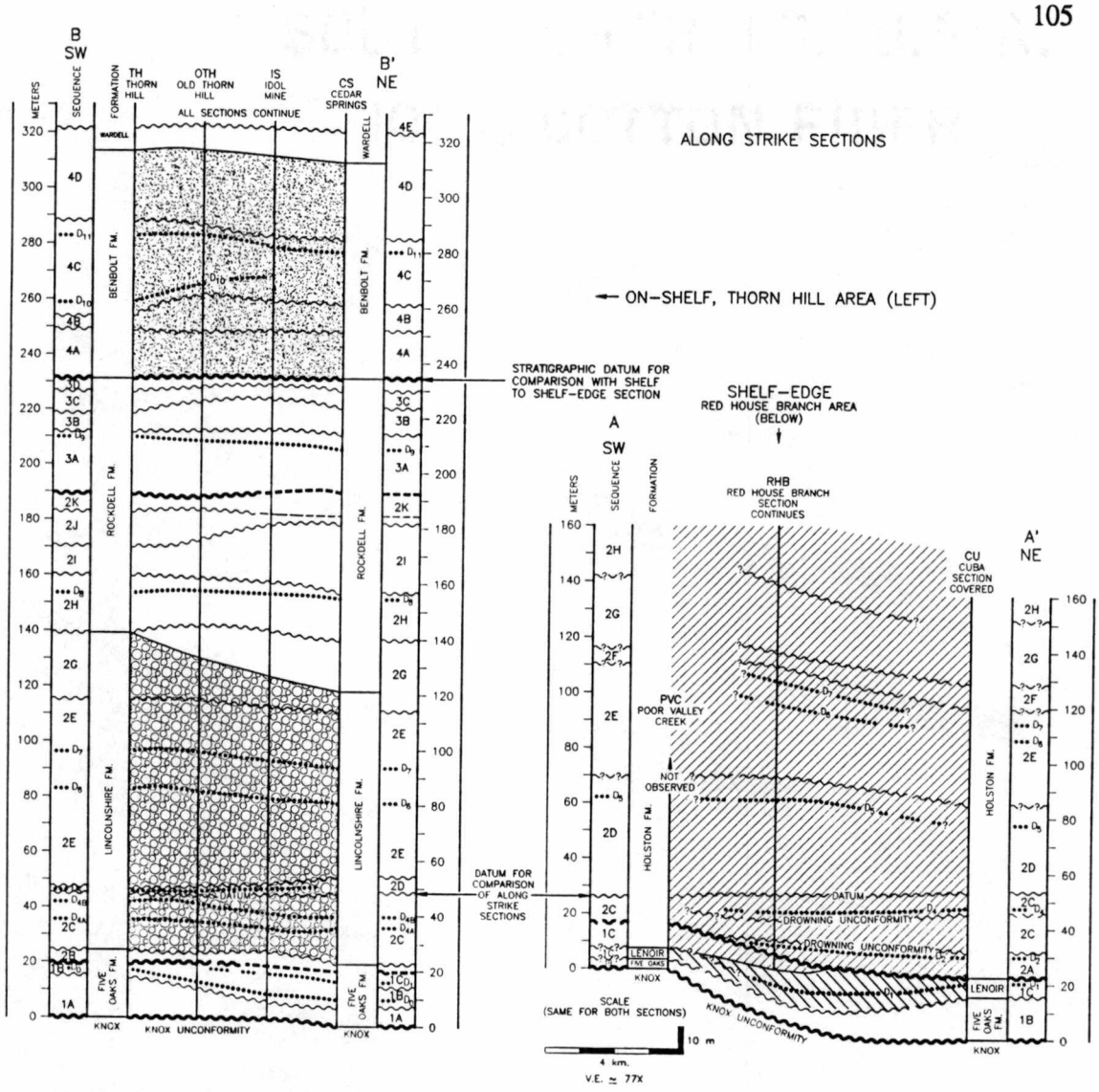
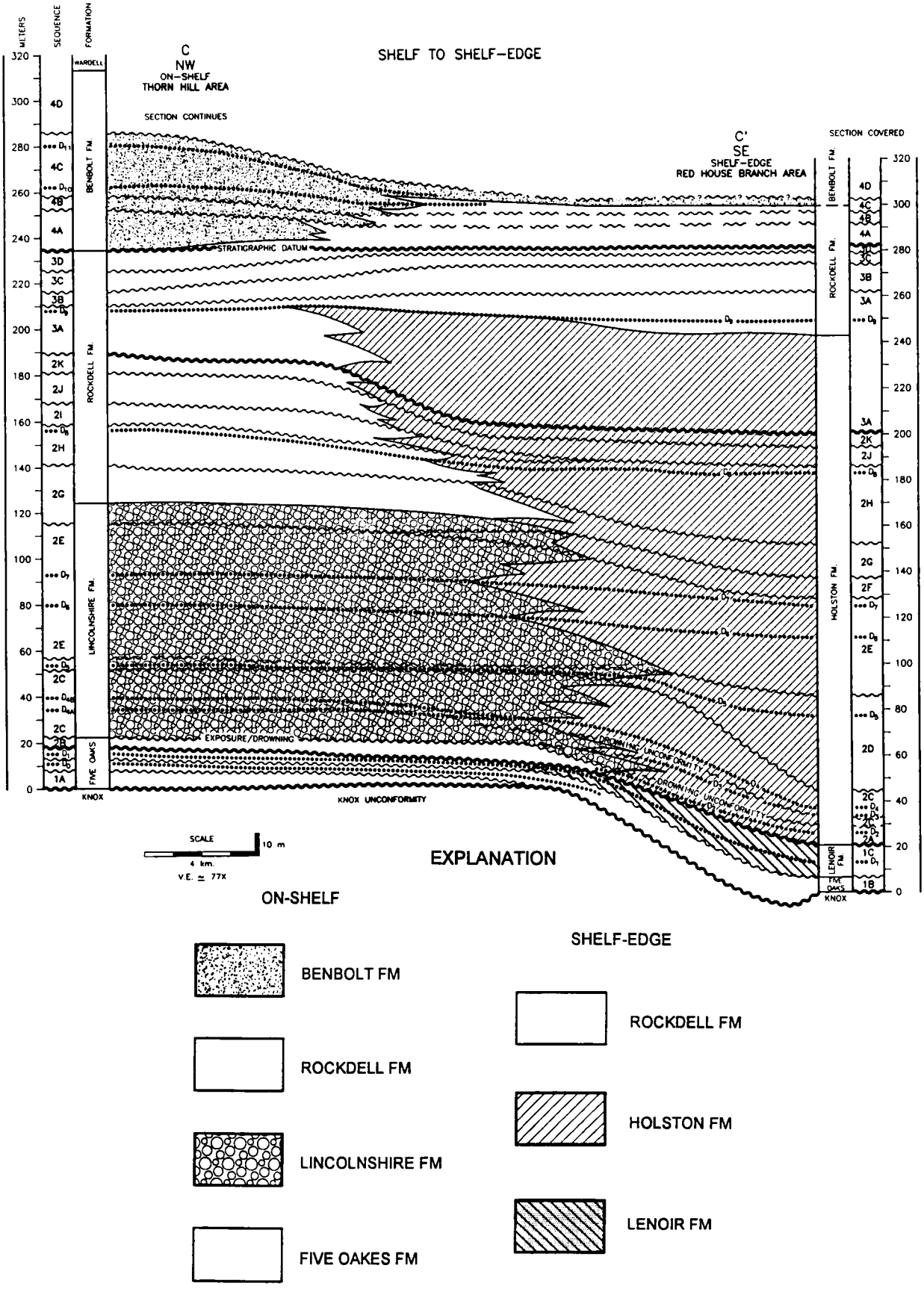



Figure 3.13. Stratigraphic subsequences 1A-4D. Cross-sections are restored along depositional strike. The shelf-edge or near shelf-edge in the Red House Branch area (left) includes from southeast to northwest: Poor Valley Creek (PVC), Red House Branch (RHB), and Cuba (CU). The on-shelf Thorn Hill area (see chapter 2) includes from southwest to northeast: Thorn Hill (TH), Old Thorn Hill (OTH), Idol Mine section (IS), and Cedar Springs (CS). Ornamentation shows location of different formations. On the shelf (diagram at left) in the Thorn Hill area, the Five Oaks Formation is shown by the white area (bottom), and is unconformably overlain by the Lincolnshire Formation indicated by circles (lower middle), followed by the Rockdell Formation in white (middle), followed by the Benbolt Formation shown by stipple (upper middle), and finally the Wardell Formation in white (top). At the shelf-edge (diagram at right) the Five Oaks Formation is show as white (bottom), followed by the Lenoir Formation shown by diagonal lines, and finally the Holston Formation indicated by opposite diagonal lines (top). Formation contacts are based on composite columnar sections (Fig. 3.12). Dotted lines labeled as $D_1$ , $D_2$ , etc., represent deepening events. Note that the sequence 2C / 2D boundary provides an appropriate stratigraphic datum for comparison of these two along strike cross-sections. The sequence 3D / 4A boundary provides a stratigraphic datum for comparison of the shelf (right) with the shelf-edge cross-section of Figure 3.14.

Figure 3.14. Stratigraphic subsequences 1A-4D, restored across depositional strike. Stratigraphic position of sequences and subsequences on the shelf in the Thorn Hill area (chapter 2; Steinhauff and Walker, in press) at left is based on the Cedar Springs (CS) section. The shelf-edge or near shelf-edge section at right is at Red House Branch. Ornamentation shows inferred distribution of different formations. The Five Oaks Formation is shown by the white area (bottom) and on the shelf (left) is unconformably overlain by the Lincolnshire Formation indicated by circles (middle), followed by the Rockdell Formation in white (middle), and finally the Benbolt Formation shown by stipple (top). At the shelf-edge (right) the Five Oaks is followed by the Lenoir Formation shown by diagonal lines and the Holston Formation indicated by opposite diagonal lines (middle). Formation contacts are based on composite columnar sections (see Fig. 3.12). Dotted lines labeled as $D_1$ , $D_2$ , etc., represent deepening events. The sequence 3 / 4 boundary provides a stratigraphic datum for comparison of the shelf (left) with the on-shelf, along depositional strike cross-section of Figure 3.13. See Figure 3.1 for location of line of section C-C'.


SHELF TO SHELF-EDGE
C
NW
ON-SHELF
THORN HILL AREA
SECTION CONTINUES
C'
SE
SHELF-EDGE
RED HOUSE BRANCH AREA
SECTION COVERED
METERS
SEQUENCE
FORMATION
WARDELL
BENBOLT FM.
ROCKDELL FM.
LINCOLNSHIRE FM.
FIVE OAKS
KNOX
STRATIGRAPHIC DATUM
EXPOSURE/DROWNING
KNOX UNCONFORMITY
HOLSTON FM.
LENOIR FM.
SCALE
10 m
4 km.
V.E. ≃ 77X
EXPLANATION
ON-SHELF
SHELF-EDGE
BENBOLT FM
ROCKDELL FM
ROCKDELL FM
HOLSTON FM
LINCOLNSHIRE FM
LENOIR FM
FIVE OAKES FM

depth changes at Poor Valley Creek are not resolved because water at Poor Valley Creek was generally deep.

## TYPES OF STRATIGRAPHIC SEQUENCES

### Third-Order Sequences

Starting with and including the Knox unconformity, seven pronounced surfaces of subaerial exposure are recognized in an approximately 600 meter thick succession of Middle Ordovician strata at on-shelf localities near Thorn Hill. These seven pronounced surfaces define seven stratigraphic sequences, numbered 1 through 7 see Fig. 1.2 of chapter 1; Fig. 3.2). The sixth surface occurs within the Moccasin Formation and has been documented by Ruppel and Walker (1982, 1984) and Simonson (1985). The uppermost (seventh) surface, followed by a pronounced deepening, is at the top of the Moccasin and separates that formation from the overlying Martinsburg Formation (Simonson, 1985; Walker, 1985). The lower five surfaces are considered in this study (about 400 meters thick).

Middle Ordovician deposition took place over a period of approximately 20 to 25 million years. This is based on the biostratigraphic work of Bergstrom and Carnes (1976) and absolute ages assigned to series boundaries as summarized by Bond et al. (1988). The interval reported on here represents about 3/4 of the entire Middle Ordovician, and had a duration of 15 to 17 million years. Thus, the estimated time for deposition of each sequence is 2.5 to a little more than 3 million years. These

sequences, then, appear to be of similar temporal duration as those commonly referred to as the products of "third-order" eustatic cycles (e.g., Vail et al., 1977).

## Fourth-Order Subsequences

Sequences bounded by pronounced exposure surfaces are subdivided by less pronounced exposure surfaces. These less pronounced exposure surfaces are correlated parallel to depositional strike (Figs. 3.8 - 3.13) and across depositional strike (Fig. 3.14). Starting above the Knox unconformity, nineteen less-pronounced exposure surfaces are recognized in the lower 400 meters (in sequences 3.1 - 3.4) of Middle Ordovician strata at on-shelf positions near Thorn Hill (Figs 3.13 and 3.14). If these nineteen less pronounced surfaces are combined with the five pronounced surfaces, 23 total surfaces are recognized in approximately 400 meters. This leads to a number of additional subsequences recognized within the previously defined and numbered third-order sequences. These subsequences bounded by less pronounced surfaces are designated alphabetically within the numbered third-order sequence in which they occur (e.g., 2A, 2B, 2C, etc.; Figs. 3.8 - 3.14). There are a total of 22 of these fourth-order subsequences. These subsequences appear to be of similar temporal duration (hundreds of thousands of years) and thickness as intervals referred to as the products of "fourth-order" sea-level cycles or "high-frequency" sea-level fluctuations (e.g., Kendall and Schlager, 1981; Read, 1989).

### Parasequences: Possible "Fifth-Order" or "Meter-Scale" Packages

Multiple shoaling events or possible exposure surfaces are indicated within many fourth-order subsequences. These are comparable in scale to the parasequences of other authors (Steinhauff and Walker, in press). Evidence for shoaling comes from inflection points noted on water-depth curves and from lithologic changes. This evidence is often only apparent in thin-section or polished slabs. Parasequences differ from sequences and subsequences in three ways. First, water-depth curve inflection points and subtle lithologic changes are not correlative across the entire 6 km on-shelf transect. Second, parasequences cannot be correlated from the shelf to the shelf-edge, whereas most fourth-order subsequences are recognized at on-shelf and shelf-edge positions. Finally, there are a variable number of parasequences at each locality. This suggests that most meter-scale parasequences are probably a result of local environmental migration. Indeed, some parasequences are capped with mud-rich sediments containing criteria suggesting supratidal and intertidal deposition. Thus, many of these parasequences are probably of autocyclic origin (in the sense of Ginsburg, 1971).

## DISCUSSION OF STRATIGRAPHIC SEQUENCES

### Third-Order Sequence 1

**Description.** Third-order Sequence 1 is comprised of fourth-order subsequences 1A, 1B, and 1C. All three fourth-order subsequences are represented on the shelf, whereas only subsequences 1B and 1C occur at the shelf-edge (Figs. 3.12, 3.13,

3.14). This is true in our study area; even though in general, conodonts indicate that Middle Ordovician deposition started earlier in southeastern fault-blocks than in northwestern blocks in the Southern Appalachians (Bergstrom, 1971, 1973, 1977; Bergstrom and Carnes 1976).

At on-shelf positions, fenestral mudstones and very thin peloidal grainstones of the Five Oaks Formation occur above the Knox unconformity. At least two exposure surfaces can be traced along the shelf within the Five Oaks Formation. These surfaces define subsequences 1A, 1B, 1C, and 2B (Steinhauff and Walker, in press; Fig. 3.8). At the shelf-edge, the Five Oaks Formation is overlain by the Lenoir Formation (Fig. 3.9). The Lenoir grades laterally into the Five Oaks to the west (Fig. 3.14). The Lenoir at Red House Branch is a fine-grained limestone with a diverse fauna including large gastropods, cephalopods, trilobites, sponges and algae. Oncoids occur in several horizons in the Lenoir Formation.

**Interpretation.** This lowermost Middle Ordovician sequence is presently being studied by Roberson (in prep.). Roberson concluded that at least two exposure surfaces within Sequence 1 are regionally diachronous and are the result of facies migration. Roberson suggested that the Five Oaks Formation within Sequence 1 represents infilling of the Knox surface with tidal flat deposits during initial Middle Ordovician transgression. He interpreted exposure surfaces in the Five Oaks to represent migration of beach ridges through a tidal flat complex (i.e., Roberson, 1987; Roberson and Foreman 1989; Roberson and Walker, 1990; Roberson, in prep).

Roberson proposes that Sequence 1 sediments filled accommodation space made available by a migrating foreland basin / peripheral bulge combination. As the pair moved toward the craton, transgression and shallow water sedimentation occurred in the forward basin, followed by regression and subaerial exposure as the trailing bulge migrated progressively northwestward (i.e., indicated at the sequence 1C / 2B boundary at on-shelf positions and the 1C / 2A boundary at shelf-edge positions) (Figs. 3.8 and 3.9).

**Correlation.** Subsequence 1A was deposited on the Knox surface within a foreland basin at on-shelf positions. A peripheral bulge occupied shelf-edge positions during this time and Sequence 1A was not deposited at the shelf-edge. As the migrating bulge passed progressively northwestward, Sequence 1B was deposited as tidal flat sediment at the shelf-edge and as very shallow-water sediment on the shelf (deepening event $D_0$). Slightly deeper, shallow-water sedimentation continued on the shelf and at the shelf-edge during deposition of Sequence 1C as indicated by deepening event $D_1$. Surfaces of subaerial exposure at the sequence 2B / 1C boundary at on-shelf positions and the 2A / 1C boundary at shelf-edge positions mark the trailing edge of Roberson's migrating peripheral bulge (Figs. 3.12, 3.13, 3.14).

## Third-Order Sequence 2

**Description.** Third-order Sequence 2 consists of eleven fourth-order subsequences labeled 2A through 2K. Subsequences 2B and 2I occur exclusively on the shelf and

subsequences 2A and 2F occur only at the shelf-edge (Figs. 3.12, 3.13, 3.14). On the shelf, Sequence 2 consists of the uppermost Five Oaks, the Lincolnshire, and the lower Rockdell formations. Sequence 2 contains eight less pronounced exposure surfaces defining nine "fourth-order" subsequences (2B through 2K). Sequence 2 consists primarily of peloidal grainstones, commonly mixed with coated-grains. The uppermost Five Oaks Formation is comprised of mudstones (facies L) and associated peloidal grainstones (facies I). The Lincolnshire Formation consists primarily of peloidal grainstones, commonly containing coated-grains. Thin mud-rich packstone, wackestone, and fenestral mudstone beds (less than 2 meters thick) occur below and along exposure surfaces separating subsequences 2C / 2D, 2D / 2E, and 2E / 2G (Fig. 3.12). The lower Rockdell Formation consists of peloidal grainstones overlain by mudstones and wackestone beds (less than 0.5 meters thick). These mud-rich intervals are up to 10 meters thick and are interbedded with amalgamated grainstone beds (less than 5 meters thick).

At the shelf-edge, Sequence 2 is comprised of the Holston Formation. Subsequences 2A through 2G of the Holston Formation consist of bryozoan bafflestones and packstones within mud-mounds, with lesser amounts of flanking skeletal grainstones (Figs. 3.9 - 3.12). Mud-rich beds are not as well-developed below and along exposure surfaces at the shelf-edge. For example, packstones and wackestones occur below and along the subsequence 1C / 2A and 2C / 2D surfaces at Red House Branch, and along the subsequence 2C / 2D surface at Cuba and Poor Valley Creek (Figs. 3.9, 3.10, 3.11). Wackestones and fenestral mudstones occur

just below the exposure surface separating subsequences 1C and 2A at Red House Branch (e.g., Figs. 3.9 and 3.12).

**Interpretation.** During deposition of Subsequence 2A, the shelf was exposed and sea-level was near the shelf-edge. Shallow-water sedimentation occurred at the shelf-edge, but not on the shelf. As relative sea-level rose, mudstones of Subsequence 2B were deposited on the shelf, but carbonate sedimentation lagged behind at the shelf-edge. As relative sea-level rose well above the shelf-edge, Subsequence 2C grainstones accumulated on the shelf and grainstones and bryozoan bafflestone were deposited at the shelf-edge (c.f., Figs. 3.8 and 3.9). The upper and lower bounding surfaces of Subsequence 2D indicate that relative sea-level twice dropped below the shelf-edge. Subsequence 2D probably represents an interval of time when sea-level was at or near the shelf-edge. A substantially thicker section was deposited at the shelf-edge (about 40 meters) as compared to the shelf (less than 5 meters thick) (e.g., Fig. 3.12). Subsequence 2E is of similar thicknesses on the shelf and at the shelf-edge. However, very shallow water sedimentation characterized by oncoid grainstones and dasycladacean algae grainstones occurred on the shelf while slightly deeper water deposition is indicated by echinoderm grainstones at the shelf-edge. Subsequence 2F occurs at the shelf-edge, but not on the shelf. Subsequence 2F suggests that sea-level dropped below the shelf-edge, and then rose, but did not cover much of the shelf and then dropped below the shelf-edge again (Fig. 3.12).

On the shelf, a displaced deep-water, thin-shelled trilobite fauna occurs within shallow-water deposits of middle Subsequence 2G (Fig. 3.12). These thin-shelled, eyeless trilobites (e.g., *Lonchodomas* sp.) are generally restricted to deep-water environments (Maitland, 1979; Walker et al., 1980). This displaced fauna suggests that the shelf was flooded during the deposition of Subsequence 2G. The boundary between subsequences 2G and 2H marks the approximate transition from the Lincolnshire into the Rockdell Formation at on-shelf positions. This transition indicates a change from homogenous, relatively open-shelf conditions, as suggested by generally mud-free peloid grainstones of the Lincolnshire Formation to a wider spectrum of high-energy tidal environments as indicated by stacked skeletal grainstones and fenestral mudstones beds of the Rockdell Formation (i.e., subsequences 2H, 2I, 2J, and 2K).

During deposition of Subsequences 2H through 2K, the shelf-edge "reef" tract of the Holston Formation prograded basinward (southeastward, Ruppel, 1979). This may have occurred in response to a long term, gradual, fall in relative sea-level. Alternatively, this relationship could have developed because sedimentation at the shelf-edge outpaced production of accommodation space by sea-level rise and / or subsidence. Under those circumstances, sediment would have been exported basinward building the shelf-edge outward toward the basin. Subsidence of the shelf-edge may have kept pace with or out-paced relative sea-level fall during deposition of subsequences 2H through 2J. Intervening surfaces of subaerial exposure, bounding

subsequences 2H through 2J, indicate that relative sea-level fell and periodically outpaced subsidence (Figs. 3.12 and 3.14).

**Correlation.** Absence of Subsequence 2A on the shelf may be due to northwestward passage of the trailing edge of the migrating peripheral bulge discussed for Sequence 1. Similarly, absence of Subsequence 2B at the shelf-edge may reflect drowning with unconformity following passage of the bulge at the shelf-edge. A second drowning unconformity (labeled deepening event $D_3$) is indicated at the shelf-edge within Subsequence 2C and is followed by deepening event $D_4$ (Fig. 3.12). Drowning unconformity $D_3$ at the shelf-edge is correlated with deepening event $D_3$ on the shelf. Deepening $D_4$ at the shelf-edge is correlated with deepening events $D_{4A}$ and $D_{4B}$ on the shelf. Similarly, deepening events $D_5$ through $D_7$ also correlate from the shelf to the shelf-edge (Figs. 3.12, 3.13, 3.14). Five meter thick Subsequence 2F occurs only at the shelf-edge between subsequences 2E and 2G. Deepening event $D_8$ occurs just below the upper Subsequence 2G surface. Because Subsequence 2I occurs on the shelf, but not at the shelf-edge, this surface probably represents a drowning unconformity at the shelf-edge and drowning followed by exposure or shoaling on the shelf.

## Third-Order Sequence 3

**Description.** Third-order Sequence 3 is comprised of four fourth-order subsequences labeled 4A through 4D. All fourth-order subsequences comprising third-order Sequence 3 occur both on-shelf and at the shelf-edge positions ( Figs. 3.12 and 3.14).

On the shelf, Subsequence 3A consists of grainstones and packstones of the uppermost Rockdell Formation. Uppermost Subsequence 3A marks establishment of well-developed Rockdell lithologies (Figs. 3.12 and 3.14). The increase in water-depth near the top of Subsequence 3A coincides with a similar increase at the top of the Holston Formation at the shelf-edge (chapter 2, see also Benedict and Walker, 1978; and Walker et al., 1980). Subsequences 3B, 3C and 3D include nodular-bedded packstones and fenestral mudstones of the Rockdell Formation (e.g, Fig. 3.12). Their lateral equivalents at the shelf-edge are skeletal grainstones of the Rockdell Formation (Ruppel, 1979) (Fig. 3.14). Spar-filled vugs with solution features and smaller cavities floored with crystal or vadose silt are abundant within mud-rich Subsequence 3A and 3C lithologies at Thorn Hill and Old Thorn Hill (Figs. 3.3 and 3.12).

At the shelf-edge, Subsequence 3A consists of grainstones and grainstone-packstones of the uppermost Holston Formation. Subsequence 3A also includes a transitional unit of fine-grained carbonate mud, marking the Holston to Rockdell transition (Fig. 3.12). Subsequence 3A consists of about 10 meters of echinoderm grainstone overlain by about 5 meters of interbedded packstones and wackestones. Subsequences 3C and 3D are both about 5 meters thick with the lower 0.5 to 1 meters consisting of wackestone grading into mudstone (facies L).

**Interpretation.** Important paleoenvironmental changes accompany deposition of Sequence 3. A substantial water-depth increase near the top of Subsequence 3A

coincides with culmination of Holston deposition at the shelf-edge (deepening event $D_9$; Fig. 3.12). Immediately upward, at the shelf-edge, a drop in relative sea-level is indicated by the exposure surface separating subsequences 3A and 3B and by additional exposure criteria within Subsequence 3B (Figs. 3.12, 3.13, 3.14). This may represent a type of drowning unconformity induced by a period of very slow deposition and then followed by exposure. Relative drop in sea-level is also indicated by mudstones of subsequences 3C and 3D.

**Correlation.** Deepening event $D_9$ occurs about 10 meters below the subsequence 3A / 3B boundary at the shelf-edge and less than one meter below this surface on the shelf (e.g., Fig. 3.14). This suggests deepening occurred somewhat earlier at the shelf-edge and somewhat later on the shelf. As deepening progressed, carbonate production was suppressed at the shelf-edge resulting in the unconformity indicated at the subsequence 3A / 3B boundary. By this time, on-shelf environments had prograded basinward to the position of Red House Branch. Thus, only a small drop in relative sea-level was needed for exposure at the subsequence 3A / 3B boundary at both shelf and shelf-edge positions. Similar exposure surfaces are correlative from on-shelf to shelf-edge at sequence boundaries 3B / 3C, 3C / 3D, and 3D / 4A (Figs. 3.12 and 3.14).

## Third-Order Sequence 4

**Description.** Third-order Sequence 4 consists of six fourth-order subsequences labeled 4A through 4F. All six subsequences are observed on the shelf and probably

occupy shelf-edge positions as well although exposures of the upper parts of the succession are poor at the latter localities. On the shelf Sequence 4 is comprised of the Benbolt, Wardell, and lowermost Bowen formations. Subsequences 4A through 4C of the lower Benbolt consist of an array of coated-grain bearing grainstones and packstones characteristic of very shallow-water deposition (Fig. 3.13). Shales, siltstone and skeletal wackestones are particularly abundant in Subsequence 4C. The Wardell Formation includes uppermost Subsequence 4D and subsequences 4E and 4F consisting of bryozoan-echinoderm wackestones and grainstone-packstones. Subsequences 4D and 4F are similar in their content of grainstone and packstone-wackestone beds, but 4D contains no mudstone or shale beds, whereas 4F has well developed mudstone, and shale beds up to several meters thick (Fig. 3.13). Mud-rich beds on the shelf and at the shelf-edge, starting with Sequence 3 and particularly within Sequence 4, are generally red to maroon in color due to iron-manganese oxide within the micritic matrix. Most of Sequence 4 is covered and not observed at the shelf-edge. Indeed, only lowermost Subsequence 4A is exposed at Red House Branch.

**Interpretation.** Shoaling sand banks of the Rockdell gave way to deeper subtidal "lagoonal" deposits of the Benbolt. Lagoonal Benbolt deposits spread eastward over the former shelf-edge (Ruppel, 1979). Sequence 4 marks the beginning of a reversal of paleobathymetry (i.e., Ruppel, 1979). This reversal continued with deeper water shelf deposits of the Wardell Formation, formed in an epeiric sea to the west. These

deeper water deposits of the Wardell prograded over lagoonal deposits of the Benbolt. On the shelf, this progradation occurred earliest at Cedar Springs and slightly later at Thorn Hill (Fig. 3.14).

Fine-grained siliciclastic detritus, derived from the east and southeast, is noted within Sequence 4, and becomes conspicuous starting in the upper Benbolt. It is not clear how this detritus entered lagoonal Benbolt environments. However, this detritus bypassed Rockdell environments at shelf-edge positions. Rockdell environments may have been bypassed by transporting the detritus through the relatively high energy Rockdell environments, or the detritus may have been transported around shelf-edge Rockdell environments through breaches in the shelf-edge north or south of the study area. This sequence apparently marks the first arrival onto this Ordovician shelf of large quantities of terrigenous mud derived from the southeast tectonic land.

**Correlation.** Correlation on the shelf, along depositional strike, is discussed and illustrated in chapter 2 and in Steinhauff and Walker (in press). Because Sequence 4 is mostly covered at the shelf-edge, correlation of fourth-order sequences from the shelf to the shelf-edge is not attempted.

## Third-Order" Sequences 5, 6, and 7

**Description.** Fourth-order subsequences within third-order sequences 5, 6, and 7 were not studied. Sequence 5 includes the uppermost Bowen, Witten and Moccasin formations (Fig. 3.2). Sequence 6 includes the upper Moccasin to the base of the

Martinsburg Formation (not shown). The Martinsburg and Juniata Formations comprise Sequence 7 (Walker, 1985; 1992). Terrigenous siltstone, calcilutites, calcarenites and shales occur in various proportions throughout sequences 5 and 6. The Bowen consists of calcareous siltstone and red calcareous claystone with mudcracks (Wedekind, 1986). The Witten is similar to the underlying Wardell. The Moccasin consists of distinctive gray limestone and red to yellow weathering calcareous shale. Ripple marks and mudcracks occur throughout the Moccasin (Simonson, 1985). The uppermost Moccasin comprises Sequence 6 which consists of peritidal deposits. Thinly laminated graptolitic, black shales of the lower Martinsburg Formation overly the sequence 6 / 7 surface.

**Interpretation.** Sequence 4 marked the beginning of a reversal of paleobathymetry (i.e., Ruppel, 1979). Eventually, the basin to the east was completely filled with tidal-flat deposits of the Bays Formation (not shown in our figures). This tidal-flat deposition prograded westward, transporting terrigenous silt and clay to the west. The result was deposition of the tidal flat complex of the Moccasin Formation with the bathymetric slope reversed in geographic position (Ruppel and Walker, 1982, 1984; Simonson, 1985). The top of the Moccasin coincides with a pronounced deepening event marked by a flooding surface described by Walker (1985; 1992).

**Correlation.** Sequences 5 and 6 are covered at the shelf-edge in our study area. However, lithostratigraphic correlation of sequence 5 and 6 sediments from the shelf

to the shelf-edge, based on study of additional stratigraphic sections, is discussed by Ruppel (1979) and Ruppel and Walker (1982, 1984). We have not investigated sequences 5 and 6 at the same level of detail as the underlying sequences. Correlation on the shelf, across depositional strike, is discussed by Steinhauff and Walker (in press). Evidence for the pronounced exposure surface separating sequence 5 and 6 is documented by Simonson (1985) in his work on the Moccasin Formation at the Thorn Hill section. Simonson noted numerous exposure criteria, especially fenestral mudstones and mudcracks, at the stratigraphic position that we have indicated for this exposure surface (Fig. 3.2). We have observed similar exposure criteria at the Idol Mine and Cedar Springs sections. Additionally, our water-depth curves (not shown) for the Moccasin, are based on a limited number of thin-sections (6 at Cedar springs and about 10 at Old Thorn Hill). Evidence observed in these thin-sections suggests very shallow-water. Finally, we should note here that a seventh third-order sequence overlies those studied here. It consists of the Upper Ordovician Martinsburg and Juniata formations in this area (Walker, 1992), but is not treated in this paper.

## DISCUSSION: EXPOSURE, DROWNING, AND MISSED BEATS

The rates and type of sedimentation, local crustal movements (including subsidence caused by episodic compaction), and eustatic sea-level are the primary controls of facies anatomy on carbonate shelves (i.e., Kendall and Schlager, 1981). Exposure, drowning, and the occurrence or absence of discrete sediment packages,

such as fourth-order sequences or cycles, are interpreted from evidence in the rock record as products of these primary controls. In this study, as in other studies, it is difficult to separate the relative importance of these three primary controls. Nevertheless, the existing stratigraphic framework combined with other lines of evidence has helped narrow the possible controls and avoid undue circular reasoning.

## Exposure

Most of the sequences I have described and illustrated in this chapter, chapter 2, and in Steinhauff and Walker (in press) lack caps containing criteria diagnostic of tidal flat accretion. Rather, subtidal grainstones and mud-rich lithologies appear to have been exposed without significant buildup of tidal flats at both on-shelf and shelf-edge positions. This pattern where subtidal sediments are subject to exposure is similar to that described for the Middle Triassic platform carbonates in Northern Italy by Goldhammer et al. (1987). However, evidence for exposure within these Middle Ordovician carbonates appears to be much more subtle than the evidence described by Goldhammer et al. for their Triassic cyclic carbonates.

## Evidence for Drowning

Abundant evidence for drowning is preserved in subtidal sediments at on-shelf and shelf-edge positions. Evidence for drowning unconformity, on the other hand, by its very nature is more circumstantial. For example, inflection points on water-depth curves that indicate water deepening are based on numerous criteria presented in

chapter 2 and Steinhauff and Walker (in press) (Fig. 3.12). These water deepening events document drowning on the shelf and are correlated with similar inflections or unconformities at the shelf-edge (Figs. 3.12 and 3.14). Fischer plots, substituting sequences for cycles, are constructed for the shelf and shelf-edge. These Fischer plots provide an alternative way in which to show correlation of deepening events (Fig. 3.15). Cephalopod-rich limestone beds overlie deeper-water subtidal limestones along drowning unconformities at the subsequence 1C / 2A boundary and within Subsequence 2C at Red House Branch and Poor Valley Creek (Fig. 3.9). Cephalopod limestone overlying shallow water carbonate is cited by Schlager (1981) as evidence for drowning unconformity within numerous Paleozoic and Mesozoic examples. Indeed, within the Middle Ordovician of East Tennessee, cephalopod-rich beds occur at several localities outside the study area (e.g., Steinhauff and Roberson, 1989; Tobin and Walker, in prep.). Black, iron-manganese oxide-rich sediment occurs within these Middle Ordovician cephalopod-rich beds (Fig. 3.4). For example, iron-manganese oxide-rich sediment associated with a coeval cephalopod-rich limestone at Douglas Lake was analyzed by Johnson (1987) using flame atomic absorption. Johnson found that whole rock samples contained more than 1000 ppm iron and manganese (in some cases up to 8000 ppm of the latter), whereas on-shelf limestones of the Lincolnshire and Rockdell formations averaged about 600 and about 200 ppm iron and manganese, respectively (see also, Chapter 6). The shelf-edge rocks also contain abundant insoluble metal-rich crusts and laminae as well. High metal contents

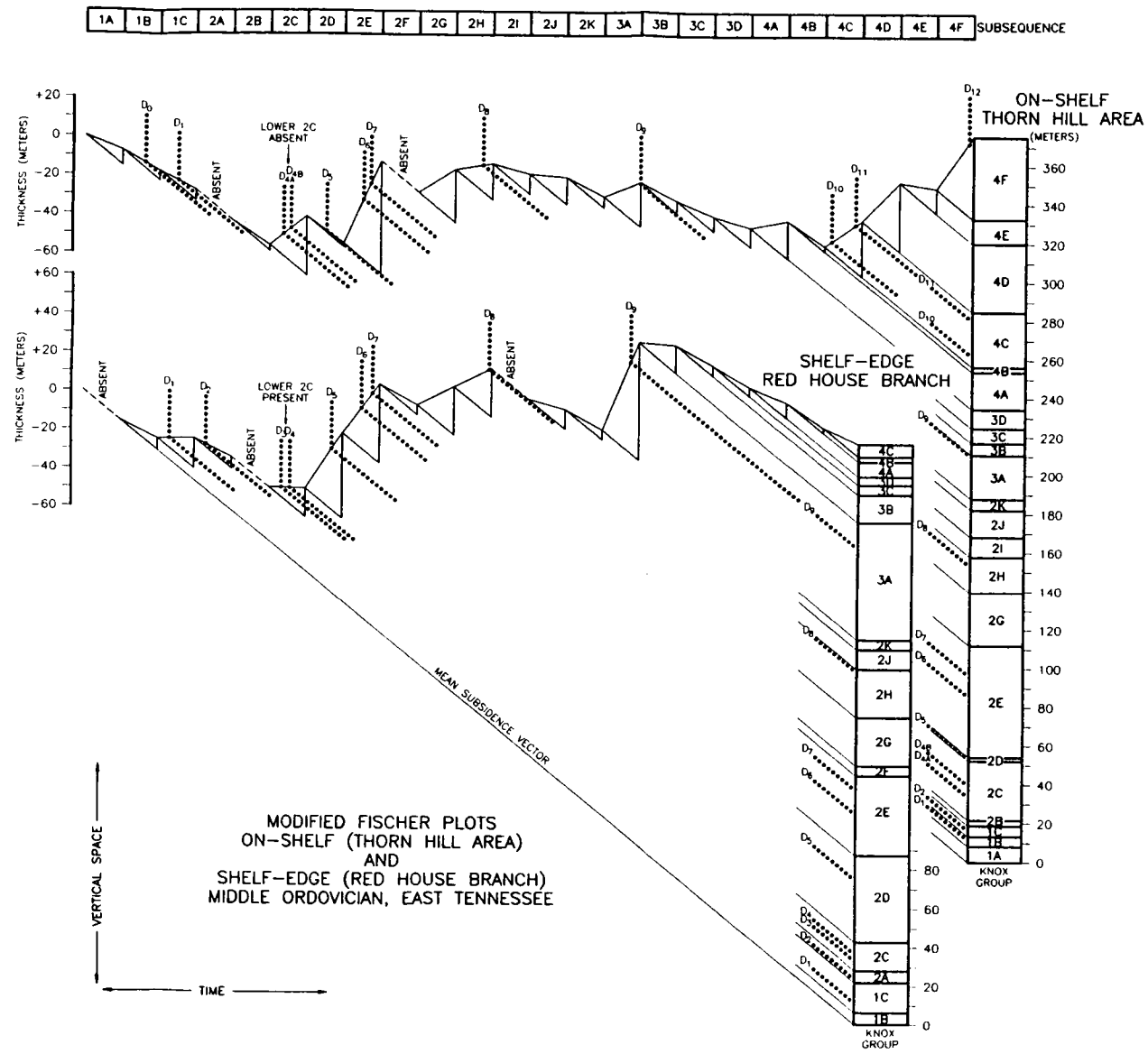



Figure 3.15. Modified Fischer plots comparing fourth-order subsequences from the composite Middle Ordovician on-shelf section for the Thorn Hill Area to the composite shelf-edge or near shelf-edge section for the Red House Branch area. Dotted lines numbered $D_1$ - $D_{12}$ indicate deepening events and are projected from the vertical stratigraphic columns (right), through the plotted sequences, to the horizontal time axis. Note that fifth-order parasequences cannot be correlated across the shelf nor from the shelf to the shelf-edge.

are characteristic of deep-sea sediments and provided additional supporting evidence for deep-water deposition and drowning unconformity (Kennett, 1982).

## Missed Beats

"Missed beats" are missing cycles of sedimentation expected to have been deposited under a Milankovitchian glacio-eustasy mechanism. Hardie et al. (1986) described two possibilities for "missed beats" in the Triassic platform carbonates of Italy. In the first, sea-level stays below the platform margin even though sea-level is oscillating. In the second, tectonic uplift exposes the platform until subsidence allows submergence and reestablishment of cyclic sedimentation. In addition, we propose drowning as third possible mechanism that may cause beats to be missed or overlooked. Indeed, beats may be missed twice during drowning. First, sediment production will lag behind initial drowning, until the "carbonate factory" can produce enough sediment to be transported on shore to build tidal flats (e.g., Hardie and Shinn, 1986). Second, sediment production will again slow down if drowning continues and the carbonate factory passes into deeper water low in the photic or into the euphotic zone (e.g., Schlager, 1981).

Fischer plots, substituting fourth-order subsequences for cycles, are constructed to show that some "beats" or subsequences are absent at on-shelf or shelf-edge positions (Fig. 3.15). For example, Subsequence 2F occurs at the shelf-edge, but not on the shelf. Subsequence 2F suggests that sea-level dropped below the shelf-edge, and then rose, but did not cover much of the shelf and then dropped below the

shelf-edge again (Figs. 3.12, 3.13, 3.14, 3.15). This situation is analogous to Hardie et al.'s (1986) first possibility for "missed beats" where sea-level stays below the platform margin even though sea-level is oscillating.

The second type of "missed beat" is illustrated by the absence of Subsequence 2A on the shelf. For this type of "missed beat," Hardie et al. (1986) proposed that tectonic uplift exposes the platform until subsidence allows submergence and reestablishment of cyclic sedimentation. For example Subsequence 2A is absent on the shelf and Subsequence 2B is absent at the shelf-edge. Absence of Subsequence 2A on the shelf may be due to northwestward passage of the trailing edge of the migrating peripheral bulge previously discussed for Sequence 1. Absence of Subsequence 2B at the shelf-edge may reflect drowning with unconformity following passage of the bulge at the shelf-edge.

At least two other sequences are absent as a result of drowning. For example, a drowning unconformity (labeled deepening event $D_3$) is indicated at the shelf-edge within Subsequence 2C. The lower portion of Subsequence 2C is missing at on-shelf positions (Fig. 3.12). In our analysis emphasizing exposure, the lower portion of Subsequence 2C is not separated from the rest of Subsequence 2C because it is bounded above and below by drowning unconformities rather than surfaces of subaerial exposure or shoaling.[1] Drowning unconformity $D_3$ is the upper surface of the lower portion of Subsequence 2C at the shelf-edge. Drowning unconformity $D_3$ is

[1] In a more traditional approach (i.e., seismic stratigraphy) this surface within Subsequence 2C, bounded above and below by drowning unconformities, would be recognized as a "sequence boundary."

plotted within the middle part of fourth order Subsequence 2C in Figure 3.15. Because the lower portion of subsequence 2C does not occur on the shelf, deepening event $D_3$ is shown to occur at the upper surface of Subsequence 2B on the shelf (Figs. 3.12 and 3.15). Similarly, Subsequence 2H occurs on the shelf, but not at the shelf-edge (Figs. 3.12, 3.13, 3.14). Subsequence 2I probably represents a drowning unconformity at the shelf-edge and drowning followed by exposure or shoaling on the shelf.

## CONCLUSIONS

1) Stratigraphic sequences, subsequences and parasequences represent shallowing-upward packages similar to cycles. However, these sequences, subsequences, and parasequences differ from many cycles in that they do not contain tidal caps and evidence for exposure and shoaling is subtle and generally revealed only through detailed microscopic examination.

2) These apparently non-cyclic carbonates have fourth-order subsequences that are grouped into third-order sequences based on the occurrence of pronounced and less pronounced exposure surfaces. When Fischer plots, substituting sequences for cycles, are constructed, it becomes apparent the subsequences may be grouped into "waves" consisting of five parts. Schwarzacher (1975) suggested existence in the geologic record of "composite cycles" consisting of five cycles superimposed to make a five part megacycle. Goldhammer et al. (1987) used time series analysis to confirm this grouping of five cycles for Middle Triassic platform carbonates of Northern Italy and suggested a Milankovitchian glacio-eustasy mechanism. Although

the data set is small and has not been tested it statistically, speculatively, it appears that similar groupings of 4 and 5 part sequences or "cycles" are present (Fig. 3.15). Within these asymmetric groupings, the basal sequence or "cycle" appears to be the thickest.

3) Detailed stratigraphic sequence analysis of shelf and shelf-edge carbonates combined with biostratigraphic data and water-depth analysis allows correlation of third-order sequences from the shelf to the shelf-edge. Such correlation reveals that some fourth-order subsequences or "beats" are missed at on-shelf or shelf-edge positions. This analysis is possible because conclusions regarding "missed beats" are made through comparison of shelf and shelf-edge successions. If one of these successions had not been studied (shelf or shelf-edge), conclusions regarding a "missed beat" would not be possible. Thus, a serious limitation of this type of analysis is that there may be still other beats that are missed at both on-shelf and shelf-edge positions. Without further temporal or biostratigraphic control, or statistical analysis, we are not able to account for such additional missed beats.

4) Meter-scale (5th-order) parasequences in this succession are seldom correlative between localities and probably do not represent widespread sea-level change. Instead, these appear to represent environmental migration and, thus, are probably of autocyclic origin.

# CHAPTER 4

## COMPARATIVE DIAGENESIS OF MIDDLE ORDOVICIAN LIMESTONES, THE COPPER CREEK ALLOCHTHON, EAST TENNESSEE


### ABSTRACT

Relative timing of different paragenetic phases at shelf-edge and on-shelf positions is compared within a nearly 400 meter thick succession of Middle Ordovician strata. Cross-cutting and competitive growth relationships observed in polished slabs and in thin-sections using conventional and cathodoluminescent petrography provide the basis for deciphering the relative timing of different phases and interpreting their diagenetic origin. Analyses of individual phases for stable isotopes of carbon and oxygen, radiogenic strontium, and trace elements provide supporting evidence.

Diagenetic pathways for sediments on the shelf were different than those for sediments at the shelf-edge. Intervals that retained porosity the longest occur below third- and fourth-order sequence surfaces at on-shelf and shelf-edge positions (Steinhauff and Walker, in press). Vugs and cavities were developed below many of these sequence boundaries during subaerial exposure. Early diagenetic phases filling these cavities represent phases precipitated during a "second-cycle" or (?) "third-cycle" of early diagenesis. Fibrous calcite ($\delta^{18}O$ = -6.0 to -4.1‰, PDB; N=89) is interpreted as marine. Bladed and clear blocky calcite are more depleted in $\delta^{18}O$ than

-6.0‰ PDB and are interpreted as meteoric. Bladed and blocky clear calcite do not show the large $\delta^{13}C$ depletions reported in meteoric phases of younger rocks. Lack of $\delta^{13}C$ depletion may be related to absence of land plants which might have provided $^{12}C$ to the groundwater.

Intermediate through late burial phases at the shelf-edge have more depleted $\delta^{18}O$ values, higher Fe and Mn contents, and are more enriched in $^{87}Sr$ than their counterparts on the shelf. If the source of fluids precipitating late burial phases was the Sevier basin to the southeast, then fluids at the shelf-edge would have encountered less carbonate rock than fluids traveling to on-shelf positions. Their Sr signature is, then, a function of their interaction with basinal siliciclastic sediments which provide more radiogenic strontium.

Analysis of temperatures assumed from burial curves, an assumed range of likely brine compositions, and known $\delta^{18}O$ values for late ferroan sparry calcite and ferroan baroque dolomite suggests that the Sevier basin is the most likely source of burial fluid that precipitated late burial phases. This analysis further suggests that burial fluids could have been generated in the Sevier basin before the end of the Middle Ordovician (ca. 450 Ma).

## INTRODUCTION

Changes in relative sea-level influence sediment type, geometry, and diagenesis of carbonate shelves and platforms. Although a wedge of carbonate sediment may be deposited from the shelf to the shelf-edge during a single rise in

relative sea-level, sediments on the shelf pass through rather different diagenetic pathways than do their coeval counterparts at the shelf-edge. The pathway ultimately followed by each is dependent on a chain of events, starting early in the diagenetic history and in many cases continuing through one or more later burial events. This chain of events largely determines the type of pore filling and whether or not porosity is retained.

Middle Ordovician carbonates of East Tennessee probably contain a record of diagenesis at least as complete as that of any Paleozoic succession and certainly much more complete than most successions of the later Paleozoic. Diagenetic products, such as marine cement, commonly fill the first available pore space. During geologic intervals such as the Middle Ordovician, calcite rather than aragonite was the favored phase precipitated in marine environments (Sandburg, 1983; Walker et al., 1990). These calcite phases occupy early pore positions and typically occlude all available pore space. In the present study, much of the pore space that these early marine phases fill was developed as a result of subaerial exposure. Furthermore, these calcite phases are relatively stable and are not readily dissolved during subsequent changes in pore fluid composition. In contrast, aragonite phases are easily dissolved. Thus, once marine calcite was precipitated in a pore, a chain of events was initiated generally resulting in a relatively simple filling of the remaining pore space with phases precipitated from freshwater and burial fluids (e.g., Walker, 1989). This chain of events were halted when the pore was completely occluded. At some stratigraphic positions, pores were completely occluded with fibrous calcite early in

the diagenetic history. In other cases, pores are successively filled with almost the entire suite of paragenetic phases, yet still retain a minor amount of porosity.

## Objectives

This study elucidates and compares the relative timing of different paragenetic phases at shelf-edge and on-shelf positions. Cross-cutting and competitive growth relationships observed in polished slabs and in thin-sections using conventional and cathodoluminescent petrography provide the basis for deciphering the relative timing of different phases and interpreting their diagenetic origin. Analysis of individual phases for stable isotopes of carbon and oxygen, $^{87}Sr/^{86}Sr$ ratios, and trace elements provides supporting evidence for interpreting the environment of origin of diagenetic phases.

This analysis of stable isotope and trace element patterns of individual phases is the most extensive ever completed for the Middle Ordovician in East Tennessee. Valuable petrographic observations made by previous workers have helped to focus geochemical sampling (i.e., Ruppel, 1979; Ruppel and Walker, 1982, 1984; Jernigan, 1987; and Johnson, 1988). This study differs from other studies using similar techniques on younger rocks because it is based on a stratigraphic succession where depositional environments, changes in water-depths, and the sequence stratigraphy are well documented both on the shelf and at the shelf-edge (chapters 2 and 3; Steinhauff and Walker, in press; in prep. a). Detailed knowledge of changes in water-depths and of the sequence stratigraphy provides the basis for understanding many complex

factors related to early diagenesis. For example, the $\delta^{13}C$ depletion trend in meteoric carbonates that other workers (e.g., Gross, 1964; Meyers and Lohmann, 1985) have documented in younger rocks is one such factor related to early diagenesis. This succession apparently lacks this trend, possibly because of the absence of land plants. The sequence stratigraphic framework also provides a context in which to compare diagenesis on the shelf with that at the shelf-edge. Such shelf to shelf-edge comparisons are particularly insightful for interpreting the possible timing and origin of late burial phases.

## Study Area

The study area consists of four on-shelf localities and three shelf-edge or near shelf-edge localities (Fig. 4.1). A regional environmental / stratigraphic framework, based on these and other sections, was developed by Walker (1977, 1980, 1985), Ruppel (1979), and Ruppel and Walker (1982, 1984). The four on-shelf localities are exposed along the northwest limb of the Copper Creek allochthon and are documented in chapter 2, and Steinhauff and Walker (in press). A more than 540 meter thick succession of Middle Ordovician (Llanvirian to Carodocian) strata ranging from the unconformity at the top of the Knox Group through the Five Oaks, Lincolnshire, Rockdell, Benbolt, Wardell, Witten and Moccasin formations is exposed. From southwest to northeast these localities include the Thorn Hill (TH), Old Thorn Hill (OTH), Idol Mine (IS), and Cedar Springs (CS) sections. Each section is separated from the other by approximately 2 km (Fig. 4.1). Strata at the three shelf-edge localities are overturned and exposed on the southeast limb of the

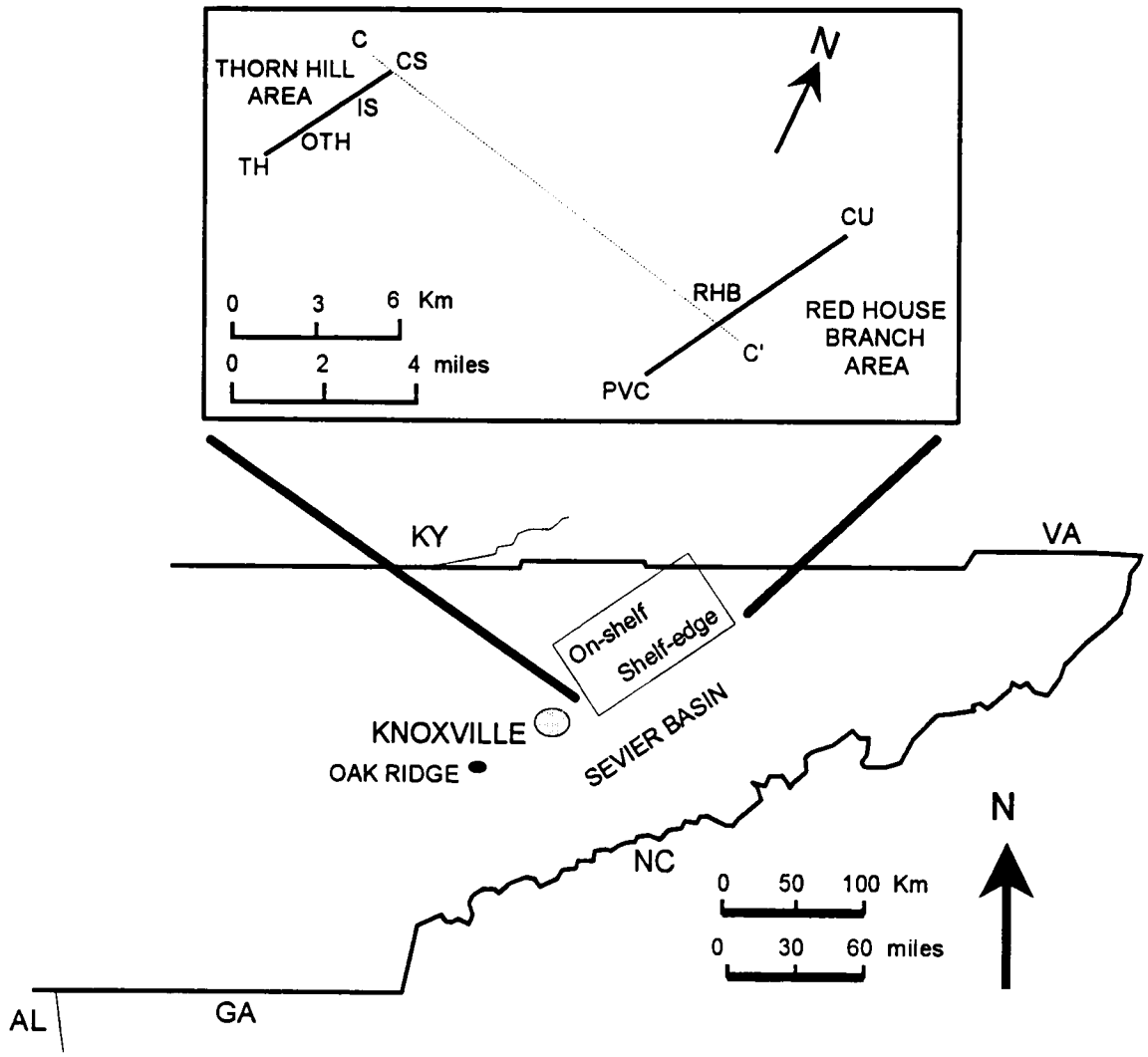
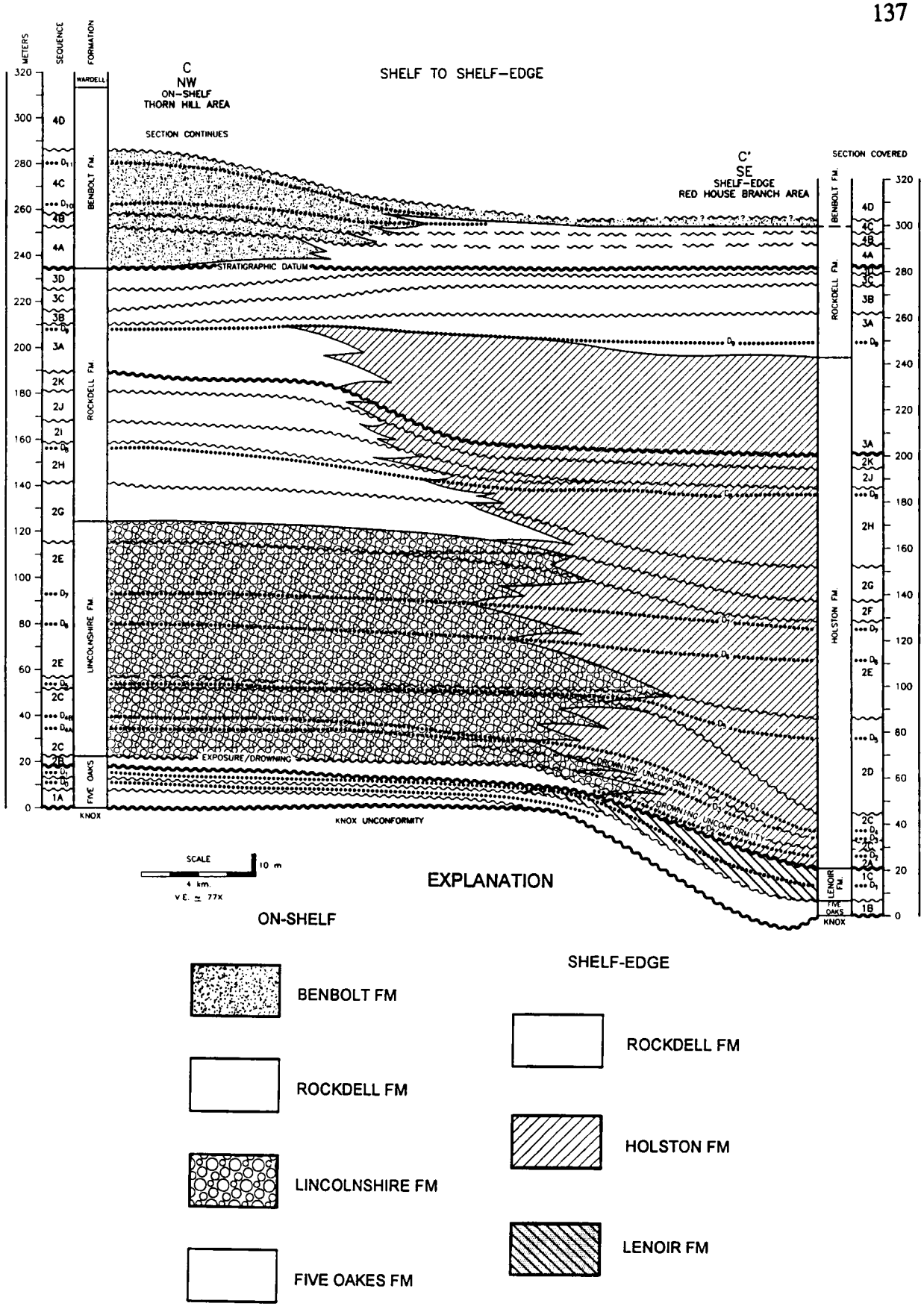



Figure 4.1 Location Map for East Tennessee. Inset (top) shows the location of on-shelf, along strike sections at the Thorn Hill section (TH), Old Thorn Hill Section (OTH), Idol Mine section (IS), and the Cedars Springs section (CS) and shelf-edge, along strike sections at Poor Valley Creek (PVC), Red House Branch (RHB), and Cuba (CU). Line of section C-C' is for the cross-section of Figure 4.2.

Figure 4.2 Fourth-order stratigraphic subsequences A-4D. Ornamentation shows inferred distribution of different formations. The Five Oaks Formation is shown by the white area (bottom) and on the shelf (left) is unconformably overlain by the Lincolnshire Formation indicated by circles (middle), followed by the Rockdell Formation in white (middle), and finally the Benbolt Formation shown by stipple (top). At the shelf-edge (right) the Five Oaks is followed by the Lenoir Formation shown by diagonal lines and the Holston Formation indicated by opposite diagonal lines (middle). Formation contacts are based on composite columnar sections (see Fig. 3.12). Dotted lines labeled as $D_1$ , $D_2$ , etc., represent deepening events. Cross-section is restored across depositional strike. See Figure 4.1 for location of line of section C-C'.


METERS
SEQUENCE
FORMATION
C
NW
ON-SHELF
THORN HILL AREA
SHELF TO SHELF-EDGE
SECTION CONTINUES
C'
SE
SHELF-EDGE
RED HOUSE BRANCH AREA
SECTION COVERED
WARDELL
BENBOLT FM.
ROCKDELL FM.
LINCOLNSHIRE FM.
FIVE OAKS
KNOX
HOLSTON FM.
LENOIR FM.
STRATIGRAPHIC DATUM
EXPOSURE/DROWNING
KNOX UNCONFORMITY
SCALE
10 m
4 km.
V.E. ≃ 77x
EXPLANATION
ON-SHELF
BENBOLT FM
ROCKDELL FM
LINCOLNSHIRE FM
FIVE OAKS FM
SHELF-EDGE
ROCKDELL FM
HOLSTON FM
LENOIR FM

Copper Creek allochthon. An approximately 300 meter thick succession of Middle Ordovician strata ranging from the Knox unconformity through the Five Oaks, Lenoir, Holston and Rockdell formations is exposed. From southwest to northeast, these localities include the Poor Valley Creek (PVC), Red House Branch (RHB), and Cuba (CU) sections (Fig. 4.1). Shelf to shelf-edge sequence stratigraphy is discussed in chapter 3, and in Steinhauff and Walker (in prep. a) and is summarized in Figure 4.2. The regional burial history is summarized in Figure 4.3.

## Previous Work

Biostratigraphic investigations by Bergstrom (1971, 1973, 1977), Bergstrom and Carnes 1976) and Anita Harris (personal communication to Keith Roberson, 1990) and lithologic correlations by Ruppel (1979) and Ruppel and Walker (1982, 1984) provide the framework for more detailed sequence stratigraphic correlations. Water-depth of deposition was established in chapters 2 and 3, and in Steinhauff and Walker (in press, in prep. a) using multiple lines of evidence to determine a range of possible water-depths (e.g., Elias , 1937; Benedict and Walker, 1978). In chapters 2 and 3 inflection points in water-depth curves were used to indicate stratigraphic intervals that also contain subtle indicators of subaerial exposure. Such indicators help deduce changes in water-depth after initial deposition. These subaerial exposure indicators include erosional truncation, mudcracks, crystal or vadose silt, calcite filled solution vugs and pendant cements observed under cathodoluminescence (Fig. 4.4). Analysis of these features has lead to a sequence stratigraphic framework in which the

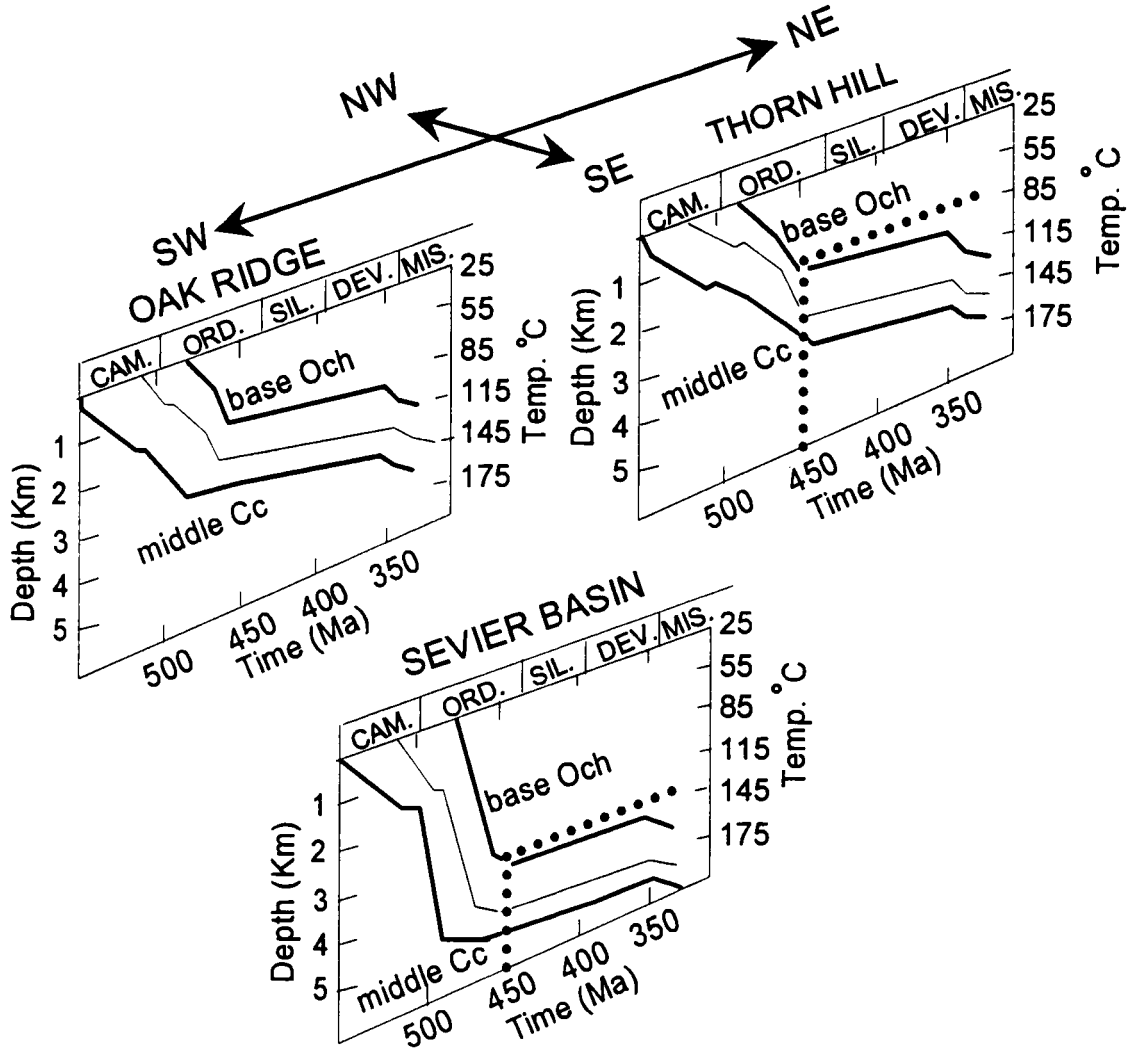



Figure 4.3 Perspective view of three burial curves for central East Tennessee. Curves for Oak Ridge and Thorn Hill are west of the Saltville fault; the curve for the Sevier basin is east of the Saltville fault. The lowermost stratigraphic datum (middle Cc) is the Middle Cambrian Conasauga Group (top of the Maryville Formation), the middle datum is the top of the Knox Group, and the uppermost datum (base Och) is the base of the Middle Ordovician Chickamauga Group (Knox unconformity). Dotted lines show that by the end of the Middle Ordovician (ca. 450 Ma) burial temperatures in the Sevier basin were probably in excess of 130°C, whereas burial temperatures at Thorn Hill were probably about 60°C. Curves modified from Walker et al. (1992) based on additional information supplied by K. Srinivasan.

Figure 4.4 Photomicrographs of diagenetic features. **A.** Fibrous calcite (f) ($\delta^{13}C$ = 0.8‰, $\delta^{18}O$ = -5.1‰ PDB, N = 6) grew along bottom of cavity followed by bladed calcite (not shown) ($\delta^{13}C$ = -0.3‰ PDB, $\delta^{18}O$ = -6.5‰ PDB, N = 5). Two generations of crystal or vadose silt (v) and ferroan blocky white calcite (c) ($\delta^{18}O$ = -7.3‰ PDB, $\delta^{13}C$ = 0.7‰ PDB, N = 1) occupy intermediate pore-filling positions followed by more ferroan blocky white calcite (c) and later coarse sparry calcite (extreme left margin of photo) , 20.6 m above Knox, Poor Valley Creek section; plane polarized light (PPL), scale bar = 1 mm. **B.** Cavity under cathodoluminescence (CL) filled with luminescent fibrous calcite (f) ($\delta^{18}O$ = -4.9‰ PDB, $\delta^{13}C$ = 0.7‰ PDB, N = 2) followed by non-luminescent, clear blocky to bladed calcite (b), and dully luminescent, clear blocky calcite (c) ($\delta^{18}O$ = -6.6‰, $\delta^{13}C$ = 0.7‰ PDB, N = 1). Some of the blocky to bladed cements have pendant like shapes, 24.6 m above Knox, Poor Valley Creek section; PPL, scale bar = 1 mm. **C.** Cavity observed under CL filled with non-luminescent, fibrous calcite (f) ($\delta^{18}O$ = -5.2‰ PDB, $\delta^{13}C$ = 0.8‰ PDB, N = 10), followed by brightly luminescent, blocky to bladed calcite (b) ($\delta^{18}O$ = -6.4‰ PDB, $\delta^{13}C$ = 0.2‰ PDB, N = 2), and moderate to dully luminescent, ferroan, coarse pink sparry calcite (c) ($\delta^{18}O$ = -11‰ PDB, $\delta^{13}C$ = 0.8‰ PDB, N = 1), 26.6 m above Knox, Poor Valley Creek section; scale bar = 1 mm. **D.** Same field as C, PPL, scale bar = 1mm. **E.** Cavity observed under CL filled with non-luminescent, fibrous calcite (f); followed by brightly luminescent, blocky to bladed calcite (b); and dully luminescent coarse blocky spar (c), same stratigraphic position as A. **F.** Cavity in E, PPL. **G.** Cavity observed under CL filled with very dully luminescent, fibrous calcite (f) ($\delta^{18}O$ = -4.7‰ PDB, $\delta^{13}C$ = 0.9‰ PDB, N = 3); followed by non-luminescent, transitional zone (t); moderately luminescent, bladed calcite (b); dully luminescent, coarse sparry calcite (c-d); and non-luminescent, coarse sparry calcite (c-n) ($\delta^{18}O$ = -8.2‰ PDB, $\delta^{13}C$ = 0.5‰ PDB, N = 2), 184.9 m above Knox, Thorn Hill section; scale bar = 1 mm. **H.** Matching polished slab for thin-section in F. Fibrous calcite (arrowed) was drilled for stable carbon and oxygen isotopes. Coarse sparry calcite (c) fills remainder of vug. Host lithology is mudstone, scale bar = 1 cm.

c
v
c
v
f
A
c
b
f
B
f
b
c
C
f
b
c
D
f
c
b
E
f
c
b
F
f
t
b
c-d
c-n
G
w
f
f
c
H

Middle Ordovician platform interior carbonate succession is correlated to the shelf-edge (chapter 3; Steinhauff and Walker, in prep. a).

## METHODS

### Thin-Sections and Slabs

A suite of 1041, 45 X 75 mm thin-sections from 784 stratigraphic intervals were used (chapters 2 and 3; Steinhauff and Walker, in press, in prep. a) to look for the presence or absence of selected Middle Ordovician water-depth criteria (appendices A, B, and C). About 700 of these thin-sections were prepared by Steinhauff using a Microtech automated thin-section machine which removes about 1 mm of material between the thin-section and the rock chip or billet. Approximately one-half of each thin-section was stained with a combined stain of potassium ferricyanide and alizarin red-S after Dickson (1965) to help identify dolomite and phases containing ferrous iron. Additionally, polished slabs from more than 325 of these stratigraphic intervals were prepared to look for criteria such as burrows, flat algal laminae, and different categories of fenestrae. These features can be difficult to discern in the field and commonly occur at a scale inappropriate for thin-section observation. Serial sections, generally two or more, were prepared for each stratigraphic interval examined. These slabs ranged in size from about 50 X 100 mm to 200 X 250 mm. These thin-sections and slabs provide the basis for observations regarding diagenetic fabrics and relative timing of different cement phases, such as those made under cathodoluminescence. Thin-sections prepared using the Microtech,

along with their corresponding billets, provide the sample materials for additional isotopic and trace elemental work.

## Cathodoluminescence

All thin-sections containing abundant calcite cements (about 300) were examined under cathodoluminescence using a Nuclide Luminoscope with a 12-14 Kv beam current at 50 $\mu$A in a helium atmosphere. Cathodoluminescence allows for observation of stratigraphic and cross-cutting relationships not otherwise observable with conventional petrography. In the present study cathodoluminescence was also used to help screen samples to ensure that only a single phase was sampled for stable carbon and oxygen isotopes and trace elements.

## Stable Isotopes of Carbon and Oxygen

**Sample Preparation.** Samples (258 samples) were drilled with a microscope-mounted microdrill from matching billets cut from these thin-sections. Drill bits consisted of a 2 mm diameter steel shank filed to a triangular point with a working diameter of about 0.2 mm. Various carbonate cement phases were milled from the billets to a depth of about 0.5 mm or less.

**Sample Extraction.** Three sample extraction techniques were used; each was selected to optimize reproduceability of different sample sizes or to separate different phases. The first technique was performed "on-line" using a common acid bath. The common acid bath extraction method was used to achieve reproducible results (less

than 0.2‰ for both carbon and oxygen) with relatively small samples in the 0.2 to 0.6 mg range. The other two techniques were performed "off line" using side-arm reaction vessels with similar or slightly better precision with samples ranging from about 0.5 to 2 mg. Selective acid extraction was used to separate $CO_2$ evolved from dolomite in samples mixed with calcite following the recommendations of Al-Aasm, et al. (1990). All samples were roasted for one hour at 375°C prior to extraction to remove any trace of organic carbon. Samples run using the common acid bath extraction method were reacted at 55°C, and unknowns and standards were later corrected for fractionization at 25°C. Unknowns and standards run using the other two techniques were individually reacted in evacuated vessels kept at 25°C.

**Instrumentation and Standards.** All stable carbon and oxygen isotope analyses were run on a VG model 903 MM gas-source stable isotopic ratio analyzer at the University of Tennessee (Appendix C). Carbon and oxygen isotope compositions were determined from $CO_2$ produced by reaction of powdered samples with 100% anhydrous phosphoric acid following McCrea (1950). All $\delta$ values are reported with respect to the PDB standard. Precision of analyses was monitored using National Bureau of Standards NBS-20 and Penn State Standard HO-CC with the common acid bath extraction method, and are precise to better than 0.2‰ for both carbon and oxygen, with the exception of 28 samples which are precise to 0.3‰ or better for both carbon and oxygen. The 28 samples which are precise 0.3‰ are considered qualified data and include 26 fibrous calcite samples, one bladed calcite sample, and

one blocky clear calcite sample. These qualified data are included because they fall within previously established fields using data that are precise to better than 0.2‰. Precision of analyses was monitored with an in-house calcite standard using standard side-arm extraction methods and was maintained to better than 0.2‰ for both carbon and oxygen (Appendix D).

## Electron Microprobe Analysis

**Sample Preparation.** Thin-sections prepared for microprobe analysis were selected from samples with corresponding billets that had previously been analyzed for stable carbon and oxygen isotopes. A glass cutter was used to select areas from existing 45 X 75 mm thin-sections and these were polished to 1 micron using a diamond wheel polisher. Thus, it is possible to match many of the phases probed for trace elements with existing isotopic data. More than 1,020 points were probed.

**Instrumentation and Operating Conditions.** Wavelength dispersive trace element analyses were performed for Mg, Mn, Fe, and Sr using a Cameca model SX-50 automated electron microprobe (Appendix E). Carbonate standards provided by the Smithsonian Institution were used to monitor precision at the beginning and end of each run. The relative proportions of these four trace elements was calculated by normalizing to 100% CaO. The following operating conditions were selected for calcite to minimize sample volatilization: 30 second count time, 15 $\mu$m beam diameter (for calcite), 10$\mu$A beam current, and 15 KeV accelerating voltage. A focused 10 $\mu$m

beam diameter was used for dolomite analysis and other operating conditions were the same as that used for calcite. Detection limits at 99% confidence are about 410 ppm for Mg, Mn, and Fe, and about 600 ppm for Sr. Analytical uncertainty, based on Poisson counting statistics, was determined to be ± 10% relative, for Mg, Fe, and Mn. All analyses showed magnesium above detection limits. Strontium was detected in less than 1% of the total analyses. About 50 analyses were rejected. These had total weight percents less than 98.5% or greater than 101.5%.

## $^{87}Sr/^{86}Sr$ Analysis

Eighteen samples were drilled from areas of billets that had previously been sampled for stable isotopes of carbon and oxygen. These samples were dissolved in nitric acid, and strontium was separated from other elements by means of ion exchange columns or by precipitation from nitric acid. Isotope ratios were measured by comparison with several standards, including standard $SrCO_3$ (NBS SRM 987) for which a ratio of 0.71014 is assumed. Measurements were performed at the University of North Carolina on a VG Sector 54 thermal ionization mass spectrometer using an internal ratio of $^{86}Sr/^{88}Sr = 0.1194$ to correct for mass fractionation and normalization to the SRM 987 Sr carbonate standard. Precision, expressed as a ratio, is estimated to be ± 0.00006 at the 95% confidence interval (Appendix F).

## DESCRIPTION OF DIAGENETIC PHASES

### Early Diagenetic, Non-Ferroan Phases

**Microcrystalline Calcite Cement.** Microcrystalline calcite cement is present in small amounts within cavities and voids, both on the shelf and at the shelf-edge. Microcrystalline calcite cement is distinguished from micrite and crystal or vadose silt by the absence of fossil material and by antigravitational fabrics (Steinhauff, 1989).

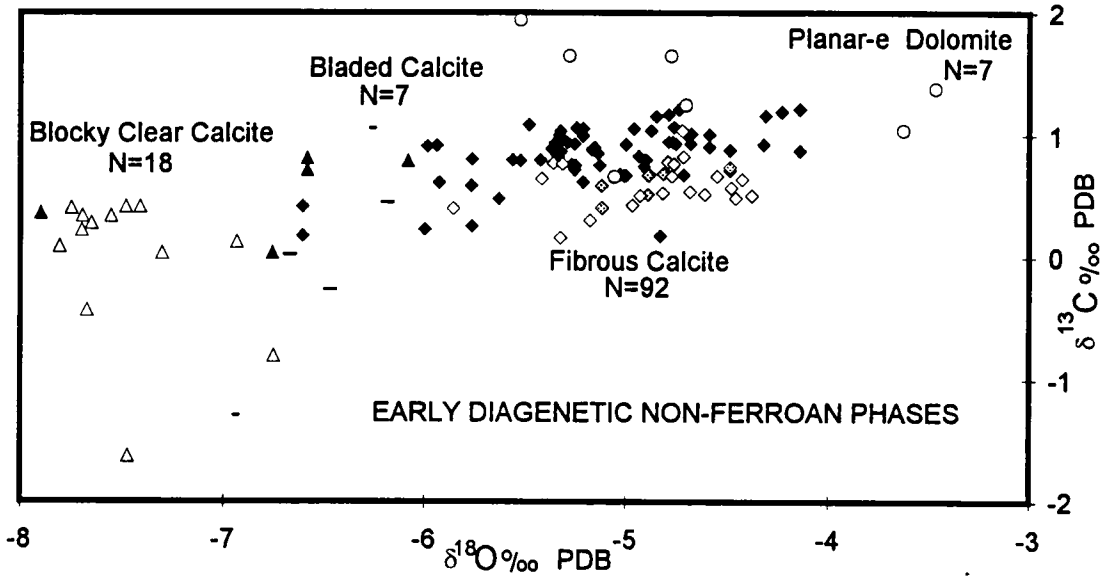
**Black, Fe/Mn Oxide-Rich Sediment, Laminae and Pavements.** Black Fe/Mn oxide-rich sediment occurs as laminae and thin (up to about 5 cm thick) pavements at the shelf-edge. Soluble sediment associated with similar Middle Ordovician pavements contains more than 3 wt % iron and almost 0.2 wt % manganese. This black sediment is cross-cut by cavities filled with fibrous calcite suggesting that at least some fibrous calcite is later than the black sediment (chapter 3; Steinhauff and Walker, in prep. a).

**Fibrous Calcite.** Abundant fibrous calcite occurs at the shelf-edge and lesser amounts occur on the shelf. Much of this fibrous calcite occurs in cavities and vugs stratigraphically below third- and fourth-order sequence boundaries (Fig. 4.3). Fibrous calcite that occurs on the shelf, is present almost exclusively as linings in cavities and vugs developed during earlier subaerial exposure (Steinhauff and Walker, in press, in prep. a).

Almost all fibrous calcite is radiaxial, but fasicular-optic fibrous calcite is also present (Jernigan , 1987). At the shelf-edge some radiaxial-fibrous subcrystals are up to 5 centimeters long, and many show alternating zones. Some zones or bands are turbid with inclusions (e.g., Steinhauff, 1989). Still other zones, observed under cathodoluminescence, are non-luminescent and alternate with dully luminescent zones (Fig.4.4G). Some shelf-edge fibrous calcite, such as that which occurs at Poor Valley Creek, are truncated by very thin (less 0.05 mm thick) reddish crusts followed by a second generation of fibrous calcite. In contrast, radiaxial-fibrous calcite subcrystals that fill cavities on the shelf are rarely more than 0.5 cm long.

The $\delta^{18}O$ of fibrous calcite falls between -6.0‰ to about -4.1‰ PDB. That which is more depleted than -6.0‰ occurs adjacent to later phases and has probably been altered (Fig. 4.5, Tables 4.1 and 4.2). Shelf-edge fibrous calcite exhibits a wider range of magnesium, manganese, and iron concentrations than does on-shelf fibrous calcite (Fig. 4.6, Tables 4.1 and 4.2). Iron concentrations for both shelf-edge and on-shelf calcite are generally less than about 0.04 wt %. However, maximum iron concentrations at the shelf-edge are almost 0.4 wt %, whereas on the shelf maximum values are below 0.1 wt %. Strontium values at both on-shelf and shelf-edge positions are below microprobe detection limits (less than 0.06 wt %). However, Jernigan (1987) and Johnson (1988) reported a mean strontium concentration of 239 ppm based on atomic absorption analysis. Ratios of $^{87}Sr/^{86}Sr$ fall close to the Middle Ordovician marine carbonate value suggested by Burke et al. (1982) (Fig. 4.7).

Figure 4.5 $\delta^{18}O$ versus $\delta^{13}C$ for early diagenetic non-ferroan phases. Shelf-edge and on-shelf fibrous calcite are isotopically similar in $\delta^{18}O$ but differ in $\delta^{13}C$. Because of stratigraphic relationships described in chapter 3, fibrous calcite at Red House Branch that occurs stratigraphically high in the section (above Sequence 2) is considered "on-shelf" fibrous calcite. By the time Sequence 3 was completely deposited, platform interior sediments had prograded to the shelf-edge. Thus, Sequence 3 at the former shelf-edge was depositionally similar to the on-shelf succession. The mean $\delta^{18}O$ for shelf-edge calcite is -5.1 $\pm$ 0.5‰ PDB, (N = 60), the mean for on-shelf fibrous calcite is -4.9 $\pm$ 0.4‰ PDB, (N = 21), and the mean for shelf-edge fibrous calcite stratigraphically equivalent to on-shelf fibrous calcite is -4.9 $\pm$ 0.2‰ PDB. In contrast, the mean $\delta^{13}C$ for shelf-edge calcite is 0.9 $\pm$ 0.2‰ PDB, (N = 60), the mean for on-shelf fibrous calcite is 0.6 $\pm$ 0.2‰ PDB, (N = 21), and the mean for shelf-edge fibrous calcite stratigraphically equivalent to on-shelf fibrous calcite is 0.7 $\pm$ 0.4‰ PDB.




- SHELF-EDGE BLADED CALCITE
- ON-SHELF BLADED CALCITE
- ▲ SHELF-EDGE BLOCKY CLEAR CALCITE
- △ ON-SHELF BLOCKY CLEAR CALCITE
- ◆ SHELF-EDGE FIBROUS CALCITE
- ◈ SHELF-EDGE FIBROUS CALCITE, EQUIVALENT TO ON-SHELF FIBROUS CALCITE
- ◇ ON-SHELF FIBROUS CALCITE
- ○ ON-SHELF PLANAR-e DOLOMITE

TABLE 4.1 SUMMARY OF GEOCHEMICAL DATA FOR SHELF-EDGE PHASES

| KEY | | SIRA RELATIVE TO PDB | | | | RADIOGENIC Sr | | ELECTRON MICROPROBE ANALYSIS | | | | |
|---|---|---|---|---|---|---|---|---|---|---|---|---|
| SYMBOL (THIS STUDY) | PHASE OR CROSS-CUTTING FEATURE | $\delta^{18}O$ ‰ Median Min. Max. | $\delta^{13}C$ ‰ Median Min. Max. | Number of Samples | Stratigraphic Intervals | $^{87}Sr/^{86}Sr$ Median | Stratigraphic Intervals | $MgCO_3$ (mole %) Median Min. Max. | Fe (wt %) Median Min. Max. | Mn (wt %) Median Min. Max. | Points Probed | Stratigraphic Intervals |
| N/A | BLACK, Fe/Mn OXIDE RICH SEDIMENT, LAM. AND PAVEMENTS | ND | ND | ND | ND | ND | ND | *see note below | 1.42* 1.33 3.19 | 0.12* 0.11 0.16 | N/A | 3 |
| ◆ | FIBROUS CALCITE (RADIAXIAL) | -5.2 -6.6 -4.1 | 0.9 0.2 1.2 | 63 | 20 | 0.708453 | 1 | 0.71 0.37 6.73 | -- -- -- 0.36 | -- -- -- 1.02 | 340 | 6 |
| ◇ | FIBROUS CALCITE, STRAT. EQUIVALENT TO ON-SHELF CALCITE** | -4.9 -5.1 -4.5 | 0.7 0.4 0.7 | 8 | 2 | ND | ND | ND | ND | ND | ND | ND |
| — | BLADED CALCITE | -6.5 -6.7 -6.2 | 0.0 -0.3 0.4 | 3 | 2 | ND | ND | 0.70 0.21 1.17 | --- --- 0.33 | 0.10 -- -- 0.68 | 62 | 2 |
| ▲ | BLOCKY CLEAR CALCITE (DRUSY) | -6.6 -7.9 -6.1 | 0.7 0.0 0.8 | 5 | 5 | ND | ND | ND | ND | ND | ND | ND |
| ✳ | FERROAN AND NON-FERROAN SYNTAXIAL OVERGROWTH CALCITE | -7.7 -8.4 -6.9 | 0.1 -0.3 0.9 | 7 | 6 | ND | ND | 0.82 0.35 7.77 | 0.15 --- --- 0.71 | -- -- -- 0.07 | 35 | 2 |
| ■ | FERROAN BLOCKY WHITE CALCITE | -7.7 -8.1 -7.3 | 0.7 0.5 0.8 | 3 | 3 | ND | ND | 1.08 0.49 1.73 | 0.04 --- --- 0.31 | -- -- -- 0.18 | 56 | 2 |
| ▩ | FERROAN VEIN CALCITE | -7.4 | 0.3 | 1 | 1 | ND | ND | 0.77 0.56 1.41 | 0.29 0.13 0.39 | 0.04 -- -- 0.07 | 14 | 1 |
| ※ | FERROAN COARSE SPARRY CALCITE | -9.5 -10.0 -8.6 | 0.6 0.1 0.9 | 7 | 5 | 0.709423 | 1 | 0.60*** | ND | 0.05*** | N/A | 1 |
| × | FERROAN COARSE PINK SPARRY CALCITE | -10.1 -11.0 -10.0 | 0.7 0.5 0.8 | 4 | 3 | 0.708568 | 2 | 1.04 0.76 1.31 | 0.24 0.05 0.35 | 0.09 -- -- 0.22 | 25 | 2 |
| ※ | FERROAN COARSE SPARRY CALCITE, (CO-PRECIPITATED WITH BAROQUE DOLOMITE) | -11.0 | -0.3 | 1 | 1 | 0.709092 | 2 | 0.80 0.20 3.11 | -- -- -- 0.37 | -- -- -- 0.10 | 24 | 1 |
| ● | FERROAN BAROQUE DOLOMITE | -7.7 -7.9 -5.7 | 1.7 1.4 1.9 | 6 | 4 | 0.709372 | 4 | 42.39 31.99 47.88 | 2.63 0.52 5.39 | 0.07 -- -- 0.55 | 106 | 4 |

* Whole-rock A.A. analysis soluble of carbonate associated with pavements at Douglas Lake by Johnson (1988). Mg ranges from about 0.53 to 0.88 wt %.

** Includes only fibrous calcite that occurs stratigraphically "high" in the section (i.e., in the Rockdell Fm).

*** A.A. analyses by Jernigan (1987) and Johnson (1988).

ND = No Data

TABLE 4.2 SUMMARY OF GEOCHEMICAL DATA FOR ON-SHELF PHASES

| KEY | | SIRA RELATIVE TO PDB | | | | RADIOGENIC Sr | | ELECTRON MICROPROBE ANALYSIS | | | | |
|---|---|---|---|---|---|---|---|---|---|---|---|---|
| SYMBOL (THIS STUDY) | PHASE OR CROSS-CUTTING FEATURE | $\delta^{18}O$ ‰ Median Min. Max. | $\delta^{13}C$ ‰ Median Min. Max. | Number of Samples | Stratigraphic Intervals | $^{87}Sr/^{86}Sr$ Median | Number of Samples | $MgCO_3$ (mole %) Median Min. Max. | Fe (wt %) Median Min. Max. | Mn (wt %) Median Min. Max. | Points Probed | Stratigraphic Intervals |
| ◇ | FIBROUS CALCITE (RADIAXIAL) | -4.8<br>-5.9 -4.4 | 0.6<br>0.2 1.0 | 21 | 3 | 0.708261 | 2 | 0.93<br>0.60 1.81 | -- --<br>-- -- 0.09 | -- --<br>-- -- 0.20 | 88 | 3 |
| ○ | PLANAR-e DOLOMITE | -4.8<br>-5.5 -3.5 | 1.4<br>0.7 1.9 | 7 | 7 | ND | ND | ND | ND | ND | ND | ND |
| - | BLADED CALCITE | -6.6<br>-7.0 -6.3 | -0.1<br>-1.3 1.2 | 2 | 2 | ND | ND | 0.71<br>0.16 2.01 | -- --<br>-- -- 0.25 | 0.10<br>-- -- 1.13 | 45 | 2 |
| △ | BLOCKY CLEAR CALCITE (DRUSY) | -7.6<br>-7.8 -6.8 | 0.2<br>-1.6 0.4 | 13 | 12 | No Run | ND | 1.12<br>0.26 2.05 | 0.07<br>-- -- 0.17 | -- --<br>-- -- 1.40 | 81 | 3 |
| + | FERROAN AND NON-FERROAN SYNTAXIAL OVERGROWTH CALCITE | -7.3<br>-8.2 -6.5 | 0.1<br>-0.8 0.5 | 7 | 6 | ND | ND | ND | ND | ND | ND | ND |
| □ | FERROAN BLOCKY WHITE CALCITE | -7.7<br>-8.4 -7.1 | 0.3<br>-1.7 0.8 | 37 | 28 | 0.708349 | 3 | 1.36<br>0.54 1.55 | 0.16<br>0.07 0.22 | 0.04<br>-- -- 0.07 | 31 | 1 |
| ⊠ | FERROAN VEIN CALCITE | -7.9<br>-10.6 -6.9 | 0.2<br>-1.0 0.5 | 12 | 11 | ND | ND | ND | ND | ND | ND | ND |
| ✳ | FERROAN COARSE SPARRY CALCITE | -8.6<br>-8.9 -8.1 | 0.5<br>-0.2 1.0 | 9 | 5 | 0.708302 | 2 | 0.65<br>0.30 3.18 | 0.09<br>-- -- 0.43 | -- --<br>-- -- 0.23 | 74 | 2 |
| ○ | FERROAN BAROQUE DOLOMITE | -8.0<br>-8.7 -7.7 | 0.5<br>-0.1 0.5 | 3 | 2 | 0.709178 | 2 | 43.52<br>41.14 45.21 | 1.86<br>0.97 2.89 | 0.10<br>-- -- 0.38 | 27 | 1 |
| N/A | COARSE CLEAR SPARRY CALCITE | -5.5 | 4.3 | 1 | 1 | ND | ND | ND | ND | ND | ND | ND |
| ⊕ | NON-FERROAN BAROQUE DOLOMITE | -6.9 | 1.4 | 1 | 1 | ND | ND | ND | ND | ND | ND | ND |

ND = No Data

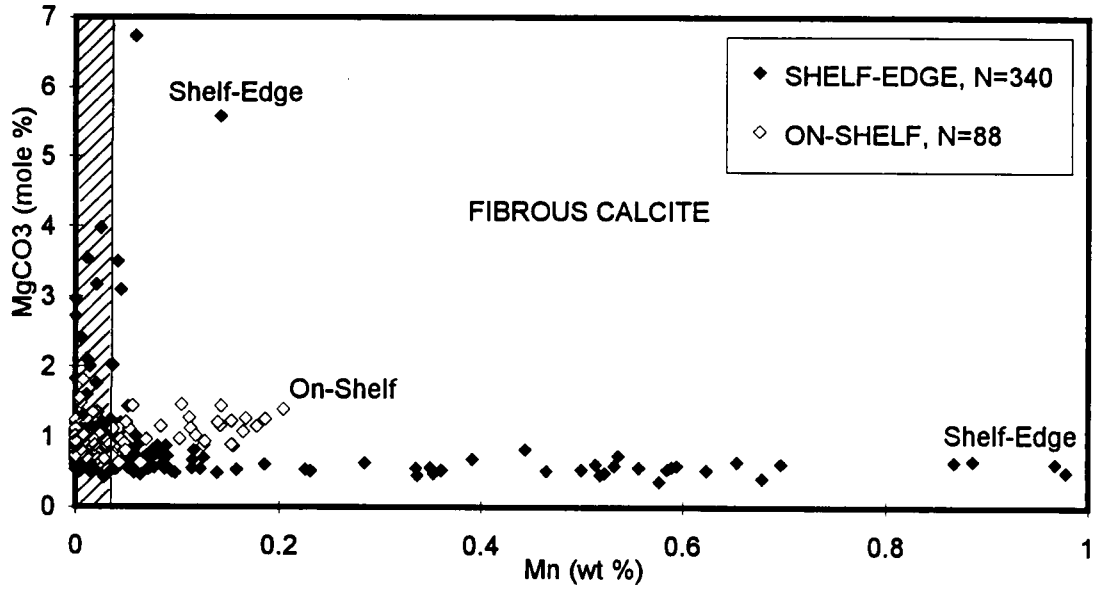
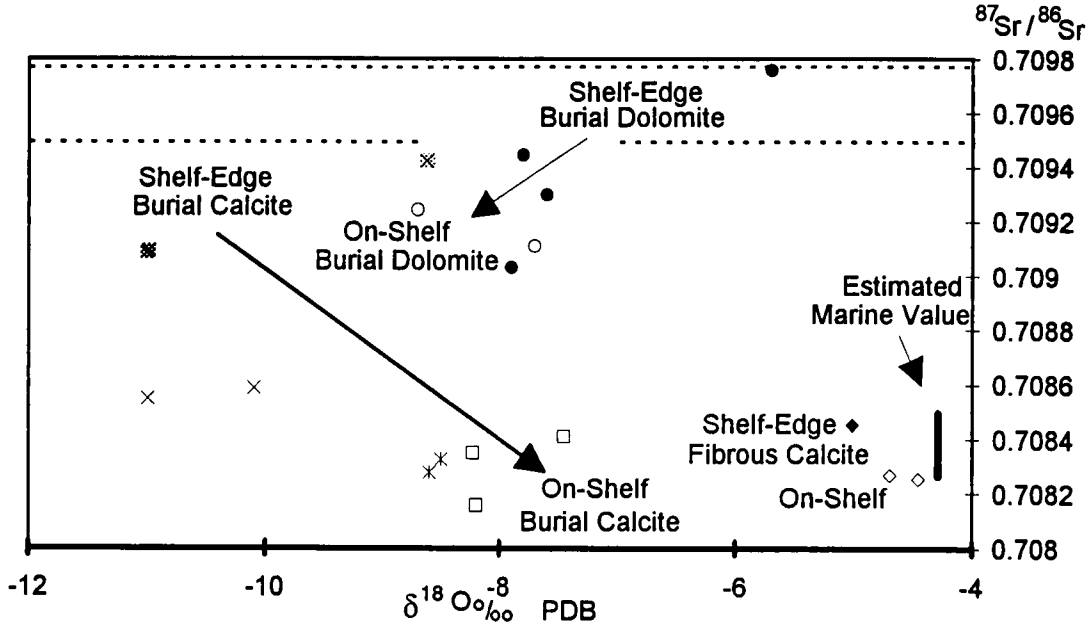



Figure 4.6 Electron microprobe analyses of weight percent manganese versus mole percent $MgCO_3$ of shelf-edge and on-shelf fibrous calcite. All analyses are above detection limits for magnesium, shaded region shows analyses below detection limits for manganese. Mean magnesium concentration of shelf-edge fibrous calcite is 0.85 $\pm$ 0.60 mole %, whereas on-shelf fibrous calcite averages 0.97 $\pm$ 0.24 mole %. Mean manganese concentration of shelf-edge fibrous calcite is about 0.07 wt %, whereas the mean concentration for on-shelf fibrous calcite is about 0.05 wt % (the median value for both are below detection limits). Jernigan (1987) and Johnson (1988) reported similar results using atomic absorption analysis on a suite of nine fibrous calcite samples from shelf-edge Holston and Rockdell Formations in the study area. Note: many authors feel that values below the detection limit should be plotted on the "zero" line. Here, however, values of manganese below the detection limit are <u>not</u> plotted on the zero line to help the reader discriminate different values of $MgCO_3$ , all of which are above the detection limit.




× SHELF-EDGE FERROAN COARSE PINK SPARRY CALICTE

▪ SHELF-EDGE COARSE SPARRY CALICTE CO-PRECIPITATED WITH FERRAON BAROQUE DOLOMITE

● SHELF-EDGE FERROAN BAROQUE DOLOMITE

○ ON-SHELF FERROAN BAROQUE DOLOMITE

◆ SHELF-EDGE FIBROUS CALCITE

◇ ON-SHELF FIBROUS CALCITE

□ ON-SHELF FERROAN BLOCKY WHITE CALCITE

※ SHELF-EDGE FERROAN COARSE SPARRY CALCITE

✳ ON-SHELF FERROAN COARSE SPARRY CALCITE

Figure 4.7 Comparison of $\delta^{18}O$ versus $^{87}Sr/^{86}Sr$ values for on-shelf and shelf-edge phases. Bar shows estimate for Middle Ordovician marine carbonate value. The $\delta^{18}O$ value of -4.2‰ PDB is based on this work, the $^{87}Sr/^{86}Sr$ value of about 0.7084 to 0.7085 is from Burke et al. (1982) and Edmond (1992). Horizontal dashed lines shows $^{87}Sr/^{86}Sr$ values for two post-ore dolomite samples from the Idol Mine reported by Kesler et al. (1988) for comparison. Mississippi Valley-type deposits occur in Lower Ordovician strata of the upper part of the Knox Group in the study area.

**Turbid, Syntaxial Rim Overgrowth Calcite.** Turbid, syntaxial rim overgrowth calcite occurs in many echinoderm grainstones. It is recognized as the first phase in optical continuity with many, but not all, echinoderm ossicles. It is best distinguished from later overgrowth calcite under cathodoluminescence. Later overgrowths are generally dully luminescent and separated from earlier non-luminescent turbid overgrowth calcite by a bright zone (e.g., Steinhauff et al., 1989, p. 128 -129).

**Crystal or Vadose Silt.** Crystal or vadose silt (Dunham, 1969) occurs as geopetal fillings within calcite filled cavities and vugs on the shelf and at the shelf-edge (Fig. 4.4A). These cavities and vugs occur stratigraphically below third- and fourth-order sequence boundaries at the shelf-edge and on the shelf. These filled cavities were probably developed during subaerial exposure (chapters 2 and 3; Steinhauff and Walker, 1992a,b; in press).

**Pendant Cement.** Pendant cement rarely occurs on the upper surfaces of calcite filled cavities and vugs. These cavities and vugs occur stratigraphically below third- and fourth-order sequence boundaries at the shelf-edge and on the shelf. Pendant cement is clear calcite. Under cathodoluminescence, pendant cements generally have one or two alternating brightly luminescent and non-luminescent zones (Steinhauff and Walker, in press; see Figs. 2.5H, 3.2H of Chapter 2).

**Planar-e Dolomite.** Planar-e dolomite (Sibley and Gregg, 1987) occurs as aggregates of non-ferroan, equant crystals, less than 0.05 mm across, within mudstones, fenestral mudstones, and other mud-rich lithologies associated with third- and fourth-order sequence boundaries on the shelf. Some of these crystal aggregates occur as thin laminations up to about 0.5 mm thick. Composite samples of planar-e dolomite from seven stratigraphic intervals on the shelf have a mean $\delta^{18}O$ value of -4.6 $\pm$ 0.8‰ PDB and a mean $\delta^{13}C$ value of 1.4 $\pm$ 0.4‰ PDB (Fig. 4.5).

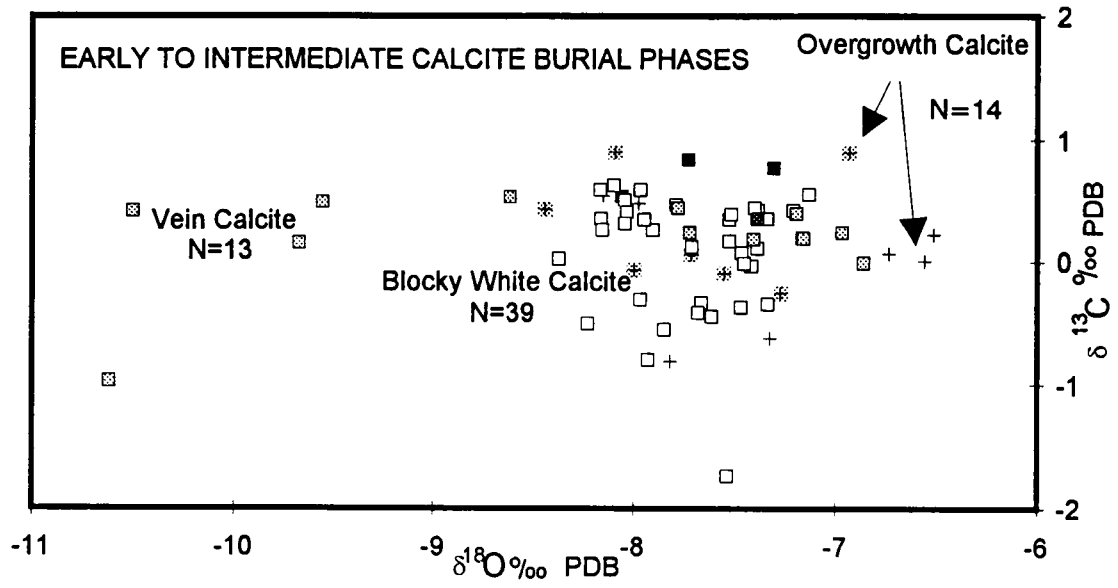
**Bladed Calcite.** Bladed calcite has a very limited stratigraphic occurrence as isopachous linings that truncate fibrous calcite in cavities and vugs. These cavities and vugs occur stratigraphically below third- and fourth-order sequence boundaries at the shelf-edge and on the shelf (chapters 2 and 3; Steinhauff and Walker, in press; in prep. a).

Bladed calcite is generally clear with planar crystal boundaries pointing toward the pore center. Length to width ratios of 3:1 to 2:1 occur at the shelf-edge, whereas bladed calcite is nearly equant on the shelf. Under cathodoluminescence, bladed calcite is bright and sometimes zoned (Figs. 4.4B-4.4G). Shelf-edge and on-shelf bladed calcite are not differentiated relative to their light stable isotopic content (Fig. 4.5). Five bladed calcite samples (3 from the shelf-edge and two from the shelf) have $\delta^{18}O$ values between -7.0‰ to -6.2‰ PDB, and $\delta^{13}C$ values between -1.3‰ to 1.2‰ PDB (Tables 4.1 and 4.2).

**Blocky, Clear Calcite.** Blocky, clear calcite generally occurs with drusy fabric in cavities and large pores on the shelf and at the shelf-edge. Many, but not all, of these blocky, clear calcite-filled cavities were probably developed during subaerial exposure (chapters 2 and 3; Steinhauff and Walker, in press; in prep. a). Under cathodoluminescence, blocky clear calcite is dully to moderately luminescent. Blocky, clear calcite is morphologically and geochemically gradational with ferroan blocky white calcite (c.f., Figs. 4.5 and 4.8). However, blocky, clear calcite is distinguished from ferroan blocky, white calcite in thin-section by its drusy fabric, relative clarity (lack of fluid inclusions), and lack of affinity for potassium ferricyanide stain. Blocky, clear calcite is generally more enriched in $\delta^{18}O$ and has a lower iron and manganese content than ferroan, blocky white calcite (Tables 4.1 and 4.2). The $\delta^{18}O$ content of blocky clear calcite at the shelf-edge (mean = -6.8 $\pm$ 0.7‰ PDB, N = 5) generally overlaps values on the shelf (mean = -7.5 $\pm$ 0.3‰ PDB, N = 13; Fig. 4.5, Tables 4.1 and 4.2). On-shelf blocky clear calcite has a mean $MgCO_3$ content of 1.1 $\pm$ 0.4 mole % (N=81), a mean iron content of about 0.07 wt % and mean manganese content of about 0.5 wt %. Trace element data are not available for shelf-edge blocky clear calcite.

## Intermediate to Early Burial Phases

**Ferroan and Non-Ferroan Overgrowth Calcite.** Ferroan and non-ferroan overgrowth calcite is a syntaxial rim overgrowth that commonly occurs as the first phase in optical continuity with echinoderm ossicles in grainstones. It is best




□ ON-SHELF FERROAN BLOCKY WHITE CALCITE

■ SHELF-EDGE FERROAN VEIN CALCITE

▨ ON-SHELF FERROAN VEIN CALCITE

✳ SHELF-EDGE FERROAN AND NON-FERROAN OVERGROWTH CALCITE

\+ ON-SHELF FERROAN AND NON-FERROAN OVERGROWTH CALCITE

■ SHELF-EDGE FERROAN BLOCKY WHITE CALCITE

Figure 4.8 $\delta^{18}O$ versus $\delta^{13}C$ for intermediate to early burial phases.

distinguished from early turbid overgrowth calcite, which may sometimes precede it, under cathodoluminescence. Later overgrowths are generally dully luminescent and separated from earlier non-luminescent turbid overgrowth calcite by a bright zone (e.g., Steinhauff et al., 1989, p. 128 -129).

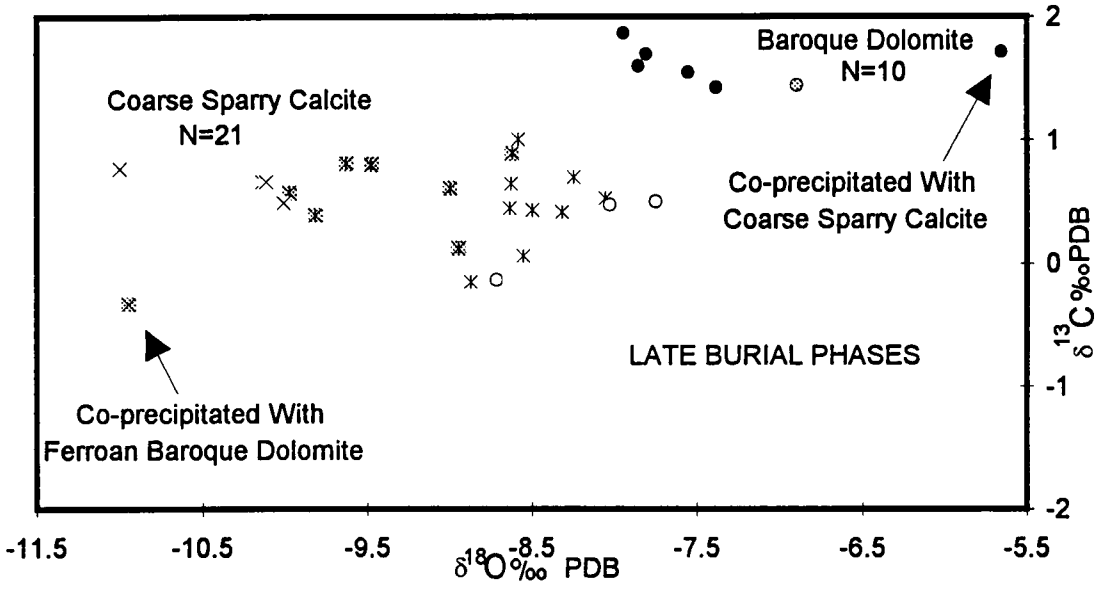
Samples for light stable isotopic analysis of overgrowth calcite were taken as a composite of smaller samples, each composite was drilled from a single 45 X 75 mm polished billet. Shelf-edge overgrowth calcite (mean = -7.7 $\pm$ 0.5‰ PDB, N= 7) appears slightly depleted in $\delta^{18}O$ compared with on-shelf overgrowth calcite (-7.3 $\pm$ 0.7‰ PDB, N = 7; Fig. 4.8).

Within many stratigraphic intervals, early overgrowths do not take a potassium ferricyanide staining, whereas later overgrowths take the stain (Jernigan, 1988; Steinhauff et al., 1989). This indicates the later overgrowths have higher iron contents than earlier overgrowths. Overgrowths from two stratigraphic intervals at the shelf-edge have iron contents that range from less than 0.04 wt % (below detection limits) to more than 0.7 wt % (Table 4.1). Manganese contents are generally below detection limits (Table 4.1).

**Ferroan, Blocky White Calcite.** Ferroan, blocky white calcite is distinguished from blocky, clear calcite in thin-section by its non-drusy fabric, high fluid inclusion content, and affinity for potassium ferricyanide stain. Under cathodoluminescence, ferroan, blocky white calcite is dully to non-luminescent. Ferroan, blocky white calcite is generally more depleted in $\delta^{18}O$ than blocky, clear calcite and contains

considerably more iron (0.15 wt % versus 0.7 wt %, for on-shelf means), and more manganese (Tables 4.1 and 4.2). This phase is also generally enriched in $\delta^{18}O$ relative to later burial phases (c.f., Figs. 4.8 and 4.9; 4.10 and 4.11). On-shelf blocky white calcite has $\delta^{18}O$ values between -8.4‰ to -7.1‰ PDB and $\delta^{13}C$ values with a mean of 0.1 $\pm$ 0.5‰ PDB (N=37; Fig. 4.9, Table 2).

**Ferroan Vein Calcite.** Ferroan calcite veins occur extensively both at the shelf-edge and on the shelf. Veins range from about 0.1 to 5 mm across. Ferroan vein calcite is non-drusy with numerous fluid inclusions and is non-luminescent. Typically, it is virtually indistinguishable from that of blocky white calcite when observed under cathodoluminescence or polarized light. In fact, many veins lead into cavities filled with blocky white calcite. Other veins contain ferroan baroque dolomite in a relationship suggesting competitive growth with the vein calcite. On-shelf ferroan vein calcite has $\delta^{18}O$ values (-10.6‰ to -6.9‰ PDB, N = 12) that overlap with blocky clear calcite (-7.8‰ to -6.8‰ PDB) and ferroan, blocky white calcite (-8.4‰ to -7.1‰ PDB; Fig. 4.8, Table 4.2). The $\delta^{18}O$ values of ferroan vein calcite are closely related to vein width, with thicker veins having relatively depleted $\delta^{18}O$ values (see chapter 5; Steinhauff and Walker, in prep. b). Trace element vein data are limited (Fig. 4.8; Tables 4.1 and 4.2). However, potassium ferricyanide staining suggests that some veins have very little iron, whereas other veins are among the most ferroan phases observed.




- SHELF-EDGE FERROAN COARSE SPARRY CALCITE
- ON-SHELF FERROAN COARSE SPARRY CALCITE
- SHELF-EDGE FERROAN COARSE PINK SPARRY CALCITE
- SHELF-EDGE FERROAN COARSE SPARRY CALCITE (CO-PPT WITH BAROQUE DOLOMITE)
- SHELF-EDGE FERROAN BAROQUE DOLOMITE
- ON-SHELF FERROAN BAROQUE DOLOMITE
- ON-SHELF NON-FERROAN BAROQUE DOLOMITE

Figure 4.9 $\delta^{18}O$ versus $\delta^{13}C$ for late burial phases.

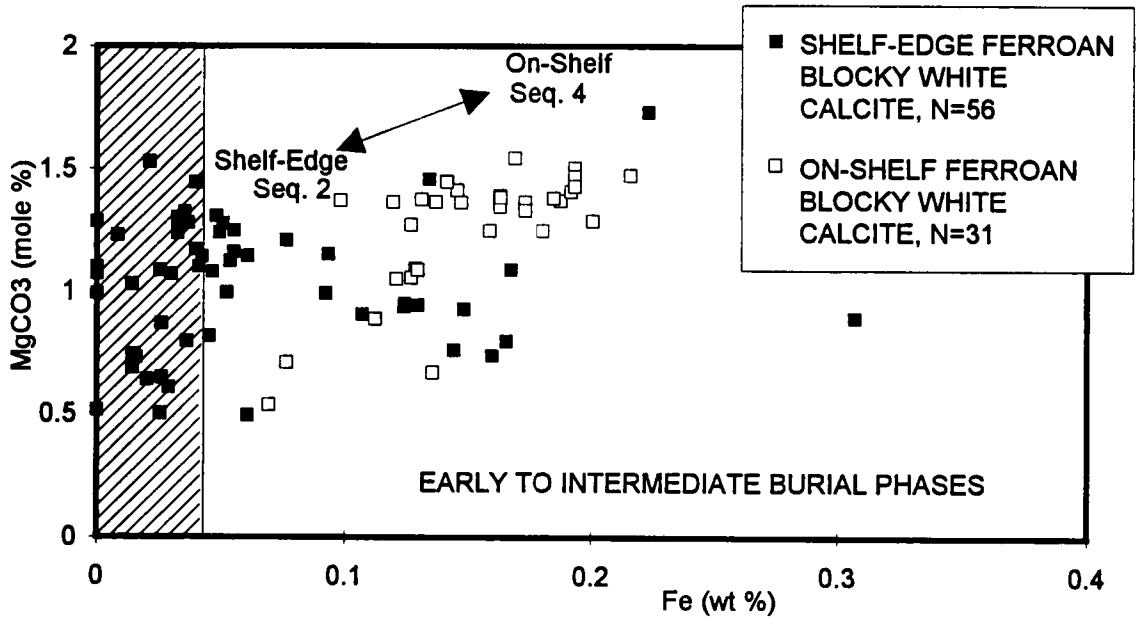



Figure 4.10 Electron microprobe analysis of weight percent iron versus mole percent $MgCO_3$ of shelf-edge and on-shelf ferroan, blocky white calcite. All analyses are above detection limits for magnesium, shaded region shows analyses below detection limits for iron. Values of iron below the detection limit are not plotted on the "zero" line to help the reader discriminate different values of $MgCO_3$ , all of which are above the detection limit.

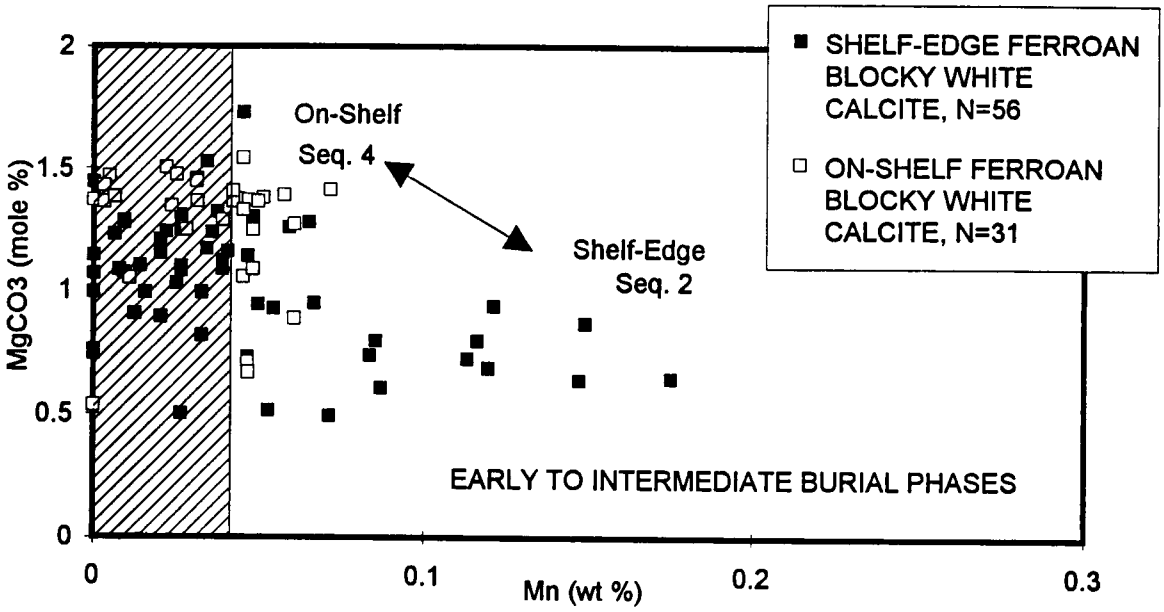



Figure 4.11 Electron microprobe analysis of weight percent manganese versus mole percent $MgCO_3$ of shelf-edge and on-shelf ferroan, blocky white calcite. All analyses are above detection limits for magnesium, shaded region shows analyses below detection limits for manganese. Values of manganese below the detection limit are not plotted on the "zero" line to help the reader discriminate different values of $MgCO_3$ , all of which are above the detection limit.

## Late Burial Phases

All late burial phases are distinguished by coarse crystal size and non-luminescence. Cross-cutting and competitive growth relationships are the basis for determining their relative timing.

**Ferroan, Coarse Sparry Calcite.** Ferroan, coarse sparry calcite occurs in cavities and vugs at the shelf-edge and on the shelf. Ferroan, coarse sparry calcite is white with fluid inclusions. Crystals are generally greater than 2 mm across with well-developed cleavage planes. Some single crystals occupy vugs that are up to 20 cm across (Steinhauff and Walker, in prep. a,b). These large crystals commonly truncate earlier phases such as crystal (vadose) silt and bladed or fibrous calcite (Figs. 4.4A, 4.4G, 4.4H).

In the absence of geochemical data, the smaller crystal variety of ferroan, coarse sparry calcite is easily confused with ferroan, blocky white calcite and coarse sparry calcite of later timing. The $\delta^{18}O$ values of ferroan, blocky calcite are enriched when compared to ferroan, coarse sparry calcite (Figs. 4.8 and 4.9, Tables 4.1 and 4.2). Ferroan sparry calcite has a mean magnesium content of 0.77 $\pm$ 0.43 mole % or about half that of ferroan blocky calcite. The iron and manganese concentrations of ferroan, coarse sparry calcite and ferroan, blocky white calcite may be similar (Figs. 4.10, 4.11, 4.12 and 4.13). Note that trace element data are not available for shelf-edge ferroan, coarse sparry calcite. On-shelf ferroan, coarse sparry calcite

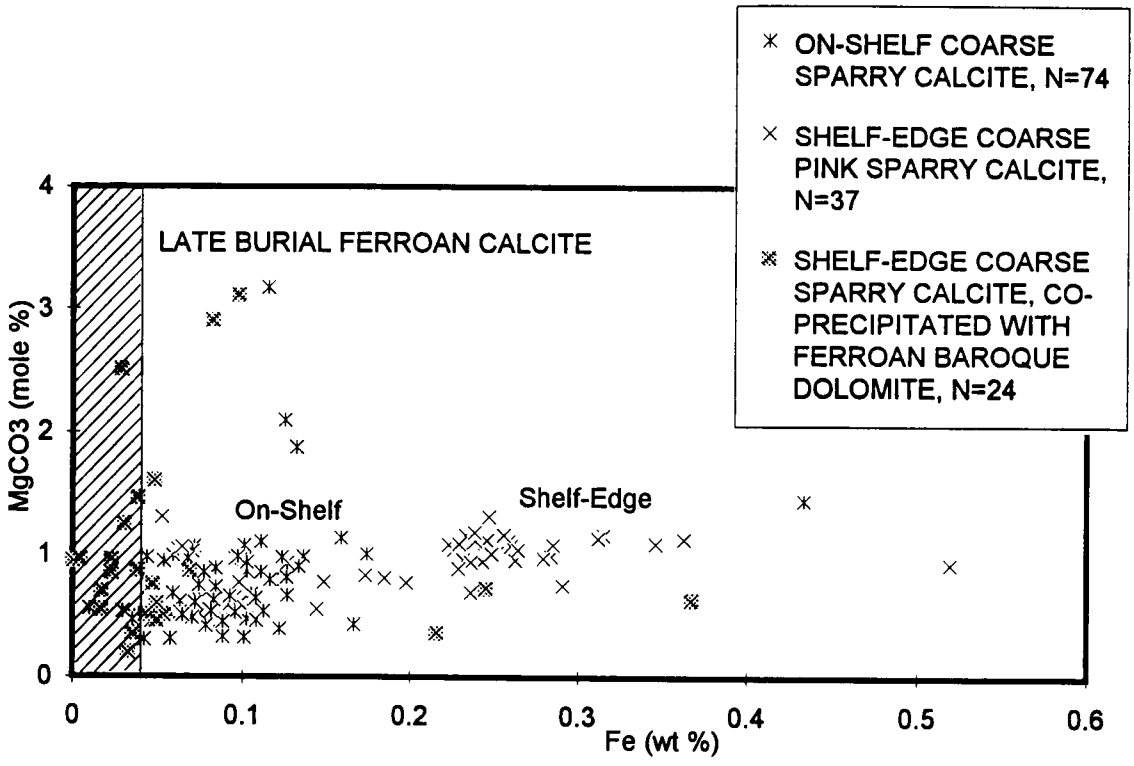



Figure 4.12 Electron microprobe analysis weight percent iron versus mole percent $MgCO_3$ for late burial ferroan calcite. All analyses are above detection limits for magnesium, shaded region shows analyses below detection limits for iron. Values of iron below the detection limit are <u>not</u> plotted on the "zero" line to help the reader discriminate different values of $MgCO_3$ , all of which are above the detection limit.

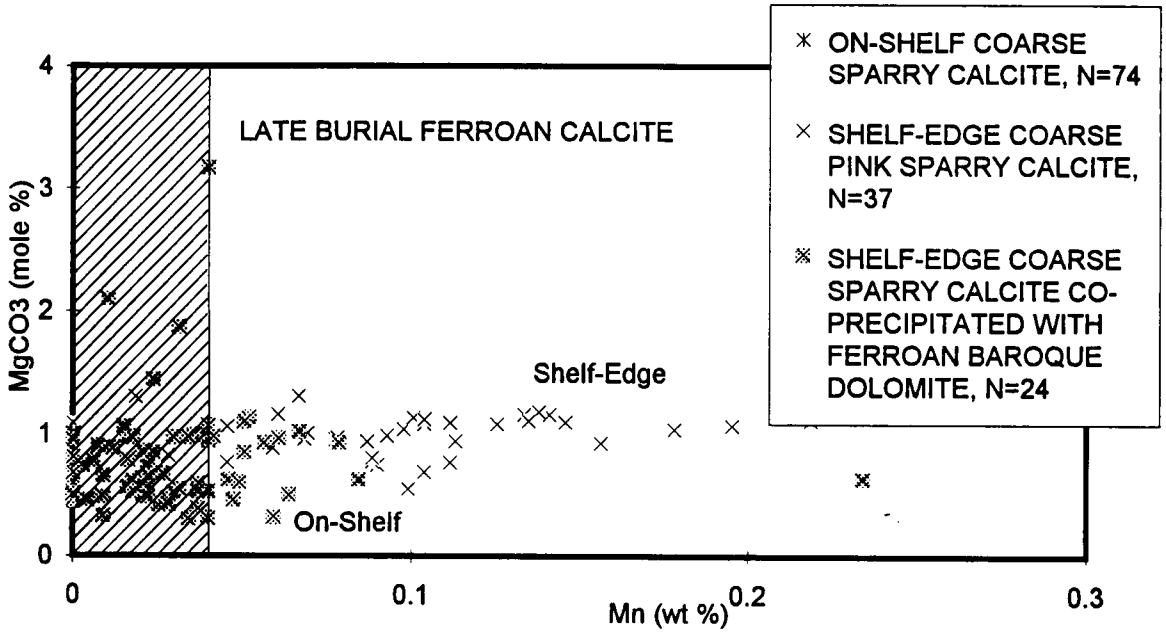



Figure 4.13 Electron microprobe analysis of weight percent manganese versus mole percent $MgCO_3$ for late burial ferroan calcite. All analyses are above detection limits for magnesium, shaded region shows analyses below detection limits for manganese. Values of manganese below the detection limit are <u>not</u> plotted on the "zero" line to help the reader discriminate different values of $MgCO_3$ , all of which are above the detection limit.

(mean = -8.5 ± 0.2‰ PDB, N=9) is enriched in $\delta^{18}O$ relative to ferroan, coarse sparry calcite at the shelf-edge ( -9.4 ± 0.5‰ PDB, N=7; Fig. 4.9).

**Ferroan, Coarse Pink Sparry Calcite.** Ferroan, coarse pink sparry calcite fills cavities and vugs only at the shelf-edge. It is whitish-pink in color and lacks visible cleavage planes. It has the most depleted $\delta^{18}O$ content of any phase sampled (-11.0‰ to -10.0‰ PDB, Fig. 4.9). However, ferroan, coarse sparry calcite co-precipitated with ferroan baroque dolomite also has a $\delta^{18}O$ value of -11.0‰ PDB (Fig. 4.9). This co-precipitated phase is milky-white and has a considerably lower iron and manganese content than ferroan, coarse pink sparry calcite (Figs. 4.12 and 4.13, Table 1). The iron content of ferroan, coarse pink sparry calcite is as high as 0.52 wt %.

**Ferroan Baroque Dolomite.** Ferroan baroque dolomite is restricted to thin (less than 5 meter thick) stratigraphic horizons below third- and fourth-order sequence surfaces on the shelf and at the shelf-edge. Cross-cutting and competitive growth relationships establish that ferroan baroque dolomite is generally the latest phase (i.e., Jernigan, 1987; Steinhauff et al., 1989). Some cavities filled with ferroan baroque dolomite retain a very small amount of residual porosity.

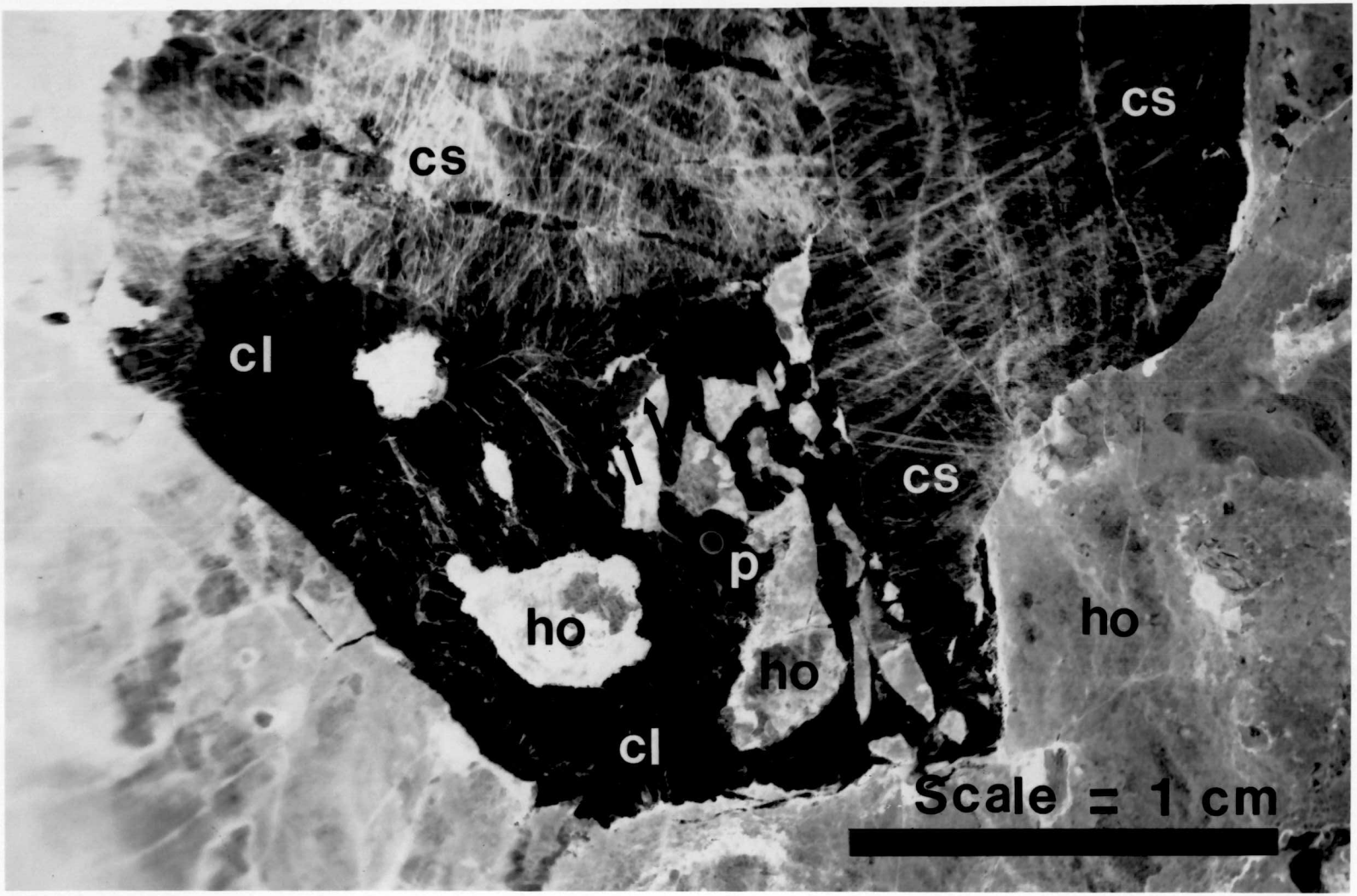
Samples for light stable isotopic analysis of ferroan baroque dolomite were taken as a composite of smaller samples, each drilled from a single 45 X 75 mm polished billet. Shelf-edge ferroan baroque dolomite is enriched in $\delta^{18}O$ (-7.9‰ to -5.7‰ PDB) relative to on-shelf ferroan baroque dolomite (-8.7‰ to -7.7‰ PDB;

Fig. 4.9, Tables 4.1 and 4.2). Similarly, shelf-edge ferroan baroque dolomite is enriched in $\delta^{13}C$ (1.4‰ to 1.9‰ PDB) relative to on-shelf ferroan baroque dolomite (-0.1‰ to 0.5‰ PDB; Fig. 4.9, Tables 4.1 and 4.2). Potassium ferricyanide staining indicates that some ferroan baroque dolomite crystals are zoned with respect to ferrous iron. The trace element content of shelf-edge and on-shelf ferroan baroque dolomite appear similar (Tables 4.1 and 4.2).

**Coarse, Clear Sparry Calcite.** A single example of coarse, clear sparry calcite occurs below the upper surface of third-order Sequence 3 on the shelf at the Idol Mine section within a ferroan sparry calcite filled vug and clearly cross-cuts this ferroan, coarse sparry calcite (Fig. 4.14). Conspicuous lack of fluid inclusions distinguish it from the later. The light stable isotopic values of coarse clear sparry calcite ($\delta^{18}O$ = -5.5‰ PDB, $\delta^{13}C$ = 4.3‰ PDB) fall outside the fields of all other phases examined (i.e., Figs. 4.5, 4.8 and 4.9).

**Non-Ferroan Baroque Dolomite.** Two examples of non-ferroan baroque dolomite are observed, both are closely associated with the upper surface of third-order Sequence 3 on the shelf at the Idol Mine section. Cross-cutting relationships suggest that it is the latest phase. The stratigraphically lowest example cross-cuts the coarse clear sparry calcite previously discussed (Fig. 4.14). The stratigraphically highest example has a $\delta^{18}O$ value of -6.9‰ PDB and $\delta^{13}C$ value of 1.4‰ PDB (Fig. 4.9).

Figure 4.14 Photo-negative shows calcite filled vug developed during subaerial exposure and / or freshwater diagenesis. Ferroan coarse sparry calcite (cs) is cut by clear sparry calcite (cl) and followed by non-ferroan baroque dolomite (arrows). Note that a small amount of porosity is indicated by the black area with an air bubble (p). The host lithology (ho) is a mudstone. Scale bar equals one centimeter.


cs
cs
cs
cl
l
p
ho
ho
ho
cl
Scale = 1 cm

## INTERPRETATION OF PARAGENETIC SEQUENCE

### Early Diagenetic Non-Ferroan Phases

Early diagenetic non-ferroan phases were precipitated or developed during marine, freshwater, and possibly very early burial diagenesis. Many stratigraphic sequences within this study experienced more than one cycle of early diagenesis (e.g., Figs. 4.15 and 4.16). On the shelf, for example, fourth-order Subsequence 3A, is overlain by several thinner fourth-order subsequences, each of which was has an upper surface that was subaerially exposed (Fig. 4.2). It is likely that Subsequence 3A experienced more than one cycle of early diagenesis. On the other hand, sediments overlain by relatively thick subsequences such as those that were deposited in the lower part of Subsequence 2E have probably not experienced a second early cycle of diagenesis. Thus, it is apparent that the early diagenesis of each subsequence is somewhat unique. I have not investigated the early diagenetic history of each subsequence (i.e., Fig. 4.2). However, two examples are presented here in which sediments have experienced a second cycle of early diagenesis.

**Marine Diagenesis.** Marine phases include (1) microcrystalline calcite cement; (2) black, Fe / Mn oxide-rich sediment, laminae and pavements; (3) fibrous calcite; and (4) turbid, syntaxial rim overgrowth calcite (Steinhauff, 1989; Steinhauff et al., 1989; Walker et al., 1990). Cross-cutting and competitive growth relationships suggest that microcrystalline calcite cement, black, Fe / Mn oxide-rich sediment, fibrous calcite, and turbid, syntaxial rim overgrowth calcite are of syndepositional marine origin.

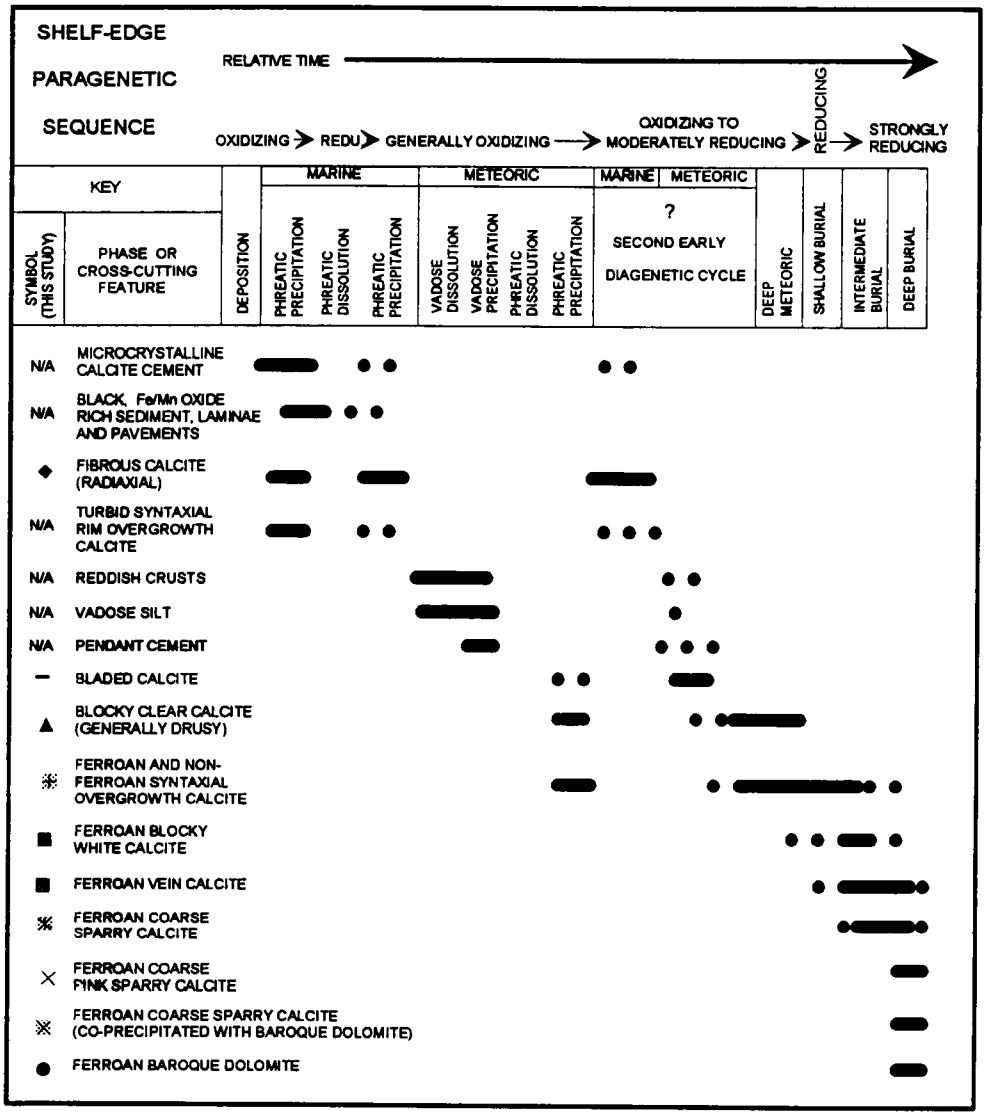



Figure 4.15 Shelf-edge paragenetic sequence. Solid bars show most commonly observed relationships, dotted lines show less commonly observed relationships.

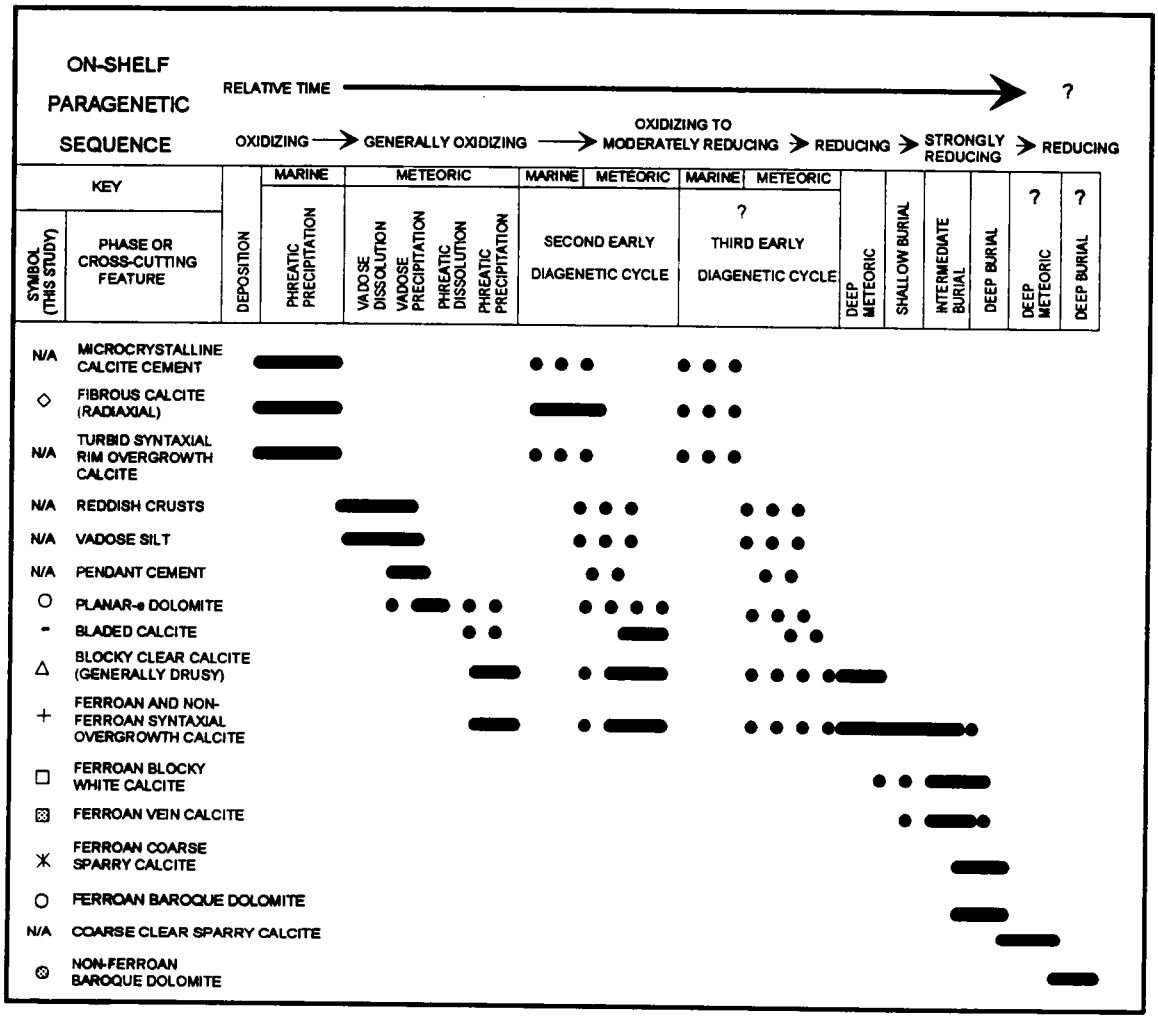



Figure 4.16 On-shelf paragenetic sequence. Solid bars show most commonly observed relationships, dotted lines show less commonly observed relationships.

The values of $\delta^{18}O$ for fibrous calcite are consistent with published values for other Middle Ordovician marine carbonates (i.e, Popp et al., 1986). The isotopically most enriched value of $\delta^{18}O$ for fibrous calcite at the shelf-edge, -4.1‰ PDB, provides an estimate of the original marine value of Middle Ordovician calcite (Fig. 4.5, Table 4.1). The slightly depleted $\delta^{13}C$ values of on-shelf fibrous calcite relative to shelf-edge fibrous calcite may be related to more frequent contact with marginal marine and / or freshwater fluids containing $CO_2$ enriched in the light $^{12}C$ isotope. Enrichment in $^{12}C$ may have occurred from decay of algal mats associated with very shallow marine and / or freshwater environments on the shelf. There is no evidence for paleosols within this succession (Steinhauff and Walker, 1992a).

Fibrous calcite is presently low magnesium calcite (Tables 4.1 and 4.2). However, Figure 4.6 shows that the distribution of magnesium within shelf-edge fibrous calcite has a wide range, with many values above 2 mole % $MgCO_3$. This wide range of magnesium content combined with low strontium content indicating original calcite mineralogy suggests that fibrous calcite has been "stabilized," and was originally a high magnesium calcite (i.e., Davies, 1977: James and Klappa, 1983; Prezbindowski, 1985). The relatively wide range of manganese content in shelf-edge fibrous calcite (less than 0.04 to 1.02 wt %) may be due to wide variations in precipitation rate, with higher manganese incorporated during times of slow or non-precipitation. Manganese may have been incorporated over relatively long periods of time when drowning unconformities were developed at the shelf-edge. In contrast, fibrous calcite on the shelf represents a much more open system with respect to

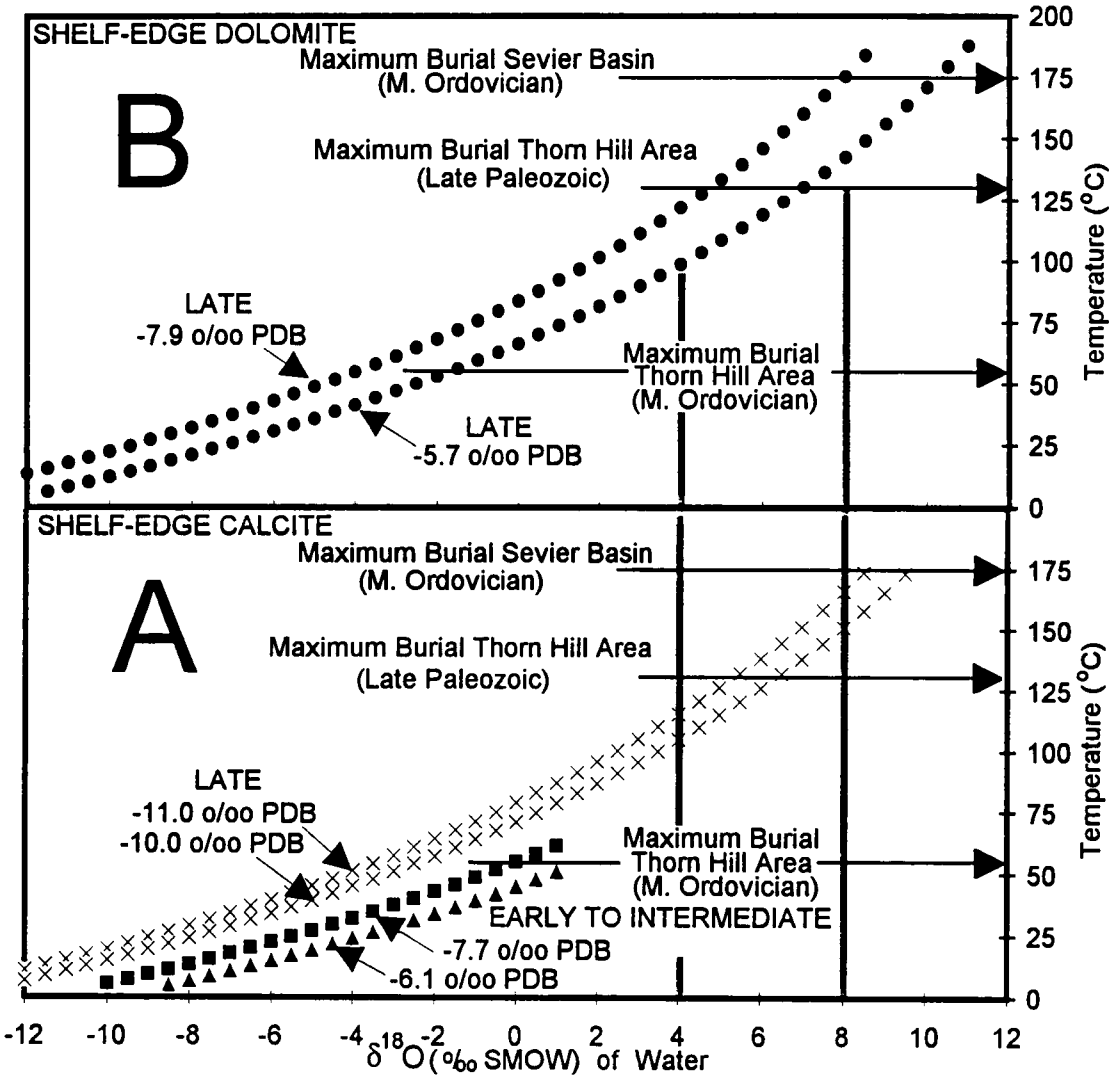
magnesium and manganese. Magnesium and manganese were probably removed from on-shelf fibrous calcite as a result of repeated and frequent subaerial exposure.

**Meteoric Diagenesis.** Crystal (vadose) silt, pendant cement, planar-e dolomite, bladed calcite, and blocky, clear calcite were probably produced during times when large parts of the shelf were exposed. Cross-cutting and competitive growth relationships observed under conventional and cathodoluminescent petrography suggest that crystal or vadose silt and pendant cements were developed early during meteoric diagenesis in the vadose zone (e.g. Dunham, 1969; Longman, 1980) and the bladed and blocky clear calcite formed somewhat later in the phreatic meteoric environment (Figs. 4.15 and 4.16).

Planar-e dolomite was probably not precipitated from meteoric fluids. However, it is listed here because it was probably formed in a supratidal setting when the shelf was exposed and experienced meteoric and / or marine vadose diagenesis (e.g., Deffeys et. al., 1965).

Bladed calcite and blocky, clear calcite have $\delta^{18}O$ and trace element values consistent with precipitation from meteoric waters (e.g., Morse and Mackenzie, 1990; Fig. 4.5, Tables 4.1 and 4.2). However, blocky, clear calcite has a wider range of $\delta^{18}O$ values than bladed calcite. The blocky, clear calcite that is most enriched in $\delta^{18}O$ (-6.1‰ PDB at the shelf-edge and -6.8‰ PDB on the shelf) could have been precipitated from freshwater with a $\delta^{18}O$ of -4.0‰ SMOW at about 25°C or less (Figs. 4.17 and 4.18). On the other hand, the isotopically most depleted blocky,

Figure 4.17 Different possible burial temperatures and burial fluid compositions are compared for calcite and dolomite at the shelf-edge. Numbers associated with the symbols plotted as curved trends show the relationship between $\delta^{18}O$ (PDB) of carbonate, $\delta^{18}O$ (SMOW) of water, and temperature, assuming $10^3 \ln\alpha_{calcite\text{-}water} = 27.8 \times 10^6 T^{-2} - 2.89$ (Friedman and O'Neil, 1977) for the lower plot (A) and $10^3 \ln\alpha_{dolomite\text{-}water} = 2.78 \times 10^6 T^{-2} + 0.91$ (Land, 1985) for the upper plot (B), where T is temperature in degrees Kelvin. Heavy vertical lines enclose a hypothetical upper bound range of possible basin brine compositions based on known values of modern brines, from 4.0‰ to 8.0‰ SMOW (e.g., Kharaka and Carothers, 1986). This should be considered an upper bound estimate because many modern brines are not this enriched (e.g., Rozkowski and Prewlocki, 1974). Burial temperatures are estimated from Figure 4.3. The lower plot (A) shows that the trend for late ferroan, coarse sparry calcite intersects this range of possible brine compositions at about 100°C, a rock temperature that could have been reached at the shelf-edge in the late Paleozoic, but probably not by the end of the Middle Ordovician. Trends for earlier blocky, white calcite and blocky, clear calcite are shown for comparison. These earlier phases could have been precipitated from waters with $\delta^{18}O$ values of less than about 1‰ SMOW before the end of the Middle Ordovician. The upper plot (B) shows that the trend for late ferroan baroque dolomite intersects this range of possible brine compositions at slightly less than 100°C, a rock temperature that could have been reached at the end of the Paleozoic. But if basin brines were involved they reached these temperatures much earlier as indicated by "maximum burial Sevier basin end of Middle Ordovician" lines on the diagram, and may have been injected into the shallower shelf sequence at this time.




- SHELF-EDGE FERROAN BAROQUE DOLOMITE (-5.7 o/oo PDB)
- SHELF-EDGE FERROAN BAROQUE DOLOMITE (-7.9 o/oo PDB)

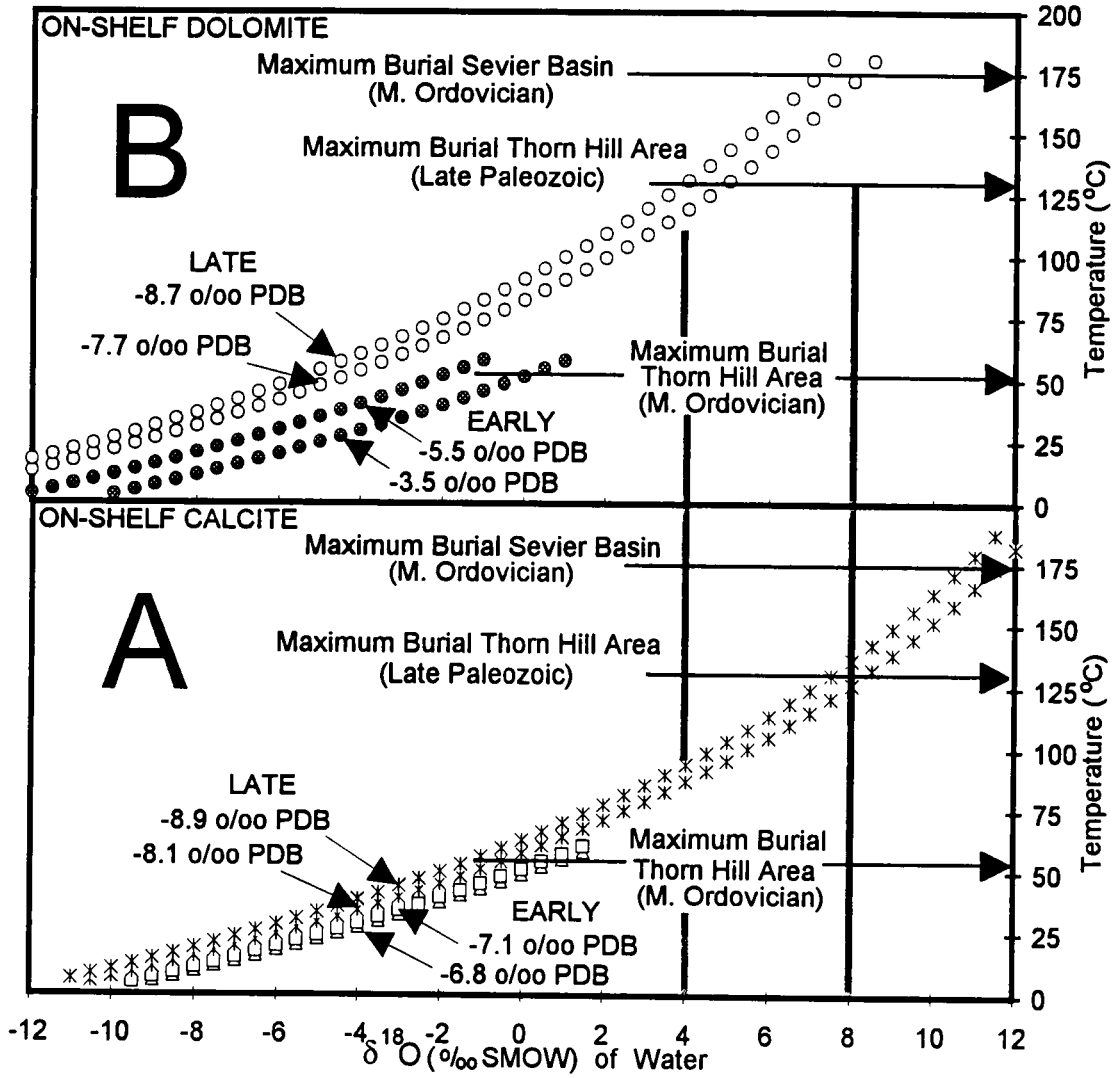
▲ SHELF-EDGE BLOCKY CLEAR CALCITE (-6.1 o/oo PDB)

■ SHELF-EDGE FERROAN BLOCKY WHITE CALCITE (-7.7 o/oo PDB)

× SHELF-EDGE FERROAN COARSE PINK SPARRY CALCITE (-11.0 o/oo PDB)

× SHELF-EDGE FERROAN COARSE PINK SPARRY CALCITE (-10.0 o/oo PDB)

Figure 4.18 Different possible burial temperatures and burial fluid compositions are compared for calcite (A) and dolomite (B) on the shelf. Numbers associated with the symbols plotted as curved trends show the same relationship discussed for Figure 4.17. Heavy vertical lines enclose a hypothetical upper bound range of possible basin brine compositions based on known values of modern brines, from 4.0‰ to 8.0‰ SMOW (e.g., Kharaka and Carothers, 1986). Burial temperatures are estimated from Figure 4.3. The lower plot (A) shows that the trend for late ferroan, coarse sparry calcite intersects this range of possible brine compositions at about 85°C, a rock temperature that could have been reached by the end of the Paleozoic, but probably not by the end of the Middle Ordovician. Trends for earlier blocky, white calcite and blocky, clear calcite are shown for comparison. These earlier phases could have been precipitated from waters with $\delta\ ^{18}O$ values of less than about 1‰ SMOW before the end of the Middle Ordovician. The upper plot (B) shows that the trend for late ferroan baroque dolomite intersects this range of possible brine compositions at more than 100°C, a rock temperature that could have been reached only at the end of the Paleozoic. Alternatively, the Sevier basin is a likely source for fluids that could have precipitated ferroan baroque dolomite from these hypothetical brines before the end of the Middle Ordovician. The trend for earlier Planar-e dolomite is shown for comparison.




- ● ON-SHELF PLANAR-e DOLOMITE (-3.5 o/oo PDB)
- ● ON-SHELF PLANAR-e DOLOMITE (-5.5 o/oo PDB)
- ○ ON-SHELF FERRAON BAROQUE DOLOMITE (-7.7 o/oo PDB)
- ○ ON-SHELF FERROAN BAROQUE DOLOMITE (-8.7 o/oo PDB)
- △ ON-SHELF BLOCKY CLEAR CALCITE (-6.8 o/oo PDB)
- □ ON-SHELF FERROAN BLOCKY WHITE CALCITE (-7.1 o/oo PDB)
- ✳ ON-SHELF FERROAN COARSE SPARRY CALCITE (-8.1 o/oo PDB)
- ✳ ON-SHELF FERROAN COARSE SPARRY CALCITE (-8.9 o/oo PDB)

clear calcite may have formed from the same fluid that precipitated the isotopically most enriched ferroan, blocky calcite. On the shelf, these phases have $\delta^{18}O$ values that overlap between -7.8‰ and -7.1 ‰ PDB, and could have been precipitated from fluids with $\delta^{18}O$ values greater than 0 SMOW at temperatures of about 50°C (Fig. 4.18)

**Early to Intermediate Burial Phases**

Early to intermediate burial phases include non-ferroan and ferroan overgrowth calcite, ferroan blocky white calcite and ferroan vein calcite (Figs. 4.15 and 4.16). Early to intermediate burial calcite has $\delta^{18}O$ values (-7‰ to -8‰ PDB) depleted relative to early diagenetic phases. If these phases were precipitated from waters with $\delta^{18}O$ values greater than 0‰ SMOW, they were probably precipitated from fluids above 50°C. If these fluids were indigenous to the shelf and near shelf-edge, they probably formed after the end of the Middle Ordovician (Figs. 4.17 and 4.18). If, on the other hand, these fluids were derived from the Sevier basin, then they may have formed before the end of the Middle Ordovician (ca. 450 Ma.; Figs. 4.3, 4.17 and 4.18). Trace element content of early to intermediate burial phases is consistent with precipitation for burial fluids of intermediate timing. For example, the iron content of overgrowth and ferroan blocky white calcite is generally lower than that which occurs in ferroan coarse sparry calcite of later timing (Tables 4.1 and 4.2). Some ferroan veins are probably of early to intermediate burial timing. However, cross-cutting and competitive growth relationships and the wide range of $\delta^{18}O$ values and iron content suggest that many veins are of late burial timing (Fig. 4.8).

## Late Burial Phases

Late burial phases include ferroan coarse sparry calcite, ferroan coarse pink sparry calcite, and ferroan baroque dolomite. Cross-cutting and competitive growth relationships of late burial phases from this succession are described and illustrated by Foreman (1989) and Steinhauff et al. (1989). The fluid inclusion content of ferroan coarse sparry calcite and the depleted $\delta^{18}O$ values and high iron content of both calcite and dolomite are indicative of burial diagenesis. Radke and Mathis (1980) have suggested that baroque dolomite is an excellent indicator of burial conditions and elevated temperatures (60° - 150°C). The Sevier basin is the most likely source for the burial fluids precipitating these phases (Figs. 4.3, 4.17 and 4.18). The smectite to illite transformation of clay minerals within the Sevier shale basin many have provided a source of iron for these ferroan phases (Johnson, 1988). Johnson (1988) suggested that these burial fluids were probably saline brines based on the relatively high whole rock sodium content he documented at the shelf-edge relative to a lower sodium content on the shelf.

Interestingly, Mississippi Valley-type deposits are hosted in the upper part of the Knox Group in the study area. Figure 4.7 shows that $^{87}Sr/^{86}Sr$ values of late burial ferroan baroque dolomite occurring within this Middle Ordovician succession are similar to values reported by Kesler et al. (1988) for post-ore dolomite in Lower Ordovician strata of the Knox Group in the study area. Could this post-ore dolomite have been precipitated from the same fluids that precipitated the late burial dolomite reported in the present study?

Limited data make interpretation of clear sparry calcite and non-ferroan calcite speculative. Cross-cutting and competitive growth relationships indicate that clear, sparry calcite and non-ferroan dolomite are the latest phases. Clear, sparry calcite is interpreted as deep meteoric based on its relative lack of fluid inclusions and anomalous stable isotope values. Non-ferroan calcite follows the clear sparry calcite and may indicate a second burial event (e.g., Radke and Mathis, 1980) (Fig. 4.15).

## DISCUSSION OF CALCITE-FILLED CAVITIES AND VUGS

Calcite-filled cavities and vugs occur below many third- and fourth-order sequence surfaces at on shelf and shelf-edge positions (e.g., chapters 2 and 3; Steinhauff and Walker, in prep. a). These filled pores, cavities, and vugs are more conspicuous and larger below third-order sequence stratigraphic surfaces than those that occur below fourth-order sequence surfaces. Many of the larger cavities and vugs that occur below third-order sequence surfaces are filled with several cement generations, yet some still retain a very small amount of porosity (Fig. 4.14).

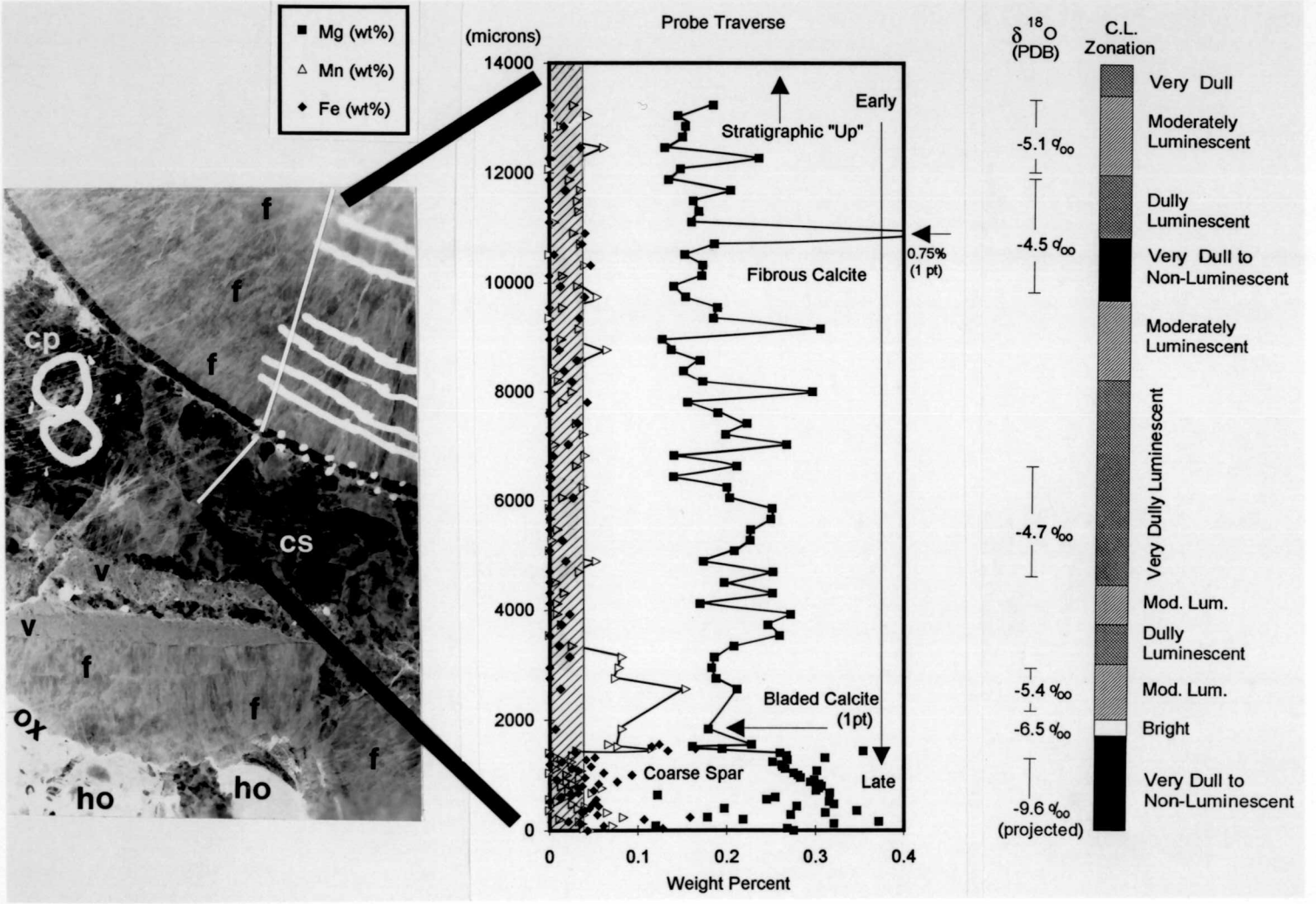
Abundant fibrous and bladed calcite occurs stratigraphically below third-order and fourth-order sequences boundaries. On the shelf, for example, these cements occur exclusively as linings in cavities and vugs developed during subaerial exposure. They must represent fillings precipitated during a "second-cycle" or in some cases perhaps a "third-cycle" of early diagenesis (Fig. 4.16). Similarly, many, but not all of the fibrous and bladed cements at the shelf-edge fill cavities and vugs developed during subaerial exposure. However, cavities are also developed as part of the

normal biological processes on the shelf-edge. Solution vugs not formed during subaerial exposure, however, have probably been developed along the middle Ordovician shelf by dissolution during relative rise in sea-level as deep marine (?), reducing, undersaturated waters impinged on the shelf-edge. Johnson (1988) has documented such examples further down the slope. Circumstantial evidence for partial dissolution exists at Poor Valley Creek, the bathymetrically deepest section in this study. Evidence for extensive marine dissolution, however, is lacking. Figures 4.19 illustrates the trace element and stable carbon and oxygen isotope distribution in vug fillings.

**Interpretation: Shelf-Edge Diagenetic Example**

A typical shelf-edge diagenetic succession within Subsequence 2C at Poor Valley Creek is illustrated in Figure 4.19. Subsequence 2C at Poor Valley Creek is a condensed section and probably also includes the condensed intervals of subsequences 2A and 2B at its base (see Fig. 3.11). The host sediment (ho) a wackestone / packstone was deposited in water at least 0.5 meters deep. A deepening event followed (probably event $D_3$ of chapters 2 and 3, and Steinhauff and Walker (in press, in prep a). Black Fe / Mn oxide-rich laminae (ox) and orthocone cephalopods were deposited during this time of slow sedimentation, producing a condensed section. Semicircular fibrous and bladed calcite in the upper right part of the photo-negative in Figure 4.19 is a cast of an orthocone cephalopod. Several generations of fibrous calcite follow. The earliest of these may have been precipitated before deepening event $D_4$ and may have been partially dissolved during that event. The

Figure 4.19 Electron microprobe traverse (right) along calcite filled cavity (photo-negative image - left) from shelf-edge locality at Poor Valley Creek, Subsequence 2C (approximately 12 to about 27 meters above the Knox unconformity). Photo-negative: narrow straight lines (white) indicate probe traverse. Uneven white lines are India ink used to help locate different phases and zones during electron microprobe analysis, ho = host sediment; ox = black, Fe / Mn oxide-rich laminae; f = fibrous calcite; v = internal sediment followed by crystal or vadose silt; b = bladed calcite; cs = ferroan coarse sparry calcite; cp = ferroan coarse pink sparry calcite. Note that serially cut thin-sections demonstrate that the two layers of internal sediment with vadose silt (v) are the same; this view is slightly oblique to the horizontal. Paragenetic relationships are discussed in the text. The black area above "cs" is a hole in the thin-section and represents material removed for A.A. trace element analysis by Jernigan (1988). Microprobe traverse: Fibrous calcite has cathodoluminescent zones ranging from non-luminescent to moderately luminescent (cathodoluminescent zones in fibrous calcite are slightly more gradational than actually depicted). Brackets next to the column that shows cathodoluminescent properties of cement indicate the position of material removed for $\delta^{18}O$ analysis. Note that $\delta^{18}O$ values, and Mg and Mn concentrations are different for different zones. The trace element values for coarse spar are not connected because this area is densely sampled. This ferroan coarse spar is intermediate in timing relative to earlier ferroan coarse sparry calcite (cs) and later coarse pink sparry calcite (cp). This coarse spar has a mean $MgCO_3$ content (about 0.97 mole %) intermediate between the mean value for ferroan coarse sparry calcite (about 0.6 mole %) and the mean value for coarse pink sparry calcite (1.01 mole %). This coarse spar has mean iron and manganese contents similar to that of coarse pink sparry calcite (about 0.27 wt % and 0.10 wt %, respectively). In contrast, ferroan coarse sparry calcite has a manganese content of 0.05 wt % and an iron content that is presumably lower as well (c.f., Table 2).

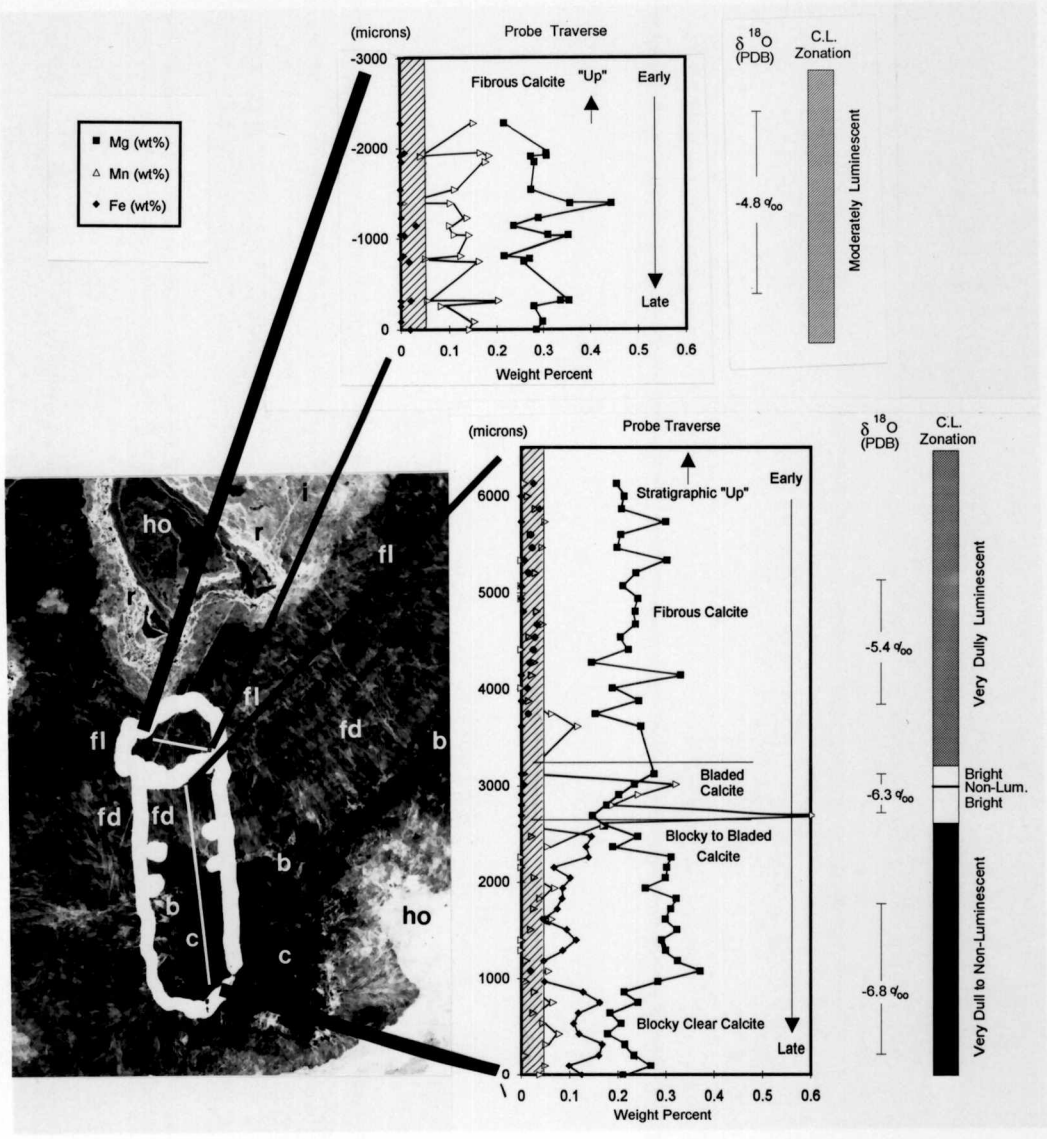

Mg (wt%)
Mn (wt%)
Fe (wt%)
cp
f
cs
v
ox
ho
Probe Traverse
(microns)
14000
12000
10000
8000
6000
4000
2000
0
Early
Stratigraphic "Up"
0.75%
(1 pt)
Fibrous Calcite
Bladed Calcite
(1pt)
Coarse Spar
Late
0
0.1
0.2
0.3
0.4
Weight Percent
δ 18O
(PDB)
C.L.
Zonation
-5.1 ‰
-4.5 ‰
-4.7 ‰
-5.4 ‰
-6.5 ‰
-9.6 ‰
(projected)
Very Dull
Moderately
Luminescent
Dully
Luminescent
Very Dull to
Non-Luminescent
Moderately
Luminescent
Very Dully Luminescent
Mod. Lum.
Dully
Luminescent
Mod. Lum.
Bright
Very Dull to
Non-Luminescent

aragonitic cephalopod skeleton was probably dissolved or replaced during this corrosive event. Precipitation of fibrous calcite probably continued following deepening event $D_4$. Internal sediment followed by crystal or vadose silt overlies this fibrous calcite. The crystal or vadose silt suggests subaerial exposure (e.g., Dunham, 1969). This exposure is probably related to that which produced the surface separating subsequences 2C and 2D (see Fig. 3.11). Reddish crusts (not shown in Figure 19) are of similar timing as crystal or vadose silt. Bladed calcite follows the silt. The $\delta^{18}O$ values of this bladed calcite fall outside the field for fibrous calcite and suggest that it is a product of freshwater diagenesis (Fig. 4.5). The remaining pore space was subsequently filled with burial phases (i.e., ferroan, coarse sparry calcite through ferroan, coarse pink sparry calcite). Note that other intervals within Subsequence 1C at Poor Valley Creek have fibrous calcite that follows the reddish crusts rather than bladed cement as shown in this example. Thus, these intervals probably experienced two early diagenetic (marine) cycles (e.g., Fig. 4.15). The first cycle is that associated with the relative sea-level rise which lead to deposition of Sequence 2C and the second cycle is that associated with the relative sea-level rise that lead to the deposition of overlying Subsequence 2D (see Fig. 3.11).

### Interpretation: On-Shelf Diagenetic Example

A typical on-shelf diagenetic pathway for Subsequence 3D at the Idol Mine section is illustrated in Figure 4.20. Subsequence 3D consists of thin, interbedded mudstone and peloidal grainstone (Fig. 4.2). The host sediment (ho), a fenestral

Figure 4.20 Electron microprobe traverse (right) along calcite filled cavity (photo-negative image - left) from on-shelf locality at Idol Mine section, Subsequence 3D (234.7 meters above the Knox unconformity). Photo-negative: narrow straight lines (white) indicate probe traverse. Uneven white lines are India ink used to help locate different phases and zones during electron microprobe analysis, ho = host sediment; r = reddish crust (hematite-rich laminae); i = internal sediment; fl = fibrous calcite, moderately luminescent; fd = fibrous calcite, dully luminescent; b = bladed calcite; c = blocky clear calcite. Paragenetic relationships are discussed in the text. Microprobe traverse: Fibrous calcite has cathodoluminescent zones ranging from non-luminescent to moderately luminescent (cathodoluminescent zones in fibrous calcite are slightly more gradational than actually depicted). Brackets show position of material removed for $\delta^{18}O$ analysis. Note that $\delta^{18}O$ values, and magnesium and manganese concentrations are different for different zones and phases.


Mg (wt%)
Mn (wt%)
Fe (wt%)
(microns)
Probe Traverse
-3000
-2000
-1000
0
Fibrous Calcite
"Up"
Early
Late
0 0.1 0.2 0.3 0.4 0.5 0.6
Weight Percent
δ 18O (PDB)
C.L. Zonation
-4.8 ‰
Moderately Luminescent
(microns)
Probe Traverse
6000
5000
4000
3000
2000
1000
0
Stratigraphic "Up"
Early
Fibrous Calcite
Bladed Calcite
Blocky to Bladed Calcite
Blocky Clear Calcite
Late
0 0.1 0.2 0.3 0.4 0.5 0.6
Weight Percent
δ 18O (PDB)
C.L. Zonation
-5.4 ‰
Very Dully Luminescent
-6.3 ‰
Bright
Non-Lum.
Bright
-6.8 ‰
Very Dull to Non-Luminescent
ho
r
i
fl
fd
b
c

mudstone, was deposited in very shallow water (less than 0.5 meters deep) and was probably exposed during low tide (Steinhauff and Walker, 1992; in press). Laminated reddish crusts (r), slightly less that one millimeter thick, cross-cut the host sediment and suggest an interval of relatively intense subaerial exposure. Note that the host sediment (ho) and reddish crusts (r) labeled in Figure 4.20 are part of a projection within a very irregular vug. These reddish crusts completely enclose the vug outside the field of view. The reddish crusts were probably developed during exposure which produced the surface separating third-order sequences 3 and 4 (Fig. 4.2; chapters 2 and 3; Steinhauff and Walker, in press, in prep. a). Internal sediment follows these reddish crusts and is followed by at least two fibrous calcite zones. The internal sediment was probably deposited during the rise in relative sea-level which lead to the deposition of Subsequence 4A (Fig. 4.2). Similarly, fibrous calcite was precipitated from marine fluids during the time that Subsequence 4A was deposited. However, deposition of Subsequence 4A was probably not a continuous process. Indeed, five, fifth-order parasequences comprise Subsequence 4A (chapter 2; Steinhauff and Walker, 1992; in press). These fifth-order parasequences probably represent autocyclic processes; changes in relative sea-level during fifth-order parasequence development were probably very minor. Bladed calcite follows the fibrous calcite. The bladed calcite consists of three cathodoluminescent zones: bright, non-luminescent, and bright. The brightly luminescent bladed calcite was probably precipitated from fresh-water during the time that the surfaces separating Subsequence 4A from Subsequence 4B and / or Subsequence 4B from Subsequence 4C were

subaerially exposed. The intervening non-luminescent zone may have been precipitated from marine fluids, possibly associated with the deposition of Subsequence 4B (Fig. 4.2). Blocky clear calcite with a somewhat drusy fabric follows the bladed calcite. This blocky clear calcite was probably precipitated from deep meteoric or shallow burial fluids. These fluids may have evolved as early as the time in which the surface separating Subsequence 4B from Subsequence 4C was subaerially exposed (Fig. 4.2).

## CONCLUSIONS

1) Diagenetic pathways for sediments on the shelf were different than those for sediments at the shelf-edge. Intervals that retained porosity the longest occur below third- and fourth-order sequence surfaces at on-shelf and shelf-edge positions (e.g., Steinhauff and Walker, 1992; in press, in prep a). Vugs and cavities were developed below many of these sequence boundaries during subaerial exposure. Detailed petrography and knowledge of the sequence stratigraphy suggests that early diagenetic phases that fill cavities and vugs represent fillings precipitated during a "second-cycle" or in some cases perhaps a "third-cycle" of early diagenesis (Figs. 4.14 and 4.15). Early diagenetic phases on the shelf were precipitated in relatively open systems, whereas early diagenetic phases at the shelf-edge were precipitated in relatively closed systems (e.g., Fig. 4.6). Early on-shelf phases probably experienced exposure more frequently than early phases at the shelf-edge (e.g., Fig. 4.2).

Intermediate through late burial phases at the shelf-edge represent more fluid dominated systems than their paragenetic counterparts on the shelf (Figs. 4.8 and 4.9). Intermediate through late burial phases at the shelf-edge have more depleted $\delta^{18}O$ values and higher iron and manganese contents than their counterparts on the shelf (Figs. 4.9 - 4.13), and are more enriched in $^{87}Sr$ than those on the shelf (Fig. 4.7). This may be explained in terms of water rock interaction. If the source of the fluids precipitating late burial phases was the Sevier basin, then fluids at the shelf-edge would have encountered less carbonate rock than those traveling to on-shelf positions.

2) Phases interpreted as meteoric in origin do not show the large depletions in $\delta^{13}C$ that other workers have observed in younger rocks. For example, Gross (1964) noted that meteoric Pleistocene carbonates from Bermuda are depleted more than 10‰ relative to shallow marine values. Similarly, Late Paleozoic meteoric carbonates studied by Meyers and Lohmann (1985) are depleted by about 5‰. Interestingly, Zempolich, et al. (1988) reported little or no $\delta^{13}C$ depletion in the phases that they interpreted as meteoric in origin within Late Proterozoic carbonates of the Beck Spring Dolomite from Southern California. Similarly, meteoric phases in the present study are depleted from marine phases by about 2‰ or less (Fig. 4.5).

Stable carbon and oxygen isotopic values of early Paleozoic marine and meteoric phases are not well known (Popp et al. , 1986). In fact, this study estimates the original $\delta^{18}O$ value of Middle Ordovician marine calcite to be about -4.2‰ PDB and the $\delta^{13}C$ value to be about 0.4‰ PDB. The apparent lack of $\delta^{13}C$ depletion in

meteoric phases relative to marine phases is either real or a sampling artifact. Bias could have been introduced because small samples (less than 0.2 mg) were not analyzed. The inability to analyze samples smaller than about 0.2 mg has precluded the sampling of thin, brightly luminescent zones (less than about 0.2 mm thick and generally much thinner). Such zones are likely to have been precipitated from meteoric fluids.

Assuming that this lack of enrichment is real, the light $^{12}C$ isotope may not have been abundant in Middle Ordovician groundwater. Meteoric cements in younger carbonate rocks derive their $^{12}C$ from the decay of plant derived organic matter (e.g., Hudson, 1977). The first major adaptive radiation of land plants was marked by the rise of the spore tetrads in the late middle Ordovician to mid-late Silurian (Caradoc to the mid-late Llandovery). This was followed by a second major radiation of the vascular plants in the mid-late Silurian (Llandovery to the Pridoli; Gray, 1984, 1985; Gensel and Andrews, 1987). In contrast, this Middle Ordovician succession is slightly older (Llanvirian to Carodocian). If land plants inhabited any of the freshwater environments represented in this Middle Ordovician succession, it is likely that they were not the vascular plants characteristic of the later Paleozoic, and that they were not very abundant. Thus, decay of plant derived organic matter may have been limited and it probably did not contribute significant amounts of the light $^{12}C$ isotope to the groundwater (e.g., Saller and Moore, 1991).

3) The Sevier basin is the most likely source of burial fluid that precipitated the late burial phases (Figs. 4.1 and 4.3). Late ferroan coarse sparry calcite and

ferroan baroque dolomite could have been generated from brines expelled from the Sevier basin before the end of the Middle Ordovician (ca. 540 Ma.). This is based an analysis of burial curves, possible temperatures, and an assumed range of likely brine compositions (Figs. 4.3, 4.17, 4.18).

# SEQUENCE STRATIGRAPHY AND COMPARATIVE DIAGENESIS OF MIDDLE ORDOVICIAN SHELF TO SHELF-EDGE LIMESTONES, THE COPPER CREEK ALLOCHTHON, EAST TENNESSEE

A Dissertation

Presented for the

Doctor of Philosophy

Degree

The University of Tennessee, Knoxville

D. Mark Steinhauff

August, 1993

VOLUME 2

# CHAPTER 5

## PRELIMINARY ANALYSIS OF DIAGENETIC TRENDS IN THIRD-ORDER STRATIGRAPHIC SEQUENCES, MIDDLE ORDOVICIAN, EAST TENNESSEE

## INTRODUCTION

This chapter draws on the shelf to shelf-edge sequence stratigraphic framework developed in chapters 2 and 3, and the diagenetic history elucidated in chapter 4 to explore diagenetic geochemical trends within that shelf to shelf-edge sequence stratigraphic framework. Most sequence stratigraphic studies do not consider diagenesis. If diagenesis is discussed at all, it is usually simplified and greatly generalized (e.g, Sarg, 1989). Likewise, diagenetic studies tend to focus on elucidating the paragenetic sequence and do not consider the sequence stratigraphy. Those diagenetic studies that have considered sequence stratigraphy generally concentrate on the effects of one or two exposure surfaces in a few tens of meters of strata (e.g., Meyers and Lohmann, 1985) and/or restrict their analysis to platform interior areas (e.g, Niemann and Read, 1988).

### Objectives

The diagenetic history of the Middle Ordovician shelf and shelf-edge successions were elucidated in chapter 4 using a "traditional" approach. The

traditional approach relies on petrographic observations made using both conventional and cathodoluminescent petrography to interpret the origin and timing of pore-fillings (e.g., Walker, 1989). Geochemical data support petrographic observations and provide corroborating evidence. The traditional approach can be (and generally has been) applied with limited knowledge of the sequence stratigraphic framework.

In contrast, emphasis in the present chapter is on how subaerial exposure that led to development of third- and fourth-order stratigraphic sequences also influenced later diagenetic trends. The present study presents specific diagenetic examples, both early and late, from on-shelf and shelf-edge positions relative to the evolution of three, third-order stratigraphic sequences (about 400 meters thick). The sequence stratigraphy (chapters 2 and 3; Steinhauff and Walker, 1992a, 1992b, in press, in prep. a) and diagenesis (chapter 4; Walker, et al. 1986; Steinhauff et al., 1989; Steinhauff and Walker, in prep. b) are well documented for this succession.

A complicating factor is that the Middle Ordovician carbonate shelf and platform has evolve through time. For example, platform interior sediments prograded to the shelf-edge and the area that was once the shelf-edge become more like the platform interior (see chapter 3). Hence, early diagenetic processes that affected the platform interior also influenced sediments deposited at the former shelf-edge. Thus, through time, the early diagenetic pathway affecting sediments at the shelf-edge was altered. Specifically, this chapter discusses how early diagenetic processes affecting third-order Sequence 2 were initially different on the shelf as compared to those at the shelf-edge. These early diagenetic trends continued to

influence later diagenesis in Sequence 2 on the shelf and at the shelf-edge. Later burial diagenetic products influenced Sequence 2 strata at the shelf-edge, but had a lesser effect on the shelf. Later, by the time Sequence 4 was deposited, platform interior sediments had prograded to the shelf-edge. Thus, early diagenetic processes in Sequence 4 were similar on the shelf and at the former shelf-edge. Hence, later diagenesis on the shelf and at the former shelf-edge was similar as well.

## Background

Middle Ordovician carbonates of East Tennessee probably contain a record of diagenesis at least as complete as that of any Paleozoic succession and certainly much more complete than most successions of the later Paleozoic. Diagenetic products, such as marine cement, commonly fill the first available pore space. During geologic intervals such as the Middle Ordovician, calcite rather than aragonite was the favored phase precipitated in marine environments (Sandburg, 1983; Walker et al., 1990). These calcite phases occupy early pore positions and commonly occlude all available pore space. In the present study, much of the pore space that these early marine phases fill was developed as a result of earlier subaerial exposure (see chapter 4; Steinhauff and Walker, in prep. b). Furthermore, these calcite phases are relatively stable and are not readily dissolved during subsequent changes in pore fluid composition. In contrast, aragonite phases are easily dissolved. Thus, once marine calcite was precipitated in a pore, a chain of events was initiated that generally resulted in a relatively simple filling of the remaining pore space with phases

precipitated from freshwater and burial fluids (e.g., Walker, 1989; Steinhauff et al., 1989). This chain of events is halted when the pore is completely occluded. In some instances pores were completely occluded with fibrous calcite very early in the diagenetic history of the succession. In other cases, pores are successively filled with almost the entire suite of paragenetic phases, yet still retain a minor amount of porosity

## Study Area

The study area was the same as that described in chapters 3 and 4. It consists of four on-shelf localities and three shelf-edge or near shelf-edge localities (see Fig. 4.1 of chapter 4). The regional environmental/stratigraphic framework and previous work are considered in chapters 2, 3, and 4.

## Methods

Stratigraphic, petrographic, and field methods are described in chapters 2 and 3, geochemical methods (stable isotope ratio analyses of carbon and oxygen, radiogenic strontium ratio analyses, and electron microprobe analyses) are described in chapter 4.

**Atomic Absorption Analysis.** Bulk samples (about 5 grams) and micro-bulk samples (0.1 to 0.2 grams) were prepared from crushed rock, weighed, and brought into solution with 25% (volume/volume) glacial acetic acid. The sample residue not dissolved was reweighed and the result was subtracted from the total weight of

carbonate dissolved. The elements Na, Mg, Fe, and Mn were analyzed on a Varian AA-475 atomic adsorption spectrophotometer using an air-acetylene flame and Sr was analyzed using a nitrous oxide-acetylene flame. Potassium was added as an ionization buffer to calibration and unknown solutions analyzed for Na, Mg, and Sr; lanthanum was added as a releasing agent to calibration and unknown solutions for Mg analyses. Concentrations were determined using the analytical curve technique. Precision was monitored with NBS 1a (SRM 2023), an argillaceous limestone and NBS-20. Additional details are described by Johnson (1988; see also, Appendix G).

## DIAGENETIC TRENDS

### On-Shelf and Shelf-Edge Fibrous and Bladed Calcite

Abundant fibrous and bladed calcite occurs stratigraphically below third-order and fourth-order sequences boundaries. On the shelf, these cements occur exclusively as linings in cavities and vugs developed during subaerial exposure. They represent fillings precipitated during a "second-cycle" or in some cases perhaps a "third-cycle" of early diagenesis (see chapter 4). Similarly, many, but not all of the fibrous and bladed cements at the shelf-edge fill cavities and vugs developed during earlier subaerial exposure.

These filled pores, cavities, and vugs are more conspicuous and larger below third-order sequence stratigraphic surfaces than those that occur below fourth-order subsequence surfaces. Many of the larger cavities and vugs that occur below third-order sequence surfaces are filled with several cement generations, yet some still

retain a very small amount of porosity. In contrast, smaller cavities and vugs associated with fourth-order surfaces contain at most three cement generations (fibrous calcite, bladed calcite, and bladed to blocky calcite). Most of these smaller cavities are completely occluded by a single phase such as fibrous or blocky calcite.

Figure 5.1 shows $\delta\ ^{18}O$ values of fibrous calcite and bladed calcite versus stratigraphic position. These values occur at discrete stratigraphic positions because fibrous and bladed calcite occurs stratigraphically below third-order and fourth-order sequences boundaries as linings in cavities and vugs developed during subaerial exposure.

## On-Shelf Blocky Calcite and Ferroan Calcite Veins

**On-Shelf Blocky Calcite.** On-Shelf blocky, clear calcite (-7.8‰ to -6.8‰ PDB) is enriched in $\delta^{18}O$ relative to ferroan on-shelf blocky, white calcite (-8.4‰ to -7.1‰ PDB; Table 4.2) with a considerable range of overlap between these two phases (Figs. 4.5 and 4.8). Indeed, taken together, $\delta^{18}O$ ranges over 1.6‰ in these on-shelf blocky calcite cements. However, when on-shelf blocky calcite is plotted within third-order sequences against stratigraphic position the range of $\delta^{18}O$ values are narrower in any one sequence (Fig. 5.2).

Figure 5.2 shows three simple linear regressions, one each for third-order sequences 2, 3, and 4. The $\delta^{18}O$ values of both blocky clear and ferroan, blocky white calcite are lumped and treated as the dependent variable plotted against stratigraphic position. Blocky clear and ferroan,blocky calcite are lumped because they are of similar paragenetic timing and appear to represent a continuum of fabrics

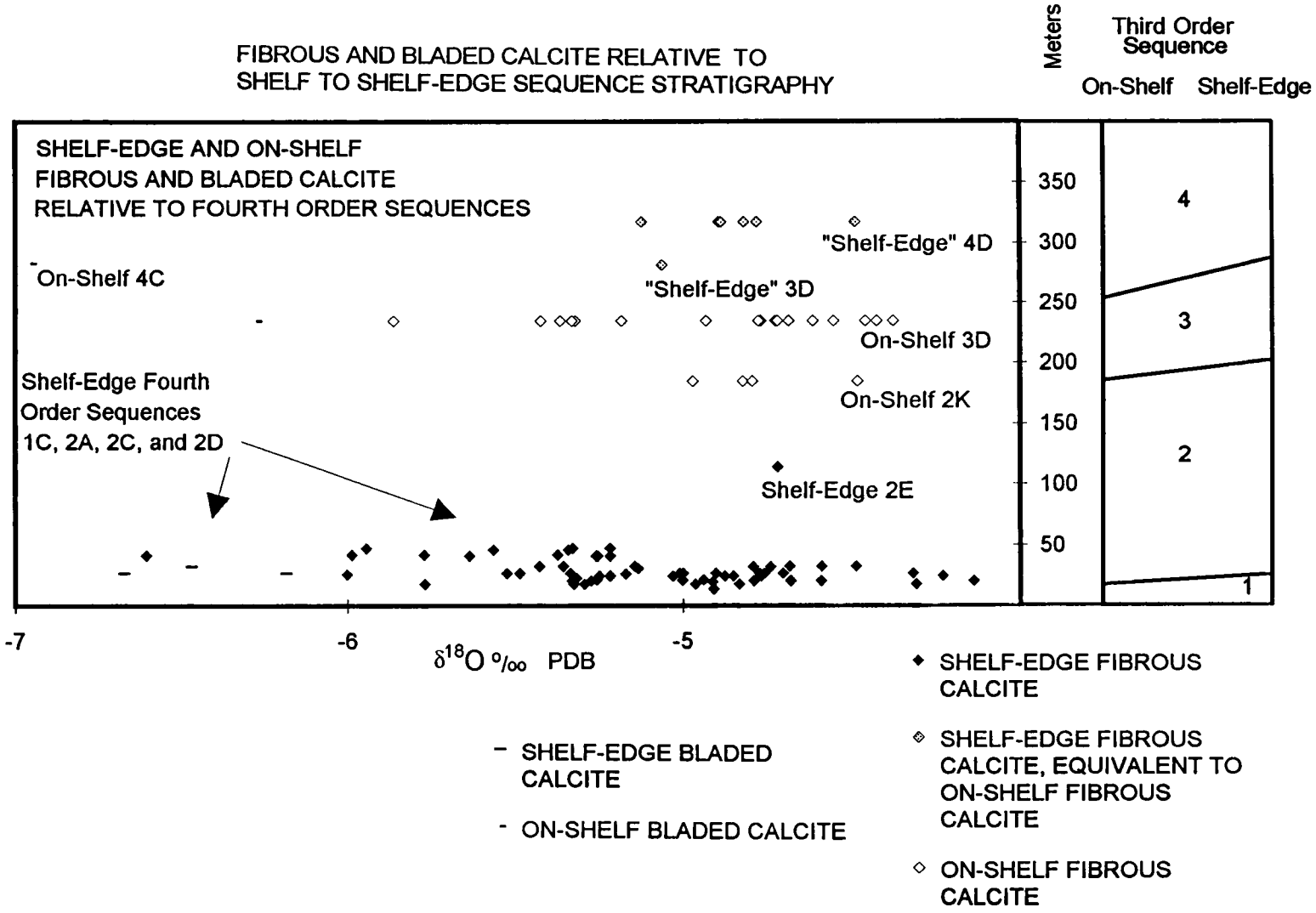



Figure 5.1. Values of $\delta^{18}O$ for fibrous and bladed calcite versus stratigraphic position above the Knox unconformity

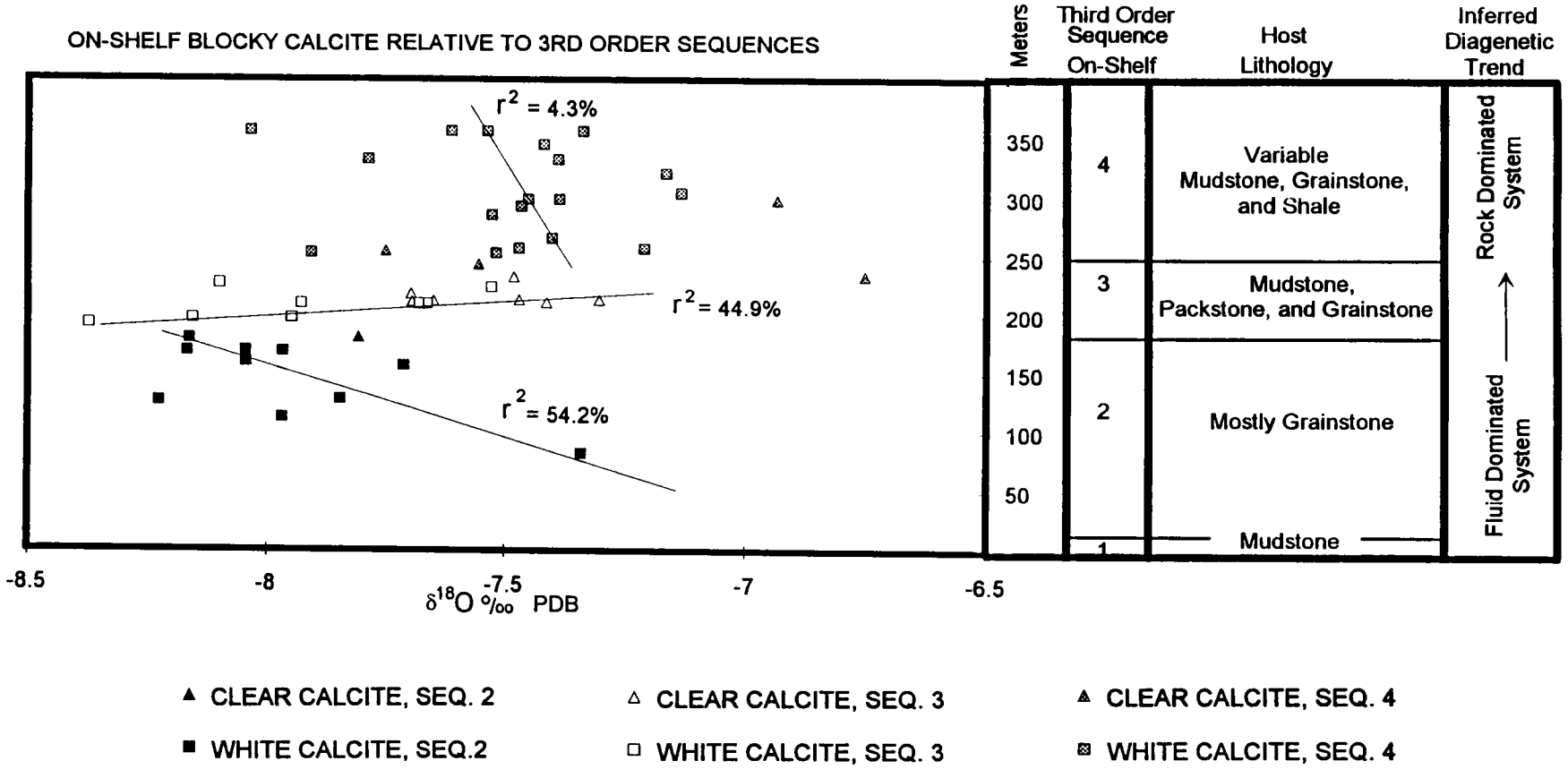



Figure 5.2. Simple linear regressions (method of least squares), for third-order sequences 2, 3, and 4 on the shelf. The dependent variable is the $\delta^{18}O$ value of both blocky clear and ferroan blocky white calcite and the independent variable is stratigraphic position. For Sequence 2, N = 12; for Sequence 3, N = 17; and for Sequence 4, N = 22. None of the R-squared values are statistically significant.

and a continuum of isotopic and trace element content. In keeping with geologic convention, stratigraphic position is displayed on the vertical axis even though it is the independent variable. The data are normally distributed. Note that the R-squared values explaining the data associated within each third-order sequence are not statistically significant.

However, the $\delta^{18}O$ values of blocky calcite distributed among stratigraphic sequences 2, 3, and 4 are statistically discernible. One-factor and two factor analysis of variance shows that all of the sample means among blocky, white calcite (compared alone and grouped with clear, blocky calcite) occurring in sequences 2, 3, and 4 are statistically discernible at the 0.05 level. Indeed, most of the means are discernible at the 0.01 level. Additionally, differences in average rank among $\delta^{18}O$ values of blocky calcite from stratigraphic sequences 2, 3, and 4 were evaluated using non-parametric statistics (Kruskal-Wallis analysis). All of the differences in rank were discernible at the 0.05 level and most were discernible at the 0.01 level.

A measure of the shift in $\delta^{18}O$ values of blocky calcite among third-order sequences 2, 3, and 4 and the interaction of $\delta^{18}O$ values with change in stratigraphic position is made through multiple regression with dummy variables (e.g., Wannacott and Wannacott, 1984). Figures 5.3 and 5.4 compare third-order sequences 2 and 3 and third-order sequences 3 and 4, respectively. The shift in $\delta^{18}O$ values of blocky calcite between sequences 2 and 3 is $1.0 \pm 0.8‰$ PDB (Fig. 5.3). The shift in $\delta^{18}O$ values of blocky calcite between sequences 3 and 4 is $-1.0 \pm 0.5‰$ PDB (Fig. 5.4). Both shifts are statistically discernible at the 0.05 level.

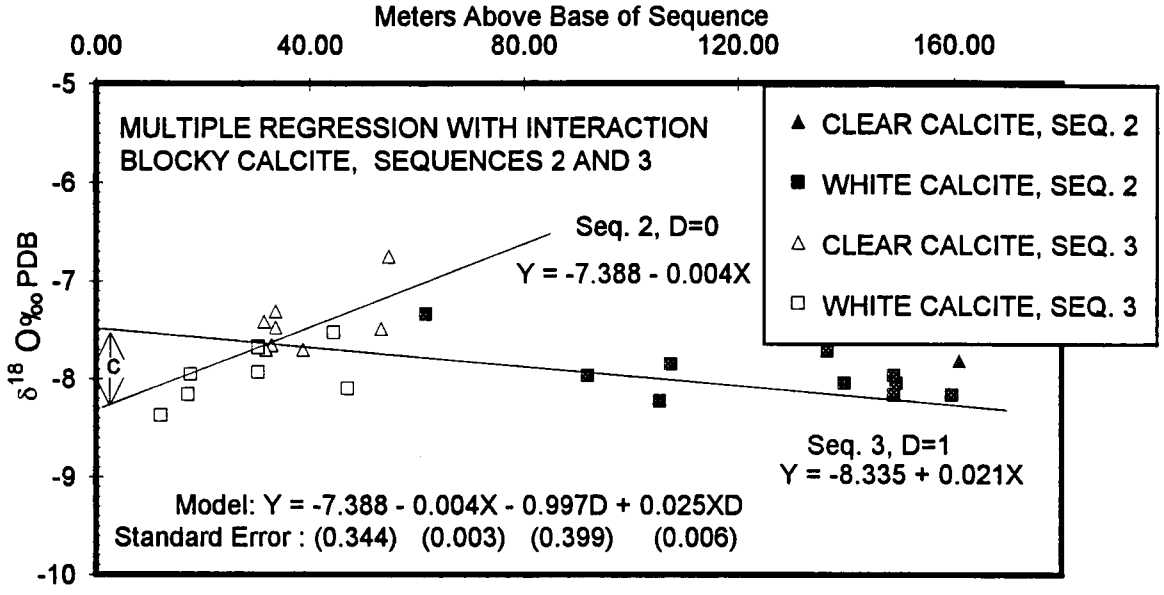



Figure 5.3. Multiple regression with interaction using stratigraphic sequences 2 and 3. The dependent variable, the $\delta^{18}O$ value of blocky calcite, is regressed on three independent regressors: (1) stratigraphic position "X" (expressed in meters above the base of the sequence), (2) the dummy variable "D", a 0-1 variable used to distinguish between the two sequences being compared, and (3) the interaction between the dummy variable and stratigraphic position "XD." The equation is of the form: $Y = a + bX + cD + eXD$. In this way its is possible to investigate how stratigraphic sequence affects $\delta^{18}O$ value of blocky calcite. This is the difference in the slope intercepts "c". Similarly, the contribution introduced by change in stratigraphic position within each sequence is evaluated as the change in slope "e" (not shown). Sequence 2 (N = 11) is compared with Sequence 3 (N = 17). The variable "c" or the shift in $\delta^{18}O$ values of blocky calcite between sequences 2 and 3 is $0.997 \pm 0.918$‰ PDB. This rounds to $1.0 \pm 0.9$‰ PDB within the analytical limits of precision. Note that values in the model are given to three significant figures to avoid showing variables that are multiplied by zero. The change in slope "e" is $0.025 \pm 0.0124$; a value that is negligible within analytical limits of precision. Similar results are obtained when the model does not account for the interaction between D and X, and when ferroan, blocky white calcite is not combined with blocky, clear calcite.

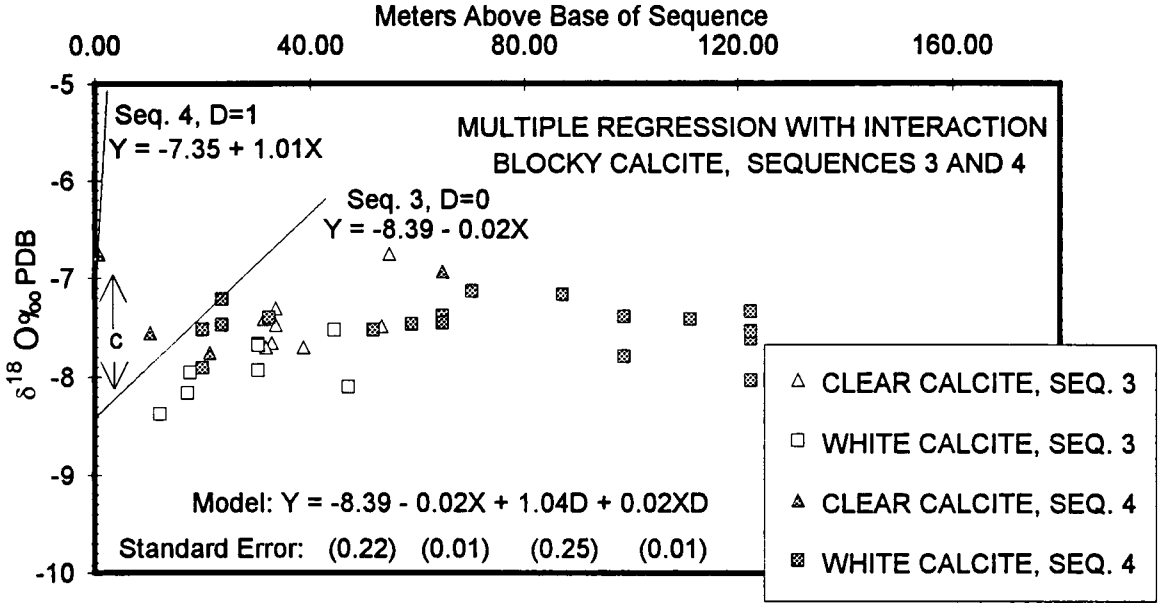



Figure 5.4. Multiple regression with interaction using stratigraphic sequences 3 and 4. Same model as described in Figure 5.3. Sequence 3 (N=17) is compared with Sequence 4 (N = 22). The shift in $\delta^{18}O$ values of blocky calcite between sequences 3 and 4, "c" is -1.0 $\pm$ 0.5‰ PDB within analytical limits of precision. The slope "e" is negligible. Both "c" and "e" are statistically discernable at the 0.05 level. Similar results are obtained when the model does not account for the interaction between D and X, and when ferroan, blocky white calcite is not combined with blocky, clear calcite.

**On-Shelf Ferroan Calcite Veins.** This vein calcite has $\delta^{18}O$ values (-10.6‰ to -6.9‰ PDB) that overlap with blocky, clear calcite (-7.8‰ to -6.8‰ PDB) and ferroan, blocky white calcite (-8.4‰ to -7.1‰ PDB; c.f., Figs. 4.5, 4.8, 5.3, 5.4; Table 4.2). Vein calcite and ferroan, blocky white calcite come from similar stratigraphic positions (c.f., Figs. 5.2 and 5.5). Cross-cutting relationships indicate that many ferroan calcite veins are of similar timing as ferroan, blocky white calcite. Indeed, vein fabric is virtually indistinguishable from that of blocky white calcite and many veins lead into cavities filled with blocky white calcite. Since different values of $\delta^{18}O$ are associated with different stratigraphic sequences, one might expect different values of $\delta^{18}O$ vein calcite to be similarly associated with different stratigraphic sequences. Although the on-shelf vein data set is small (N = 12), stratigraphic associations similar to those observed for blocky calcite are not apparent when $\delta^{18}O$ values are plotted against stratigraphic position (c.f., Figs. 5.2 and 5.5). Rather, regression of $\delta^{18}O$ values against vein width explains about 83% of the data (Fig. 5.6).

**Discussion.** Depletion and enrichment of $\delta^{18}O$ values in blocky calcite relative to stratigraphic sequences can be explained in terms of water-rock interaction (Fig. 5.2). Third-order Sequence 2 consists predominantly of massive grainstone that would have retained significant porosity during early to intermediate burial diagenesis. In contrast, third-order Sequence 3 consists of mudstones, packstones, and grainstones which would have retained less porosity than Sequence 2 during early to late burial

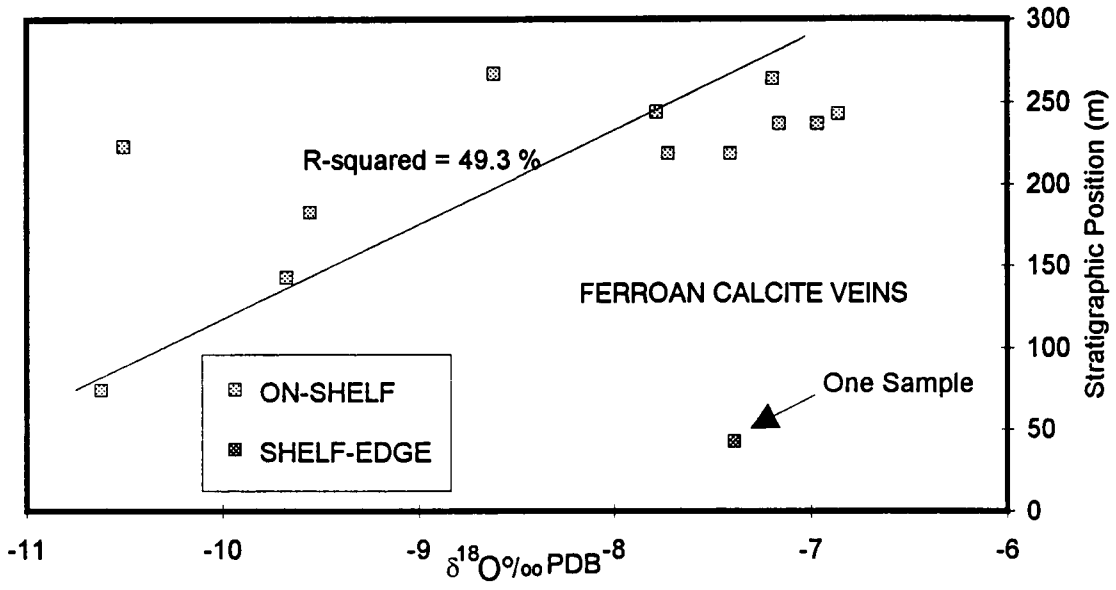



Figure 5.5 On-shelf vein calcite $\delta^{18}O$ values are plotted against stratigraphic position (N=12). Shelf-edge vein calcite is shown for comparison, but is not included in the least-squares regression.

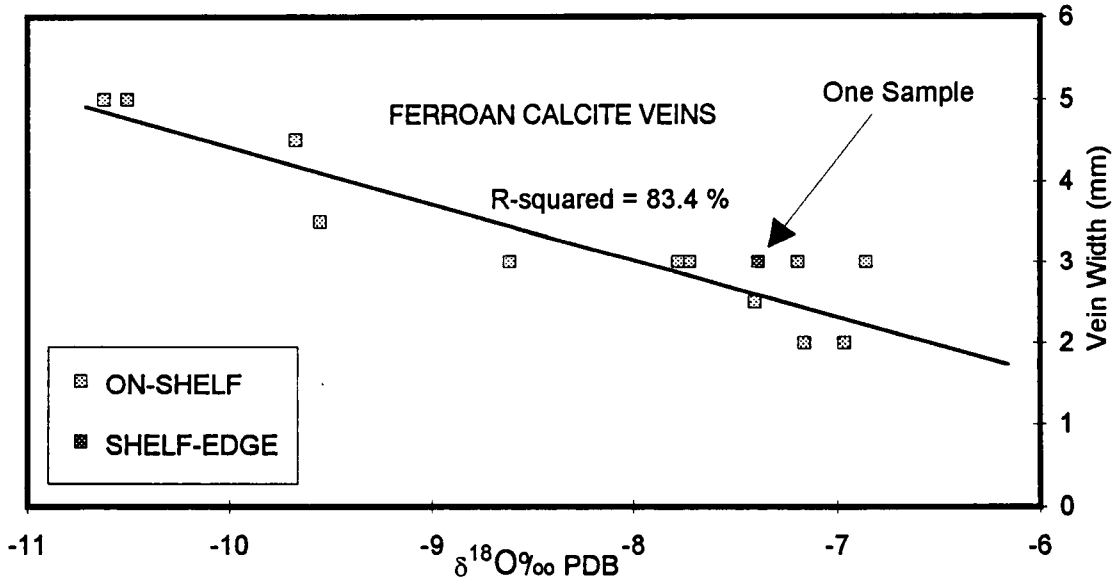
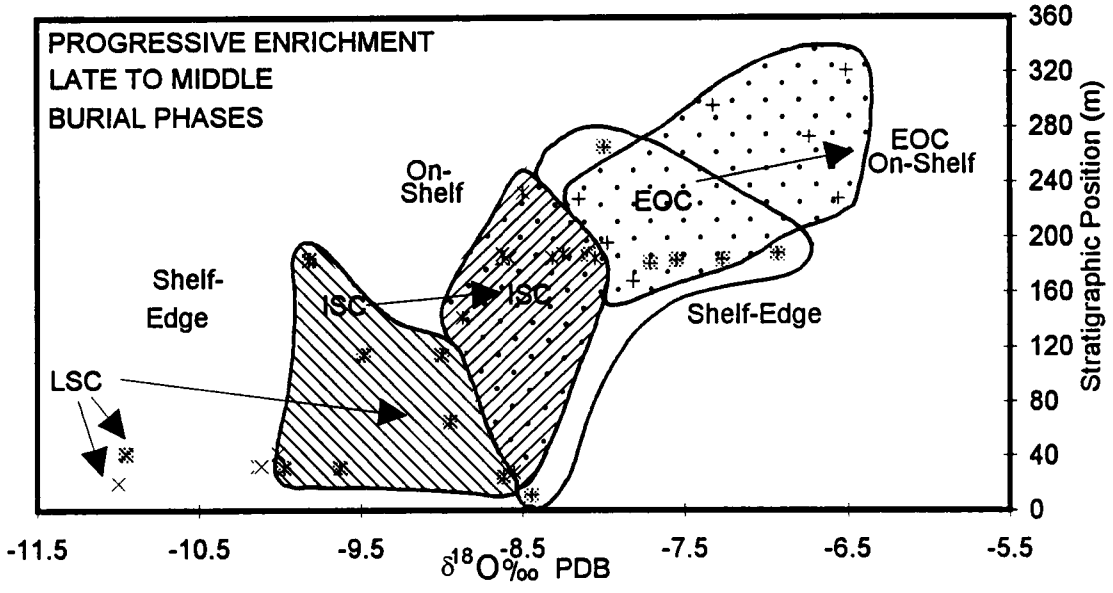



Figure 5.6. On-shelf vein calcite $\delta^{18}O$ values against vein width. Shelf-edge vein calcite is plotted for comparison, but is not included in the least squares regression.

diagenesis. Finally, third-order Sequence 4 consisting of mudstone, grainstone and shale probably retained even less porosity during early to intermediate burial than either Sequence 2 of Sequence 3. Also, the presence of shale beds and laminae in Sequence 4 probably reduced vertical (across-layering) fluid transmissivity greatly. Thus, Sequence 2 probably represented a fluid-dominated system, Sequence 4 a rock-dominated system, and Sequence 3 an intermediate or transitional system. Calcite filled veins, on the other hand, probably represent fluid rock systems of their own. Wider veins acted as fluid-dominated systems, whereas narrower veins represent rock-dominated systems. Stratigraphic position, and presumably the host lithology as well, appear to be less important in buffering $\delta^{18}O$ values of vein calcite.

## Progressive Shelf-Edge to On-Shelf Enrichment of $\delta^{18}O$ in Late to Middle Burial Phases

**Enrichment Trends.** Progressive enrichment in $\delta^{18}O$ values of late to middle burial phases of similar paragenetic timing occurs among phases occupying on-shelf positions when compared to their paragenetic counterparts at the shelf-edge. Figure 5.7 shows $\delta^{18}O$ values of earlier overgrowth calcite (EOC), intermediate sparry calcite (ISC), and late sparry calcite (LSC) plotted against stratigraphic position. This progressive enrichment is best illustrated by ferroan coarse sparry calcite of intermediate paragenetic timing (ISC). Intermediate sparry calcite is enriched in $\delta^{18}O$ on the shelf (median = -8.6‰ PDB, N=7) relative to that at the shelf-edge (median = -9.5‰ PDB, N=9).




- ON-SHELF FERROAN COARSE SPARRY CALCITE
- SHELF-EDGE FERROAN COARSE PINK SPARRY CALCITE
- SHELF-EDGE COARSE SPARRY CALCITE, CO-PRECIPITATED WITH FERROAN BAROQUE DOLOMITE
- SHELF-EDGE FERROAN AND NON-FERROAN SYNTAXIAL OVERGROWTH CALCITE
- ON-SHELF FERROAN AND NON-FERROAN SYNTAXIAL OVERGROWTH CALCITE
- SHELF-EDGE FERROAN COARSE SPARRY CALCITE

Figure 5.7. $\delta^{18}O$ values for different types of burial calcite are plotted against stratigraphic position. Early overgrowth calcite (EOC) at the shelf-edge is depleted in $\delta^{18}O$ relative to EOC on the shelf. Similarly, intermediate sparry calcite (ISC) is depleted in $\delta^{18}O$ relative to ISC on the shelf. Late sparry calcite (LSC) occurs only at the shelf-edge. It should be noted that "earlier overgrowth calcite" is early only relative to other burial phases. It is a relatively late phase in the overall paragenetic sequence.

Earlier overgrowth calcite may also show this type of progressive enrichment. For example, earlier overgrowth calcite on the shelf (median = -7.1‰ PDB, N=7) is enriched in $\delta^{18}O$ relative to earlier overgrowth calcite at the shelf-edge (median = -7.7‰ PDB, N=7). However, these differences are not statistically significant. The three on-shelf overgrowth calcite samples that fall within the shelf-edge overgrowth field have higher relative iron contents (based on potassium ferricyanide staining) than do their more $\delta^{18}O$ enriched counterparts. Thus, these $\delta^{18}O$ depleted on-shelf overgrowths may have been precipitated slightly later than their on-shelf $\delta^{18}O$ enriched counterparts that fall well outside of the shelf-edge field. Detailed sampling at a finer scale may help to show that overgrowth calcite on the shelf is indeed enriched in $\delta^{18}O$ relative to its shelf-edge counterpart of similar paragenetic timing. Late sparry calcite occurs exclusively at the shelf-edge and consists of ferroan coarse pink sparry calcite and coarse sparry calcite co-precipitated with ferroan baroque dolomite.

**Depletion trends.** A progressive depletion in $\delta^{18}O$ values occurs from earlier precipitated phases to later precipitated phases at the shelf-edge and on the shelf (Figs.4.7, 4.9 and 5.5, Tables 4.1 and 4.2). For example, earlier overgrowth calcite at the shelf-edge is depleted in $\delta^{18}O$ when compared to intermediate sparry calcite also at the shelf-edge (paragenetically the next latest phase). Similarly, intermediate sparry calcite at the shelf-edge is depleted relative to late sparry calcite at the shelf-edge.

**Discussion.** Progressive enrichment in $\delta^{18}O$ values of burial phases occupying on-shelf positions as compared to their paragenetic counterparts at the shelf-edge can be explained in terms of both water-rock interaction and temperature. If the Sevier basin is the likely source for the fluids precipitating these burial phases (see chapter 4), then the shelf-edge along the Sevier basin probably received a greater quantity of these fluids than did the succession on the shelf. Larger quantities of fluid alone probably best explain the relatively deleted $\delta^{18}O$ values of burial phases at the shelf-edge as compared with those on the shelf.

A temperature gradient, with higher temperatures at the shelf-edge as compared to the shelf could also explain the relatively depleted $\delta^{18}O$ values at the shelf-edge. This might have occurred if burial fluids from the basin exchanged their heat with cooler deep freshwater fluids on the shelf. Such an exchange might have been possible during early burial diagenesis, but appears improbable during later burial diagenesis. During late burial diagenesis, both the shelf and shelf-edge sections may have been buried as deep as 3 km (Fig. 4.3). Fluid expelled from a basin into a succession at such depths would have retained most of its heat.

Progressive depletion in $\delta^{18}O$ values from earlier precipitated phases to later precipitated phases is the trend normally seen as carbonate rocks undergo progressive burial diagenesis (e.g., Morse and Mackenzie, 1990). Depletion in $\delta^{18}O$ occurs with increasing burial temperature.

## Whole-Rock Trace Element Values in Third-Order Stratigraphic Sequences

Whole-rock trace element distributions on the shelf and at the shelf-edge are presented and discussed within the context of previous interpretations made based isotopic ($\delta^{18}O$, $\delta^{13}C$, $^{87}Sr/^{86}Sr$) and electron microprobe analysis of trace elements (Mg, Mn, Fe, Sr) of individual carbonate phases (i.e., Chapter 4). Whole-rock trace element values presented without such supporting evidence are difficult, if not impossible to interpret. However, combined with additional evidence, such as that provided in chapter 4, it may be possible to speculate about the distribution of trace elements in whole-rock samples within different stratigraphic sequences at on-shelf and shelf-edge positions.

Changes in whole-rock trace element values from Sequence 2 to Sequence 4 are discussed relative to sequence stratigraphic development on the shelf. Third-order Sequence 4 is covered at the shelf-edge. However, trace element data from the lower part of on-shelf Sequence 4 can be compared with on-shelf and shelf-edge data from Sequence 3. Whole rock trace element values are normally distributed throughout the succession. Whole rock analyses of 68 samples from sequence 2 and 3 were performed by Johnson (1988). Analyses of 11 samples from Sequence 4 were performed by Steinhauff.

**Strontium.** Strontium concentrations on the shelf in Sequence 2 are higher relative to those that occur at the shelf-edge in Sequence 2. Differences in sample means are

discernible at better than the 0.01 level. Strontium averages slightly less than 200 ppm throughout the entire succession. Sample means for strontium concentrations are statistically similar on the shelf and at the shelf-edge in Sequence 3 as compared with Sequence 4 on the shelf.

Johnson (1988) attributed differences in strontium and magnesium ratios in Middle Ordovician carbonates to the relative openness of the carbonate system (e.g., Brand and Veizer, 1980). Thus, on the shelf, Sequence 2 may have represented a relatively closed system and a more open system at the shelf-edge. Sequence 2 represents the time during which environmental differences between the shelf and shelf-edge were most pronounced and thus the resultant sediment types in the two areas were most different (see chapter 3). Johnson suggested that reducing waters were probably responsible for the relative openness of the system at the shelf-edge. Indeed, Sequence 2 experienced several significant increases in water-depth. These may have put shelf-edge sediments in contact with deep-marine reducing waters. Such deep-marine reducing waters were likely undersaturated with respect to calcium carbonate. This undersaturation may have led to dissolution at the shelf-edge and subsequently may have helped these sediments retain significant porosity. During late burial diagenesis shelf-edge sediments probably experienced additional contact with reducing waters, this time in the form of hot metal-rich brines that precipitated late burial phases within the remaining pore space.

**Sodium.** Johnson (1988) noted that sodium concentrations in acid soluble whole-rock fractions are higher in shelf-edge samples when compared to samples on the shelf (Fig. 5.8). Shelf-edge limestone from Red House Branch averages 190 $\pm$ 36 ppm in Sequence 2 and 219 $\pm$ 66 ppm in Sequence 3, while on-shelf limestone from Cedar Springs averages 112 $\pm$ 74 ppm in Sequence 2 and 140 $\pm$ 36 ppm in Sequence 3. Differences in sample means of shelf-edge versus on-shelf sodium concentration are statistically discernible at better than the 0.01 level in Sequence 2 and at the 0.03 level in Sequence 3.

Veizer et al. (1977) found that hypersaline facies are separated from normal marine facies at about 230 ppm sodium. Maximum sodium values exceed 300 ppm sodium in both sequences 2 and 3 at the shelf-edge (Fig. 5.8). Johnson (1988) noted that the shelf-edge facies at Red House Branch were not originally deposited in a hypersaline environment, but still have sodium values above 230 ppm. Thus, he speculated that saline brines were responsible for diagenetic enrichment in sodium at the shelf-edge. This also agrees with the fact that burial diagenetic phases are more abundant in shelf-edge facies as compared to on-shelf facies (Walker et al., 1986; Jernigan, 1987; Johnson, 1988; Steinhauff et al., 1989).

**Magnesium.** On-shelf magnesium concentrations are higher relative to those that occur at the shelf-edge (Fig. 5.8). Magnesium concentrations on the shelf average 4164 $\pm$ 1889 ppm for Sequence 2 and 2582 $\pm$ 184 ppm for Sequence 3, whereas Mg concentrations at the shelf-edge average 2881 $\pm$ 1424 ppm for Sequence 2 and 2011

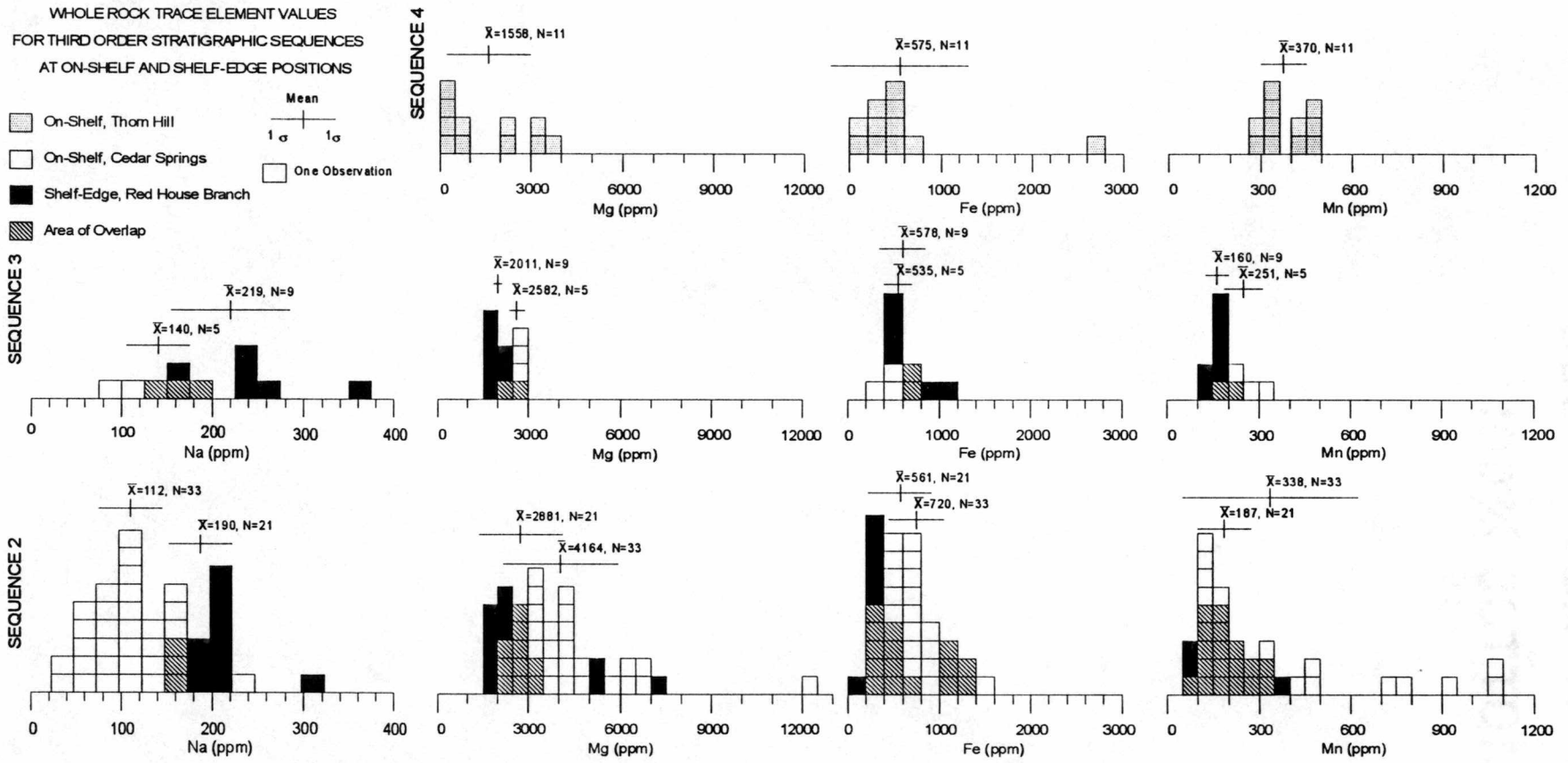



Figure 5.8. Whole rock trace element values relative to third-order stratigraphic sequences at on-shelf and shelf-edge positions. Analyses of 68 samples from sequences 2 and 3 was performed by Johnson (1988) and analyses of 11 samples from lowermost Sequence 4 was performed by Steinhauff.

± 356 ppm for Sequence 3. Differences in sample means of on-shelf versus shelf-edge magnesium concentration are statistically discernable at the 0.01 level in Sequence 2 and better than the 0.01 level in Sequence 3. Additionally, kurtosis (degree of flatness) of magnesium concentrations on the shelf are higher relative to those at the shelf-edge. For example, standardized kurtosis of on-shelf values is 10.5 and 0.6 for sequences 2 and 3 respectively, whereas shelf-edge values are 3.9 and 0.1 for sequences 2 and 3, respectively. Similarly, standardized skewness (lack of symmetry) of on-shelf Mg concentrations in Sequence 2 (6.0) is greater than that of shelf-edge Sequences 2 (3.9). Skewness of on-shelf and shelf-edge magnesium concentrations in Sequence 3 are similar. These differences indicate that there is a greater dispersion of magnesium concentration on the shelf in sequences 2 and 3 as compared to the shelf-edge in sequences 2 and 3.

Since the dolomite fraction was not excluded from these analyses, the distribution of these data can tentatively be attributed to the relative absence of microdolomite at the shelf-edge and to the relative abundance of microdolomite on the shelf (or shelf equivalent strata, i.e. shelf-edge Sequence 3).

**Iron.** The iron concentration of all sample means are statistically the same (at the 0.05 level; Fig. 5.8). This strongly suggests that whole rock iron content is primarily a result of syndepositional processes and that large amounts of iron were not remobilization during diagenesis (e.g., Johnson. 1988).

**Manganese.** Manganese concentrations in the soluble fraction on the shelf are higher relative to those that occur at the shelf-edge (Fig. 5.8). Manganese concentrations on the shelf average 338 ± 289 ppm for Sequence 2 and 251 ± 59 ppm for Sequence 3, whereas manganese concentrations at the shelf-edge average 187 ± 87 ppm for Sequence 2 and 160 ± 30 ppm for Sequence 3. Differences in sample means of on-shelf versus shelf-edge manganese concentration are statistically discernible at the 0.02 level in Sequence 2 and better than the 0.01 level in Sequence 3. Furthermore, kurtosis (degree of flatness) of manganese concentrations on the shelf are higher relative to those at the shelf-edge. For example standardized kurtosis of on-shelf values are 1.6 and 0.2 for sequences 2 and 3, respectively, whereas shelf-edge values are -0.7 and -0.5 for sequences 2 and 3, respectively. Similarly, standardized skewness (lack of symmetry) of on-shelf manganese concentrations in Sequence 2 (3.6) is greater than that of shelf-edge Sequence 2 (1.1). Skewness of on-shelf and shelf-edge manganese concentrations in Sequence 3 are similar. Thus, there is greater dispersion of manganese concentrations on the shelf in sequences 2 and 3 as compared to those at the shelf-edge in sequences 2 and 3.

Manganese concentrations were not originally the same in sediments deposited on the shelf and at the shelf-edge. Rather, manganese is concentrated in black Fe / Mn oxide-rich sediments and pavements associated with slow deep-water sedimentation and drowning unconformities at the shelf-edge and along the basin slope (e.g., Ruppel and Walker, 1982; Johnson, 1988; Steinhauff et. al., 1989, 1992; Steinhauff and Walker, in prep. b). Black Fe /M n-rich crusts and pavements that

occur at the shelf-edge at Red House Branch (see Fig. 3.4D) were intentionally not included as part of the whole rock trace element analysis (Fig. 5.8). Thus, whole rock manganese trace element concentrations at the shelf-edge reflect manganese concentrations in sediments deposited during times of "normal" sediment accumulation rather than during times of slow deposition. Greater dispersion of manganese concentrations on the shelf in sequences 2 and 3 as compared to those at the shelf-edge in sequences 2 and 3 is tentatively attributed to differential distribution of manganese by post-depositional and diagenetic processes.

## CONCLUSIONS

1) Most fibrous calcite occupies pores, cavities and vugs developed or enhanced by subaerial exposure during earlier lowstands in relative-sea levels. Cement filled pores, cavities and vugs developed below third-order sequence stratigraphic surfaces are more conspicuous, larger and contain more cement phases than those that occur below fourth-order sequence surfaces. Thus, significant porosity was retained the longest below third-order stratigraphic sequence surfaces than anywhere else in the stratigraphic succession. Indeed, a minor amount of porosity is still retained below some third-order sequence boundaries.

2) On-shelf clear, blocky calcite and ferroan, blocky white calcite precipitated during early to intermediate burial diagenesis have different, statistically discernible, $\delta^{18}O$ values depending on the third-order stratigraphic sequence into which they were emplaced. The $\delta^{18}O$ values of veins that fed many of these blocky calcite cavities, on

the other hand, do not appear to be dependent on the stratigraphic sequence into which the veins were emplaced. Rather, different $\delta^{18}O$ values of veins are explained by vein width. Water-rock interaction can explain the different distributions of $\delta^{18}O$ values in blocky calcite relative to third-order stratigraphic sequences and the distribution of $\delta^{18}O$ in coeval veins. Each stratigraphic sequence is dominated by a different lithology. Grainstone-rich Sequence 2 probably retained porosity the longest and thus represents a fluid-dominated system. Mudstone, grainstone and shale of Sequence 4 were probably deposited with little or no porosity and thus represent a rock-dominated system. Veins, on the other hand, probably represent their own water-rock systems. Wider veins acted as fluid-dominated systems, whereas narrower veins acted as rock-dominated systems.

3) Progressive enrichment in $\delta^{18}O$ values of burial phases occupying on-shelf positions as compared to their paragenetic counterparts at the shelf-edge is best explained in terms of water-rock interaction. The shelf-edge along the Sevier basin probably received a greater quantity of warm burial fluids than did the succession on the shelf. Progressive depletion in $\delta^{18}O$ values from earlier precipitated phases to later precipitated phases occurs with increasing burial temperature.

4) Whole-rock trace element distributions of Sr, Na, Mg, and Mn are different in sequences 2 and/or 3 at the shelf-edge when compared to those on the shelf. Higher strontium concentration on the shelf in Sequence 2 as compared to the shelf-edge in Sequence 2 is attributed to a relatively more open system at the shelf-edge in Sequence 2. Higher sodium concentrations occur at the shelf-edge as

compared to the shelf. These are probably a result of saline brines in contact with the shelf-edge during burial diagenesis. In contrast, early diagenetic processes associated with changes in relative sea-level may have affected the distribution of magnesium and manganese. Sediments on the shelf were exposed more frequently than those at the shelf-edge. This may have lead to dispersal of magnesium and manganese concentrations on the shelf.

In general, distribution of strontium, magnesium iron, and manganese in lowermost Sequence 4 is similar to distribution of these elements in both the on-shelf and shelf-edge successions of Sequence 3. By the time Sequence 4 was deposited, platform interior sediments had prograded to the shelf-edge. Thus, early diagenetic processes in Sequence 4 were similar on the shelf and at the former shelf-edge. Hence, later diagenesis on the shelf and at the former shelf-edge was similar as well.

# CHAPTER 6

## CONCLUSIONS

### SUMMARY

1) Stratigraphic sequences, subsequences, and parasequences represent shoaling-upward sediment packages similar to cycles. However, sequences, subsequences, and parasequences of this study differ from the usually described cycles elsewhere in that evidence for exposure and shoaling is subtle and generally revealed only through detailed microscopic examination of numerous thin-sections and polished slabs.

2) The apparently non-cyclic, largely subtidal sequences of this study are different from the subtidal cyclic successions described by Osleger (1991) and Osleger and Read (1991). The subtidal cycles of Osleger (1991, p. 917) " ... are distinguished by an upward increase in grain size, bed thickness, and cross-bedding and other high-energy sedimentary structures. Subtidal cycles are not capped by intertidal lithologies, nor do any of the subtidal cycles exhibit exposure features such as microkarst or vadose dissolution or cementation." In this study we have illustrated many similar features. However, the distinguishing features described by Osleger (1991) and Osleger and Read (1991) do not appear to be systematically arranged in the subtidal rocks of the present study. Furthermore, evidence for subaerial exposure

within most of the sequences described in this study are illustrated in figures 2.12 - 2.18.

3) Sequence, subsequence, and parasequence lithologies differ both vertically and horizontally. They comprise a facies mosaic and cannot be generalized. Thus, a representation of the entire succession is presented in figures 2.12 through 2.18, rather than an idealized sequence.

4) Meter-scale (5th-order) parasequences in this succession are seldom correlative between localities and probably do not represent widespread sea-level change. Indeed, parasequences are only recognized on the shelf. Instead, parasequences appear to represent environmental migration and are probably of autocyclic origin.

5) Non-cyclic carbonates are amenable to the use of Fischer plots. If one applies a standard interpretation (i.e., Read and Goldhammer, 1988) to the Fischer plot (Fig. 2.19), the plot supports broad interpretations previously made for this succession based on other lines of evidence (i.e., Ruppel, 1979; Ruppel and Walker, 1982, 1984). Thus, relative sea-level rises appear as positive departures from the horizontal and relative sea-level falls appear as negative departures from the horizontal.

6) Detailed stratigraphic sequence analysis of shelf and shelf-edge carbonates combined with biostratigraphic data and water-depth analysis allows for correlation of third-order sequences from the shelf to the shelf-edge. Such correlation reveals that some fourth-order subsequences or "beats" are missed at on-shelf or shelf-edge

positions. This analysis is possible because conclusions regarding "missed beats" are made through comparison of shelf and shelf-edge successions. If one of these successions had not been studied (shelf or shelf-edge), conclusions regarding a "missed beat" would not be possible. A serious limitation of this type of analysis is that there may be still other beats that are missed at both on-shelf and shelf-edge positions. Even with further temporal or biostratigraphic control, or statistical analysis, it would probably not be possible to identify such additional missed beats because of their likely very short duration.

7) Phases interpreted as meteoric in origin do not show the large depletions in $\delta^{13}C$ that other workers have observed in younger rocks. Stable carbon and oxygen isotopic values of early Paleozoic marine and meteoric phases have not previously been well known (Popp et al. , 1986). In fact, this study estimates the original $\delta^{18}O$ value of Middle Ordovician marine calcite to be about -4.2‰ and the $\delta^{13}C$ value to be about 0.4‰. The apparent lack of $\delta^{13}C$ depletion in meteoric phases relative to marine phases is either real or a sampling artifact. Bias could have been introduced because small samples (less than 0.2 mg) were not analyzed. On the other hand, this lack of $^{12}C$ shows up in all size samples run by the carbonate research group at the University of Tennessee. Assuming that this lack of enrichment is real, a sufficient amount of the light $^{12}C$ isotope may not have been available in Middle Ordovician groundwater. Meteoric cements in younger carbonate rocks derive their $^{12}C$ from the decay of plant derived organic matter (e.g., Hudson, 1977). The first major adaptive radiation of land plants was marked by the rise of the spore tetrads in the late middle

Ordovician to mid-late Silurian (Caradoc to the mid-late Llandovery). This was followed by a second major radiation of the vascular plants in the mid-late Silurian (Llandovery to the Pridoli; Gray, 1984, 1985; Gensel and Andrew, 1987). In contrast, this Middle Ordovician succession is slightly older (Llanvirian to Carodocian). Thus, decay of plant derived organic matter may have been limited and it probably did not contribute significant large amounts of the light $^{12}C$ isotope to the groundwater (e.g., Saller and Moore, 1991).

8) Diagenetic pathways for sediments on the shelf were different from those for sediments at the shelf-edge. Intervals that retained porosity the longest occur below third- and fourth-order sequence surfaces at on-shelf and shelf-edge positions. Vugs and cavities were developed below many of these sequence boundaries during subaerial exposure. Detailed petrography and knowledge of the sequence stratigraphy suggests that early diagenetic phases that fill cavities and vugs represent fillings precipitated during a "second-cycle" or in some cases perhaps a "third-cycle" of early diagenesis (Figs. 4.14 and 4.15). Early diagenetic phases on the shelf were precipitated in relatively open systems, whereas early diagenetic phases at the shelf-edge were precipitated in relatively closed systems (e.g., Fig. 4.6). Early on-shelf phases probably experienced exposure more frequently than early phases at the shelf-edge (e.g., Fig. 4.2). Intermediate through late burial phases at the shelf-edge represent more fluid dominated systems than their paragenetic counterparts on the shelf (Figs. 4.8 and 4.9). Intermediate through late burial phases at the shelf-edge have more depleted $\delta^{18}0$ values and higher iron and manganese contents than their

counterparts on the shelf (Figs. 4.9 - 4.13), and are more enriched in $^{87}Sr$ than those on the shelf (Fig. 4.7). This may be explained in terms of water-rock interaction. If the source of the fluids precipitating late burial phases was the Sevier basin, then fluids at the shelf-edge would have encountered less carbonate rock than those traveling to on-shelf positions.

9) The Sevier basin is the most likely source of burial fluid that precipitated the late burial phases (Figs. 4.1 and 4.3). Late, ferroan coarse sparry calcite and ferroan baroque dolomite could have been generated from brines expelled from the Sevier basin before the end of the Middle Ordovician. This is based an analysis of burial curves, possible temperatures, and an assumed range of likely brine compositions (Figs. 4.3, 4.17, 4.18).

10) On the shelf, clear, blocky calcite and ferroan, blocky white calcite precipitated during early to intermediate burial diagenesis have different, statistically discernible, $\delta^{18}O$ values depending on the third-order stratigraphic sequence into which they were emplaced. The $\delta^{18}O$ values of veins that fed many of these blocky calcite cavities, on the other hand, do not appear to be dependent on the stratigraphic sequence into which the veins were emplaced. Rather, different $\delta^{18}O$ values of veins are explained by vein width. Water-rock interaction can explain the different distributions of $\delta^{18}O$ values in blocky calcite relative to third-order stratigraphic sequences and the distribution of $\delta^{18}O$ in coeval veins. Each stratigraphic sequence is dominated by a different lithology. Grainstone-rich Sequence 2 probably retained porosity the longest and thus represents a fluid dominated system. Mudstone,

grainstone and shale of Sequence 4 were probably deposited with little or no porosity and thus represent a rock-dominated system. Veins, on the other hand, probably represent their own water-rock systems. Wider veins acted as fluid-dominated systems, whereas narrower veins acted as rock-dominated systems.

11) Progressive enrichment in $\delta^{18}O$ values of burial phases occupying on-shelf positions as compared to their paragenetic counterparts at the shelf-edge is best explained in terms of water-rock interaction. The shelf-edge along the Sevier basin probably received a greater quantity of burial fluids than did the succession on the shelf. Progressive depletion in $\delta^{18}O$ values from earlier precipitated phases to later precipitated phases occurs with increasing burial temperature.

12) Whole-rock trace element distributions of Sr, Na, Mg, and Mn are different in sequences 2 and/or 3 at the shelf-edge when compared to those on the shelf. Higher strontium concentration on the shelf in Sequence 2 as compared to the shelf-edge in Sequence 2 is attributed to a relatively more open system at the shelf-edge in Sequence 2. Higher sodium concentrations occur at the shelf-edge as compared to the shelf. These are probably a result of saline brines in contact with the shelf-edge during burial diagenesis. In contrast, early diagenetic processes associated with changes in relative sea-level may have affected the distribution of magnesium and manganese. Sediments on the shelf were exposed more frequently than those at the shelf-edge. This may have lead to dispersion of magnesium and manganese concentrations on the shelf. In general, distribution of strontium, magnesium, iron and manganese in lowermost Sequence 4 is similar to distribution of these elements in

both the on-shelf and shelf-edge successions of Sequence 3. By the time Sequence 4 was deposited, platform interior sediments had prograded to the shelf-edge. Thus, early diagenetic processes in Sequence 4 were similar on the shelf and at the former shelf-edge. Hence, later diagenesis on the shelf and at the former shelf-edge was similar as well.

## FUTURE WORK

### Is Present Day Groundwater Flow Influenced by Depositional and Diagenetic Features?

A depositional and diagenetic model in the form of detailed three-dimensional restored cross-sections and paragenetic sequences for the Lincolnshire, Rockdell, Holston, and Benbolt formations is presented in chapters 2 and 3. These formations have widespread distribution throughout East Tennessee and southeast Virginia. For example, the X-10 facility of the Oak Ridge National Laboratory (ORNL), a major government installation with serious groundwater contamination, is located on the Rockdell through Moccasin Formations within the White Oak Mountain thrust sheet. Past and present hydrogeologic concepts of groundwater flow at ORNL have assumed that "groundwater flow paths are mainly through joints and other fractures in bedrock." (Moore 1988, p. 21; Soloman et al., 1992). No one doubts that significant amounts of groundwater occur in joints and fractures. However, this work (particularly chapters 2 and 4) suggests that this groundwater philosophy may need to be revised to include concepts of stratabound flow. Chapters 2, 3, and 4

show that a small amount of residual porosity is retained below some third-order and fourth-order sequence boundaries. The hypotheses that (1) *residual porosity retained below ancient exposure surfaces might be solution enhanced within the present day groundwater regime* should be investigated. Furthermore, (2) *solution enhancement should be expected to be especially pronounced where these zones of residual porosity intersect later joints and fractures.*

Interestingly, recent studies on the Oak Ridge Reservation suggest that there is indeed a significant groundwater component that is stratabound within selected stratigraphic units (i.e., Lee and Ketelle, 1987). In fact Ketelle and Lee (1992) have identified stratabound flow within the lowermost part of Stockdale's (1951) Unit E of the Chickamauga Group at the X-10 facility. The lower part of Stockdale's Unit E is approximately equivalent to the lower Benbolt Formation (Table 6.1). Figure 2.15 of chapter 2 suggests that this interval within the lower Benbolt at Thorn Hill (in the Copper Creek allochthon) was affected by a relative lowstand in sea-level. Chapter 4 further notes that residual porosity is retained in strata at on-shelf positions within the lower Benbolt Formation (upper part of Sequence 3 and the lower part of Sequence 4) at Thorn Hill. Subaerial exposure features can be observed in thin-sections collected by Eric Weiss (1981) from the lower part of the Benbolt Formation at Solway Bridge within the White Oak Mountain thrust Sheet about 12 km north east of the X-10 facility (ORNL). It is likely that the boundary between third-order stratigraphic Sequence 3 and third-order Sequence 4 coincides closely with the Rockdale / Benbolt contact at Solway Bridge and at the X-10 facility. Furthermore, the Benbolt within

Table 6.1

Stratigraphic Nomenclature For The Chickamauga Group In The White Oak Mountain Thrust Sheet And Probable 3rd-Order Stratigraphic Sequences

| Stockdale (1951) | Weiss (1981) & Lemiszki (1992) Formation Names of Cooper and Prouty (1943) | Steinhauff and Walker (1992a,b) Approximate 3rd-Order Sequences M. Ordovician Strata, East TN | Thickness (Meters)[1] at X-10 |
|---|---|---|---|
| N/A | Cooper Creek Thrust | N/A | ± 6 |
| H | Moccasin Formation | Sequence 6 | 100-170 |
| G | Witten Formation | Sequence 5 | 105-110 |
| F | Bowen Formation | Sequence 4 and 5 | 5-10 |
| E | Benbolt/Wardell Fms[2] | Sequence 4 | 110-115 |
| C and D | Rockdell Formation | Sequence 2 and 3 | 80-85 |
| B | Fleanor and Hogskin Mbs of Lincolnshire Fm | Sequence 2 | 75-85 |
| A | Five Oaks Fm and Eidson Mb of the Lincolnshire Fm | Sequences 1 and 2 | 70-80 |
| N/A | Post - Knox Unconformity | N/A | 0-5 |

[1] Thickness reported by Lee and Ketelle (1988) and Lemiszki (1992).
[2] Lemiszki (1992) was not able to differentiate the Benbolt Formation from the Wardell Formation at X-10.

the White Oak Mountain thrust sheet represents strata that were deposited further on the shelf as compared to the lower Benbolt at Thorn Hill (e.g., Weiss, 1981). Thus, Benbolt strata located in the White Oak Mountain thrust sheet may have had a greater potential for enhancement of residual porosity during subaerial exposure than coeval strata in the Copper Creek allochthon.

If the component of stratabound flow in the lower Benbolt described by Ketelle and Lee (1992) occurs along fourth-order stratigraphic subsequences associated with the exposure surface separating sequences 3 and 4, then it should be possible to predict the stratigraphic and lateral extent of these potential zones of stratabound groundwater flow. If a sequence stratigraphic framework similar to the one presented in chapter 2 were constructed for the Middle Ordovician of the Oak Ridge Reservation, it might be possible to use this framework to predict zones having high potential for stratabound flow. Such a model could probably be tested using existing groundwater data.

## Sequence Stratigraphic Correlation

The water-depth curves, Fischer plots, and the sequence stratigraphic framework developed in chapters 2 and 3 provide a new means for correlation of Middle Ordovician strata. This sequence stratigraphic framework could be extended within East Tennessee and the Southern Appalachians. Comparison of water-depth curves and Fischer plots from different localities can be used to test different assumptions regarding changes in relative sea-level. For example, subaerial exposure or increases in water-depth caused by normal faulting along the Middle Ordovician

shelf-edge should not produce stratigraphic sequences that correlate over great distances (i.e., more than several tens of kilometers). In contrast, eustatic changes in sea-level should produce stratigraphic sequences that can be correlated throughout East Tennessee and possibly to other parts of the world.

## Relationship to Mississippi Valley-Type Deposits?

This study provides evidence for the timing of late burial diagenesis and the introduction of hot metal bearing brines from the Sevier basin to the shelf-edge and into the Middle Ordovician carbonate platform. This diagenetic event could have occurred before the end of the Middle Ordovician (about 435 Ma). Thus, this Middle Ordovician succession is uniquely positioned, geographically and temporally, between the area that other workers have proposed as the starting point for Mississippi Valley-Type deposits (the Sevier basin) in East Tennessee and at least one of the end points for that mineralization, namely the Idol (zinc) Mine (e.g., Kesler et al., 1988). Comparative petrographic and geochemical work should be conducted to investigate the possible relationship between late diagenetic phases preserved within this Middle Ordovician succession and similar phases recorded in gangue and ore minerals of the Idol Mine (i.e., Lu, J. and Craig, J.R., 1992).

## Paleoecology

This work provides a wealth of material (more than 1,000 thin-sections) for paleoecologic study of Middle Ordovician strata within a sequence stratigraphic

framework. For example, ceolobites are organisms that occupy submarine cavities and caves. Coelobite faunas, consisting of bryozoans and sponges, occur within cavities on the shelf at Thorn Hill. If a description of these faunas were to be published, it would represent the first published account of coelobite faunas from the Middle Ordovician.

# REFERENCES


Aissaoui, D.M., 1988, Magnesian calcite cements and their diagenesis: dissolution and dolomitization, Mururoa Atoll: Sedimentology, v. 35, p. 821-841.

Al-Aasm, I., Taylor, B.E., and South, B., 1990, Stable isotope analysis of multiple carbonate samples using selective acid extraction: Chemical Geology, v. 80, p. 119-125.

Allen, J.R., 1967, Depth indicators of clastic sequences: Marine Geology, v. 5., 429-446.

Bachtadse, V., Van der Voo, R., Haynes, F.M., and Kesler, S.E., 1987, Late Paleozoic magnetization of mineralization of mineralizing and unmineralizing Ordovician Carbonates from East Tennessee: Evidence for a post-ore chemical event: Journal of Geophysical Research, v. 92, p. 14165-14176.

Bathurst, R.G.C., 1967, Depth indicators in sedimentary carbonates: Marine Geology, v. 5,. p. 447-471.

Baturin, G.N., 1982, Phosphorites on the sea floor: origin, composition, and distribution: New York, Elsevier, 343 p.

Benedict, G.L., and Walker, K.R., 1978, Paleobathymetric analysis in Paleozoic sequences and its geodynamic significance: American Journal of Science, v. 278, p. 579-607.

Berger, W.H., 1974, Deep-sea sedimentation, in Burk, C.A., and Drake, C.D., eds., The Geology of Continental Margins: New York, Springer-Verlag, p. 213-241.

Bergstrom, S.M., 1971, Conodont biostratigraphy of the Middle and Upper Ordovician of Europe and eastern North America: Geological Society of America Memoir 127, p. 83-162.

Bergstrom, S.M., 1973, Biostratigraphy and facies relationships in the lower Middle Ordovician of easternmost Tennessee: American Journal of Science, v. 273-A, p. 261-293.

Bergstrom, S.M., 1977, Early Paleozoic conodont biostratigraphy in the Atlantic Borderland, in Swain, F.M., ed., Stratigraphic micropaleontology of Atlantic Basin Borderlands: Elsevier, New York, p. 85-110.

Bergstrom, S.M., and Carnes, J., 1976, Conodont biostratigraphy and paleoecology of the Holston Formation (Middle Ordovician) and associated strata in Eastern Tennessee, in Barnes, C,R., (ed.), Conodont Paleoecology: Geological Association of Canada Special Publication 15, p. 27-58.

Berry, W.B.N., 1987, Phylum Hemichordata (including Graptolithina), in Boardman, R.S., Cheetham, A.H., and Rowell, A.J., eds., Fossil Invertebrates: Palo Alto, Blackwell Scientific Publications, p. 612-635.

Bond, G.C., Kominz, M.A., and Grotzinger, J.P., 1988, Cambro-Ordovician eustasy: Evidence from geophysical modelling of subsidence in Cordilleran and Appalachian passive margins, in Kloinspehn, K., and Paola, C., eds., New Perspectives in Basin Analysis: New York, Springer Verlag, p. 131-160.

Bosence, D.W.J., 1983, Description and classification of rhadoliths (rhodoids, rhodolites), in Peryt, T.M., ed., Coated Grains: Berlin, Springer-Verlag, p. 217-242.

Breland, F.C., 1980, Stratigraphy, Paleoenvironmental, and Echinoderm Distributional Patterns in an Unfaulted Middle Ordovician (Chickamauga Group) Shelf-Edge to On-Shelf Transect in East Tennessee [unpublished doctoral dissertation]: Knoxville, University of Tennessee, 217 p.

Brick, JL., 1986, Precision K-Rb-Sr isotope analysis: application to Pb-Sr chronology: Chemical Geology , v. 56, p. 73-83.

Bromley, R.G., 1967, Marine phosphorites as depth indicators: Marine Geology, v. 5, p. 503-509.

Budd, D.A., and Perkins, R.D., 1980, bathymetric zonation and paleoecologic significance of microborings in Puerto Rican shelf and slope sediments: Journal of Sedimentary Petrology, v. 50, no. 3, p. 881-994.

Burk, W.H., Denison, R.E., Hetherington, R.B., Koepnick, R.B., Nelson, H.F., and Otto, J.B., 1982, Variation of seawater $^{87}Sr/^{86}Sr$ through Phanerozoic time: Geology, v. 10, p.516-519.

Byerly, D.W., Walker, K.R., Diehl, W.W., Ghazizadeh, M, Johnson, R.E., Lutz, C.T., Schoner, A.K., Simmons, W.A., Simonson, J.C.B., Weber, L.J., and Wedekind, J.E., 1986, Thorn Hill: A classic Paleozoic stratigraphic section in Tennessee, in Neathering, T.L. (ed.) Southeastern Section of the Geological Society of America Centennial Field Guide, v. 6, no. 28., p. 131-136.

Cantrell, D.L., 1982, Anatomy, Diagenesis, and geochemistry of a Middle Ordovician Oolite Shoal, Eastern Tennessee [unpublished M.S. thesis]: Knoxville, University of Tennessee, 153 p.

Cantrell, D.L., and Walker, K.R., 1985, Depositional and diagenetic patterns, ancient oolite, Middle Ordovician, eastern Tennessee: Journal of Sedimentary Petrology, v. 55, p. 518-531.

Carnes, J.B., 1975, Conodont biostratigraphy in the lower Middle Ordovician of the western Appalachian thrust-belts in northeastern Tennessee [unpublished doctoral dissertation]: Columbus, The Ohio State University, 291 p.

Cathles, L.M., and Smith, A.T., 1983, Thermal constraints on the formation of Mississippi Valley-type lead-zinc deposits and their implications for episodic basin dewatering and deposit genesis: Economic Geology, v. 59, p. 161-170.

Chayes, F., 1956, Petrographic Modal Analysis: New York, John Wiley.

Churnet, H.G., Misra, K.C., and Walker, K.R., 1982, Deposition and dolomitization of upper Knox carbonate sediments, Cooper Ridge district, East Tennessee: Geological Society of America Bulletin, v. 93, p. 76-86.

Clarkson, E.N.K., 1967, Environmental significance of eye-reduction in trilobites and Recent Arthropods: Marine Geology, v. 5, p. 367-375.

Cocks, L.R.M., and Mckerrow, W.S., 1978, Ordovician, in Mckerrow, W.S., ed., The Ecology of Fossils: London, Duckworth and Co., p. 62-92.

Cook, H.E., and Mullins, H.T., 1983, Basin Margin Environment, in Scholle, P.A., Bebout, D.G., and Moore, C.H., eds., Carbonate Depositional Environments: American Association of Petroleum Geologists Memoir 33, p. 540-617.

Cooper, G.A. and Prouty, C.E., 1943, Stratigraphy of the lower Middle Ordovician of Tazewell County, Virginia: Geological Society of America Bulletin, v. 43, p. 819-886.

Cronan, D.S., 1977, Deep-sea nodules: distribution and geochemistry, in Glasby, G.P., Marine Manganese Deposits: New York, Elsevier, p. 11-44.

Davies, 1977, former magnesium calcite and aragonite submarine cements in upper Paleozoic reefs of the Canadian Arctic a summary: Geology, v. 5, p. 11-15.

Deffeyes, K.S., Lucia, F.J., Weyl. P.K., 1965, Dolomitization of Recent and Plio-Pleistocene sediments by marine evaporite waters in Bonaire, Netherlands Antilles, in Pray, L.C., and Murray R.C., eds., Dolomitization and Limestone Diagenesis a Symposium, Society of Economic Paleontologists and Mineralogists Special Publication 13, p. 71-88.

Dickson, J.A.D., 1965, Modified staining technique for carbonates in thin section: Nature, v. 205, p. 587.

Dickson, J.A.D., 1966, Carbonate identification and genesis as revealed by staining: Journal of Sedimentary Petrology, v. 36, p. 491-505.

Dunham, R.J., 1969, Early vadose silt in Townsend mound (reef), New Mexico: Society of Economic Paleontologists and Mineralogists Special Publication 14, p. 139-182.

Dunham, R.J., 1962, Classification of carbonate rocks according to depositional texture: American Association of Petroleum Geologists Memoir 1, p. 108-121.

Ebers, M.L., and Kopp, O.C., 1979, Cathodoluminescent microstratigraphy in gangue dolomite, the Mascot-Jefferson City district, Tennessee: Economic Geology, v. 74, p. 735-739.

Edmond, J., 1992, Himalayan tectonics, weathering processes, and the strontium isotope record in marine limestones: Science, v. 258, p. 1594-1597.

Ekdale, A.A., Bromley, R.G., and Pemberton, S.G., 1984, Ichnology: The use of Trace Fossils in Sedimentology and Stratigraphy: Society of Economic Paleontologists and Mineralogists Short Course 15, 317 p.

Elias, M.K., 1937, Depth of deposition of the Big Blue (Late Paleozoic) sediments in Kansas: Geological Society of America Bulletin, v. 48, p. 403-432.

Elliot, C.W., and Aronson, J.L., 1987, Alleghanian episode of K-bentonite illitization in the Southern Appalachian Basin, v. 15, p. 735-739.

Elrick, M. and Read, J.F, 1991, Cyclic ramp-to-basin carbonate deposits, Lower Mississippian, Wyoming and Montana: A combined field and computer modeling study, in Fischer, A.G., et al. (eds.), Orbital Variations and Sedimentary Sequences: Journal of Sedimentary Petrology, v. 61, no. 7, p. 1194-1224.

Emery, K.O., 1945, Entrainment of air in beach sand: Journal of Sedimentary Petrology, v. 15, no. 2, p. 39-49.

Esteban, M., and Klappa, C.F., 1983, Subaerial exposure environment, in Scholle, P.A., Bebout, D.G., and Moore, C.H., eds., Carbonate Depositional Environments: American Association of Petroleum Geologists Memoir 33, p. 1-54.

Fell, B.H., 1966, Ecology of crinoids, in Boolootian, R.A., ed., Physiology of Echinodermata, p. 49 -62.

Fetzer, J.A., 1973, Biostratigraphic evaluation of some Middle Ordovician bentonite complexes in eastern North America [unpublished M.S. thesis]: Columbus, The Ohio State University, 165 p.

Fischer, A.G., 1964, The Lofer cyclothem of the Alpine Triassic: Kansas Geological Survey Bulletin 169, p. 107-149.

Flugel, E., 1978, Mikrofazielle Untersuchugsmethoden von Kalken: Berlin, Springer-Verlag.

Flugel, E., 1982, Microfacies Analysis of Limestones: New York, Springer-Verlag, 633 p.

Foreman, J.L., 1989, Chapter 7: Burial cements, in Walker, K.R., ed., The Fabric of Cements in Paleozoic Limestone: University of Tennessee Studies in Geology No. 20, p. 66-77.

Freeman, T., 1962, Quiet water oolites from Laguna Madre, Texas: Journal of Sedimentary Petrology, v. 32, no. 3., p. 475-483.

Friedman, I., and O'Neil, J.R., 1977, Compilation of stable isotope fractionation factors of geochemical interest: U.S. Geological survey Professional Paper 440K, 12 p.

Furman, F.C., 1990, Strontium isotope geochemistry of Mississippi Valley-type deposits, east Tennessee: Implications for age and source of mineralizing brines: Discussion and reply: Geological Society of America Bulletin, v. 102, p. 1600-1602.

Gensel, P.G., and Andrews, H.N., 1987, The evolution of early land plants: American Scientist, v. 75, p. 478-489.

Ginsburg, R.N., 1971, Landward movement of carbonate mud: New model for regressive cycles in carbonates [abstract]: American Association of Petroleum Geologists Bulletin, v. 55, p. 340.

Ginsburg, R.N., Hardie. L.A., Bricker, O.P., Garrett, P., and Wanless, H.R., 1977, Exposure index: a quantitative approach to defining position within the tidal zone, in Hardie, L.A., ed., Sedimentation on Modern Tidal Flats of Andros Island: Johns Hopkins Studies in Geology 22, p. 7-11.

Goldhammer, R.K., Dunn, P.A., and Hardie, L.A., 1987, High frequency glacio-eustatic sea-level oscillations with Malankovitch characteristics recorded in Middle Triassic platform carbonates in northern Italy: American Journal of Science, v. 287, p. 853-892.

Goldhammer, R.K., Dunn, P.A., and Hardie. L.A., 1990, Depositional cycles, composite sea-level changes, cycle stacking patterns, and the hierarchy of stratigraphic forcing: Examples from Alpine Triassic platform carbonates: Geological Society of America Bulletin, v. 102, p. 535-562.

Golubic, S., and Perkins, R.D., and Lukas, K.J., 1975, Boring microorganisms and microborings in carbonate substrates, in Fery, R.W., The study of trace Fossils: New York, Springer-Verlag, p. 229-259.

Gray, J., 1985, The microfossil record of early land plants: advances in understanding of early terrestrialization, 1970-1984: Philosophical Transactions of the Royal Society of London, v. B 309, p. 167-195.

Gray, J., 1984, Ordovician-Silurian land plants: The interdependence of ecology and evolution, in Basset, M.G., and Lawson, J.D., Autecology of Silurian Organisms: London, The Paleontological Association of London, Special Papers in Paleontology No. 32, p.281-285.

Gross, G.M., 1964, Variations in the $O^{18}/O^{16}$ and $C^{13}/C^{12}$ ratios of diagenetically altered limestones in the Bermuda Islands: Journal of Geology, v. 3, p.19-22.

Grover, G., and Read, J.F., 1978, Fenestral and associated vadose diagenetic fabrics of tidal flat carbonates, Middle Ordovician New Market Limestone, Southwestern Virginia: Journal of Sedimentary Petrology, v. 48, no. 2., p. 453-973.

Evamy, B.D., 1969, the precipitation environment and correlation of some calcite cements deduced from artificial staining: Journal of Sedimentary Petrology, v. 39, p. 787-793.

Hall, G.M. and Amick, H.C., 1934, The section on the west side of Clinch Mountain: Tennessee Academe of Sciences Journal, v. 9, p. 157-168, 195-220.

Hardie, L.A. (ed.), 1977, Sedimentation of Modern Carbonate Tidal Flats of Northwest Andros Island, Bahamas: John Hopkins University Studies in Geology 22, 202 p.

Hardie, L.A., Boselli, A., and Goldhammer, R.K., 1986, Repeated subaerial exposure of subtidal carbonate platforms: Evidence for high frequency sea-level oscillations on a $10^4$ year scale: Paleoceanography, v. 1, p. 447-457.

Hardie, L.A., and Shinn, E.A., 1986, Carbonate depositional environments, modern and ancient, 3, Tidal Flats: Colorado School of Mines Quarterly, v. 81, no. 1, 74 p.

Hardie, L.A., Dunn, P.A., and Goldhammer, R.K., 1991, Field and modeling studies of Cambrian carbonate cycles, Virginia Appalachians - Discussion: Journal of Sedimentary Petrology, v. 61, p. 636-646.

Hill, W., T., and Wedow, 1971, An early Middle Ordovician age for collapse breccias in the East Tennessee zinc districts as indicated by compaction and porosity features: Economic Geology, V. 66, p. 725-734.

Hudson, J.D., 1977, Stable isotopes and limestone lithification: Journal of Geological Society of London, v. 133, p. 637-660.

Illing, L.V., 1954, Bahamian calcareous sand: American Association of Petroleum Geologists Bulletin, v. 38, no. 1, p. 1-95.

Illing, L.V., Wells, A.J., and Taylor, J.C., 1965, Penecontemporary dolomite in the Persian Gulf, in Pray, L.C., and Murray , R.C., eds., Dolomitization and Limestone Diagenesis a Symposium: Society of Economic Paleontologists and Mineralogists Special Publication 13, p. 89-111.

James, N.P., 1972, Holocene and Pleistocene calcareous crust (caliche) profiles: criteria for crust subaerial exposure: Journal of Sedimentary Petrology, v. 42, no. 4, p. 817-836.

James, N.P., and Choquette, P.W., 1984, Diagenesis 9 - Limestones - the meteoric diagenetic environment: Geoscience Canada, v. 11, p. 161-194.

James and Klappa, 1983, Petrogenesis of early Cambrian reef limestone, Labrador, Canada: Journal of Sedimentary Petrology, v. 53, p. 1051-1-96.

Jernigan, D.G., 1987, Comparative Diagenetic Histories of the Holston and Rockdell Formations, Middle Ordovician of Northeastern Tennessee: [unpublished M.S. thesis]: Knoxville, University of Tennessee, 234 p.

Johnson, R.E., 1988, Petrogenesis of Carbonate Lithofacies along an Evolving Paleozoic Shelf, Lower Chickamauga Group and Equivalents, Middle Ordovician, Northeastern Tennessee [unpublished doctoral dissertation]: Knoxville, University of Tennessee, 391 p.

Kendall, C. St. G., and Schlager, W., 1981, Carbonates and relative changes in sea level: Marine Geology, v. 44, p. 181-212.

Kennett, J.P., 1982, Marine Geology: Englewood Cliffs, New Jersey, Prentice-Hall, 813 p.

Kesler, S.E., Jones, L.M., and Ruiz, J., 1988, Strontium isotope geochemistry of Mississippi Valley-type deposits, East Tennessee: Implication for age and source of mineralizing brines: Geological Society of America Bulletin, v. 100, p. 1300-1307.

Ketelle, R.H., and Lee, R.R., 1992, Migration of a Groundwater Contaminate Plume be Stratabound Flow in Waste Area Grouping 1 at Oak Ridge National Laboratory, Oak Ridge, Tennessee: ORNL/ER-126, Oak Ridge National Laboratory, Oak Ridge, Tennessee, 21 p.

Kharaka, Y.K., and Carothers, W.W., 1986, Oxygen and hydrogen isotopic geochemistry of deep basin brines, in Fritz, P. and Fontes, J. Ch., eds., Handbook of Environmental Isotope Geochemistry, v..2: New York, Elsevier, 305-360 p.

Klein, G. DeV., 1970, Depositional and dispersal dynamics of intertidal sand bars: Journal of Sedimentary Petrology, v. 40, no. 4, p. 1095-1127.

Koerschner, W.F.,III, and Read, J.F., 1989, Field and modelling studies of Cambrian carbonate cycles, Virginia Appalachians: Journal of Sedimentary Petrology, v. 59, p. 654-687.

Koerschner, W.F.,III, and Read, J.F., 1990, Field and modelling studies of Cambrian carbonate cycles, Virginia Appalachians - Reply: Journal of Sedimentary Petrology, v. 60, p. 795-796.

Kozar, M.G., Weber, L.J., and Walker, K.R., 1990, Field and Modelling in Cambrian carbonate cycles, Virginia Appalachians - Discussion: Journal of Sedimentary Petrology, v. 60, p. 790-794.

Krumbein, W.C. and Sloss, L.L., 1951, Stratigraphy and Sedimentation: San Francisco, W.H. Freeman, 660.

Canaan, P.H., 1967, Emplacement of Flask-type sand beds: Sedimentology, v. 9, p. 203- 243.

Land, L.S., 1985, The origin of massive dolomite: Journal of Geological Education, v. 33, p. 112-125.

Land, L.S., Behrens, E.W., and Frishman, S.A., 1979, The ooids of Baffin Bay, Texas, Journal of Sedimentary Petrology, v. 49, p. 1261-1278.

Lee, R.R., and Ketelle, R.H., 1987, Stratigraphic Influence on Deep Groundwater Flow in the Knox Group Copper Ridge Dolomite on the West Chesnut Ridge Site: ORNL/TM-10479 Oak Ridge National Laboratory, Oak Ridge, Tennessee.

Lee, R.R., and Ketelle, R.H., 1988, Subsurface Geology of the Chickamauga Group at Oak Ridge National Laboratory: ORNL/TM-10749 Oak Ridge National Laboratory, Oak Ridge, Tennessee, 31 p.

Lemiszki, P.J., 1992, Geology of the Bethel Valley Quadrangle - Part of the Department of Energy Oak Ridge Reservation on the Southern Appalachian Foreland Fold-Thrust Belt and Fracture Mechanics Modeling of Extension Fracture Growth During Basin Subsidence and Buckle Folding [unpublished doctoral dissertation]: Knoxville, University of Tennessee, 353 p.

Lewis, J.B. 1965, A preliminary description of some marine benthic communities from Barbados, West Indies: Canadian Journal of Zoology, v. 43, p. 1094-1074.

Logan, B.W., Rezak, R., and Ginsburg, R.N., 1964, Classification and environmental significance of algal stromatolites: Journal of Geology, v. 72, no. 1, p. 68-83.

Logan, B.W., Hoffman, P. and Gebelein, C.D., 1974, Algal Mats, Cryptalgal Fabrics, and structures, Hamelin Pool, Western Australia, in Logan, B.W., Read, J.F., Gregory, M.H., Hoffman, P., brown, R.G., Woods, P.J., and Gebelein, C.D., Evolution and Diagenesis of Quaternary Carbonate Sequences, Shark Bay, Western Australia: American Association of Petroleum Geologists Memoir 22, p. 140-194.

Longman, M.W., 1980, Carbonate diagenetic textures from near-surface diagenetic environments: American Association of Petroleum Geologists Bulletin, v. 64, p. 461-478.

Lu, J. and Craig, J.R., 1992, Zinc mineralization and paragenesis at the Idol Mine, Copper Ridge district, East Tennessee [abstract]: Geological Society of America Abstracts with Programs, v. 24, no. 7, p. A234.

Maitland, M.R., 1979, The Paleobathymetric and Paleoenvironmental distribution of Middle Ordovician Trilobites within a portion of the Valley and Ridge of East Tennessee [unpublished M.S. Thesis]: Knoxville, University of Tennessee, 140 p.

McCrea, J.M., 1950, The isotope chemistry of carbonates and a paleotemperature scale: Journal of Chemistry and Physics, v. 18, 849-857.

Meyers, W.J., and Lohmann, K.C., 1985, Isotope geochemistry of regionally extensive calcite cement zones and marine components in Mississippian limestones, New Mexico, in Schnidermann, N. and Harris, P.M., eds., Carbonate Cements: Society of Economic Paleontologists and Mineralogists Special Publication No. 36, p. 223-239.

Misra, K.C., and Fulweiler, R.E., Zinc Deposits of the Mascot-Jefferson City district, East Tennessee, in Misra, K.C., Fulweiler, R.E., and Walker, K.R., 1992, Zinc Deposits in East Tennessee: Society of Economic Geologists Guidebook Series, v. 14, p, 9-24.

Mitchum, R.M., and Van Wagoner, J.C., 1991, High-frequency sequences and their stacking patterns: sequence-stratigraphic evidence of high-frequency eustatic cycles: Sedimentary Geology, v. 70, p. 131-160.

Moore, G.K., 1988, Concepts of Groundwater Occurrence and Flow Near Oak Ridge National Laboratory, Tennessee: ORNL/TM-10969 Oak Ridge National Laboratory, Oak Ridge Tennessee, 92 p.

Moore, N.K., 1978, Taxonomy and Paleoenvironmental Distribution of the Benthic Algal flora from Middle Ordovician Carbonate Rocks of East Tennessee [Doctoral Dissertation]: Knoxville, University of Tennessee, 148 p.

Moore, R.C., ed., 1955, Treatise on Invertebrate Paleontology, Part V, Graptolithina: Lawrence, University of Kansas Press, Geological Society of America.

Moore, R.C., 1959, Treatise on Invertebrate Paleontology, Part O, Arthropoda 1: Lawrence, University of Kansas Press, Geological Society of America, 559 p.

Morse, J.W., and Mackenzie, F.T., 1990, Geochemistry of Sedimentary Carbonates, Developments in Sedimentology 48: New York, Elsevier, 707 p.

Niemann, J.C., and Read, J.F., 1988, Regional cementation from unconformity-recharge aquifer and burial fluids, Mississippian Newman Limestone, Kentucky: Journal of Sedimentary Petrology, v. 58, p. 688-705.

Osleger, D.A., 1990, Cyclostratigraphy of Late Cambrian Cyclic Carbonates: An Interbasinal Field and Modeling Study, U.S.A. [unpublished doctoral dissertation]: Blacksburg, Virginia Polytechnic Institute, 303 p.

Osleger, D.A, 1991, Subtidal carbonate cycles: Implications for allocyclic vs. autocyclic controls: Geology, v. 19, no. 9, p. 917-920.

Osleger, D.A., and Read, J.F., 1991, Relation of eustacy to stacking patterns of meter-scale carbonates, Late Cambrian, U.S.A.: Journal of Sedimentary Petrology, v. 16, no. 7, p. 1225-1252.

Peryt, T.M., 1983, Oncoids: comment to recent developments, in Peryt, T.M., ed., Coated Grains: New York, Springer-Verlag.

Presbindowski, D.R., 1985, Burial cementation -- Is it important?, in Scheidermann, N., and Harris, P.M., eds., Carbonate Cements: Society of Economic Paleontologists and Mineralogists Special Publication 36, p. 241-264.

Popp, B.N., Anderson, T.F., and Sandberg, P.A., 1986, Brachiopods as indicators of original isotopic compositions in some Paleozoic limestones: Geological Society of America Bulletin, v. 97, p. 1262-1269.

Price, N.B., 1967, Some geochemical observations on Manganese-iron oxide nodules from different environments: Marine Geology, v. 5, p. 511-538.

Prudy, E.G., 1963, Recent calcium carbonate facies of the Great Bahama Bank, part 2, sedimentary facies: Journal of Geology, v. 71, 472-497 p.

Radke, R.M., and Mathis, R.L., 1980, On the formation of saddle dolomite: Journal of Sedimentary Petrology. v. 50, p. 1149-1168.

Ramsay, T.A. 1974, The distribution of calcium carbonate in deep sea sediments, in Hay, W.W., ed., studies in Paleoceanography: Society of Economic Paleontologists and Mineralogists Special Publication 22, p. 58-76.

Read, 1989, Controls on evolution of Cambrian-Ordovician passive margin, U.S. Appalachians, in Crevello, P.D., Sarg, J.F., Wilson, J.L., and Read, J.F., eds., Controls on Carbonate Platform and Basin Development: Society of Economic Paleontologists and Mineralogists Special Publication 44, p. 147-165.

Read, J.F., and Goldhammer, 1988, Use of Fischer plots to define third-order sea-level curves in Ordovician peritidal carbonates, Appalachians: Geology, v. 16, 895-899.

Read, J.F., Grotzinger, J.P., Bova, J.A., and Koerschner, W.F., 1986, Models for generation of carbonate cycles: Geology, v. 14, p. 107-110.

Reineck, H.E., and Singh, I.B., 1973, Depositional Sedimentary Environments: New York, Springer-Verlag, 439 p.

Riding, R., 1975, *Girvanella* and other algae as depth indicators: Lethaia, v. 8, p. 173 - 179.

Rhoads, D.C., 1974, The paleoecological and environmental significance of trace fossils, in Fery, R.W., The Study of Trace Fossils: New York, Springer-Verlag, p. 147-159.

Roberson, K.E., 1987, Tidal flat stromatactis from the Middle Ordovician of Alabama [abstract]: Society of Economic Paleontologists and Mineralogists (SEPM) Annual Midyear Meeting Abstracts, v. IV, p.71.

Roberson, K.E., in prep., Stratigraphy and Depositional History of Middle Ordovician Peritidal Carbonate Rocks Overlying the Post-Knox Unconformity, East Tennessee [unpublished doctoral dissertation]: Knoxville, University of Tennessee.

Roberson, K.E., and Foreman, J.L., 1989, Sedimentology and diagenesis of tidal flat Stromatactis, Middle Ordovician, Alabama, in Walker, K.R., ed., The Fabric of Cements in Paleozoic Limestones: University of Tennessee Studies in Geology 20, p. 105-117.

Roberson, K. E., and Walker, K. R., 1990, Regional Appalachian disconformity produced solely by environmental migration within a Chazy (Middle Ordovician) transgressive sedimentary sequence [abstract]: Geological Society of America, Abstracts with Programs, v. 22, p. 334.

Rozkowski, A., and Rezewlocki, K., 1974, Application of stable environmental isotopes in mine hydrology taking Polish coal basins as an example, in Isotope Techniques in Groundwater Hydrology, V. 1, Proceedings of a symposium organized by the international atomic Energy Agency and held in Vienna, 11-15 March, 1974, p. 481-502.

Rowell, A.J., and Grant, R.E., 1987, Phylum Brachiopoda, in Boardman, R.S., Cheetham, A.H., and Rowell, A.J., eds., Fossil Invertebrates: Palo Alto, Blackwell Scientific Publications, p. 445.

Rudwick, M.J.S., 1970, Living and Fossil Brachiopods: London, Hutchinson and Co., 199 p.

Ruppel, S.C., 1979, The Stratigraphy, Carbonate Petrology, and Depositional Environments of the Chickamauga Group (Middle Ordovician) of Northern East Tennessee [unpublished doctoral dissertation]: Knoxville, University of Tennessee, 231 p.

Ruppel, S.C., and Walker, K.R., 1982, Sedimentology and distinction of platformal and downslope carbonate buildups: Middle Ordovician, East Tennessee: Journal of Sedimentary Petrology, v. 52, no. 4, p. 1055-1071.

Ruppel, S.C., and Walker, K.R., 1984, Petrology and depositional history of a Middle Ordovician carbonate platform: Chickamauga Group, northeastern Tennessee: Geological Society of America Bulletin, v. 95, p. 568-583.

Saller, A., H., and Moore, C.H., Geochemistry of meteoric calcite cements in some Pleistocene limestones: Sedimentology, v. 38, p. 601-621.

Sandburg, P.A., 1983, An oscillation trend in Phanerozoic non-skeletal carbonate mineralogy: Nature, v. 305, p. 19-22.

Sarg, J.F., 1988, Carbonate sequence stratigraphy, in Wilgus, C.K., Hastings, B.S., Kendall, C.G. St. C., Postamentier, H.W., Ross, C.A., and Van Wagoner, J.C., eds., Sea-Level Changes: An Integrated Approach: Society of Economic Paleontologists and Mineralogists Special Publication No. 42, p. 155-181.

Schlager, W., 1981, The paradox of drowned reefs and carbonate platforms: Geological Society of America Bulletin, v. 92, p. 197-211.

Schlager, W., and James, N.P., 1978, Low-magnesian calcite limestones forming at the deep-sea-floor, Tongue of the Ocean, Bahamas: Sedimentology, v. 25., p. 675-702.

Scholle, P.A., Arthur, M.A., and Ekdale, A.A., 1983, Pelagic environment, in Scholle, P.A., Bebout, D.G., and Moore, C.H., eds., Carbonate Depositional Environments: American Association of Petroleum Geologists Memoir 33, p. 620-691.

Schopf, T.J., 1969, Paleoecology of ectoprocts (bryozoans): Journal of Paleontology, v. 43, p. 234-244.

Schwarzacher, W., 1975, Sedimentation Models and Quantitative Stratigraphy: Developments in Sedimentology 19: New York, Elsevier, 382 p.

Shanmugam, G., and Walker, K.R., 1980, Sedimentation, subsidence, and evolution of a foredeep basin in the Middle Ordovician, Southern Appalachians: American Journal of Science, v. 280, p. 479-496.

Shinn, E.A., 1968, Practical significance of birdseyes structures in limestones: Journal of Sedimentary Petrology, v. 38, p. 215-223.

Shinn, E.A., 1983a, Birdseyes, fenestrae, shrinkage pores, and loferites: a reevaluation: Journal of Sedimentary Petrology, v. 53, no. 2, p. 619-628.

Shin, E.A., 1983b, Tidal Flat, in Scholle, P.A., Bebout, D.G., and Moore, C.H., eds., Carbonate Depositional Environments: American Association of Petroleum Geologists Memoir 33, p. 172-210.

Shinn, E.A., Ginsburg, R.N., and Lloyd, R.M., 1965, Recent supratidal Dolomite from Andros Island, Bahamas, in Pray, L.C., and Murray R.C., eds., Dolomitization and Limestone Diagenesis a Symposium, Society of Economic Paleontologists and Mineralogists Special Publication 13, p. 112-123.

Sibley, D.F., and Greg, J.M., 1987, Classification of dolomite rock textures: Journal of sedimentary Petrology, v. 57, No. 6, p. 967-975.

Simonson, J.B.C., 1985, The Stratigraphy, Carbonate Petrology, Depositional Environments, and Paleoecology of the Middle Ordovician Moccasin Formation Near Thorn Hill, Tennessee:[unpublished M.S. thesis] Knoxville, University of Tennessee, 279 p.

Sloss, L.L., 1963, Sequences in the cratonic interior of North America: Geologic Society of America Bulletin, v. 74, p. 93-113.

Solomon, D.K., Moore, G.K., Toran, L.E., Dreier, R.B., and McMaster, W.M., 1992, Status Report: A Hydrologic Framework for the Oak Ridge Reservation: Oak Ridge National Laboratory, Environmental Sciences Division Publication No. 3815.

Stockdale, P.B., 1951, Geologic Conditions at the Oak Ridge National Laboratory (X-10) Area Relevant to the Disposal of Radioactive Waste: ORO-58 U.S. Atomic Energy Commission, Oak Ridge Operations, Oak Ridge, Tennessee, 78 p.

Srinivasan, K., Foreman, J.L., Johnson, R.E., Walker, K.R., and Steinhauff, D.M., 1989, Chapter 4: A brief review of staining, luminescence microscopy, and geochemical methods in study, of carbonate cements, in Walker, K.R., ed., The Fabric of Cements in Paleozoic Limestones: Knoxville, University of Tennessee Studies in Geology, no. 20, p. 19-36.

Steinhauff, D.M., 1989, Chapter 5: Marine cements, in Walker, K.R., ed., The Fabric of Cements in Paleozoic Limestones: Knoxville, University of Tennessee Studies in Geology, no. 20, p. 37-53.

Steinhauff, D.M., in prep., Sequence Stratigraphy and Comparative Diagenesis of Middle Ordovician Shelf to Shelf-Edge Limestones, The Copper Creek Allochthon, East Tennessee [unpublished doctoral dissertation]: Knoxville, University of Tennessee.

Steinhauff, D. M., Jernigan, D.G., and Walker, K.R., 1989a, Chapter 11: Stratigraphic patterns of cementation in the Middle Ordovician Holston and Rockdell formations, East Tennessee, in Walker, K.R., ed., The Fabric of Cements in Paleozoic Limestones: Knoxville, University of Tennessee Studies in Geology 20, p. 118-138.

Steinhauff, D.M., and Roberson, K.E., 1989, Stop 7 - Uppermost Knox Group, the Knox unconformity, and Middle Ordovician transition between shallow shelf and deeper basin near Dandridge, Tennessee, in Walker, K.R.; Read, J.F., and Hardie, L.A., eds., Cambro-Ordovician Carbonate Banks and Siliclastic Basins of the United States Appalachians, Field Trip Guidebook T161, Knoxville Tennessee to Hagerstown, Maryland, June 30 - July 9, 1989, 28th International Geological Congress: Washington D.C., American Geophysical Union, p. 24 -27.

Steinhauff, D.M., Walker, K.R., and Foreman, J.L., 1989b, Relevance of textural criteria for identifying diagenetic phases: Petrographic and isotopic evidence, Middle Ordovician Holston and Rockdell formations, East Tennessee [abstract]: Geological Society of America Abstracts with Programs, St. Louis, Missouri, November, 6-9, v. 21, no. 6, p. A259.

Steinhauff, D.M., and Walker, K.R., 1987, Carbonate Cement Sequences in the Middle Ordovician Five Oaks, Lincolnshire, and Rockdell Formations (Chickamauga Group) East Tennessee [Abstract]: Geological Society of America Abstracts with Programs, Norfolk, Virginia, March 25-27, v. 19, no. 2, p. 131.

Steinhauff, D.M., and Walker, K.R., 1992a, Sequence stratigraphy of an apparently non-cyclic carbonate succession: Recognizing subaerial exposure in largely subtidal sequences, Middle Ordovician , East Tennessee [Abstract]: Geological Society of America Abstracts with Programs, Annual Meeting, Cincinnati, OH, v. 24, no. 7, p. A318.

Steinhauff, D.M., and Walker, K.R., 1992b, Third order sequence boundary in apparently non-cyclic carbonates: Middle Ordovician Rockdell and Benbolt formations near Idol, TN, in Driese, S.G., Mora, C.I., and Walker, K.R., eds., Paleosols, Paleoweathering, Surfaces, and Sequence Boundaries: University of Tennessee Department of Geological Sciences Studies in Geology 21, prepared for the 10th Annual Field Trip of the Midcontinent section of the Society for Sedimentary Geology (SEPM) Knoxville, Tennessee, October, 1992, p. 19-25.

Steinhauff, D.M., and Walker, K.R., in press, Sequence stratigraphy of an apparently non-cyclic carbonate succession: Recognizing subaerial exposure in largely subtidal stratigraphic sequences, Middle Ordovician, East Tennessee, in Witzke, B.J., and Ludvigson, G., eds., Paleozoic Sequence Stratigraphy: Geological Society of America Special Paper, manuscript 19 p., 2 tables, 19 figures.

Steinhauff, D.M., and Walker, K.R., submitted, Recognizing exposure, drowning, and "missed beats": Shelf to shelf-edge sequence stratigraphy of Middle Ordovician non-cyclic carbonates, East Tennessee: Bulletin American Association of Petroleum Geologists, manuscript 19 p., 15 figs., 2 tables.

Steinhauff, D.M., and Walker, K.R., in prep. b, Comparative diagenesis of Middle Ordovician shelf to shelf-edge limestones, the Copper Creek allochthon, East Tennessee, manuscript 17 p., 21 figs., 2 tables.

Swinchatt, J.P., 1969, Algal boring: a possible depth indicator in carbonate rocks and sediments: Geological Society of America Bulletin, v. 80, p. 1391-1396.

Tobin, K.J., and Walker, K.R., in prep., The Anatomy of an Ordovician marine-flooding surface: Top of the Holston Formation near Knoxville, Tennessee.

Vail, P.R., Mitchum, R.M., Jr., and Thompson, S., III, 1977, Seismic stratigraphy and global changes of sea-level, part three: relative changes of sea level from coastal onlap: American Association of Petroleum Geologists Memoir 26, p. 63-82.

Vail, P.R., Mitchum, R.,M., Jr., Todd, R.G., Wildmier, J.M., Thompson, S.. III, Sangree, J.B., Bubb, J.N., and Hatfield, W.G., 1977, Seismic stratigraphy and global changes of sea level, in Payton, C.E., Seismic Stratigraphy - applications to hydrocarbon exploration: American Association of Petroleum Geologists, Memoir 26, p. 49-212.

Van der Plas, L., and Tobi, A.C., 1965, A chart for judging the reliability of point counting results: American Journal of Science, v. 263, p. 87-90.

Veizer, J, Lemieux, J., Jones, B., Gibling, M.R., and Savelle, J., 1977, Sodium: paleosalinity indicator in ancient rocks: Geology, v. 5, p. 177-179.

Walker, K.R., 1977, A Brief Introduction to the Ecostratigraphy of the Middle Ordovician of Tennessee (southern Appalachians, U.S.A.), in Ruppel, S.C., and Walker, K.R., eds., The Ecostratigraphy of the Middle Ordovician of the Southern Appalachians (Kentucky, Tennessee, and Virginia), U.S.A.: A Field Excursion: Knoxville, University of Tennessee Department of Geological Sciences Studies in Geology 1, p. 12-17.

Walker, K.R., 1980, Introduction to the stratigraphy and paleoenvironments of the Middle Ordovician of Tennessee, in Walker, K.R., Broadhead, T.W., and Keller, F.B., eds., Middle Ordovician Carbonate Shelf to Deep Water Basin Deposition in the Southern Appalachians, Field Trip 10, Geological Society of America Annual Meeting, Atlanta, 1980: University of Tennessee Studies in Geology 4, p. 4-12.

Walker, K.R., ed., 1985, The Geologic History of the Thorn Hill Paleozoic Section (Cambrian - Mississippian), Eastern Tennessee: Knoxville, University of Tennessee Studies in Geology 10, 128 p.

Walker, K.R., 1989, Chapter 2: Petrographic criteria for interpreting the origin of pore fillings, in Walker, K.R., ed., The Fabric of Cements in Paleozoic Limestone: University of Tennessee Studies in Geology No. 20, p.4-10

Walker, K.R., 1992, Marine flooding interval between the Moccasin and Overlying "Martinsburg" Formations: A 3rd order sequence boundary, in Driese, S.G, Mora, C.I., and Walker, K.R., eds., Paleosols, Paleoweathering Surfaces, and Sequence Boundaries: University of Tennessee Department of Geological Sciences Studies in Geology 21, p.26-34.

Walker, K.R., Broadhead, T.W., and Keller, F.B., eds., 1980, Middle Ordovician Carbonate Shelf to Deep Water Basin Deposition in the Southern Appalachians, field Trip 10, Geological Society of America Annual Meeting, Atlanta, 1980: University of Tennessee Studies in Geology 4, 120 p.

Walker, K.R., and Foreman, J.L, 1990, Early diagenetic history controls burial alteration: comparison of Cambrian and Ordovician carbonates in the S. Appalachians, U.S.A., [abstract]: 13th International Sedimentological Congress Papers, p. 582.

Walker, K.R., Foreman, J.L., Roberson, K.E., Srinivasan, K., and Steinhauff, D.M., 1989, Cambrian original marine-calcite carbon and oxygen isotopic composition determined from unaltered ooids and fibrous cements [abstract]: Geological Society of America Abstracts with Programs, St. Louis, Missouri, November 6-9, v. 21, no. 6, p. A222.

Walker, K.R., Jernigan, D.G., and Steinhauff, D.M., 1986, Analysis of pore histories in Paleozoic rocks: an example from the Middle Ordovician of the Southern Appalachians: Appalachian Basin Industrial Associates, v. 12, p. 101-116.

Walker, K.R., Jernigan, D.G., and Steinhauff, D.M., 1987a, Fluid-flow timing and pathway prediction across carbonate shelf margins: The lower Paleozoic of the Southern Appalachians as a natural laboratory [abstract]: Appalachian Petroleum Geology Symposium, Morgantown, West Virginia, March 23-25, 1987.

Walker, K.R., Jernigan, D.G., and Steinhauff, D.M., 1987b, Fluid-flow timing and pathway prediction across carbonate shelf margins: The lower Paleozoic of the Southern Appalachians as a natural laboratory, in Rifts, Ramps, Reefs and Royalties: West Virginia Geological and Economic Survey, Circular C-40, p. 105-118.

Walker, K.R., Jernigan, D.G., and Steinhauff, D.M., 1987c, Fluid-flow timing and pathway prediction in carbonate sequences: Examples from Middle Ordovician of Southern Appalachians [Abstract]: Society of Economic Paleontologists and Mineralogists, Midyear Meeting, Austin, Texas, v. 4, p. 88.

Walker, K.R., Jernigan, D.G., and Weber, 1990, Petrographic criteria for the recognition of marine, syntaxial overgrowths, and their distribution in geologic time: Carbonates and Evaporites, v. 5, No. 2, p. 141-151.

Walker, K.R., Shanmugam, G., and Ruppel, S.C., 1983, A model for carbonate to terrigenous clastic sequences: Geological Society of America Bulletin, v. 95, p. 100-110.

Walker, K.R., Steinhauff, D.M., and Roberson, K.E., 1992, Stop 5: Uppermost Knox Group, The Knox unconformity, the Middle Ordovician transition from shallow shelf to deeper basin near Dandridge, Tennessee, and a possible source for mineralizing fluids, in Misra, K.C., Fulweiler, R.E., and Walker, K.R., eds., Zinc Deposits in East Tennessee: Society of Economic Geologists, Guidebook Series v. 14, p. 66-73.22

Walker, R.G., ed., 1984, Facies Models, 2nd edition: Geoscience Canada, Reprint Series 1, 317 p.

Weber, L.J., 1988, Paleoenvironmental analysis and test of stratigraphic cyclicity in the Nolichucky Shale and Maynardville Limestone (Upper Cambrian) in central East Tennessee [unpublished doctoral dissertation]: Knoxville, University of Tennessee, 389 p.

Wedekind, J.E., 1986, The stratigraphy, Depositional Environments, Bryozoan Paleoecology, and taphonomy of the Middle Chickamauga Group near Thorn Hill, Grainger County, Tennessee [unpublished M.S. Thesis]: Knoxville, University of Tennessee, 200 p.

Weiss, E.A., 1981, Environmental Sedimentology of the Middle Ordovician and Paleoecology of a Portion of the Witten Formation at Solway, Tennessee [unpublished M.S. thesis]: Knoxville, University of Tennessee, 229 p.

Wilson, J.L., 1975, Carbonate Facies in Geologic History: New York, Springer-Verlag, 471 p.

Wonnacott, T.H, and Wonnacott, R.J., 1984, Introductory Statistics for Business and Economics, Third Edition: New, York, John Wiley and Sons. 746.

Wrey, J.L., 1977, Calcareous Algae: New York, Elsevier, 185 p.

Zempolich, W.G., Wilkinson, B.H., and Lohmann, K.C., 1988, Diagenesis of Late Proterozoic Carbonates: the Beck Spring Dolomite of Eastern California: Journal of Sedimentary Petrology, v. 58, no. 4, p. 656-672.

# APPENDICES

# APPENDIX A

## MEASUREMENT CONVENTIONS AND DESCRIPTION OF STRATIGRAPHIC SECTIONS

## MEASUREMENT CONVENTIONS AND DEFINITIONS

Field descriptions are given in ascending order, oldest to youngest. Appendix A is intended to provide field descriptions of each measured section. However, petrographic criteria and inferences made to help place sequence boundaries are discussed where appropriate.

### Field Descriptions

**Bed Thickness.**

| | |
|---|---|
| Very thick bedded | greater than 1.0 m |
| Thick bedded | 0.3 to 1.0 m |
| Medium bedded | 0.1 to 0.3 m |
| Thin bedded | 0.03 to 0.1 m |
| Very thin bedded | 0.01 to 0.003 m |
| Laminated | 003 to 0.01 m |
| Thin laminated | less than 0.003 m |

**Grain Size.**

| | |
|---|---|
| Coarse grained | grains visible to unaided eye and readily identifiable(approximately greater than 1 mm across). |
| Medium grained | grains visible but not readily identifiable (approximately 0.25 to 1.0 mm across). |
| Fine grained | grains visible only with 10X hand lens (approximately 0.1 to 0.25 mm across). |
| Very fine grained | grains not visible even with a hand lens (generally less than 0.1 mm across). |

### Additional Descriptions

**Color.** Descriptive color terms follow the Munsell system. Unless otherwise stated, all references to color apply to fresh or non-weathered specimens.

**Lithologic Terminology and Facies.** Limestone names are after Dunham (1962). Letters assigned to 15 facies are modified from Wilson (1975), see Tables 2.1 and 2.2

of Chapter 2. Lithologies or facies are interpreted and listed for each thin-section. For example, "facies E" is echinoderm grainstone. In many cases, transitional lithologies are recognized; these are indicated by two letters separated by a slash. The dominate lithology is listed first and represents an estimated proportion of the allochems or lithology present in the thin-section (generally more than 1/2 and up to 2/3 of the dominate lithology). The subordinate lithology is listed second, and represents less than 1/2, but at least 1/3 of this lithology in the thin-section. For example "facies E/I" indicates an echinoderm grainstone with 1/2 to 1/3 of its allochems as peloids (see Tables 2.1 and 2.1 of Chapter 2).

**Third-Order Sequences and Fourth-Order Subsequences.** Third-order stratigraphic sequence are correlative across the shelf and from the shelf to the shelf-edge. Third-order sequence boundaries are recognized by pronounced surfaces of subaerial exposure (some of which are coincident with drowning unconformities). Fourth-order subsequences are correlative across the shelf, but not all subsequences are correlative from the shelf to the shelf-edge. Fourth-order subsequence are recognized by less pronounced surfaces of subaerial exposure (see, Chapter 2).

**Parasequences or Possible Fifth-Order Sequences.** Parasequences are not laterally continuous across the shelf and can not be recognized or resolved at the shelf-edge. Furthermore, these parasequences are inferred from inflection points on depth-curves and from subtle lithologic changes. Parasequences generally can not be resolved in the field. Consequently, not all parasequences are inferred at each stratigraphic section. Fifth order parasequences are numbered consecutively (1 through 44; e.g., Fig. 2.18). The stratigraphic position of the upper surface of each parasequence occurring within a fourth-order subsequence is summarized following discussion of each fourth-order subsequence.

**Water-Depth Deepening Events.** Water-depth deepening events are similar to subsequences and parasequences in that they are inferred from maximum inflections on water-depth curves and from subtle lithologic changes. Consequently, not all water-depth deepening events can be identified at each stratigraphic section. The stratigraphic position of water-depth deepening events occurring within fourth-order subsequences are summarized following discussion of each fourth-order subsequence.

**Sample Numbering.** Samples collected by the author (50 X 75 mm, thin-sections) are identified in a three part format indicating location, year of collection, and a unique number (generally the order of collection). For example, Sample TH-89-7A was the seventh sample collected from the Thorn Hill section in 1989: two thin-sections, named A and B, were cut from the same billet or rock chip (i.e., a serially cut section). All thin-sections were cut perpendicular to bedding. Samples with different unique numbers, but occupying the same stratigraphic position represent two thin-sections cut from different billets or rock chips. Such thin-sections were prepared when different lithologies were observed to occur at the same stratigraphic position

(i.e., a grainstone lens within a packstone or wackestone). The terms "Top," "Bottom," and "N" are used to refer to thin-sections cut from the same limestone slab. "Top" indicates a thin-section cut from the top of the slab, "Bottom," a thin-section from the bottom of the slab, and "N" a thin-section cut normal to the slab. Because different parts of some sections were collected at different times, these unique numbers are usually, but not necessarily in stratigraphic order.

## DESCRIPTION OF STRATIGRAPHIC SECTIONS

### Thorn Hill Section (TH)

The Thorn Hill or "New" Thorn Hill section is exposed in a road cut along the eastern and western portions of Dixie Highway (U.S. Route 25 East) at its intersection with State Route 131 (formerly State Route 66), near Thorn Hill, Grainger County, Tennessee (between lat 36°21'08''N to 36°21'29''N and long 83°25'48''W to 83°26'18''W). This area lies in approximately the NE 1/4, NW 1/4, SW 1/4 of the Avondale 7.5 minute topographic quadrangle. This is the same stratigraphic section described in *The Geologic History of the Thorn Hill Paleozoic Section (Cambrian - Mississippian), East Tennessee* edited by K.R. Walker (1985); This section is also described by Byerly et al. (1986). It should be noted that before the Dixie Highway was opened in the 1970's, the section located immediately to the east (Old Thorn Hill Section of this work) was known as the "Thorn Hill section" (e.g., Hall and Amick, 1934 ; Carnes, 1975; Ruppel, 1979). This work represents the first time that the Lincolnshire and Rockdell formations have been systematically sampled and studied at the "New" Thorn Hill section.

The Middle Ordovician Thorn Hill section was collected in four separate, but overlapping parts. These are indicated as thick black bars in Figure 2.1. Only the first three parts are used in this work. 1) Samples from 23 to 32 meters above the Knox unconformity were obtained from the northernmost part of the section, on the east side of Dixie Highway. A covered interval occurs from about 32 to 77 meters. 2) Samples from about 77 to 137 meters were collected along the western branch of Forked Deer Creek on the west side of Dixie Highway, starting at the culvert that passes under the Highway. These samples were collected all the way up to and along the south side of State Route 131. Much of this part of the section was covered with debris after sampling when the intersection of Dixie Highway and State Route 131 was improved in 1991. 3) Samples from 137 to 320 meters were obtained along the western branch of Forked Deer Creek and from the pasture on the west side of Dixie Highway, starting north of State Route 131 and continuing to Thorn Hill Church Road which crosses the creek about 0.4 km south of State Route 131. 4) The southernmost and stratigraphically highest portion of the section was collected along the eastern side of Dixie Highway by James Wedekind (1986) and John Simonson (1985). Wedekind studied the Benbolt Formation and collected samples from about

235 to about 430 meters above the Knox. Simonson studied the Moccasin Formation and collected samples from about 425 to 610 meters above the Knox. Descriptions made by Wedekind and Simonson were consulted; however, thin-sections cut by each were not used to construct any of the water-depth curves of this work.

Approximately 430 m (1,410 ft.) of the Chickamauga Group comprising the Five Oaks, Lincolnshire, Rockdell, Benbolt, Bowen, and Witten formations are exposed from the Knox/Chickamauga contact (best located on the hill side on the side of Dixie Highway about 2.5 km north of State Route 131) to the base of Moccasin Formation. All samples described from the Thorn Hill section (below) were collected and prepared by the author. Description of additional Chickamauga Group samples collected from the Benbolt and Moccasin Formations are provided by Wedekind (1986) and Simonson (1985), respectively.

**KNOX GROUP**

Unconformity

| Sequence/ Cycle | | | **CHICKAMAUGA GROUP** |
|---|---|---|---|
| 2nd Ord. | Seq. Thk (m) | Cumul. Thk (m) | |
| O-S | 1,384 | 1,384 | **Tippecanoe Sequence (Sloss, 1963).** Other Synonyms: Ordovician-Silurian (O-S) Second Order Cycle or Supercycle (Vail, et al., 1977), and Paleozoic Sequence II, Middle Ordovician to Lower Devonian, Walker (1985) and Byerly et al. (1986). |
| 3rd & 4th Ord. | Seq. Thk (m) | Cumul. Thk (m) | |
| 1A-2B | 23.0 | 23.0 | **Five Oaks Formation.** The interval from 0 to 23 m (Five Oaks Formation) is well exposed along Dixie Highway: However, it was not sampled for this study. Fourth Order Sequence 1C is not recognized at this section but is recognized at the Old Thorn Hill, Idol Mine, and Cedar Springs sections. The Five Oaks Formation is recognized by its three major lithologies, dolostone (facies P), wackestone/mudstone (facies L), and peloidal grainstone (facies I). Fresh examples of these |

lithologies range from pale-yellowish-brown to dark-yellowish-brown and are generally very fine- to fine-grained. Peloidal grainstones are generally fine- to medium-grained and darkest in color, approaching dusky-brown. The same color hues are observed in weathered out crop, but the chroma or saturation is generally altered. Wackestones and mudstones tend to weather to lower chroma or saturation (darker colors), whereas grainstones tend to weather to a higher chroma (lighter colors). Ostracodes are the only fauna present in large numbers.

| | | | |
|---|---|---|---|
| 1 | 18.5 | 18.5 | **Third-Order Sequence 1 (lower to upper Five Oaks Formation).** |
| Estimated 1A | 14.5 | 14.5 | Fourth-Order Subsequence 1A (Blackford Member of the Five Oaks Formation). |
| | 14.5 | 14.5 | Parasequence 1 (0 to 14.5 m): The first two to three meters of strata developed above the Knox consists of pale-brown, pale-yellowish- brown, and dark-yellowish-brown, medium- to thick-bedded, massive dolostone. The lower contact with the Knox is gradational. These massive dolostones grade upward into thick- to very-thick bedded wackestone/mudstone (facies L) of similar color.<br><br>Stratigraphic Positions Interpreted from Water-Depth Curves:<br>Upper Parasequence Surfaces: Parasequence 1, 14.5 m (estimated).<br>Deepening Events: None. |
| Estimated 1B | 4.0 | 18.5 | Fourth-Order Subsequence 1B (Five Oaks Formation, continued). |
| | 4.0 | 18.5 | Parasequence 2 (14.5 to 18.5 m): Pale-brown, pale-yellowish-brown, and dark-yellowish-brown, thick- to very-thick bedded wackestone/mudstone (facies L) as in Subsequence 1A<br><br>Stratigraphic Positions Interpreted from Water-Depth Curves:<br>Upper Parasequence Surfaces: Parasequence 2, 18.5 m (estimated).<br>Deepening Event: $D_0$, (exact position not resolved) |

| | | | |
|---|---|---|---|
| 1C | N/A | N/A | Fourth-Order Subsequence 1C (Five Oaks Formation, continued). Subsequence 1C and its contained parasequence 3 are not presently recognized at the Thorn Hill section; however, additional analysis of thin-sections from the Five Oaks at the Thorn Hill Section may help to define this subsequence.<br><br>Stratigraphic Positions Interpreted from Water-Depth Curves:<br>Upper Parasequence Surfaces: N/A.<br>Deepening Event: $D_1$, (exact position not resolved). |
| 2 | 165.0 | 188.0 | **Third-Order Sequence 2 (Five Oaks and Lincolnshire formations).** |
| 2A | N/A | N/A | Fourth-Order Subsequence 2A. Subsequence 2A does not occur on the shelf (see Chapter 3). |
| Estimated 2B | 4.5 | 23.0 | Fourth-Order Subsequence 2B (Five Oaks Formation, total thickness 23.0 m). |
| | 4.5 | 23.0 | Parasequence 4 (18.5 to 23.0 m): Parasequence 4 consists of thick- to very-thick bedded wackestone/mudstone (facies L) as in Subsequence 1B. Sharp contact occurs with overlying Subsequence 2C. Exposure is inferred at the top of Subsequence 2B based on a change in lithology and by comparison with the Old Thorn Hill section.<br><br>Stratigraphic Positions Interpreted from Water-Depth Curves:<br>Upper Parasequence Surfaces: Parasequence 4, 23.0 m (estimated).Deepening Events: None. |
| 2C-2G | 115.5 | 138.5 | **Lincolnshire Formation:** The Five Oaks Lincolnshire contact is sharp and occurs directly above the upper surface of Subsequence 2B. The Lincolnshire Formation is distinguished from the underlying Five Oaks by its well developed, thick, and laterally extensive grainstone beds. In contrast, grainstone beds in the Five Oaks are almost entirely peloidal, considerably thinner, and generally lensoidal.<br><br>The Lincolnshire consists of peloid-rich grainstones (facies I and J) and echinoderm-rich grainstones (facies E, K, and D) |

intercalated with lesser amounts of mud-rich lithologies (facies B and F). Fresh examples of peloid-rich grainstones are generally grayish-brown to grayish-orange-pink and fine- to medium-grained. Echinoderm-rich grainstones range in color from moderate-orange-pink, grayish-orange-pink, light-brown, to moderate-brown (rare). Echinoderm grainstones are always coarse-grained. Mud-rich lithologies range from moderate-brown, to dusky-brown. The wackestones and mudstones tend to weather to a lower chroma or saturation (darker colors), whereas the grainstones tend to weather to higher chromas (lighter colors).

| | Estimated | | |
|---|---|---|---|
| 2C | 30.8 | 53.8 | Fourth-Order Subsequence 2C (Lincolnshire Formation). |
| | 15 | 38.0 | Parasequence 5 (23.0 to about 38.0 m): The basal Lincolnshire (1.5 meters thick) consists of thick-bedded, coarse- to medium-grained, nodular echinoderm/bryozoan packstones and echinoderm grainstones. These basal packstones and grainstones are overlain by about 4.5 meters of thick bedded, fine- to medium-grained, crossbedded grainstones with aggregate-grains and peloids (from about 24.5 to 29.0 m). These crossbedded grainstones grade into about 3.5 m of very thick-bedded peloidal grainstone (from 29 to 32 m). The exact position of the upper surface of Parasequence 5 is not resolved. Thin-sections: TH-90-555A, 23.0 m, facies F; TH-90-555B, 23.0 m, facies E; TH-90-556, 24.4 m, facies J; TH-90-557, 27.6 m, facies J. |
| | 15.8 | 53.8 | Parasequence 6 (about 38.0 to 53.8 m): The peloidal grainstones occurring at approximately the top of Parasequence 5 are sharply overlain by 3 meters of very thick-bedded, massive to crossbedded echinoderm grainstone (from 32 to 35 m). These grainstones are medium-bedded above about 34.5 meters. The section is covered above 35 meters. Thin-sections: TH-90-558, 30.4 m, facies I; TH-90-559, 32.4 m, facies E; TH-90-560A, 35.0 m, facies E; TH-90-560B, 35.0 m, facies E. |

Stratigraphic Positions Interpreted from Water-Depth Curves:
Upper Parasequence Surfaces: Parasequence 5, about 38 meters (exact position not resolved); Parasequence 6, 53.8 m (estimated).
Deepening Events: $D_{4A}$, 35.0 m; $D_{4B}$ (exact position not resolved).

| | | | |
|---|---|---|---|
| 2D | 2.7 | 56.5 | Fourth-Order Subsequence 2D (Lincolnshire Formation, continued). Subsequence 2D is covered. Subsequence 2D and its contained Parasequence 7 is inferred to occur between about 53.5 to 56.5 meters above the Knox.<br><br>Stratigraphic Positions Interpreted from Water-Depth Curves:<br>Upper Parasequence Surfaces: Parasequence 7, 56.5 meters (estimated).<br>Deepening Event: $D_5$ (exact position not resolved). |
| Approximate 42 | | 75 | COVERED INTERVAL |
| 2E | 59.0 | 115.5 | Fourth-Order Subsequence 2E (Lincolnshire Formation, continued). |
| | 21.8 | 78.3 | Parasequence 8 (about 56.5 to 78.3 m): Subsequence 2E and its contained Parasequence 8 are covered below about 77 meters. The lower part of Subsequence 2E is inferred to consist of thick- to very thick-bedded echinoderm grainstone (facies E). This is based on the occurrence of such grainstones at the Old Thorn Hill and Idol Mine sections. Thick-to-very thick-bedded, medium- to coarse-grained grainstones with coated bioclasts occur from 77 to about 79.5 meters. Thin-section: TH-90-450, 77.0 m, facies D. |
| | 8.7 | 87.0 | Parasequence 9 (78.3 to about 87.0 m): The section is not well exposed from 79.5 to 80.5 meters. Thick-bedded, coarse-grained dasyclad grainstone is interbedded with thin-to medium-bedded packstone and medium- to coarse-grained grainstone with coated bioclasts (from 80.5 to about 88 m). Massive to amalgamated crossbeds are common, especially in within the grainstone beds of this interval. Thin-sections: TH-90-449, 78.5 m, facies D/J; TH-90-448, 80.4 m, facies K; TH-90-447, 81.8 m, facies F; TH-90-446.1, 83.6 m, facies K; TH-90-446.2, 84.4 m, facies D; TH-90-444, 86.2 m, facies K; TH-90-445, 85.2 m, facies K, TH-89-444, 86.2 m, facies K; TH-89-1, 86.2 m, facies D. |
| | 7.6 | 94.6 | Parasequence 10 (about 87 to 94.6 m): The section is poorly exposed from about 87 to 89.5 meters. Very thick-bedded, coarse-grained, massive to amalgamated cross-bedded echinoderm grainstone occurs from about 89.5 to 95.5 meters. |

Thin-sections:TH-89-2, 91.5 m, facies E; TH-89-3A, 92.3 m, facies E; TH-89-3B, 92.3 m, facies I/J.

20.9 115.5 Parasequence 11 (94.6 to 115.5 m): These crossbeds are gradational with and are overlain by about 4.5 meters of very thick-bedded, fine-grained, massive bioclastic wackestone/packstone (95.5 to 100 m). The section is covered from about 100 to 112 meters. Very thick-bedded, fine-grained, massive bioclastic wackestone/packstone occurs from about 112 to 114.5 meters. These very thick- bedded wackestones and packstones become thick- to medium-bedded above about 113.5 meters, where they grade into medium-bedded nodular wackestone/mudstone. Subsequence 2E is capped with about 0.5 meters of this nodular wackestone (facies L). Exposure is inferred based on this capping wackestone lithology and by comparison with vadose features observed at this stratigraphic position at the Old Thorn Hill section. Thin-sections: TH-89-4, 94.7 m, facies F/M; TH-89-5, 95.1 m, facies B; TH-89-6, 97.2 m, facies B; TH-89-7, 99.2 m, facies B; TH-89-8, 113.6 m, facies B; TH-89-8N, 113.6 m, facies B; TH-89-9, 115.1 m, facies L.

Stratigraphic Positions Interpreted from Water-Depth Curves:
Upper Parasequence Surfaces: Parasequence 8, 78.3 m; Parasequence 9 (exact position not resolved); Parasequence 10, 94.6 m; Parasequence 11, 115.5 m.
Deepening Events: $D_6$, 80.4 m; $D_7$, 94.7 m.

2F N/A N/A Fourth-Order Subsequence 2F. Subsequence 2F is not recognized on the shelf.

Stratigraphic Positions Interpreted from Water-Depth Curves:
Upper Parasequence Surfaces: N/A
Deepening Events: N/A

2G 23.0 138.5 Fourth-Order Subsequence 2G (Lincolnshire Formation, total thickness 115.5 m).

<3.5 <119 Parasequence 12 (115.5 to <119 m): The contact with the underlying wackestone is gradational and occurs within thin- to medium-bedded nodular wackestones about 115.1 to 115.9 meters above the Knox. A thin- to medium-bedded oncoid-

bearing wackestone/packstone interval persists from about 115.5 to about 117 meters. This wackestone/packstone is overlain by about 2 meters of thin-bedded grainstone/packstone containing aggregate-grains and peloids (from about 117 to 119 m). These grainstone/packstones grade into about 2 meters of oncoid-bearing wackestone/packstone, thick-bedded in the first meter and thin-bedded in second meter (from about 119 to 120 m). Thin-sections: TH-89-10, 115.9 m, facies N; TH-89-11, 116.9 m, facies J/N; TH-89-12, 117.3 m, facies J/N.

>8.1 127.1 Parasequence 13 (<119 to 127.1 m): The interval from 119 meters to the top of Subsequence 2G, (about 138.5 m), was never well exposed. Much of Parasequence 13 is now covered by construction debris. The approximately 8 meter thick Parasequence 13 consists predominately of medium-bedded grainstones with aggregate-grains and peloids. Some of these beds contain partially coated-grains. Two thin beds of trilobite (*Lonchodomas* sp.) grainstone (lumped with facies E) occur between about 125.4 and 125.5 meters. Shoaling is indicated at the top of Parasequence 13 by the occurrence of about two meters of thin- to medium-bedded aggregate-grain, grainstone containing peloids and coated grains (facies J). Thin-sections: TH-89-13, 118.8 m, facies J and N; TH-89-14, 119.2 m, facies N; TH-89-15, 119.6 m, facies N; TH-89-16, 120.9 m, facies J; TH-89-17N, 121.4 m, facies J; TH-89-18, 122.2 m, facies J; TH-89-19, 122.6 m, facies J/N; TH-89-20, 122.9 m, sample lost; TH-89-21, 123.2 m, facies J; TH-89-23, 123.3 m, facies J; TH-89-22, 123.7 m, facies I; TH-89-24, 123.7 m, facies J; TH-89-25, 125 m, facies I; TH-89-26A, 125.4 m, facies E (but with more trilobite fragments than echinoderm fragments); TH-89-26B, 125.4 m, facies E - but with more trilobite fragments than echinoderm fragments; TH-89-27A, 125.5 m, facies E; TH-89-27B, 125.5 m, facies E; TH-89-28, 125.7 m, facies E; TH-89-29, 126.9 m, facies J; TH-89-30, 127.1 m, facies J.

7 134.1 Parasequence 14 (127.1 to 134.1 m): This approximately 8 meter thick parasequence consists almost entirely of thin- to medium-bedded aggregate-grain, grainstone containing peloids and coated-grains (facies J). Shoaling is indicated by an increase in partially coated-grains and by *Girvanella* oncolites. The problematic algae *Nuia* is particularly abundant at the top of Parasequence 14. Thin-sections: TH-89-31, 128.6 m, facies J; TH-89-32, 129.1 m, facies J; TH-89-33, 129.4 m, facies J/N; TH-89-34, 129.5 m, facies J; TH-90-35, 131.8 m, sample lost;

TH-89-36, 132.0 m, facies J/N; TH-89-37, 133.7 m, facies J; TH-89-38, 133.9 m, facies J; TH-89-39A, 134.1 m, facies I/J; TH-89-39B, 134.1 m, facies J/I.

4 138.5 Parasequence 15 (134.1 to 138.5 m): The final 4.5 m of this parasequence also consists almost entirely of thin- to medium-bedded aggregate-grain, grainstone containing peloids and coated-grains (facies J). Shoaling is indicated by the appearance of well-developed *Girvanella* oncolites. *Nuia* is also particularly abundant at the top of Parasequence 15. Exposure is inferred at the top of Subsequence 2G based on the occurrence of crystal or vadose silt in thin-section TH-89-42 from 136.7 meters, and by comparison with similar vadose features observed at the Old Thorn Hill section. Thin-sections: TH-89-40, 134.7 m, facies J; TH-89-41, 134.9 m, facies J; TH-89-42, 136.7 m, facies J; TH-89-43, 136.7 m, facies J/I.

Stratigraphic Positions Interpreted from Water-Depth Curves: Upper Parasequence Surfaces: Parasequence 12, < 199 m (exact position not resolved); Parasequence 13, 127.1 m; Parasequence 14, 134.1 m; Parasequence 15, 138.5 m. Deepening Events: None.

2H-3D 95.3 233.8 **Rockdell Formation.** The occurrence of the first "pink" grainstone beds has been used to mark the Lincolnshire/Rockdell contact (e.g., Ruppel, 1979). This contact or transition represents a facies change. At the Thorn Hill section this transition is gradational over at least 10 meters. The upper surface of Subsequence 2G is selected as the Lincolnshire/Rockdell contact because the transition from beds dominated by darker colored peloidal grainstones (Lincolnshire Formation) into beds containing "pink" echinoderm-rich grainstones (Rockdell Formation) closely coincides with the stratigraphic position of the upper surface of Sequence 2G.

The Rockdell consists of an assemblage of grainstone-packstones and mud-rich lithologies, all medium- to very thick-bedded. The Rockdell is further characterized by its echinoderm (pelmatozoan) - bryozoan fauna and an algal assemblage that includes *Contexta* and *Vermiporella*. Grainstones facies include facies C, D, I, J, and E. Fresh examples of facies C, D, J, and E range from pale- to moderate-yellowish-brown through grayish-orange-pink. In outcrop these grainstones tend to

weather to higher "values" (lightness) of orange-pink and grayish-orange. The most important packstone lithology is facies F, echinoderm/bryozoan packstone. Below about 220 meters, fresh examples of facies F are generally grayish-orange-pink to light-brown; whereas above about 220 meters specimens of facies F are dusky- to grayish -brown through blackish- to dusky-red. In outcrop, the orange and brown varieties characteristic of the lower part of the Rockdell weathers to higher "values" (lightness) of orange and brown. The brown to red variety characteristic of the upper Rockdell tends to retain its color in the weathered condition. Mud-rich lithologies include facies A, B, and L. Fresh examples of these mud-rich facies are pale-yellowish-brown and weather to a slightly lower chroma or saturation (darker color).

2H 20.4 158.9 Fourth-Order Subsequence 2H (Rockdell Formation).

20.4 158.9 Parasequence 16 (138.5 to 158.9 m): Medium-bedded grainstones with aggregate-grains and peloids continue from the base of Subsequence 2H to about 144.5 meters. The section is covered from about 144.5 to 152 meters. The interval from 152.5 to 154.5 meters is characterized by thin- to medium-bedded, medium-grained grainstones containing coated- and worn- bioclasts, aggregate-grains, and peloids. This interval is overlain by about 3.5 meters of very thick-bedded echinoderm/bryozoan packstones containing grainstone lenses (from 154.5 to 158.0 m). These mud-rich beds thicken upward and become fine-grained in the final meter below the top of Subsequence 2H (158.9 m). The upper surface of Subsequence 2H is also defined by a single 0.2 meter thick grainstone and mudstone bed consisting of medium-grained peloids in a sparry matrix admixed with fenestral mudstone (Facies L) (159.7 m). Exposure is inferred based on the occurrence of vadose silt in wackestone and mudstones capping Subsequence 2H. (i.e., samples TH-89-62, 156.5 m, and TH-89-63, 157.1 m). Thin-sections: TH-89-44, 139.9 m, facies J; TH-89-45, 140.9 m, facies J; TH-89-46, 141.3 m, facies J; TH-89-47, 141.6 m, facies J; TH-89-48, 142.2 m, facies J; TH-89-49A, 142.8 m, facies J; TH-89-49B, 142.8 m, facies J; TH-89-50, 143.1 m, facies J; TH-89-51, 143.9 m, facies I/J; TH-89-52, 144.4 m, facies I; TH-89-53A, 152.3 m, facies D; TH-89-53B, 152.3 m, facies C; TH-89-53C, 152.3 m, facies D; TH-89-54, 152.7 m, facies J; TH-89-55, 153.2 m, facies D; TH-89-56, 153.5 m,

facies J; TH-89-57, 153.9 m, facies B; TH-89-58N, 154.5 m, facies F/J; TH-89-58, 154.4 m, facies F; TH-89-60N, 155.3 m, facies E; TH-89-60N, 155.3 m, facies E; TH-89-61, 155.8 m, facies B; TH-89-62, 156.5 m, facies F; TH-89-59, 156.8 m, facies E/J; TH-89-63, 157.1 m, facies F; TH-89-64, 158.4 m, facies B.

Stratigraphic Positions Interpreted from Water-Depth Curves:
Upper Parasequence Surface: Parasequence 16, 158.9 m.
Deepening Event: $D_8$, about 154.6 m.

| | | | |
|---|---|---|---|
| 2I | 10.2 | 169.1 | Fourth-Order Sequence 2I (Rockdell Formation, continued). |
| | 3.6 | 162.5 | Parasequence 17 (158.9 to 162.5 m): About 3.5 meters of very thick-bedded wackestone/mudstone overlies the inferred upper surface of Subsequence 2H (from about 159.8 to 162.5 m). Fenestral fabrics and calcite filled vugs occur within this interval and indicate the approximate upper surface of Parasequence 17. This interval is lithologically similar to the uppermost part of underlying Subsequence 2H. However, water-depth analysis suggests that these mudstones were deposited in slightly deeper water than were the mudstones of the underlying Subsequence 2H. Thin-sections: TH-89-65, 158.8 m, facies L/I; TH-89-66Bottom, 159.5 m, facies I/J; TH-89-66Top, 159.7 m, facies L - fenestral; TH-89-67, 160.9 m, facies L/B; TH-89-68, 161.4 m, facies L or A; TH-89-69, 162.0 m, facies L. |
| | 0.5 | 163.0 | Parasequence 18 (162.5 to about 163 m): The wackestones and mudstones of underlying Parasequence 17 continue to about 163 meters where they are sharply truncated by echinoderm grainstone. Thin-section: TH-89-70, 162.9 m, facies L. |
| | 4.8 | 167.8 | Parasequence 19 (about 163 to 167.8 m). About 4 meters of very thick-bedded, coarse-grained, crossbedded echinoderm grainstone overlies Parasequence 18 (from about 163 to 167 m). This echinoderm grainstone grades into a very thick-bedded, medium-grained grainstone with aggregate grains and peloids (facies J) in the uppermost part of Parasequence 19 (slightly less than 1 meter thick). Coated-grains and superficial ooids occur within this aggregate-grain, grainstone and indicate shoaling at the top of Parasequence 19. Thin-sections: TH-89-71, 163.9 m, facies E; TH-89--72, 164.4 m, facies E; TH-89-73, 165.9 m, facies E/I; TH-89-74, 166.6 m, facies F; TH-89-75, 167.8 m, facies J/E. |

1.3 169.1 Parasequence 20 (167.8 to 169.1 m): A single fenestral wackestone and mudstone bed, slightly more than one meter thick, sharply overlies the aggregate grain, grainstone at the top of Parasequence 19. Exposure at the top of Parasequence 20 and Subsequence 2I is recognized by the occurrence of fenestral fabrics, crystal or vadose silt, and calcite filled vugs within the capping wackestone and mudstone. Thin-sections: TH-89-76Bottom, 168.1 m, facies F/E; TH-89-76Top, 168.2 m, facies L/A; TH-89-77A, 168.8 m, facies L - fenestral; TH-89-77B, 168.8 m, facies L/B.

Stratigraphic Positions Interpreted from Water-Depth Curves:
Upper Parasequence Surfaces: Parasequence 17, 163.0 m, Parasequence 18, 163.5 m (approximate); Parasequence 19, 167.8 m; Parasequence 20, 169.1 m.
Deepening Events: None.

2J 12.7 181.8 Fourth-Order Subsequence 2J (Rockdell Formation, continued).
8 177.1 Parasequence 21 (169.1 to 177.1 m): Wackestones and mudstones of the underlying Subsequence 2I are sharply truncated by almost 10 meters of very thick-bedded, coarse-grained, massive to crossbedded echinoderm grainstones and packstones (from about 169 to 179 m). Within these echinoderm grainstones, the upper surface of Parasequence 21 is indicated by an increase in mud content and the occurrence of partially coated-grains at 177.1 meters. Thin-sections: TH-89-78, sample lost; TH-89-79, 169.3 m, facies f (bottom of thin-section), facies E (top of thin-section); TH-89-80, 170.0 m, facies E/I; TH-89-81, 170.4 m, facies E; TH-89-82A, 170.8 m, facies E/I; TH-89-82B, 170.8 m, facies I; TH-89-83, 172.4 m, facies E/I; TH-89-84A, 175.2 m, facies F; TH-89-85, 176.3 m, facies F; TH-89-86A, 177.1 m, facies E/I; TH-89-86B, 177.1 m, facies E/I.

4.7 181.8 Parasequence 22 (177.1 to 181.8 m): About two meters of echinoderm grainstone and grainstone/packstone overlie the inferred upper surface of Parasequence 21. A bioclastic wackestone and packstone bed (facies B), about 0.1 m thick, sharply truncates these grainstones and packstones. This bioclastic wackestone/packstone is followed upward by about 3 meters of very thick-bedded massive wackestone/mudstone (facies L). Algal laminae and fenestral fabrics indicate very shallow water conditions marking the top of Parasequence 21.

The very thick-bedded wackestone/packstone continues upward to 182.5 meters. The contact with overlying Subsequence 2K is indicated by a subtle lithologic change from wackestone/mudstone (facies L) grading into bioclastic wackestone packstone (facies B). The occurrence of crystal or vadose silt in thin-section TH-89-92 (180.9 m) suggests exposure at the top of Sequence 2J and is also used to help infer the position of the contact with overlying Subsequence 2K. Thin-sections: TH-89-87A, 177.2 m, facies F/E; TH-89-87B, 177.2 m, facies F/E; TH-89-88, 177.7 m, facies F; TH-89-89A, 178.5 m, facies F; TH-89-89B, 178.5 m, facies F; TH-89-90, 179.0 m, facies B/E; TH-89-91A, 179.5 m, facies L; TH-89-91B, 179.5 m, facies L/B; TH-89-92A, 180.9 m, facies L - laminated (bottom of thin-section), facies L (top of thin-section); TH-89-92B, 180.9 m, facies L - fenestral).

Stratigraphic Positions Interpreted from Water-Depth Curves:
Upper Parasequence Surfaces: Parasequence 21, 177.1 m, Parasequence 22, 181.8 m.
Deepening Events: None.

2K 6.2 188.0 Fourth-Order Subsequence 2K (Rockdell Formation, continued).

6.2 188.0 Parasequence 23 (181.8 to 188.0 m): Subsequence 2K consists of about 6 meters of very thick-bedded, generally massive, wackestone/mudstone. A one meter thick bed of massive, bioclastic wackestone/packstone (facies B) occurs from about 187 to 188 meters. Vadose features, including crystal or vadose silt, calcite filled vugs lined with reddish crusts, and fenestral fabrics are ubiquitous throughout in the lower 2/3 and uppermost 0.5 meters (above and below the bioclastic wackestone/packstone bed) of Subsequence 2K. The upper surface of Subsequence 2K is very sharply truncated by echinoderm grainstones of overlying Subsequence 3A. Thin-sections: TH-89-93, 182.8, facies B; TH-89-94, 183.1 m, facies L - fenestral; TH-89-95A, 184.9 m, facies L; TH-89-95B, 184.9 m, facies L - with calcite filled vugs; TH-89-95C, 184.9 m, mud-rich facies; TH-89-96, 185.5 m, facies L - fenestral and laminated; TH-89-97A, 185.9 m, facies L - fenestral; TH-89-97B, 185.9 m, facies L - fenestral and laminated; TH-89-98A, 187.1 m, facies B/F; TH-89-98B, 187.1 m, facies B; TH-89-99, 187.6 m, facies B/L; TH-89-100A, 187.8 m, facies L - calcite

filled vug, matrix laminated with dolomite; TH-89-100B, 187.8 m, facies L - calcite filled vug, matrix laminated with dolomite.

Stratigraphic Positions Interpreted from Water-Depth Curves:
Upper Parasequence Surface: Parasequence 23, 188.0 m.
Deepening Events: None.

3 45.8 233.8 **Third-Order Sequence 3 (Rockdell Formation, continued).**

3A 23.6 211.6 Fourth-Order Subsequence 3A (Rockdell Formation, continued).

8.3 196.3 Parasequence 24 (188.0 to 196.3 m): About 4 meters of very thick-bedded, coarse-grained, massive echinoderm grainstone sharply overlies the top of Subsequence 2K (from about 188 to 192 m). The section is covered from about 192 to 195.5 meters. The top of Parasequence 24 is marked by a discontinuous horizon, about 0.8 meters thick, developed above the top of the covered interval. This horizon consists of echinoderm grainstone and packstone containing lenses or small cavities (up to about 0.5 meters long and 0.2 meters thick). These lenses or cavities consist of, or are filled with fenestral to slightly laminated mudstone. Thin-sections: TH-89-101, 188.3 m, facies E/I; TH-89-102, 189.3 m, facies I; TH-89-103, 189.6 m, facies E; TH-89-104, 190.6 m, facies E; TH-89-105A, 191.7 m, facies G; TH-89-105B, 191.7 m, facies G; TH-89-106, 195.7 m, facies E; TH-89-107, 196.1 m, facies F (bottom of thin-section, represents material from bottom of lens or cavity), facies L (top of thin-section, represents material from upper portion of lens or cavity); TH-89-108, 196.1 m, facies E (represents material surrounding the mudstone lenses or cavities).

15.3 211.6 Parasequence 25 (196.3 to 211.6 m): About 5 meters of grainstone and packstone beds are gradational with, and developed above the horizon described at the top of Parasequence 24 (from 196.3 to about 201.5 m). Within these 5 meters, the lowermost 2 meters consists of very thick-bedded grainstone/packstones. In contrast, the beds in the uppermost 3 meters thin upward (into thick- to medium-beds) and are more mud-rich. This succession is sharply overlain by about 0.5 meters of pale-olive-green shale (possibly a bentonite bed). This

shale bed comprises the base of an approximately 10 meter thick succession consisting of 0.5 to 2 meter thick, thin- to medium-bedded, carbonate units intercalated with 0.5 to 1 meter thick beds of pale-olive-green shale (from 201.5 to 211.6 m). The carbonate beds of this interval consist of either thin-bedded bioclastic wackestone/packstone or medium bedded wackestones with whole fossils rooted in micrite. The contact with overlying Sequence 3B appears to be gradational. It is inferred to be an exposure surface. Numerous vadose features including crystal or vadose silt and calcite filled vugs occur below the position of this inferred surface (located at approximately 211.6 m). Thin-sections: TH-89-109, 196.6 m, facies F/E; TH-89-110, 197.6 m, facies F; TH-89-111A, 198.7 m, facies F; TH-89-111B, 198.7 m, facies F; TH-89-112, 199.1 m, facies F; TH-89-113A, 200.5 m, facies F; TH-89-113B, 200.5 m, facies F; TH-89-114, 201.3 m, facies E/F; TH-89-115, 202.9 m, facies B; TH-89-116, 203.8 m, facies F/E; TH-89-117, 204.3 m, facies B; TH-89-118, 204.5 m, facies B; TH-89-119, 205.6 m, facies A; TH-89-120, 208.2 m, facies A; TH-89-121, 209.6 m, facies B; TH-89-122, 210.2 m, facies B/L; TH-89-123, 211.3, facies B.

Stratigraphic Positions Interpreted from Water-Depth Curves:
Upper Parasequence Surfaces: Parasequence 24, 196.3 m; Parasequence 25, 211.6 m.
Deepening Event: $D_9$, 210.2 m.

3B 5.9 217.5 Fourth-Order Subsequence 3B (Rockdell Formation, continued). Sequence 3B is similar to the carbonate and shale succession described for the upper 10 meters of Subsequence 3A. The mud-rich carbonate portion of this approximately 6 meter thick succession contains burrows or borings filled with (?) reworked pale-olive-green, very fine-grained carbonate. Some of these borings or burrows also contain bryozoans in life position. Calcite filled vugs and cavities, some of which contain crystal or vadose silt occur throughout the entire subsequence.

3.3 214.9 Parasequence 26 (211.6 to 214.9 m): The top of the succession comprising Parasequence 26 is tentatively identified by a single grainstone/packstone bed, about 0.1 meters thick, occurring at

214.9 meters within the mud-rich succession of Sequence 3B. This bed marks a facies change, indicating either a slight deepening or shoaling. Thin-sections: TH-89-124, 211.7 m, facies A/B; TH-89-125, 212.3 m, facies B; TH-89-126, 212.8

m, facies A/B; TH-89-127, 213.5 m, facies B/A; TH-89-128, 214.1 m, facies B; TH-89-129, 214.9 m, facies E/F.

2.6 217.5 Parasequence 27 (214.9 to 217.5 m): The top of Subsequence 3B is defined by the occurrence of abundant crystal or vadose silt trapped within cavities contained within wackestone beds below the Subsequence 3B surface. Thin-sections: TH-89-130, 216.4 m, facies B; TH-89-131, 217.2 m, facies A/B; TH-89-132, 217.2 m, facies B/A.

Stratigraphic Positions Interpreted from Water-Depth Curves:
Upper Parasequence Surfaces: Parasequence 26, 214.9 m; Parasequence 27, 217.5 m.
Deepening Events: None.

3C 8.25 225.7 Fourth-Order Subsequence 3C (Rockdell Formation, continued).

8.05 225.7 Parasequence 28 (217.7 to 225.75 m): Subsequence 3C and its contained parasequence comprises an approximately 7 meter thick succession of thin- to medium-bedded wackestones, packstones, and grainstones. The lower approximately 5 meters consists of bioclastic wackestone/packstone. This grades upward into packstone/grainstone. A 0.5 meter thick bed of olive-green shale (? bentonite) occurs from about 120.0 to 120.5 meters. The upper surface of Subsequence 3C is recognized by the occurrence of two, thin grainstone beds. The lower grainstone bed contains coated- and worn- bioclasts (facies C) and is assigned as the uppermost bed of Subsequence 3C. The upper grainstone bed is a conglomerate with worn grains that are blackened and iron stained (facies H). It is interpreted as a lag deposit and is assigned as the lowermost bed of overlying Subsequence 3D. Thin-sections: TH-89-133, 217.9 m, sample lost; TH-89-134; 218.6 m, facies A; TH-89-135, 219.7 m, facies B; TH-89-136, 220.6 m, facies A; TH-89-137A, 221.2 m, facies B; TH-89-137B, 221.2 m, facies B; TH-89-138, 221.5 m, facies B/A; TH-89-139, 223.1 m, facies E/F; TH-89-140, 223.3 m, facies B/F; TH-89-141A, 224.2 m, facies F/A; TH-89-141B, 224.2 m, facies F/A; TH-89-142, 224.4 m, facies F; TH-89-143, 224.9 m, facies E; TH-89-144, 225.5 m, facies F; TH-89-145A, 225.7 m, facies C; TH-89-145B, 225.7 m, facies C.

Stratigraphic Positions Interpreted from Water-Depth Curves:
Upper Parasequence Surface: Parasequence 28, 225.75 m.
Deepening Events: None.

3D 8.05 233.8 Fourth Order-Subsequence 3D (Rockdell Formation, total thickness 95.3 m).

8.05 233.8 Parasequence 29 (225.75 to 233.8 m): Subsequence 3D and its contained parasequence is only about 8 meters thick. It consists of about 7 meters of medium- to thin-bedded echinoderm grainstone and dusky-red packstone. A grainstone bed, about 0.1 meters thick, consisting of coated- and worn-grains occurs at about 230.6 meters. This bed marks the transition to more mud-rich lithologies of the uppermost 3 meters. The upper most 3 meters consists of about 1 meter of medium-bedded, whole fossil (bryozoan) wackestone followed by about 1.5 meters of medium-bedded to thick bedded packstone. The subsequence is capped with slightly more than 0.5 meters of thick-bedded whole fossil wackestone. Exposure is inferred from calcite filled vugs and crystal or vadose silt filled cavities contained within the capping wackestone. Thin-sections: TH-89-146, 225.8 m, facies H; TH-89-147, 226.0 m, facies B; TH-89-148, 226.9 m, facies E/F; TH-89-149, 227.1 m, facies E; TH-89-150, 228.0 m, facies F/G; TH-89-151, 228.4 m, facies F; TH-89-152, 229.0 m, facies F; TH-89-153, 229.5 m, facies F; TH-89-154, 229.6 m, facies E; TH-89-155, 230.6 m, facies C (bottom of thin-section), facies F/E (top of thin-section); TH-89-156A, 230.9 m, facies L/A; TH-89-156B, 230.9 m, facies A; TH-89-157, 231.2 m, facies A; TH-89-158, 231.9 m, facies E/F; TH-89-159, 232.2 m, facies F/B; TH-89-160N, 233.3 m, facies A/B.

Stratigraphic Positions Interpreted from Water-Depth Curves:
Upper Parasequence Surface: Parasequence 29, 233.8 m.
Deepening Events: None.

4 139.5 373.3 **Third-Order Sequence 4 (Benbolt, Wardell, and lowermost Bowen formations).**

Approximate
4A-4D 81.2 315 **Benbolt Formation.** The Benbolt Formation is recognized by the occurrence of the first "light grey, fossiliferous medium

bedded, stylolitic wackestone" (Wedekind, 1986). Wedekind placed the Rockdell/Benbolt contact at 235.1 meters above the Knox. This work places this contact at 233.8 meters above the Knox so as to coincide with the Sequence 3/4 surface (same as the 3D/4A surface). The Benbolt is characterized by grainstones intercalated with mud-rich lithologies. The two most important grainstone lithologies are echinoderm grainstone (facies E) and echinoderm-bearing grainstone with coated- and worn-grains (facies C). Facies E tends to lack the "pink" color characteristic of this lithology lower in the section. Rather, fresh examples are generally pale-yellowish-brown and weathered samples are yellowish-grey. Facies C generally occurs as a grainstone/packstone mixture. It contains dusky-red mud. Fresh and weathered examples tend to retain this reddish color. Similarly, mud-rich lithologies which include bioclastic wackestone/packstone (facies B), echinoderm/bryozoan packstone (facies F), and oncoid-bearing wackestone/packstone (facies N) have dusky-red colors. Additional description of the Benbolt is provided by Wedekind (1986).

4A 20.9 254.7 Fourth-Order Subsequence 4A (Benbolt Formation). Subsequence 4A is about 20.5 meters thick and contains five parasequences, numbered 30 through 34. Parasequence 30 (233.8 to 236.7 m): The basal 1 meter of pale-olive to dusky yellow-shale sharply overlies the whole fossil wackestone of underlying Subsequence 3D. Approximately 8 meters of medium- to thick-bedded packstones interbedded with grainstones sharply overlies this basal shale (from about 234.8 to above 236.7 m). The top of Parasequence 30 is recognized within these packstone beds at about 236.7 meters. Abundant *Girvanella* oncolites, the red algae *Solenopora* (P), and other encrusting red algae indicate shoaling at the top of Parasequence 30. Thin-sections: TH-89-161, 234.0 m, facies A; TH-89-162, 235.6 m, facies F; TH-89-163, 236.2 m, facies F; TH-89-164A, 236.7 m, facies F/E; TH-89-164B, 236.7 m, facies E/F.

7.6 244.2 Parasequence 31 (236.6 to 244.2 m): Very thick-bedded massive packstone beds continue to about 240 meters. These very thick-bedded packstones are overlain by about 2 meters of medium-to thin-bedded mud-rich rocks. Mud content increases upward in this two meter thick interval, starting with packstones and ending with mudstones and wackestones (from 240.0 to about 242.0). About 1 meter of massive oncoid grainstone sharply

overlies these mud-rich rocks (from about 242 to 243 m). Finally, this oncoid grainstone bed is sharply overlain by a slightly more than 1 meter thick bed of massive oncoid-bearing wackestone/packstone. Red and green algae (including *Kazakhstanelia* are abundant within the upper portion of this wackestone packstone bed. These shallow water features all indicate shoaling and mark the top of Parasequence 31. Thin-sections: TH-89-165, 239.3. m, facies F; TH-89-166, 240.3 m, facies F; TH-89-167, 241.0 m, facies C/G; TH-89-168, 241.5 m, facies N; TH-89-169, 242.8 m, facies G/C; TH-89-170, 244.2 m, facies N.

3.9 248.1 Parasequence 32 (244.2 to 248.1 m): The interval from 244.2 to about 248.1 meters consists of thick- to very thick-bedded mud-rich lithologies (i.e., facies N, F, and A) interbedded with thin grainstone beds and lenses (i.e., facies E and C). The occurrence of cavities filled with crystal or vadose silt contained within oncoid-bearing wackestone/packstone at 247.6 meters suggests shoaling and exposure at the top of Parasequence 32. Thin-sections: TH-89-171, 244.5 m, facies C/G; TH-88-4, 244.6 m, facies N (bottom of thin-section), facies C (top of thin-section); TH-88-5, 245.3 m, thin-section lost, billet retained; TH-89-172, 246.4 m, facies F; TH-88-6, 247.6 m, facies N/A.

1.6 249.7 Parasequence 33 (248.1 to 249.7 m): This 1.6 meter thick interval is characterized by thick to -medium-bedded oncoid-bearing wackestone/packstone containing grainstone lenses up to about 0.1 meters thick. Abundant and well developed *Girvanella* oncolites occur between 249.3 to 249.7 meters and indicate very shallow water conditions. The top of Parasequence 33 is placed at 249.7 meters based on the occurrence of these shallow water indicators. Thin-sections: TH-89-173, 248.7 m, facies N/C; TH-88-8, 249.3 m, facies N/C; TH-88-7, 249.3 m, facies A; TH-88-9A, 249.7 m, facies C; TH-88-9B, 249.7 m, facies C.

5.0 254.7 Parasequence 34 (249.7 to 254.7 m): The interval above 249.7 meters to about 254.2 meters is also characterized by thick- to medium-bedded oncoid-bearing wackestone/packstone containing grainstone lenses. However, these grainstone lenses thicken considerably (to about 0.5 m thick) near the top of Parasequence 34. Subsequence 4A and Parasequence 34 are capped with about 0.5 meters of dark-reddish-brown silty shale. An exposure surface is inferred to occur within the thick-bedded

packstone developed just above this silty shale. Cavities filled with crystal or vadose silt occur above and below the silty shale. Thin-sections: TH-89-174, 250.0 m, facies N; TH-88-10A, 250.8 m, facies A; TH-88-10B, 250.8 m, facies A; TH-88-11, 250.8 m, facies C; TH-88-12, 251.6 m, facies N/C; TH-89-175, 252.4 m, facies C; TH-89-176, 252.7 m, facies C/H; TH-89-177, 252.9 m, facies B; TH-89-178, 253.8 m, facies C (bottom of thin-section), facies F (top of thin-section); TH-89-179, 254.6 m; facies F/E.

Stratigraphic Positions Interpreted from Water-Depth Curves: Upper Parasequence Surfaces: Parasequence 30, 236.7 m; Parasequence 31, 244.2 m; Parasequence 32, 248.1 m; Parasequence 33, 249.7 m; Parasequence 34, 254.7 m. Deepening Events: None.

4B 2.9 257.6 Fourth-Order Subsequence 4B (Benbolt Formation, continued).

2.9 257.5 Parasequence 35 (254.7 to 257.6 m): Three meter thick Subsequence 4B and its contained parasequence consist mostly of medium- to very thick-bedded bioclastic packstone (facies B). The subsequence is capped by a 0.5 meter thick bed of dasyclad algae grainstone (facies K). The top of Subsequence 4B is inferred from the presence of green algae indicating very shallow water. Thus, the top of Subsequence 4B may not have been entirely exposed at the Thorn Hill section. Thin-sections: TH-89-180, 255.2 m, facies B/A; TH-89-181, 256.7 m, facies B; TH-89-181, 256.7 m, facies B; TH-89-182, 256.7 m, facies B; TH-89-183, 257.5 m, facies K; TH-89-183, 257.5 m, facies K.

Stratigraphic Positions Interpreted from Water-Depth Curves: Upper Parasequence Surfaces: Parasequence 35, 257.6 m. Deepening Events: None.

4C 30.1 287.7 Fourth-Order Subsequence 4C (Benbolt Formation, continued). Subsequence 4C comprises an approximately 30 meter thick succession. A lower interval of about 7.5 meters of mud-rich lithologies is followed by a middle interval of about 9.5 meters of grainstone and mud-rich lithologies, a 6 meter thick covered interval, and by an upper 3 meter thick interval of mud-rich lithologies.

26.0 283.6 Parasequence 36 (257.6 to 283.6 m):

7.5 265.5 Lower Interval (258 to 265.5 m): About 1 meter of very thick-bedded massive bioclastic wackestone/packstone sharply overlies the approximately 0.5 meter thick dasyclad algae grainstone bed marking the top of Subsequence 4B. This bioclastic wackestone/packstone is gradational with an approximately 2 meter thick package of massive oncoid-rich packstone. An approximately 0.5 meter thick echinoderm grainstone bed sharply overlies this oncoid-rich packstone. This is followed by about 3 meters of thick-bedded echinoderm/bryozoan packstones interbedded with thick-bedded bioclastic wackestone and packstone. About 1 meter of yellow- to green-shale sharply overlies these wackestones and packstones and completes the lower 7.5 meters (about 264.5 to 265.5 m). Thin-sections: TH-89-184, 257.8 m, facies B; TH-89-184, facies B; TH-89-185A, 258.2 m, facies B; TH-89-185B, 258.2 m, facies B/A; TH-89-186, 258.4 m, facies B/F; TH-89-186, 258.4 m, facies B/F; TH-89-186, 258.4 m, facies F/B; TH-89-187, 258.7 m, facies N/C; TH-89-188, 260.1 m, facies C/N; TH-89-189A, 260.5 m, facies F/N; TH-89-189B, 260.5 m, facies F/N; TH-89-190A, 261.6 m, facies B/F; TH-89-190B, 261.6 m, facies B/F; TH-89-191A, 262.5 m, facies F/E; TH-89-191B, 262.5 m, facies E/F; TH-89-191C, 262.5 m, facies E/F; TH-89-191D, 262.5 m, facies F/E; TH-89-192A, 263.4 m, facies B; TH-89-192B, 263.4 m, facies B; TH-89-193A, 264.1 m, facies N; TH-89-193B, 264.1 m, facies N.

9.5 275.0 Middle Interval (265.5 to 275 m): About 1.5 meters of very thick- to thick-bedded bioclastic wackestone/packstone sharply overlies the shale. This is followed by about 3.5 meters of very thick-bedded echinoderm grainstone which sharply overlies the bioclastic wackestone/packstone (from about 266.5 to 270.0 m). An approximately 0.2 meter thick grainstone lens containing coated- and worn-bioclasts occurs at the base of this grainstone package. This package of grainstone consists of amalgamated crossbeds. A packstone lens, about 0.5 meters thick, occurs within the middle portion of this grainstone package. This grainstone package is sharply overlain by about 1 meter of wackestone containing whole bryozoan fossils and fragments (from 270 to 271 m). About 3.5 meters of thick-bedded echinoderm grainstone with amalgamated crossbeds sharply overlies the wackestone (from about 271 to 274.5 m). These grainstones grade into packstones just below the covered interval

(starting at about 275 m). Thin-sections: TH-89-194, 266.3 m, facies B; TH-89-195A, 266.7 m, facies C/E; TH-89-195B, 266.7 m, facies C/E; TH-89-196, 267.2 m, facies E; TH-90-197, 268.4 m, facies E/F; TH-90-198, 269.4 m, facies E; TH-90-199, 271.0 m, facies A/B; TH-90-200, 272.5 m, facies E; TH-90-201, 273.3 m, facies E.

6.0 281.0 Covered Interval (275 to 281 m): No thin-sections recovered.

3.0 283.6 Upper Interval (281.0 to 283.6 m): More than 2.6 meters of very thick-bedded echinoderm/bryozoan packstone occurs above the covered interval. The upper surface of Parasequence 26 is placed just above horizontal cavities and fenestrae that occur within a packstone bed at 283.6 meters. Thin-sections: TH-90-202, 275.1 m, facies E; TH-90-203, 282.2 m, facies E/F; TH-90-204, 283.6 m, facies F.

4.1 287.7 Parasequence 37 (283.6 to 287.7 m): The packstone beds at the top of Parasequence 37 continue upwards to about 288 meters. Thus, about 3.5 meters of very thick-bedded echinoderm/bryozoan packstone occurs above the covered section of Parasequence 36. These packstones then grade into about 0.5 meters of thick-bedded bioclastic wackestone/packstone and then into whole fossil wackestone. Subsequence 4C and Parasequence 37 are capped with about 3 meters of very thick-bedded whole fossil wackestone (facies A). Exposure is inferred at the top of Subsequence 4C based on the occurrence of cavities filled with crystal or vadose silt contained within the uppermost 5 meters of packstone and wackestone. Thin-sections: TH-90-205A, 285.8 m, facies A/B; TH-90-205B. 285.8 m, facies A/B; TH-90-206, 287.6 m, facies A/B.

Stratigraphic Positions Interpreted from Water-Depth Curves:
Upper Parasequence Surfaces: Parasequence 36, 283.6 m; Parasequence 37, 287.7 m.
Deepening Events: $D_{10}$, 263.3 m; $D_{11}$, 282.2 m.

Estimated
4D 33.0 321.0 Fourth-Order Subsequence 4D (Benbolt Formation, total thickness 81.2 m; Lowermost Wardell Formation).
Subsequence 4D is at least 32 meters thick at the Thorn Hill section.

8.3 296 Parasequence 38 (287.7 to about 296 m): Parasequence 38 consists of about 8 meters of thick- to very thick-bedded echinoderm/bryozoan packstone beds. An approximately 0.2 meter thick grainstone lens (facies C) occurs at approximately and 296 meters. This grainstone lens contains coated- and worn-grains indicating shoaling. Thus, the upper surface of Parasequence 38 is place just above this lens. Thin-sections: TH-90-207, 289.8 m, facies F/B; TH-90-208, 292.9 m, facies F/A; TH-90-209A, 293.8 m, facies B/F; TH-90-209B, 293.8 m, facies B/A; TH-90-10, 295.6, facies C.

65 231 Parasequence 39 (about 296 to about 321 m): Thick- to very thick-bedded echinoderm/bryozoan packstone beds continue from underling Parasequence 38 (to about 306 m). An approximately 0.2 meter thick echinoderm grainstone bed occurs at approximately 299 meters. The section is not well exposed above about 306 meters. This poorly exposed interval consists of medium bedded packstones and wackestone/packstones. The upper surface of Subsequence 4D and Parasequence 39 is probably covered. Its position is inferred based on comparison with the Old Thorn Hill section. Thin-sections: TH-90-211, 295.8 m, facies E, TH-90-212A, 298.8 m, facies F/B (25 X 45 mm polished thin-section); TH-90-212B, 298.8 m, facies F/B (bottom of thin-section), facies F (top of thin-section); TH-90-213, 304.3 m, facies E; TH-90-214, 308.8 m, facies B; TH-90-215, 311.8 m, facies F/B; TH-90-216, 313.1 m, facies F; TH-90 -217A and B, 314.3 m, facies B; TH-90-218A and B, 318.0 m, facies B/F; TH-90-219A and B, 319.9 m, facies E/C.

Stratigraphic Positions Interpreted from Water-Depth Curves:
Upper Parasequence Surfaces: Parasequence 38 (about 296 m, exact position not resolved); Parasequence 39, 321 m (estimated).
Deepening Events: None.

Approximate
4D-4F 27 343 **Wardell Formation.** This work follows Wedekind (1986) and places the Benbolt/Wardell contact at about 315.7 meters. This contact occurs where "the lowermost stratum of Wardell forms a rather prominent ledge of medium to coarse grained rock which is readily distinguished from the fine grained shale [brown shale] of the Benbolt" (Wedekind, 1986). Thus, a facies change marks the contact. This contact occurs in the upper two-thirds

of Subsequence 4D and is at approximately the same position as the upper Parasequence 38 surface. The Wardell is an argillaceous lime mudstone intercalated with thin (generally less than 0.2 meters thick) wackestone and packstone beds. Additional description of the Wardell is provided by Wedekind (1986).

COVERED INTERVAL

| | | Approximate | |
|---|---|---|---|
| 4E | 50 | 392 | Fourth-Order Subsequence 4E (Wardell Formation, total thickness about 50 m). The remaining portion of Sequence 4 (4E and 4D) and overlying Sequence 5 are covered within the western branch of Forked Deer Creek on the west side of Dixie Highway. However, this section is exposed on the eastern side of Dixie Highway and has been sampled by Wedekind (1987) and Simonson (1985). |

Additional Thin-sections prepared as part of a 1988 carbonates class project (stratigraphic positions unknown): TH-88-1, TH-88-2, TH-88-3.

## Old Thorn Hill Section (OTH)

The Old Thorn Hill Section is exposed in a road cut along the eastern and western portions of old U.S. Route 25 E at Thorn Hill, Grainger County, Tennessee (between lat 36°21'07''N to 36°21'55''N and long 83°25'00''W to 83°25'34''W). Old U.S. 25E follows the eastern branch of Forked Deer Creek. This area lies in approximately the NE 1/4, NW 1/4, NE 1/4 of the Avondale 7.5 minute topographic quadrangle. Before the Dixie Highway was opened in the 1970's, this section was known as the "Thorn Hill Section" (i.e., Hall and Amick, 1934 ;Ruppel, 1979). The Old Thorn Hill section should not be confused with the "New" Thorn Hill section (e.g., Walker, 1985; Byerly et al., 1986). The Old Thorn Hill section has been measured and described by Hall and Amick (1934) and Ruppel (1979). However, this work represents the first time that thin-sections and polished slabs have been systematically collected, prepared, and studied from the Lincolnshire, Rockdell, and Benbolt formations at this section. Thin-sections from the Five Oaks Formation were provided by Keith Roberson.

The Knox/Chickamauga contact is located within and adjacent to the old quarry located on the east side of the old highway, about 750 meters north of Thorn Hill (the intersection State Route 131 and the old highway). More than 530 meters of Chickamauga Group consisting of the Five Oaks, Lincolnshire, Rockdell, Benbolt, Bowen, Witten, and Moccasin formations are exposed from the Knox/Chickamauga contact along the old highway and in adjacent fields and pastures north, south, and within the settlement of Thorn Hill.

**KNOX GROUP**

Unconformity

**CHICKAMAUGA GROUP**

| Sequence/ Cycle | 2nd Ord. | Seq. Thk (m) | Cumul. Thk (m) | |
|---|---|---|---|---|
| O-S | | 1,384 | 1,384 | **Tippecanoe Sequence (Sloss, 1963).** Other Synonyms: Ordovician-Silurian (O-S) Second Order Cycle or Supercycle (Vail, et al., 1977), and Paleozoic Sequence II, Middle Ordovician to Lower Devonian, Walker (1985) and Byerly et al. (1986). |

| 3rd & 4th Ord. | Seq. Thk (m) | Cumul. Thk (m) | |
|---|---|---|---|
| 1A-2B | 22.2 | 22.2 | **Five Oaks Formation.** The interval from 0 to 22.2 meters above the Knox (Five Oaks Formation) is exposed in the old quarry located on the east side of the old highway, about 750 meters south of Thorn Hill (the intersection State Route 131 and the old highway). The Five Oaks was sampled by Keith Roberson. Twenty-two thin-sections were prepared from just below the Knox unconformity to about 22.4 meters above the Knox by Keith Roberson. Numbers associated with these thin-sections are placed within quotation marks because they reflect Roberson's thin-section numbering scheme (i.e., he used the prefix "TH" rather than "OTH" for samples that he prepared from this "Old Thorn Hill" section).<br><br>The Five Oaks Formation is recognized by its three major lithologies, dolostone (facies P), wackestone/mudstone (facies L), and peloidal grainstone (facies I). Fresh examples of these lithologies range from pale-yellowish-brown to dark-yellowish-brown and are generally very fine- to fine-grained. The peloidal grainstones are generally fine- to medium-grained and darkest in color, approaching dusky-brown. The same color hues are observed in weathered outcrop, but the chroma or saturation is generally altered. Wackestones and mudstones tend to weather to lower chroma or saturation (darker colors), whereas grainstone tend to weather to a higher chroma (lighter colors). Ostracodes are the only fossils present in large numbers. |
| 1 | 22.2 | 22.2 | **Third-Order Sequence 1 (lower to upper Five Oaks Formation).** |
| 1A | 9.0 | 9.0 | Fourth-Order Sequence 1A (Blackford Member of the Five Oaks Formation). |
| | 9.0 | 9.0 | Parasequence 1 (0 to 9.0 m): The first meter of strata developed on and above the Knox consists of pale-brown, pale-yellowish- brown, and dark-yellowish-brown, medium- to thick-bedded, dolostone. The lower contact with the Knox is gradational. These massive dolostones grade upward into thick- to very-thick bedded fenestral wackestone/mudstone (facies L) of similar color. Thin-sections: "TH-1.1", -0.3 m (just below Knox unconformity), facies P; "TH-2.4", 1.0 m, facies L |

(fenestral); "TH-3.0", 1.6 m, facies L (fenestral); "TH-4.4", 3.) m, facies L (fenestral); "TH-5.7", 4.3 m, facies L (fenestral); "TH-6.8", 5.4 m, facies L (fenestral); "TH-7.4", 6.0 m, facies L (fenestral); "TH-9.4", 8.0 m, facies L (fenestral); "TH-10.4", 9.0 m, facies L (fenestral).

Stratigraphic Positions Interpreted from Water-Depth Curves:
Upper Parasequence Surfaces: Parasequence 1, 9.0 m.
Deepening Events: None.

1B 5.6 14.6 Fourth-Order Subsequence 1B (Five Oaks Formation, continued).

5.6 14.6 Parasequence 2 (9.0 to 14.6 m): About 3.6 meters of pale-brown, pale-yellowish- brown, and dark-yellowish-brown, thick- to very-thick bedded wackestone/mudstone (facies L) are developed above Subsequence 1A (from 9.0 to about 12.6 m). A pale-olive-green (?) silicified bed, possibly a bentonite bed, less than 0.1 meters thick occurs between about 11 and 12 m above the Knox within the fenestral mudstone interval. About 2 meters of medium and thin-bedded peloidal grainstone and dasyclad algae grainstone gradationally overlie the fenestral mudstones. The top of Subsequence 1B and its contained Parasequence 2 are recognized by the transition where peloidal grainstones and mudstones pass upward into fenestral mudstones. Thin-sections: "TH-10.6", 10.6 m, facies L; "TH-13.2A", 11.8 m, facies L (fenestral); "TH-13.2B", 11.8 m, facies L (fenestral); "TH-14.0", 12.6 m, facies I/K; "TH-14.1", 12.7 m, facies K/O; "TH-15.0, 13.6 m, facies I/O; "TH-16.0", 14.6 m, facies L (fenestral)/I.

Stratigraphic Positions Interpreted from Water-Depth Curves:
Upper Parasequence Surfaces: Parasequence 2, 14.6 m.
Deepening Event: $D_0$, 11.8 m.

1C 4.3 18.9 Fourth-Order Subsequence 1C (Five Oaks Formation, continued).

4.3 18.9 Parasequence 3 (14.6 to 18.9 m): Subsequence 1C and its contained Parasequence 3 consists of a 4 meter thick interval of thin- to medium-bedded fenestral mudstone. A mud-rich bed, less than 0.2 meters thick, containing lithoclasts in a

packstone/grainstone matrix marks the approximate upper surface of Subsequence 1C and its contained Parasequence 3.
Thin-sections: "TH-16.3", 14.9 m, facies L (fenestral); "TH-20.3", 18.9 m, facies L (fenestral)/O.
Stratigraphic Positions Interpreted from Water-Depth Curves:
Upper Parasequence Surfaces: 18.9 m.
Deepening Event: $D_1$, 14.9 m.

2 172.1 191.0 **Third-Order Sequence 2 (Five Oaks and Lincolnshire formations).**

2B 3.3 22.2 Fourth-Order Subsequence 2B (Five Oaks Formation, total thickness 22.2 m).

3.3 22.2 Parasequence 4 (18.9 to 22.2 m): Subsequence 2B and its contained Parasequence 4 sharply overlie Subsequence 1C. Subsequence 2B consists of slightly more than 3 meters of thin- to medium-bedded wackestone/mudstone (facies L). Exposure is inferred at the top of Subsequence 2B based on an upward change in lithology and by comparison with the Thorn Hill section. Thin-sections: "TH-21.6", 20.2 m, facies L (fenestral); "TH-22.6", 21.2 m, facies L (fenestral); "TH-23.4", 22.0 m, facies L (fenestral); "TH-23.6", 22.2 m, facies L (fenestral).

Stratigraphic Positions Interpreted from Water-Depth Curves:
Upper Parasequence Surfaces: Parasequence 4, 22.2 m.
Deepening Events: None.

2C-2G 19.2 141.4 **Lincolnshire Formation.** The Five Oaks/Lincolnshire contact is sharp and occurs directly above the upper surface of Subsequence 2B. The general description for the Lincolnshire Formation at the Old Thorn Hill section is the same as that given for the Lincolnshire at the "New" Thorn Hill or Thorn Hill section.

2C 31.6 53.8 Fourth-Order Subsequence 2C (Lincolnshire Formation).

15.8 38.0 Parasequence 5 (22.2 to about 38.0 m): The basal Lincolnshire (1.5 meters thick) consists predominately of thin-bedded, medium-to fine-grained peloidal and peloid-bearing grainstones

intercalated with thin-bedded, coarse- to medium-grained, nodular echinoderm/bryozoan packstone and echinoderm grainstone. The interval from approximately 22.4 meters to above 38 meters is not as well studied as are the intervals above and below. However, field observations suggest that this interval consists mostly of very thick- to thick-bedded, massive to crossbedded, medium-to fine-grained peloidal and peloid-bearing grainstones. Coarse- to medium-grained, echinoderm grainstones are rare within this interval. The exact position of the upper surface of Parasequence 5 is not resolved. Thin-section: "TH-23.8", 22.4 m, facies I; OTH-90-0A, 28.1 m, facies I; OTH-90-0B, 28.1 m, facies I.

15.8 53.8 Parasequence 6 (about 38.0 to 53.8 m): Very thick to thick-bedded peloidal grainstones of Parasequence 5 continue to about 45 meters above the Knox. Very thick to thick-bedded grainstones continue upwards from about 45 meters to about 50.5 meters. However, the peloid content within these grainstones decreases upwards and gradually gives way to more echinoderm-rich grainstones and packstones. These echinoderm-rich grainstones and packstones are sharply overlain by about 2 meters of medium- to thin-bedded mud-rich beds. Bioclastic wackestone/packstone (facies B) occurs above this sharp contact and grades upward into echinoderm/bryozoan packstone (facies F) (from 50.5 to about 52.6 m). Finally, these mud-rich rocks are overlain by slightly more than 1 meter of medium-bedded peloid and aggregate grain-bearing echinoderm grainstone (from about 52.6 to 53.8 m). The upper surface of Subsequence 2C and Parasequence 6 are inferred by the occurrence of crystal or vadose silt filled cavities contained with in the capping grainstone and mud-rich lithologies. Thin-sections: OTH-90-299, 40.6 m, facies I; OTH-90-300, 48.1 m, facies E/I; OTH-90-301, 49.5 m, facies F/J; OTH-90-302, 50.5 m, facies E/J; OTH-90-303, 50.7 m, facies B/F; OTH-90-304, 52.5 m, facies F/E; OTH-90-305, 53.7 m, facies E/J.

Stratigraphic Positions Interpreted from Water-Depth Curves:
Upper Parasequence Surfaces: Parasequence 5 (about 38 m, exact position not resolved); Parasequence 6, above about 50 meters, but probably below 53.8 m (exact position not resolved).
Deepening Events: $D_{4A}$, about 35 m; $D_{4B}$, about 41 m.

2D 2.7 56.5 Fourth-Order Subsequence 2D (Lincolnshire Formation, continued).

>6.5 56.5 Parasequence 7 (>50 to 56.5 m): Sequence 2D and its contained Parasequence 7 consist of medium-bedded peloid and aggregate grain-bearing echinoderm grainstone. Poorly-developed, one-sided coated-grains occur with in these grainstones at 55.4 meters and suggest shoaling. However, evidence for exposure at the top of Subsequence 2D at the Old Thorn Hill section is generally lacking. The upper surface of Subsequence 2D is placed at about 56.5 meters based on a sharp contact (at about 56.5 m). Relatively "pure," very thick-bedded echinoderm grainstones overlie transitional peloidal- to echinoderm grainstones of uppermost Subsequence 2D along this sharp contact. Comparison of this interval with its counterpart at the Idol Mine section, where there is evidence of exposure, is also used to inferred the upper surface of Sequence 2D. Thin-sections: OTH-90-306, 54.9 m, facies E; OTH-90-307A, 55.4 m, facies E/J; OTH-90-307B, 55.4 m, facies E/J.

Stratigraphic Positions Interpreted from Water-Depth Curves: Upper Parasequence Surfaces: Parasequence 7, 56.5 m. Deepening Event: $D_5$, 54.9 m.

2E 59.0 115.5 Fourth-Order Subsequence 2E (Lincolnshire Formation, continued).

21.5 78.0 Parasequence 8 (about 56.5 to about 78 m): Subsequence 2E and its contained Parasequence 8 consists of about 13.5 meters of very thick-bedded, massive to crossbedded, coarse-grained, echinoderm grainstone (facies E) (from 56.5 to about 70 m). Echinoderm grainstone continue upwards, becoming thick- to medium-bedded from 70 to about 76 meters. The beds are not well exposed above 76 meters. The upper surface of Parasequence 8 is not resolved at the Old Thorn Hill section. Thin-sections: OTH-90-308, 58.4 m, facies E; OTH-90-309, 60.4 m, facies E; OTH-90-1, 62.6 m, facies E; OTH-90-2A, facies E; OTH-90-2B, 74.1 m, facies E.

11.4 89.4 Parasequence 9 (about 78 to about 89.4 m): The section is not well exposed from 78 to about 80 meters. This interval is inferred to consist of echinoderm grainstone (facies E). About 2 meters of thick-bedded, coarse-grained echinoderm grainstone occurs from 80 to 82 meters. A 7.4 meter thick interval

consisting of thin-bedded peloidal grainstones (at the base) grades into medium-bedded peloid bearing echinoderm grainstone (near the top; from 82 to 89.4 m). The upper Parasequence 9 surface is difficult to resolve on the basis of water-depth curve inflection points. However, the facies occurring near this inferred surface represent water-depths that are shallower than those occurring above or below this position. Thin-sections: OTH-90-3, 80.7 m, facies E; OTH-90-4, 84.5 m, facies E; OTH-90-5A, 87.2 m, facies E/I; OTH-90-5B, 87.2 m, facies E/I.

16.4 105.4 Parasequence 10 (89.4 to 105.8 m): About 5 meters of very-thick bedded grainstones occur from 89 to 94.3 meters. These are peloid-bearing echinoderm grainstones in the first meter, grading into about 3 meters of peloidal grainstone, followed by about 1 meter of an aggregate-grain, grainstone. These are followed by nearly 10 meters of thick- to medium-bedded, massive to crossbedded echinoderm grainstone and peloid-bearing echinoderm grainstone from 94.3 to about 104 meters. The facies change from echinoderm grainstone into overlying peloidal grainstone is used to infer the upper surface of Parasequence 10. However, this surface is difficult to resolve on the basis of water-depth curve inflection points. Thin-sections: OTH-90-6, 89.5 m, facies E/I; OTH-90-7, 94.2 m, facies J; OTH-90-8, 94.9 m, facies E; OTH-90-9, 96.7 m, facies E/I; OTH-90-10, 100.7 m, facies E; OTH-90-11, 105.8 m, facies I.

7.4 113.2 Parasequence 11 (105.8 to 113.2 m): About 6 meters of very thick-bedded, massive to crossbedded peloidal grainstone occurs from 105.8 to 111.8 meters. A very thick-bedded, massive bioclastic wackestone and packstone (facies B) interval overlies these peloidal grainstones. The upper Subsequence 2E and Parasequence 11 surface is placed at the top of this wackestone and packstone interval. Calcite filled vugs and fractures occur in the lower third of this approximately 1.4 meter thick wackestone and packstone interval. These vugs and fractures are filled with equant calcite and (?) crystal or vadose silt. Thin-section: OTH-90-12, 111.9 m, facies B.

Stratigraphic Positions Interpreted from Water-Depth Curves: Upper Parasequence Surfaces: Parasequence 8, about 78 m (exact position not resolved); Parasequence 9, about 89.4 m (exact position not resolved); Parasequence 10, 105.8 (exact

position not resolved); Parasequence 11, 113.2 m.
Deepening Events: $D_6$, 80.8 m; $D_7$, 94.9 m.

2 N/A N/A Fourth-Order Subsequence 2F. Subsequence 2F is not recognized on the shelf (see Chapter 3).

Stratigraphic Positions Interpreted from Water-Depth Curves:
Upper Parasequence Surfaces: N/A
Deepening Events: N/A

2G 28.2 141.4 Fourth-Order Subsequence 2G (Lincolnshire Formation, total thickness of Lincolnshire Formation 119.2 m).

4.8 118.0 Parasequence 12 (113.2 to 118.0 m): About 3 meters of thick- to medium-bedded, cross-bedded, peloidal grainstone sharply overlies the very thick-bedded, massive bioclastic wackestone

and packstone interval (from 133.2 to 116.2 m). These peloidal grainstones are overlain by about 1.8 meters of medium-bedded bioclastic wackestone/packstone (from 116.2 to 118.0 m). The upper surface of Parasequence 12 is recognized at 118.0 meters by a sharp contact with overlying peloid-rich echinoderm grainstones. Thin-sections: OTH-90-13, 114.3 m, facies I; OTH-90-14, 116.3 m, facies B.

11.9 129.9 Parasequence 13 (118.0 to 129.9 m): The interval from 118 to 122 meters consists of medium-bedded peloidal grainstone. These peloidal grainstones grade into thin-bedded packstones and thin into thin-bedded bioclastic wackestone (from 122 to 125 meters). This mud-rich interval is sharply overlain by about 5 meters of very thick-bedded echinoderm grainstone. The top of Subsequence 2G, at about 129.9 meters, is indicated by an increase in coated-grain content (suggesting shoaling) observed just below 129.9 meters (i.e., TH-90-17, 127.4 m). Thin-sections: OTH-90-15, 118.3 m, facies E/I; OTH-90-16, 121.9 m, facies I; OTH-90-17, 127.4 m, facies E/J; OTH-90-18, 129.9 m, facies E.

1.5 131.4 Parasequence 14 (129.9 to 131.4 m): This approximately 1.5 meter thick parasequence consists of very thick-bedded echinoderm grainstone. An approximately 7 meter thick covered interval occurs above 131.4 meters. The exact position

of the upper Parasequence 14 surface is not resolved. Thin-section: OTH-90-19, 131.4 m, facies E.

7 138.4 COVERED INTERVAL

10 141.4 Parasequence 15 (131.4 to 141.4 m): The section is covered below about 140 meters. The capping 1.4 meters of Subsequence 2G and parasequence 15 is medium-bedded and consists of about 0.8 meters of oncoid-bearing wackestone/packstone, overlain by about 0.6 meters of *Spongiostrome* mudstone with a tufted algal fabric. Calcite and crystal or vadose silt filled vugs and cavities are conspicuous in the oncoid bearing wackestone/packstone. Thin-sections: OTH-90-20A, 140.4 m, facies N; OTH-90-20B, 140.4 m, facies N; OTH-90-21, 141.3 m, facies M.

Stratigraphic Positions Interpreted from Water-Depth Curves: Upper Parasequence Surfaces: Parasequence 12, 118.0 m; Parasequence 13, 129.9 m; Parasequence 14, 131.4 m (exact position not resolved); Parasequence 15, 141.4 m.
Deepening Events: None.

97.6 239 **Rockdell Formation.** The occurrence of the first "pink" grainstone beds has been used to mark the Lincolnshire/Rockdell contact. This contact or transition represents a facies change. At the Old Thorn Hill section this transition appears to occur within an approximately 37 meter thick covered interval. Thus, the upper surface of Subsequence 2G is selected as the Lincolnshire/Rockdell contact. The general description given for the Rockdell at the Thorn Hill section also applies to the Rockdell at the Old Thorn Hill section with two notable exceptions. First, dusky- to grayish brown through blackish to dusky-red colored packstones and wackestones are generally lacking in the Rockdell the Old Thorn Hill section. Second, little or no shale occurs in the Rockdell at the Old Thorn Hill section.

2H 20.4 158.9 Fourth-Order Sequence 2H (Rockdell Formation).

| | | | |
|---|---|---|---|
| | 17.5 | 158.9 | Parasequence 16 (141.4 to 158.9 m): About 0.5 meters of Thick-bedded peloidal grainstone sharply overlies the Subsequence 2G surface. The rest of Subsequence 2G and Parasequence 16 are covered. Thin-section: OTH-90-22, 141.6 m, facies I.<br><br>Stratigraphic Positions Interpreted from Water-Depth Curves:<br>Upper Parasequence Surface: Parasequence 16, 158.9 (estimated, exact position not resolved).<br>Deepening Event: $D_8$ (no data). |
| Approximate 2I | 10.2 | 169.1 | Fourth-Order Subsequence 2I (Rockdell Formation, continued). Subsequence 2I is covered. |
| | 3.6 | 162.5 | Parasequence 17 (about 158.9 to about 162.5 m). |
| | 0.5 | 163 | Parasequence 18 (about 162.5 to about 163 m). |
| | 4.8 | 167.8 | Parasequence 19 (about 163 to about 167.8 m). |
| | 1.3 | 169.1 | Parasequence 20 (about 167.8 to about 169.1 m).<br>Stratigraphic Positions Interpreted from Water-Depth Curves:<br>Upper Parasequence Surfaces: Parasequence 17, 162.5 m (exact position not resolved); Parasequence 18, about 163 m (exact position not resolved); Parasequence 19, 167.8 m (exact position not resolved); Parasequence 20, 169.1 m (exact position not resolved).<br>Deepening Events: None. |
| Approximate | 30 | 175 | COVERED INTERVAL |
| 2J | 11.6 | 180.7 | Fourth-Order Subsequence 2J (Rockdell Formation, continued).<br>Parasequence 21 (about 169.1 to 179.1 m): About 0.5 m of thin-bedded aggregate-grain grainstone occurs just above the covered interval at 179.1 meters. Very shallow water indicators, including well developed *Girvanella* oncolites and the problematic alga *Nuia*, occur within this grainstone. Thin-section: OTH-90-23, 179.1 m, facies J. |
| | 1.6 | 180.7 | Parasequence 22 (179.1 to 180.7 m): About 1.5 meters of thin-bedded, medium- to coarse-grained, peloid and aggregate grain- |

bearing grainstone overlie Parasequence 21. Echinoderm packstone/grainstone lenses, about 0.1 meter thick, occur within the peloidal grainstones near the top of this interval. Partially coated algal oncolites and other coated-grains indicate shallow water at the top of this interval. The upper surface of Subsequence 2J and Parasequence 22 is selected based a sharp contact (at about 180.7 m) with overlying bioclastic wackestones and packstones. Overlying facies represent slightly deeper water-depths than do the underlying grainstone. Thin-section: OTH-90-24, 180.6 m, facies j (left side of thin-section), facies F (right side of thin-section).

Stratigraphic Positions Interpreted from Water-Depth Curves:
Upper Parasequence Surfaces: Parasequence 21, 179.1 m, Parasequence 22, 180.7 m.
Deepening Events: None.

2K 10.3 191.0 Fourth-Order Subsequence 2K (Rockdell Formation, continued). Parasequence 23 (180.7 to 191.0 m): Subsequence 2K consists of about 10.3 meters of mud-rich and peloidal grainstone lithologies. About 5 meters of medium- to thin-bedded bioclastic wackestone/packstone (facies B) gradationally overlies Subsequence 2J (form 180.7 to 185.7 m). This wackestone/mudstone grades into about 0.5 meters of very thin- to thin-bedded aggregate-grain grainstone (facies J) mixed with packstone. These thin beds are sharply overlain by about 1.6 meters of very thick-bedded aggregate-grain grainstone (facies J). Very shallow water indicators, including well developed *Girvanella* oncolites and the problematic algae *Nuia*, occur within this grainstone. This grainstone is sharply overlain (at about 187.6 m) by slightly less than 3 meters of very thin-bedded bioclastic wackestone/packstone (facies B) (from 187.6 to 190.6 m). This sharp contact might possibly qualify as a parasequence boundary; although, one is not presently recognized here. Subsequence 2K and its contained Parasequence 23 are capped by slightly less than one meter of aggregate-grain grainstone. The upper Subsequence 2K and Parasequence 23 surface is inferred to occur within this capping grainstone at about 191.0 meters. Very shallow water indicators, including well developed *Girvanella* oncolites, the problematic alga *Nuia*, and other problematic green algae occur within this grainstone. Thin-sections: OTH-90-25, 183.1 m, facies B; OTH-90-26, 186.5 m, facies J (approx. upper part of

thin-section) and facies N (lower portion of thin-section); OTH-90-27, 186.7 m, facies J; OTH-90-28, 186.9 m, facies J; OTH-90-29, 187.5 m, facies J; OTH-90-30, 190.1 m, facies B; OTH-90-31, 191.0 m, facies J.

Stratigraphic Positions Interpreted from Water-Depth Curves:
Upper Parasequence Surface: Parasequence 23, 191.0 m.
Deepening Events: None.

3 48.0 239 **Third-Order Subsequence 3 (Rockdell Formation, continued).**

3A 20.8 211.8 Fourth-Order Subsequence 3A (Rockdell Formation, continued).

5.0 196.0 Parasequence 24 (191.0 to 196.0 m): About 4.4 m of thin- to very thin-bedded bioclastic wackestone/packstone comprises Parasequence 24. Blackened and iron-stained grains occur in the lower 2 meters of this secession. The top of Parasequence 24 is marked by a sharp contact with overlying peloidal grainstones. Thin-sections: OTH-90-32, 192.5 m, facies B/H; OTH-90-33, 193.2 m, facies B/H.

15.8 211.8 Parasequence 25 (196.0 to 211.8 m): About 2.5 meters of medium-bedded peloidal grainstone sharply overlies the top of Parasequence 24 (from 196.0 to about 198.0 m). These peloidal grainstones grade into about 3 meters of aggregate-grain grainstone (facies J) (from 198 to 102 m). An approximately 1 meter thick bed of bioclastic wackestone/packstone containing aggregate-grains occurs above the grainstone. An approximately 5 meter thick succession of very thick-bedded grainstone beds gradationally overlies the wackestone/packstone (from 203 to about 208 m). The lower 2 meters of this 5 meter thick succession consist of aggregate-grain bearing echinoderm grainstone. This is followed by about 2.5 meters of massive to crossbedded echinoderm grainstone. A bioclastic wackestone/packstone lens, about 0.2 meters thick, occurs at about 206.1 meters. The upper 0.5 meters of this succession consist of medium-bedded echinoderm grainstone/packstone. These grainstone/packstones are gradationally overlain by about 3.5 meters of thick- to medium bedded peloidal and aggregate-grain, grainstones. A bioclastic wackestone/packstone lens, about 0.1 meters thick, occurs at

about 208.9 meters. The upper surface of Subsequence 3A and Parasequence 25 is indicated by an approximately 0.2 meter thick wackestone/mudstone (facies L) bed sharply overlying the grainstones. Cavities filled with crystal or vadose silt and calcite filled vugs occur within the uppermost mudstone and grainstones beds. Thin-sections: OTH-90-34, 196.4 m, facies I; OTH-90-35A, 199.9 m, facies J; OTH-90-35B, 199.9 m, facies J; OTH-90-35.25, 201.2 m, facies J; OTH-90-35.5, 202.5 m, facies B/J; OTH-90-36, 202.6 m, facies B; OTH-90-36.5 202.7 m, facies J; OTH-90-37, 203.3 m, facies E/J; OTH-90-38A, 203.6 m, facies E; OTH-90-38B, 203.6 m, facies E; OTH-90-38C, 203.6 m, facies E; OTH-90-38D, 203.6 m, facies E; OTH-90-39, 204.0 m, facies E/I; OTH-90-40A, 205.0 m, facies J; OTH-90-40B, 205.0 m, facies J; OTH-90-41, 206.1 m, facies B/J (this facies represents an approximately 0.5 meter thick lens); OTH-90-41.5, 206.8 m, facies J (bottom of thin-section), facies F(top of thin-section); OTH-90-42, 207.6 m, facies I/J; OTH-90-43, 208.8 m, facies B and facies I; OTH-90-44, 210.7 m, facies J; OTH-90-45, 211.1 m, facies I/J and facies F; OTH-90-46A, 211.7 m, facies L; OTH-90-46B, 211.7 m, facies L.

Stratigraphic Positions Interpreted from Water-Depth Curves:
Upper Parasequence Surfaces: Parasequence 24, 196.0 m; Parasequence 25, 211.8 m.
Deepening Event: $D_9$, 208.8 m.

3B 10.8 222.6 Fourth-Order Subsequence 3B (Rockdell Formation, continued). Subsequence 3B can be divided into three parts. The lower part consists of about 3.5 meters of medium- to thick-bedded peloidal grainstone. The middle part sharply overlies the lower part and is comprised of 3.5 meters of thin- to very thick-bedded, massive to crossbedded echinoderm grainstone and packstone. The upper part consists of almost 4 meters of peloidal grainstones.

5.0 216.8 Parasequence 26 (211.8 to 216.8 m): Thin-bedded echinoderm grainstones are truncated by massive echinoderm grainstone beds at about 216.8 meters. The upper surface of Parasequence 26 is tentatively placed at this position within the echinoderm grainstones of the middle portion of Sequence 3B. Thin-sections: OTH-90-46.5A, 213.3 m, facies I; OTH-90-46.5B, 213.3 m, facies I; OTH-90-47, 213.3 m, facies J; OTH-90-48,

214.1 m, facies I; OTH-90-49, 215.0 m, facies E/F; OTH-90-50, 215.8, facies F/E; OTH-90-51, 216.7 m, facies E/F.

5.8 222.6 Parasequence 27 (216.8 to 222.6 m): The top of Subsequence 3B is marked by an erosional surface developed above the upper peloidal grainstone portion of Subsequence 3B. A lens, ranging from about 0.1 to 0.4 meters thick, consisting of wackestone/mudstone (facies L) and bioclastic wackestone sharply overlies this erosional surface. The upper Subsequence 3B and Parasequence 27 surface is placed at the top of this wackestone/mudstone lens (not sampled). Thin-sections: OTH-90-52A, 218.6 m, facies I; OTH-90-52B, 218.6 m, facies I; OTH-90-53, 220.3 m, facies I; OTH-90-54, 220.7 m, facies I/J; OTH-90-55, 222.3 m, facies I/J.

Stratigraphic Positions Interpreted from Water-Depth Curves:
Upper Parasequence Surfaces: Parasequence 26, 216.8 m (exact position not resolved); Parasequence 27, 222.6 m.
Deepening Events: None.

3C 4.8 227.4 Fourth-Order Subsequence 3C (Rockdell Formation, continued).

4.8 227.4 Parasequence 28 (222.6 to 227.4 m): Subsequence 3C and its contained parasequence comprise an approximately 4.8 meter thick succession of thick to medium-bedded grainstones. The lower approximately 2 meters consists of aggregate-grain grainstone. This grades upward into about 3.4 meters of packstone/grainstone. The upper surface of Sequence 3C is recognized by the occurrence of an approximately 0.2 meter thick bed of bioclastic wackestone/packstone containing well-developed coated-grains. Thin-sections: OTH-90-56, 223.0 m, facies J; OTH-90-56N, 223.0 m, facies J; OTH-90-57, 225.0 m, facies E/C; OTH-90-58A, 227.0, facies E/F; OTH-90-58B, 227.0, facies F/E; OTH-90-59, 227.4 m, facies B/F.

Stratigraphic Positions Interpreted from Water-Depth Curves:
Upper Parasequence Surface: Parasequence 28, 227.4 m.
Deepening Events: None.

| | | | |
|---|---|---|---|
| 3D | 11.6 | 239 | Fourth-Order Subsequence 3D (Rockdell Formation, continued). |
| | 11.6 | 239.0 | Parasequence 29 (227.4 to about 239 m): Subsequence 3D and its contained parasequence are about 11.6 meters thick. It consists of about 9 meters of very thick- to thick-bedded echinoderm grainstone. The uppermost 2.6 meters is not well exposed, but probably consists of packstone grading into wackestone and mudstone (from about 236 to 239 m). Exposure is inferred based on the occurrence of fenestral mudstone at the top of Subsequence 3D. Thin-sections: OTH-90-60, 227.8 m, facies F/E; OTH-90-61, 228.3 m, facies F and facies I; OTH-90-62, 230.4 m, facies E; OTH-90-63, 231.4 m, facies E/I; OTH-90-64, 233.7 m, facies E/C; OTH-90-65, 235.5 m, facies E.<br><br>Stratigraphic Positions Interpreted from Water-Depth Curves:<br>Upper Parasequence Surface: Parasequence 29, about 239 m (exact position not resolved).<br>Deepening Events: None. |
| Approximate 4A-4D | 76 | 315 | **Benbolt Formation.** This work places the Rockdell/Benbolt contact at about 238 meters so as to coincide with the subsequence 3D/4A surface. The Benbolt at the Old Thorn Hill section is characterized by the same suite of lithologies that occur at the "New" Thorn Hill or Thorn Hill (i.e., echinoderm grainstone, facies E; echinoderm-bearing grainstone with coated- and worn-grains, facies C; bioclastic wackestone/packstone, facies B; echinoderm/bryozoan packstone, facies F; and oncoid-bearing wackestone/packstone, facies N). However, at least one important difference exists between these two sections. Namely, the middle portion of the Benbolt at Old Thorn Hill is characterized by shaly beds intercalated with thin wackestone/packstone and grainstone beds (generally less than 0.2 meters thick). In contrast, this shale is generally absent from the Benbolt at the Thorn Hill section. |
| 4 | 134.3 | 373.3 | **Third-Order Sequence 4 (Benbolt, Wardell, and lowermost Bowen formations).** |

4A 14.1 253.1 Fourth-Order Subsequence 4A (Benbolt Formation). Subsequence 4A is about 14 meters thick and contains five parasequences, numbered 30 through 34. Subsequence 4A has not been sampled at the same level of detail as the underlying strata. Sampling in Subsequence 4A averages about 1 sample for every 3 to 4 meters; whereas the underlying strata were sampled about every meter. Thus, the position of parasequence boundaries are not as well constrained in Subsequence 4A as they are in the underlying sequences.

1.5 240.5 Parasequence 30 (about 239 to 240.5 m): The basal approximately 1.5 meters consists of thick-bedded, massive wackestone/mudstone (faces L). Placement of this 1.5 meter thick basal portion within lowermost Subsequence 4A, rather than uppermost Subsequence 3D is somewhat arbitrary because this facies transition is not well sampled. The top of Parasequence 30 is indicated at 240.5 meters where the wackestone/mudstone beds are sharply truncated by echinoderm grainstones. This contact is irregular. Thin-sections: OTH-90-66, 240.5 m, facies L; OTH-90-67, 240.5 m, facies E.

3.5 244.0 Parasequence 31 (about 240.5 to about 244 m): Very thick-bedded, massive to crossbedded echinoderm grainstone and peloid-bearing echinoderm grainstone beds overlie Parasequence 30. The top of Parasequence 31 is not resolved at the Old Thorn Hill section. An approximate position for the top of Parasequence 31 at about 244 meters is suggested by way of comparison with the Thorn Hill section. Thin-section: OTH-90-68, 242.1 m, facies E/I.

4.0 248.0 Parasequence 32 (about 244 to about 248 m): The interval from 244 to about 248 meters also consists of very thick-bedded massive to crossbedded echinoderm grainstone and peloid-bearing echinoderm grainstone beds. The top of Parasequence 32 is also not resolved at the Old Thorn Hill section. An approximate position for the top of Parasequence 32 at about 248 meters is suggested by way of comparison with the Thorn Hill section. Thin-section: OTH-90-69, 246.1 m, sample lost.

2.5 250.5 Parasequence 33 (about 248 to about 250.5 m): This approximately 2.5 meter thick parasequence is characterized by very thick- to thick-bedded, massive to crossbedded echinoderm grainstone and peloid-bearing echinoderm grainstone beds. The top of Parasequence 33 is not resolved at the Old Thorn Hill

section. Thin-sections: OTH-90-70A, 249.4 m, facies E/I; OTH-90-70B, 249.4 m, facies E.

2.6 253.1 Parasequence 34 (about 250.5 to about 253.1 m): The interval above 250.5 meters is also characterized by thick- to very thick to thick-bedded, massive to crossbedded echinoderm grainstone and peloid-bearing echinoderm grainstone beds. The top of Subsequence 4A and Parasequence 33 are not resolved at the Old Thorn Hill section. An approximate position for the top of Subsequence 4A is suggested at 253.1 meters through comparison with the Thorn Hill and Idol Mine sections. The top of Subsequence 4A may not have experienced exposure at the Old Thorn Hill Section. Thin-sections: None.

Stratigraphic Positions Interpreted from Water-Depth Curves: Upper Parasequence Surfaces: Parasequence 30, 240.5 m; Parasequence 31, about 244 m (exact position not resolved); Parasequence 32, about 248 m (exact position not resolved); Parasequence 33, about 250.5 m (exact position not resolved); Parasequence 34, about 253.1 m (exact position not resolved). Deepening Events: None.

4B 8.1 261.2 Fourth-Order Subsequence 4B (Benbolt Formation, continued). Parasequence 35 (about 253.1 to 261.2 m): Subsequence 4B and its contained parasequence consist of very thick- to thick-bedded massive to crossbedded echinoderm grainstone and peloid-bearing echinoderm grainstone beds (from about 253.1 to 260.8 m). Parasequence 35 is capped by about 0.4 meters of wackestone/mudstone with poorly developed fenestrae. Thin-sections: OTH-90-71, 255.3 m, facies E/I; OTH-90-72, 257.6 m, facies E/I; OTH-90-73, 260.6 m, facies E; OTH-90-74, 261.1 m, facies A.

Stratigraphic Positions Interpreted from Water-Depth Curves: Upper Parasequence Surfaces: Parasequence 35, 261.2 m. Deepening Events: None.

4C 26.5 287.7 Fourth-Order Subsequence 4C (Benbolt Formation, continued). Subsequence 4C comprises an approximately 26.5 meter thick succession. The section is covered above about 275 meters.

21.8 283.0 Parasequence 36 (261.2 to about 283 m): About 14 meters of very thick to thick-bedded, massive to crossbedded echinoderm grainstone and packstone occur from about 261 to 275 meters. The uppermost 5 meters of this 14 meter thick succession consists mostly of thick-bedded packstones and are not well exposed. The section is covered above 275 meters. Thin-sections: OTH-90-74.25, 262.4 m, facies E; OTH-90-74.5, 262.6 m, facies E/F; OTH-90-75, 264.5 m, facies F/E; OTH-90-76, 266.1 m, facies E; OTH-90-77, 267.1 m, facies E; OTH-90-77.25, 268.2 m, facies E/F; OTH-90-77.5, 268.5 m, facies E/F; OTH-90-268.8 m, facies E/F; OTH-90-79, 270.6 m, facies E/F; OTH-90-80, 272.5 m, facies E/F, OTH-90-81A, 274.4 m, facies E; OTH-90-81B, 274.4 m, facies E.

3.4 287.0 Parasequence 37 (about 283.6 to about 287 m): This part of the section is covered.

Stratigraphic Positions Interpreted from Water-Depth Curves: Upper Parasequence Surfaces: Parasequence 36, about 283 m (estimated by comparison with other sections); Parasequence 37, about 287 (estimated by comparison with other sections). Deepening Events: $D_{10}$, 268.5; $D_{11}$, (not resolved, section covered).

Approximate
24 302 COVERED INTERVAL

4D 34.1 321.0 Fourth-Order Subsequence 4D (Benbolt Formation, continued, and lowermost Wardell Formation).

13 296 Parasequence 38 (about 283 to about 296 m): Parasequence 38 is covered.

52.1 321.1 Parasequence 39 (about 296 to about 321.1 m): The section is covered from about 275 to at about 303.5 meters. Thick- to medium-bedded, massive to crossbedded echinoderm grainstone occurs above 303.5 meters. The occurrence of red alga *Solenopora* (P) and well-developed coated-grains within echinoderm grainstone (facies E) at about 321.1 meters suggests shoaling. Shallow-water indicators are used to infer the position of the upper surface of Subsequence 4D and Parasequence 39. Thin-sections: OTH-90-82, 304.1 m, facies E; OTH-90-83, 305.8 m, facies E; OTH-90-84A, 308.1 m, facies E; OTH-90-

84B, 308.1 m, facies E; OTH-90-85, 312.4 m, facies E; OTH-90-86, 315.4 m, facies E; OTH-90-87, 317.9 m, facies E; OTH-90-88, 320.5 m, facies E/F; OTH-90-89, 321.1 m, facies E.

Stratigraphic Positions Interpreted from Water-Depth Curves: Upper Parasequence Surfaces: Parasequence 38 (about 296 m, exact position not resolved); Parasequence 39, 321.1 m. Deepening Events: None.

4E 15.1 336.2 Fourth-Order Subsequence 4E (Wardell Formation, continued).
11.6 332.7 Parasequence 40 (321.1 to 332.7 m). Parasequence 39 is overlain by about 4 meters of very thick-bedded, massive echinoderm grainstone (from 321.1 to about 325 m). An approximately 0.6 meter thick bed of bioclastic wackestone/packstone occurs from about 325.0 to 325.6 meters. About 7 meters of thick- to medium-bedded echinoderm grainstone overlies this wackestone/packstone bed (from about 325.6 to 332.5 m). Several discontinuous lenses, less than 0.2 meters thick, consisting of wackestone/mudstone (facies L ) and bioclastic wackestone/packstone (facies B) mark the upper surface of Parasequence 40. Cavities filled with vadose silt occur within the wackestones and mudstones of these lenses. Thin-sections: OTH-90-90, 322.9 m, facies E; OTH-90-91, 324.5 m, facies E; OTH-90-92, 325.1 m, facies B; OTH-90-93, 325.7 m, facies E; OTH-90-94, 326.3 m, facies E; OTH-90-95, 327.7 m, facies E; OTH-90-96, 328.6 m, facies E; OTH-90-97, 329.6 m, facies E; OTH-90-98, 330.2 m, facies E; OTH-90-99, 331.8 m, facies E; OTH-90-100, 332.6 m, facies B; OTH-90-101A, 332.6 m, facies B (bottom of thin-section), facies L (top of thin-section); OTH-90-101B, 332.6 m, facies B (bottom of thin-section), facies L (top of thin-section); OTH-90-102, 332.6 m, facies F (bottom of thin-section), facies F/I (top of thin-section).

Stratigraphic Positions Interpreted from Water-Depth Curves: Upper Parasequence Surfaces: Parasequence 40, 332.7 m. Deepening Events: None.

Approximate
27 343 **Wardell Formation.** This work follows Wedekind (1986) in placement of the Benbolt/Wardell contact at about 315.7 meters. The Wardell is an argillaceous lime mudstone intercalated with

thin (generally less than 0.2 meters thick) wackestone and packstone beds. Additional description of the Wardell is provided by Wedekind (1986).

4F 40.6 373.3 Fourth-Order Subsequence 4F (uppermost Wardell and Bowen formations).

3.5 336.2 Parasequence 41 (332.7 to 336.2 m). About 3.5 meters of thick-bedded echinoderm grainstone overlies Parasequence 41. The upper surface of Parasequence 41 is tentatively placed at the top of an approximately 0.2 meter thick grainstone/packstone bed. Thin-sections: OTH-90-103, 332.8 m, facies E; OTH-90-104, 334.1 m, facies E; OTH-90-105, 336.2 m, facies E/F.

9.8 346.0 Parasequence 42 (336.2 to 346 m). Parasequence 42 is not well exposed. About 9.8 meters of very thick-bedded echinoderm grainstone beds intercalated with thin- to medium-bedded packstones overlies Parasequence 41. A facies change from echinoderm grainstone and packstone into peloidal grainstone tentatively marks the he upper surface of Parasequence 41. The upper surface of Parasequence 42 is placed at the top of an approximately 0.2 meter thick grainstone/packstone bed. An approximately 3 meter thick covered interval occurs above this bed. Thin-sections: OTH-90-106, 336.7 m, facies E; OTH-90-107, 340.1 m, facies E/F; OTH-90-108, 341.3 m, facies E; OTH-90-109, 342.3 m, facies F; OTH-90-110, 343.2 m, facies E; OTH-90-111, 345.1 m, facies E; OTH-90-112A, 345.6 m, facies E/F; OTH-90-112B, 345.6 m, facies E/F; OTH-90-112N, 345.6 m, facies E/F.

3 349.0 COVERED INTERVAL

3 371.5 COVERED INTERVAL

27.3 373.3 Parasequence 43 (346 to 373.3 m). A covered interval occurs from about 346 to about 349 meters. About 12 .5 meters of medium- to thin-bedded peloidal grainstone and aggregate-grain grainstone occurs from about 349 to 361.5 meters. These grainstones are gradationally overlain by about 7 meters of medium- to thin-bedded bioclastic wackestone/packstone and echinoderm grainstone/packstone (from 361.5 to 368.3 m). An

approximately 3 meter thick covered section occurs from 368.3 to about 371.5. Sequence 4F and Parasequence 43 are capped by at least 2 meters of thin-bedded fenestral wackestone/mudstone (facies L). Thin-sections: OTH-90-113, 348.9 m, facies I; OTH-90-114A, 356.4 m, facies I; OTH-90-114B, 356.4 m, facies I; OTH-90-115, 358.7 m, facies J/I; OTH-90-116, 360.2 m, facies I/F; OTH-90-117, 362.3 m, facies B; OTH-90-118, 362.9 m, facies B (right side of thin-section), facies F (left side of thin-section); OTH-90-119, 365.8 m, facies F/J; OTH-90-120, 367.1 m, facies B; OTH-90-121, 368.2 m, facies B; OTH-90-122, 372.4 m, facies L.

Stratigraphic Positions Interpreted from Water-Depth Curves:
Upper Parasequence Surfaces: Parasequence 41 336.2 m; Parasequence 42, 346 m (exact position not resolved); Parasequence 43, 373.3 m.
Deepening Events: $D_{12}$, about 370 m; $D_{14}$, about 400.0 m.

4 375 **Bowen Formation.** This work assigns the Bowen Formation to an approximately 4 meter thick interval at the Old Thorn Hill section. The Bowen comprises the rocks immediately above and below the Sequence 4/5 boundary. The Bowen consists of shaly limestone interbedded with wackestone and mudstone. Mud cracks occur within many of the shaly beds.

Approximate
57 430 **Witten Formation.** The Witten overlies the Bowen and is lithologically similar to the underlying Wardell Formation.

Estimated
5 152 525 Third-Order Sequence 5.

13.7 387 Parasequence 44 (373.3 to about 387 m): Parasequence 44 is not well exposed. Shaly limestone is gradational with the fenestral wackestone/mudstone developed at the top of Subsequence 4E. Three thin-bedded intervals, each up to about 0.3 meters thick, consisting of bioclastic wackestones and peloidal grainstones occur within this approximately 9 meter thick shaly limestone (i.e., OTH-90-123, 377.4 m; OTH-90-124, 379.0 m; OTH-90-125, 382.0 m). The approximate upper surface of Parasequence 44 is indicated by a thin-bedded peloidal grainstone interval, about 0.2 meters thick, within the shaly limestone at about 387 meters. Calcite filled vugs, similar to those observed lower in the section, occur within these

peloidal grainstones. Thin-sections: OTH-90-123, 377.4 m, facies B (bottom of thin-section), facies I (top of thin-section); OTH-90-124, 379.0 m, facies B/N; OTH-90-125, 382.0 m, facies B; OTH-90-126, 387.0 m, facies I.

Additional thin-sections from Sequence 5 (Witten formation continued): OTH-90-127, 394.0 m, facies N/J; OTH-90-128, 398.5 m, facies G; OTH-90-129, 401.5 m, facies L (laminated); OTH-90-130, 500.8 m, facies L (fenestral and laminated); OTH-90-131A, 508.6 m, facies L; OTH-90-131B, 508.6 m, facies L (laminated and fenestral); OTH-90-132A, 517.8 m, facies I/L; OTH-90-132B, 517.8 m, facies L (laminated); OTH-90-133, facies 521.4 m, facies J; OTH-90-134, 524.8 m, facies L (laminated and fenestral); OTH-90-135, 528.9 m, facies F (bottom of thin-section), facies J (top of thin-section).

Approximate
180 610 **Moccasin Formation.** The Moccasin gradationally overlies the Witten and consists largely of very thin-bedded mud-rich limestones intercalated with yellow weathering clay shale. Ripple marks and mudcracks characterize many intervals within the Moccasin. Complete description of the Moccasin is provided by Simonson (1986). Thin-section: OTH-90-136, 532.3 m, facies L.

## Idol Mine Section (IS)

The Idol Mine section (IS) is located along the road leading north from State Route 131 to the Union Zinc Co. "Idol Mine," in Grainger County, Tennessee from lat 36°22'03''to 36°22'18''N and long 83°52'53'' to 83°26'03'' W (approximately the NE1/4, NE1/4, NW1/4 of the Avondale 7.5' topographic quadrangle). The intersection of the road leading to the Idol Mine with State Route 131 is located about 1.8 km (1.1 mi.) northeast of Thorn Hill. About 340 m of Chickamauga Group strata are exposed in the road cut, in adjacent fields, and along Joe Mill Creek. Samples for, thin-sections (50 X 75 mm) were collected by three people. Ruppel (1979) was the first to sample this section. His samples are denoted as "IS" followed by his unit number and the sample number from that unit (e.g, his second sample from his Unit 2 is "IS-2-2"). Roberson provided samples from the Five Oaks Formation and lowermost Lincolnshire formations. Roberson's samples are labeled with the prefix "ISR." Steinhauff remeasured the section in 1990 and collected additional samples above the Five Oaks Formation to help fill gaps in the section. Samples collected by Steinhauff are labeled "IS-90," followed by a unique number. Samples are given with thickness above the Knox unconformity.

**KNOX GROUP**

Unconformity

| Sequence/ Cycle | | | **CHICKAMAUGA GROUP** |
|---|---|---|---|
| 2nd Ord. | Seq. Thk (m) | Cumul. Thk (m) | |
| O-S | 1,384 | 1,384 | **Tippecanoe Sequence (Sloss, 1963).** Other Synonyms: Ordovician-Silurian (O-S) Second Order Cycle or Supercycle (Vail, et al., 1977), and Paleozoic Sequence II, Middle Ordovician to Lower Devonian, Walker (1985) and Byerly et al. (1986). |
| 3rd & 4th Ord. | Seq. Thk (m) | Cumul. Thk (m) | |
| 1A-2B | 26.0 | 26.0 | **Five Oaks Formation.** The lower approximately 8 meters (Ruppel's Units 1 and 2) of the Five Oaks at the Idol Mine section consists predominately of dolostone and dolomitic limestone. Two lithologies, wackestone/mudstone (facies L) and |

peloidal grainstone (facies I), dominate the Five Oaks above about 8 meters (Ruppel's Unit 3). Ruppel (1979) noted fine laminations throughout the upper Five Oaks. He also noted that the mudstone and the grainstone lithologies are often separated by sharp contacts and that the peloidal lithologies are locally fossiliferous and contain gastropods, trilobites, and ostracodes.

1 19.4 19.4 **Third-Order Sequence 1 (lower Five Oaks Formation).**

1A 3.5 3.5 Fourth-Order Sequence 1A (Blackford Member of the Five Oaks Formation).

3.5 3.5 Parasequence 1 (0 to 3.5 m): Parasequence 1 is a fine-grained dolomite and dolomitic limestone. The upper surface of Subsequence 1A and Parasequence 1 is indicated by the occurrence of mudstone. Thin-sections: ISR-1, 0.0 m, facies P; ISR-3, 0.9 m, facies P; IS-1-1, 1.0 m, facies P; IS-1-2, 1.5 m, facies P; ISR-4, 1.9 m, facies P; ISR-6, 3.4 m, facies P; IS-2-1, 3.5 m, sample lost.

Stratigraphic Positions Interpreted from Water-Depth Curves:
Upper Parasequence Surfaces: Parasequence 1, 3.5 m.
Deepening Events: None.

1B 12.5 16.0 Fourth-Order Subsequence 1B (Five Oaks Formation, continued).

12.5 16.0 Parasequence 2 (3.5 to 16.0 m): A thin interval of lithoclastic grainstone (less than 0.5 meters thick) overlies Parasequence 1. This is followed upward by dolomitic limestone and mudstones. The upper surface of Sequence 1B and Parasequence 2 is marked by fenestral mudstone (facies L). Thin-sections: ISR-9, 6.1 m, facies O; IS-2-2, 7.9 m, sample missing; IS-3-1, 8.1 m, facies L (fenestral); ISR-11, 10.0 m, facies L (fenestral); IS-3-2, 10.0 m, sample lost; ISR-12, 10.2 m, facies L (fenestral); ISR-13, 10.3 m, facies L (fenestral); ISR-14, 10.6 m, facies L

(fenestral); ISR-15, 10.9 m, facies L (fenestral); ISR-16, 12.6 m, facies L (fenestral).

Stratigraphic Positions Interpreted from Water-Depth Curves:
Upper Parasequence Surfaces: Parasequence 2, 16.0 m.
Deepening Event: $D_0$, 11.9 m.

1C 3.4 19.4 Fourth-Order Sequence 1C (Five Oaks Formation, continued). Subsequence 1C comprises the middle to upper part of Ruppel's Unit 3.

3.4 19.4 Parasequence 3 (16.0 to 19.4 m): Subsequence 1C and Parasequence 3 consist of about 2 meters of thick-bedded wackestone/mudstone (facies L) gradationally overlain by slightly more than 1 meter of ooid-bearing packstone. This packstone grades into an interval dominated by peloidal grainstone at the top of Subsequence 1C. Thin-sections: IS-3-3, 16.0 m, facies L; ISR-18, 16.2 m, facies L (fenestral); ISR-20, 18.8 m, facies I; IS-3-4, 19.0 m, sample lost; ISR-21, 19.3 m, facies I.

Stratigraphic Positions Interpreted from Water-Depth Curves:
Upper Parasequence Surfaces: Parasequence 3, 19.4 m.
Deepening Event: $D_1$, 16.1 m.

2 165.0 188.0 Third-Order Subsequence 2 (Five Oaks and Lincolnshire formations).

2A N/A N/A Fourth-Order Subsequence 2A. Subsequence 2A is not recognized at on-shelf positions.

Stratigraphic Positions Interpreted from Water-Depth Curves:
Upper Parasequence Surfaces: N/A.
Deepening Events: N/A.

2B 6.6 26.0 Fourth-Order Subsequence 2B (Five Oaks Formation, total thickness 26.0 m). Comprises the upper part of Ruppel's Unit 3.

3.4 19.4 Parasequence 4 (16.0 to 19.4 m): Subsequence 2B consists of very thick- to thick-bedded wackestone/mudstone mixed with peloidal grainstone and overlies the packstone developed at the

top of Subsequence 1C. Thin-bedded mudstones are developed at the top of Subsequence 2B and its contained Parasequence 4. These thin beds grade into peloidal grainstones of overlying Subsequence 2C. Thin-sections: IS-3-5, 21.0 m, sample lost; ISR-23, 24.3 m, facies L (fenestral); IS-3-6, 24.8 m, facies L (fenestral)/I; ISR-25, 25.9 m, facies I/L (fenestral); ISR-26, 26.0 m, facies I/J.

Stratigraphic Positions Interpreted from Water-Depth Curves: Upper Parasequence Surfaces: Parasequence 4, 19.4 m. Deepening Event: None.

| | | | |
|---|---|---|---|
| Approximate 2C-2G | 115.4 | 141.1 | Lincolnshire Formation. Lincolnshire lithologies at the Idol Mine section are similar to those described for the Thorn Hill and Old Thorn Hill sections. Additional description is provided by Ruppel (1979, Units 4 through 13). Chapters 2 and 3 of the present study place the Lincolnshire/Rockdell contact at 115.4 meters above the Knox unconformity to coincide with the surface separating Sequence 2G from 2H. |
| 2C | 21.7 | 47.7 | Fourth-Order Subsequence 2C (Lincolnshire Formation, continued). Subsequence 2C comprises Ruppel's Units 4, 5, and 6. |
| | 10.5 | 36.5 | Parasequence 5 (26.0 to about 36.5 m): Slightly less than 6 meters of very thick-bedded, massive to crossbedded peloidal grainstone (facies I) are developed at the base of Subsequence 2C (from 26.0 to 31.9 m). About 4.5 meters of very thick-bedded, massive to crossbedded peloid-bearing echinoderm grainstone sharply overlies the peloidal grainstones (from 31.9 to about 36.5 m). Thin-sections: ISR-27, 26.5 m, facies E/I; IS-4-1, 27.0 m, sample lost; IS-90-0A, 28.1 m, facies I; IS-90-0B, 28.1 m, facies I; ISR-29, 28.6 m, facies I/J; IS-4-2, 30.0 m, facies I; IS-90-13, 31.7 m, facies I; IS-90-1, 35.1 m, facies E/I; IS-90-2, 35.3 m, facies E/I; IS-4-3, 35.5 m, sample missing. |
| | 11.2 | 47.7 | Parasequence 6 (about 36.5 to 47.7 m): These very thick-bedded grainstones of the underlying parasequence are sharply overlain by about 3.5 meters of thin-bedded aggregate grain-bearing echinoderm grainstone (36.5 to 40.0 m). These thin-beds are sharply overlain by about 7.7 meters of very thick- |

bedded, massive to crossbedded echinoderm grainstone (from 40.0 to 47.7 m). The top of Sequence 2C and Parasequence 6 is marked by a sharp contact with an overlying wackestone/packstone bed (about 0.5 meters thick). Thin-sections: IS-90-14, 37.4 m, facies E/J; IS-5, 38.0 m, facies E/J; IS-90-3, 39.9 m, facies E/J; IS-6, 40.2 m, sample missing; IS-90-4, 40.6 m, facies E; IS-90-5, 45.5 m, facies E/D.

Stratigraphic Positions Interpreted from Water-Depth Curves: Upper Parasequence Surfaces: Parasequence 5, about 36.5 m (exact position not resolved); Parasequence 6, 47.7 m. Deepening Events: $D_{4A}$, about 35.2 m; $D_{4B}$, about 40.6 m.

2D 3 50.7 Fourth-Order Subsequence 2D (Lincolnshire Formation, continued). Subsequence 2D corresponds to Ruppel's Units 6 and 7.

3 47.7 Parasequence 7 (47.7 to 50.7 m): About 0.5 meters of massive wackestone/packstone sharply overlies Subsequence 2C and grades into an approximately 2.5 meter thick, thick-bedded interval of massive grainstone (from about 48.2 to 50.7 m). This grainstone interval consists of aggregate grain-bearing echinoderm grainstone at the base and peloidal grainstone at the top Parasequence 7. Thin-sections: IS-90-15, 48.2 m, facies B; IS-7-1, 48.5 m, sample lost; IS-7-2A, 49.0 m, facies F/J; IS-7-2B, 49.0 m, facies E/F; IS-7-3, 50.0 m, sample lost.

Stratigraphic Positions Interpreted from Water-Depth Curves: Upper Parasequence Surfaces: Parasequence 7, about 50.7 m. Deepening Event: $D_5$, about 48.2 m.

Approximate
2E 62.5 113.2 Fourth-Order Subsequence 2E (Lincolnshire Formation, continued). Subsequence 2E comprises Ruppel's Units 8-13 and the lower part of his Unit 14.

27.3 78.0 Parasequence 8 (50.7 to about 78 m): Very thick-bedded, massive to cross-bedded grainstone occurs from about 50.7 to 70 meters. The interval from about 70 to 76.5 meters is not well exposed, but probably consists mostly of peloidal grainstone (facies I). This is followed by very thick-bedded grainstone and packstone (from about 76.5 to 78 m). The transition from Parasequence 8 into Parasequence 9 occurs at about 78 meters where echinoderm grainstone is gradationally

overlain by echinoderm/bryozoan packstone/grainstone. Thin-sections: IS-90-6, 50.8 m, facies I (bottom of thin-section), facies E (top of thin-section); IS-8-1, 57.0 m, facies E; IS-8-2, 62.0 m, facies E; IS-90-8, 63.3 m, facies E/I; IS-9, 63.5 m, facies E/I; IS-90-16, 67.3 m, facies E; IS-10, 65.0 m, sample lost; IS-90-9, 68.6 m, facies E/C; IS-90-10, 72.3 m, facies I; IS-11-1, 77.0 m, facies E; IS-90-17, 77.5 m, facies E/I.

9.0 87.0 Parasequence 9 (about 78 to about 87 m): This approximately 9 meter thick interval is not well exposed. However, it consists mostly of thick- to medium-bedded echinoderm grainstone. Thin-sections: IS-90-11, 78.4 m, facies E; IS-11-2, 79.5 m, facies F (bottom of thin-section), facies F/B (top of thin-section); IS-90-12, 80.2 m, facies E; IS-12-1, 80.3 m, sample lost; IS-90-18, 84.6 m, facies E; IS-90-18N, 84.6 m, facies E; IS-90-19, 86.9 m, facies F/I.

26.2 113.2 Parasequences 10 and 11 (about 87 to 113.2 m): The upper portion of Sequence 2E is very poorly exposed or covered. Thin-sections: IS-12-2, 87.7 m, sample lost; IS-13, 92.0 m, facies E; IS-90-20, 92.4 m, facies E/J; IS-14-1, 98.4 m, sample lost.

Stratigraphic Positions Interpreted from Water-Depth Curves:
Upper Parasequence Surfaces: Parasequence 8, about 78 m (exact position not resolved); Parasequence 9, about 87 m (exact position not resolved); Parasequence 10, covered; Parasequence 11, covered.
Deepening Events: $D_6$, about 81 m; $D_7$, about 95 m.

Estimated, Approximate

2G 28.2 141.4 <u>Fourth-Order Subsequence 2G (Lincolnshire Formation, total thickness 115.4 m)</u>. Approximately the upper part of Ruppel's Unit 14. This part of the section comprising parasequences 12, 13, 14, and 15 is very poorly exposed or covered. Thin-section: IS-14-2, 128.0 m, sample lost.

Stratigraphic Positions Interpreted from Water-Depth Curves:
Upper Parasequence Surfaces: Parasequences 12, 13, 14, and 15 are covered.
Deepening Events: None.

2H-3D 96.2 237.6 **Rockdell Formation.** The present work places the Lincolnshire/Rockdell contact at the surface separating Subsequence 2G from 2H at about 141 meters above the Knox. This contact is covered at the Idol Mine section.

Estimated, Approximate

2H 17.5 159 Fourth-Order Subsequence 2H (Rockdell Formation). Approximately the uppermost part of Ruppel's Unit 14 and lower part of Ruppel's Unit 15. This part of the section comprising Parasequence 16 is poorly exposed or covered. The interval from 151 to about 156 meters consists is generally mud-rich and consists of oncoid-bearing wackestone/packstone (facies N). Thin-sections: IS-15-1, 145.0 m, sample lost; IS-15-2, 152 m, facies N; IS-15-3, 155.0 m, facies N.

Stratigraphic Positions Interpreted from Water-Depth Curves:
Upper Parasequence Surfaces: Parasequence 16 is covered or poorly exposed.
Deepening Events: $D_8$, (covered).

Approximate

74 170 COVERED INTERVAL

2I 16 175.0 Fourth-Order Subsequence 2I (Rockdell Formation, continued). Approximately the upper part of Ruppel's Unit 15. The lower part of Subsequence 2I comprising parasequences 17 and 18 is poorly exposed or covered.

4.5 172.5 Parasequence 19 (about 168 to 172.5 m): Parasequence 19 overlies a poorly exposed interval. Parasequence 19 consists of about 4.5 meters of medium- to thin- bedded aggregate-grain grainstone (facies J). Mud and oncoids (i.e. an oncoid-bearing packstone/grainstone) occurs in the upper approximately 0.5 meters of Parasequence 19. Thin-sections: IS-90-21, 170.0 m, facies J; IS-90-22, 172.4 m, facies J/N.

2.5 175.0 Parasequence 20 (about 172.5 to 175.0 m): Parasequence 20 gradationally overlies Parasequence 19 and consists of about 2.5 meters of oncoid-bearing wackestone/packstone (facies N, from 172.5 to 175 m). A thin lens (less than 0.5 meter thick) consisting of bioclastic wackestone/packstone and overlies the oncoid-bearing wackestone/packstone and 0.1 to 0.2 meters of aggregate-grain grainstone erosionally overlies this

wackestone/packstone lens. The top of Sequence 2I and Parasequence 20 is paced at the top of this wackestone packstone lens. Thin-sections: IS-15-4, 173.0 m, facies N; IS-90-23, 174.6 m, facies B; IS-90-24, 175.0 m, facies E/J; IS-16-1, 175.0 m, facies J.

Stratigraphic Positions Interpreted from Water-Depth Curves:
Upper Parasequence Surfaces: Parasequences 17, and 18 are covered; Parasequence 19, 172.5 m; Parasequence 20, 175.0 m.
Deepening Events: None.

2J 6 181 Fourth-Order Subsequence 2J (Rockdell Formation, continued). Subsequence 2J corresponds to the lowest part of Ruppel's interval "Units 16-19."

6 181 Parasequence 21 and 22 (from 175 to about 180 m) are not differentiated: About 0.1 to 0.2 meters of aggregate-grain grainstone erosionally overlies the wackestone/packstone lens developed at the top of Sequence 2I. This aggregate-grain grainstone grades abruptly (over less than 2 meters) into very thick-bedded, massive to crossbedded echinoderm grainstone. This crossbedded echinoderm grainstone continues to about 184 meters. The top of Parasequence 22 is inferred to occur at about 181 meters where a lower set of echinoderm grainstone crossbeds is observed to truncate an upper set of echinoderm grainstone crossbeds. Comparison with facies patterns observed at the Old Thorn Hill and Cedar Springs section are also used to infer the approximate position for the top of Sequence 2J and Parasequence 22. Thin-sections: IS-90-25, 179.8 m, facies E; IS-16-2, 180.0 m, sample lost.

Stratigraphic Positions Interpreted from Water-Depth Curves:
Upper Parasequence Surfaces: Parasequence 21, (exact position not resolved); Parasequence 22, about 181 m (exact position not resolved).
Deepening Events: None.

2K 9.8 190.8 Fourth-Order Subsequence 2K (Rockdell Formation, continued). Subsequence 2K corresponds to the lower to middle part of Ruppel's interval "Units 16-19."

| | | | |
|---|---|---|---|
| | 9.8 | 190.8 | Parasequence 23 (about 181 to 190.8 m): About 3.8 meters of very thick-bedded, massive to crossbedded echinoderm grainstone continues above the inferred upper surface of Subsequence 2J (from 181 to 184.8 meters). An approximately 1 meter thick bioclastic wackestone/packstone (facies B) bed sharply overlies these grainstones. This bed grades vertically into wackestone/mudstone (facies L) over about 0.5 meters. This massive wackestone/mudstone is about 4.5 meters thick. An aggregate-grain grainstone lens (about 0.5 m thick) occurs within this wackestone/mudstone at about 186.8 meters. The top of Subsequence 2K and Parasequence 23 is recognized at about 190.8 meters were these wackestone/mudstones contain *Spongiostroma* and are erosionally overlain by very thin- to thin-bedded echinoderm grainstone. Thin-sections: IS-90-26, 185.2 m, facies B; IS-90-27, 186.8 m, facies J and L; IS-90-28A, 190.8 m, facies E/J; IS-90-28B, 190.8 m, facies E. |
| | | | Stratigraphic Positions Interpreted from Water-Depth Curves: Upper Parasequence Surfaces: Parasequence 23, 190.8 m. Deepening Events: None. |
| 3 | 46.8 | 237.6 | **Third-Order Sequence 3 (Rockdell Formation, continued).** |
| 3A | 21.5 | 212.3 | Fourth-Order Subsequence 3A (Rockdell Formation, continued). Subsequence 3A corresponds to the middle part of Ruppel's interval "Units 16-19." |
| | 3.0 | 193.8 | Parasequence 24 (about 190.8 to about 193.8 m): Parasequence 24 sharply overlies mudstones of Subsequence 2K. Parasequence 24 consists of a basal 0.5 meter thick interval of thin- to very-thin-bedded echinoderm grainstone followed by about 1 meter of thick-bedded aggregate grain-bearing echinoderm grainstone. This echinoderm grainstone is overlain by about 0.5 meters of aggregate-grain, grainstone (facies J). About 2 meters of bioclastic wackestone/packstone (facies B) occurs at the top of Parasequence 24. The contact with Parasequence 25 is covered. IS-90-29, 191.4 m, facies E/J; IS-90-30, 192.0 m, facies J. |
| | 18.5 | 212.3 | Parasequence 25 (about 193.8 to 212.3 m): About 3.5 meters of grainstone and packstone overlies the 0.5 meter thick covered interval at the top of Parasequence 24 (from 94.5 to 97 m). |

This packstone passes upwards into a poorly exposed, 4.5 meter thick interval of wackestone/packstone (facies B) (from about 97 to 201.5 m). About 5.5 meters of medium to thick-bedded aggregate-grain-bearing echinoderm grainstone occurs from 201.5 to 206.5 meters. These grainstones are followed by about 4 meters of poorly exposed wackestone/packstone (from 206.5 to 210.5 m). About 1.8 meters of aggregate-grain and cortoid-bearing echinoderm grainstone occurs at the top of Sequence 3A and Parasequence 25. A few superficial ooids occur in IS-90-36 (211.2) and indicate very shallow water deposition. Thin-sections: IS-90-31, 196.7 m, facies E/F; IS-90-32, 197.1 m, facies C/B; IS-17.1 m, facies 198.0 m, facies B; IS-17-2, 200.0 m, sample lost; IS-18-1, 202.0 m, facies E/J; IS-90-33, 202.0 m, facies E/J; IS-90-34, 205.6 m, facies E/J; IS-90-35, 206.6 m, facies E/J; IS-17-3, 208.0 m, facies B; IS-90-36, 211.2 m, facies E/C.

Stratigraphic Positions Interpreted from Water-Depth Curves:
Upper Parasequence Surfaces: Parasequence 24, 193.8 m; Parasequence 25, 212.3 m.
Deepening Events: $D_9$, 208.0 m.

3B 10.7 223.0 Fourth-Order Subsequence 3B (Rockdell Formation, continued). Subsequence 3B corresponds to the middle to upper part of Ruppel's interval "Units 16-19."

10.7 223.0 Parasequences 26 and 27 (about 212.3 to about 223.0 m): About 8.7 meters of very thick-bedded, massive to crossbedded echinoderm grainstone overlies Subsequence 3A (from 212.3 to about 221 m). An approximately 2 meter thick covered interval occurs at the top of Subsequence 3B. Thin-sections: IS-90-37, 216.2 m, facies E; IS-90-37, 216.2 m, facies E/I.

Stratigraphic Positions Interpreted from Water-Depth Curves:
Upper Parasequence Surfaces: Parasequence 26, about 217 m (exact position not resolved); Parasequence 27, 223.0 m (exact position not resolved).
Deepening Events: None.

3C 7.0 230.0 Fourth-Order Subsequence 3C (Rockdell Formation, continued). Subsequence 2K corresponds to the middle to upper part of Ruppel's interval "Units 16-19."

7.0 230.0 Parasequence 28 (about 223.0 to about 230.0 m): About 2 meters of very thick-bedded echinoderm grainstone overlies Subsequence 3B and Parasequence 27. This interval is gradationally overlain by about 5 meters of cortoid-bearing echinoderm grainstone. These grainstones are overlain by an approximately 0.5 meter thick lens consisting of about 0.1 meters of peloidal grainstone at the base grading into about 0.4 meters of wackestone/packstone (facies B). This lens marks the upper surface of Subsequence 3C and Parasequence 28. Thin-sections: IS-90-38, 226.1 m, facies E/C; IS-90-39, 228.7 m, facies E/C; IS-18-2, 230.0 m, sample lost; IS-90-40, 230.0 m, facies E/C; IS-90-41, 230.0 m, facies I.

Stratigraphic Positions Interpreted from Water-Depth Curves: Upper Parasequence Surfaces: Parasequence 28, about 230.0 m.

Deepening Events: None.

3D 7.6 237.6 Fourth-Order Subsequence 3D (Rockdell Formation, continued). Subsequence 3D corresponds to the upper part of Ruppel's interval "Units 16-19."

7.5 237.6 Parasequence 29 (about 230.0 to 237.6 m): About 2 meters of thick-bedded peloidal grainstone/packstone overlies Subsequence 3C. This grainstone/packstone grades into about 1 meter of wackestone/mudstone (facies L) containing vugs, up to 0.1 m across, filled with sparry calcite. This wackestone/mudstone is sharply overlain by about 0.5 meters of medium-bedded peloidal grainstone. An approximately 3.5 meter thick interval consisting of thick-bedded mudstones and wackestone occurs from 233.5 to 237 meters. Vugs filled with fibrous and sparry calcite and cavities filled with vadose silt occur with in the mudstones of this interval. An approximately 0.2 meter thick bed or lens of peloidal grainstone overlies this interval. The upper surface of Subsequence 3D and Parasequence 29 is placed at the top of an approximately 0.5 meter thick wackestone/packstone bed (facies B). Thin-sections: IS-90-42, 232.1 m, facies I/B; IS-90-43A1, 232.9 m, facies L or A (with calcite filled vugs); IS-90-43A, 232.9 m, facies L or A (with

calcite filled vugs); IS-90-43B, 232.9 m, facies L or A (with calcite filled vugs); IS-90-43B1, 232.9 m, facies L or A (with calcite filled vugs); IS-90-43C, 232.9 m, facies L or A (with calcite filled vugs); IS-90-43C1, 232.9 m, facies L or A (with calcite filled vugs); IS-90-43C2, 232.9 m, facies L or A (with calcite filled vugs); IS-90-43C3, 232.9 m, facies L or A (with calcite filled vugs); IS-90-43C4, 232.9 m, facies L or A (with calcite filled vugs); IS-90-44, 233.6 m, facies I; IS-90-45, 234.2 m, facies B and B/I; IS-90-46, 234.6 m, facies L; IS-90-47A, 234.7 m, facies L; IS-90-47B, 234.7 m, facies L. Stable carbon and oxygen isotopes sampled from the following polished slabs (these slabs do not have corresponding thin-sections): IS-90-47b (Slab), 234.7 m, facies L; IS-90-47b1 (Slab), 234.7 m, facies L; IS-90-47b2 (Slab), 234.7 m, facies L; IS-90-47c (Slab), 234.7 m, facies L.

Thin-sections, continued: IS-19-1A, 236.0 m, facies B; IS-19-1B, 236.0 m, facies B; IS-90-48, 236.6 m, facies L; IS-90-2A, 237.0 m, facies I and B; IS-90-2B, 237.0 m, facies I and B; IS-90-49A, 237.5 m, facies I/B; IS-90-49B, 237.5 m, facies I/B. Stratigraphic Positions Interpreted from Water-Depth Curves: Upper Parasequence Surfaces: Parasequence 29, 237.6 m. Deepening Events: None.

4A-4D 74.6 312.2 **Benbolt Formation.** The general description for the Benbolt at the Idol Mine section is similar to that given for the Thorn Hill and Old Thorn Hill sections. One important difference, however, is that shaly limestone occurs about 25 meters lower in the section at the Idol Mine locality when compared to the Thorn Hill and Old Thorn Hill localities. Additionally, the packstone lithologies in the lower part of the Benbolt have dusky-red colors. This work places the base of the Benbolt at the surface separating Subsequence 3D from Subsequence 4A. Thus, the Benbolt recognized here corresponds to Ruppel's Units 16 through 24.

Approximate
4 136 374 **Third Order Subsequence 4 (Benbolt Formation).** Evidence regarding the contact/exposure surface separating sequences 3 and 4 is discussed by Steinhauff and Walker (1992a,b).

| | | | |
|---|---|---|---|
| 4A | 16.4 | 254.0 | Fourth-Order Subsequence 4A (Benbolt Formation). Subsequence 4A corresponds to the uppermost Unit 19 and lowermost Unit 20 of Ruppel (1978). |
| | 3.6 | 241.2 | Parasequence 30 (237.6 to 241.2 m) Thin-sections: An approximately 1 meter thick bed of bioclastic wackestone/packstone (facies B, probably a bryozoan mud-mound) is developed above the Sequence 3D surface. This wackestone/packstone is overlain by slightly less than 2 meters of peloid-bearing echinoderm grainstone and echinoderm grainstone (facies E) (from 238.8 to about 240.4 m). The interval from about 240 to 422 meters is not well exposed. A bed of bioclastic wackestone/packstone bed (less than about 0.3 meters thick) occurs at about 241 meters. Small cavities filled with crystal or vadose silt occur within this bed. Thus, the top of Parasequence 30 is placed at the top of this bed. Thin-sections: IS-90-50A and B, 238.5 m, facies B; IS-90-51A and B, 238.9 m, facies E/I; IS-19-3, 241.0 m, facies L. |
| | 2.8 | 244.0 | Parasequence 31 (241.2 to about 244 m): The interval comprising Parasequence 31 consists of very thick- to thick-bedded echinoderm grainstone. The upper surface of Parasequence 31 is not well defined. It is placed at about 244 meters, where echinoderm grainstones is overlain by thick-bedded packstone and grainstone/packstone. Thin-section: IS-90-52A and B, 243.1 m, facies E. |
| | <8.0 | 252.0 | Parasequence 32 and 33 (above 244 m to about 252 m): About 7.5 meters of medium- to thin-bedded packstone and packstone/grainstone overlie parasequence (from 244 to 251.5 m). A transition from packstone into shaly carbonate occurs from about 251.5 to 252 meters. The upper surface of Parasequence 33 is placed within this 0.5 meters of section. Thin-sections: IS-90-53A, 245.3 m, facies E/F; IS-90-53B, 245.3 m, facies E; IS-90-54A and B, 248.1 m, facies E/F; IS-19-4, 249.0 m, sample lost; IS-90-55A and B, 248.9 m, facies E; IS-90-56A, 249.2 m, facies E/F; IS-90-56B, 249.2 m, facies F/E. |
| | 2.0 | 254.0 | Parasequence 34 (about 252 to 254.0 m): About 11 meters of shale and shaly carbonate occurs from about 252 to about 263 meters. A few thin flaggy carbonate beds (less than 0.2 meters thick) occur within the lower most 5 meters of this shaly interval. These flaggy beds consist of packstone beds followed |

by peloidal grainstones beds. Crystal or vadose silt occurs within cavities contained within one of these thin peloidal grainstone beds at about 253.9 meters. Thus, the top of Sequence 4A and Parasequence 34 is placed at the top of this bed. Thin-sections: IS-20, 253.0 m, facies F; IS-90-57A and B, 253.0 m, facies F (bottom of thin-section), facies E (top of thin-section); IS-90-58A, 253.9 m, facies I/J; IS-90-58B, 253.9 m, facies I/J.

Stratigraphic Positions Interpreted from Water-Depth Curves:
Upper Parasequence Surfaces: Parasequence 30, 241.2 m; Parasequence 31, about 244 m (exact position not resolved); Parasequence 32 (not resolved); Parasequence 33, about 252 m (exact position not resolved); Parasequence 34, 254.0 m.
Deepening Events: None.

| | | | |
|---|---|---|---|
| Approximate 4B | 82 | 62 | Fourth-Order Subsequence 4B (Benbolt Formation, continued). Probably corresponds to Units 20, 21, and 22 of Ruppel (1979). |
| | 8.0 | 262.0 | Parasequence 35 (254.0 to about 262 m): About 9 meters of shale and shaly carbonate intercalated with very thin-bedded peloidal grainstone beds occurs between 254 to 263 meters. The section is covered between about 263 and 267 meters. The top of sequence 4B is inferred to occur within this covered interval based on comparison with the sections at Old Thorn Hill and Cedar Springs. Thin-sections: None. |

Stratigraphic Positions Interpreted from Water-Depth Curves:
Upper Parasequence Surfaces: Parasequence 35, about 262 m (exact position not resolved).
Deepening Events: None.

| | | | |
|---|---|---|---|
| | 8 | 268 | COVERED INTERVAL |
| Approximate 4C | 26 | 288 | Fourth-Order Sequence 4C (Benbolt Formation, continued). Corresponds to Ruppel's Units 22, 23, and 24. |
| | <26.0 | 288.0 | Parasequences 36 and 37 (above 262 to about 288 m): Sequence 4C consists of shaly carbonate and shale intercalated with very thin peloidal grainstone beds. The thin-sections indicated below are representative of these thin peloidal |

grainstone beds. The top of sequence 4C is inferred to occur at the top of one of these thin peloidal grainstone beds at 288 meters. The selection of this bed is based on comparison with the sections at Old Thorn Hill and Cedar Springs. Thin-sections: IS-90-59A and B, 269.0 m, facies I; IS-21, 256.5 m, sample lost; IS-22, 259.0 m, sample lost; IS-90-60A and B, 277.5 m, facies I/L; IS-90-60.5A, 280.9 m, facies B; IS-90-60.5B, 280.9 m, facies B; IS-24-3, 280.0 m, facies I; IS-90-61A and B, 281.4 m, facies I/B; IS-90-62A and B, 282.2 m, facies J/I; IS-90-63A and B, 282.7 m, facies I/J; IS-24-2A and B, 288.0 m, facies I.

Stratigraphic Positions Interpreted from Water-Depth Curves: Upper Parasequence Surfaces: Parasequence 36 (not resolved); Parasequence 37, about 288 m (exact position not resolved). Deepening Events: $D_{11}$, 282.2 m.

4D 35 323 Fourth-Order Subsequence 4D (Benbolt Formation, continued; and lowermost Wardell Formation). Corresponds to Ruppel's Units 24 and 25.

8.7 296.7 Parasequence 38 (about 288 to 296.7 m): About 5 meters of shaly carbonate and shale intercalated with very thin peloidal grainstone beds overlies Subsequence 4C (from 288 to 293 m). A transition from shale and shaly carbonate beds into grainstone beds occurs in the upper most 3.7 meters of Parasequence 38. These grainstone beds are peloidal and very thin in the lowest part of this transitional interval. They grade into medium to thick-bedded aggregate-grain, grainstone and echinoderm grainstone in the upper part of this interval. Shoaling is indicated at about 296.7 meters by the occurrence of coated-grains and superficial ooids. Thus, the top of Parasequence 38 is placed about 296.7 meters. Thin-sections: IS-90-64A and B, 293.6 m, facies J; IS-90-65A and B, 294.9 m, facies F/E; IS-90-66A and B, 295.9 m, facies J; IS-90-67A, 296.7 m, facies I/J; IS-90-67B, 296.7 m, facies I/J.

26.3 323.0 Parasequence 39 (296.7 to 323.0 m): About 6.6 meters of thin- to medium- bedded peloidal and echinoderm grainstone overlies Parasequence 38 (from 296.7 to 303.3 m). Thin beds (less than 0.2 meters thick) of shale and shaly carbonate are intercalated with these grainstone beds in the upper half of this 6.6 meter thick interval. About 2.6 meters of medium- to very

thin-bedded peloidal and echinoderm grainstones occur from 303.3 to about 305.9 meters. Slightly more than 8 meters of very thick bedded, massive to crossbedded echinoderm grainstone follows from 305.9 to about 314 meters. An approximately 3 meter thick, poorly exposed interval consisting of bioclastic wackestone/packstone (facies B) follows from 314 to about 317 meters. Very thick- bedded, massive to crossbedded peloidal-bearing echinoderm grainstone follows from 317 to 318.5 meters. The section is covered from 318.5 to 320.5 meters. About 2.5 meters of medium-bedded peloid-bearing echinoderm grainstone occurs from 320.5 to 323 meters. The section is poorly exposed or covered above about 323 meters and is inferred to consist mostly of wackestones and packstones. The upper surface of Sequence 4D and Parasequence 39 is placed just below the covered part of this section. Thin-sections: IS-90-68A and B, 297.6 m, facies E/I; IS-90-69A and B, 298.3 m, facies E; 298.8 m, IS-90-70A and B, facies I/J; IS-90-71A and B, 300.6 m, facies I; IS-90-72A and B, 304.0 m, facies E/I; IS-90-73A and B, 305.1 m, facies E; IS-90-74, 306.7 m, ? facies I or B; IS-90-75A and B, 306.9 m, facies E; IS-24-1A and B, 311.0 m, facies E/I; IS-90-76A and B, 311.9 m, facies E; IS-90-25, 313.0 m, sample lost; IS-26A and B, 315.0 m, facies B; IS-90-77A and B, 317.4 m, facies E; IS-27, 318.0 m, sample lost; IS-28-1A and B, 321.0 m, facies E/I; IS-90-78A and B, 322.8 m, facies E.

Stratigraphic Positions Interpreted from Water-Depth Curves:
Upper Parasequence Surfaces: Parasequence 38, 296.7 m; Parasequence 39, 323.0 m.
Deepening Events: None.

Approximate
27 343 **Wardell Formation (from about 312.2 to about 343 m).** The Wardell is generally covered at the Idol Mine section. The Wardell is an argillaceous lime mudstone intercalated with thin (generally less than 0.2 meters thick) wackestone and packstone beds. The reader is referred to Wedekind (1986) for additional description of the Wardell.

Approximate
4E 12 335 Fourth-Order Subsequence 4E (Wardell Formation, continued). Approximately Units 25-29 of Ruppel (1978).

| | | | |
|---|---|---|---|
| | 12.0 | 335.0 | Parasequence 40 (323.0 to about 335 m): Thin-sections: IS-90-79A and B, 325.4 m, facies F; IS-90-80, 327.3 m, facies E; IS-29, 328.0 m, sample missing.<br><br>Stratigraphic Positions Interpreted from Water-Depth Curves:<br>Upper Parasequence Surfaces: Parasequence 38, 296.7 m; Parasequence 39, 323.0 m.<br>Deepening Events: None. |
| Approximate | >100 | 425 | COVERED INTERVAL |
| Estimated | | | |
| 5 | 152 | 525 | **Third-Order Sequence 5.** Covered at the Idol Mine section. |
| | 4 | 375 | **Bowen Formation.** The Bowen is covered at the Idol Mine Section. The Bowen consists of shaly limestone interbedded with wackestone and mudstone where it is observed at other localities. |
| Approximate | 57 | 430 | **Witten Formation.** The Witten overlies the Bowen and is lithologically similar to the underlying Wardell Formation. The lower Witten is generally covered or poorly exposed at the Idol Mine Section. Thin-section: IS-90-81, approximately 425.0 m, facies G. |

## Cedar Springs Section (CS)

The Cedar Springs section was collected by Steve Ruppel as part of his dissertation. All the thin-sections reported here are described by Ruppel (1979). Access to this section is by way of Ceder Springs Road. Cedar Springs Road intersects the north side of State Route 131 (formerly State Route 66) about 4.8 km (3.0 mi.) northeast of Thorn Hill in Grainger County, East Tennessee. This section is exposed along Cedar Springs Creek in pastures on either side of Cedar Springs Church road from lat 36°22'47''to 36°23'07''N and long 83°22''13''to 83°22'30''W (SW1/4, SW1/4, SW1/4 of the Swan Island 7.5' topographic quadrangle). Ruppel noted that "approximately 425 m (1392 ft.) of the Chickamauga Group are exposed from the Knox/Chickamauga contact (near the church) to the lower part of the Moccasin Formation." Stratigraphic sequence boundaries and facies interpreted as part of this work are indicated below; the reader is referred to Ruppel (1979) for detailed description of this section. Sample numbers (thin-sections) are Ruppel's original numbers. These are given with measured thickness from the base of the section along with the facies interpretation (made by Steinhauff). Analysis of fifth-order parasequences are not as complete as at the other sections.

**KNOX GROUP**

Unconformity

| Sequence/ Cycle | | | **CHICKAMAUGA GROUP** |
|---|---|---|---|
| 2nd Ord. | Seq. Thk (m) | Cumul. Thk (m) | |
| O-S | 1,384 | 1,384 | **Tippecanoe Sequence (Sloss, 1963).** Other Synonyms: Ordovician-Silurian (O-S) Second Order Cycle or Supercycle (Vail, et al., 1977), and Paleozoic Sequence II, Middle Ordovician to Lower Devonian, Walker (1985) and Byerly et al. (1986). |
| 3rd & 4th Ord. | Seq. Thk (m) | Cumul. Thk (m) | |
| 1A-2B | 23.5 | 23.5 | **Five Oaks Formation.** The Five Oaks Formation recognized in this work is the same as that recognized by Ruppel (1978) (i.e., Ruppel's Units 1-19). |

| | | | |
|---|---|---|---|
| 1 | 20.7 | 20.7 | **Third-Order Sequence 1 (lower Five Oaks Formation).** |
| 1A | 7.0 | 7.0 | Fourth-Order Subsequence 1A (Five Oaks Formation). Subsequence 1A comprises Units 1-12 of Ruppel (1979). Thin-sections: CS-1-1, approximately 0.0 m, facies L; CS-1-2, approximately 0.0 m, facies P (polished slab, no thin-section); CS-1-3, approximately 1 m, facies P (polished slab, no thin-section); CS-2, 1.5 m, facies P; CS-3, 2.0 m, facies L; CS-4, 2.5 m, facies J; CS-5, 3.0 m, facies I; CS-6, 4.0 m, facies I; CS-7, 4.5 m, facies L; CS-8, 5.5 m, facies I; CS-9, 6.0 m, facies J; CS-10, 6.3 m, facies I; CS-11, 6.7 m, facies I; CS-12, sample lost. |
| 1B | 9.0 | 16.0 | Fourth-Order Subsequence 1B (Five Oaks Formation, continued). Subsequence 1B comprises approximately Units 13-16 of Ruppel (1979). Thin-sections: CS-13, 7.3 m, facies L; CS-14, 7.8 m, facies L; CS-15, 8.9 m, facies L; CS-15, 8.9 m, facies L; CS-16, 10.6 m, facies I; CS-17, 11.5 m, facies L (laminated and fenestral); CS-18, 13.3 m, facies L (fenestral); CS-19, 14.5 m, facies L (fenestral).;<br><br>Stratigraphic Positions Interpreted from Water-Depth Curves: Deepening Event: $D_0$, 7.3 m. |
| 1C | 4.7 | 20.7 | Fourth-Order Subsequence 1C (Five Oaks Formation, continued). Subsequence 1C comprises approximately Units 17 and 18 of Ruppel (1979). Thin-sections: CS-20, 16.0m, facies L (laminated); CS-21, 16.3 m, facies J; CS-22, 18.0 m, facies I/J.<br>Stratigraphic Positions Interpreted from Water-Depth Curves: Deepening Events: $D_1$, 16.3 m. |
| 2 | 172.9 | 193.6 | **Third-Order Sequence 2 (Five Oaks and Lincolnshire formations).** |
| 2A | N/A | N/A | Fourth-Order Subsequence 2A. Subsequence 2A does not occur on the shelf (see Chapter 3). |

| | | | |
|---|---|---|---|
| 2B | 2.8 | 23.5 | Fourth-Order Subsequence 2B (Five Oaks Formation, total thickness 23.5 m). Subsequence 2B comprises approximately Ruppel's Unit 19. Thin-sections: CS-23, 20.7 m, facies I; CS-24, 22.0 m, facies I. |
| Approximate 2C-2G | 116.5 | 140 | **Lincolnshire Formation.** The Lincolnshire comprises approximately Units 20-37 of Ruppel (1979). The present work places the Lincolnshire/Rockdell contact at about 140 meters above the Knox to coincide with the surface separating subsequences 2G and 2H. In contrast, Ruppel (1979) placed this contact at a slightly lower stratigraphic position (about 212.5 meters above the Knox) based on a gradual lithologic change (over tens of meters) from underlying "pinkish gray " grainstone into overlying "brownish gray ... nodular weathering" mud-rich lithologies. Lincolnshire lithologies at Cedar Springs are similar to those described for the Thorn Hill and Old Thorn Hill sections. |
| 2C | 25.5 | 49.0 | Fourth-Order Subsequence 2C (Lincolnshire Formation). Comprises about the lower part of Ruppel's interval "Units 22-27." Thin-sections: CS-25, 24.0 m, facies F; CS-26, 25.5 m, sample lost; CS-27, 29.0 m, facies E/J; CS-28, 33.0 m, facies B (bottom of thin-section) stromatolite boundstone (top of thin-section); CS-29, 35.0 m, facies J; CS-30, 38.8 m, facies D/J; CS-31, 39.5 m, facies D; CS-32, 40.5 m, facies D; CS-33, 46.4 m, facies D; CS-34, 47.0 m, sample lost.<br><br>Stratigraphic Positions Interpreted from Water-Depth Curves: Deepening Events: $D_{4A}$, about 35.0 m; $D_{4B}$, 39.5 m. |
| Approximate 2D | 7.5 | 56.5 | Fourth-Order Subsequence 2D (Lincolnshire Formation, continued). Subsequence 2D comprises the upper part of Ruppel's interval "Units 22-27." Thin-section: CS-35, 56.5 m, facies J.<br><br>Stratigraphic Positions Interpreted from Water-Depth Curves: Deepening Events: $D_5$, not resolved. |
| 2E | 55.9 | 112.5 | Fourth-Order Subsequence 2E (Lincolnshire Formation, continued). Subsequence 2E comprises the upper part of Ruppel's interval "Units 22-27" and the lower part of Ruppel's |

"Units 28-35." Thin-sections: CS-36, 57.0 m, sample lost; CS-37, 65.0 m, facies D; CS-38, 67.0 m, facies E; CS-39, 68.9 m, facies E/F; CS-40, 70.0 m, facies E; CS-41, 73.4 m, facies C; CS-42, 80.4 m, facies C; CS-43, 88.3 m, facies E/C; CS-44, 91.8 m, facies E; CS-45 99.4 m, facies E; CS-46, 101.0 m, facies D; CS-47, 102.5 m, facies J; CS-48, 109.0 m, facies D/J; CS-49, 112.0 m, facies N.

Stratigraphic Positions Interpreted from Water-Depth Curves: Deepening Events: $D_6$, about 80.0 m; $D_7$, about 95 m.

2F N/A N/A Fourth-Order Subsequence 2F. Subsequence 2F was not deposited on the shelf (see Chapter 3).

2G 27.5 140.0 Fourth Order Subsequence 2G (Lincolnshire Formation, total thickness, 116.5 m). Comprises approximately upper part of Ruppel's "Units 28-35" and Units 36, 37, and 38. Thin-sections: CS-50, 115.3 m, facies G; CS-51, 117.1 m, facies L; CS-52, 121.5 m, facies G; CS-53, 125.5 m, facies E/C; CS-54, 128.3 m, facies L (laminated and fenestral - bottom of thin-section), facies N (top of thin-section); CS-55, 133.0 m, facies G; CS-56, 136.2 m, facies C; CS-57, 139.3 m, facies A/B.

Stratigraphic Positions Interpreted from Water-Depth Curves: Upper Parasequence Surfaces: Parasequence 12, about 117.0 m.

Deepening Events: None.

Approximate
2H-3D 101 241 **Rockdell Formation.** The present work places the Rockdell/Benbolt contact to coincide with the exposure surface separating third order sequences 3 and 4 at about 241 m above the Knox. There are three reasons for moving the contact: 1) The surface separating sequences 3 and 4 appears to be a more consistent stratigraphic datum than the first occurrence of medium gray limestone beds. 2) Using this surface helps keep many of the already busy diagrams from getting even more complicated. 3) This keeps the exposure surfaces or unconformities from "crossing" formational contacts. Exposure surfaces that "cross" formation contacts do not violate the definition of a formation. However, some geologists who reviewed an early presentation of this material were bothered by this. In contrast, Ruppel (1979) placed the Rockdell/Benbolt

contact at about 218.6 meters above the Knox based on the first occurrence of "medium gray, medium to coarse grained limestone . . . " The Rockdell recognized here includes Ruppel's Units 37 through 47.

2H 15.6 155.6 Fourth-Order Subsequence 2H (Rockdell Formation). Subsequence 2H includes Ruppel's Units 37 through 40. Thin-sections: CS-58, 140.7 m, facies C/E; CS-59, 146.4 m, facies J; CS-60, 153.0 m, facies C; CS-61, 153.2 m, facies J; CS-62, 154.0 m, facies L/B; CS-63, 155.2 m; CS-64, 155.2 m, facies L (fenestral); CS-64, 155.5 m, facies C.

Stratigraphic Positions Interpreted from Water-Depth Curves: Deepening Events: $D_8$, 155.2 m.

Approximate
2I 8.2 163.8 Fourth-Order Subsequence 2I (Rockdell Formation, continued). Subsequence 2I corresponds to approximately Ruppel's interval "Units 40-41." Thin-section: CS-65, 161.2 m, facies L/A.

Approximate
2J 112.0 170.0 Fourth-Order Subsequence 2J (Rockdell Formation, continued). Subsequence 2J comprises approximately the lower part of Ruppel's interval "Units 42-44." No thin-sections.

2K 18.6 193.6 Fourth-Order Subsequence 2K (Rockdell Formation, continued). Subsequence 2K comprises approximately the middle to upper part of Ruppel's interval "Units 42-44." Thin-sections: CS-66, 174.4 m, facies J/E; CS-67, 175.0 m, facies L (fenestral, bottom of thin-section), facies B (top of thin-section); CS-68, 166.5 m, facies F/E; CS-69, 168.0 m, facies F/E; CS-69, 168.0 m, facies F/E; CS-70, 170.0 m, facies E/F; CS-71, 174.8 m, facies 9; CS-72, 180 .9 m, facies C; CS-73, 190.3 m, facies C.

Approximate
3 43.4 237 **Third-Order Sequence 3 (Rockdell Formation, continued).**

3A 21.3 214.9 Fourth-Order Subsequence 3A (Rockdell Formation, continued). Subsequence 3A comprises approximately the uppermost part of Ruppel's interval "Units 42-44." Thin-sections: CS-74, 193.6 m,

facies A; CS-75, 206.5 m, facies C; CS-76, 207.9 m, facies F; CS-77, 211.3 m, facies F.

Stratigraphic Positions Interpreted from Water-Depth Curves: Deepening Events: $D_9$, about 210.0 m.

| | | | |
|---|---|---|---|
| | 2.4 | 218.6 | COVERED INTERVAL |
| 3B | 10.0 | 224.7 | Fourth-Order Subsequence 3B (Rockdell Formation, continued). Subsequence 3B comprises approximately Units 46 and 47 of Ruppel (1978). Thin-sections: CS-78, 217.2 m, facies E; CS-79, 224.0 m, facies C. |
| Approximate 3C | 4.3 | 229 | Fourth-Order Subsequence 3C (Rockdell Formation, continued). Subsequence 3C is covered. |
| | 13.1 | 237.8 | COVERED INTERVAL |
| Approximate 3D | 8 | 237 | Fourth-Order Subsequence 3D (Rockdell Formation, total thickness, about 101 m). Subsequence 3D corresponds to the upper part of Ruppel's Unit 47. This part of the section not well exposed. Thin-sections: CS-80, recovered from float, approximate stratigraphic position 231 m, facies E/F. |
| 4 | 140 | 377 | **Third-Order Sequence 4 (Benbolt, Wardell, and lower Bowen formations).** |
| Approximate 4A-4 | 72.3 | 313.3 | **Benbolt Formation.** The general description for the Benbolt at Cedar Springs is similar to that given for the Idol Mine and Old Thorn Hill sections. The present work places the base of the Benbolt at the surface separating Subsequence 3D from Subsequence 4A. Thus, the Benbolt recognized here corresponds approximately to Ruppel's Units 48 through 52. |
| 4A | 16.5 | 253.5 | Fourth-Order Subsequence 4A (Benbolt Formation). Subsequence 4A corresponds to approximately Units 47 and 48 |

of Ruppel (1979). Thin-sections: CS-81, 238.5 m, facies E/F; CS-82, 241.3 m, facies E/C; CS-83, 248.7 m, facies E/J; CS-85, 250.5 m, facies E; CS-86, 253.5 m, facies B.

| | | | |
|---|---|---|---|
| Approximately 4B | 8.5 | 262 | Fourth-Order Subsequence 4B (Benbolt Formation, continued). Subsequence 4B includes approximately Units 49 and 50 of Ruppel (1979). Thin-section: CS-87, 255.3 m, facies B/L. |
| 7.2 | 280.6 | | COVERED INTERVAL |
| Approximate 4C | 25.6 | 287.6 | Fourth-Order Subsequence 4C (Benbolt Formation, continued). Subsequence 4C includes approximately Units 51 and 52 of Ruppel (1979). Thin-sections: CS-88, 264.8 m, facies 9; CS-89, 268.1 m, facies B/H; CS-90, 272.8 m, facies E; CS-91, 281.0 m, facies E/F; CS-92, 282. 5 m, facies E/I; CS-93, 287.3 m, facies E. |
| | | | Stratigraphic Positions Interpreted from Water-Depth Curves: Deepening Events: $D_{10}$, ? about 265 m; $D_{11}$, 281.5 m. |
| 4D | 35.2 | 322.8 | Fourth-Order Subsequence 4D (Benbolt Formation, total thickness, about 72.3 m; lowermost Wardell Formation). Subsequence 4D includes approximately Units 52 and 53 of Ruppel (1979). Thin-sections: CS-94, 290.7 m, facies E; CS-95, 294.9 m, facies E; CS-96, 302.6 m, facies E/J; CS-97, 307.4 m, facies E/F; CS-98, 309.2 m, facies E/F; CS-99, 310.8 m, facies E; CS-100, 312.6 m, facies E/J; CS-101, 313.14 m, facies F; CS-102, 313.9 m, facies B/A; CS-103, 315.7 m, facies F/N; CS-104, 321.3 m, facies B; CS-104A, 322.5 m, facies E/J. |
| 4E | 11.5 | 334.3 | Fourth-Order Subsequence 4E (Wardell Formation, continued). Comprises approximately Unit 54 of Ruppel (1979). Thin-sections: CS-105, 323.1 m, facies B; CS-106, 328.0 m, facies B; CS-107, 332.8 m, facies B/L; CS-108, 334.3 m, facies B/L. |
| 4.3 | | 355.1 | COVERED INTERVAL |

4D-4F 55.2 368.5 **Wardell Formation.** The Wardell comprises the same interval recognized by Ruppel (1979) (i.e., Units 54 trough 58).

5.5 374.0 COVERED INTERVAL

Approximate
4F 42.7 377 Fourth-Order Subsequence 4F (Wardell Formation, total thickness, 55.2 m; lower Bowen Formation). Subsequence 4F comprises approximately Units 55 through 58 of Ruppel (1979). Thin-sections: CS-109, 342.0 m, facies L (laminated); CS-110, 349.0 m, facies B; CS-111, 356.0 m, facies L (laminated); CS-112A, recovered from float, approximate stratigraphic position 362.5 m, facies F/E; CS-112B, recovered from float, approximate stratigraphic position 362.5 m, facies F/E; CS-113, recovered from float, approximate stratigraphic position 364.0 m; CS-114, recovered from float, approximate stratigraphic position 365.5 m, facies H; CS-115, 367.1 m, facies B/H; CS-116, 375.0 m, facies I; CS-117, 375.9 m, facies L (laminated) mixed with facies I.

Stratigraphic Positions Interpreted from Water-Depth Curves: Deepening Event: $D_{12}$, about 375 m.

Approximate
4F 8.5 377 **Lower Bowen Formation.** Lower Bowen comprises approximately the lower part of Ruppel's Unit 59. Thin-sections: CS-116, CS-117.

Estimated
5 152 525 **Third-Order Sequence 5 (upper Bowen, Witten and lower Moccasin formations).** Third order Sequence 5 is not subdivided into fourth order sequences.

5 1.9 378.9 **Upper Bowen Formation.** Total thickness of Bowen Formation, about 10.4 m. Comprises the upper part of Ruppel's Unit 59. Thin-section: CS-118, 377.8 m, facies I.

5 45.5 424.3 **Witten Formation.** The Witten comprises the same interval recognized by Ruppel (1979) (i.e., Units 60-64). Thin-sections: CS-119, 382.5 m, facies N; CS-120, recovered from float, approximate stratigraphic position 387 m; facies G; CS-121,

392.5 m, facies E; CS-122, 394.0 m, facies N; CS-123, 398.0 m, facies N; CS-124, 409.4 m, facies L (laminated); CS-125, 414.0 m, facies I; CS-126A, 420.1 m, facies E; CS-126B, 420.1 m, facies B; CS-127, 421.9 m, facies J; CS-128A, 424.0 m, facies B; CS-128B, 424.0 m, facies C; CS-129A, 422.1 m, facies B/N; CS-129B, 422.1 m, facies B/N.

Stratigraphic Positions Interpreted from Water-Depth Curves: Deepening Event: $D_{13}$, about 398 m.

| | | | |
|---|---|---|---|
| Estimated 5 | 180 | 610 | **Moccasin Formation.** Thin-section: CS-130, sample lost. |

## Poor Valley Creek Section (PVC)

About 40 meters of Chickamauga Group limestones are exposed on the southwest side of the Poor Valley Creek embayment of Cherokee Lake (Holston River), southwest of the US 11W bridge. This area is about 1.2 km (0.75 mi.) east of the intersection of US 11W and Flat Gap Road (State Road 31) at Mooresburg, Hawkins County, Tennessee (lat 36°20'41" to 36°20'45" N and 83°12'12" to 83°12'18"W). This area lies in the N1/2, SE1/4, NW1/4, NW1/4 of the Russellville 7.5' topographic quadrangle. The section is overturned, incomplete and possibly structurally complicated. It lies close to the Saltville Fault. Thin-sections and samples were collected by Steve Ruppel (SCR) and Greg Jernigan (DGJ). Their original sample numbers are given from the base of the section.

**KNOX GROUP**

Unconformity

| Sequence/ Cycle | | | **CHICKAMAUGA GROUP** |
|---|---|---|---|
| 2nd Ord. | Seq. Thk (m) | Cumul. Thk (m) | |
| O-S | >40.0> | 40.0 | **Tippecanoe Sequence (Sloss, 1963).** Other Synonyms: Ordovician-Silurian (O-S) Second Order Cycle or Supercycle (Vail, et al., 1977), and Paleozoic Sequence II, Middle Ordovician to Lower Devonian, Walker (1985), Byerly et al. (1986). |
| 3rd & 4th Ord. | Seq. Thk (m) | Cumul. Thk (m) | |
| 1 | 17.6 | 17.6 | **Third-Order Sequence 1 (Five Oaks and Lenoir formations).** Sequence 1 corresponds to Units 1 and 2 of Ruppel (1978) |
| 1A | N/A | N/A | Fourth-Order Subsequence 1A. Subsequence 1A is not recognized at shelf-edge positions (see Chapter 3). |

| | | | |
|---|---|---|---|
| 1B | 3.4 | 3.4 | Fourth-Order Subsequence 1B (Five Oaks Formation, total thickness 3.4 m): Subsequence 1B corresponds to the lower part of Unit 1 of Ruppel (1979). The Five Oaks Formation consists largely of fenestral wackestone/mudstone (facies L), dolomitic limestone and dolomite. Thin-sections: None. |
| | 3.2 | 6.6 | COVERED INTERVAL (? Lenoir Formation). |
| 1C | 14.2 | 17.6 | Fourth-Order Subsequence 1C (Lenoir Formation, total thickness, 3.2 m; Holston Formation). Subsequence 1C corresponds to the upper part of Ruppel's Unit 1 and the lower to upper-middle part of Unit 2. Subsequence 1C consists of mostly of echinoderm grainstone (facies E) and packstone (facies F). Crystal or vadose silt occurs in cavities contained with packstones of the upper few meters. Thin-sections: PVC'-1A-T (DGJ), 11.6 m, facies E; PVC'-1A-B (DGJ), 11.6 m, facies E; PVC'-1B-1 (DGJ), 13.6 m, facies E; PVC'-1B-2 (DGJ), 13.8 m, facies E; PVC'-2E-2S (DGJ), 16.0 m, facies F.<br><br>Additional thin-sections with less certain ($\pm$ 4 m) stratigraphic positions: PVC-1 (SCR), 13.5 to 20.1 m, facies E; PVC-2 (SCR), 13.5 to 20.1 m, facies F;<br><br>Additional Thin-sections from Subsequence 1C: PVC-1B-R (DGJ), facies E; PVC-2A (DGJ), facies F; PVC-2C-MR (DGJ), facies F; PVC-2A-C2-R (DGJ), facies F; PVC-2C-b2 (DGJ), facies F; PVC-2D (DGJ), facies F; PVC-2Db (DGJ), facies F.<br><br>Stratigraphic Positions Interpreted from Water-Depth Curves: Deepening Event: $D_1$, not resolved. |
| Approximate 2 | >40.0 | 40.0 | **Third-Order Subsequence 2 (Holston Formation).** Corresponds to Units 3 and 4 of Ruppel (1978). |
| 2A | 2.2 | 24.2 | Fourth-Order Subsequence 2A (Holston Formation). Subsequence 2A appears to be absent from the section at Poor Valley Creek. It is possibly represented as a drowning unconformity occurring between underlying Sequence 1C and overlying Subsequence 2C. Thus, condensed Sequence 2B may be superimposed on condensed Subsequence 2A. |

Stratigraphic Positions Interpreted from Water-Depth Curves: Deepening Event: $D_2$, not resolved.

2B N/A N/A Fourth-Order Subsequence 2B. Subsequence 2B is not recognized at shelf-edge positions. However, a drowning unconformity, separating Subsequence 1C from overlying Subsequence 2C, is inferred to occur at about 24 meters above the Knox. This unconformity is interpreted as the condensed Subsequence 2B at the shelf-edge.

2C 11.0 28.6 Fourth-Order Subsequence 2C (Holston Formation, continued). Subsequence 2C is approximately equivalent to Ruppel's Unit 3. It consists mostly of bryozoan packstone and is interpreted as reef core fill. Large cephalopods and encrusting bryozoans are common. Many cavities are lined with botryoidal fibrous calcite cement and floored with internal sediment. Many of these cavities are also filled with crystal or vadose silt. Stromatactis is developed in the middle of the unit, subparallel to bedding. Thin-sections: PVC'-1C (DGJ), 18.6 m, facies E; PVC-4-1 (SCR), about 20.1 m, facies F; PVC-2Ca (DGJ), 20.6 m, facies F; PVC-2Cb (DGJ), 20.6 m, facies F; PVC'-2Cc (DGJ), 20.6 m, facies F; PVC-2C-1a, 20.6 m, facies F; PVC-2H (DGJ), 21.0 m, facies F; PVC-2D-1 (DGJ), 21.6 m, facies F; PVC-2D-2 (DGJ), 21.6 m, facies F; PVC-2D-3 (DGJ), 21.6 m, facies F; PVC-2D-a (DGJ), 21.6 m, facies F; PVC-2D-b (DGJ), 21.6 m, facies F; PVC-2A-C1-MR (DGJ), 24.6 m, facies F; PVC-2A-C1-ML (DGJ), 24.6 m, facies F; PVC-2A-C1-L (DGJ), 24.6 m, facies F; PVC-2A-C1-R (DGJ), 24.6 m, facies F; PVC-2A-C2 (DGJ), 24.9 m, facies F; PVC-2A-C2a (DGJ), 24.9 m, facies F; PVC-2A-C2b (DGJ), 24.9 m, facies F; PVC'-2G (DGJ), 26.6 m, facies F; PVC'-2H (DGJ), 27.6 m, facies F; PVC-3 (SCR), about 28.6 m, facies F.

Additional thin-sections with less certain ($\pm$ 4 m) stratigraphic positions: PVC-2A-1a (DGJ), about 24.6 m, facies F; PVC-2A-1b (DGJ), about 24.6 m, facies F; PVC'-2A-LM (DGJ), 20.1 to 28.6 m, facies F; PVC'-2C (DGJ), 20.1 to 28.6 m, facies F; PVC'-2C-1a (DGJ), 20.1 to 28.6 m, facies F; PVC'-2F (DGJ), 20.1 to 28.6 m, facies F; PVC'-2Gb (DGJ), 20.1 to 28.6 m, facies F; PVC'-2G(Bill) (DGJ), 20.1 to 28.6 m, facies F; PVC'-2J (DGJ), 20.1 to 44 m, facies F;

Stratigraphic Positions Interpreted from Water-Depth Curves: Deepening Events: $D_3$, not resolved; $D_4$, not resolved m.

2D >11.8 >40.3 Fourth-Order Subsequence 2D (Holston Formation, continued). Subsequence 2D is approximately equivalent to Ruppel's Unit 4. It consists of bryozoan packstone and echinoderm grainstone. Thin-sections: PVC-3Aa (DGJ), 39.6 m, facies F; PVC-3Ab (DGJ), 39.6 m, facies E; PVC-3A-T (DGJ), 39.6 m, facies E; PVC-3A-B (DGJ), 39.6 m, facies E.

Additional thin-sections with less certain ($\pm$ 4 m) stratigraphic positions: PVC'-2K-S2 (DGJ), 20.1 to 44 m, facies F; PVC-7 (SCR), > 28.6 m, facies E; PVC-8 (SCR), > 28.6 m, facies E.

Stratigraphic Positions Interpreted from Water-Depth Curves: Deepening Event: $D_5$, covered.

COVERED INTERVAL

## Red House Branch Section (RHB)

The Red House Branch section is located on both sides of the Red House Branch Embayment of Cherokee Lake (Holston River), southeast of U.S. 11W in Hawkins County, Tennessee (lat 36°22'00'' to 36°23'28'' N and 83°10'38''to 83°10'54''W). The section is overturned. This area lies in approximately the NE1/4, NW1/4, of the Russellville 7.5, topographic quadrangle. The northeast side of the exposure is adjacent to Lakemont Cabin Area at Mooresburg, Tennessee.

Samples (50 X 75 mm thin-sections) were collected by Ruppel (1978), Jernigan (1987), and Johnson (1988). The original sample numbers assigned by each worker are given along with stratigraphic position from the base of the section and facies interpretation (made by Steinhauff). Samples collected by each worker are identified by each workers initials in parenthesis: Steve Ruppel (SCR), Greg Jernigan (DGJ), and Eric Johnson (REJ).

**KNOX GROUP**

Unconformity

Sequence/ Cycle — **CHICKAMAUGA GROUP**

| 2nd Ord. | Seq. Thk (m) | Cumul. Thk (m) | |
|---|---|---|---|
| O-S | >423 | >423 | **Tippecanoe Sequence (Sloss, 1963).** Other Synonyms: Ordovician-Silurian (O-S) Second Order Cycle or Supercycle (Vail, et al., 1977), and Paleozoic Sequence II, Middle Ordovician to Lower Devonian, Walker (1985) and Byerly et al. (1986). |
| 3rd & 4th Ord. | Seq. Thk (m) | Cumul. Thk (m) | |
| 1 | 22 | 22 | **Third-Order Sequence 1 (Five Oaks and Lenoir formations).** Corresponds to Units 1 and 2 of Ruppel (1978) |
| 1A | N/A | N/A | Fourth-Order Subsequence 1A. Subsequence 1A is not recognized at shelf-edge positions (see Chapters 2 and 3). |

1B 5.2 5.2 Fourth-Order Subsequence 1B (Five Oaks Formation, total thickness 5.2 m): Subsequence 1B corresponds to Unit 1 of Ruppel (1979). The Five Oaks Formation consists largely of fenestral wackestone/mudstone (facies L), and bioclastic wackestone/packstone with peloidal grainstone. The upper surface of Subsequence 1B is recognized by a relatively sharp upper contact with the overlying peloidal grainstone. Thin-sections: RHB-1-1 (SCR), 0.0 m, facies L (fenestral); RHB-2-1 (SCR), 0.5 m, facies B/I; RHB-1-2 (SCR), 1.0 m, facies L (fenestral); RHB-2 (REJ), 3.0 m, facies L (fenestral); RHB-3 (REJ), 4.8 m, facies L (fenestral).

1C 16.8 22.0 Fourth-Order Subsequence 1C (Lenoir Formation, total thickness, 16.8 m). Subsequence 1C corresponds to Ruppel's Unit 2. Subsequence 1C consists of at least 1 meter of peloidal grainstone (facies I) grading upwards into at least 6 meters of bioclastic wackestone/packstone (facies B). Stromatoporiod boundstone occurs at about 17 meters. The uppermost 6 to 7 meters consists of echinoderm/bryozoan packstone (facies F). The upper surface of Subsequence 1B is recognized by a relatively sharp upper contact with the overlying echinoderm grainstones. Peloidal grainstone mixed with bioclastic wackestone/packstone occurs along or just below this inferred surface. Thin-sections: RHB-4 (REJ), 6.6 m, facies I; RHB-5 (REJ), 9.7 m, facies B; RHB-6 (REJ), 13.0 m, facies B; RHB-7 (REJ), 16.3 m, facies - Stromatoporoid boundstone.

Stratigraphic Positions Interpreted from Water-Depth Curves: Deepening Event: $D_1$, about 12 m.

Approximate
2 177 199 **Third-Order Sequence 2 (Holston Formation).** Corresponds to Units 3 through about 8 of Ruppel (1979).

2A-3A 218.5 240.5 **Holston Formation.** See Ruppel (1979) for description or the Holston Formation.

2A 5.2 27.2 Fourth-Order Subsequence 2A (Holston Formation). Thin-sections: Subsequence 2A is approximately equivalent to the lowest part of part of Ruppel's Unit 3. Subsequence 2A consists mostly of echinoderm grainstone (facies E) with

bryozoan packstone (facies F). A drowning unconformity or condensed section is inferred to occur just above a bryozoan boundstone interval at about 27.2 m. Orthocone cephalopods are observed within the grainstone of the overlying beds. RHB-8 (REJ), 17.0, facies F/B; RHB-LCa (DGJ) B, about 21.9 m, facies I/B (bottom of thin-section); RHB-2-4 (SCR), 22.0 m, facies F; RHB-LCa (DGJ) B, about 22.1 m, facies E (top of thin-section); RHB-LCb (DGJ), 22.0 m, facies E; RHB'-1 (DGJ), 22.5 m, facies E; RHB-1A (DGJ), 24.5 m, facies E; RHB-9-1A (REJ), 25.7 m, facies E; RHB'-1A-L (DGJ), 27.0 m, facies E; RHB-2-2 (SCR), 27.0 m, facies - stromatoporoid boundstone.

Stratigraphic Positions Interpreted from Water-Depth Curves: Deepening Events: $D_2$, 22.5 m.

2B N/A N/A Fourth-Order Subsequence 2B. Subsequence 2B is not recognized at shelf-edge positions. However, a drowning unconformity, separating Subsequence 2A from overlying Subsequence 2C, is inferred to occur at about 27.2 meters above the Knox. This unconformity is interpreted as the condensed Subsequence 2B at the shelf-edge (see Chapter 3).

Approximate
2C 14.8 42.0 Fourth-Order Subsequence 2C (Holston Formation, continued). Subsequence 2C is approximately equivalent to the upper part of Ruppel's Unit 3 and the lower part of Unit 4. This interval consists mostly of echinoderm grainstone. Water-depth analysis suggests relatively deep-water (at least 2 meters deep and possibly more than 150 meeters deep) at about 36.0 meters. Shallow-water indicators, including coated-grains, occur a few meters above and below the proposed deep-water interval at about 36.0 meters. These indicators suggest relatively shallow water-depths (generally 0.5 to 10 meters deep) above and below about 36.0 meters above the top of the Knox. Straight, orthocone cephalopods occur within this proposed deep-water part of the section. On the basis of this evidence, a condensed section, possibly a drowning unconformity, is inferred to occur at about 36.0 meters. Whole fossil bryozoans rooted in mud occur at about 39.6 meters. The upper surface of Subsequence 2C is indicated by a substantial increase in mud content from about 39 to 41.7 meters. Crystal or vadose silt fills cavities

within the bioclastic wackestone/packstone at the top of Subsequence 2C.

Thin-sections: RHB-10 (REJ), 30.8 m, facies E; RHB-1B (DGJ), 32.5 m, facies E; RHB'-1C (DGJ), 36.0 m, facies E; RHB-12 (REJ), 39.6 m, facies B. RHB-2G-B (DGJ), 42.0 m, facies F/E.

Additional thin-sections with less certain ($\pm$ 3 m) stratigraphic positions: RHB-2B-L (DGJ), about 41.3 m, facies E/H (bottom of thin-section), facies F (top of thin-section); RHB-2B-1C (DGJ), about 41.3 m, facies E; RHB-2C-B (DGJ), about 41.5 m, facies E; RHB'-2C-TR (DGJ), about 41.4 m, facies E.

Stratigraphic Positions Interpreted from Water-Depth Curves: Deepening Events: $D_3$, about 35.0 m; $D_4$, 36.0 m.

5.0 50.0 COVERED INTERVAL

2D 43.5 85.3 Fourth-Order Subsequence 2D (Holston Formation, continued). Subsequence 2D is approximately equivalent to the uppermost part of Ruppel's Unit 4, the overlying 5.0 meter thick covered interval, and the lower part of Unit 5. Very shallow-water indicators are occur above Subsequence 2C. Stromatactis occurs within mud-rich lithologies just above the inferred upper surface of Subsequence 2C. Roberson and Foreman (1989) have made a strong argument that at least some stromatactis is of very shallow-water origin. Other, less controversial, evidence for shallow-water includes blackened-grains and well-developed oncolites within grainstone (facies D) at about 44.0 meters. Above about 44 meters, Subsequence 2D consists of a complex mixture of echinoderm grainstone (facies E), grainstone/packstones, and bryozoan packstone (facies F). The upper surface of Subsequence 2D is recognized by the occurrence of spar fill vugs and cavities filled with crystal or vadose silt contained with the mud-rich lithologies that occur immediately below about 85 meters. Thin-sections: RHB-2H (DGJ), 42.0 to 42.5 m, facies ?B (stromatactis); RHB-2I-S2 (DGJ), 42.0 to 42.5 m, facies ?B (stromatactis); RHB'-2B-S2-TR (DGJ), 44.8 m, facies E; RHB'-2B-S2-TL (DGJ), 44.8 m, facies E; RHB'-2A-R (DGJ), 50.5 m, facies F/A; RHB-'-2A-L (DGJ), 50.5 m, facies E/A; RHB'-3A-R (DGJ), 50.5, facies

F/E; RHB'-3A-L (DGJ), 50.5 m, facies E/F; RHB'-3A (DGJ), 50.5 m, facies E/F; RHB'-3A-4I (DGJ), 50.5 m, facies E; RHB'-3B-S1 (DGJ), 54.8 m, facies E/F; RHB'-3B-S2 (DGJ), 54.8 m, facies E/F; RHB'-3Ca (DGJ), 57.0 m, facies F; RHB'-3Cb (DGJ), 57.0 m, facies F; RHB'-3D-LD (R) (DGJ), 60.3 m, facies E/F; RHB'-3D-1B (DGJ), 60.3 m, facies E; RHB'-3D-S2 (DGJ), 60.3 m, facies E/F; RHB'-3D-LD (L) (DGJ), 60.3 m, facies E (with ? stromatoporoid boundstone);RHB'-3D-S1, 60.3 m, facies E; RHB-21 (REJ), 61.0 m, facies E; RHB'-3E-B (DGJ), 62.7 m, facies E; RHB'-3E (DGJ), 62.7 m, facies E;RHB'-3F-SI (DGJ), 65.0 m, facies E; RHB'-3F-S3 (DGJ), 65.0 m, facies E; RHB'-3F-S2 (DGJ), 65.0 m, facies E; RHB'-3F-SI (DGJ), 65.0 m, facies E; RHB-23a (REJ), 74.0 m, facies F; RHB-23b (REJ), 74.0 m, facies E; RHB'-3G (DGJ), 75.8 m, facies F; RHB-24 (REJ), 79.5 m, facies F; RHB'-3H(R) (DGJ), 81.2 m, facies B/F; RHB'-3H-L (DGJ), 81.2 m, facies F; RHB-25 (REJ), 83.3 m, facies F/E; RHB'-3I-T (DGJ), 85.0 m, facies F/E; RHB'-3I-G (DGJ), 85.0 m, facies F.

Additional thin-sections with less certain ($\pm$ 3 m) stratigraphic positions: RHB-2G-BL (DGJ), about 42.0 m, facies E; RHB-2J-S1 (DGJ), about 42.5 m, facies B; RHB-2J-S2 (DGJ), about 42.5 m, facies B; RHB'-2K (DGJ), 42 to 50 m, facies ?B (stromatactis); RHB-4-1 (DGJ), about 44.0 m, facies D; RHB-3 (REJ), 38 to 45 m; facies O (bottom of thin-section), facies - bryozoan boundstone (top of thin-section); RHB'-2I-S2 (DGJ) - polished slab only, 45 to 50 m, facies ?B (stromatactis).

Additional thin-sections from Subsequence 2D, exact stratigraphic positions uncertain: RHB-2E-S2 (DGJ), facies F/B; RHB-2F-R (DGJ), facies E/F; RHB-2Ga (DGJ), facies E/F; RHB-2G-BLa (DGJ), facies E; RHB-2G-BLb (DGJ), facies E; RHB-2G-B1 (DGJ), facies E/F; RHB-3D-b1 (DGJ), facies F; RHB-3D-b2 (DGJ), facies F; RHB-3F (DGJ), facies E; RHB-3J (DGJ), facies B.

Stratigraphic Positions Interpreted from Water-Depth Curves: Deepening Event: $D_5$, 75.8 m.

21.0 112.5 COVERED INTERVAL

2E 42.0 127.2 Fourth-Order Subsequence 2E (Holston Formation, continued). Subsequence 2E is approximately equivalent to the upper part of Ruppel's Unit 5 and the lower part of Unit 6. Sequence 2E is dominated by echinoderm grainstone (facies E) and contains lesser amounts of bryozoan packstone (facies F). The upper surface of Subsequence 2E is indicated by a facies change from echinoderm grainstone into bryozoan packstone in the uppermost few meters of Subsequence 2E. Crystal or vadose silt partial fills cavities within packstones that occur just below the upper surface of Subsequence 2E. Thin-sections: RHB'-4A-S2-BR (DGJ), 113.9 m facies E (thin-section lost); RHB'4A-S2-TR (DGJ), 113.9 m, facies F; RHB'-4A-S1-R (DGJ), 113.9 m, facies E; RHB'-4A-S1-L (DGJ), 113.9 m, facies E; RHB-27 (REJ), 121.0 m, facies E; RHB'-4B-S1 (DGJ), 122.4 m, facies E/F; RHB-28a (REJ), 127.0 m, facies F; RHB-28b (REJ), 127.0 m, facies F.

Additional thin-sections with less certain (generally less than $\pm$ 3 m) stratigraphic positions: RHB-3R-a2 (DGJ), 85 to 113 m, facies E/F; RHB-6-2 (SCR), about 121.5 m, facies E; RHB-6-1 (SCR), about 121.5 m, facies F.

Additional thin-sections from Sequence 2E, exact stratigraphic positions uncertain: RHB'-4A-S2-BL (DGJ), facies F; RHB'-4B-S2-BL (DGJ), facies E.

Stratigraphic Positions Interpreted from Water-Depth Curves: Deepening Events: $D_6$, about 114 m; $D_7$, about 122.5 m.

2F 3.4 130.6 Fourth-Order Subsequence 2F (Holston Formation, continued). Approximately equivalent to the upper part of Ruppel's Unit 6. Subsequence 2F consists largely of echinoderm grainstone. The upper surface of Subsequence 2F is indicated by the occurrence of coated-grains suggesting very shallow water at about 130.3 meters. Crystal or vadose silt partially fills cavities within grainstones at this position just below the upper surface of Subsequence 2F. Thin-sections: RHB-29 (REJ), 129.0 m, facies E; RHB-30, 129.8 m, facies E; RHB'-4D-L (DGJ), 130.3 m, facies F; RHB'-4D-R (DGJ), 130.3 m, facies F; RHB'-4Da (DGJ), 130.3 m, facies F; RHB-4Db (DGJ), 130.3 m, facies F; RHB'-4E-R (DGJ), 131.0 m, facies E; RHB-4E-L (DGJ), 131.0 m, facies E.

| | | | |
|---|---|---|---|
| Approximate 2G | 26.4 | 157 | Fourth-Order Subsequence 2G (Holston Formation, continued). Subsequence 2G is approximately equivalent to Ruppel's Unit 7. Subsequence 2G is dominated by echinoderm grainstone with lesser amounts of packstone. Subsequence 2G is not well exposed. The position of the upper surface of Subsequence 2G is estimated by comparison with the section at Cuba. Thin-sections: RHB-31 (REJ), 142.7 m, facies E; RHB'-5A (DGJ), 144.0 m, facies E/F. |
| Approximate 2H | 26.4 | 183.4 | Fourth-Order Subsequence 2H (Holston Formation, continued). Subsequence 2H is approximately equivalent to the middle to lower part of Ruppel's Unit 8. Subsequence 2H consists mostly of echinoderm grainstones. The upper surface of Subsequence 2H is indicated by a subtle increase in mud content and the occurrence of algal *Girvanella* oncolites and coated-grains at about 183.4 meters, suggesting very shallow-water. However, evidence for profound exposure is lacking. Thin-sections: RHB-32 (REJ), 179.8 m, facies E; RHB'-6A-BR (DGJ), 181.0 m, facies E; RHB'-6A-BL (DGJ), 181.0 m, facies E; RHB'-6A-TR (DGJ), 181.0 m, facies E; RHB'-6A-TL (DGJ), 181.0 m, facies E; RHB-33 (REJ), 181.8 m, facies E; RHB-34 (REJ), 182.8 m, facies E; RHB'-6B-BL (DGJ), 183.4 m, facies E; RHB'-6B-BR (DGJ), 183.4 m, facies E/F; RHB'-6B-T (DGJ), 183.4 m, facies F.<br><br>Stratigraphic Positions Interpreted from Water-Depth Curves: Deepening Event: $D_8$, about 181 m. |
| 2I | N/A | N/A | Fourth-Order Subsequence 2I. Subsequence 2I is not recognized at shelf-edge positions (see Chapter 3). |
| 2J | 10.1 | 193.5 | Fourth-Order Subsequence 2H (Holston Formation, continued). Subsequence 2J is approximately equivalent to the middle to upper part of Ruppel's Unit 8. Subsequence 2H consists mostly of echinoderm grainstones with lesser amounts of packstone. The upper surface of Subsequence 2H is indicated by a subtle increase in mud content and the occurrence of algal *Girvanella* oncolites and coated-grains at about 193.5 meters, suggesting very shallow-water. Evidence for profound exposure is lacking. Thin-sections: RHB'-6Ca (DGJ), 184.0 m, facies E; RHB'-6Cb |

(DGJ), 184.0 m, facies E; RHB'-6D-M (DGJ), 188.0 m, facies E/F; RHB'-6D-R (DGJ), 188.0 m, facies F; RHB'-6D-L (DGJ), 188.0 m, facies E; RHB-35 (REJ), 192.0 m, facies E; RHB'-6E-TR (DGJ), 193.5 m, facies E; RHB'-6E-TL (DGJ), 193.5 m, facies E; RHB'-6E-R (DGJ), 193.5 m, facies E.

2J 5.5 199 Fourth-Order Subsequence 2H (Holston Formation, continued). Subsequence 2J is approximately equivalent to the upper part of Ruppel's Unit 8. It Consists of echinoderm grainstones and packstones. Exposure is inferred from the occurrence of crystal or vadose silt contained within calcite filled cavities developed in packstone at about 198.8 meters. Thin-sections: RHB-36 (REJ), 198.8 m, facies F.

30 240.5 COVERED INTERVAL

3 82.3 281.3 **Third Order Sequence 3.**

3A 61.2 260.2 Fourth-Order Subsequence 3A (Holston Formation, total thickness 220 m). Subsequence 3A is approximately equivalent to the upper part of Ruppel's Unit 8, Unit 9, and the lower part of Unit 10. It consists largely of echinoderm grainstone and bryozoan packstone. The upper surface of Subsequence 3A is recognized by a general facies change from grainstone to packstone (from about 258 to 260.2 m). Shallow-water indicators including superficial ooids, coated-grains and an arthropod-mollusk faunal association occur within the uppermost packstones. Cavities filled with crystal or vadose silt are contained with the mud-rich lithologies that occur immediately below about 260 meters. Thin-sections: RHB'-6F-R (DGJ), 199.6 m, facies F; RHB'-6F-L (DGJ), 199.6 m, facies F; RHB-37 (REJ), 247.2 m, facies E; RHB'-7A-S2 (DGJ), 248.5 m, facies E; RHB'-7A-S1 (DGJ), 248.5 m, facies E; RHB'-7B-B (DGJ), 249.0 m, facies E; RHB'-7B-T (DGJ), 249.0 m, facies E; RHB-39 (REJ), 258.0, facies E/F; RHB'-8A (DGJ), 259.4 m, facies F/E; RHB-40 (REJ), 260.0 m, facies E/F.

Stratigraphic Positions Interpreted from Water-Depth Curves: Deepening Event: $D_9$, 247.2 m.

| | | | |
|---|---|---|---|
| Estimated 3A-4D | >42 | >302 | **Benbolt Formation.** |
| 3B | 12.8 | 273 | Fourth-Order Subsequence 3B (Benbolt Formation). Subsequence 3B is approximately equivalent to the middle part of Ruppel's Unit 10. Subsequence 3B consists largely of echinoderm grainstone at its base and grades upward into packstones and fenestral mudstones. Spar filled vugs and cavities also contain crystal or vadose silt, especially within the mud-rich lithologies from about 271 to 273 meters. Thin-sections: RHB-41 (REJ), 264.0 m, facies E; RHB'-8C-L (DGJ) 265.0 m, facies E; RHB'-8C (DGJ), 265.4 m, facies E; RHB-42 (REJ), 270.0 m, facies F; RHB'-8D-S2-R (DGJ), 271.4 m, facies F/B; RHB'-8D-S1 (DGJ), 271.4 m, facies B; RHB'-8D-S2-L (DGJ), 271.4 m, facies F/B; RHB-43 (REJ), 271.5 m, facies F; RHB-8E-R (DGJ), 272.8 m, facies F/E; RHB'-8E (DGJ), 272.8 m, facies B.<br><br>Additional thin-sections from Subsequence 3B, exact stratigraphic positions uncertain: RHB'-8B (DGJ), facies F; RHB'-8D-S2-L (DGJ), facies ?F. |
| 3C | 5 | 278 | Fourth-Order Subsequence 3C (Benbolt Formation, continued). Subsequence 3C is approximately equivalent to the upper part of Ruppel's Unit 10. Subsequence 3C consists mostly of wackestone/mudstone (facies L). Stromatactis occurs within mud-rich lithologies just below the inferred upper surface of Subsequence 3C. The mudstones immediately below the inferred upper surface of Subsequence 3C have fenestral fabrics. Stromatactis, spar filled vugs, and cavities filled with crystal or vadose silt occur within these mudstones. This stromatactis is interpreted as shallow water in origin (e.g., Roberson and Foreman, 1989). Thin-sections: RHB'-8E-SL1 (DGJ), 277.4 m, facies L (fenestral); RHB'-8E-SL2 (DGJ), 277.4 m, facies L (fenestral)/B; RHB'-8F-S1 (DGJ), 277.4 m, facies B; RHB'-8F-S2 (DGJ), 277.4 m, facies L (fenestral)/B; RHB-10 (SCR), 278.0, facies ?B (stromatactis). |
| 3D | 3.3 | 281.3 | Fourth-Order Subsequence 3D (Benbolt Formation, continued). Subsequence 3D is approximately equivalent to the uppermost part of Ruppel's Unit 10. Subsequence 3D consists largely of |

packstone with lesser amounts of echinoderm grainstone. Fenestral fabrics and cavities filled with crystal or vadose silt occur within mud-rich lithologies immediately below the inferred upper surface of Subsequence 3D. Thin-sections: RHB-45 (REJ), 279 m, facies F; RHB-1--1 (SCR), 280.0 m, facies L (fenestral); RHB'-8G-TR (DGJ), 280.9 m, facies F/E; RHB'-8G-BR (DGJ), 280.9 m, facies F; RHB'-8G (DGJ), 280.9 m, facies E/F; RHB'-8G-BL(DGJ), 280.9 m, facies F.

| | | | |
|---|---|---|---|
| 4 | >9.7 | >291 | **Third-Order Sequence 4.** |
| Approximate 4A | 9.7 | 291 | Fourth-Order Subsequence 4A (Benbolt Formation, continued). Subsequence 4A is approximately equivalent to the lower part of Ruppel's Unit 11. It consists largely of bryozoan packstone and echinoderm grainstone. The upper part of Subsequence 4A is covered or poorly exposed. Thin-sections: RHB'-8H (DGJ), 281.4 m, facies L (stromatactis); RHB'-8H-W2-S2 (DGJ), 281.4 m, facies L (stromatactis); RHB'-8K-1 (DGJ), 284.1 m, facies E; RHB'-8K-R (DGJ), 284.1 m, facies E; RHB-47 (REJ), 283.0 m, facies E; RHB-11 (SCR), 284.0 m, facies F.<br><br>Additional thin-section from Subsequence 4A, exact stratigraphic positions uncertain: RHB'-8H-W2-R (DGJ), facies L (stromatactis). |
| Estimated 4B | 2 | 293 | Fourth-Order Subsequence 4B (Benbolt Formation, continued). Subsequence 4B is approximately equivalent to the lower to the middle part of Ruppel's Unit 11. Thin-sections: None. |
| Estimated 4C | 9 | 302 | Fourth-Order Subsequence 4C (Benbolt Formation, continued). Subsequence 4C is approximately equivalent to the upper part of Ruppel's Unit 11. Thin-sections: None. |
| Estimated 4D-4E | 39 | 341 | Fourth-Order Subsequence 4D (Benbolt Formation, total thickness greater than 61.5 m, but less than 84.5 m; Wardell Formation). Subsequence 4D is probably equivalent to Ruppel's Unit 12 and the overlying 15 meter thick covered interval. Thin-section: RHB'-8H-WL-S1 (DGJ), 317.4 m, facies ?L (stromatactis). |

15.5 341.2 COVERED INTERVAL

Estimated
4E 72.2 397.2 Fourth-Order Subsequence 4E (Wardell Formation, continued). Subsequence 4E is probably equivalent to Ruppel's Unit 13. Thin-sections: RHB-31-1 (SCR), 380.0 m, facies F; RHB-13-2 (SCR), 390.0 m, facies F.

5 >26 >423 **Third-Order Sequence 5 (? Bowen Formation, total thickness probably less than about 10 m).**

26.0 423.2 **Witten Formation.** The Witten corresponds to Unit 14 of Ruppel (1978). Thin-sections: RHB-14-1 (SCR), 410.0 m, facies F; RHB-14-2 (SCR), 420.0 m, thin-section lost.

**Moccasin Formation.**

## Cuba Section (CU)

The Cuba section is exposed in a field north of the Gill's Baptist Church on U.S. 11W at Cuba, Hawkins County, Tennessee (lat 36°22'53'' to 36°23'25'' N and 83°07'30'' to 83°07'59''W). The Cuba section occupies the SE1/4, SE1/4, SE1/4 of the Lee Valley 7.5' topographic quadrangle. About 239 meters of Chickamauga Group strata are exposed from the Knox/Chickamauga contact to the base of the Moccasin Formation. According to Ruppel (1979), this section has been shortened due to thrusting. However, most of this shortening appears to have occurred relatively high in the section (above the Holston Formation). Only the lower approximately 50 meters are considered here, even though the section thickness of this section is 167.3 meters. The lower 50 meters of the Cuba section appears to be structurally competent.

The conodont biostratigraphy of this section has been studied by Carnes (1975) and the lithostratigraphy by Ruppel (1979). All the samples (50 X 75 mm, thin-sections) reported here are those collected and prepared by Steve Ruppel. Stratigraphic sequence boundaries and facies interpreted as part of this work are indicated below; the reader is referred to Ruppel (1979) for detailed description of this section. Sample numbers (thin-sections) are Ruppel's original numbers. These are given with measured thickness from the base of the section along with the facies interpretation (made by Steinhauff).

**KNOX GROUP**

Unconformity

| Sequence/ Cycle(s) | | | **CHICKAMAUGA GROUP** |
|---|---|---|---|
| 2nd Ord. | Seq. Thk (m) | Cumul. Thk (m) | |
| O-S | >239 | >239 | **Tippecanoe Sequence (Sloss, 1963).** Other Synonyms: Ordovician-Silurian (O-S) Second Order Cycle or Supercycle (Vail, et al., 1977), and Paleozoic Sequence II, Middle Ordovician to Lower Devonian, Walker (1985) and Byerly et al. (1986). |

| 3rd & 4th Ord. | Seq. Thk (m) | Cumul. Thk (m) | |
|---|---|---|---|
| 1 | 20.2 | 20.2 | **Third-Order Sequence 1 (Five Oaks and Lenoir formations). Corresponds to Units 1, 2 and the lower part of Unit 3 of Ruppel (1978).** |
| 1A | N/A | N/A | Fourth-Order Subsequence 1A. Subsequence 1A is not recognized at shelf-edge positions (see Chapter 3). |
| 1B | 16.0 | 16.0 | Fourth-Order Subsequence 1B (Five Oaks Formation, total thickness 16.0 m): Subsequence 1B corresponds to Units 1 and 2 of Ruppel (1979). The Five Oaks Formation consists largely of fenestral wackestone/mudstone (facies L), and bioclastic wackestone/packstone with peloidal grainstone. The upper surface of Subsequence 1B is recognized by a relatively sharp upper contact with the overlying peloidal grainstone. Thin-sections: CU-1, 0.5 m, facies P (fibrous calcite within dolomitic fabric); CU-2, 5.0 m, facies L (fenestral and laminated)/I; CU'3, 16.0 m, facies E/F. |
| 1C | 4.2 | 20.2 | Fourth-Order Subsequence 1C (Lenoir Formation, total thickness, 4.2 m). Subsequence 1C corresponds to the lower part of Ruppel's Unit 3. Subsequence 1C consists of echinoderm grainstone (facies E) grading upwards into bryozoan packstone (facies F). Oncolites (up to 1 cm across) occur in the upper part of this sequence. The upper surface of Subsequence 1C is recognized as a gradational contact with the overlying peloidal grainstone of Subsequence 2A. Thin-section: CU'-3S-2, 19.0 m, facies F.<br><br>Stratigraphic Positions Interpreted from Water-Depth Curves: Deepening Event: $D_1$, about 19.5 m. |
| Approximate 2 | >140 | >160 | **Third-Order Sequence 2 (Holston Formation).** Sequence 2 corresponds to Units 4 through about Units 8 or 9 of Ruppel (1978). |

| | | | |
|---|---|---|---|
| Approximate 2A | 13.8 | 34 | Fourth-Order Subsequence 2A (Holston Formation). Subsequence 2A is approximately equivalent to Unit 4 and the he lowest part of part of Ruppel's Unit 5. Subsequence 2A<br><br>consists of peloidal grainstone (facies I) grading upwards into echinoderm grainstone (facies E). The upper surface of Subsequence 2A is inferred to occur at about 34 meters above the Knox where echinoderm grainstone grades vertically and laterally into bryozoan packstone. This surface is interpreted as a poorly developed drowning unconformity or an interval of slow deposition. Thin-sections: CU-4-1, 20.7 m, facies I/J; CU-4-3, 26.2 m, facies E; CU-5-1, 31.5 m, facies E.<br><br>Stratigraphic Positions Interpreted from Water-Depth Curves: Deepening Events: $D_2$, about 30 m. |
| 2B | N/A | N/A | Fourth-Order Subsequence 2B. Subsequence 2B is not recognized at shelf-edge positions. However, a drowning unconformity, separating Subsequence 2A from overlying Subsequence 2C, is inferred to occur at about 27.2 meters above the Knox. This unconformity is interpreted as the condensed Subsequence 2B at the shelf-edge. |
| Approximate 2C | 21 | 55 | Fourth-Order Subsequence 2C (Holston Formation, continued). Subsequence 2C is approximately equivalent to the upper part of Ruppel's Unit 4, all of Unit 5, and the lower part of Unit 6. Subsequence 2C consists almost exclusively of bryozoan packstone (facie F). Deepening events $D_3$ and $D_4$ are inferred to occur along the gradational contact between Ruppel's Units 4 and 5. This contact is recognized by a change in bed thickness, from relative thick beds occurring in Unit 4 to relatively thinner beds in overlying Unit 5. Thin-sections: CU-5-2, 42.0 m, facies F; CU-6A, 52.0 m, facies F; CU-7-1, facies F/C.<br><br>Stratigraphic Positions Interpreted from Water-Depth Curves: Deepening Events: $D_3$ and $D_4$ (superimposed), about 44 m. |
| Approximate 2D | 30 | 85 | Fourth-Order Subsequence 2D (Holston Formation, continued). Subsequence 2D is approximately equivalent to the uppermost part of Ruppel's Units 6 and 7. Subsequence 2D consists of a |

complex mixture of packstones and grainstones. Thin-sections: None.

Stratigraphic Positions Interpreted from Water-Depth Curves: Deepening Event: $D_5$, probably occurs at the facies change from underlying echinoderm grainstone into overlying bryozoan packstone at about 75 m; however, water-depth curves were not constructed for this part of the section.

| | | | |
|---|---|---|---|
| Approximate 2E | 36.5 | 121.5 | Fourth-Order Subsequence 2E (Holston Formation, continued). Subsequence 2E is approximately equivalent to Ruppel's units 7, 8, and 9. Subsequence 2E consists mostly on echinoderm grainstone (facies E) with encrusting bryozoans. Thin-sections: None. |

Stratigraphic Positions Interpreted from Water-Depth Curves: Deepening Event: $D_6$, no data.

| | | |
|---|---|---|
| 12.6 | 120.1 | COVERED INTERVAL |

| | | | |
|---|---|---|---|
| Approximate 2F | 6.5 | 128.0 | Fourth-Order Subsequence 2F (Holston Formation, continued. Subsequence 2F is approximately equivalent to the lower part of Ruppel's Unit 10. Subsequence 2F consists mostly of bioclastic (bryozoan) wackestone/packstone (facies B). Ruppel (1978) interpreted these mud-rich lithologies ar "reef core." The upper surface of Subsequence 2F is inferred to occur along the relatively sharp upper contact with Subsequence 2G. Thin-sections: None. |
| Approximate 2G | >32 | >160 | Fourth-Order Subsequence 2G (Holston Formation, continued). Subsequence 2G is approximately equivalent to Ruppel's Units 11 and 12. Subsequence 2G consists mostly of bioclastic (bryozoan) wackestone/packstone (facies B). Thin-sections: None. |

| | | |
|---|---|---|
| 19.8 | 167.3 | COVERED INTERVAL |

# APPENDIX B

## PETROGRAPHIC CONSTITUENT ANALYSES

## EXPLANATION

Appendix B compares point-count data with facies interpretations presented in ternary diagrams of figures 2.8 and 2.9 of Chapter 2, and figures 3.5 and 3.6 of chapter 3. Petrographic constituent analyses were preformed by Ruppel (1979), Breland (1980), and Jernigan (1987) using 50 X 75 mm thin-sections. The details of petrographic constituent analysis conducted by each author differ slightly with respect to constituents recognized. The tables in this appendix account for these minor differences. Furthermore, the tables are presented in the same format. Thus, it is possible to compare the results of each authors work. Facies interpretation was made by Steinhauff.

Thin-sections counted by Ruppel (1979) and Breland (1980) are based on 200 points counted per thin-section. Jernigan (1987) counted 800 points per thin-section using a "cement priority" point counting technique (see figure 2.8 of chapter 2; see also Steinhauff et al., 1989). Shaded rows indicate rejected analyses. Some of the analyses made by Breland (1980), based on thin-sections from the Knoxville area, may not reflect depositional environments represented in the study area. These analyses were rejected (i.e., those from the Tumbez, Chapman Ridge, Ottosee, and Witten formations). Other analyses were rejected if the thin-section was lost or if the total volume percent was greater than 105% or less than 95%.

Key to Abbreviations

| | |
|---|---|
| Sample Number: | |
| CS | Cedar Springs section |
| DG | Dry Gap section |
| GA | Graveston section |
| HC | Halls Crossroads section |
| HR | Harbison section |
| IS | Idol Mine section |
| PVC | Poor Valley Creek section |
| RHB | Red House Branch Section |
| Strat. Position | Stratigraphic position in meters above the Knox unconformity |
| Fm | Formation (recognized in this report) |
| Ch. Ridge | Chapman Ridge Formation |
| Linc. | Lincolnshire Formation |
| Dom. Facies | Dominant facies (see Appendix A) |
| Sub. Facies | Subordinate facies (see Appendix A) |
| Mic | Micrite |
| Spar | Sparry calcite (undifferentiated) |

Key to Abbreviations (continued)

| | |
|---|---|
| Intra | Intraclasts |
| Pel | Peloids |
| Oo | Ooids |
| Brach | Brachiopods |
| Gast | Gastropods |
| Ostra | Ostracodes |
| Tri | Trilobites |
| Ech | Echinoderms |
| Bry | Bryozoans |
| Alg | Algae |
| On | Oncoids |
| Sp | Sponge debris |
| Other Foss. | Other fossils |
| Dolo | Dolomite (undifferentiated) |
| Qtz | Quartz (detrital and authigenic) |
| Other | Other constituents (e.g., stylocmulate, opaque mineral, etc.) |
| T | Trace constituent |

| Comparative Point-Count Data In Volume Percent From The Knoxville Area, After Breland (1980) | | | | | | | | | | | | | | | | | | | | | | | |
|---|---|---|---|---|---|---|---|---|---|---|---|---|---|---|---|---|---|---|---|---|---|---|---|
| Sample Number | Strat. Position | Fm. | Dom. Facies | Sub. Facies | Mic | Spar | Intra | Pel | Oo | Brach | Gast | Ostra | Tri | Moll | Ech | Bry | Alg | On | Sp | Other Foss | Dolo | Qtz | Oth |
| DG1A | 0 | Five Oaks | 19f | | 5.0 | 5.5 | 5.5 | 62.5 | 0.0 | 0.5 | 0.0 | 7.0 | 0.0 | 1.0 | 0.0 | 1.0 | 0.0 | 0.0 | 0.0 | 0.0 | 0.0 | 12.0 | 0.0 |
| DG3A | 158 | Rockdell | 12p | | 46.0 | 0.5 | 0.0 | 0.0 | 0.0 | 1.5 | T | 1.5 | T | 2.0 | 13.0 | 22.5 | 0.0 | 0.0 | 0.0 | 0.0 | 2.0 | 0.5 | 10.5 |
| DG4A | 165 | Rockdell | 12g | | 10.0 | 27.5 | 0.0 | 0.0 | 2.5 | 0.0 | 0.0 | 0.5 | T | 0.0 | 54.0 | 3.5 | 0.0 | 0.0 | 0.0 | 0.0 | 0.5 | 0.5 | 1.0 |
| DG5B | 187 | Rockdell | 9 | | 49.0 | 8.0 | 0.0 | 0.0 | 0.0 | 0.0 | T | 8.0 | 1.5 | 3.0 | 7.5 | 2.0 | 0.5 | 0.0 | 9.0 | 0.0 | 1.5 | 0.0 | 10.0 |
| DG6A | 209 | Rockdell | 17 | | 32.0 | 22.5 | 0.0 | 7.5 | 0.0 | 0.5 | T | 8.5 | 2.5 | 0.5 | 10.0 | 4.0 | 6.0 | P | 0.0 | 0.0 | 1.5 | 0.0 | 4.5 |
| DG6C | 215.5 | Rockdell | 12g | | 7.5 | 39.5 | 0.0 | 1.0 | 0.0 | 1.5 | 2.5 | 13.0 | 2.5 | 1.5 | 26.0 | 4.0 | T | 0.0 | 0.0 | 0.0 | 1.0 | 0.0 | 0.0 |
| DG7B | 232.5 | Rockdell | 11 | | 14.5 | 36.0 | 0.0 | 3.0 | 0.0 | T | T | 3.0 | 2.0 | 2.5 | 24.5 | 12.5 | 0.0 | 0.0 | 0.5 | 0.0 | 0.5 | 0.0 | 1.0 |
| DG7D | 240 | Rockdell | 12g | | 1.0 | 31.0 | 0.0 | 0.0 | 0.0 | 0.0 | 0.0 | 0.5 | 2.5 | 0.0 | 36.5 | 28.5 | 0.0 | 0.0 | 0.0 | 0.0 | 0.0 | 0.0 | 0.0 |
| DG8C | 255 | Rockdell | 12g | | 1.5 | 24.5 | 0.0 | 0.0 | 0.0 | 0.0 | T | 0.5 | 1.5 | 0.0 | 44.0 | 28.0 | 0.0 | 0.0 | 0.0 | 0.0 | 0.0 | 0.0 | 0.0 |
| DG9A | 263 | Rockdell | 14 | 9 | 24.5 | 10.5 | 0.0 | 4.0 | 0.0 | 0.0 | 0.5 | 3.5 | 1.5 | 1.5 | 30.0 | 13.5 | 2.0 | 0.0 | 0.0 | 0.0 | 4.5 | 0.0 | 4.0 |
| DG9C | 269 | Rockdell | 19f | | 79.5 | 4.0 | 0.0 | 8.5 | 0.0 | 0.0 | 0.0 | 1.5 | 1.0 | 0.5 | T | 5.0 | 0.0 | 0.0 | T | 0.0 | 0.0 | 0.0 | 0.0 |
| DG9G | 278 | Rockdell | 12p | | 25.5 | 14.0 | 0.0 | 8.5 | 0.0 | T | 5.5 | 1.5 | 0.5 | 1.0 | 24.5 | 10.5 | 2.5 | P | 0.0 | 0.0 | 0.0 | 0.0 | 5.0 |
| DG10C | 286 | Rockdell | 22 | 14 | 38.5 | 8.0 | 0.0 | 4.5 | 0.0 | 0.5 | 0.0 | 2.0 | 1.0 | 1.5 | 21.5 | 17.0 | 0.5 | P | T | 0.0 | 0.0 | 0.0 | 5.0 |
| DG10E | 292 | Rockdell | 9 | 12g | 54.0 | 8.0 | 0.0 | 1.5 | 0.0 | 0.5 | T | 1.0 | 2.0 | 2.5 | 14.0 | 16.5 | 0.0 | 0.0 | T | 0.0 | 0.0 | 0.0 | 0.0 |
| DG11A | 304 | Benbolt | 12g | | 4.5 | 22.0 | 0.0 | 0.0 | 0.0 | 0.5 | 0.0 | 4.5 | 1.0 | 0.0 | 47.0 | 19.5 | 0.0 | 0.0 | 0.0 | 0.0 | 0.0 | 0.0 | 1.0 |
| DG12C | 313 | Wardell | 19 | 9 | 79.0 | 0.0 | 0.0 | 0.0 | 0.0 | 0.0 | 0.0 | 1.0 | 1.0 | 0.5 | 5.5 | 8.5 | 0.0 | 0.0 | 3.0 | 0.0 | 0.5 | 0.0 | 1.0 |
| DG13C | 319 | Wardell | 19 | 9 | 88.0 | 0.0 | 0.0 | 0.0 | 0.0 | T | 0.5 | 1.5 | 1.0 | 1.0 | 3.5 | 0.5 | 0.5 | P | 0.0 | 0.0 | 0.0 | 0.0 | 3.5 |
| DG13F | 333 | Wardell | 9 | | 67.5 | 1.5 | 0.0 | 1.0 | 0.0 | T | 1.5 | 1.5 | 0.5 | 1.5 | 14.0 | 5.0 | 4.5 | P | 0.5 | 0.0 | 1.0 | 0.0 | 0.0 |
| DG14A | 350 | Witten | 9 | 17 | 47.0 | 4.5 | 0.0 | 0.0 | 0.0 | 1.5 | T | 1.0 | 2.5 | 0.5 | 6.0 | 11.5 | 14.0 | 0.0 | 0.0 | 0.0 | 3.5 | 0.0 | 8.0 |
| DG14C | 355 | Witten | ?19 | | 79.5 | 2.0 | 0.0 | T | 0.0 | T | 2.0 | 1.5 | 3.0 | 0.0 | 2.5 | 6.0 | T | 0.0 | 0.5 | 0.0 | 2.0 | 0.0 | 1.0 |

| Sample Number | Strat. Position | Fm. | Dom. Facies | Sub. Facies | Mic | Spar | Intra | Pel | Oo | Brach | Gast | Ostra | Tri | Moll | Ech | Bry | Alg | On | Sp | Other Foss | Dolo | Qtz | Oth |
|---|---|---|---|---|---|---|---|---|---|---|---|---|---|---|---|---|---|---|---|---|---|---|---|
| DG15A | 358 | Witten | 9 | | 70.0 | 4.0 | 0.0 | 2.0 | 0.0 | 0.5 | 0.5 | 0.0 | 1.0 | 1.5 | 9.0 | 2.5 | T | 0.0 | 0.5 | 0.0 | 2.0 | 0.0 | 6.5 |
| DG15C | 362 | Witten | 9 | | 51.0 | 6.5 | 0.0 | 4.0 | 0.0 | 3.5 | 1.0 | 1.0 | 0.5 | 3.0 | 18.5 | 2.5 | 2.0 | 0.0 | T | 0.0 | 4.0 | 0.0 | 2.5 |
| DG15F | 371 | Witten | 16 | | 13.5 | 12.0 | 0.0 | 53.0 | 0.0 | 2.0 | 0.0 | 0.5 | 2.5 | T | 4.0 | 5.0 | 4.0 | 0.0 | 0.0 | 0.0 | 2.5 | 0.5 | 0.5 |
| DG15G | 372 | Witten | 19l | | 44.5 | 2.0 | 0.0 | 39.0 | 0.0 | 0.0 | T | 0.5 | T | 0.0 | 1.5 | 0.0 | 0.0 | 0.0 | 0.0 | 0.0 | 5.0 | 0.5 | 7.0 |
| DG16A | 372.5 | Witten | 9 | | 54.5 | 11.5 | 1.0 | 6.5 | 0.0 | 1.0 | 1.5 | 2.0 | 1.0 | 0.5 | 13.5 | 5.0 | 0.5 | 0.0 | 0.5 | 0.0 | 1.0 | 0.0 | 0.0 |
| DG17B | 381 | Witten | 16 | | 0.0 | 29.5 | 0.0 | 23.0 | 4.5 | 1.5 | 0.0 | 3.0 | 2.5 | 1.0 | 29.5 | 4.0 | 0.5 | 0.0 | 0.0 | 0.0 | 1.0 | 0.0 | 0.0 |
| DG17C | 383 | Witten | 12p | 17 | 20.5 | 18.0 | 0.5 | 6.0 | 0.0 | 1.0 | T | 1.0 | 2.0 | 0.5 | 36.5 | 9.5 | 2.5 | 0.0 | 0.0 | 0.0 | 0.0 | 0.0 | 2.0 |
| HC1A | 3 | Tumbez | 12g | | 17.0 | 20.0 | 0.0 | 0.0 | 0.0 | T | 0.0 | 0.5 | 0.5 | 0.0 | 55.0 | 5.0 | 0.0 | 0.0 | 0.0 | 0.0 | 0.0 | 0.0 | 0.0 |
| HC1B | 10.5 | Tumbez | 12g | 17 | 15.0 | 6.5 | 0.0 | 15.0 | 0.0 | 1.5 | T | T | 0.0 | 1.5 | 27.5 | 21.0 | 11.5 | 0.0 | 0.0 | 0.0 | 0.0 | 0.0 | 0.5 |
| HC1D | 20 | Tumbez | lost | | 14.5 | 6.0 | 0.0 | 0.0 | 0.0 | T | 0.0 | T | 1.0 | 0.0 | 18.0 | 41.5 | 15.5 | 0.0 | 0.0 | 0.0 | 1.0 | 0.0 | 2.5 |
| HC1E | 27 | Tumbez | 8 | | 57.5 | 3.0 | 0.0 | 0.0 | 0.0 | 0.5 | T | 1.5 | T | 0.5 | 2.0 | 32.0 | 0.0 | 0.0 | 2.0 | 0.0 | 0.0 | T | 0.0 |
| HC2A | 129 | Rockdell | 8 | | 60.5 | 3.0 | 0.0 | 0.0 | 0.0 | T | 0.0 | T | 1.5 | 1.5 | 18.5 | 15.0 | T | 0.0 | T | 0.0 | 0.0 | 0.0 | 0.0 |
| HC2B | 131 | Rockdell | 8 | 9 | 49.0 | 1.5 | 0.0 | 0.0 | 0.0 | T | 0.0 | 1.0 | T | 0.0 | 1.5 | 47.0 | 0.0 | 0.0 | T | 0.0 | T | T | 0.0 |
| HC3A | 133 | Rockdell | 12p | | 27.0 | 14.5 | 0.0 | 0.0 | 0.0 | 0.0 | T | 0.0 | 0.0 | 0.0 | 14.5 | 39.5 | 4.0 | 0.0 | 0.0 | 0.0 | 0.0 | 0.0 | 0.5 |
| HC3C | 136 | Rockdell | 9 | | 35.5 | 2.0 | 0.0 | 0.0 | 0.0 | 0.0 | 0.0 | T | T | T | 1.5 | 53.0 | 6.5 | 0.0 | 1.5 | 0.0 | 0.0 | 0.0 | 0.0 |
| HC3D | 140.5 | Rockdell | 12g | | 3.0 | 25.5 | 1.0 | 0.0 | 0.0 | 1.5 | 0.5 | 0.5 | 1.0 | 0.0 | 47.0 | 8.0 | 12.0 | 0.0 | 0.0 | 0.0 | 0.0 | 0.0 | 0.0 |
| HC3E | 141 | Rockdell | 12p | 14 | 34.0 | 0.5 | 0.0 | 0.0 | 0.0 | 1.5 | 0.0 | T | 1.0 | 0.0 | 22.5 | 35.5 | 1.0 | 0.0 | 2.5 | 0.0 | 0.0 | 0.0 | 2.0 |
| HC4B | 147 | Rockdell | 9 | 19 | 82.5 | 0.0 | 0.0 | 0.0 | 0.0 | 0.0 | 0.0 | T | T | 0.5 | 6.5 | 10.0 | 0.0 | 0.0 | 0.5 | 0.0 | 0.0 | T | 0.0 |
| HC4C | 158 | Rockdell | 12g | | 24.0 | 19.0 | 2.5 | 0.0 | 0.0 | 0.0 | 0.5 | 0.0 | T | 0.0 | 34.5 | 15.0 | 3.5 | 0.0 | 0.0 | 0.0 | 0.0 | 0.0 | 0.0 |
| HC4E | 169 | Rockdell | 9 | | 67.5 | 2.5 | 0.0 | 6.0 | 0.0 | T | T | T | 1.0 | 1.5 | 5.0 | 10.5 | T | 0.0 | 6.0 | 0.0 | 0.0 | 0.0 | 0.0 |
| HC5B | 174 | Rockdell | 8 | 9 | 75.0 | 2.5 | 0.0 | 1.5 | 0.0 | 0.5 | 0.0 | T | T | 1.5 | 1.5 | 14.5 | 0.0 | 0.0 | 0.5 | 0.0 | 0.5 | 0.5 | 1.5 |

| Sample Number | Strat. Position | Fm. | Dom. Facies | Sub. Facies | Mic | Spar | Intra | Pel | Oo | Brach | Gast | Ostra | Tri | Moll | Ech | Bry | Alg | On | Sp | Other Foss | Dolo | Qtz | Oth |
|---|---|---|---|---|---|---|---|---|---|---|---|---|---|---|---|---|---|---|---|---|---|---|---|
| HC5C | 184 | Rockdell | 10 | | 35.5 | 16.5 | 1.0 | 0.0 | 0.0 | 0.5 | 0.5 | 0.5 | 0.0 | 1.0 | 31.5 | 6.5 | 1.0 | P | 0.0 | 0.0 | 2.0 | 0.0 | 4.5 |
| HC5E | 193 | Rockdell | 9 | | 73.5 | 1.0 | 0.0 | 0.0 | 0.0 | 0.0 | 0.0 | T | T | T | 2.0 | 15.0 | 0.5 | 0.0 | 7.0 | 0.0 | T | 0.0 | 1.0 |
| HC6A | 195 | Rockdell | 9 | 8 | 35.5 | 4.0 | 0.0 | 17.5 | 0.0 | 0.0 | 0.0 | T | T | 3.5 | 12.5 | 13.5 | 3.0 | 0.0 | T | 0.0 | 5.0 | T | 5.5 |
| HC6C | 205 | Rockdell | 9 | | 59.5 | 2.5 | 0.0 | 0.0 | 7.5 | 0.5 | 0.5 | T | 1.5 | 1.0 | 13.5 | 10.5 | 0.0 | 0.0 | 0.5 | 0.0 | 0.0 | 0.0 | 2.5 |
| HC7A | 216 | Rockdell | 9 | | 68.0 | 4.5 | 0.0 | 0.0 | 0.0 | 0.0 | 0.0 | T | T | 0.5 | 14.0 | 5.0 | 0.0 | 0.0 | 3.0 | 0.0 | 0.0 | 0.0 | 5.0 |
| HC8A | 224 | Rockdell | 8 | 19 | 55.0 | 3.0 | 0.0 | 0.0 | 0.0 | 0.0 | 0.0 | 0.5 | 0.5 | 0.5 | 0.5 | 10.5 | T | 0.0 | T | 26.5 | 0.0 | 0.0 | 1.5 |
| HC8C | 234 | Rockdell | 12g | | 13.5 | 25.0 | 1.5 | 8.0 | 0.0 | 4.0 | 0.5 | 1.0 | T | 0.5 | 28.0 | 13.0 | T | 0.0 | 0.0 | 0.0 | 5.0 | 0.0 | 0.0 |
| HC9A | 276 | Rockdell | 9 | 12p | 58.5 | 3.5 | 0.0 | 0.0 | 0.0 | 0.5 | T | T | 0.5 | 1.0 | 14.0 | 21.0 | 1.0 | 0.0 | 0.0 | 0.0 | 0.0 | 0.0 | 0.0 |
| HC9C | 288 | Rockdell | 9 | | 64.5 | 2.5 | 3.0 | 0.0 | 0.0 | 0.0 | T | T | T | 3.0 | 17.5 | 10.5 | 0.5 | 0.0 | 1.5 | 0.0 | 0.0 | 0.0 | 0.0 |
| HC10A | 311 | Ch. Ridge | 12p | 9 | 41.0 | 4.5 | 0.0 | 0.0 | 0.0 | 0.0 | 0.0 | T | T | 0.0 | 17.5 | 37.0 | 0.0 | 0.0 | 0.0 | 0.0 | 0.0 | 0.0 | 0.0 |
| HC11A | 327 | Ch. Ridge | 9 | | 67.5 | 2.0 | 0.0 | 10.0 | 0.0 | 0.0 | 0.0 | T | T | T | 3.0 | 10.0 | 4.5 | 0.0 | 3.0 | 0.0 | 0.0 | 0.0 | 0.0 |
| HC11B | 335 | Ch. Ridge | 9 | 8 | 57.5 | 8.5 | 0.0 | 0.0 | 0.0 | 0.0 | T | T | 1.0 | 1.0 | 7.0 | 22.0 | 1.5 | 0.0 | 1.5 | 0.0 | 0.0 | 0.0 | 0.0 |
| HC11D | 356 | Ch. Ridge | 12p | | 63.0 | 1.5 | 0.0 | 0.0 | 0.0 | 0.0 | 0.0 | 0.5 | 1.0 | 0.0 | 19.0 | 10.5 | T | 0.0 | T | 0.0 | 0.0 | 0.0 | 4.5 |
| HC12A | 359 | Ch. Ridge | 9 | | 68.5 | 0.0 | 0.0 | 6.5 | 0.0 | 0.0 | 3.0 | 1.5 | T | 1.5 | 4.5 | 10.5 | 0.5 | 0.0 | 3.5 | 0.0 | 0.0 | 0.0 | 0.0 |
| HC12D | 368 | Ch. Ridge | 22 | | 37.0 | 6.5 | 0.0 | 0.0 | 0.0 | 0.5 | 1.0 | 0.5 | T | 5.0 | 10.0 | 31.0 | 8.0 | 0.0 | 0.5 | 0.0 | 0.0 | 0.0 | 0.0 |
| HC13A | 371 | Ch. Ridge | 12p | | 42.0 | 9.5 | 0.0 | 0.0 | 0.0 | 0.0 | 0.5 | 0.0 | 0.0 | T | 32.0 | 7.5 | 7.5 | 0.0 | T | 0.0 | 0.0 | 0.0 | 1.0 |
| HC13C | 377 | Ch. Ridge | 19 | | 77.5 | 0.5 | 0.0 | 5.0 | 0.0 | 0.0 | T | T | T | 1.5 | 7.0 | 3.5 | 0.0 | 0.0 | 5.0 | 0.0 | 0.0 | 0.0 | 0.0 |
| HC13D | 381 | Ch. Ridge | 12p | | 24.0 | 34.5 | 0.0 | 0.0 | 0.0 | T | T | 0.5 | 0.5 | 1.0 | 22.5 | 15.5 | 1.5 | 0.0 | 0.0 | 0.0 | 0.0 | 0.0 | 0.0 |
| HC13F | 388 | Ch. Ridge | 9 | | 64.0 | 5.0 | 0.0 | 6.5 | 0.0 | T | T | T | T | 2.5 | 9.0 | 5.5 | 0.0 | 0.0 | 7.5 | 0.0 | 0.0 | 0.0 | 0.0 |
| HC13H | 399 | Ch. Ridge | 9 | | 67.5 | 0.5 | 0.0 | 1.0 | 0.0 | 1.0 | T | 0.5 | 2.0 | 3.0 | 8.0 | 11.0 | 5.0 | 0.0 | 0.5 | 0.0 | 0.0 | 0.0 | 0.0 |
| HC14B | 438 | Ottosee | 9 | 8 | 67.5 | 2.5 | 0.0 | 2.5 | 0.0 | 0.0 | 0.0 | 0.5 | 0.0 | 0.0 | 3.5 | 19.0 | 0.0 | 0.0 | 2.5 | 0.0 | 0.0 | 0.0 | 0.0 |

| Sample Number | Strat. Position | Fm. | Dom. Facies | Sub. Facies | Mic | Spar | Intra | Pel | Oo | Brach | Gast | Ostra | Tri | Moll | Ech | Bry | Alg | On | Sp | Other Foss | Dolo | Qtz | Oth |
|---|---|---|---|---|---|---|---|---|---|---|---|---|---|---|---|---|---|---|---|---|---|---|---|
| HC14C | 440 | Ottosee | 12p | | 32.5 | 11.5 | 2.0 | 0.0 | 0.0 | 0.0 | T | T | 0.0 | 0.0 | 30.0 | 24.0 | 0.0 | 0.0 | 0.0 | 0.0 | 0.0 | 0.0 | 0.0 |
| HC14E | 444 | Ottosee | 9 | 12p | 73.0 | 2.0 | 0.0 | 2.0 | 0.0 | 0.0 | T | 0.5 | 0.5 | 1.5 | 9.0 | 9.5 | T | 0.0 | 2.0 | 0.0 | 0.0 | 0.0 | 0.0 |
| HC14F | 446 | Ottosee | 12g | 17 | 16.5 | 32.5 | 13.5 | 0.0 | 0.0 | 0.0 | 0.0 | T | T | 0.0 | 33.0 | 4.5 | 0.0 | 0.0 | 0.0 | 0.0 | 0.0 | 0.0 | 0.0 |
| HC15C | 459 | Ottosee | 9 | | 66.5 | 4.0 | 0.0 | 4.0 | 0.0 | T | 0.0 | 0.5 | 1.0 | 2.0 | 6.0 | 15.5 | 0.0 | 0.0 | T | 0.0 | 0.0 | 0.0 | 0.0 |
| HC15E | 463 | Ottosee | 9 | | 73.5 | 2.0 | 0.0 | 3.5 | 0.0 | 0.0 | T | 0.5 | T | 2.5 | 9.5 | 7.0 | 0.0 | 0.0 | T | 0.0 | 0.5 | 0.0 | 0.0 |
| HC16B | 474 | Benbolt | 19 | 9 | 82.0 | 7.5 | 0.0 | 0.0 | 0.0 | T | 0.0 | T | T | 1.5 | T | 3.5 | 0.0 | 0.0 | 3.0 | 0.0 | 0.0 | 0.0 | 2.5 |
| HC17B | 479 | Benbolt | 13 | | 8.5 | 30.0 | 5.0 | 0.0 | 0.0 | 0.0 | 0.5 | T | T | 0.0 | 20.0 | 3.0 | 25.5 | P | 0.0 | 0.0 | 7.5 | 0.0 | 0.0 |
| HC17D | 485 | Benbolt | 9 | | 72.5 | 4.5 | 0.0 | 2.5 | 0.0 | T | 0.0 | T | 0.0 | 0.0 | 2.5 | 2.0 | T | 0.0 | 15.0 | 0.0 | 0.5 | 0.0 | 0.0 |
| HC17E | 490 | Benbolt | 9 | 16 | 60.5 | 3.0 | 2.5 | 14.0 | 0.0 | 1.0 | T | 1.5 | 1.5 | 2.5 | 4.5 | 6.5 | 0.0 | 0.0 | T | 0.0 | T | 0.0 | 2.5 |
| HC17G | 498 | Benbolt | 9 | | 87.0 | 0.0 | 0.0 | 0.0 | 0.0 | 0.5 | T | T | 0.5 | 1.5 | 4.5 | 3.0 | T | 0.0 | 0.0 | 0.0 | 1.0 | 0.0 | 2.0 |
| HC18A | 501 | Witten | 9 | | 87.0 | 0.0 | 0.0 | 0.0 | 0.0 | T | T | 1.5 | T | 2.0 | 3.0 | 0.5 | 1.0 | 0.0 | 0.0 | 0.0 | 2.0 | 0.0 | 2.5 |
| HC18B | 511 | Witten | 19 | | 89.5 | 0.0 | 0.0 | 3.0 | 0.0 | T | T | 0.0 | 0.0 | 0.5 | 2.5 | 0.0 | 0.0 | 0.0 | 0.0 | 0.0 | 0.0 | 0.0 | 4.5 |
| HC20A | 533 | Witten | 9 | 17 | 34.5 | 14.0 | 0.0 | 1.5 | 0.0 | 1.5 | 0.5 | 0.5 | T | 4.0 | 15.5 | 6.0 | 21.0 | P | 0.0 | 0.0 | 0.5 | 0.0 | 0.5 |
| HC21A | 544 | Witten | 9 | Bound | 58.0 | 0.0 | 0.0 | 0.0 | 0.0 | 0.0 | 1.5 | 0.5 | 0.5 | 2.0 | 2.5 | 1.0 | 4.0 | 0.0 | 0.0 | 30.0 | 0.0 | 0.0 | 0.0 |
| HC21D | 547 | Witten | 9 | | 65.0 | 0.5 | 0.0 | 0.0 | 0.0 | 0.0 | 5.0 | T | 0.5 | 1.0 | 3.0 | 24.0 | 1.0 | 0.0 | 0.0 | T | 0.0 | 0.0 | 0.0 |
| HR1A | 5 | Five Oaks | 16 | 191 | 0.0 | 0.0 | 0.0 | 97.5 | 0.0 | 0.0 | 2.0 | 0.5 | 0.0 | 0.0 | 0.0 | 0.0 | 0.0 | 0.0 | 0.0 | 0.0 | 0.0 | 0.0 | 0.0 |
| HR2A | 10 | Linc. | 17 | | 2.0 | 15.5 | 0.0 | 7.5 | 0.0 | 0.0 | 0.0 | 2.5 | 4.5 | 0.0 | 50.0 | 15.0 | 1.0 | 0.0 | 0.0 | 0.0 | 0.0 | 0.0 | 2.0 |
| HR2B | 14.5 | Linc. | 9 | 17/191 | 28.5 | 10.0 | 0.0 | T | 0.0 | 0.0 | 0.5 | 1.5 | 1.0 | 0.0 | 9.5 | 6.5 | 42.5 | P | 0.0 | 0.0 | 0.0 | 0.0 | 0.0 |
| HR3B | 36 | Linc. | 12g | | 0.0 | 27.0 | 0.0 | 4.0 | 0.0 | 0.0 | 0.0 | 3.5 | 3.5 | 0.0 | 46.0 | 16.0 | 0.0 | 0.0 | 0.0 | 0.0 | 0.0 | 0.0 | 0.0 |
| HR4A | 43 | Linc. | 17 | 13 | 5.0 | 21.0 | 0.0 | 10.0 | 0.0 | 0.0 | 0.0 | T | T | 0.0 | 42.0 | 14.0 | 7.5 | P | T | 0.0 | 0.0 | 0.0 | 0.5 |
| HR5A | 63 | Linc. | 17 | 13 | 3.5 | 13.5 | 0.0 | 6.0 | 0.0 | 0.0 | 0.0 | 3.0 | 1.5 | 0.0 | 38.0 | 27.5 | T | 0.0 | 4.0 | 0.0 | 3.0 | 0.0 | 0.0 |

| Sample Number | Strat. Position | Fm. | Dom. Facies | Sub. Facies | Mic | Spar | Intra | Pel | Oo | Brach | Gast | Ostra | Tri | Moll | Ech | Bry | Alg | On | Sp | Other Foss | Dolo | Qtz | Oth |
|---|---|---|---|---|---|---|---|---|---|---|---|---|---|---|---|---|---|---|---|---|---|---|---|
| HR6A | 70 | Rockdell | 9 | 22 | 52.0 | 3.0 | 0.0 | 0.0 | 0.0 | 0.0 | 0.5 | 3.0 | 0.5 | 0.0 | 9.0 | 21.0 | 10.0 | 0.0 | 1.0 | 0.0 | 0.0 | 0.0 | 0.0 |
| HR6B | 77 | Rockdell | 12g | | 0.5 | 36.0 | 0.0 | 0.0 | 0.0 | 0.0 | 0.0 | 1.5 | 1.5 | 0.0 | 30.5 | 29.5 | 0.5 | 0.0 | 0.0 | 0.0 | 0.0 | 0.0 | 0.0 |
| HR6C | 78 | Rockdell | 12g | 17 | 1.5 | 29.0 | 0.0 | 0.0 | 0.0 | T | 0.0 | 0.5 | 1.0 | 0.0 | 33.0 | 34.5 | T | 0.0 | 0.0 | 0.0 | 0.0 | 0.0 | 0.5 |
| HR6E | 85 | Rockdell | 12g | 17 | 15.5 | 22.5 | 0.0 | 0.0 | 0.0 | T | 0.0 | T | 1.0 | 0.0 | 28.0 | 24.5 | 3.5 | 0.0 | 0.0 | 0.0 | 0.0 | 0.0 | 0.0 |
| HR6G | 89 | Rockdell | 12g | 17 | 22.0 | 21.5 | 0.0 | 0.0 | 0.0 | 0.0 | 0.0 | 1.5 | 1.0 | 0.0 | 28.5 | 24.5 | 1.0 | 0.0 | 0.0 | 0.0 | 0.0 | 0.0 | 0.0 |
| HR6H | 92 | Rockdell | 12g | 17 | 4.0 | 22.0 | 0.0 | 0.0 | 0.0 | 0.0 | 0.0 | 0.5 | T | 0.0 | 26.0 | 35.0 | 0.5 | 0.0 | 0.0 | 0.0 | 0.0 | 0.0 | 2.0 |
| HR6I | 96 | Rockdell | 9 | | 52.5 | 4.5 | 0.0 | 0.0 | 0.0 | 0.0 | 0.0 | 0.5 | 0.0 | 0.0 | 11.5 | 9.5 | 21.0 | 0.0 | 0.5 | 0.0 | 0.0 | 0.0 | 0.0 |
| HR6J | 97 | Rockdell | 9 | | 54.0 | 1.5 | 0.0 | 2.0 | 0.0 | 0.0 | T | 2.0 | 0.0 | T | 6.5 | 28.5 | 0.5 | 0.0 | 5.0 | 0.0 | 0.0 | 0.0 | 0.0 |
| HR7C | 98 | Rockdell | 17 | | 34.5 | 12.0 | 0.0 | 1.5 | 0.0 | 0.0 | 1.0 | 1.0 | 0.5 | 0.0 | 15.0 | 10.0 | 19.0 | 0.0 | T | 0.0 | 3.0 | 0.0 | 0.0 |
| HR7D | 108 | Rockdell | 9 | | 74.5 | 4.5 | 0.0 | 0.0 | 0.0 | 0.0 | T | 0.0 | 0.0 | T | 7.5 | 10.5 | T | 0.0 | T | 0.0 | 0.0 | 0.0 | 3.0 |
| HR8A | 114 | Rockdell | 12g | | 12.0 | 28.5 | 0.0 | 0.0 | 0.0 | T | 0.0 | 0.5 | 1.5 | 0.0 | 36.0 | 21.0 | 0.5 | 0.0 | T | 0.0 | 0.0 | 0.0 | 0.0 |
| HR8C | 123 | Rockdell | 9 | | 78.0 | 1.5 | 0.0 | 0.0 | 0.0 | T | 0.0 | 0.5 | T | T | 8.5 | 9.5 | T | 0.0 | 0.0 | 0.0 | T | T | 0.0 |
| HR9A | 130 | Rockdell | 12g | | 9.5 | 26.0 | 1.5 | 1.5 | 0.0 | 0.0 | 0.0 | 1.5 | T | 0.0 | 29.0 | 29.0 | 1.5 | 0.0 | 0.0 | 0.0 | T | T | 0.0 |
| HR9C | 140.5 | Rockdell | 12g | 17 | 13.0 | 23.5 | 1.5 | 0.0 | 0.0 | T | 1.5 | 1.5 | 0.5 | 1.0 | 17.0 | 39.0 | 1.5 | P | 0.0 | 0.0 | 0.0 | 0.0 | 0.0 |
| HR9D | 144 | Rockdell | lost | | 71.0 | 4.5 | 0.0 | 0.0 | 0.0 | T | 0.0 | 1.0 | 0.5 | 0.0 | 15.0 | 7.5 | T | P | 0.5 | 0.0 | 0.0 | 0.0 | 2.0 |
| HR9E | 146 | Rockdell | lost | | 65.0 | 3.0 | 0.0 | 16.0 | 0.0 | 0.0 | 0.0 | 1.5 | 0.0 | T | 2.0 | 7.5 | T | 0.0 | 5.0 | 0.0 | 0.0 | 0.0 | 0.0 |
| HR10A | 159 | Rockdell | lost | | 65.0 | 3.0 | 0.0 | 16.0 | 0.0 | 0.0 | 0.0 | 1.5 | 0.0 | T | 2.0 | 7.5 | T | 0.0 | 5.0 | 0.0 | 0.0 | 0.0 | 0.0 |
| HR10B | 161 | Rockdell | lost | | 31.0 | 5.5 | 0.0 | 2.0 | 0.0 | 0.5 | 0.0 | 0.5 | 1.0 | 0.0 | 28.0 | 30.0 | 1.5 | 0.0 | T | 0.0 | 0.0 | 0.0 | 0.0 |
| HR10D | 167 | Rockdell | 12p | | 43.5 | 8.5 | 0.0 | 2.0 | 0.0 | 1.5 | 0.0 | 0.5 | 1.0 | 0.0 | 26.5 | 12.0 | T | 0.0 | 0.5 | 0.0 | 1.5 | 0.0 | 2.5 |
| HR11A | 185 | Rockdell | 12p | | 36.5 | 10.0 | 0.0 | 0.0 | 0.0 | 0.5 | T | 2.5 | 0.0 | 0.5 | 24.0 | 20.0 | 6.0 | 0.0 | 0.0 | 0.0 | 0.0 | 0.0 | 0.0 |
| HR11B | 190 | Rockdell | 12g | | 5.5 | 25.0 | 0.0 | 0.0 | 0.0 | 0.0 | 0.0 | 0.0 | 1.5 | 0.0 | 48.5 | 19.0 | 0.0 | 0.0 | 0.0 | 0.0 | 0.0 | 0.0 | 0.0 |

| Sample Number | Strat. Position | Fm. | Dom. Facies | Sub. Facies | Mic | Spar | Intra | Pel | Oo | Brach | Gast | Ostra | Tri | Moll | Ech | Bry | Alg | On | Sp | Other Foss | Dolo | Qtz | Oth |
|---|---|---|---|---|---|---|---|---|---|---|---|---|---|---|---|---|---|---|---|---|---|---|---|
| HR11F | 204 | Rockdell | 9 | | 5.5 | 3.0 | 0.0 | 2.5 | 0.0 | 0.0 | 0.0 | 0.0 | 0.5 | 0.0 | 21.5 | 9.5 | 0.0 | 0.0 | 5.0 | 0.0 | 0.0 | 0.0 | 3.0 |
| HR12A | 232 | Rockdell | 12p | | 47.5 | 12.5 | 0.0 | 0.0 | 0.0 | 0.5 | T | 2.0 | 0.5 | 0.0 | 21.0 | 16.0 | 0.0 | T | 0.0 | 0.0 | 0.0 | 0.0 | |
| HR13A | 258 | Rockdell | 12p | | 19.5 | 14.5 | 0.0 | 14.5 | 0.0 | 0.5 | 0.0 | 0.5 | 0.5 | T | 30.5 | 19.0 | 0.0 | 0.0 | 0.0 | 0.5 | 0.0 | 0.0 | |
| HR13C | 264 | Rockdell | 9 | 16 | 59.0 | 7.0 | 0.0 | T | 0.0 | 0.5 | 0.0 | T | T | 0.0 | 24.5 | 9.0 | 0.0 | 0.0 | 0.0 | 0.0 | 0.0 | 0.0 | 0.0 |
| HR13D | 267 | Rockdell | 9 | | 57.0 | 5.0 | 0.0 | 0.0 | 0.0 | 0.0 | T | T | 1.0 | 0.5 | 14.5 | 22.0 | 0.0 | 0.0 | T | 0.0 | 0.0 | 0.0 | 0.0 |
| HR13F | 275 | Rockdell | 12p | | 12.0 | 23.0 | 0.0 | 0.0 | 0.0 | T | 0.0 | T | 1.0 | 0.0 | 58.0 | 6.0 | 0.0 | 0.0 | T | 0.0 | 0.0 | 0.0 | 0.0 |
| HR14B | 287 | Rockdell | 19f | 8 | 80.0 | 4.0 | 0.0 | 0.0 | 0.0 | 0.0 | 0.0 | T | 0.0 | 0.0 | 1.0 | 11.0 | 0.0 | 0.0 | 4.0 | 0.0 | 0.0 | 0.0 | 0.0 |
| HR14D | 292 | Rockdell | 9 | | 59.5 | 3.0 | 0.0 | 0.0 | 0.0 | 0.0 | 0.5 | 0.5 | T | 0.0 | 1.0 | 28.0 | 0.0 | 0.0 | 0.5 | 0.0 | 0.0 | 0.0 | 0.0 |
| HR15C | 310 | Ch. Ridge | 9 | | 63.0 | 5.0 | 0.0 | 0.0 | 0.0 | 0.0 | 1.0 | 1.5 | T | 0.0 | 14.0 | 15.5 | 0.0 | 0.0 | 0.0 | 0.0 | 0.0 | 0.0 | 0.0 |
| HR16B | 326 | Ch. Ridge | 9 | | 65.5 | 0.5 | 0.0 | 0.0 | 0.0 | 0.0 | 0.0 | 0.5 | T | 0.0 | 20.0 | 9.5 | 0.0 | 0.0 | 2.5 | 0.0 | 0.0 | 0.0 | 1.5 |
| HR16E | 332 | Ch. Ridge | 8 | 9 | 70.5 | 2.5 | 0.0 | 18.0 | 0.0 | 0.0 | 0.0 | T | T | 0.0 | 2.0 | 7.0 | 0.0 | 0.0 | 0.0 | 0.0 | 0.0 | 0.0 | 0.0 |
| HR17A | 336 | Benbolt | 19f | | 56.0 | 3.0 | 0.0 | 0.0 | 0.0 | 0.0 | 0.0 | T | 0.0 | 0.0 | 0.0 | 2.0 | 0.0 | 0.0 | 39.0 | 0.0 | 0.0 | 0.0 | 0.0 |
| HR17D | 344 | Benbolt | 12g | 17 | 48.5 | 13.0 | T | 8.0 | 0.0 | 0.5 | 0.5 | 0.5 | T | 0.0 | 25.5 | 2.5 | 0.0 | 0.0 | T | 0.0 | 0.0 | 0.0 | 1.0 |
| HR17F | 352 | Benbolt | 9 | | 83.0 | 0.0 | 0.0 | 0.0 | 0.0 | 0.5 | t | 0.5 | t | 0.5 | 6.5 | 8.5 | 0.0 | 0.0 | t | 0.0 | 0.0 | 0.0 | 0.0 |
| HR18A | 354 | Benbolt | 9 | 8 | 87.0 | 5.5 | 0.0 | 0.0 | 0.0 | 0.0 | 0.0 | 0.0 | T | 0.0 | 0.5 | 3.5 | 0.0 | 0.0 | 3.5 | 0.0 | 0.0 | 0.0 | 0.0 |
| HR18C | 362 | Benbolt | 12p | 14 | 74.5 | 1.5 | 0.0 | 2.5 | 0.0 | 0.5 | 1.5 | 3.0 | 1.5 | 1.0 | 9.5 | 1.5 | 0.0 | 0.0 | 0.0 | 0.0 | 1.5 | 0.0 | 1.5 |
| HR18D | 365 | Benbolt | 9 | 16 | 87.0 | 0.0 | 0.0 | 1.5 | 0.0 | 1.0 | 0.5 | 1.0 | 0.5 | 0.5 | 4.0 | 2.0 | 0.0 | 0.0 | 0.0 | 0.0 | 0.0 | 0.0 | 2.0 |
| HR18F | 371 | Benbolt | 12p | | 45.0 | 1.0 | 0.0 | 43.5 | 0.0 | T | 0.0 | 0.0 | T | 0.0 | 5.0 | 3.0 | 0.0 | 0.0 | 0.0 | 0.0 | 2.5 | 0.0 | 0.0 |
| HR19A | 372 | Benbolt | 19 | | 97.0 | 0.0 | 0.0 | 3.0 | 0.0 | 0.0 | 0.0 | 0.0 | 0.0 | 0.0 | 0.0 | 0.0 | 0.0 | 0.0 | 0.0 | 0.0 | 0.0 | 0.0 | 0.0 |
| HR19C | 378 | Benbolt | 12g | 16 | 6.0 | 20.0 | 0.0 | 6.0 | 0.0 | 0.0 | 0.0 | 0.0 | 1.0 | 0.0 | 59.0 | 8.0 | 0.0 | 0.0 | 0.0 | 0.0 | 0.0 | 0.0 | 0.0 |
| HR19E | 383 | Benbolt | 22 | | 45.5 | 10.0 | 0.0 | 9.0 | 0.0 | 3.0 | T | 0.5 | 1.0 | 4.5 | 13.0 | 5.5 | 8.0 | P | T | 0.0 | 0.0 | 0.0 | 0.0 |

| Sample Number | Strat. Position | Fm. | Dom. Facies | Sub. Facies | Mic | Spar | Intra | Pel | Oo | Brach | Gast | Ostra | Tri | Moll | Ech | Bry | Alg | On | Sp | Other Foss | Dolo | Qtz | Oth |
|---|---|---|---|---|---|---|---|---|---|---|---|---|---|---|---|---|---|---|---|---|---|---|---|
| HR19F | 386 | Benbolt | 22 | | 59.5 | 1.5 | 0.0 | 0.0 | 0.0 | T | T | 0.5 | 1.5 | 0.5 | 5.5 | 4.5 | 25.5 | P | 0.0 | 0.0 | 0.0 | 0.0 | 1.5 |
| HR20B | 395 | Wardell | ?19l | | 0.0 | 0.0 | 0.0 | 90.0 | 0.0 | 0.0 | 0.0 | T | 0.0 | 0.0 | T | 0.0 | 0.0 | 0.0 | 0.0 | 0.0 | 7.0 | 2.5 | 0.0 |
| HR20C | 398 | Wardell | 22 | | 77.0 | 0.5 | 0.0 | 0.0 | 0.0 | 2.5 | 0.0 | T | T | 0.0 | 10.0 | 3.0 | 5.5 | P | 0.0 | 0.0 | 0.0 | 0.0 | 0.0 |
| HR21D | 421 | Witten | 19l | | 0.0 | 9.0 | 0.0 | 87.0 | 0.0 | 0.0 | 0.0 | 0.0 | 0.0 | 0.0 | 0.0 | 0.0 | 0.0 | 0.0 | 0.0 | 0.0 | 0.0 | 0.0 | 4.0 |
| GA1A | 0.5 | Linc. | 13 | | 5.5 | 38.0 | 0.0 | 0.0 | 0.0 | 0.5 | 0.0 | 1.5 | 1.0 | 0.0 | 20.5 | 3.5 | 29.5 | P | 0.0 | 0.0 | 0.0 | 0.0 | 0.0 |
| GA2C | 5 | Linc. | 17 | | 2.0 | 33.5 | 0.0 | 0.0 | 0.0 | T | 0.0 | 2.0 | 2.0 | 0.0 | 13.5 | 9.0 | 37.0 | P | 0.0 | 0.0 | 1.0 | 0.0 | 0.0 |
| GA3A | 28 | Linc. | 17 | | 10.0 | 20.5 | 0.0 | 0.0 | 0.0 | 0.0 | 0.0 | 1.0 | 0.5 | 1.0 | 16.0 | 12.5 | 38.0 | P | 0.0 | 0.0 | 0.0 | T | 0.5 |
| GA4D | 63 | Rockdell | 12p | | 37.0 | 27.0 | 0.0 | 0.0 | 0.0 | T | 0.0 | 1.5 | 0.5 | 0.0 | 12.5 | 20.0 | 1.0 | 0.0 | 0.5 | 0.0 | 0.0 | 0.0 | 0.0 |
| GA5A | 67.5 | Rockdell | lost | | 15.5 | 25.5 | 0.0 | 0.0 | 0.0 | 1.0 | 0.0 | 3.0 | 0.5 | 0.0 | 38.0 | 9.5 | 4.5 | P | 0.0 | 0.0 | 2.5 | 0.0 | 0.0 |
| GA6A | 74.5 | Rockdell | 12g | | 4.0 | 25.0 | 0.0 | 0.0 | 0.0 | 0.0 | 0.0 | 0.5 | 0.5 | 0.0 | 55.0 | 13.5 | 1.5 | 0.0 | 0.0 | 0.0 | T | 0.0 | 0.0 |
| GA7A | 75.5 | Rockdell | 12g | | 2.0 | 29.5 | 0.0 | 0.0 | 0.0 | 0.0 | T | T | 0.0 | 0.0 | 50.0 | 16.5 | 2.0 | 0.0 | 0.0 | 0.0 | 0.0 | 0.0 | 0.0 |
| GA8A | 76.5 | Rockdell | 12g | | 1.0 | 25.0 | 0.0 | 0.0 | 0.0 | 0.0 | 0.0 | 2.0 | 0.5 | 0.0 | 45.0 | 22.0 | 3.5 | 0.0 | 0.0 | 0.0 | 1.0 | 0.0 | 0.0 |
| GA8F | 84 | Rockdell | 10 | | 27.0 | 17.5 | 1.5 | 0.0 | 0.0 | 0.0 | 9.0 | 0.5 | 0.5 | 0.0 | 14.5 | 10.0 | 17.5 | 0.0 | T | 2.0 | 0.0 | 0.0 | 0.0 |
| GA9A | 85.5 | Rockdell | lost | | 6.5 | 16.5 | 0.0 | 29.5 | 0.0 | 0.0 | T | 0.0 | 0.0 | 0.0 | 39.0 | 5.5 | 0.5 | 0.0 | 0.0 | 0.0 | T | 0.0 | 0.0 |
| GA11B | 95.5 | Rockdell | 12p | | 26.5 | 5.0 | 0.0 | 0.0 | 0.0 | T | 0.0 | 1.0 | T | 0.0 | 29.5 | 32.5 | 0.5 | 0.0 | 0.0 | 0.0 | 0.5 | 0.5 | 4.5 |
| GA12A | 98 | Rockdell | lost | | 29.0 | 1.5 | 1.5 | 0.0 | 0.0 | T | T | 0.5 | 1.0 | 0.0 | 31.0 | 10.0 | 0.0 | 0.0 | 0.0 | 0.0 | 4.5 | 8.5 | 12.5 |
| GA12C | 98 | Rockdell | 9 | | 66.0 | 3.5 | 0.0 | 5.0 | 0.0 | 0.5 | 1.0 | T | 1.0 | 0.0 | 2.5 | 11.0 | 2.5 | 0.0 | 0.0 | 0.0 | 0.5 | 1.0 | 5.5 |
| GA13A | 102.5 | Rockdell | 12p | | 8.0 | 7.5 | 2.0 | 0.0 | 0.0 | 1.0 | 0.0 | 0.0 | 1.5 | 0.0 | 46.0 | 29.5 | 2.0 | 0.0 | 0.0 | 0.0 | 2.0 | 0.5 | 2.0 |
| GA14C | 105.5 | Rockdell | 12g | | 21.5 | 22.0 | 0.0 | 0.0 | 0.0 | 0.5 | 1.0 | 0.5 | 1.5 | 0.0 | 30.5 | 16.0 | 5.0 | 0.0 | 0.0 | 0.0 | 1.5 | 0.0 | 0.0 |
| GA15C | 109.5 | Rockdell | 12g | 17 | 18.5 | 20.5 | 0.0 | 0.0 | 0.0 | t | 0.0 | 1.5 | 1.5 | 0.0 | 39.0 | 12.0 | 0.5 | 0.0 | 0.0 | 0.0 | 6.0 | 0.0 | 0.5 |
| GA16B | 114 | Rockdell | 9 | 8 | 77.5 | 5.0 | 0.0 | 3.5 | 0.0 | 0.0 | t | t | t | t | 1.0 | 12.0 | 0.0 | 0.0 | 0.5 | 0.0 | 0.0 | 0.0 | 0.5 |

| Sample Number | Strat. Position | Fm. | Dom. Facies | Sub. Facies | Mic | Spar | Intra | Pel | Oo | Brach | Gast | Ostra | Tri | Moll | Ech | Bry | Alg | On | Sp | Other Foss | Dolo | Qtz | Oth |
|---|---|---|---|---|---|---|---|---|---|---|---|---|---|---|---|---|---|---|---|---|---|---|---|
| GA16C | 117 | Rockdell | 12p | | 29.5 | 13.5 | 1.5 | t | 0.0 | 0.0 | 1.5 | 0.0 | t | 0.0 | 39.5 | 13.5 | 1.0 | 0.0 | 0.0 | 0.0 | 0.0 | 0.0 | 0.0 |
| GA17C | 118.5 | Rockdell | 12g | 17 | 19.5 | 22.5 | t | 0.0 | 0.0 | 0.5 | t | 2.0 | 1.0 | 0.5 | 38.0 | 11.5 | 2.5 | 0.0 | 0.0 | 0.0 | 1.0 | 0.0 | 1.0 |
| GA18B | 122.5 | Rockdell | 12g | 17 | 18.0 | 23.0 | 0.0 | 1.5 | 0.0 | 0.0 | 0.0 | 2.5 | 0.5 | t | 37.0 | 13.5 | 0.0 | 0.0 | 0.0 | 0.0 | 4.0 | 0.0 | 0.0 |
| GA19C | 143.5 | Rockdell | 12g | 16 | 8.5 | 30.5 | 0.0 | 16.5 | 0.0 | 1.0 | 0.0 | 4.0 | 1.0 | 0.5 | 23.5 | 12.0 | 0.0 | 0.0 | 0.0 | 0.0 | 2.5 | 0.0 | 0.0 |
| GA19E | 150 | Rockdell | 17 | | 5.5 | 48.0 | 0.0 | 0.0 | 0.0 | t | 0.0 | 5.5 | 2.5 | 1.5 | 13.0 | 22.0 | t | 0.0 | 0.0 | 0.0 | 0.5 | 0.0 | 1.5 |
| GA20A | 156 | Rockdell | 9 | 17 | 42.5 | 12.0 | t | t | 0.0 | 1.0 | 0.0 | t | t | 1.0 | 17.5 | 14.0 | 0.0 | 0.0 | 0.0 | 0.0 | 8.0 | 0.0 | 4.0 |
| GA21C | 164 | Rockdell | lost | | 10.5 | 33.0 | 2.0 | 7.5 | ## | 1.0 | 0.0 | 0.5 | 1.0 | 0.0 | 19.5 | 6.0 | 0.0 | 0.0 | 0.0 | 0.0 | 0.0 | 0.0 | 0.0 |
| GA21E | 167 | Rockdell | 9 | | 56.0 | 17.0 | 0.0 | 9.0 | t | 0.0 | 0.0 | 0.5 | 1.0 | 0.0 | 3.0 | 7.0 | 0.0 | 0.0 | 0.0 | 0.0 | 6.5 | 0.0 | 0.0 |
| GA22C | 173 | Rockdell | ?12g | 16 | 6.5 | 31.0 | 0.0 | 0.0 | 0.0 | 0.5 | 0.0 | 1.5 | 1.0 | 0.0 | 32.5 | 24.0 | 0.0 | 0.0 | 0.0 | 0.0 | 0.5 | 0.0 | 2.5 |
| GA23A | 176 | Rockdell | 12g | | 1.5 | 34.0 | 1.0 | 0.0 | 0.0 | 0.0 | t | 1.0 | 0.0 | 0.0 | 48.0 | 14.0 | t | 0.0 | 0.0 | 0.0 | 0.5 | 0.0 | 0.0 |
| GA24D | 188 | Rockdell | 12p | | 15.5 | 28.0 | 0.0 | 0.0 | 0.0 | 0.0 | 0.0 | 0.5 | 3.0 | 0.0 | 46.0 | 7.0 | 0.0 | 0.0 | 0.0 | 0.0 | 0.0 | 0.0 | 0.0 |
| GA25A | 198.5 | Rockdell | 12p | | 26.0 | 16.5 | 0.0 | 5.0 | 0.0 | 0.5 | 0.0 | 0.5 | 1.5 | 0.0 | 30.0 | 16.0 | 1.0 | 0.0 | 0.0 | 0.0 | 0.0 | 0.0 | 3.0 |
| GA26C | 220 | Rockdell | 9 | | 40.5 | 10.0 | 0.0 | 0.0 | 0.0 | 0.0 | 0.0 | 1.0 | t | 0.5 | 22.5 | 18.0 | 2.0 | 0.0 | 0.0 | 0.0 | 0.5 | 1.0 | 4.0 |
| GA27A | 225 | Rockdell | lost | | 39.0 | 15.5 | 0.5 | 3.0 | 0.0 | 0.0 | t | 0.5 | 0.0 | 0.0 | 24.5 | 16.5 | 0.0 | 0.0 | t | 0.0 | 0.0 | 0.0 | 0.5 |
| GA28A | 249.5 | Benbolt | 12p | | 50.0 | 17.0 | 0.0 | 0.0 | 0.0 | 0.5 | 0.0 | t | 1.0 | 1.5 | 12.5 | 17.5 | 0.0 | 0.0 | 0.0 | 0.0 | 0.0 | 0.0 | 0.0 |
| GA28D | 266 | Benbolt | 19 | 9 | 70.0 | 6.5 | 0.0 | 22.5 | 0.0 | 0.0 | 0.0 | 0.0 | 0.0 | 0.0 | T | 1.0 | 0.0 | 0.0 | 0.0 | 0.0 | 0.0 | 0.0 | 0.0 |
| GA29B | 270.5 | Benbolt | 9 | | 62.0 | 13.5 | 0.0 | 0.0 | 0.0 | 0.0 | 0.5 | 2.5 | 2.5 | 1.0 | 13.0 | 0.5 | T | 0.0 | 0.0 | 0.0 | 0.0 | 0.0 | 4.5 |
| GA30A | 278 | Benbolt | 9 | | 77.5 | 2.0 | 0.0 | 0.0 | 0.0 | T | T | 2.5 | 1.0 | 0.5 | 2.5 | 0.5 | 11.0 | 0.0 | 0.0 | 0.0 | 0.0 | 0.0 | 2.5 |
| GA31C | 299.5 | Benbolt | 191 | | 0.5 | 3.0 | 0.0 | 92.5 | 0.0 | T | 0.0 | 1.0 | 0.0 | 0.0 | 1.0 | T | 0.0 | 0.0 | 0.0 | 0.0 | 2.0 | 0.0 | 0.0 |
| GA31D | 301 | Benbolt | 19 | 9 | 56.0 | 13.5 | 4.0 | 4.0 | 0.0 | 0.5 | 0.0 | 3.0 | 0.5 | 0.5 | 8.0 | 3.0 | 0.0 | 0.0 | 0.0 | 0.0 | 6.5 | 0.5 | 0.0 |
| GA32A | 309.5 | Wardell | 8 | | 75.5 | 13.0 | 0.0 | 0.0 | 0.0 | 0.0 | 0.5 | 1.5 | 1.0 | 0.5 | 1.5 | 1.5 | 4.0 | 0.0 | T | 0.0 | 1.0 | 0.0 | 0.0 |

| Sample Number | Strat. Position | Fm. | Dom. Facies | Sub. Facies | Mic | Spar | Intra | Pel | Oo | Bracl | Gast | Ostra | Tri | Moll | Ech | Bry | Alg | On | Sp | Other Foss | Dolo | Qtz | Oth |
|---|---|---|---|---|---|---|---|---|---|---|---|---|---|---|---|---|---|---|---|---|---|---|---|
| GA34C | 357 | Wardell | 19f | | 28.5 | 11.5 | 0.0 | 57.0 | 0.0 | 0.0 | 0.0 | 0.5 | 0.0 | 0.0 | 0.0 | 0.0 | 0.0 | 0.0 | 0.5 | 0.0 | 0.0 | 0.0 | 2.0 |
| GA34D | 361 | Wardell | 19l | 16 | 22.0 | 15.5 | 0.0 | 38.0 | 0.0 | 0.0 | 0.0 | 10.0 | 0.5 | 5.0 | 1.5 | T | 0.0 | 0.0 | 0.0 | 0.0 | 3.5 | 3.0 | 1.0 |
| GA34E | 364 | Bowen | 19l | | 0.0 | 3.0 | 0.0 | 81.5 | 0.0 | 0.0 | 0.0 | 2.0 | 0.0 | 2.0 | 0.0 | T | 0.0 | 0.0 | 0.0 | 0.0 | 8.0 | 0.5 | 3.0 |
| GA35B | 384 | Witten | 17 | 9 | 11.5 | 11.0 | 3.5 | 55.5 | 0.0 | 1.0 | T | 4.0 | 2.0 | 0.0 | 2.5 | 5.0 | 0.0 | 0.0 | 0.0 | 0.0 | 3.5 | 0.0 | 0.5 |

| Shelf and Shelf-Edge Point-Count Data From The Thorn Hill Area, After Jernigan (1987) | | | | | | | | | | | | | | | | | | | | | | | |
|---|---|---|---|---|---|---|---|---|---|---|---|---|---|---|---|---|---|---|---|---|---|---|---|
| Sample Number | Strat. Position | Fm. | Dom. Facies | Sub. Facies | Mic | Spar | Intra | Pel | Oo | Brach | Gast | Ostra | Tri | Moll | Ech | Bry | Alg | On | Sp | Other Foss | Dolo | Qtz | Oth |
| RHB-1 | 22.5 | Holston | 12g | | 0.0 | 35.1 | 0.0 | 0.0 | 0.0 | 0.0 | N/A | 0.6 | 0.1 | 0.0 | 21.7 | 38.0 | 0.0 | 0.0 | 0.0 | 2.9 | 0.7 | 0.0 | 1.0 |
| RHB-1A | 24.5 | Holston | 12g | | 0.0 | 29.8 | 0.0 | 0.0 | 0.0 | 0.7 | N/A | 1.0 | 1.1 | 0.0 | 29.4 | 33.6 | 0.0 | 0.0 | 0.0 | 2.3 | 0.1 | 0.0 | 2.1 |
| RHB-1B | 32.5 | Holston | 12g | | 0.4 | 29.3 | 0.0 | 0.0 | 0.0 | 1.2 | N/A | 0.0 | 0.2 | 0.0 | 34.1 | 30.7 | 0.0 | 0.0 | 0.0 | 2.8 | 0.1 | 0.0 | 1.2 |
| RHB-2A | 41 | Holston | Lost | | 39.6 | 26.2 | 0.0 | 1.6 | 0.0 | 0.1 | N/A | 0.1 | 0.3 | 0.2 | 5.0 | 15.9 | 0.0 | 0.0 | 9.1 | 0.4 | 0.0 | 0.2 | 1.2 |
| RHB-2C | 41.5 | Holston | 12g | | 2.0 | 45.2 | 0.0 | 0.0 | 0.0 | 0.3 | N/A | 0.0 | 0.9 | 0.0 | 22.1 | 24.8 | 0.0 | 0.0 | 0.0 | 1.7 | 0.0 | 0.0 | 2.9 |
| RHB-2G | 42 | Holston | 12g | | 7.4 | 59.8 | 0.0 | 0.0 | 0.0 | 1.2 | N/A | 0.0 | 1.2 | 0.0 | 7.6 | 17.7 | 0.0 | 0.0 | 0.0 | 1.4 | 0.0 | 0.0 | 3.7 |
| RHB-2J- | 42.5 | Holston | 12g | | 41.6 | 30.5 | 0.2 | 0.4 | 0.0 | 0.0 | N/A | 1.0 | 0.1 | 0.7 | 2.3 | 16.0 | 0.0 | 0.0 | 2.4 | 1.1 | 0.0 | 0.0 | 3.6 |
| RHB-2K | 43 | Holston | Lost | | 39.4 | 49.5 | 0.0 | 0.0 | 0.0 | 0.0 | N/A | 0.2 | 0.0 | 0.0 | 0.0 | 0.4 | 0.0 | 0.0 | 7.4 | 0.2 | 0.0 | 0.0 | 3.0 |
| RHB-3A | 50.5 | Holston | 12g | 12p | 5.2 | 36.2 | 0.0 | 0.0 | 0.0 | 0.1 | N/A | 0.3 | 0.7 | 0.0 | 22.8 | 22.1 | 0.0 | 0.0 | 0.0 | 1.9 | 2.8 | 0.0 | 8.0 |
| RHB-3B | 54.8 | Holston | 12p | 12p | 14.9 | 37.5 | 0.0 | 0.0 | 0.0 | 0.9 | N/A | 0.3 | 4.9 | 0.0 | 11.2 | 24.0 | 0.0 | 0.0 | 0.0 | 1.1 | 0.0 | 0.0 | 4.8 |
| RHB-3C | 57 | Holston | 12g | | 30.2 | 30.7 | 0.0 | 0.3 | 0.0 | 1.6 | N/A | 0.2 | 1.7 | 0.0 | 9.9 | 21.1 | 0.0 | 0.0 | 0.0 | 1.0 | 0.0 | 0.0 | 3.3 |
| RHB-3D | 60.3 | Holston | 12g | | 15.1 | 32.3 | 0.0 | 0.6 | 0.0 | 0.4 | N/A | 0.1 | 0.2 | 1.0 | 21.1 | 21.1 | 0.0 | 0.0 | 0.0 | 1.1 | 0.0 | 0.0 | 7.0 |
| RHB-3E- | 62.7 | Holston | 12g | | 1.3 | 44.8 | 0.0 | 0.1 | 0.0 | 0.1 | N/A | 0.0 | 2.3 | 0.0 | 13.9 | 32.6 | 0.0 | 0.0 | 0.0 | 1.8 | 0.8 | 0.0 | 2.4 |
| RHB-3F- | 65 | Holston | 12g | | 10.9 | 52.7 | 0.0 | 0.0 | 0.0 | 0.0 | N/A | 0.0 | 0.4 | 0.0 | 1.8 | 32.0 | 0.0 | 0.0 | 0.0 | 0.2 | 0.0 | 0.0 | 2.0 |
| RHB-3G | 75.8 | Holston | 12g | | 25.8 | 22.5 | 0.0 | 0.1 | 0.0 | 0.0 | N/A | 0.0 | 0.4 | 0.0 | 3.7 | 35.1 | 0.0 | 0.0 | 0.0 | 0.0 | 3.9 | 0.0 | 8.6 |
| RHB-3H | 81.2 | Holston | 12g | | 21.3 | 42.6 | 0.0 | 0.0 | 0.0 | 0.0 | N/A | 0.1 | 0.5 | 0.0 | 12.0 | 23.1 | 0.0 | 0.0 | 0.0 | 0.4 | 0.0 | 0.0 | 0.0 |
| RHB-3I- | 85 | Holston | Lost | | 17.5 | 28.0 | 0.0 | 0.0 | 0.0 | 0.0 | N/A | 0.0 | 0.6 | 0.0 | 3.5 | 30.9 | 0.0 | 0.0 | 0.0 | 0.4 | 16.4 | 0.0 | 2.7 |
| RHB-4A | 113.9 | Holston | 12g | | 12.8 | 44.0 | 0.0 | 0.0 | 0.0 | 1.6 | N/A | 0.5 | 2.7 | 0.0 | 9.3 | 25.6 | 0.0 | 0.0 | 0.0 | 0.9 | 0.0 | 0.0 | 2.6 |
| RHB-4B | 122.4 | Holston | Lost | | 0.5 | 38.9 | 0.0 | 0.0 | 0.0 | 0.7 | N/A | 0.0 | 1.4 | 0.0 | 30.3 | 27.2 | 0.0 | 0.0 | 0.0 | 0.8 | 0.0 | 0.0 | 0.3 |
| RHB-4C | 128.3 | Holston | Lost | | 35.5 | 28.1 | 0.0 | 0.9 | 0.0 | 0.3 | N/A | 0.4 | 1.4 | 0.0 | 6.4 | 23.8 | 0.0 | 0.0 | 0.0 | 0.6 | 0.0 | 0.0 | 2.7 |
| RHB-4D | 130.3 | Holston | 12p | | 24.7 | 33.7 | 0.0 | 1.8 | 0.0 | 0.1 | N/A | 0.1 | 0.7 | 0.0 | 5.5 | 24.6 | 0.0 | 0.0 | 0.0 | 0.8 | 0.0 | 0.0 | 8.0 |
| RHB-4E- | 131 | Holston | 12g | | 5.2 | 34.9 | 0.0 | 0.0 | 0.0 | 0.5 | N/A | 1.1 | 4.9 | 0.0 | 21.5 | 28.8 | 0.0 | 0.0 | 0.0 | 1.1 | 0.0 | 0.0 | 2.0 |

| Sample Number | Strat. Position | Fm. | Dom. Facies | Sub. Facies | Mic | Spar | Intra | Pel | Oo | Brach | Gast | Ostra | Tri | Moll | Ech | Bry | Alg | On | Sp | Other Foss | Dolo | Qtz | Oth |
|---|---|---|---|---|---|---|---|---|---|---|---|---|---|---|---|---|---|---|---|---|---|---|---|
| RHB-5A | 144 | Holston | 12g | 12p | 2.7 | 20.6 | 0.0 | 0.0 | 0.0 | 0.1 | N/A | 0.4 | 0.0 | 0.0 | 28.6 | 37.9 | 1.8 | 0.0 | 0.0 | 0.2 | 3.6 | 0.0 | 6.1 |
| RHB-6A | 181 | Holston | 12g | | 6.5 | 44.2 | 1.1 | 0.0 | 0.0 | 0.0 | N/A | 0.1 | 0.1 | 0.0 | 30.1 | 13.3 | 0.0 | 0.0 | 0.0 | 0.4 | 2.5 | 0.0 | 1.7 |
| RHB-6B | 183.4 | Holston | 12g | 12p | 14.6 | 38.4 | 1.4 | 0.0 | 0.0 | 0.0 | N/A | 0.4 | 0.3 | 0.0 | 28.3 | 15.7 | 0.0 | 0.0 | 0.0 | 0.6 | 0.0 | 0.0 | 0.4 |
| RHB-6C | 184 | Holston | 12g | | 1.2 | 32.7 | 0.2 | 0.0 | 0.0 | 0.0 | N/A | 0.4 | 0.9 | 0.0 | 32.2 | 22.4 | 0.0 | 0.0 | 0.0 | 0.7 | 6.1 | 0.0 | 3.2 |
| RHB-6D | 188 | Holston | 12g | 12p | 14.7 | 38.4 | 0.6 | 0.2 | 0.0 | 0.0 | N/A | 0.1 | 1.0 | 0.1 | 29.7 | 9.7 | 0.0 | 0.0 | 0.0 | 1.8 | 0.4 | 0.0 | 3.3 |
| RHB-6E- | 193.5 | Holston | 12g | | 4.0 | 39.7 | 1.6 | 0.3 | 0.0 | 0.2 | N/A | 0.2 | 0.0 | 0.0 | 32.0 | 14.7 | 0.0 | 0.0 | 0.0 | 0.3 | 3.5 | 0.0 | 3.5 |
| RHB-6F- | 199.6 | Holston | 12g | | 39.1 | 16.0 | 1.4 | 0.2 | 0.0 | 0.0 | N/A | 0.0 | 0.5 | 0.6 | 17.7 | 23.0 | 0.0 | 0.6 | 0.8 | 0.0 | 0.1 | 0.0 | 0.1 |
| RHB-7A | 248.5 | Rockdell | 12g | | 4.2 | 32.8 | 1.9 | 0.2 | 0.0 | 0.0 | N/A | 0.4 | 0.1 | 0.4 | 35.4 | 19.7 | 0.0 | 0.0 | 0.0 | 3.5 | 0.1 | 0.0 | 1.2 |
| RHB-7B | 249 | Rockdell | 12g | | 1.7 | 38.8 | 1.3 | 0.0 | 0.0 | 0.0 | N/A | 0.0 | 0.9 | 0.0 | 28.9 | 19.7 | 0.0 | 0.0 | 0.0 | 2.7 | 0.0 | 0.0 | 5.9 |
| RHB-8A | 259.4 | Rockdell | 12p | 12g | 16.3 | 33.2 | 1.1 | 0.0 | 0.0 | 2.2 | N/A | 0.0 | 0.0 | 0.1 | 13.2 | 22.3 | 0.0 | 0.2 | 0.0 | 1.3 | 0.1 | 7.1 | 2.9 |
| RHB-8B | 261.4 | Rockdell | Lost | | 16.5 | 45.0 | 0.1 | 0.0 | 0.0 | 0.0 | N/A | 0.6 | 0.1 | 0.0 | 18.9 | 15.2 | 0.0 | 0.0 | 0.0 | 2.1 | 0.0 | 0.0 | 1.4 |
| RHB-8- | 265.4 | Rockdell | 12g | | 5.3 | 38.0 | 0.7 | 0.1 | 0.0 | 0.4 | N/A | 0.0 | 0.1 | 0.0 | 25.1 | 21.0 | 0.1 | 0.3 | 0.0 | 0.7 | 0.0 | 0.3 | 7.9 |
| RHB-8D | 271.4 | Rockdell | | 9.0 | 49.9 | 28.4 | 0.4 | 1.4 | 0.0 | 0.1 | N/A | 0.1 | 0.6 | 0.1 | 2.0 | 10.9 | 0.2 | 0.0 | 2.4 | 0.4 | 3.2 | 0.0 | 0.0 |
| RHB-8E | 272.8 | Rockdell | | 9.0 | 31.5 | 16.7 | 0.2 | 0.5 | 0.0 | 0.4 | N/A | 0.5 | 0.1 | 0.2 | 8.8 | 26.3 | 0.0 | 0.1 | 1.2 | 1.3 | 4.6 | 0.0 | 7.7 |
| RHB-8F- | 277.4 | Rockdell | 9 | 19f | 61.0 | 13.0 | 0.0 | 1.0 | 0.0 | 0.0 | N/A | 0.2 | 0.0 | 0.0 | 1.9 | 4.4 | 0.0 | 0.0 | 7.9 | 1.1 | 7.6 | 0.0 | 1.9 |
| RHB-8G | 280.9 | Rockdell | 12g | 12p | 24.6 | 31.1 | 0.0 | 1.1 | 0.0 | 1.2 | N/A | 0.1 | 0.2 | 0.4 | 11.1 | 24.5 | 0.0 | 0.0 | 0.4 | 1.1 | 0.0 | 0.0 | 4.4 |
| RHB-8H | 281.4 | Rockdell | Lost | | 53.9 | 35.6 | 0.0 | 2.0 | 0.0 | 0.0 | N/A | 0.1 | 0.0 | 0.0 | 0.5 | 0.3 | 0.0 | 0.0 | 6.4 | 0.4 | 0.0 | 0.0 | 0.9 |
| RHB-8K | 284.1 | Rockdell | 12g | | 0.0 | 41.1 | 0.0 | 0.0 | 0.0 | 1.2 | N/A | 0.0 | 0.9 | 0.0 | 35.6 | 15.3 | 0.0 | 0.0 | 0.0 | 1.5 | 0.0 | 0.0 | 4.5 |
| PVC-1A | 11.6 | Holston | 12g | | 1.9 | 52.3 | 0.0 | 0.0 | 0.0 | 0.0 | N/A | 0.4 | 0.2 | 0.0 | 5.9 | 34.5 | 0.0 | 0.0 | 0.0 | 3.0 | 1.9 | 0.0 | 0.0 |
| PVC-1B- | 13.6 | Holston | 12g | | 3.3 | 44.8 | 0.0 | 0.0 | 0.0 | 0.1 | N/A | 0.0 | 0.7 | 0.0 | 6.1 | 41.5 | 0.0 | 0.0 | 0.0 | 1.4 | 0.0 | 0.0 | 2.0 |
| PVC-1B- | 13.8 | Holston | 12g | | 0.8 | 51.8 | 0.0 | 0.0 | 0.0 | 0.0 | N/A | 0.0 | 0.8 | 0.0 | 0.9 | 39.6 | 0.0 | 0.0 | 0.0 | 1.3 | 0.0 | 0.0 | 4.9 |
| PVC-1C | 18.6 | Holston | 12g | | 1.6 | 41.1 | 0.0 | 0.0 | 0.0 | 0.3 | N/A | 0.3 | 0.7 | 0.0 | 22.9 | 27.4 | 0.0 | 0.0 | 0.0 | 2.2 | 0.3 | 0.0 | 3.4 |
| PVC-2C | 20.6 | Holston | 12p | | 35.4 | 30.2 | 0.0 | 0.5 | 0.0 | 0.1 | N/A | 1.8 | 2.4 | 0.0 | 2.1 | 1.1 | 0.0 | 0.1 | 16.8 | 1.2 | 0.2 | 0.0 | 8.0 |

| Sample Number | Strat. Position | Fm. | Dom. Facies | Sub. Facies | Mic | Spar | Intra | Pel | Oo | Brach | Gast | Ostra | Tri | Moll | Ech | Bry | Alg | On | Sp | Other Foss | Dolo | Qtz | Oth |
|---|---|---|---|---|---|---|---|---|---|---|---|---|---|---|---|---|---|---|---|---|---|---|---|
| PVC-2D | 21.6 | Holston | 12p | | 54.9 | 21.2 | 0.0 | 0.1 | 0.0 | 0.1 | N/A | 0.1 | 1.7 | 0.2 | 0.7 | 2.9 | 0.0 | 0.0 | 13.4 | 0.9 | 0.0 | 0.0 | 3.7 |
| PVC-2E- | 22.6 | Holston | 12p | | 38.6 | 36.5 | 0.0 | 0.4 | 0.0 | 0.0 | N/A | 3.2 | 0.9 | 0.2 | 0.6 | 11.2 | 0.0 | 0.0 | 2.9 | 1.6 | 0.0 | 0.0 | 3.9 |
| PVC-2A | 24.6 | Holston | 12p | | 38.0 | 37.8 | 0.0 | 0.3 | 0.0 | 0.9 | N/A | 0.3 | 0.0 | 0.0 | 5.0 | 12.9 | 0.0 | 0.0 | 2.1 | 0.5 | 0.0 | 0.0 | 2.5 |
| PVC-2A | 24.9 | Holston | 12p | | 46.9 | 32.2 | 0.0 | 0.6 | 0.0 | 0.4 | N/A | 0.0 | 1.5 | 0.2 | 6.4 | 9.7 | 0.0 | 0.0 | 0.7 | 0.4 | 0.0 | 0.0 | 1.0 |
| PVC-2G | 26.6 | Holston | 12p | | 22.0 | 56.7 | 0.0 | 0.0 | 0.0 | 0.0 | N/A | 0.5 | 1.8 | 0.3 | 0.8 | 12.2 | 0.0 | 0.0 | 2.3 | 0.8 | 0.0 | 0.0 | 2.5 |
| PVC-2H | 27.6 | Holston | 12p | | 31.5 | 30.5 | 0.0 | 0.7 | 0.0 | 0.0 | N/A | 0.4 | 0.0 | 0.0 | 0.2 | 27.5 | 0.0 | 0.0 | 4.7 | 2.1 | 0.0 | 0.0 | 2.5 |
| CS-37 | 121.6 | Linc. | 11 | | 14.9 | 42.1 | 0.0 | 0.0 | 0.0 | 0.3 | N/A | 1.0 | 0.7 | 0.3 | 9.2 | 5.0 | 3.0 | 0.0 | 0.0 | 4.2 | 0.0 | 0.5 | 19.1 |
| CS-40 | 132.3 | Linc. | 12g | | 6.3 | 41.0 | 0.0 | 1.4 | 0.0 | 0.2 | N/A | 0.4 | 2.2 | 0.0 | 23.8 | 12.3 | 2.7 | 2.0 | 0.0 | 3.4 | 0.4 | 0.5 | 3.6 |
| CS-41 | 136.3 | Linc. | 10 | | 13.5 | 43.1 | 0.0 | 0.2 | 0.0 | 0.2 | N/A | 0.4 | 0.7 | 0.0 | 19.6 | 11.3 | 0.0 | 0.0 | 0.0 | 3.8 | 0.2 | 0.0 | 7.1 |
| CS-43 | 138.2 | Linc. | 12g | 10.0 | 11.0 | 45.2 | 1.3 | 1.3 | 0.0 | 0.2 | N/A | 0.2 | 0.6 | 0.0 | 24.5 | 12.3 | 0.4 | 0.0 | 0.0 | 2.4 | 0.0 | 0.0 | 0.7 |
| CS-42 | 141.1 | Rockdell | 10 | | 51.1 | 21.5 | 0.0 | 0.2 | 0.0 | 0.0 | N/A | 0.2 | 0.0 | 0.2 | 0.7 | 21.5 | 0.0 | 0.0 | 0.0 | 0.9 | 0.0 | 0.0 | 3.6 |
| CS-44 | 143.5 | Rockdell | 12g | | 49.4 | 29.8 | 0.0 | 0.0 | 0.0 | 0.0 | N/A | 0.0 | 0.0 | 0.0 | 6.9 | 9.5 | 0.7 | 0.0 | 0.5 | 1.6 | 0.2 | 0.0 | 1.4 |
| CS-45 | 152.4 | Rockdell | 12g | | 13.4 | 42.2 | 1.1 | 0.2 | 0.0 | 0.0 | N/A | 0.4 | 0.4 | 0.4 | 27.2 | 6.1 | 0.0 | 0.0 | 0.0 | 4.5 | 0.2 | 0.0 | 4.1 |
| CS-49 | 174.7 | Rockdell | 22 | | 52.8 | 29.5 | 0.0 | 0.0 | 0.0 | 0.0 | N/A | 0.2 | 0.0 | 0.0 | 2.5 | 10.9 | 0.0 | 0.0 | 1.4 | 2.7 | 0.0 | 0.0 | 0.0 |
| CS-51 | 179.7 | Rockdell | 19l | | 51.8 | 26.6 | 0.0 | 0.7 | 0.0 | 0.2 | N/A | 0.0 | 0.2 | 0.2 | 9.6 | 8.2 | 0.0 | 0.0 | 0.0 | 1.4 | 0.0 | 0.0 | 1.0 |
| CS-52 | 182.4 | Rockdell | 13 | | 41.5 | 49.2 | 0.0 | 0.7 | 0.0 | 0.2 | N/A | 0.0 | 0.0 | 0.0 | 0.0 | 3.3 | 0.0 | 0.0 | 0.0 | 1.4 | 0.0 | 0.0 | 3.6 |
| CS-53 | 188.2 | Rockdell | 12g | 10.0 | 46.6 | 37.6 | 0.0 | 0.0 | 0.0 | 0.0 | N/A | 0.5 | 0.5 | 0.0 | 3.0 | 9.4 | 0.0 | 0.0 | 0.2 | 1.6 | 0.0 | 0.0 | 0.7 |
| CS-54 | 193.3 | Rockdell | 22 | 19l/19 | 10.6 | 50.6 | 0.0 | 0.0 | 0.0 | 0.6 | N/A | 0.8 | 0.4 | 0.2 | 16.9 | 16.5 | 0.0 | 0.0 | 0.0 | 0.0 | 3.0 | 0.0 | 0.6 |
| CS-55 | 197.9 | Rockdell | 13 | | 22.0 | 43.7 | 0.0 | 0.6 | 0.0 | 0.4 | N/A | 0.2 | 0.6 | 0.2 | 12.3 | 14.0 | 0.0 | 0.0 | 0.4 | 3.4 | 0.0 | 0.0 | 2.4 |
| CS-58 | 204.5 | Rockdell | 10 | 12g | 13.3 | 52.8 | 0.0 | 0.9 | 0.0 | 0.2 | N/A | 0.9 | 0.5 | 0.0 | 12.9 | 14.4 | 0.2 | 0.0 | 0.0 | 2.1 | 0.5 | 0.0 | 1.2 |
| CS-59 | 208.1 | Rockdell | 17 | | 4.6 | 39.6 | 0.9 | 0.0 | 0.0 | 0.4 | N/A | 0.2 | 1.5 | 0.0 | 35.7 | 9.0 | 0.0 | 0.0 | 0.0 | 3.7 | 0.6 | 0.0 | 4.0 |
| CS-57 | 209.7 | Rockdell | 8 | 9.0 | 51.9 | 41.2 | 0.0 | 1.6 | 0.0 | 1.2 | N/A | 0.0 | 0.0 | 0.0 | 0.5 | 1.4 | 0.0 | 0.0 | 0.0 | 2.1 | 0.0 | 0.0 | 0.2 |
| CS-60 | 212.9 | Rockdell | 10 | | 7.8 | 42.3 | 0.0 | 0.0 | 0.0 | 0.4 | N/A | 0.9 | 1.1 | 0.0 | 18.8 | 24.0 | 0.0 | 0.0 | 0.0 | 2.6 | 0.0 | 0.0 | 2.2 |

| Shelf and Shelf-Edge Point-Count Data In Volume Percent From The Thorn Hill Area, After Ruppel (1979) | | | | | | | | | | | | | | | | | | | | | | |
|---|---|---|---|---|---|---|---|---|---|---|---|---|---|---|---|---|---|---|---|---|---|---|
| Sample Number | Strat. Position | Fm. | Dom. Facies | Sub. Facies | Mic | Spar | Intra | Pel | Oo | Brach | Gast | Ostra | Tri | Moll | Ech | Bry | Alg | On | Sp | Other Foss | Dolo | Qtz | Oth |
| CS-1 | <1.5 | Five Oak | 19 | | 48.3 | 31.0 | | | | | | | | | | | | | | | 20.8 | | |
| CS-8 | 5.5 | Five Oak | 16 | | 8.3 | 24.3 | | | | | 37.5 | 0.3 | | | 0.3 | | 0.3 | | | 6.5 | 20.5 | | |
| CS-20 | 16 | Five Oak | 19l | 19f | 45.3 | 47.3 | | | | | | | | | 0.5 | 0.3 | | | | 5.0 | | | 1.8 |
| CS-25 | 24 | Linc. | 12p | | 9.8 | 31.3 | | 2.0 | | | | 0.8 | | | 34.3 | 6.5 | 15.4 | | | | | | |
| CS-32 | 40.5 | Linc. | 11 | | 5.0 | 40.5 | | | | 0.8 | | | 1.3 | | 21.3 | 13.3 | 15.0 | | | | 1.8 | | 1.3 |
| CS-33 | 46.5 | Linc. | 11 | | 5.8 | 41.3 | | | | | | | 1.5 | | 34.0 | 16.5 | 1.0 | | | | | | |
| CS-38 | 67 | Linc. | 12g | | 5.5 | 32.3 | | | | | | | 1.0 | | 14.3 | 46.8 | 0.3 | | | | | | |
| CS-55 | 133 | Linc. | 13 | | 9.0 | 33.5 | | | | | 0.3 | 0.8 | 1.5 | 0.5 | 23.0 | 12.8 | 13.3 | | | | 3.8 | | 1.8 |
| CS-64 | 155.5 | Rockdell | 10 | | 15.3 | 28.0 | 5.0 | 4.3 | | | 1.5 | 2.0 | | | 30.5 | 11.8 | 1.8 | | | | | | |
| CS-69 | 168 | Rockdell | 12p | 12g | 39.0 | 20.8 | | | | 0.5 | 1.8 | 0.8 | 0.5 | | 18.5 | 13.0 | | | | 0.5 | 4.8 | | 4.8 |
| CS-81 | 238.5 | Benbolt | 12g | 12p | 14.0 | 51.5 | | | | 0.8 | | 0.3 | 1.3 | | 19.8 | 7.3 | | | | 2.0 | | | 0.8 |
| CS-87 | 255.3 | Benbolt | 9 | ?19 | 57.3 | 22.3 | | | | 2.5 | | 3.8 | 4.5 | | 5.8 | | | | 1.3 | 1.0 | | | 3.8 |
| CS-92 | 282.5 | Benbolt | 12g | 16.0 | 4.5 | 46.5 | 1.8 | | | | 2.3 | 6.5 | 0.3 | | 30.5 | 6.5 | | | | 1.3 | | | |
| CS-103 | 315.7 | ?Wardell | 12p | 22.0 | 35.0 | 10.8 | | | | 0.3 | | 1.3 | 0.8 | | 20.8 | 24.3 | | | T | 2.8 | 0.5 | | 3.8 |
| CS-104 | 321.3 | Wardell | 9 | 47.75 | 8.5 | | | | | | | 0.8 | 0.3 | | 12 | 8 | | | 15 | | | | 8.5 |
| CS-107A | 332.8 | Wardell | 9 | 19 | 11 | 30 | | | | 0.3 | 0.3 | 3.8 | 1.5 | | 38 | 16 | | | 0.3 | 1 | | | |
| CS-120 | <393 | Witten | 22 | | 16.0 | 38.3 | | | | 3.5 | 0.8 | 2.8 | 3.8 | | 9.0 | 16.3 | | | 1.0 | 3.0 | | 5.7 | |
| CS-123 | 398 | Witten | 22 | | 53.8 | 2.8 | | | | 0.3 | 0.8 | 2.0 | 2.0 | | 10.8 | 13.8 | | 0.5 | | 9.3 | | | 4.0 |
| CS-129 | 422.1 | Witten | 9 | 22.0 | 30.5 | 5.0 | | | | 0.5 | | 1.8 | 0.8 | | 16.5 | 39.8 | | | 3.3 | 2.0 | | | |
| IS-17-3 | 208 | Rockdell | 9 | | 44.0 | 21.8 | | | | | | | 0.5 | | 9.3 | 15.3 | | | | 9.3 | | | |
| IS-24-1 | 311 | Benbolt | 12g | 16.0 | 16.8 | 34.5 | | 0.5 | | 1.0 | 0.8 | 2.8 | 6.0 | | 25.8 | 8.5 | | | 3.5 | | | | |
| RHB-6-1 | <130.5 | Holston | 12p | | 24.8 | 7.5 | | | | 0.3 | | | 0.8 | | 7.8 | 50.0 | | | | 0.5 | 0.5 | | 8.0 |

| Sample Number | Strat. Position | Fm. | Dom. Facies | Sub. Facies | Mic | Spar | Intra | Pel | Oo | Brach | Gast | Ostra | Tri | Moll | Ech | Bry | Alg | On | Sp | Other Foss | Dolo | Qtz | Oth |
|---|---|---|---|---|---|---|---|---|---|---|---|---|---|---|---|---|---|---|---|---|---|---|---|
| RHB-6-2 | <130.5 | Holston | 12g | | | 2.5 | | | | | | | 0.8 | | 12.0 | 70.0 | | | | | 0.8 | | 14.0 |
| PVC-2 | <20.1 | Holston | 12p | | 35.0 | 22.8 | | | | 1.8 | | 0.3 | 1.0 | | 14.0 | 20.8 | | | | 1.3 | 0.3 | | 3.0 |
| PVC-3 | <20.1 | Holston | 12p | | 61.3 | 6.8 | | | | | | 1.0 | T | | 8.8 | 21.5 | | | | 1.5 | | | 1.3 |
| PVC-8 | <45.0 | Holston | 12g | | | 48.0 | | | | | | | | | 22.3 | 27.5 | | | | | | | 2.3 |

# APPENDIX C

## INTERPRETED WATER-DEPTHS

## EXPLANATION

A range of possible water-depths during the time of deposition was determined for each thin-section using the criteria presented in figures 2.2 and 2.3 of Chapter 2. Possible water-depth ranges are presented graphically in figures 2.4A, 2.4B, and 2.12 through 2.18 of Chapter 2; and figures 3.8 through 3.12 of Chapter 3. Appendix C expressed these possible water-depth ranges numerically as "Depth Minimum" and "Depth Maximum."

| Thorn Hill Section Sample Number | Stratigraphic Position (m) | Depth Minimum | Depth Maximum | Dominant Facies | Subordinate Facies |
|---|---|---|---|---|---|
| TH-90-555A | 23.0 | 0.0 | -20.0 | 12g | |
| TH-90-555B | 23.0 | 0.0 | -20.0 | 12p | |
| TH-90-556 | 24.4 | -2.0 | -10.0 | 17 | |
| TH-90-557 | 27.6 | 0.0 | -2.0 | 17 | |
| TH-90-558 | 30.4 | 0.0 | -30.0 | 16 | |
| TH-90-559 | 32.4 | 0.0 | -15.0 | 12g | |
| TH-90-560A and B | 35.0 | -0.5 | -30.0 | 12g | |
| TH-90-450 | 77.0 | -0.5 | -20.0 | 11 | |
| TH-90-449 | 78.5 | 0.0 | -3.0 | 11 | 17 |
| TH-90-448 | 80.4 | -15.0 | -30.0 | 18 | |
| TH-90-447 | 81.8 | 0.0 | -20.0 | 12p | |
| TH-90-446 | 83.6 | 0.0 | -15.0 | 18 | |
| TH-90-446.5 | 84.4 | -2.0 | -10.0 | 11 | |
| TH-90-445 | 85.2 | -0.5 | -15.0 | 18 | |
| TH-90-444 | 86.2 | -0.5 | -15.0 | 11 | |
| TH-89-1 | 86.2 | -0.5 | -15.0 | 18 | |
| TH-89-2 | 91.5 | -0.5 | -15.0 | 12g | |
| TH-89-3A | 92.3 | -0.5 | -10.0 | 12g | |
| TH-89-3B | 92.3 | -4.0 | -10.0 | 16 | 17 |
| TH-89-4 | 94.7 | -2.0 | -30.0 | 12p | 21 |
| TH-89-5 | 95.1 | -4.0 | -15.0 | 9 | |
| TH-89-6 | 97.2 | 0.0 | -20.0 | 9 | |
| TH-89-7 | 99.2 | -0.5 | -30.0 | 9 | |
| TH-89-8 | 113.6 | -10.0 | -15.0 | 9 | |
| TH-89-9 | 115.1 | 0.0 | -15.0 | 19 | |
| TH-89-10 | 115.9 | -2.0 | -4.0 | 22 | |
| TH-89-11 | 116.9 | -0.5 | -4.0 | 17 | 22 |
| TH-89-12 | 117.3 | -1.0 | -4.0 | 17 | 22 |
| TH-89-13 | 118.8 | -1.0 | -4.0 | 17 | 22 |
| TH-89-14 | 119.2 | -1.0 | -4.0 | 22 | |
| TH-89-15 | 119.6 | -1.0 | -4.0 | 22 | |
| TH-89-16 | 120.9 | -1.0 | -4.0 | 19 | |
| TH-89-17N | 121.4 | -1.0 | -4.0 | 17 | |
| TH-89-18 | 122.2 | -1.0 | -4.0 | 17 | |
| TH-89-19 | 122.6 | -1.0 | -4.0 | 17 | 22 |

| Sample Number | Position (m) | Minimum | Maximum | Facies | Facies |
|---|---|---|---|---|---|
| TH-89-20 | 122.9 | 0.0 | 0.0 | | Lost |
| TH-89-21 | 123.2 | -2.0 | -4.0 | 17 | |
| TH-89-23 | 123.3 | -2.0 | -15.0 | 17 | |
| TH-89-22 | 123.7 | -0.5 | -10.0 | 16 | |
| TH-89-24 | 123.7 | -0.5 | -4.0 | 17 | |
| TH-89-25 | 125.0 | -0.5 | -10.0 | 16 | |
| TH-89-26 | 125.4 | -4.0 | -6.0 | 12g | |
| TH-89-27 | 125.5 | -4.0 | -20.0 | 12g | |
| TH-89-28 | 125.7 | -1.0 | -2.0 | 12g | |
| TH-89-29 | 126.9 | -1.0 | -10.0 | 17 | |
| TH-89-30 | 127.1 | 0.0 | -10.0 | 17 | |
| TH-89-31 | 128.6 | -0.5 | -4.0 | 17 | |
| TH-89-32 | 129.1 | -1.0 | -4.0 | 17 | |
| TH-89-33 | 129.4 | -0.5 | -4.0 | 17 | 22 |
| TH-89-34 | 129.5 | -0.5 | -4.0 | 17 | |
| TH-89-35 | 129.5 | 0.0 | 0.0 | | Lost |
| TH-89-36 | 132.0 | -1.0 | -4.0 | 17 | 22 |
| TH-89-37 | 133.7 | -0.5 | -2.0 | 17 | |
| TH-89-38 | 133.9 | -1.0 | -2.0 | 17 | |
| TH-89-39A | 134.1 | 0.0 | -4.0 | 16 | 17 |
| TH-89-39B | 134.1 | 0.0 | -4.0 | 16 | 17 |
| TH-89-40 | 134.7 | -0.5 | -2.0 | 17 | |
| TH-89-41 | 134.9 | -1.0 | -4.0 | 17 | |
| TH-89-42 | 136.7 | -1.0 | -4.0 | 17 | |
| Dog leg in section | | 0.0 | 0.0 | | |
| TH-89-43 | 136.7 | -1.0 | -3.0 | 17 | 16 |
| TH-89-44 | 139.9 | -1.0 | -4.0 | 17 | |
| TH-89-45 | 140.9 | -1.0 | -2.0 | 17 | |
| TH-89-46 | 141.3 | -2.0 | -3.0 | 17 | |
| TH-89-47 | 141.6 | -1.0 | -6.0 | 17 | |
| TH-89-48 | 142.2 | -1.0 | -3.0 | 17 | |
| TH-89-49A | 142.8 | -0.5 | -2.0 | 17 | |
| TH-89-49B | 142.8 | -0.5 | -2.0 | 17 | |
| TH-89-50 | 143.1 | -0.5 | -4.0 | 17 | |
| TH-89-51 | 143.9 | -1.0 | -10.0 | 16 | |
| TH-89-52 | 144.4 | 0.0 | -10.0 | 16 | |

| Sample Number | Position (m) | Minimum | Maximum | Facies | Facies |
|---|---|---|---|---|---|
| TH-89-53 | 152.3 | -0.5 | -4.0 | 11 | |
| TH-89-54 | 152.7 | -1.0 | -2.0 | 17 | |
| TH-89-55 | 153.2 | -1.0 | -6.0 | 11 | |
| TH-89-56 | 153.5 | -0.5 | -10.0 | 17 | |
| TH-89-57 | 153.9 | -2.0 | -6.0 | 9 | |
| TH-89-58 | 154.5 | -0.5 | -6.0 | 12p | |
| TH-89-58N | 154.5 | -0.5 | -6.0 | 12p | 17 |
| TH-89-59 | 156.8 | -0.5 | -3.0 | 12p | 17 |
| TH-89-60 | 155.3 | -0.5 | -15.0 | 12g | |
| TH-89-61 | 155.8 | -0.5 | -2.0 | 9 | |
| TH-89-62 | 156.5 | -0.5 | -6.0 | 12p | |
| TH-89-63 | 157.1 | -2.0 | -3.0 | 12p | |
| TH-89-64 | 158.4 | -1.0 | -6.0 | 9 | |
| TH-89-65 | 158.8 | 0.0 | -2.0 | 19 | 16 |
| TH-89-66B | 159.5 | -2.0 | -2.0 | 16 | 19 |
| TH-89-66T | 159.7 | -0.5 | -6.0 | 19f | |
| TH-89-67 | 160.9 | 0.0 | -6.0 | 19 | 9 |
| TH-89-68 | 161.4 | 0.0 | -2.0 | 19 | |
| TH-89-69 | 162.0 | 1.0 | -2.0 | 19 | |
| TH-89-70 | 162.9 | 1.0 | -2.0 | 19 | |
| TH-89-71 | 163.9 | -0.5 | -6.0 | 12g | |
| TH-89-72 | 164.4 | 0.0 | -20.0 | 12g | |
| TH-89-73 | 165.9 | -0.5 | -6.0 | 12g | 16 |
| TH-89-74 | 166.6 | 1.0 | -0.5 | 12p | |
| TH-89-75 | 167.8 | -0.5 | -4.0 | 17 | 12g |
| TH-89-76B | 168.1 | -0.5 | -6.0 | 12p | 12g |
| TH-89-76T | 168.2 | 1.0 | -6.0 | 19 | 8 |
| TH-89-77A | 168.8 | -0.5 | -2.0 | 19f | |
| TH-89-77B | 168.8 | -0.5 | -2.0 | 19 | 9 |
| TH-89-78 | N/A | N/A | N/A | Lost | |
| TH-89-79 | 169.3 | -0.5 | -6.0 | 12g | 12p |
| TH-89-80 | 170.0 | -0.5 | -6.0 | 12 | 16 |
| TH-89-81 | 170.4 | -0.5 | -15.0 | 12g | |
| TH-89-82 | 170.8 | -0.5 | -4.0 | 16 | |
| TH-89-83 | 172.4 | -1.0 | -4.0 | 12 | 16 |
| TH-89-84A | 175.2 | -0.5 | -3.0 | 12p | |

| Sample Number | Position (m) | Minimum | Maximum | Facies | Facies |
|---|---|---|---|---|---|
| TH-89-85 | 176.3 | -0.5 | -10.0 | 12p | |
| TH-89-86 | 177.1 | -0.5 | -10.0 | 12g | 16 |
| TH-89-87A | 177.2 | -2.0 | -2.0 | 12p | 12g |
| TH-89-87B | 177.2 | -2.0 | -2.0 | 12p | 12g |
| TH-89-88 | 177.7 | -0.5 | -15.0 | 12p | |
| TH-89-89A | 178.5 | -0.5 | -2.0 | 12p | |
| TH-89-89B | 178.5 | -0.5 | -2.0 | 12p | |
| TH-89-90 | 179.0 | -0.5 | -15.0 | 9 | 12 |
| TH-89-91A | 179.5 | 0.0 | -2.0 | 19 | |
| TH-89-91B | 179.5 | 0.0 | -2.0 | 19 | 9 |
| TH-89-92A | 180.9 | 0.0 | -2.0 | 19l | |
| TH-89-92B | 180.9 | 0.0 | -2.0 | 19f | |
| TH-89-93 | 182.8 | -0.5 | -6.0 | 9 | |
| TH-89-94 | 183.1 | 0.0 | -2.0 | 19f | |
| TH-89-95A | 184.9 | 0.0 | -2.0 | 19 | |
| TH-89-95B | 184.9 | 0.0 | -2.0 | 19 | |
| TH-89-95C | 184.9 | 0.0 | -2.0 | 19 | ?A |
| TH-89-96 | 185.5 | 0.0 | -2.0 | 19fl | |
| TH-89-97A | 185.9 | 0.0 | -2.0 | 19f | |
| TH-89-97B | 185.9 | 0.0 | -2.0 | 19f | 19l |
| TH-89-98A | 187.1 | -0.5 | -6.0 | 9 | 12p |
| TH-89-98B | 187.1 | -0.5 | -6.0 | 9 | |
| TH-89-99 | 187.6 | 1.0 | -6.0 | 9 | 19 |
| TH-89-100A | 187.8 | 0.0 | -2.0 | 16 | 19l |
| TH-89-100B | 187.8 | 0.0 | -2.0 | 16 | 19l |
| TH-89-101 | 188.3 | 0.0 | -15.0 | 12g | 16 |
| TH-89-102 | 189.3 | -2.0 | -4.0 | 16 | |
| TH-89-103 | 189.6 | 0.0 | -15.0 | 12g | |
| TH-89-104 | 190.6 | -0.5 | -3.0 | 12g | |
| TH-89-105A | 191.7 | 0.0 | -2.0 | 13 | |
| TH-89-105B | 191.7 | 0.0 | -2.0 | 13 | |
| TH-89-106 | 195.7 | -2.0 | -20.0 | 12g | |
| TH-89-107B | 196.1 | -0.5 | -15.0 | 12p | |
| TH-89-107T | 196.1 | -0.5 | -15.0 | 19 | |
| TH-89-108 | 196.1 | 1.0 | -6.0 | 12g | |
| TH-89-109 | 196.6 | -0.5 | -20.0 | 12p | 12g |

| Sample Number | Position (m) | Minimum | Maximum | Facies | Facies |
|---|---|---|---|---|---|
| TH-89-110 | 197.6 | -0.5 | -6.0 | 12p | |
| TH-89-111A | 198.7 | -0.5 | -20.0 | 12p | |
| TH-89-111B | 198.7 | -0.5 | -20.0 | 12p | |
| TH-89-112 | 199.1 | -0.5 | -20.0 | 12p | |
| TH-89-113A | 200.5 | -0.5 | -6.0 | 12p | |
| TH-89-113B | 200.5 | -0.5 | -6.0 | 12p | |
| TH-89-114 | 201.3 | -0.5 | -20.0 | 12g | 12p |
| TH-89-115 | 202.9 | -0.5 | -20.0 | 9 | |
| TH-89-116 | 203.8 | -2.0 | -4.0 | 12p | 12g |
| TH-89-117 | 204.3 | -2.0 | -15.0 | 9 | |
| TH-89-118 | 204.5 | -2.0 | -20.0 | 9 | |
| TH-89-119 | 205.6 | -30.0 | -20.0 | 8 | |
| TH-89-120 | 208.2 | -2.0 | -20.0 | 8 | |
| TH-89-121 | 209.6 | -2.0 | -30.0 | 9 | |
| TH-89-122 | 210.2 | -0.5 | -30.0 | 9 | 19 |
| TH-89-123 | 211.3 | -15.0 | -15.0 | 9 | |
| TH-89-124 | 211.7 | -2.0 | -6.0 | 8 | 9 |
| TH-89-125 | 212.3 | -2.0 | -6.0 | 9 | |
| TH-89-126 | 212.8 | -0.5 | -6.0 | 8 | 9 |
| TH-89-127 | 213.5 | -2.0 | -6.0 | 9 | 8 |
| TH-89-128 | 214.1 | -2.0 | -6.0 | 9 | |
| TH-89-129 | 214.9 | -0.5 | -15.0 | 12g | 12p |
| TH-89-130 | 216.4 | -2.0 | -15.0 | 9 | |
| TH-89-131 | 217.2 | -0.5 | -6.0 | 8 | 9 |
| TH-89-132 | 217.2 | -2.0 | -6.0 | 9 | 8 |
| TH-89-133 | 217.9 | N/A | N/A | Lost | |
| TH-89-134 | 218.4 | 0.0 | -6.0 | 8 | |
| TH-89-135 | 219.7 | -2.0 | -6.0 | 9 | |
| TH-89-136 | 220.6 | -2.0 | -6.0 | 8 | |
| TH-89-137A | 221.2 | -2.0 | -6.0 | 9 | |
| TH-89-137B | 221.2 | -2.0 | -6.0 | 9 | |
| TH-89-138 | 221.5 | -0.5 | -15.0 | 9 | 8 |
| TH-89-139 | 223.1 | -0.5 | -15.0 | 12g | 12p |
| TH-89-140 | 223.3 | -2.0 | -15.0 | 9 | 12p |
| TH-89-141A | 224.2 | -0.5 | -20.0 | 12p | 8 |
| TH-89-141B | 224.2 | -0.5 | -20.0 | 12p | 8 |

| Sample Number | Position (m) | Minimum | Maximum | Facies | Facies |
|---|---|---|---|---|---|
| TH-89-142 | 224.4 | -0.5 | -15.0 | 12p | |
| TH-89-143 | 224.9 | -0.5 | -15.0 | 12g | |
| TH-89-144 | 225.5 | -0.5 | -15.0 | 12p | |
| TH-89-145A | 225.7 | 0.0 | -20.0 | 10 | |
| TH-89-145B | 225.7 | 0.0 | -20.0 | 10 | |
| TH-89-146 | 225.8 | -0.5 | -15.0 | 14 | |
| TH-89-147 | 226.0 | -0.5 | -15.0 | 9 | |
| TH-89-148 | 226.9 | -0.5 | -15.0 | 12g | 12p |
| TH-89-149 | 227.1 | -1.0 | -15.0 | 12g | |
| TH-89-150 | 228.0 | -0.5 | -6.0 | 12p | 12g |
| TH-89-151 | 228.4 | -0.5 | -6.0 | 12p | |
| TH-89-152 | 229.0 | -0.5 | -20.0 | 12p | |
| TH-89-153 | 229.5 | -0.5 | -15.0 | 12p | |
| TH-89-154 | 229.6 | 0.0 | -20.0 | 12g | |
| TH-89-155B | 230.6 | -0.5 | -6.0 | 10 | |
| TH-89-155T | 230.6 | -0.5 | -6.0 | 12p | 12g |
| TH-89-156A | 230.9 | -0.5 | -2.0 | 19 | 8 |
| TH-89-156B | 230.9 | -0.5 | -2.0 | 8 | |
| TH-89-157 | 231.2 | -0.5 | -15.0 | 8 | |
| TH-89-158 | 231.9 | -1.0 | -15.0 | 12g | 12p |
| TH-89-159 | 232.2 | -0.5 | -6.0 | 12p | 9 |
| TH-89-160N | 233.3 | 0.0 | -6.0 | 8 | 9 |
| TH-89-161 | 234.0 | -0.5 | -15.0 | 8 | |
| TH-89-162 | 235.6 | -1.0 | -20.0 | 12p | |
| TH-89-163 | 236.2 | -1.0 | -15.0 | 12p | |
| TH-89-164A | 236.7 | -0.5 | -2.0 | 12p | 12g |
| TH-89-164B | 236.7 | -0.5 | -2.0 | 12p | 12g |
| TH-89-165 | 239.3 | -1.0 | -3.0 | 12p | 12g |
| TH-89-166 | 240.3 | -0.5 | -3.0 | 12p | |
| TH-89-167 | 241.0 | -0.5 | -6.0 | 10 | 13 |
| TH-89-168 | 241.5 | -0.5 | -3.0 | 22 | |
| TH-89-169 | 242.8 | -0.5 | -10.0 | 13 | 10 |
| TH-89-170 | 244.2 | -0.5 | -6.0 | 22 | |
| TH-89-171 | 244.5 | -2.0 | -3.0 | 10 | |
| TH-88-4B | 244.6 | -0.5 | -4.0 | 22 | |
| TH-88-4T | 244.6 | -0.5 | -4.0 | 10 | |

| Sample Number | Position (m) | Minimum | Maximum | Facies | Facies |
|---|---|---|---|---|---|
| TH-88-5 | 245.3 | N/A | N/A | N/A | ?22 |
| TH-89-172 | 246.4 | 0.0 | -6.0 | 12p | |
| TH-88-6 | 247.6 | -0.5 | -6.0 | 22 | 8 |
| TH-89-173 | 248.7 | 0.0 | -20.0 | 22 | 10 |
| TH-88-7 | 249.3 | -0.5 | -30.0 | 8 | |
| TH-88-8 | 249.3 | 0.0 | -2.0 | 22 | 10 |
| TH-89-9A | 249.7 | -0.5 | -15.0 | 10 | |
| TH-89-9B | 249.7 | -0.5 | -4.0 | 10 | |
| TH-89-174 | 250.0 | -0.5 | -4.0 | 22 | |
| TH-88-10A | 250.8 | -0.5 | -6.0 | 8 | |
| TH-88-10B | 250.8 | -0.5 | -6.0 | 8 | |
| TH-88-11 | 250.8 | -0.5 | -4.0 | 10 | |
| TH-88-12 | 251.6 | -0.5 | -3.0 | 22 | 10 |
| TH-89-175 | 252.4 | -0.5 | -4.0 | 10 | |
| TH-89-176 | 252.7 | -0.5 | -3.0 | 10 | 14 |
| TH-89-177 | 252.9 | -0.5 | -4.0 | 8 | 9 |
| TH-89-178 | 253.8 | -0.5 | -3.0 | 12p | 10 |
| TH-89-179 | 254.6 | -0.5 | -4.0 | 12p | 12g |
| TH-89-180 | 255.2 | 0.0 | -15.0 | 9 | 8 |
| TH-89-181 | 256.7 | -0.5 | -4.0 | 9 | |
| TH-89-182 | 256.7 | -0.5 | -6.0 | 9 | |
| TH-89-183 | 257.5 | 0.0 | -3.0 | 18 | |
| TH-89-184 | 257.8 | -2.0 | -6.0 | 9 | |
| TH-89-185A | 258.2 | -2.0 | -10.0 | 9 | |
| TH-89-185B | 258.2 | -2.0 | -10.0 | 9 | 8 |
| TH-89-186 | 258.4 | 0.0 | -15.0 | 12p | 9 |
| TH-89-187 | 258.7 | 0.0 | -4.0 | 22 | 10 |
| TH-89-188 | 260.1 | -0.5 | -3.0 | 10 | 22 |
| TH-89-189A | 260.5 | -0.5 | -3.0 | 12p | 22 |
| TH-89-189B | 260.5 | -0.5 | -3.0 | 12p | 22 |
| TH-89-190A | 261.6 | -0.5 | -6.0 | 9 | 12p |
| TH-89-190B | 261.6 | -0.5 | -6.0 | 9 | 12p |
| TH-89-191A | 262.5 | -0.5 | -15.0 | 12p | 12g |
| TH-89-191B | 262.5 | -0.5 | -15.0 | 12p | 12g |
| TH-89-192A | 263.4 | -1.0 | -30.0 | 9 | |
| TH-89-192B | 263.4 | -1.0 | -30.0 | 9 | |

| Sample Number | Position (m) | Minimum | Maximum | Facies | Facies |
|---|---|---|---|---|---|
| TH-89-193A | 264.1 | -2.0 | -2.0 | 22 | |
| TH-89-193B | 264.1 | -2.0 | -2.0 | 22 | |
| TH-89-194 | 266.3 | 0.0 | -15.0 | 9 | |
| TH-89-195A | 266.7 | -0.5 | -10.0 | 10 | 12g |
| TH-89-195B | 266.7 | -0.5 | -10.0 | 10 | 12g |
| TH-89-196 | 267.2 | -0.5 | -20.0 | 12g | |
| TH-90-197 | 268.4 | -0.5 | -15.0 | 12g | 12p |
| TH-90-198 | 269.4 | -2.0 | -15.0 | 12g | |
| TH-90-199 | 271.0 | -0.5 | -6.0 | 8 | 9 |
| TH-90-200 | 272.5 | -0.5 | -20.0 | 12g | |
| TH-90-201 | 273.3 | -0.5 | -15.0 | 12g | |
| TH-99-202 | 275.1 | -1.0 | -20.0 | 12p | |
| TH-90-203 | 282.2 | -0.5 | -15.0 | 12g | 12p |
| TH-90-204 | 283.6 | 1.0 | -0.5 | 12p | |
| TH-90-205A | 285.8 | 0.0 | -0.5 | 8 | 9 |
| TH-90-205B | 285.8 | 0.0 | -0.5 | 8 | 9 |
| TH-90-206 | 287.6 | 0.0 | -0.5 | 8 | 9 |
| TH-90-207 | 289.8 | 0.0 | -20.0 | 12p | |
| TH-90-208 | 292.9 | -0.5 | -6.0 | 12p | 18 |
| TH-90-209A | 293.8 | -0.5 | -15.0 | 9 | 12p |
| TH-90-209B | 293.8 | -0.5 | -15.0 | 9 | 8 |
| TH-90-210 | 295.6 | -0.5 | -15.0 | 10 | |
| TH-90-211 | 295.8 | 0.0 | -15.0 | 12g | |
| TH-90-212A | 298.8 | -0.5 | -15.0 | 12p | 9 |
| TH-90-212B | 298.8 | -0.5 | -15.0 | 12p | |
| TH-90-213 | 304.3 | -0.5 | -15.0 | 12p | |
| TH-90-214 | 308.8 | -0.5 | -6.0 | 9 | |
| TH-90-215 | 311.8 | -1.0 | -4.0 | 12p | 9 |
| TH-90-216 | 313.1 | -1.0 | -30.0 | 12p | |
| TH-90-217A | 314.3 | -2.0 | -30.0 | 9 | |
| TH-90-217B | 314.3 | -2.0 | -30.0 | 9 | |
| TH-90-218A | 318.0 | -2.0 | -6.0 | 9 | 12p |
| TH-90-218B | 318.0 | -2.0 | -6.0 | 9 | 12p |
| TH-90-219A | 319.9 | -0.5 | -20.0 | 12g | 10 |
| TH-90-219A | 319.9 | -0.5 | -20.0 | 12g | 10 |

| Old Thorn Hill Section Sample Number | Stratigraphic Position (m) | Depth Minimum | Depth Maximum | Dominant Facies | Subordinate Facies |
|---|---|---|---|---|---|
| "TH-1.1" | -0.3 | 1.5 | 0.0 | dolo | |
| "TH-2.4" | 1.0 | 1.5 | 0.0 | 19f | |
| "TH-3.0" | 1.6 | 1.5 | 0.0 | 19f | |
| "TH-4.4" | 3.0 | 1.5 | 0.0 | 19f | |
| "TH-5.7" | 4.3 | 1.5 | 0.0 | 19f | |
| "TH-6.8" | 5.4 | 1.5 | 0.0 | 19f | |
| "TH-7.4" | 6.0 | 1.5 | 0.0 | 19f | |
| "TH-9.4" | 8.0 | 1.5 | 0.0 | 19f | |
| "TH-10.4" | 9.0 | 1.5 | 0.0 | 19f | |
| "TH-13.2" | 11.8 | 1.5 | -15.0 | 19f | |
| "TH-13.2" | 11.8 | 1.5 | -6.0 | 19f | |
| "TH-14.0" | 12.6 | -0.5 | -10.0 | 16 | 18 |
| "TH-14.1" | 12.7 | -0.5 | -10.0 | 18 | 24 |
| "TH-15.0" | 13.6 | -0.5 | -6.0 | 16 | 24 |
| "TH-16.0" | 14.6 | 1.5 | -0.5 | 19f | 16 |
| "TH-16.3" | 14.9 | 1.5 | -15.0 | 19f | |
| "TH-20.3" | 18.9 | 1.5 | -0.5 | 19f | 24 |
| "TH-21.6" | 20.2 | 1.5 | -0.5 | 19f | |
| "TH-22.6" | 21.2 | 1.5 | -0.5 | 19f | |
| "TH-23.4" | 22.0 | 1.5 | -0.5 | 19f | |
| "TH-23.6" | 22.2 | 1.5 | -0.5 | 19f | |
| "TH-23.8" | 22.4 | -0.5 | -10.0 | 16 | |
| OTH-90-0A | 28.1 | -0.5 | -10.0 | 16 | |
| OTH-90-0B | 28.1 | -0.5 | -10.0 | 16 | |
| OTH-90-299 | 40.6 | 0.0 | -10.0 | 16 | |
| OTH-90-300 | 48.1 | -0.5 | -6.0 | 12 | 16 |
| OTH-90-301 | 49.5 | -0.5 | -20.0 | 12p | 17 |
| OTH-90-302 | 50.5 | -0.5 | -20.0 | 12 | 17 |
| OTH-90-303 | 50.7 | 0.0 | -20.0 | 9 | 12p |
| OTH-90-304 | 52.5 | -0.5 | -20.0 | 12pg | |
| OTH-90-305 | 53.7 | -0.5 | -10.0 | 12 | 17 |
| OTH-90-306 | 54.9 | -0.5 | -20.0 | 12g | |
| OTH-90-307A | 55.4 | -0.5 | -10.0 | 12g | 17 |
| OTH-90-307B | 55.4 | -0.5 | -20.0 | 12g | 17 |
| OTH-90-308 | 58.4 | -0.5 | -20.0 | 12g | |

| Sample Number | Position (m) | Minimum | Maximum | Facies | Facies |
|---|---|---|---|---|---|
| OTH-90-309 | 60.4 | -0.5 | -20.0 | 12g | |
| OTH-90-90-1 | 62.6 | -0.5 | -20.0 | 12g | |
| OTH-90-2A | 74.1 | -2.0 | -20.0 | 12g | |
| OTH-90-2A | 74.1 | -2.0 | -20.0 | 12g | |
| OTH-90-3 | 80.7 | -0.5 | -20.0 | 12g | |
| OTH-90-4 | 84.5 | -0.5 | -10.0 | 12g | |
| OTH-90-5A | 87.2 | -1.0 | -15.0 | 12 | 16 |
| OTH-90-5B | 87.2 | -1.0 | -15.0 | 12 | 16 |
| OTH-90-6 | 89.5 | -0.5 | -20.0 | 12 | 16 |
| OTH-90-7 | 94.2 | -0.5 | -6.0 | 17 | |
| OTH-90-8 | 94.9 | -0.5 | -20.0 | 12g | |
| OTH-90-9 | 96.7 | -0.5 | -20.0 | 12g | 16 |
| OTH-90-10 | 100.7 | -0.5 | -20.0 | 12g | |
| OTH-90-11 | 105.8 | 0.0 | -15.0 | 16 | |
| OTH-90-12 | 111.9 | -1.0 | -3.0 | 9 | |
| OTH-90-13 | 114.3 | 0.0 | -15.0 | 16 | |
| OTH-90-14 | 116.3 | 0.0 | -20.0 | 9 | |
| OTH-90-15 | 118.3 | -0.5 | -10.0 | 12g | 16 |
| OTH-90-16 | 121.9 | -0.5 | -10.0 | 16 | |
| OTH-90-17 | 127.4 | -1.0 | -15.0 | 12 | 17 |
| OTH-90-18 | 129.9 | -0.5 | -15.0 | 12 | |
| OTH-90-19 | 131.4 | -0.5 | -15.0 | 12g | |
| OTH-90-20A | 140.4 | -0.5 | -2.0 | 22 | |
| OTH-90-20B | 140.4 | -0.5 | -2.0 | 22 | |
| OTH-90-21 | 141.3 | 0.0 | -2.0 | 21 | |
| OTH-90-22 | 141.6 | 0.0 | -10.0 | 16 | |
| OTH-90-23 | 179.1 | -1.0 | -2.0 | 17 | |
| OTH-90-24 | 180.6 | -1.0 | -4.0 | 17 | 12p |
| OTH-90-25 | 183.1 | 0.0 | -10.0 | 9 | |
| OTH-90-26 | 186.5 | -2.0 | -4.0 | 17 | 22 |
| OTH-90-27 | 186.7 | -1.0 | -2.0 | 17 | |
| OTH-90-28 | 186.9 | -1.0 | -4.0 | 17 | |
| OTH-90-29 | 187.5 | -1.0 | -4.0 | 17 | |
| OTH-90-30 | 190.1 | 0.0 | -4.0 | 9 | |
| OTH-90-31 | 191.0 | 0.0 | -2.0 | 17 | |
| OTH-90-32 | 192.5 | -1.0 | -6.0 | 9 | 14 |

| Sample Number | Position (m) | Minimum | Maximum | Facies | Facies |
|---|---|---|---|---|---|
| OTH-90-33 | 193.2 | -1.0 | -4.0 | 9 | 14 |
| OTH-90-34 | 196.4 | -1.0 | -10.0 | 16 | |
| OTH-90-35A | 199.9 | 0.0 | -4.0 | 17 | |
| OTH-90-35B | 199.9 | -1.0 | -4.0 | 17 | |
| OTH-90-35.25 | 201.2 | -0.5 | -6.0 | 17 | |
| OTH-90-35.5 | 202.5 | -0.5 | -6.0 | 9 | 17 |
| OTH-90-36 | 202.6 | -2.0 | -10.0 | 9 | |
| OTH-90-36.5 | 202.7 | -0.5 | -10.0 | 10 | |
| OTH-90-37 | 203.3 | -0.5 | -10.0 | 12 | 17 |
| OTH-90-38A | 203.6 | -0.5 | -15.0 | 12g | |
| OTH-90-38B | 203.6 | -0.5 | -15.0 | 12g | |
| OTH-90-38C | 203.6 | -0.5 | -15.0 | 12g | |
| OTH-90-38D | 203.6 | -0.5 | -15.0 | 12g | |
| OTH-90-39 | 204.0 | -0.5 | -10.0 | 12g | 16 |
| OTH-90-40A | 205.0 | -2.0 | -10.0 | 12g | |
| OTH-90-40B | 205.0 | -2.0 | -10.0 | 12g | |
| OTH-90-41 | 206.1 | -2.0 | -10.0 | 9 | 16 |
| OTH-90-41.5 | 206.8 | -0.5 | -10.0 | 12p | 16 |
| OTH-90-42 | 207.6 | -2.0 | -10.0 | 16 | 17 |
| OTH-90-43 | 208.8 | -0.5 | -20.0 | 16 | 9 |
| OTH-90-44 | 210.7 | -0.5 | -20.0 | 17 | |
| OTH-90-45 | 211.1 | -0.5 | -10.0 | 16 | 17 |
| OTH-90-46A | 211.7 | -2.0 | -6.0 | 19 | |
| OTH-90-46B | 211.7 | -2.0 | -6.0 | 19 | |
| OTH-90-46.5A | 213.3 | -0.5 | -10.0 | 16 | |
| OTH-90-46.5B | 213.3 | -0.5 | -10.0 | 16 | |
| OTH-90-47 | 213.3 | -0.5 | -6.0 | 17 | |
| OTH-90-48 | 214.1 | -0.5 | -10.0 | 16 | |
| OTH-90-49 | 215.0 | -0.5 | -20.0 | 12gp | |
| OTH-90-50 | 215.8 | -0.5 | -20.0 | 12pg | |
| OTH-90-51 | 216.7 | -0.5 | -15.0 | 12gp | |
| OTH-90-52A | 218.6 | -0.5 | -10.0 | 16 | |
| OTH-90-52B | 218.6 | -0.5 | -10.0 | 16 | |
| OTH-90-53 | 220.3 | -0.5 | -15.0 | 16 | |
| OTH-90-54 | 220.7 | -0.5 | -10.0 | 16 | 17 |
| OTH-90-55 | 222.3 | -0.5 | -10.0 | 16 | 17 |

| Sample Number | Position (m) | Minimum | Maximum | Facies | Facies |
|---|---|---|---|---|---|
| OTH-90-56 | 223.0 | -0.5 | -2.0 | 17 | |
| OTH-90-56N | 223.0 | -0.5 | -2.0 | 17 | |
| OTH-90-57 | 225.0 | -0.5 | -15.0 | 12g | 10 |
| OTH-90-58A | 227.0 | -0.5 | -10.0 | 12g | 12p |
| OTH-90-58B | 227.0 | -0.5 | -10.0 | 12p | 12g |
| OTH-90-59 | 227.4 | -2.0 | -6.0 | 9 | 12p |
| OTH-90-60 | 227.8 | -0.5 | -10.0 | 12p | 12g |
| OTH-90-61 | 228.3 | -0.5 | -15.0 | 12p & 16 | |
| OTH-90-62 | 230.4 | -0.5 | -15.0 | 12g | |
| OTH-90-63 | 231.4 | -0.5 | -10.0 | 12g | 16 |
| OTH-90-64 | 233.7 | -0.5 | -10.0 | 12g | 10 |
| OTH-90-65 | 235.5 | -0.5 | -10.0 | 12g | |
| OTH-90-66 | 240.5 | -0.5 | -6.0 | 19 | |
| OTH-90-67 | 240.5 | -0.5 | -10.0 | 12g | |
| OTH-90-68 | 242.1 | -0.5 | -15.0 | 12g | 16 |
| OTH-90-69 | 246.1 | N/A | N/A | Lost | |
| OTH-90-70A | 249.4 | -0.5 | -10.0 | 12g | 16 |
| OTH-90-70B | 249.4 | -0.5 | -20.0 | 12g | |
| OTH-90-71 | 255.3 | -0.5 | -10.0 | 12g | 16 |
| OTH-90-72 | 257.6 | -0.5 | -15.0 | 12g | 16 |
| OTH-90-73 | 260.6 | -0.5 | -15.0 | 12g | |
| OTH-90-74 | 261.1 | -0.5 | -10.0 | 8 | |
| OTH-90-74.25 | 262.4 | -0.5 | -10.0 | 12g | |
| OTH-90-74.5 | 262.6 | -0.5 | -10.0 | 12g | 12p |
| OTH-90-75 | 264.5 | -0.5 | -15.0 | 12p | 12g |
| OTH-90-76 | 266.1 | -0.5 | -10.0 | 12g | |
| OTH-90-77 | 267.1 | -0.5 | -15.0 | 12g | |
| OTH-90-77.25 | 268.2 | -0.5 | -15.0 | 12gp | |
| OTH-90-77.5 | 268.5 | -0.5 | -15.0 | 12gp | |
| OTH-90-78 | 268.8 | -2.0 | -20.0 | 12gp | |
| OTH-90-79 | 270.6 | -0.5 | -20.0 | 12gp | |
| OTH-90-80 | 272.5 | -0.5 | -20.0 | 12gp | |
| OTH-90-81A | 274.4 | -0.5 | -15.0 | 12g | |
| OTH-90-81B | 274.4 | -2.0 | -15.0 | 12g | |
| OTH-90-82 | 304.1 | -0.5 | -15.0 | 12g | |
| OTH-90-83 | 305.8 | -0.5 | -10.0 | 12g | |

| Sample Number | Position (m) | Minimum | Maximum | Facies | Facies |
|---|---|---|---|---|---|
| OTH-90-84A | 308.1 | -0.5 | -15.0 | 12g | |
| OTH-90-84B | 308.1 | -0.5 | -15.0 | 12g | |
| OTH-90-85 | 312.4 | -0.5 | -15.0 | 12g | |
| OTH-90-86 | 315.4 | -0.5 | -15.0 | 12g | |
| OTH-90-87 | 317.9 | -0.5 | -15.0 | 12g | |
| OTH-90-88 | 320.5 | -2.0 | -15.0 | 12gp | |
| OTH-90-89 | 321.1 | -0.5 | -10.0 | 12g | |
| OTH-90-90 | 322.9 | -0.5 | -15.0 | 12g | |
| OTH-90-91 | 324.5 | -0.5 | -15.0 | 12g | |
| OTH-90-92 | 325.1 | -2.0 | -15.0 | 9 | |
| OTH-90-93 | 325.7 | -0.5 | -20.0 | 12g | |
| OTH-90-94 | 326.3 | -0.5 | -15.0 | 12g | |
| OTH-90-95 | 327.7 | -0.5 | -15.0 | 12g | |
| OTH-90-96 | 328.6 | -0.5 | -15.0 | 12g | |
| OTH-90-97 | 329.6 | -0.5 | -15.0 | 12g | |
| OTH-90-98 | 330.2 | -0.5 | -20.0 | 12g | |
| OTH-90-99 | 331.8 | -0.5 | -15.0 | 12g | |
| OTH-90-100 | 332.6 | -2.0 | -20.0 | 9 | |
| OTH-90-101A | 332.6 | 0.0 | -6.0 | 19 | 9 |
| OTH-90-101B | 332.6 | 0.0 | -6.0 | 19 | 9 |
| OTH-90-102 | 332.6 | 0.0 | -2.0 | 12p | 16 |
| OTH-90-103 | 332.8 | -0.5 | -20.0 | 12g | |
| OTH-90-104 | 334.1 | -0.5 | -15.0 | 12g | |
| OTH-90-105 | 336.2 | -0.5 | -15.0 | 12g | 12p |
| OTH-90-106 | 336.7 | -0.5 | -15.0 | 12g | |
| OTH-90-107 | 340.1 | -0.5 | -10.0 | 12gp | |
| OTH-90-108 | 341.3 | -0.5 | -15.0 | 12g | |
| OTH-90-109 | 342.3 | -0.5 | -15.0 | 12p | |
| OTH-90-110 | 343.2 | -2.0 | -15.0 | 12g | |
| OTH-90-111 | 345.1 | -0.5 | -15.0 | 12g | |
| OTH-90-112A | 345.6 | -0.5 | -15.0 | 12g | 12p |
| OTH-90-112B | 345.6 | -0.5 | -15.0 | 12g | 12p |
| OTH-90-112N | 345.6 | -0.5 | -15.0 | 12g | 12p |
| OTH-90-113 | 348.9 | 0.0 | -10.0 | 16 | |
| OTH-90-114A | 356.4 | -0.5 | -10.0 | 16 | |
| OTH-90-114B | 356.4 | -0.5 | -10.0 | 16 | |

| Sample Number | Position (m) | Minimum | Maximum | Facies | Facies |
|---|---|---|---|---|---|
| OTH-90-115 | 358.7 | -0.5 | -20.0 | 17 | 16 |
| OTH-90-116 | 360.2 | -1.0 | -10.0 | 16 | 12p |
| OTH-90-117 | 362.3 | -2.0 | -6.0 | 9 | |
| OTH-90-118 | 362.9 | -2.0 | -15.0 | 12p | 9 |
| OTH-90-119 | 365.8 | -1.0 | -15.0 | 12p | 17 |
| OTH-90-120 | 367.1 | -2.0 | -20.0 | 9 | |
| OTH-90-121 | 368.2 | -2.0 | -20.0 | 9 | |
| OTH-90-122 | 372.4 | 1.5 | -6.0 | 19 | |
| OTH-90-123 | 377.4 | -2.0 | -10.0 | 16 | 9 |
| OTH-90-124 | 379.0 | -2.0 | -6.0 | 9 | 22 |
| OTH-90-125 | 382.0 | -2.0 | -20.0 | 9 | |
| OTH-90-126 | 387.0 | 0.0 | -10.0 | 16 | |
| OTH-90-127 | 394.0 | -0.5 | -10.0 | 22 | 17 |
| OTH-90-128 | 398.5 | -30.0 | -2000.0 | 3 | |
| OTH-90-129 | 401.5 | -30.0 | -2000.0 | 3 | |
| OTH-90-130 | 500.8 | 1.0 | -0.5 | 19fl | |
| OTH-90-131A | 508.6 | 1.0 | -0.5 | 19 | |
| OTH-90-131B | 508.6 | 1.0 | -0.5 | 19lf | |
| OTH-90-132A | 517.8 | 1.5 | -100.0 | 16 | 19 |
| OTH-90-132B | 517.8 | 1.5 | -100.0 | 19l | |
| OTH-90-133 | 521.4 | -0.5 | -10.0 | 17 | |
| OTH-90-134 | 524.8 | 0.0 | -30.0 | 19 | |
| OTH-90-135 | 528.9 | -0.5 | -10.0 | 17 | 12p |
| OTH-90-136 | 532.3 | 1.5 | 0.0 | | |
| | | | | | |
| | | | | | |
| | | | | | |
| | | | | | |

| Idol Mine Section Sample Number | Stratigraphic Position (m) | Depth Minimum | Depth Maximum | Dominant Facies | Subordinate Facies |
|---|---|---|---|---|---|
| ISR-1 | 0.0 | 1.5 | 0.0 | Dolostone | |
| ISR-3 | 0.9 | 1.5 | 0.0 | Dolostone | |
| IS-1-1 | 1.0 | 1.5 | 0.0 | Dolostone | |
| IS-1-2 | 1.5 | 1.5 | 0.0 | Dolostone | |
| ISR-4 | 1.9 | 1.5 | 0.0 | Dolostone | |
| ISR-6 | 3.4 | 1.5 | 0.0 | Dolostone | |
| ISR-9 | 6.1 | 0.0 | -10.0 | 24 | |
| ISR-3-1 | 8.1 | 1.5 | -10.0 | 19f | |
| ISR-11 | 10.0 | 1.5 | -0.5 | 19f | |
| ISR-12 | 10.2 | 1.5 | -0.5 | 19f | |
| ISR-13 | 10.3 | 1.5 | -0.5 | 19f | |
| ISR-14 | 10.6 | 1.5 | -0.5 | 19f | |
| ISR-15 | 10.9 | 1.5 | -6.0 | 19f | |
| ISR-16 | 12.6 | 1.5 | -0.5 | 19f | |
| IS-3-3 | 16.0 | 1.5 | -30.0 | 19 | |
| ISR-18 | 16.2 | 0.0 | -20.0 | 19 | |
| ISR-20 | 18.8 | 1.5 | -10.0 | 16 | |
| ISR-21 | 19.3 | 1.5 | -15.0 | 16 | |
| ISR-23 | 24.3 | 1.5 | -6.0 | 19f | |
| IS-3-6 | 24.8 | 0.0 | -2.0 | 19f | |
| ISR-25 | 25.9 | 1.5 | -0.5 | 16 | 19f |
| ISR-26 | 26.0 | -0.5 | -10.0 | 16 | 17 |
| ISR-27 | 26.5 | -0.5 | -4.0 | 12g | 16 |
| IS-90-0A | 28.1 | -0.5 | -10.0 | 16 | |
| IS-90-0B | 28.1 | -0.5 | -10.0 | 16 | |
| ISR-29 | 28.6 | -0.5 | -10.0 | 16 | 17 |
| ISR-4-2 | 30.0 | 0.0 | -10.0 | 16 | |
| IS-90-13 | 31.7 | 0.0 | -10.0 | 16 | |
| IS-90-1 | 35.1 | -2.0 | -15.0 | 12g | 16 |
| IS-90-2 | 35.3 | -2.0 | -15.0 | 12g | 16 |
| IS-90-14 | 37.4 | 0.0 | -6.0 | 12g | 17 |
| IS-5 | 38.0 | 0.0 | -3.0 | 12g | 17 |
| IS-90-3 | 39.9 | -2.0 | -3.0 | 12g | 17 |
| IS-90-5 | 40.6 | -0.5 | -15.0 | 12g | |
| IS-90-4 | 45.5 | -0.5 | -3.0 | 12g | 11 |

| Sample Number | Position (m) | Minimum | Maximum | Facies | Facies |
|---|---|---|---|---|---|
| IS-90-15 | 48.2 | -0.5 | -6.0 | 9 | |
| IS-90-7-2A | 49.0 | -0.5 | -2.0 | 12p | 17 |
| IS-90-7-2B | 49.0 | -0.5 | -2.0 | 12p | 17 |
| IS-90-6 | 50.8 | -2.0 | -10.0 | 16 | 12g |
| IS-90-7 | 52.2 | -0.5 | -15.0 | 12g | |
| IS-8-1 | 57.0 | 0.0 | -15.0 | 12g | |
| IS-8-2 | 62.0 | -0.5 | -15.0 | 12g | |
| IS-90-8 | 63.3 | -0.5 | -20.0 | 12g | 16 |
| IS-9 | 63.5 | -0.5 | -10.0 | 12g | 16 |
| IS-90-16 | 67.3 | -0.5 | -15.0 | 12g | |
| IS-90-9 | 68.6 | -0.5 | -15.0 | 12g | 10 |
| IS-90-10 | 72.3 | -0.5 | -15.0 | 16 | |
| IS-11-1 | 77.0 | -0.5 | -10.0 | 12g | |
| IS-90-17 | 77.5 | -0.5 | -15.0 | 12g | 16 |
| IS-90-11 | 78.4 | -0.5 | -15.0 | 12g | |
| IS-11-2 | 79.5 | -0.5 | -6.0 | 12pg | |
| IS-90-12 | 80.2 | -0.5 | -6.0 | 12g | |
| IS-90-18 | 84.6 | -0.5 | -20.0 | 12g | |
| IS-90-18N | 84.6 | -0.5 | -20.0 | 12g | |
| IS-90-19 | 86.9 | -0.5 | -10.0 | 12p | 16 |
| IS-13 | 92.0 | 0.0 | -15.0 | 12g | |
| IS-90-20 | 92.4 | 0.0 | -15.0 | 12g | 17 |
| IS-15-2 | 152.0 | -0.5 | -4.0 | 22 | |
| IS-15-3 | 155.0 | -0.5 | -4.0 | 22 | |
| IS-90--21 | 170.0 | -0.5 | -2.0 | 17 | |
| IS-90-22 | 172.4 | -0.5 | -3.0 | 17 | 22 |
| IS-15-4 | 173.0 | -2.0 | -3.0 | 22 | |
| IS-90-23 | 174.6 | -2.0 | -6.0 | 9 | |
| IS-90-24 | 175.0 | -0.5 | -6.0 | 12g | 17 |
| IS-16-1 | 175.0 | 0.0 | -10.0 | 17 | |
| IS-90-25 | 179.8 | 0.0 | -4.0 | 12g | |
| IS-90-26 | 185.2 | -2.0 | -6.0 | 19 | 9 |
| IS-90-27 | 186.8 | -2.0 | -10.0 | 16 | 19 |
| IS-90-28A | 190.8 | -0.5 | -3.0 | 12g | |
| IS-90-28B | 190.8 | -0.5 | -3.0 | 12g | |
| IS-90-29 | 191.4 | -0.5 | -4.0 | 12g | 17 |

| Sample Number | Position (m) | Minimum | Maximum | Facies | Facies |
|---|---|---|---|---|---|
| IS-90-30 | 192.0 | -0.5 | -10.0 | 17 | |
| IS-90-31 | 196.7 | -0.5 | -3.0 | 12pg | |
| IS-90-32 | 197.1 | -0.5 | -3.0 | 10 | 9 |
| IS-17-1 | 198.0 | -0.5 | -6.0 | 9 | |
| IS-18-1 | 202.0 | -0.5 | -10.0 | 12g | 17 |
| IS-90-33 | 202.0 | -0.5 | -10.0 | 12g | 17 |
| IS-90-34 | 205.6 | -0.5 | -10.0 | 12g | 16 |
| IS-90-35 | 206.6 | -0.5 | -10.0 | 12g | 17 |
| IS-17-3 | 208.0 | -0.5 | -10.0 | 9 | |
| IS-90-36 | 211.2 | -0.5 | -4.0 | 12g | 10 |
| IS-90-37 | 216.2 | -0.5 | -10.0 | 12g | |
| IS-90-38 | 226.1 | -0.5 | -10.0 | 12g | 10 |
| IS-90-39 | 228.7 | -0.5 | -15.0 | 12g | 10 |
| IS-90-40 | 230.0 | -0.5 | -10.0 | 12g | 10 |
| IS-90-41 | 230.0 | -0.5 | -3.0 | 16 | |
| IS-90-42 | 232.1 | -2.0 | -20.0 | 16 | 9 |
| IS-90-43A1 | 232.9 | 1.5 | -0.5 | 19 | |
| IS-90-43A | 232.9 | 1.5 | -0.5 | 19 | |
| IS-90-43B | 232.9 | 1.5 | -0.5 | 19 | |
| IS-90-43B1 | 232.9 | 1.5 | -0.5 | 19 | |
| IS-90-43C | 232.9 | 1.5 | -0.5 | 19 | |
| IS-90-43C1 | 232.9 | 1.5 | -0.5 | 19 | |
| IS-90-43C2 | 232.9 | 1.5 | -0.5 | 19 | |
| IS-90-43C3 | 232.9 | 1.5 | -0.5 | 19 | |
| IS-90-43C4 | 232.9 | 1.5 | -0.5 | 19 | |
| IS-90-44 | 233.6 | -0.5 | -10.0 | 16 | |
| IS-90-45 | 234.2 | -0.5 | -10.0 | 9 | 16 |
| IS-90-46 | 234.6 | 1.0 | -0.5 | 19 | |
| IS-90-47A | 234.7 | 0.0 | -2.0 | 19 | |
| IS-90-47B | 234.7 | 0.0 | -2.0 | 19 | |
| IS-19-1A | 236.0 | 0.0 | -20.0 | 9 | |
| IS-19-1B | 236.0 | 0.0 | -20.0 | 9 | |
| IS-90-48 | 236.6 | -0.5 | -6.0 | 19 | |
| IS-90-2A | 237.0 | -0.5 | -15.0 | 16 | 9 |
| IS-90-2B | 237.0 | -0.5 | -15.0 | 16 | 9 |
| IS-90-49A | 237.5 | 0.0 | -3.0 | 16 | 9 |

| Sample Number | Position (m) | Minimum | Maximum | Facies | Facies |
|---|---|---|---|---|---|
| IS-90-47B | 237.5 | 0.0 | -6.0 | 16 | 9 |
| IS-90-50A and B | 238.5 | -0.5 | -20.0 | 9 | |
| IS-90-51A and B | 238.9 | -0.5 | -15.0 | 12g | 16 |
| IS-19-3 | 241.0 | -2.0 | -30.0 | 19 | |
| IS-90-52A and B | 243.1 | -0.5 | -15.0 | 12g | |
| IS-90-53A | 245.3 | -0.5 | -15.0 | 12g | 12p |
| IS-90-53B | 245.3 | -0.5 | -15.0 | 12g | |
| IS-90-54A and B | 248.1 | -0.5 | -15.0 | 12gp | |
| IS-90-55A and B | 248.9 | -0.5 | -15.0 | 12g | |
| IS-56-A and B | 249.2 | -0.5 | -15.0 | 12gp | |
| IS-90-57A and B | 253.0 | -0.5 | -20.0 | 12g | 19 |
| IS-20 | 253.0 | -0.5 | -20.0 | 19 | |
| IS-90-58A | 253.9 | -6.0 | -10.0 | 16 | 17 |
| IS-90-58B | 253.9 | -0.5 | -10.0 | 16 | 17 |
| IS-90-59A and B | 269.0 | -1.0 | -10.0 | 16 | |
| IS-90-60A and B | 277.5 | -2.0 | -10.0 | 16 | 9 |
| IS-24-3A and B | 280.0 | -2.0 | -10.0 | 16 | |
| IS-90-60.5A | 280.9 | -2.0 | -100.0 | 9 | |
| IS-90-60.5B | 280.9 | -0.5 | -100.0 | 9 | |
| IS-90-61A and B | 281.4 | -1.0 | -15.0 | 16 | 9 |
| IS-90-62A and B | 282.2 | -2.0 | -30.0 | 17 | 16 |
| IS-90-63A and B | 282.7 | 0.0 | -10.0 | 16 | 17 |
| IS-24-2A and B | 288.0 | -2.0 | -10.0 | 16 | |
| IS-90-64A and B | 293.6 | -2.0 | -20.0 | 17 | |
| IS-90-65A and B | 294.9 | -0.5 | -20.0 | 12pg | |
| IS-90-66A and B | 295.9 | -2.0 | -20.0 | 17 | |
| IS-90-67A | 296.7 | 0.0 | -15.0 | 16 | 17 |
| IS-90-67B | 296.7 | -0.5 | -15.0 | 16 | 17 |
| IS-9068A and B | 297.6 | -2.0 | -20.0 | 12g | 16 |
| IS-90-69A and B | 298.3 | -0.5 | -20.0 | 12g | |
| IS-90-70A and B | 298.8 | -2.0 | -10.0 | 16 | 17 |
| IS-90-71 A and B | 300.6 | 0.0 | -20.0 | 16 | |
| IS-90-72A and B | 304.0 | -0.5 | -20.0 | 12g | 16 |
| IS-90-73A and B | 305.1 | -0.5 | -20.0 | 12g | |
| IS-90-75A and B | 306.9 | -0.5 | -15.0 | 12g | |
| IS-24-1A and B | 311.0 | -0.5 | -20.0 | 12g | 16 |

| Sample Number | Position (m) | Minimum | Maximum | Facies | Facies |
|---|---|---|---|---|---|
| IS-90-76A and B | 311.9 | -0.5 | -15.0 | 12g | |
| IS-26A and B | 315.0 | -0.5 | -15.0 | 9 | |
| IS-90-77A and B | 317.4 | -0.5 | -15.0 | 12g | |
| IS-28-1A and B | 321.0 | -0.5 | -15.0 | 12g | 16 |
| IS-90-78A and B | 322.8 | -2.0 | -15.0 | 12g | |
| IS-90-79A and B | 325.4 | -0.5 | -20.0 | 12p | |
| IS-90-80A and B | 327.3 | -0.5 | -15.0 | 12g | |
| IS-90-81 | 452.0 | -2.0 | -100.0 | 24 | |

| Cedar Springs Section Sample Number | Stratigraphic Position (m) | Depth Minimum | Depth Maximum | Dominant Facies | Subordinate Facies |
|---|---|---|---|---|---|
| N/A | 0.0 | 1.5 | 0.0 | | |
| CS-1-1 | 1.0 | 1.5 | -6.0 | 19 | |
| CS-1-2 (slab) | 1.5 | 1.0 | 0.0 | 19 | |
| CS-3 (slab) | 2.0 | 0.0 | -10.0 | 19 | |
| CS-4 | 2.5 | 0.0 | -2.0 | 17 | |
| CS-5 | 3.0 | 1.0 | -0.5 | 16 | |
| CS-6 | 4.0 | -0.5 | -6.0 | 16 | |
| CS-7 | 4.5 | -1.0 | -4.0 | 19 | |
| CS-8 | 5.5 | 0.0 | -2.0 | 16 | |
| CS-9 | 6.0 | 1.5 | -0.5 | 17 | |
| CS-10 | 6.3 | 1.0 | -0.5 | | |
| CS-11 | 6.7 | 0.0 | -2.0 | 16 | |
| CS-13 | 7.3 | 0.0 | -15.0 | 19 | |
| CS-14 | 7.8 | 1.5 | -6.0 | 19 | |
| CS-15 | 8.9 | -0.5 | -6.0 | 19 | |
| CS-16 | 10.6 | -0.5 | -3.0 | 16 | |
| CS-17 | 11.5 | 1.5 | -6.0 | 17 | |
| CS-18 | 13.3 | 0.0 | -2.0 | 19f | |
| CS-19 | 14.5 | -0.5 | -0.5 | 19f | |
| CS-20 | 16.0 | 1.5 | -0.5 | 19l | 19f |
| CS-21 | 16.3 | -2.0 | -6.0 | 17 | |
| CS-22 | 18.0 | 1.5 | -6.0 | 16 | 17 |
| CS-23 | 20.7 | 0.0 | -10.0 | 16 | |
| CS-24 | 22.0 | 0.0 | -10.0 | 16 | |
| CS-25 | 24.0 | 0.0 | -2.0 | 12p | |
| CS-27 | 29.0 | 0.0 | -2.0 | 12g | 17 |
| CS-28 | 29.0 | 0.0 | -2.0 | 12g | 17 |
| CS-29 | 33.0 | 1.0 | -0.5 | 9 | |
| CS-30 | 35.0 | -0.5 | -4.0 | 17 | |
| CS-31 | 38.0 | -0.5 | -4.0 | 11 | 17 |
| CS-32 | 39.5 | -0.5 | -4.0 | 11 | |
| CS-33 | 40.5 | -0.5 | -4.0 | 11 | |
| CS-34 | 47.0 | -0.5 | -4.0 | 11 | |
| CS-35 | 56.5 | -0.5 | -4.0 | 17 | |
| CS-37 | 65.0 | -0.5 | -2.0 | 11 | |

| Sample Number | Position (m) | Minimum | Maximum | Facies | Facies |
|---|---|---|---|---|---|
| CS-38 | 67.0 | -0.5 | -20.0 | 12g | |
| CS-39 | 68.5 | -0.5 | -20.0 | 12g | 12p |
| CS-40 | 70.0 | -0.5 | -20.0 | 12g | |
| CS-41 | 73.4 | -0.5 | -20.0 | 10 | |
| CS-42 | 80.4 | -0.5 | -20.0 | 10 | |
| CS-43 | 88.3 | -0.5 | -10.0 | 12g | 10 |
| CS-44 | 91.8 | -0.5 | -10.0 | 12g | |
| CS-45 | 99.4 | -0.5 | -20.0 | 12g | |
| CS-46 | 101.0 | -0.5 | -3.0 | 11 | |
| CS-47 | 102.5 | -0.5 | -4.0 | 17 | |
| CS-48 | 109.0 | 0.0 | -2.0 | 11 | 17 |
| CS-49 | 112.0 | 0.0 | -4.0 | 22 | |
| CS-50 | 115.3 | -0.5 | -2.0 | 13 | |
| CS-51 | 117.1 | 0.0 | -2.0 | 19l | |
| CS-52 | 121.5 | -0.5 | -4.0 | 13 | |
| CS-53 | 125.5 | -0.5 | -10.0 | 12g | 10 |
| CS-54 | 128.3 | -0.5 | -2.0 | 22 | 19f |
| CS-55 | 133.0 | -0.5 | -4.0 | 13 | |
| CS-56 | 136.2 | -0.5 | -10.0 | 10 | |
| CS-57 | 139.3 | 0.0 | -6.0 | 8 | 9 |
| CS-58 | 140.7 | 0.0 | -10.0 | 10 | 12g |
| CS-59 | 146.4 | 0.0 | -10.0 | 17 | |
| CS-60 | 153.0 | -0.5 | -4.0 | 10 | |
| CS-61 | 153.2 | -0.5 | -2.0 | 17 | |
| CS-62 | 154.0 | -0.5 | -6.0 | 19 | 9 |
| CS-63 | 155.2 | -0.5 | -20.0 | 19f | |
| CS-64 | 155.5 | -0.5 | -6.0 | 10 | |
| CS-65 | 161.2 | -0.5 | -2.0 | 19 | 8 |
| CS-66 | 174.4 | -0.5 | -6.0 | 17 | 12g |
| CS-67 | 175.0 | -0.5 | -30.0 | 9 | 19f |
| CS-68 | 166.5 | 0.0 | -2.0 | 12g | 12g |
| CS-69 | 168.0 | -0.5 | -20.0 | 12p | 12g |
| CS-70 | 170.0 | -0.5 | -6.0 | 10g | 10p |
| CS-71 | 174.8 | 1.5 | -6.0 | 9 | |
| CS-72 | 180.9 | -0.5 | -10.0 | 10 | |
| CS-73 | 190.3 | -0.5 | -20.0 | 10 | |

| Sample Number | Position (m) | Minimum | Maximum | Facies | Facies |
|---|---|---|---|---|---|
| CS-74 | 193.6 | 1.5 | -0.5 | 8 | |
| CS-75 | 206.5 | -0.5 | -20.0 | 10 | |
| CS-76 | 207.9 | -0.5 | -20.0 | 12p | |
| CS-77 | 211.3 | -0.5 | -20.0 | 12p | |
| CS-78 | 217.2 | -0.5 | -20.0 | 12g | |
| CS-79 | 224.0 | -0.5 | -6.0 | 10 | |
| CS-80 | 231.2 | -0.5 | -20.0 | 12g | 12p |
| CS-81 | 238.5 | -0.5 | -20.0 | 12g | 12p |
| CS-82 | 241.3 | -2.0 | -20.0 | 12g | 10 |
| CS-84 | 248.7 | -2.0 | -20.0 | 12g | 17 |
| CS-85 | 250.5 | -2.0 | -20.0 | 12g | |
| CS-86 | 253.5 | -2.0 | -10.0 | 9 | |
| CS-87 | 255.3 | -2.0 | -15.0 | 9 | 19 |
| CS-88 | 264.8 | -2.0 | -15.0 | 9 | |
| CS-89 | 268.1 | -0.5 | -20.0 | 9 | 14 |
| CS-90 | 272.8 | -2.0 | -20.0 | 12g | |
| CS-91 | 281.0 | -2.0 | -20.0 | 12g | 12p |
| CS-92 | 282.5 | -0.5 | -15.0 | 12g | 16 |
| CS-93 | 287.5 | -0.5 | -15.0 | 12g | |
| CS-94 | 290.7 | -0.5 | -15.0 | 12g | |
| CS-95 | 294.9 | -0.5 | -15.0 | 12g | |
| CS-96 | 302.6 | -0.5 | -10.0 | 12g | 17 |
| CS-97 | 307.4 | -0.5 | -15.0 | 12g | 12p |
| CS-98 | 309.2 | -0.5 | -15.0 | 12g | 12p |
| CS-99 | 310.8 | -0.5 | -15.0 | 12g | |
| CS-100 | 312.6 | 0.0 | -15.0 | 12g | 17 |
| CS-101 | 313.1 | -2.0 | -20.0 | 12p | |
| CS-102 | 313.9 | -2.0 | -20.0 | 9 | 8 |
| CS-103 | 315.7 | -2.0 | -20.0 | 12p | 22 |
| CS-104 | 321.3 | -2.0 | -15.0 | 9 | |
| CS-104A | 322.5 | -0.5 | -20.0 | 12g | 17 |
| CS-105 | 323.1 | -2.0 | -20.0 | 9 | |
| CS-106 | 328.0 | -1.0 | -15.0 | 9 | |
| CS-107 | 332.8 | -0.5 | -20.0 | 9 | 19 |
| CS-108 | 334.3 | -0.5 | -2.0 | 9 | 19 |
| CS-109 | 342.0 | -2.0 | -20.0 | 19l | |

| Sample Number | Position (m) | Minimum | Maximum | Facies | Facies |
|---|---|---|---|---|---|
| CS-110 | 349.0 | -2.0 | -20.0 | 9 | |
| CS-111 | 356.0 | -15.0 | -15.0 | 19l | |
| CS-112A | 362.5 | -0.5 | -20.0 | 12p | 12g |
| CS-112B | 362.5 | -0.5 | -20.0 | 12p | 12g |
| CS-113 | 364.0 | -2.0 | -20.0 | 22 | |
| CS-114 | 365.5 | -0.5 | -10.0 | 17 | |
| CS-115 | 367.1 | -0.5 | -4.0 | 9 | 14 |
| CS-116 | 375.0 | 1.5 | -15.0 | 16 | |
| CS-117 | 375.9 | 1.5 | -15.0 | 19l | 16 |
| CS-118 | 377.8 | 1.5 | -6.0 | 16 | |
| CS-119 | 382.5 | -0.5 | -4.0 | 22 | |
| CS-120 | 397.1 | -0.5 | -4.0 | 22 | |
| CS-121 | 392.5 | -0.5 | -10.0 | 12g | |
| CS-122 | 394.0 | -0.5 | -2.0 | 22 | |
| CS-123 | 398.0 | -2.0 | -20.0 | 22 | |
| CS-124 | 409.4 | -15.0 | -100.0 | 19l | |
| CS-125 | 414.0 | 0.0 | -100.0 | 16 | |
| CS-126A | 420.1 | -0.5 | -6.0 | 12g | |
| CS-126B | 420.1 | -0.5 | -6.0 | 9 | |
| CS-127 | 421.9 | -0.5 | -4.0 | 17 | |
| CS-128A | 424.0 | -0.5 | -6.0 | 9 | |
| CS-128B | 424.0 | -0.5 | -3.0 | 9 | |
| CS-129A | 422.1 | -0.5 | -6.0 | 9 | |
| CS-129B | 422.1 | -0.5 | -6.0 | 9 | |

| Poor Valley Creek Section Sample Number | Stratigraphic Position (m) | Depth Minimum | Depth Maximum | Dominant Facies | Subordinate Facies |
|---|---|---|---|---|---|
| PVC-1A-B | 7.1 | -0.5 | -30.0 | 12g | |
| PVC-1A-T | 7.1 | -0.5 | -30.0 | 12g | |
| PVC-1B-1 | 13.6 | -0.5 | -30.0 | 12g | |
| PVC-1B-2L | 13.8 | -0.5 | -30.0 | 12g | |
| PVC-1Ca | 18.6 | -0.5 | -30.0 | 12g | |
| PVC-2Cb | 20.6 | -0.5 | -30.0 | 12p | |
| PVC-2Cc | 20.6 | -0.5 | -30.0 | 12p | |
| PVC-2C-1a | 20.6 | -0.5 | -30.0 | 12p | |
| PVC-2H | 21.0 | -0.5 | -30.0 | 12p | |
| PVC-2D-1 | 21.6 | -0.5 | -30.0 | 12p | |
| PVC-2D-2 | 21.6 | -0.5 | -30.0 | 12p | |
| PVC-2D-3 | 21.6 | -0.5 | -30.0 | 12p | |
| PVC-2D-a | 21.6 | -0.5 | -30.0 | 12p | |
| PVC-2D-b | 21.6 | -0.5 | -30.0 | 12p | |
| PVC-2A-C1-MR | 24.6 | -0.5 | -30.0 | 12p | |
| PVC-2A-C1-ML | 24.6 | -0.5 | -30.0 | 12g | |
| PVC-2A-C1-L | 24.6 | -0.5 | -30.0 | 12p | |
| PVC-2A-C1-R | 24.6 | -0.5 | -30.0 | 12p | |
| PVC-2A-C2 | 24.9 | -0.5 | -30.0 | 12p | |
| PVC-2A-C2a | 24.9 | -0.5 | -30.0 | 12p | |
| PVC-2A-C2b | 24.9 | -0.5 | -30.0 | 12p | |
| PVC'-2G | 26.6 | -0.5 | -30.0 | 12p | |
| PVC'-2H | 27.6 | -0.5 | -30.0 | 12p | |
| PVC-3 | 28.6 | -0.5 | -30.0 | 12p | |
| PVC-3Aa | 39.6 | -0.5 | -30.0 | 12p | |
| PVC-3Ab | 39.6 | -0.5 | -30.0 | 12p | |
| PVC-3A-T | 39.6 | -0.5 | -30.0 | 12p | |
| PVC-3A-B | 39.6 | -0.5 | -30.0 | 12p | |

| Red House Branch Section Sample Number | Stratigraphic Position (m) | Depth Minimum | Depth Maximum | Dominant Facies | Subordinate Facies |
|---|---|---|---|---|---|
| RHB-1-1 (SCR) | 0.0 | 1.5 | 0.0 | 19F | |
| RHB-2-1 (SCR) | 0.5 | -0.5 | -2.0 | 9 | 16 |
| RHB-1-2 (SCR) | 1.0 | 1.5 | 0.0 | 19F | |
| RHB-2 (REJ) | 3.0 | 1.5 | 0.0 | 19F | |
| RHB-3 (REJ) | 4.8 | 1.5 | 0.0 | 19F | |
| RHB-4 (REJ) | 6.6 | -5.0 | -2.0 | 16 | |
| RHB-5 (REJ) | 9.7 | -0.5 | -10.0 | 9 | |
| RHB-6 (REJ) | 13.0 | -0.5 | -10.0 | 9 | |
| RHB-7 (REJ) | 16.3 | 0.0 | -10.0 | | |
| RHB-8 (REJ) | 17.0 | -0.5 | -10.0 | 12p | 9 |
| RHB-LCa (DGJ) B | 21.9 | 1.5 | -2.0 | 16 | 9 |
| RHB-2-4 (SCR) | 22.0 | -0.5 | -30.0 | 12p | |
| RHB-LCb (DGJ) T | 22.0 | -2.0 | -10.0 | 12g | |
| RHB-LCa (DGJ) T | 22.1 | -2.0 | -10.0 | 12g | |
| RHB'-1 (DGJ) | 22.5 | -0.5 | -150.0 | 12g | |
| RHB-1A (DGJ) | 24.5 | -2.0 | -150.0 | 12g | |
| RHB-9 (REJ) | 25.7 | N/A | N/A | 12g | |
| RHB'-1A-L (DGJ) | 27.0 | -0.5 | -30.0 | 12g | |
| RHB-2-2 (SCR) | 27.0 | -0.5 | -30.0 | Boundstone | |
| RHB-10 (REJ) | 30.8 | -0.5 | -30.0 | 12g | |
| RHB-1B (DGJ) | 32.5 | -0.5 | -10.0 | 12g | |
| RHB'-1C (DGJ) | 36.0 | -2.0 | -150.0 | 12g | |
| RHB-12 (REJ) | 39.6 | -0.5 | -30.0 | 8 | |
| RHB-2B-L (DGJ) B | 41.3 | -0.5 | -30.0 | 12g | 14 |
| RHB-2B-L (DGJ) T | 41.3 | -0.5 | -2.0 | 12p | |
| RHB'-2C-TR (DGJ) | 41.5 | -0.5 | -30.0 | 12g | |
| RHB-2C-B (DGJ) | 41.5 | -0.5 | -30.0 | 12g | |
| RHB-2G-BL (DGJ) | 42.0 | -0.5 | -30.0 | 12g | |
| RHB-2G-B (DGJ) | 42.0 | -2.0 | -30.0 | 12p | 12g |
| RHB-2H (DGJ) | 42.0 | -0.5 | -30.0 | 12p (Stromatactis) | |
| RHB-2I-S2 (DGJ) | 42.0 | -0.5 | -30.0 | 12p (Stromatactis) | |
| RHB-2J-S1 (DGJ) | 42.5 | -0.5 | -30.0 | 9 | |
| RHB-2J-S2 (DGJ) | 42.5 | -0.5 | -30.0 | 9 | |
| RHB-4-1 (SCR) | 44.0 | -0.5 | -2.0 | 11 | |
| RHB'-2A-L (DGJ) | 50.5 | -0.5 | -30.0 | 12p | 8 |

| Sample Number | Position (m) | Minimum | Maximum | Facies | Facies |
|---|---|---|---|---|---|
| RHB'-2A-R (DGJ) | 50.5 | -0.5 | -30.0 | 12p | 8 |
| RHB-3A (DGJ) | 50.5 | -0.5 | -30.0 | 12g | 12p |
| RHB-3A-4I (DGJ) | 50.5 | -0.5 | -30.0 | 12g | |
| RHB-3A-L (DGJ) | 50.5 | -0.5 | -30.0 | 12g | 12p |
| RHB-3A-R (DGJ) | 50.5 | -2.0 | -30.0 | 12p | 12g |
| RHB'-3B-S1 (DGJ) | 54.8 | -2.0 | -30.0 | 12g | 12p |
| RHB'-3B-S2 (DGJ) | 54.8 | -2.0 | -30.0 | 12g | 12p |
| RHB'-3B-S2 (DGJ) | 54.8 | -2.0 | -30.0 | 12g | |
| RHB-3Ca (DGJ) | 57.0 | -0.5 | -30.0 | 12p | |
| RHB-3Cb (DGJ) | 57.0 | -2.0 | -30.0 | 12p | |
| RHB'-3D-LD(R) (DGJ) | 60.3 | -0.5 | -30.0 | 12g | 12p |
| RHB-3D-S1 (DGJ) | 60.3 | -2.0 | -30.0 | 12g | |
| RHB-3D-S2 (DGJ) | 60.3 | -0.5 | -30.0 | 12g | 12p |
| RHB'-3D-LD(L) (DGJ) | 60.3 | -0.5 | -30.0 | 12g (? Stromatoporoid bo | |
| RHB-3D-S1B (DGJ) | 60.3 | -2.0 | -30.0 | 12g | |
| RHB-21 (REJ) | 61.0 | -2.0 | -30.0 | 12g | |
| RHB'-3E-B (DGJ) | 62.7 | -0.5 | -30.0 | 12g | |
| RHB-3E-B (DGJ) | 62.7 | -0.5 | -30.0 | 12g | |
| RHB'-3F-SI (DGJ) | 65.0 | -0.5 | -30.0 | 12g | |
| RHB'-3F-S2 (DGJ) | 65.0 | -0.5 | -30.0 | 12g | |
| RHB'-3F-S3 (DGJ) | 65.0 | -0.5 | -30.0 | 12g | |
| RHB'-2F-SI (DGJ) | 65.0 | -0.5 | -30.0 | 12g | |
| RHB-23a (REJ) | 74.0 | -0.5 | -30.0 | 12p | |
| RHB-23b (REJ) | 74.0 | -0.5 | -30.0 | 12g | |
| RHB'-3G (DGJ) | 75.8 | -0.5 | -150.0 | 12p | |
| RHB-24 (REJ) | 79.5 | -0.5 | -30.0 | 12p | |
| RHB'-3H-(R) (DGJ) | 81.2 | -0.5 | -30.0 | 9 | 12p |
| RHB'-3H-L (DGJ) | 81.2 | -0.5 | -30.0 | 12p | |
| RHB-25 (REJ) | 83.3 | -0.5 | -30.0 | 12p | 12g |
| RHB'-3I-G (DGJ) | 85.0 | -0.5 | -30.0 | 12p | |
| RHB'-3I-T (DGJ) | 85.0 | -0.5 | -30.0 | 12p | 12g |
| RHB'-4A-S2-TR (DGJ) | 113.9 | -2.0 | -30.0 | 12g | |
| RHB'-4A-S1-L (DGJ) | 113.9 | -0.5 | -30.0 | 12p | |
| RHB'-4A-S2-BR (DGJ) | 113.9 | -0.5 | -30.0 | 12g | |
| RHB'-4A-S1-R (DGJ) | 113.9 | -0.5 | -30.0 | 12g | |
| RHB-27 (REJ) | 121.0 | -0.5 | -30.0 | 12g | |

| Sample Number | Position (m) | Minimum | Maximum | Facies | Facies |
|---|---|---|---|---|---|
| RHB-6-2 (SCR) | 121.5 | -0.5 | -30.0 | 12g | |
| RHB-6-1 (SCR) | 121.5 | -0.5 | -30.0 | 12p | |
| RHB'-4B-S1 (DGJ) | 122.4 | -0.5 | -30.0 | 12g | 12p |
| RHB-28a (REJ) | 127.0 | -2.0 | -30.0 | 12p | |
| RHB-28b (REJ) | 127.0 | -0.5 | 0.0 | 12p | |
| RHB-29 (REJ) | 129.0 | -0.5 | -30.0 | 12g | |
| RHB-30 (REJ) | 129.8 | -0.5 | -30.0 | 12g | |
| RHB'-4D-L (DGJ) | 130.3 | -0.5 | -30.0 | 12p | |
| RHB'-4D-R (DGJ) | 130.3 | -0.5 | -30.0 | 12p | |
| RHB'-4Da (DGJ) | 130.3 | -0.5 | -30.0 | 12p | |
| RHB'-4Db (DGJ) | 130.3 | -0.5 | -30.0 | 12p | |
| RHB'-4E-L (DGJ) | 131.0 | -0.5 | -30.0 | 12g | |
| RHB'-4E-R (DGJ) | 131.0 | -0.5 | -30.0 | 12g | |
| RHB-31 (REJ) | 142.7 | N/A | N/A | 12g | |
| RHB'-5A (DGJ) | 144.0 | -0.5 | -3.0 | 12g | 12p |
| RHB-6A-TR (DGJ) | 181.0 | -0.5 | -150.0 | 12g | |
| RHB-6A-TL (DGJ) | 181.0 | -0.5 | -150.0 | 12g | |
| RHB-6A-BR (DGJ) | 181.0 | -2.0 | -150.0 | 12g | |
| RHB-6A-BL (DGJ) | 181.0 | -2.0 | -150.0 | 12g | |
| RHB-33 (REJ) | 181.8 | -0.5 | -30.0 | 12g | |
| RHB-34 (REJ) | 182.8 | -0.5 | -30.0 | 12g | |
| RHB-6B-BR (DGJ) | 183.4 | -0.5 | -30.0 | 12g | 12p |
| RHB-6B-BL (DGJ) | 183.4 | -2.0 | -30.0 | 12g | |
| RHB-6B-T (DGJ) | 183.4 | -0.5 | -4.0 | 12p | |
| RHB'-6Ca (DGJ) | 184.0 | -0.5 | -30.0 | 12g | |
| RHB'-6Ca (DGJ) | 184.0 | -0.5 | -30.0 | 12g | |
| RHB'-6D-L (DGJ) | 188.0 | -0.5 | -30.0 | 12g | |
| RHB'-6D-M (DGJ) | 188.0 | -0.5 | -30.0 | 12g | |
| RHB'-6D-R (DGJ) | 188.0 | -0.5 | -30.0 | 12g | 12p |
| RHB-35 (REJ) | 192.0 | -0.5 | -30.0 | 12g | |
| RHB-6E-TR (DGJ) | 193.5 | -0.5 | -30.0 | 12g | |
| RHB-6E-R (DGJ) | 193.5 | -0.5 | -4.0 | 12g | |
| RHB-6E-TL (DGJ) | 193.5 | -0.5 | -4.0 | 12g | |
| RHB-36 (REJ) | 198.8 | -0.5 | -30.0 | 12p | |
| RHB-6F-R (DGJ) | 199.6 | -0.5 | -30.0 | 12p | |
| RHB-6F-R (DGJ) | 199.6 | -0.5 | -30.0 | 12p | |

| Sample Number | Position (m) | Minimum | Maximum | Facies | Facies |
|---|---|---|---|---|---|
| RHB-37 (REJ) | 247.2 | -0.5 | -150.0 | 12g | |
| RHB'-7A-S1 (DGJ) | 248.5 | -0.5 | -6.0 | 12g | |
| RHB'-7A-S2 (DGJ) | 248.5 | -0.5 | -6.0 | 12g | |
| RHB'-7B (DGJ) | 249.0 | -0.5 | -30.0 | 12g | |
| RHB'-7B-T (DGJ) | 249.0 | -0.5 | -30.0 | 12g | |
| RHB-39 (REJ) | 258.0 | -0.5 | -30.0 | 12g | 12p |
| RHB'-8A (DGJ) | 259.4 | -2.0 | -30.0 | 12p | 12g |
| RHB-40 (REJ) | 260.0 | -0.5 | -30.0 | 12g | 12p |
| RHB-41 (SCR) | 264.0 | -0.5 | -30.0 | 12g | |
| RHB-8C (DGJ) | 265.4 | -0.5 | -30.0 | 12g | |
| RHB-8C-L (DGJ) | 265.4 | -2.0 | -30.0 | 12g | |
| RHB-72 (REJ) | 270.0 | -0.5 | -30.0 | 12p | |
| RHB-8D-S2-R (DGJ) | 271.4 | -0.5 | -6.0 | 12p | 9 |
| RHB-8D-S2-L (DGJ) | 271.4 | -0.5 | -6.0 | 12p | 9 |
| RHB-8D-S1 (DGJ) | 271.4 | -0.5 | -6.0 | 9 | |
| RHB-43 (REJ) | 271.5 | -0.5 | -30.0 | 12p | |
| RHB'-8E (DGJ) | 272.8 | -0.5 | -30.0 | 9 | |
| RHB'-8E-R (DGJ) | 272.8 | -0.5 | -30.0 | 12p | 12g |
| RHB'-8F-SL1 (DGJ) | 277.4 | -0.5 | -6.0 | 9 | |
| RHB'-8F-S2 (DGJ) | 277.4 | -0.5 | -6.0 | 19F | 9 |
| RHB'-8F-S1 (DGJ) | 277.4 | -0.5 | -6.0 | 19F | |
| RHB-45 (REJ) | 279.0 | -0.5 | -30.0 | 12p | |
| RHB-10-1 (SCR) | 280.0 | 0.0 | -6.0 | 19F (Stromatactis) | |
| RHB'-8G (DGJ) | 280.9 | -0.5 | -30.0 | 12g | 12p |
| RHB'-8G-BR (DGJ) | 280.9 | -0.5 | -30.0 | 12p | 12g |
| RHB'-8G-BL (DGJ) | 280.9 | -0.5 | -30.0 | 12p | |
| RHB'-8G-TR (DGJ) | 280.9 | -0.5 | -30.0 | 12p | |
| RHB'-8H-WL-S1 | 281.4 | 0.0 | -1000.0 | 19 (Stromatactis) | |
| RHB'-8H-W2-S2 | 281.4 | 0.0 | -1000.0 | 19 (Stromatactis) | |
| RHB'-8K-R | 281.4 | 0.0 | -1000.0 | 12g | |
| RHB'-8K-1 | 281.4 | 0.0 | -1000.0 | 12g | |
| RHB-47 (REJ) | 284.1 | -0.5 | -200.0 | 12g | |
| RHB-11 (SCR) | 284.1 | -0.5 | -200.0 | 12g | |
| RHB-13-1 (SCR) | 380.0 | -40.0 | -100.0 | 12p | |
| RHB-13-2 (SCR) | 390.0 | -2.0 | -30.0 | 12p | |
| RHB-14-1 (SCR) | 410.0 | -2.0 | -20.0 | 12p | |

| Cuba Section Sample Number | Stratigraphic Position (m) | Depth Minimum | Depth Maximum | Dominant Facies | Subordinate Facies |
|---|---|---|---|---|---|
| CU-1 | 0.5 | 1.5 | 0.0 | Dolostone | |
| CU-2 | 5.0 | 1.5 | 0.0 | 19f | 16 |
| CU-3-S1 | 16.0 | -0.5 | -10.0 | 12g | 12p |
| CU-3S2 | 19.0 | -0.5 | -30.0 | 12p | |
| CU-4-1 | 20.7 | 0.0 | -2.0 | 16 | 17 |
| CU-4-3 | 26.2 | -0.5 | -10.0 | 12g | |
| CU-4L | ? | -0.5 | -30.0 | 12p | 12g |
| CU'-4R | ? | -2.0 | -30.0 | 12g | 12p |
| CU-5-1 | 31.5 | -0.5 | -30.0 | 12g | |
| CU-5-2 | 42.0 | -0.5 | -30.0 | 12p | |
| CU-5-R | ? | -0.5 | -10.0 | 12g | |
| CU-6A | 52.0 | -0.5 | -30.0 | 12p | |
| CU-6L | ? | -0.5 | -30.0 | 12g | |
| CU--6R | ? | -2.0 | -30.0 | 12g | |
| CU-7-1 | 53.0 | -0.5 | -30.0 | 12p | |

# APPENDIX D

## STABLE ISOTOPE RATIO ANALYSES OF CARBON AND OXYGEN

## EXPLANATION

Appendix D presents stable carbon and oxygen isotope data in the order in which each unknown was run along with the standards run with each sample. The standards are included so that any questions regarding data quality can be independently evaluated. Analyses run in December of 1988 and early in 1989 were among the first that were run at the stable isotope laboratory at the Department of Geological Sciences, University of Tennessee.

### Standards and Reference Gases

The HO-CC (Penn State) standard or NBS-20 was used as a standard run with samples and/or to make reference gas from December 1988 through October, 1989. The Chicc (Chihuahua Calcite) standard was used as a standard and was run with samples to make reference gas after October, 1988. Additional, National Bureau of Standards (NBS), standards were used to periodically evaluate laboratory performance. NBS-20 (Solenhofen limestone) was used as an additional standard from December 1988 though December 1990. Standards NBS-19 and NBS-20 were used in October of 1990 to evaluate performance of on-line common acid bath extraction techniques (results are available in the stable isotope laboratory at the University of Tennessee).

### "Known" or Accepted Values for Standards

Values for NBS standards are based on an unpublished letter written by L.I. Barnes (National Bureau of Standards) in 1986. Values for the HO-CC and Chicc standards are based on personal communications and on records of analyses kept the stable isotope facility at the University of Tennessee.

| Reference Material | (25oC) δ13C vs. PDB | (25oC) δ18O vs. PDB |
|---|---|---|
| HO-CC (Penn State Std) | -5.5 | -9.37 |
| Chicc (Chihuahua Calcite) | -10.6 | -9.4 |
| NBS-18 | -5.00 | -23.00 |
| NBS-19 | 1.92 | -2.19 |
| NBS-20 (Solenhofen limestone) | -1.06 | -4.14 |

## Data Quality

Precision was evaluated within each run by comparing the results of each standard run that was run with unknowns to the accepted value for that standard. Each run is indicated by date and the temperature at which the standards and unknowns were run. Standards run at 55° ± 0.1°C were corrected for fractionation by averaging the results of all standards run at the same temperature during a run and then taking the difference of that average value from the accepted value. This difference was used to "correct" the values of unknowns run at 55°C to that which would be expected if they had been run at 25°C. Precision was evaluated between runs by comparing the mean value for each standard that was used to its accepted value. The standard deviation associated with these mean values is considered a measurement of precision. These means and standard deviations are as follows:

| | $\delta^{13}C$ | $\delta^{18}O$ | N |
|---|---|---|---|
| HO-CC Standard (at 55°C) | -5.4±0.3‰ | -10.9±0.3‰ | 22 |
| Chicc Standard (at 25°C) | -10.6±0.1‰ | -9.2±0.1‰ | 69 |

A precision of ± 0.2‰ is generally considered acceptable. Nearly all of the data presented in this appendix that were run using side-arm extraction methods at 25°C and are within ± 0.2‰. All of the data are within 0.3‰. All of the data run using the on-line extraction technique at 55°C using the HO-CC standard are within 0.3‰ and most of these data are within 0.2‰.

## Rejected and Qualified Data

Three types of qualified data are considered. The first type of qualified data have precision between 0.2‰ and 0.3‰ and include 25 fibrous calcite samples, 1 bladed calcite sample, and 1 blocky-clear calcite sample. The second type of qualified data are the analyses of December, 1988. These data appear to be within 0.2‰, but only three NBS-20 standards were run. Thus, it is difficult to evaluate the standard deviation associated with this run. The third type of qualified data are three analyses (mass spectrometer numbers 1718, 1722, and 1723) that represent the calcite portion of a mixed sample extracted using the method of Al Aasm et al. (1990). Precision associated with these samples is better than ± 0.2‰. However, these analyses are qualified because the method of extraction differs slightly from that used to extract all other calcite samples. All qualified data fall within fields previously established for these phases using data that are precise to ± 0.2‰. Qualified data

are indicated by light shading. Data that represent more than one phase were rejected. Data that have precision between 0.2‰ and 0.3‰, other than those considered above, were rejected. Rejected data are indicated by dark shading.

**Key to Abbreviations**

| | |
|---|---|
| D O18 | The value of $\delta^{18}O$ at 25°C |
| D C13 | The value of $\delta^{13}C$ at 25°C |
| Wt. mg. | Sample weight in milligrams |
| meters | Stratigraphic position in meters above Knox unconformity |
| STD | Indicates that a standard was run |
| Mass Spec Number | A four digit number or a letter followed by three digits. Mass spectrometer numbers are archived at the stable isotope facility at the University of Tennessee and are recorded at the time of the analysis. Mass spectrometer numbers that have a letter followed by three digits were archived retroactively. Entries with multiple mass spectrometer numbers have averaged $\delta^{13}C$ and $\delta^{18}O$ values. |
| Extraction Numbers | Samples run after October 15, 1990 have numbers that reference an archived record of sample extraction. "C1" refers to "Carbonate Line, Book 1" and "BL" refers to "Boat Launcher, Book 1." These archived records are maintained at the stable isotope facility at the University of Tennessee. These book numbers are followed by "RV" or "boat" and a number or letter which indicates the respective reaction vessel or boat in which each sample was extracted. |
| Sample I.D. | The sample identification number indicates the thin-section (actually, its corresponding rock chip or billet) from which each sample was drilled. This numbering scheme is consistent with those in Appendices A, B, C, E, and F. |

Key to Abbreviations (continued)

| | |
|---|---|
| TH | Thorn Hill Section |
| OTH | Old Thorn Hill Section |
| IS | Idol Mine Section |
| PVC | Poor Valley Creek Section |
| RHB | Red House Branch Section |
| AL | Alcoa Highway Section (Cantrell, 1982) |
| LN | L & N Railroad Section |
| OTT | Ottosee oolite |

Phase Name and "Zone" — Abbreviations for the sample phase follow below. Quotation marks enclose "Zone" because numbers that follow the phase indicate that a unique area of the phase was sampled. However, trimming relationships are not implied.

| | |
|---|---|
| (Ech) | Echinoderm Skeleton |
| (Bry) | Bryozoan Skeleton |
| Ooid | Ooid from the Ottosee Oolite, Middle Ordovician, Aloca Highway, East Tennessee. These data are shown for comparative purposes. They are not considered in the text. |
| Fib | Fibrous Calcite |
| Eqdol (calcite split) | The "calcite" portion or the first part of a mixed sample extracted following the method of Al Aasm et al. (1990). This portion of the sample was usually a mixture of two or more calcite phases and was generally rejected. |
| Eqdol (dolo. split) | Planer-e Dolomite. This is the "dolomite" portion or the second part of a mixed sample that was extracted following the method of Al Aasm et al. (1990). |
| Bladed | Bladed Calcite |
| Blocky-clear | Blocky Clear Calcite |

Key to Abbreviations (continued)

| | |
|---|---|
| Ovg or FeOvg | Non-Ferroan and Ferroan Syntaxial Overgrowth Calcite |
| Blocky-white Fe | Ferroan Blocky-White Calcite |
| Vein | Ferroan Vein Calcite |
| Csc-Fe | Ferroan Coarse Sparry Calcite |
| Csc-pink | Ferroan Coarse Pink Sparry Calcite |
| Csc-Fe (Co-ppt) | Ferroan coarse Sparry Calcite Co-Precipitated With Ferroan Baroque Dolomite |
| Bardol (calcite split) | This is the "calcite" portion or the first portion of the sample extracted following the method of Al Aasm et al. (1990). This portion of the sample was usually a mixture of two or more calcite phases and was generally rejected. |
| Bardol (dolo. split) | Ferroan Baroque Dolomite. This is the "dolomite portion or the second part of a mixed sample that was extracted following the method of Al Aasm et al. (1990). |
| Clear Spar | Coarse Clear Sparry Calcite |
| Bardol Nf (cal. split) | This is the "calcite" portion or the first portion of the sample extracted following the method of Al Aasm et al. (1990). This portion of the sample was usually a mixture of two or more calcite phases and was rejected. |

Bardol Nf (dolo. split) Non-Ferroan Baroque Dolomite. This is the "dolomite" portion or the second part of a mixed sample that was extracted following the method of Al Aasm et al. (1990).

Finally, to summarize, the shaded columns in the subsequent table represent the following:

| | | |
|---|---|---|
| Dark Shaded Rows | = | Rejected Data |
| Light Shaded Rows | = | Qualified Data |
| Non-shaded Rows | = | Data that are precise to better than $\pm$ 0.2% for both carbon and oxygen. |

| Stable Carbon And Oxygen Isotope Data Relative To PDB | | | | |
|---|---|---|---|---|
| Mass Spec Number and Sample I.D. | Meters | Wt. mg. | D C13 | D O18 |
| **Run 4-11 Dec 88 (Foreman), 55 deg. C** | | | | |
| A002 & A003 RHB-4A-S2-BR Fib 1 | 113.9 | 1.8 | 0.7 | -4.7 |
| A004 & A005 RHB-2C-B Fib 1 | 41.5 | 1.8 | 0.4 | -6.6 |
| A006, A007, A008 Solenh. Stand.(NBS-20) | STD | 1 | -1.3 | -4.2 |
| A009 & A010 RHB-2I-S2 Fib. 1 | 45 to 50 | 1.1 | 0.9 | -5.9 |
| A011 & A012 Solenh. Stand. (NBS-20) | STD | ?1 | -1.2 | -4.1 |
| A013 & A014 PVC-2E-S2 Fib 1 | 22.6 | 2 | 1.0 | -5.3 |
| A015 & A016 RHB-2I-S2 Fib 2 | 45 to 50 | 1.8 | 1.0 | -5.3 |
| A017 & A018 RHB-3F-S1 Blocky-white Fe 1 | 65 | 1.1 | 0.8 | -6.6 |
| A019 & A020 Solenh. Stand. (NBS-20) | STD | 0.8 | -1.1 | -4.1 |
| **Run 18-21 Jan 89 (Foreman), 55 deg. C** | | | | |
| B001 HO-CC Stand. | STD | 2.3 | -5.7 | -9.7 |
| B002 HO-CC Stand. | STD | 2.3 | -5.7 | -9.6 |
| B003 HO-CC Stand. | STD | 2.3 | -5.7 | -9.6 |
| B004 HO-CC Stand. | STD | 1.2 | -5.6 | -9.9 |
| B005 HO-CC Stand. | STD | 1.2 | -5.6 | -9.8 |
| B006 HO-CC Stand. | STD | 1.8 | -5.5 | -9.4 |
| B007 HO-CC Stand. | STD | 1.8 | -5.6 | -9.6 |
| B008 HO-CC Stand. | STD | 1.8 | -5.6 | -9.6 |
| B009 HO-CC Stand. | STD | 1.8 | -5.6 | -9.6 |
| B010, B011, B012 RHB-6B-BL Csc Fe | 183.4 | 0.9 | 0.4 | -9.8 |
| B013, B014 RHB-3F-S1 Csc Fe 2 | 65 | 0.3 | 0.1 | -9.0 |
| B015 HO-CC Stand. | STD | 1.6 | -5.6 | -9.7 |
| B016 HO-CC Stand. | STD | 1.6 | -5.6 | -9.7 |
| B017 & B018 RHB-4A-S1-R Csc Fe 1 | 113.9 | 2.7 | 0.8 | -9.5 |
| B019, B020, B021, B022 PVC-2J Csc Fe 1 | 21 to 41 | 2.2 | 0.6 | -10.0 |
| B023, B024, B025 PVC-2J Csc Fe 2 | 21 to 41 | 2.6 | 0.8 | -9.6 |
| B026 & B027 RHB-3F-S1 Blocky-white Fe 1 | 65 | 1.3 | 0.5 | -8.1 |
| B028 & B029 RHB-4A-S1-R Csc Fe 2 | 113.9 | 1.2 | 0.6 | -9.0 |
| B030 & B031 RHB-4A-S2BR Blocky-clear | 113.9 | 0.9 | 0.4 | -7.9 |
| **Run 17-20 March 1989, 55 deg.** | | | | |
| C001 HO-CC Stand. | STD | 9.92 | -5.7 | -10.4 |
| C002 PVC-1A-B Ovg | 11.6 | 0 | 0.4 | -8.4 |
| C003 RHB'-6A-BL Vein | 181 | 2.39 | 1.0 | -6.6 |
| C004 RHB'-6A-BR Ovg | 181 | 2.5 | 0.1 | -7.7 |

| Mass Spec Number and Sample I.D. | Meters | Wt. mg. | D C13 | D O18 |
|---|---|---|---|---|
| C005 RHB'-6D-M Ovg | 188 | 1.81 | 0.9 | -6.9 |
| C006 HO-CC Stand | STD | 10.94 | -5.6 | -9.4 |
| C007 RHB-6C Ovg | 184 | 1.12 | -0.3 | -7.3 |
| C008 RHB-6D-R Ovg | 188 | 0.84 | 0.9 | -8.1 |
| C009 RHB-3I-T (Bry) | 85 | 0.37 | 0.7 | -5.9 |
| C010 HO-CC Stand | STD | 0.96 | -5.7 | -9.7 |
| C011 RHB-3I-T (Bry) | 148 | 0.02 | -0.4 | -6.8 |
| C012 RHB-8C-L Ovg. | 265.4 | 0.38 | -0.1 | -8.0 |
| C013 RHB'-6B-T ?Ovg | 183.4 | ?0 | -0.1 | -7.6 |
| C014 RHB'-6B-T (Ech) | 183.4 | 0.76 | 0.2 | -6.5 |
| C015 HO-CC Stand. | STD | 1.03 | -5.2 | -9.0 |
| **Run 7 June 1989 (Class Proj.); 55 deg. C** | | | | |
| D001 HO-CC Stand. | STD | 1? | -5.8 | -9.4 |
| D002 HO-CC Stand. | STD | 1? | -5.8 | -9.4 |
| D003 HO-CC Stand. | STD | 1? | -5.6 | -9.4 |
| D004 HO-CC Stand. | STD | 1? | -5.6 | -9.3 |
| D005 HO-CC Stand. | STD | 1? | -5.5 | -9.4 |
| D006 HO-CC Stand. | STD | 1? | -5.5 | -9.3 |
| D007 HO-CC Stand. | STD | 1? | -5.4 | -9.4 |
| D008 HO-CC Stand. | STD | 1? | -5.4 | -9.4 |
| D009 HO-CC Stand. | STD | 1? | -5.4 | -9.4 |
| D014 & D015 OTT-89-2 Ooids | ? | <1 | 0.0 | -7.3 |
| D020 & D021 AL-89-4 Ooids | ? | <1 | -0.7 | -7.4 |
| D026 & D027 AL-89-4 Ooids | ? | <1 | -0.9 | -8.0 |
| **Run 25 June 1989 (Class Proj.); 55 deg. C** | | | | |
| E001 HO-CC Stand. | STD | 1? | -5.3 | -9.2 |
| E002 HO-CC Stand. | STD | 1? | -5.3 | -9.3 |
| E003 HO-CC Stand. | STD | 1? | -5.6 | -9.6 |
| E004 HO-CC Stand. | STD | 1? | -5.6 | -9.6 |
| E005 HO-CC Stand. | STD | 1? | -5.6 | -9.6 |
| E006 HO-CC Stand. | STD | 1? | -5.4 | -9.3 |
| E007 HO-CC Stand. | STD | 1? | -5.4 | -9.3 |
| E008 HO-CC Stand. | STD | 1? | -4.9 | -9.1 |
| E009 HO-CC Stand. | STD | 1? | -5.5 | -9.3 |
| E010 & E011 AL-89-5 Ooids | ? | <1 | -0.1 | -6.9 |
| **Run 10 October 1989 (Foreman) 55 deg. C** | | | | |

| Mass Spec Number and Sample I.D. | Meters | Wt. mg. | D C13 | D O18 |
|---|---|---|---|---|
| 0161 HO-CC Stand. | STD | 0.78 | -5.9 | -9.5 |
| 0168 HO-CC Stand. | STD | 1.86 | -5.1 | -9.3 |
| 0172 RHB-2C-B Fib 2 | 41.5 | 2.28 | 0.6 | -5.8 |
| 0173 PVC'-2H Fib 1 | 21 | 2.57 | -1.0 | -5.2 |
| 0176 HO-CC Stand. | STD | 0.56 | -4.7 | -9.4 |
| **Run 16-17 October 1989 (Class Proj.); 55 deg. C** | | | | |
| F001 HO-CC Stand. | STD | <1 | -5.7 | -9.3 |
| F003 HO-CC Stand. | STD | <1 | -5.8 | -9.4 |
| F004 AL-89-4.1 Ooids | ? | <1 | -0.8 | -7.2 |
| F005 AL-89-4.2 Ooids | ? | <1 | -0.3 | -7.4 |
| F006 AL-89-1.1 Ooids | ? | <1 | -0.1 | -7.1 |
| F007 AL-89-1.2 Ooids | ? | <1 | -0.1 | -7.3 |
| F008 & F009 AL-89-3 Ooids | ? | <1 | -0.1 | 10.6 |
| F010 & F011 AL-89-2.2 Ooids | ? | <1 | -0.2 | -8.0 |
| F012 LN-89-2a Ooids | ? | <1 | 0.2 | -7.4 |
| F013 AL-89-2.1 Ooids | ? | <1 | 0.0 | -7.4 |
| F014 AL-89-4.3 Ooids | ? | <1 | -0.1 | -7.5 |
| F019 HO-CC Stand. | STD | <1 | -5.4 | -9.4 |
| F020 HO-CC Stand. | STD | <1 | -5.4 | -9.5 |
| F021 LN-1A Ooids | ? | <1 | 0.3 | -7.1 |
| F022 HO-CC Stand. | STD | <1 | -4.6 | -9.4 |
| F023 HO-CC Stand. | STD | <1 | -4.6 | -9.3 |
| **Run 24 October 1989; 55.15 deg. C** | | | | |
| 0132 HO-CC Stand. | STD | 1.47 | -5.5 | -10.0 |
| 0133 HO-CC Stand. (Dup) | STD | 1.47 | -5.6 | -10.5 |
| 0134 & 0135 PVC'-2K-S2 Fib | >27.6<33.6 | 1.78 | 0.8 | -5.1 |
| 0136 PVC'-2A-1a Fib 1 | 24.6 | 1.22 | 0.6 | -5.2 |
| 0137 PCV-2A-1b Fib 1 | 24.6 | 1.54 | 0.7 | -5.0 |
| 0138 PVC-2A-1b Blocky-clear | >18.6<20.6 | 1.21 | 0.7 | -6.6 |
| 0139 PVC'-2D-a Fib 1 | 21.6 | 1.11 | 0.9 | -5.3 |
| 0140 PVC'-2Gb Fib 1 | 26.6 | 1.08 | 0.9 | -4.3 |
| 0141 PVC'-2H Fib 2 | 21 | 1.14 | 0.7 | -5.0 |
| 0142 PVC'-2D-b Fib 1 | 21.6 | 1.11 | 0.8 | -4.9 |
| 0143 PVC'-2A-LM Fib 1 | >18.6<20.6 | 2.43 | 0.7 | -4.9 |
| 0144 RHB-2C-B Fib 3 | 41.5 | 3.49 | 0.3 | -7.7 |
| 0145 RHB-2H Fib 1 | ?26.85 | 3.25 | 0.9 | -5.9 |

| Mass Spec Number and Sample I.D. | Meters | Wt. mg. | D C13 | D O18 |
|---|---|---|---|---|
| 0146 & 0147 RHB-2I-S2 Fib 2 | 45 to 50 | 3.6 | 1.1 | -5.2 |
| 0148 HO-CC Stand. | STD | 3.15 | -5.1 | -8.7 |
| 0149 HO-CC Stand. | STD | 15 | -5.7 | -9.6 |
| **Run 15-Oct-90, 25 deg. C** | | | | |
| 1443 C1-136 RV16 Chicc STD | STD | 15.01 | -10.6 | -9.1 |
| 1444 C1-135 RV1 TH-89-93 Vein 1 | 182.8 | 16.29 | 0.5 | -9.6 |
| 1445 C1-135 RV18 OTH-90-56 Vein 1 | 223 | 9.86 | 0.4 | -10.5 |
| 1446 C1-135 RV 14 OTH-90-52a Vein 1 | 218.6 | 19.66 | 0.2 | -7.4 |
| 1447 C1-135 RVB TH-89-160N Blocky-clear 1 | 233.3 | 16.85 | 0.4 | -7.5 |
| 1448 C1-136 RV16 Chicc STD | STD | 15.01 | -10.6 | -9.1 |
| 1449 C1-136 RV3 TH-89-124 Blocky-clear | 211.7 | 11.45 | 0.3 | -7.7 |
| 1450 C1-136 RV15 TH-89-164 Vein1 | 236.7 | 10.69 | 0.2 | -7.0 |
| 1452 C1-136 RVC TH-89-77b Blocky-white Fe 1 | 168.8 | 11.59 | 0.6 | -8.2 |
| 1453 C1-137 RV13 TH-89-164, Vein 2 | 236.7 | 8.28 | 0.2 | -7.2 |
| 1454 C1-137 RV10 OTH-90-21 Csc-. Fe 1 | 141.3 | 13.63 | -0.2 | -8.9 |
| 1455 C1-138 RV1 HOCC | STD | 6.12 | -5.6 | -9.4 |
| 1456 C1-137 RV18 Chicc STD | STD | 19.33 | -10.5 | -9.2 |
| 1457 C1-137 RV18 Chicc STD, Repeat | STD | 19.33 | -10.6 | -9.1 |
| 1458 C1-137 RV5 OTH-90-52b, Vein 1 | 218.6 | 10.5 | 0.2 | -7.7 |
| 1459 C11-137 RV11 TH-89-123, Blocky-clear 1 | 211.3 | 11.56 | 0.4 | -7.4 |
| 1461 C1-137 IS-90-43b Csc Fe 1R | 232.9 | 23.1 | 0.4 | -8.5 |
| 1462 C1 138 RV1 HOCC Std | STD | 6.12 | -5.7 | -9.3 |
| 1463 C1 137 RVB TH-89-95a Csc-. Fe | 184.90 | 19.09 | 0.4 | -8.3 |
| 1464 C1-138 RV15 Chicc STD | STD | 27.16 | -10.6 | -9.2 |
| 1465 C1-138 RV12 TH-89-170a Vein Comp. 1 | 244.20 | 9.05 | 0.4 | -7.8 |
| 1466 C1 138 RVA TH-89-170a, Blocky-clear 1 | 244.20 | 6.44 | 0.3 | -7.6 |
| 1466' C1 138 RV15 Chicc STD | STD | 27.16 | -10.6 | -9.3 |
| 1467 C1 RVC TH-89-77a, Blocky-white Fe 1 | 168.80 | 12.01 | 0.6 | -8.0 |
| 1468 C1-139 RVD TH-89-95a Csc-Fe 1 | 184.90 | 2.65 | 0.5 | -8.1 |
| 1468'C1-139 RV11 Chicc STD | STD | 6.21 | -10.6 | -9.3 |
| 1469 C1-139 RV13 TH-89-100a Csc-Fe 2a | 184.90 | 18.87 | 1.0 | -8.6 |
| 1470 C1-139 RV10 TH-89-95b Csc-Fe 1 | 184.90 | 10.53 | 0.5 | -8.6 |
| 1471 C1-139 RV16 TH-89-126 Blocky-clear | 212.80 | 15.01 | 0.3 | -7.7 |
| 1472 C1-139 RV5 Chicc STD | STD | 17.07 | -10.6 | -9.2 |
| **Run 20-Oct-90, 25 deg. C** | | | | |
| 1500 C1-141 RV11 Chicc STD | STD | 3.72 | -10.7 | -9.6 |

| Mass Spec Number and Sample I.D. | Meters | Wt. mg. | D C13 | D O18 |
|---|---|---|---|---|
| 1501 C1-141 RV11 Chicc STD | STD | 3.72 | -10.8 | -9.6 |
| 1511 C1-142 RV13 TH-89-169 vein 1 | 242.80 | 5.51 | 0.0 | -6.9 |
| 1512 C1-142 RV15 TH-89-134 Blocky-clear 1 | 218.60 | 6 | 0.2 | -7.7 |
| 1513 C1-142 RV3 Chicc STD | STD | 15.87 | -10.6 | -9.3 |
| 1515 C142 RV14 TH-89-178 Blocky-white Fe 1 | 253.80 | 9.42 | 0.3 | -7.9 |
| 1516 C1-142 RV18 TH-90-212a (slab) Blocky-clear 1 | 298.80 | 15.84 | 0.1 | -6.9 |
| 1517 C1-143 RV11 TH-89-100a Csc-Fe 2b | 187.80 | 5.8 | 0.7 | -8.6 |
| 1518 C1-1433 RV10 TH-89-180 Blocky-clear 1 | 255.20 | 15.89 | 0.4 | -7.8 |
| 1519 C1-143 RV9 TH-89-100a Csc Fe 1 | 187.80 | 22.13 | 0.7 | -8.3 |
| 1520 C1-143 RV7 Chicc STD | STD | 14.34 | -10.6 | -9.2 |
| 1521 C1-14 RV5 TH-89-193 Vein 1 | 264.10 | 11.79 | 0.4 | -7.2 |
| 1522 C1-144 RV16 TH-89-196 Vein 1 | 267.20 | 8.7 | 0.5 | -8.6 |
| 1523 C1-144 RV1 TH-89-142a Blocky-white Fe1 | 224.40 | 5.68 | 0.3 | -7.5 |
| 1524 C1-144 RVC TH-89-178 Blocky-white Fe | 253.80 | 8.52 | 0.4 | -7.5 |
| 1525 C1-143 RV7 Chicc STD | STD | 14.34 | -10.5 | -9.2 |
| 1526 C1-144 RVA TH-90-213 Blocky-white Fe 1 | 304.30 | 19.18 | 0.5 | -7.1 |
| 1527 C1-144 RV15 Chicc STD | STD | 6.1 | -10.6 | -9.3 |
| 1532 C1-142 RV3 Chicc STD | STD | 15.87 | -10.6 | -9.3 |
| **Run 24-Oct-90, 25 deg. C** | | | | |
| 1544 C1-147 RV12 Chicc STD | STD | 3.13 | -10.7 | -9.0 |
| 1545 C1-146 RVD OTH-90-58b Blocky-white Fe | 227.00 | 6.71 | 0.6 | -8.1 |
| 1546 C1-147 RV7 OTH-101b, Blocky-white Fe 1a | 332.60 | 4.69 | 0.5 | -7.8 |
| 1547 C1-147 RV3 OTH-90-111, Blocky-white Fe | 345.10 | 4.93 | 0.0 | -7.4 |
| 1548 C1-147 RV9 IS-90-46 Fib. 1 | 234.60 | 3.33 | 1.0 | -4.7 |
| 1549 C1-147 RV13 Chicc STD | STD | 4.7 | -10.6 | -9.2 |
| 1550 C1-147 RV16 OTH-90-114a Blocky-white Fe 1a | 356.40 | 5.93 | -0.3 | -7.3 |
| 1551 C1-147 RVB IS-90-63 Blocky to Bladed | 282.70 | 4.38 | -1.3 | -7.0 |
| 1552 C1-147 RVC IS-90-43b2 Clear Spar 1 | 232.90 | 9.04 | 4.3 | -5.5 |
| 1553 C1-148 RV10 Chicc STD | STD | 7.85 | -10.4 | -9.0 |
| 1554 C1-148 RV18 IS-90-47a Fib. | 234.70 | 7.13 | 0.5 | -4.4 |
| 1555 C1-148 RV11 OTH-90-101b, Blocky-white Fe 1b | 332.60 | 5.66 | 0.4 | -8.0 |
| 1556 C1-148 RV14 OTH-90-114a Blocky-white Fe 1b | 356.40 | 6.17 | -0.4 | -7.6 |
| 1557 C1-148 RV1 Chicc STD | STD | 7.5 | -10.6 | -9.3 |
| **Run 11-Nov-90, 25 deg. C** | | | | |
| 1567 C1-149 RV11 Chicc STD | STD | 2.31 | -10.8 | -9.5 |
| 1568 C1-149 RV11 Chicc STD | STD | 2.31 | -10.7 | -9.5 |

| Mass Spec Number and Sample I.D. | Meters | Wt. mg. | D C13 | D O18 |
|---|---|---|---|---|
| 1569 C1-148 RV5 TH-89-95 (slab) Fib. 1 | 184.9 | 1.66 | 0.4 | -5.0 |
| 1570 C1-149 RV3 TH-89-95 (slab) Fib. 2 | 184.9 | 2.33 | 0.5 | -4.8 |
| 1571 C1-149 RVD RHB-8H-W2 Fib. 1 | 281.4 | 2.6 | 0.7 | -5.1 |
| 1572 C1-149 RV16 PVC-2C Fib. 1 | 14 | 2.52 | 0.8 | -4.9 |
| 1573 C1-149 RV15 RHB-2K-Fib. 1 | 42.5 to 50 | 2.98 | 0.8 | -5.6 |
| 1574 C1-149 RV13 Chicc STD | STD | 3.6 | -10.6 | -9.4 |
| 1575 C1-149 RV1 PVC-3A-B Blocky-clear | 39.6 | 9.41 | 0.8 | -6.6 |
| 1576 C1-149 RV9 RHB-2B-C1 Fib.1 | 41.25 | 2.7 | 1.0 | -5.2 |
| 1577 C1-150 RV12 PVC-2F Blocky-clear | 13.5 to 22 | 3.02 | 0.8 | -6.1 |
| 1578 C1-150 RV14 Chicc STD | STD | 2.33 | -10.6 | -9.2 |
| 1579 C1-150 RV18 PVC-2F Fib 1 | 13.5 to 22 | 4.26 | 1.1 | -5.0 |
| 1580 C1-150 RV7 Chicc STD | STD | 6.88 | -10.6 | -9.4 |
| **Run 18-Nov-90, deg. C** | | | | |
| 1601 C1-154 RV Chicc STD | STD | 3.83 | -10.5 | -9.3 |
| 1602 C1-153 RVA RHB-2K Fib 2 | 42.5 to 50 | 4.23 | 0.8 | -5.3 |
| 1603 C1-153-RV5 PVC-2Gb Fib 2 | 20 | 5.63 | 1.0 | -6.6 |
| 1604 C1-153 RV18 PVC-2A-1b Fib 2 | 24.60 | 2.95 | 1.1 | -4.8 |
| 1605 C1-153 RV15 PVC-2A-1a Fib 2 | 24.60 | 3.94 | 1.2 | -4.9 |
| 1606 C1-153 RV9 TH-89-95 (slab) Fib 3 | 184.90 | 3.84 | 0.8 | -4.8 |
| 1607 C1-154-RV10 Chicc STD | STD | 3.7 | -10.6 | -9.2 |
| 1608 C1-153 RV13 IS-90-47a Fib 2 | 234.70 | 2.29 | 0.8 | -5.4 |
| 1609 C1-154 RV7 RHB-2H Fib 3 | 42 to 42.5 | 3.03 | 0.9 | -6.0 |
| 1610 C1-153 RVD TH-89-95 (slab) Fib 4 | 184.90 | 3.96 | 0.6 | -4.5 |
| 1611 C1-154 RV12 Chicc STD | STD | 2.95 | -10.5 | -8.8 |
| 1612 C1-156 RV16 Chicc STD | STD | 11.13 | -10.5 | -9.1 |
| 1613 C1-154 RVB-PVC-2K-S2 Fib 2 | 20.1 to 44 | 6.55 | 1.2 | -4.8 |
| 1614 C1-154 RVC PVC-2AL-LM Fib 2 | 13.5 to 22 | 5.36 | 0.2 | -4.8 |
| 1615 C1-155 RV11 PVC-2F Fib 2 | 13.5 to 22 | 3.19 | 1.2 | -4.3 |
| 1616 C1-155 RV14 RHB-2H Fib 2 | 42 to 42.5 | 4.83 | 0.9 | -5.4 |
| 1617 C1-156 RV16 Chicc STD | STD | 11.13 | -10.5 | -9.1 |
| 1618 C1-155 RV1 PVC-2G (Bill) Csc-pink | 20.00 | 24 | 0.8 | -11.0 |
| 1619 C1-155 RV18 PVC-2A-1b Fib 3 | 24.60 | 3.65 | 1.0 | -4.9 |
| 1620 C1-155 RV5 PVC-2K-S2 Fib 3 | 20.1 to 44 | 6 | 1.2 | -4.7 |
| 1621 C1-156 RVD PVC-2A-1a Fib 3 | 24.60 | 3.9 | 1.2 | -4.2 |
| 1622 C1-156 RV3 PVC-2A-1a Csc-Fe | 24.60 | 8.48 | 0.9 | -8.6 |
| 1623 C1-154 RV16 Chicc STD | STD | 21.48 | -10.6 | -9.4 |

| Mass Spec Number and Sample I.D. | meters | Wt. mg. | D C13 | D O18 |
|---|---|---|---|---|
| **Run 24-Nov-90, 25 deg. C.** | | | | |
| 1626 C1-158 RV18 NBS-20 STD | STD | 18.64 | -1.1 | -4.0 |
| 1627 C1-157 RVA PVC-2C-1a Fib 1 | 20.60 | 4.68 | 0.9 | -4.1 |
| 1628 C1-157 RV12 PVC-2C-1a Fib 2 | 20.60 | 2.39 | 0.8 | -5.3 |
| 1629 C1-157 RV9 RHB-2I-S2 Blocky-clear 1 | 45 to 50 | 3.69 | 0.4 | -6.2 |
| 1630 C1-158 RV11 Chicc STD | STD | 5.56 | -10.6 | -8.8 |
| 1631 C1-158 RV11 Chicc STD | STD | 5.56 | -10.6 | -9.0 |
| 1632 C1-157 RV5 RHB-8H-WL Fib 2 | 317.40 | 2.87 | 0.5 | -4.9 |
| 1633 C1-157 RHB-2B-C1 Fib 3 | 41.25 | 2.22 | 0.7 | -5.3 |
| 1634 C1-157 RVD RHB-8H-WL Fib 3 | 317.40 | 2.13 | 0.4 | -5.1 |
| 1635 C1-157 RV15 PVC-2C-1a Blocky-White Fe 1 | 20.60 | 6.01 | 0.8 | -6.9 |
| 1636 C1-157 RHB-2H Vein 2 | 42 to 42.5 | 4.58 | 0.7 | -7.4 |
| 1637 C1-158 NBS-20 STD | STD | 18.64 | -1.1 | -4.1 |
| 1638 C1-159 RV1 Chicc STD | STD | 4.69 | -10.7 | -8.9 |
| 1639 C1-159 RV1 Chicc STD | STD | 4.69 | -10.7 | -9.1 |
| 1640 C1-158 RVB IS-90-46 Fib 2 | 234.60 | 2.21 | 0.8 | -5.3 |
| 1641 C1-158 RV3 IS-90-47a Blocky 1(?Bladed) | 234.70 | 1.99 | 1.1 | -6.3 |
| 1642 C1-158 RHB-2C-B Csc-pink 1 | 41.50 | 3 | -1.1 | -10.5 |
| 1643 C1-158 RV7 RHB-2B-C1 Fib 2 | 41.25 | 1.68 | 0.3 | -5.8 |
| 1644 C1-158 RV14 Chicc STD | STD | 4.42 | -10.7 | -8.6 |
| 1645 C1-158 R14 Chicc STD | STD | 4.42 | -10.7 | -8.9 |
| 1646 C1-159 RVD PVC-2J Fib 3 | 21 to 44 | 1.72 | 0.6 | -5.9 |
| 1647 C1-159 RV3 PVC-2J Fib 1 | 21 to 44 | 3.75 | 0.9 | -4.5 |
| 1648 C1-159 RV12 Chicc STD | STD | 5.23 | -10.6 | -8.8 |
| 1649 C1-159 RV12 Chicc STD | STD | 5.23 | -10.7 | -9.0 |
| 1650 C1-59 PVC-2G(Bill) Fib 2 | 26.60 | 2.99 | 0.9 | -4.8 |
| 1651 C1-159 RV15 PVC-2G((Bill) Fib 1 | 26.60 | 1.37 | 0.8 | -5.5 |
| 1652 C1-159 RV13 PVC-2J Csc-pink 1 | 21 to 44 | 3.7 | 0.5 | -10.1 |
| 1653 C1-159 PVC-2J Fib 4 | 21 to 44 | 1.68 | 0.8 | -5.4 |
| 1654 C1-RVC Chicc STD | STD | 2.23 | -10.8 | -9.1 |
| **Run 28-Nov-90, 25 deg. C** | | | | |
| 1672 C1-160 RV16 Chicc STD | STD | 17.96 | -10.7 | -9.2 |
| 1673 C1-160 RV16 Chicc STD | STD | 17.96 | -10.6 | -9.2 |
| 1674 C1-161 RVA PVC-2G (Bill) Fib 4 | 26.40 | 3.46 | 0.9 | -5.2 |
| 1675 C1-161 RV3 PVC-2J Fib 6 | 21 to 44 | 6.96 | 0.9 | -4.6 |
| 1676 C1-161 RV1 PVC-2G (Bill) Fib 3 | 26.60 | 3.76 | 1.0 | -4.7 |

| Mass Spec Number and Sample I.D. | Meters | Wt. mg. | D C13 | D O18 |
|---|---|---|---|---|
| 1677 C1-161 RV15 PVC-2J Fib 8 | 21 to 44 | 6.8 | 0.9 | -5.4 |
| 1678 C1-161-RV12 PVC-2J Fib 5 | 21 to 44 | 4.09 | 0.9 | -5.1 |
| 1679 C1-162 RV14 Chicc STD | STD | 4.15 | -10.7 | -9.2 |
| 1680 C1-162 RV14 Chicc STD | STD | 4.15 | -10.8 | -9.2 |
| 1681 C1-161 PVC-2C-a1 Fib 4 | 20.60 | 4.4 | 1.0 | -4.7 |
| 1682 C1-161 RV5 PVC-2C-1a Blocky-white Fe 2 | 20.60 | 4.98 | 0.8 | -7.3 |
| 1683 C1-162 RVB PVC-2J Csc-pink 2 | 21 to 44 | 5.4 | 0.7 | -10.1 |
| 1684 C1-162 RV16 Chicc STD | STD | 4.67 | -10.7 | -9.2 |
| **Run 2-Dec-90, 25 deg. C** | | | | |
| 1691 C1-160 RV16 | STD | 17.96 | -10.6 | -9.1 |
| 1692 C1-162 RV5 PVC-2C-1a Fib 6 | 20.60 | 4.03 | 1.0 | -4.6 |
| 1693 C1-162 RV14 Chicc STD | STD | 4.15 | -10.7 | -8.6 |
| 1694 C1-162 RV14 Chicc STD | STD | 4.15 | -10.7 | -9.1 |
| 1695 C1-161 RV7 PVC-2J Fib 7 | 21 to 44 | 9.89 | 0.9 | -4.7 |
| 1696 C1-162 RV16 Chicc STD | STD | 4.67 | -10.4 | -8.4 |
| 1697 C1-162 RV18 Chicc STD | STD | 4.76 | -10.7 | -8.9 |
| 1698 C1-162 RV18 Chicc STD | STD | 4.76 | -10.7 | -9.1 |
| 1699 C1-162 RV3 PVC-2C-1a Fib 3 | 20.60 | 3.61 | 1.0 | -4.8 |
| 1700 C1-162 PVC-2A-1a Fib 4 | 24.60 | 3.36 | 1.1 | -5.2 |
| 1701 C1-163 RV12 RHB-8H-WL-S1 Fib 4 | 317.40 | 3.15 | 0.7 | -4.5 |
| 1702 C1-163 RVD Chicc STD | STD | 4.29 | -10.7 | -9.3 |
| 1703 C1-160 RV16 Chicc STD | STD | 17.96 | -10.6 | -9.1 |
| 1704 C1-163 RV1 RHB-2I-S2 Blocky-clear 2 | 45 to 50 | 3.13 | 0.0 | -6.8 |
| 1705 C1-163 RVD Chicc STD | STD | 4.29 | -10.6 | -9.0 |
| 1706 C1-163 Chicc STD | STD | 4.29 | -10.6 | -9.1 |
| 1707 C1-63 RV9 IS-90-46 Fib 3 | 234.60 | 2.64 | 0.8 | -4.7 |
| 1708 C1163 RV13 RHB-8H-WL Fib 5 | 317.40 | 2.58 | 0.7 | -4.8 |
| 1709 C1-163 RVB RHB-2H Vein 3 | 42 to 42.5 | 3.95 | 0.3 | -7.4 |
| 1710 C1-164 RV7 Chicc STD | STD | 2.05 | -10.7 | -9.3 |
| 1711 C1-163 RV15 RHB-2C-B Csc-spar 2 | 41.50 | 3.78 | 0.5 | -10.0 |
| 1712 C1-164 RV5 RHB-2B-C1 Fib 4 | 41.25 | 1.78 | 0.8 | -5.3 |
| 1713 C1-164 RVC RHB-2B-C1 Fib 5 | 41.25 | 1.26 | 0.5 | -5.6 |
| 1714 C1-164 RVA Chicc STD | STD | 1.8 | -10.7 | -9.6 |
| 1716 C1-164 Chicc STD | STD | 1.8 | -10.8 | -9.6 |
| 1717 C1-164 Chicc STD | STD | 1.8 | -10.8 | -9.5 |
| 1718 C1-164 RVA OTH-90-2A Bardol 1(cal. = vein) | 74.10 | 7.81 | -1.0 | -10.6 |

| Mass Spec Number and Sample I.D. | Meters | Wt. mg. | D C13 | D O18 |
|---|---|---|---|---|
| 1719 C1-165 RV14 RHB-2B-C1 Bardol 1 (cal.= Blk-wht Fe | 41.25 | 10.41 | 0.8 | -7.7 |
| 1720 C1-164 RV16 Chicc STD | STD | 3.77 | -10.6 | -9.2 |
| 1721 C1-164 RV1 PVC-1A-T Bardol 1(calcite split) | 11.60 | 11.06 | 1.0 | -8.3 |
| 1722 C1-165 RV16 IS-90-0A Bardol 1(cal. = Csc Fe) | 28.10 | 12.82 | 0.1 | -8.6 |
| 1723 C1-165 RV9 RHB-2C-B Bardol 1(calcite split) | 41.50 | 8.36 | 1.1 | -6.6 |
| 1724 C1-163 RVD Chicc STD | STD | 4.29 | -10.6 | -9.0 |
| 1725 C1-160 RV16 Chicc STD | STD | 17.96 | -10.6 | -9.1 |
| 1726 C1-166 RHB-6B-T Bardol 1(calicte split) | 183.40 | 8.65 | 1.4 | -7.5 |
| 1727 C1-166 RV5 IS-90-0B Bardol 1(calcite split) | 28.10 | 16.25 | 0.3 | -8.8 |
| 1728 C1-164 RV7 Chicc STD | STD | 2.5 | -10.7 | -9.3 |
| **Run 5-Dec-90, 25 deg. C** | | | | |
| 1746 C1-160 RV13 NBS-20 STD | STD | 15.2 | -1.1 | -4.1 |
| 1747 C1-164 RVA OTH-90-2A Bardol 1(dolo. split) | 74.10 | 7.81 | -0.1 | -8.7 |
| 1748 C1-165 RV7 Chicc STD | STD | 9 | -10.6 | -9.0 |
| 1749 C1-165 RV7 Chicc STD | STD | 9 | -10.6 | -9.0 |
| 1750 C1-166 RVD Chicc STD | STD | 10.45 | -10.7 | -9.2 |
| 1751 C1-164 RV1 PVC-1A-T Bardol 1(dolo. split) | 11.60 | 11.06 | 1.7 | -7.8 |
| 1752 C1-164 RV1 PVC-1A-T Bardol 1(dolo. split) | 11.60 | 11.06 | 1.6 | -7.9 |
| 1753 C1-165 RV14 RHB-2B-C1 Bardol 1 (dolo. split) | 41.25 | 10.41 | 1.4 | -7.4 |
| 1754 C1-165 RV9 RHB-2C-B Bardol 1(dolo. split) | 41.50 | 8.36 | 1.7 | -5.7 |
| 1755 C1-165 RV16 IS-90-0A Bardol 1 (dolo. split) | 28.10 | 12.82 | 0.5 | -7.7 |
| 1756 C1-166 RV1 Chicc STD | STD | ?>10 | -10.7 | -9.2 |
| 1757 C1-166 RHB-6B-T Bardol 1(dolo. split) | 183.40 | 8.65 | 1.9 | -7.9 |
| 1758 C1-166 RV5 IS-90-0B Bardol 1 (dolo. split) | 28.10 | 16.25 | 0.5 | -8.0 |
| 1759 C1-165 RV13 RHB-3R-a2 Bardol 1(dolo. split) | 85 to 114 | 12.14 | 1.6 | -7.6 |
| 1760 C1-166 RV3 Chicc STD | STD | 12.62 | -10.6 | -9.1 |
| **Run 8-Dec-90, 25 deg. C** | | | | |
| 1761 C1-166 RVD Chicc STD | STD | 10.4 | -10.6 | -9.1 |
| 1762 C1-166 RVD Chicc STD | STD | 10.4 | -10.7 | -9.1 |
| 1763 C1-160 RV13 NBS-20 | STD | 15.2 | -1.0 | -4.0 |
| 1764 C1-169 RV9 IS-90-37 Eqdol 1(calcite split) | 216.20 | 11.23 | 0.8 | -6.1 |
| 1765 C1-168 RVA TH-89-84a Eqdol 1(clacite split) | 175.20 | 16.55 | 0.7 | -5.8 |
| 1766 C1-168 RVA TH-89-84a Eqdol 1(clacite split) | 175.20 | 16.55 | 0.7 | -5.9 |
| 1767 C1-168 RVA TH-89-84a Eqdol 1(clacite split) | 175.20 | 16.55 | 0.7 | -5.9 |
| 1768 C1-168 RV13 IS-90-29 Bardol Nf1(calcite split) | 191.40 | 12.88 | 0.9 | -7.1 |
| 1769 C1-166 RV15 Chicc STD | STD | >10 | -10.7 | -9.3 |

| Mass Spec Number and Sample I.D. | meters | Wt. mg. | D C13 | D O18 |
|---|---|---|---|---|
| 1770 C1-166 RV15 Chicc STD | STD | >10 | -10.7 | -9.2 |
| 1771 C1-RV12 TH-89-67 Eqdol 1 (clacite split) | 160.90 | 13.37 | 0.2 | -6.5 |
| 1772 C1-168 RV14 OTH-90-62 Eqdol 1(dolo. split) | 230.40 | 13.58 | 0.7 | -5.1 |
| 1773 C1-RV12 TH-89-67 Eqdol 1(dolo. split) | 160.90 | 13.37 | 1.4 | -3.5 |
| 1774 C1-168 RV16 OTH-90-87 Eqdol 1 (dolo. split) | 317.90 | 9.03 | 1.2 | -4.7 |
| 1775 C1-166 RV3 Chicc STD | STD | 12.62 | -10.6 | -9.2 |
| 1776 C1-166 RV3 Chicc STD | STD | 12.62 | -10.6 | -9.2 |
| 1777 C1-169 RV9 IS-90-37 Eqdol 1 (dolo. split) | 216.20 | 11.23 | 1.7 | -5.3 |
| 1778 C1-168 RV13 IS-90-29 Bardol Nf 1 (dolo. split) | 191.40 | 12.88 | 1.4 | -6.9 |
| 1779 C1-168 RVA TH-89-84a Eqdol 1 (dolo. split) | 175.20 | 16.55 | 1.7 | -4.8 |
| 1780 C1-169 Chicc STD | STD | 16.51 | -10.6 | -9.2 |
| 1781 C1-169 Chicc STD | | 16.51 | -10.7 | -9.2 |
| **Run 10-Dec-90, 25 deg. C** | | | | |
| 1782 C1-169 RVC Chicc STD | STD | 16.51 | -10.7 | -9.1 |
| 1783 C1-169 RVC Chicc STD | STD | 16.51 | -10.7 | -9.2 |
| 1784 C1-166 RV3 Chicc STD | STD | 12.62 | -10.6 | -9.0 |
| 1785 C1-166 RV3 Chicc STD | STD | 12.62 | -10.6 | -9.0 |
| 1786 C1-171 RVB PVC-2F Fib 4 | 13.5 to 22 | 4.04 | 0.8 | -5.8 |
| 1787 C1-71 RV1 PVC-2F Fib 3 | 13.5 to 22 | 3.33 | 0.9 | -5.3 |
| 1788 C1-171 RV1 PVC-2F Fib 3 | 13.5 to 22 | 3.33 | 0.9 | -5.3 |
| 1789 C1-171 RV5 PVC-2G (Bill) Fib 6 | 26.60 | 2.28 | 0.9 | -5.0 |
| 1790 C1-169 RVD Chicc STD | STD | 16.29 | -10.7 | -9.0 |
| 1791 C1-169 RVD Chicc STD | STD | 16.29 | -10.7 | -9.0 |
| 1792 C1-169 RVD Chicc STD | STD | 16.29 | -10.7 | -9.0 |
| 1793 C1-16 RV13 NBS-20 STD | STD | 15.2 | -1.1 | -4.1 |
| 1794 C1-16 RV13 NBS-20 STD | STD | 15.2 | -1.1 | -4.1 |
| 1795 C1-171 RV7 PVC-2G (Bill) Fib 5 | 26.60 | 1.76 | 1.1 | -5.5 |
| 1796 C1-172 RV10 Chicc STD | STD | 3.13 | -10.7 | -9.2 |
| 1797 C1-172 RV10 Chicc STD | STD | 3.13 | -10.7 | -9.3 |
| 1798 C1-171 RVC PVC-2C-1a Fib 8 | 20.60 | 2.3 | 1.0 | -5.3 |
| 1799 C1-172 RV16 Chicc STD | STD | 2.2 | -10.7 | -9.3 |
| 1800 C1-169 RV7 Chicc STD | STD | 12.89 | -10.6 | -9.1 |
| 1801 C1-169 RV7 Chicc STD | STD | 12.89 | -10.7 | -9.3 |
| 1802 C1-172 RVV9 PVC-2G (Bill) Fib 8 | 26.60 | 2.6 | 0.9 | -4.8 |
| 1803 C1-172 RV13 PVC-2G (Bill) Fib 9 | 26.60 | 1 | 1.0 | -5.3 |
| 1804 C1-171 RVD PVC-2G (Bill) Fib 7 | 26.60 | 1.96 | 0.7 | -5.0 |

| Mass Spec Number and Sample I.D. | meters | Wt. mg. | D C13 | D O18 |
|---|---|---|---|---|
| 1805 C1-171 RVD PVC-2G (Bill) Fib 7 | 26.60 | 1.96 | 0.8 | -4.9 |
| 1806 C1-169 RV18 Chicc STD | STD | 16.79 | -10.7 | -9.3 |
| 1807 C1-172 RV14 RHB-8H-WL-S1 Fib 6 | 317.40 | 3.28 | 0.7 | -4.8 |
| 1808 C1-172 RV11 RHB-8H-WL-S1 Fib 8 | 317.40 | 2 | 0.7 | -4.9 |
| 1809 C1-173 RHB-8H-WL-S1 Fib 9 | 317.40 | 1.88 | 0.6 | -5.1 |
| 1810 C1-169 RV15 Chicc STD | STD | 10.63 | -10.7 | -9.2 |
| 1811 C1-169 RV15 Chicc STD | STD | 10.63 | -10.7 | -9.1 |
| **Run 14 Dec. 1990; 55.00deg. C** | | | | |
| 1812 C1-169 RV7 Chicc STD | STD | 12.89 | -10.6 | -9.1 |
| 1813 C1-169 RV7 Chicc STD | STD | 12.89 | -10.6 | -9.1 |
| 1814 BL1-5 Boat 5 Chicc STD | STD | 1 | -11.1 | -9.8 |
| 1815 BL1-5 Boat 5 Chicc STD | STD | 1 | -11.1 | -9.7 |
| 1816 BL1-5 Boat 6 Chicc STD | STD | 0.62 | Lost | Lost |
| 1817 BL1-5 Boat 7 PVC-2G (Bill) Bladed 1 | 26.6 | 1.89 | 0.0 | -6.7 |
| 1818 BL1-5 Boat 8 Chicc STD | STD | 1.55 | -10.5 | -9.4 |
| 1819 BL1-5 Boat 9 Chicc STD | STD | 1.55 | -10.5 | -9.3 |
| 1820 BL1-5 Boat 9 IS-90-47a Blocky-clear to white 3 | 234.7 | 1.04 | -0.8 | -6.8 |
| 1821 BL1-5 Boat 10 PVC-2J Bladed 1 | 21 to 44 | 0.72 | -0.3 | -6.5 |
| 1822 BL1-5 Boat 11 NBS-20 STD | STD | 0.99 | -1.5 | -4.3 |
| 1823 BL1-5 Boat 11 NBS-20 STD | STD | 0.99 | -1.5 | -4.3 |
| 1824 BL1-5 Boat 12 TH-89-92 Blocky-clear 1 | 180.9 | 0.52 | 0.1 | -7.8 |
| 1825 BL1-5 Boat 13 TH-89-62 Blocky-white Fe 1 | 156.5 | 2.41 | 0.1 | -7.7 |
| 1826 BL1-5 Boat 14 PVC-2G (Bill) Bladed 2 | 26.6 | 0.53 | 0.4 | -6.2 |
| 1827 BL1-5 Boat 15 Chicc STD | STD | 0.76 | -10.3 | -9.0 |
| 1828 BL1-5 Boat 15 Chicc STD | STD | 0.76 | -10.3 | -8.8 |
| 1829 BL1-5 Boat 16 Chicc STD | STD | 0.64 | -10.8 | -9.5 |
| 1830 BL1-5 Boat 16 Chicc STD | STD | 0.64 | -10.8 | -9.7 |
| 1831 C1-169 RVC Chicc STD | STD | 16.51 | -10.6 | -9.1 |
| 1832 C1-169 RVC Chicc STD | | 16.51 | -10.6 | -9.1 |
| **Run 15-Dec-90, 25 deg. C** | | | | |
| 1833 C1-169 RV15 Chicc STD | STD | 10.63 | -10.6 | -9.0 |
| 1834 C1-169 RV15 Chicc STD | STD | 10.63 | -10.7 | -9.0 |
| 1835 C1-169 RV15 Chicc STD | STD | 10.63 | -10.7 | -9.0 |
| 1836 C1-169 RV18 Chicc STD | STD | 16.79 | -10.6 | -9.1 |
| 1837 C1-169 RV18 Chicc STD | STD | 16.79 | -10.6 | -9.1 |
| 1838 C1-173 RV10 IS-90-30 Eqdol 1 | 192.00 | 22.72 | 0.0 | -5.3 |

| Mass Spec Number and Sample I.D. | meters | Wt. mg. | D C13 | D O18 |
|---|---|---|---|---|
| 1839 C1-173 RV14 TH-89-100a Eqdol 1 | 187.80 | 33.67 | 0.8 | -7.1 |
| 1840 C1-173 RV5 TH-90-212 Blocky-white Fe 1 | 298.80 | 5.62 | 0.4 | -7.4 |
| 1841 C1-174 R11 IS-89-49b Vein 1 | 142.80 | 10.16 | 0.1 | -9.7 |
| 1842 C1-173 RV18 Chicc STD | STD | 17.66 | -10.6 | -9.2 |
| 1843 C1-173 RV18 Chicc STD | STD | 17.66 | -10.6 | -9.2 |
| 1844 C1-174 RV15 TH-89-110 Blocky-white Fe 1 | 197.60 | 5.01 | 0.3 | -7.9 |
| 1845 C1-173 RV10 IS-90-30 Blocky-white Fe 1 | 192.00 | 3.79 | 0.0 | -8.4 |
| 1846 C1-174 RV7 OTH-90-12 Blocky-white Fe 1 | 111.90 | 7.39 | -0.3 | -8.0 |
| 1847 C1-169 RVC Chicc STD | STD | 16.51 | -10.6 | -9.1 |
| 1848 C1-169 RVC Chicc STD | STD | 16.51 | -10.7 | -9.1 |
| 1849 C1-174 RV3 TH-89-91a Blocky-white Fe 1 | 179.50 | 3.85 | 0.3 | -8.2 |
| 1850 C1-174 RV12 TH-89-26 Blocky-white Fe 1 | 125.40 | 4.75 | -0.5 | -8.2 |
| 1851 C1-174 Chicc STD | STD | 3.45 | -10.6 | -9.2 |
| 1852 C1-174 Chicc STD | STD | 3.45 | -10.6 | -9.3 |
| 1853 C1-173 RV14 TH-89-100a Eqdol 1 | 187.80 | 33.67 | 1.9 | -5.5 |
| 1854 C1-173 RV10 IS-90-30 Eqdol 1 | 192.00 | 22.72 | 1.0 | -3.6 |
| 1855 C1-175 RVB Chicc STD | STD | 3.53 | -10.7 | -9.4 |
| 1856 C1-175 RVB Chicc STD | STD | 3.53 | -10.7 | -9.4 |
| **Run #1, 20 Dec. 1990; 55.00 deg. C** | | | | |
| 1882 C1-169 RVC Chicc STD | STD | 11.23 | -10.6 | -8.9 |
| 1883 C1-169 RVC Chicc STD | STD | 11.23 | -10.6 | -8.9 |
| 1884 C1-169 RV18 Chicc STD | STD | 16.79 | -10.6 | -9.0 |
| 1885 C1-169 RV18 Chicc STD | STD | 16.79 | -10.6 | -9.0 |
| 1886 BL1-7 Boat 5 Chicc STD | STD | 1.87 | -10.9 | -9.3 |
| 1887 BL1-7 Boat 5 Chicc STD | STD | 1.87 | -11.0 | -9.4 |
| 1888 BL1-7 Boat 6 Chicc STD | STD | 1.24 | -11.0 | -9.4 |
| 1889 BL1-7 Boat 6 Chicc STD | STD | 1.24 | -10.9 | -9.4 |
| 1890 BL1-7 Boat 6 Chicc STD | STD | 1.24 | -10.9 | -9.3 |
| 1892 BL1-7 Boat 8 OTH-90-60 Ovg 1 | 227.8 | 0.79 | 0.0 | -6.6 |
| 1893 BL1-7 Boat 9 Chicc STD | STD | 0.83 | -10.1 | -9.2 |
| 1894 BL1-7 Boat 9 Chicc STD | STD | 0.83 | -10.1 | -9.1 |
| 1895 BL1-7 Boat 10 TH-89-183 Blocky-white Fe 1 | 257.5 | 0.67 | -0.4 | -7.5 |
| 1896 BL1-7 Boat 11 TH-89-208 Blocky-white Fe 1 | 292.9 | 0.98 | 0.1 | -7.5 |
| 1897 BL1-7 Boat 12 TH-89-127 Blocky-clear to white 1 | 213.5 | 0.38 | 0.0 | -7.3 |
| 1898 BL1-7 Boat 13 Chicc STD | STD | 1.28 | -10.6 | -9.4 |
| 1899 BL1-7 Boat 13 Chicc STD | STD | 1.28 | -10.6 | -9.4 |

| Mass Spec Number and Sample I.D. | meters | Wt. mg. | D C13 | D O18 |
|---|---|---|---|---|
| 1900 BL1-7 Boat 14 TH-90-200 FeOvg 1 | 272.5 | 2.26 | 0.1 | -6.7 |
| 1901 BL1-7 Boat 15 OTH-90-17 Blocky-white Fe 1 | 127.4 | 1.94 | -0.6 | -7.8 |
| 1902 BL1-7 Boat 16 Chicc STD | STD | 1.68 | -10.3 | -9.1 |
| 1903 BL1-7 Boat 16 Chicc STD | STD | 1.68 | -10.3 | -9.2 |
| 1904 BL1-7 Boat 17 TH-89-127 Blocky-clear to white 2 | 213.5 | 0.3 | -1.6 | -7.5 |
| 1905 BL1-7 Boat 18 Chicc STD | STD | 1.23 | -10.7 | -9.2 |
| 1906 BL1-7 Boat 18 Chicc STD | STD | 1.23 | -10.6 | -9.2 |
| 1907 BL1-7 Boat 19 Chicc STD | STD | 1.84 | -10.8 | -9.3 |
| 1908 BL1-7 Boat 19 Chicc STD | STD | 1.84 | -10.9 | -9.4 |
| **Run #2, 20 Dec. 1990; 55.00 deg. C** | | | | |
| 1909 C1-169 RV18 Chicc STD | STD | 16.79 | -10.6 | -9.0 |
| 1911 BL1-9 Boat 5 Chicc STD | STD | 1.06 | -11.1 | -9.8 |
| 1912 BL1-9 Boat 5 Chicc STD | STD | 1.06 | -11.2 | -9.8 |
| 1913 BL1-9 Boat 6 Chicc STD | STD | 0.72 | -11.0 | -9.5 |
| 1914 BL1-9 Boat 6 Chicc STD | STD | 0.72 | -11.0 | -9.6 |
| 1915 BL1-9 Boat 7 TH-90-210 FeOvg 1 | 295.6 | 0.5 | -0.6 | -7.3 |
| 1916 BL1-9 Boat 9 Chicc STD | STD | 2.07 | -10.7 | -9.3 |
| 1917 BL1-9 Boat 9 Chicc STD | STD | 2.07 | -10.7 | -9.3 |
| 1918 BL1-9 Boat 8 TH-89-156 Blocky 1 | 230.9 | 0.91 | -1.3 | -7.4 |
| 1920 BL1-9 Boat 11 TH-88-12 Blocky 1 | 251.6 | 0.59 | -0.1 | -6.8 |
| 1921 BL1-9 Boat 12 OTH-90-89 Blocky-white Fe 1 | 321.1 | 0.39 | 0.2 | -7.2 |
| 1922 BL1-9 Boat 13 Chicc STD | STD | 0.75 | -10.4 | -9.4 |
| 1924 BL1-9 Boat 15 OTH-90-90 Blocky 1 | 322.9 | 1.04 | 0.2 | -7.2 |
| 1925 BL1-9 Boat 16 Chicc STD | STD | 2.52 | -10.7 | -9.2 |
| 1926 BL1-9 Boat 17 TH-89-125 Blocky 1 | 212.3 | 0.63 | -1.3 | -6.8 |
| 1927 BL1-9 Boat 18 Chicc STD | STD | 1.56 | -10.6 | -9.0 |
| **Run 23-Dec-90, 25 deg. C** | | | | |
| 1948 ?C1-183-A Chicc STD | STD | ?10.88 | -10.6 | -9.2 |
| 1949 ?C1-183-A Chicc STD | STD | ?10.88 | -10.7 | -9.2 |
| 1950 C1-185 RV3 TH-89-128 Blocky-clear 1 | 214.10 | 4.56 | 0.3 | -7.4 |
| 1951 C1-184 RVB TH-90-447 Blocky-white Fe 1 | 81.80 | 4.75 | 0.3 | -7.3 |
| 1952 C1-184 RV5 IS-90-47b2 (slab) Fib 5 | 234.70 | 4.49 | 0.3 | -5.2 |
| 1953 C1-184 RV7 IS-90-32 Blocky-white Fe 1 | 197.1 | 2.23 | 0.3 | -8.2 |
| 1954 C1-184 RV18 OTH-90-102 Blocky-white Fe 1 | 332.60 | 6.4 | 0.1 | -7.4 |
| 1955 C1-185 RV14 TH-89-194 Blocky-white Fe 1 | 266.30 | 3.72 | 0.4 | -7.4 |
| 1956 C1-185 RV11 IS-90-46c (slab) Fib 1 | 234.60 | 4.04 | 0.7 | -4.6 |

| Mass Spec Number and Sample I.D. | meters | Wt. mg. | D C13 | D O18 |
|---|---|---|---|---|
| 1957 C1-185 RVA Chicc STD | STD | 3.48 | -10.7 | -9.3 |
| 1958 C1-185 RVA Chicc STD | STD | 3.48 | -10.7 | -9.3 |
| 1959 C1-186 IS-90-47b1 (slab) Fib 1 | 234.70 | 4.8 | 0.5 | -4.7 |
| 1960 C1-185 RV10 TH-89-66T Blocky-white Fe 1 | 159.70 | 2.15 | 0.3 | -8.0 |
| 1961 C1-185 RVD Chicc STD | STD | 2.76 | -10.8 | -9.2 |
| 1962 C1-185 RVD Chicc STD | STD | 2.76 | -10.7 | -9.2 |
| 1963 C1-185 RVC TH-89-79 Blocky-white Fe 1 | 169.30 | 5.53 | 0.5 | -8.0 |
| 1964 C1-186 RVB IS-90-47b1 (slab) Fib 4 | 234.70 | 4.15 | 0.4 | -5.9 |
| 1965 C1-185 RVA Chicc STD | STD | 3.48 | -10.7 | -9.2 |
| 1966 C1-185 RVA Chicc STD | STD | 3.48 | -10.8 | -9.3 |
| 1967 C1-185 RVD Chicc STD | STD | 2.76 | -10.7 | -9.2 |
| 1968 C1-185 RVD Chicc STD | STD | 2.76 | -10.8 | -9.1 |
| 1969 C1-187 RV16 IS-90-47b2 (slab) Fib 1 | 234.70 | 3.83 | 0.6 | -4.4 |
| 1970 C1-186 RV18 IS-90-47b2 (slab) Fib 2 | 234.70 | 4.32 | 0.6 | -5.4 |
| 1971 C1-186 RV15 IS-90-47b1 (slab) Fib 2 | 234.70 | 4.39 | 0.5 | -4.6 |
| 1972 C1-187 RV5 IS-90-47b1 (slab) Fib 3 | 234.70 | 5.27 | 0.5 | -4.9 |
| 1973 C1-185 RVA Chicc STD | STD | 3.48 | -10.7 | -9.2 |
| 1974 C1-185 RVA Chicc STD | STD | 3.48 | -10.7 | -9.3 |
| 1975 C1-187 RVA IS-90-47b2 (slab) Fib 4 | 234.70 | 2.19 | 0.2 | -5.3 |
| 1976 C1-187 RV7 IS-90-46b (slab) Fib 2 | 234.60 | 3.8 | 0.8 | -4.8 |
| 1977 C1-187 RVC TH-89-106 FeOvg 1 | 195.70 | 5.91 | 0.5 | -8.0 |
| 1978 C1-187 IS-90-46b (slab) Fib 1 | 234.60 | 4.24 | 0.7 | -4.8 |
| 1979 C1-86 RV12 Chicc STD | STD | 2.61 | -10.8 | -9.5 |
| 1980 C1-86 RV12 Chicc STD | STD | 2.61 | -10.8 | -9.2 |
| 1981 C1-86 RV12 Chicc STD | STD | 2.61 | -10.8 | -9.3 |
| 1982 C1-188 RV3 OTH-90-60 Ovg 2 | 227.80 | 4.46 | 0.5 | -8.2 |
| 1983 C1-187 RV14 TH-89-183 Blocky-white Fe 2 | 257.50 | 4.1 | 0.4 | -7.2 |
| 1984 C1-188 RV10 IS-90-47b2 (slab) Fib 3 | 234.70 | 2.73 | 0.5 | -4.5 |
| 1985 C1-186 RV9 Chicc STD | STD | 9.31 | -10.6 | -9.2 |
| **26 Dec. 1990; 55.00 deg. C** | | | | |
| 1986 C1-185 RVD Chicc STD | STD | 2.76 | -10.6 | -8.9 |
| 1987 C1-185 RVD Chicc STD | STD | 2.76 | -10.6 | -8.9 |
| 1988 C1-188 RVD Chicc STD | STD | 19.33 | -10.7 | -9.2 |
| 1989 C1-188 RVD Chicc STD | STD | 19.33 | -10.7 | -9.2 |
| 1990 BL1-11 Boat 5 Chicc STD | STD | 0.68 | -11.3 | -10.1 |
| 1991 BL1-11 Boat 6 Chicc STD | STD | 0.58 | -11.0 | -9.4 |

| Mass Spec Number and Sample I.D. | Meters | Wt. mg. | D C13 | D O18 |
|---|---|---|---|---|
| 1992 BL1-11 Boat 6 Chicc STD | STD | 0.58 | -10.9 | -9.3 |
| 1993 BL1-11 Boat 6 Chicc STD | STD | 0.58 | -10.8 | -9.2 |
| 1994 BL1-11 Boat 7 TH-89-75 Ovg 2 | 167.8 | 0.59 | -0.8 | -7.8 |
| 1995 BL1-11 Boat 8 TH-89-122 Blocky-clear to white 2 | 210.2 | 0.42 | -0.4 | -7.7 |
| 1996 BL1-11 Boat 9 OTH-90-89 Ovg 1 | 321.1 | 0.69 | 0.2 | -6.5 |
| 1997 BL1-11 Boat 10 Chicc STD | STD | 0.51 | -9.6 | -9.4 |
| 1998 BL1-11 Boat 11 TH-89-122 Blocky-white Fe 3 | 210.2 | 1.07 | -0.8 | -7.9 |
| 1999 BL1-11 Boat 12 TH-89-122 Blocky-white Fe 4 | 210.2 | 0.3 | -0.3 | -7.7 |
| 2000 BL1-11 Boat 13 Chicc STD | STD | 0.87 | 13.7 | 25.9 |
| 2001 BL1-11 Boat 14 TH-90-122 Blocky-white Fe 5 | 210.2 | 0.97 | -0.4 | -7.7 |
| 2002 BL1-11 Boat 15 TH-90-212 (slab) Blocky-white Fe | 298.8 | 0.73 | 0.0 | -7.5 |
| 2003 BL1-11 Boat 16 TH-90-205A Blocky-white Fe 1 | 285.8 | ?0.27 | 0.2 | -7.5 |
| 2004 BL1-11 Boat 17 TH-89-104 Ovg 1 | 190.6 | 0.66 | 0.7 | -8.3 |
| 2005 BL1-11 Boat 18 Chicc STD | STD | 2.45 | -10.6 | -9.3 |
| 2006 BL1-11 Boat 18 Chicc STD | STD | 2.45 | -10.5 | -9.2 |
| 2007 BL1-11 Boat 19 OTH-90-114b Blocky-white Fe 1 | 356.4 | 0.69 | -1.7 | -7.5 |
| 2008 BL1-11 Boat 20 Chicc STD | STD | 1.14 | -10.5 | -9.2 |
| 2009 BL1-11 Boat 20 Chicc STD | STD | 1.14 | -10.5 | -9.2 |
| **Run 25-Dec-92 (analyses by Ken Tobin), 25 deg. C** | | | | |
| 4766 & 4766 C2-37-S2 RHB-2C-B Fib 4 | 41.50 | 4.28 | 0.2 | -6.0 |
| 4768 C2-37-AS Chicc STD | STD | 5.57 | -10.6 | -9.3 |
| 4791 C2-375-S16 RHB-2C-B Csc-Fe (Co-ppt) 3 | 41.50 | 5.42 | -0.3 | -11.0 |
| 4803 C2-38-AS Chicc STD | STD | 1.86 | -10.6 | -9.3 |
| 4804 C2-38-3-S17 PVC-2J Csc-pink 4 | 32.50 | 6.6 | 0.7 | -10.1 |

# APPENDIX E

## ELECTRON MICROPROBE ANALYSES OF TRACE ELEMENTS

## EXPLANATION

Electron microprobe analyses are presented by phase in Appendix E. The sample identification number indicates the thin-section (actually, its corresponding rock chip or billet) from which each sample was drilled. This numbering scheme is consistent with those in Appendices A, B, C, D and F. Phase name abbreviations are give in Appendix D. "Zone" generally refers to a unique area of the phase that was sampled. Zones indicated in Appendix E do not correspond to those indicated in Appendix D. Analyses with total weight percents greater than 100.5% and less than 98.5% were rejected and are not shown in Appendix E.

Detection limits are as follows:

Mg = 410 ppm

Fe = 410 ppm

Mn = 410 ppm

Sr = 600 ppm

Values below detection limit are reported in the following table, but those values should be understood to indicate only that the element, if present in the table, is present in an amount below the detection limit for that element.

| Shelf-Edge Fibrous Calcite | | | | | | Mole % |
|---|---|---|---|---|---|---|
| Sample I.D. and Zone | Wt % Mg | Wt % Ca | Wt % Mn | Wt % Fe | Wt % Sr | MgCO3 |
| PVC-2K-S2 Fib Zone 1a | 0.1339 | 39.9335 | 0.0170 | 0.0085 | 0.0000 | 0.5498 |
| PVC-2K-S2 Fib Zone 1a | 0.1737 | 40.0564 | 0.0000 | 0.0183 | 0.0121 | 0.7096 |
| PVC-2K-S2 Fib Zone 1a | 0.1378 | 40.1231 | 0.0124 | 0.0141 | 0.0059 | 0.5623 |
| PVC-2K-S2 Fib Zone 1a | 0.2494 | 40.0858 | 0.0278 | 0.0028 | 0.0214 | 1.0148 |
| PVC-2K-S2 Fib Zone 1a | 0.1648 | 39.8542 | 0.0216 | 0.0001 | 0.0152 | 0.6767 |
| PVC-2K-S2 Fib Zone 1a | 0.2098 | 39.8875 | 0.0309 | 0.0183 | 0.0286 | 0.8584 |
| PVC-2K-S2 Fib Zone 1a | 0.2094 | 40.1880 | 0.0000 | 0.0000 | 0.0000 | 0.8519 |
| PVC-2K-S2 Fib Zone 1a | 0.1916 | 39.6126 | 0.0356 | 0.0169 | 0.0251 | 0.7900 |
| PVC-2K-S2 Fib Zone 1b, 2a | 0.1750 | 39.9930 | 0.0248 | 0.0001 | 0.0129 | 0.7153 |
| PVC-2K-S2 Fib Zone 1b, 2a | 0.1578 | 39.9831 | 0.0108 | 0.0001 | 0.0215 | 0.6465 |
| PVC-2K-S2 Fib Zone 1b, 2a | 0.1971 | 39.4782 | 0.0000 | 0.0113 | 0.0494 | 0.8156 |
| PVC-2K-S2 Fib Zone 1b, 2a | 0.1326 | 39.6938 | 0.0402 | 0.0000 | 0.0390 | 0.5467 |
| PVC-2K-S2 Fib Zone 1b, 2a | 0.1678 | 39.8860 | 0.0000 | 0.0451 | 0.0251 | 0.6888 |
| PVC-2K-S2 Fib Zone 1b, 2a | 0.1879 | 40.0030 | 0.0000 | 0.0254 | 0.0137 | 0.7677 |
| PVC-2K-S2 Fib Zone 1b, 2a | 0.1760 | 39.8517 | 0.0001 | 0.0056 | 0.0308 | 0.7226 |
| PVC-2K-S2 Fib Zone 1b, 2a | 0.2942 | 40.0447 | 0.0001 | 0.0451 | 0.0323 | 1.1951 |
| PVC-2K-S2 Fib Zone 1b, 2a | 0.2029 | 39.9438 | 0.0001 | 0.0001 | 0.0016 | 0.8301 |
| PVC-2K-S2 Fib Zone 3 | 0.1749 | 39.4463 | 0.0001 | 0.0028 | 0.0295 | 0.7253 |
| PVC-2K-S2 Fib Zone 3 | 0.1774 | 39.8095 | 0.0108 | 0.0169 | 0.0047 | 0.7292 |
| PVC-2K-S2 Fib Zone 3 | 0.1680 | 39.7792 | 0.0001 | 0.0001 | 0.0204 | 0.6911 |
| PVC-2K-S2 Fib Zone 3 | 0.1571 | 40.1246 | 0.0062 | 0.0099 | 0.0065 | 0.6419 |
| PVC-2K-S2 Fib Zone 3 | 0.1639 | 40.0294 | 0.0232 | 0.0085 | 0.0052 | 0.6702 |
| PVC-2K-S2 Fib Zone 4, 5 | 0.1514 | 39.8885 | 0.0186 | 0.0310 | 0.0295 | 0.6216 |
| PVC-2K-S2 Fib Zone 4, 5 | 0.1328 | 39.8952 | 0.0325 | 0.0183 | 0.0227 | 0.5452 |
| PVC-2K-S2 Fib Zone 4, 5 | 0.2047 | 39.2524 | 0.0526 | 0.0803 | 0.0028 | 0.8509 |
| PVC-2K-S2 Fib Zone 4, 5 | 0.1227 | 39.6068 | 0.0944 | 0.0071 | 0.0403 | 0.5071 |
| PVC-2K-S2 Fib Zone 4, 5 | 0.1950 | 39.8198 | 0.0031 | 0.0028 | 0.0052 | 0.8009 |
| PVC-2K-S2 Fib Zone 4, 5 | 0.1717 | 39.9309 | 0.0046 | 0.0001 | 0.0176 | 0.7032 |
| PVC-2K-S2 Fib Zone 4, 5 | 0.1993 | 39.5474 | 0.0757 | 0.0001 | 0.0140 | 0.8229 |
| PVC-2K-S2 Fib Zone 4, 5 | 0.2077 | 39.6818 | 0.0325 | 0.0339 | 0.0217 | 0.8543 |
| PVC-2K-S2 Fib Zone 4, 5 | 0.1379 | 39.9819 | 0.0773 | 0.0001 | 0.0145 | 0.5649 |
| PVC-2K-S2 Fib Zone 4, 5 | 0.2509 | 39.2872 | 0.0170 | 0.0001 | 0.0240 | 1.0414 |
| PVC-2K-S2 Fib Zone 4, 5 | 0.1902 | 39.5574 | 0.0001 | 0.0268 | 0.0070 | 0.7858 |
| PVC-2K-S2 Fib Zone 4, 5 | 0.2582 | 39.7226 | 0.0170 | 0.0324 | 0.0173 | 1.0588 |
| PVC-2K-S2 Fib Zone 4, 5 | 0.1429 | 39.9655 | 0.0356 | 0.0001 | 0.0114 | 0.5855 |

| Sample I.D. and Zone | Wt % Mg | Wt % Ca | Wt % Mn | Wt % Fe | Wt % Sr | MgCO3 |
|---|---|---|---|---|---|---|
| PVC-2K-S2 Fib Zone 4, 5 | 0.1740 | 39.9647 | 0.0093 | 0.0001 | 0.0093 | 0.7125 |
| PVC-2J Fib Zone 1a | 0.1271 | 40.1925 | 0.2306 | 0.0014 | 0.0217 | 0.5161 |
| PVC-2J Fib Zone 1a | 0.1257 | 40.0271 | 0.0340 | 0.0001 | 0.0336 | 0.5142 |
| PVC-2J Fib Zone 1a | 0.1691 | 39.6916 | 0.0325 | 0.0001 | 0.0001 | 0.6971 |
| PVC-2J Fib Zone 1a | 0.1307 | 39.3948 | 0.1579 | 0.0564 | 0.0001 | 0.5422 |
| PVC-2J Fib Zone 1a | 0.1614 | 40.0538 | 0.0387 | 0.0099 | 0.0001 | 0.6591 |
| PVC-2J Fib Zone 1a | 0.1759 | 39.4377 | 0.0898 | 0.0099 | 0.0207 | 0.7290 |
| PVC-2J Fib Zone 1a | 0.1975 | 40.1037 | 0.0573 | 0.0001 | 0.0166 | 0.8049 |
| PVC-2J Fib Zone 1a | 0.1896 | 39.4272 | 0.0759 | 0.0071 | 0.0114 | 0.7851 |
| PVC-2J Fib Zone 1a | 0.1817 | 39.7639 | 0.0449 | 0.0183 | 0.0155 | 0.7471 |
| PVC-2J Fib Zone 1a | 0.2158 | 40.0297 | 0.0001 | 0.0085 | 0.0001 | 0.8807 |
| PVC-2J Fib Zone 1a | 0.1616 | 39.7177 | 0.0248 | 0.0001 | 0.0001 | 0.6661 |
| PVC-2J Fib Zone 1a | 0.1583 | 40.1111 | 0.0511 | 0.0001 | 0.0016 | 0.6453 |
| PVC-2J Fib Zone 1a | 0.1868 | 39.5237 | 0.0727 | 0.0254 | 0.0044 | 0.7724 |
| PVC-2J Fib Zone 1a | 0.2223 | 39.2964 | 0.0000 | 0.0099 | 0.0137 | 0.9241 |
| PVC-2J Fib Zone 1a | 0.1826 | 40.1832 | 0.0697 | 0.0452 | 0.0005 | 0.7423 |
| PVC-2J Fib Zone 1a | 0.2057 | 40.1052 | 0.0263 | 0.0000 | 0.0176 | 0.8379 |
| PVC-2J Fib Zone 1a | 0.1409 | 39.9363 | 0.0371 | 0.0465 | 0.0001 | 0.5773 |
| PVC-2J Fib Zone 1a | 0.1208 | 40.1834 | 0.0155 | 0.0254 | 0.0001 | 0.4924 |
| PVC-2J Fib Zone 1a | 0.1722 | 40.1090 | 0.0572 | 0.0338 | 0.0233 | 0.7018 |
| PVC-2J Fib Zone 1a | 0.2282 | 39.8353 | 0.0108 | 0.0056 | 0.0210 | 0.9350 |
| PVC-2J Fib Zone 1a | 0.1600 | 39.6629 | 0.0310 | 0.0042 | 0.0127 | 0.6609 |
| PVC-2J Fib Zone 1a | 0.1858 | 39.3127 | 0.0279 | 0.0014 | 0.0171 | 0.7727 |
| PVC-2J Fib Zone 1a | 0.1455 | 40.2575 | 0.0433 | 0.0001 | 0.0001 | 0.5918 |
| PVC-2J Fib Zone 1a | 0.1546 | 39.8846 | 0.0139 | 0.0169 | 0.0028 | 0.6350 |
| PVC-2J Fib Zone 1a | 0.1512 | 39.7593 | 0.0001 | 0.0001 | 0.0001 | 0.6232 |
| PVC-2J Fib Zone 1a | 0.1310 | 39.8301 | 0.0619 | 0.0353 | 0.0001 | 0.5387 |
| PVC-2J Fib Zone 1b | 0.2369 | 39.6172 | 0.0031 | 0.0001 | 0.0013 | 0.9770 |
| PVC-2J Fib Zone 1b | 0.1485 | 39.8661 | 0.0001 | 0.0240 | 0.0026 | 0.6095 |
| PVC-2J Fib Zone 1b | 0.1353 | 39.9969 | 0.0232 | 0.0001 | 0.0186 | 0.5547 |
| PVC-2J Fib Zone 1b | 0.2051 | 39.8954 | 0.0356 | 0.0183 | 0.0225 | 0.8395 |
| PVC-2J Fib Zone 1b | 0.1631 | 40.0306 | 0.0325 | 0.0001 | 0.0365 | 0.6664 |
| PVC-2J Fib Zone 1b | 0.1691 | 39.5954 | 0.0341 | 0.0001 | 0.0034 | 0.6987 |
| PVC-2J Fib Zone 2a | 0.1742 | 39.8783 | 0.0433 | 0.0001 | 0.0060 | 0.7148 |
| PVC-2J Fib Zone 2a | 0.1761 | 40.0160 | 0.0093 | 0.0183 | 0.0031 | 0.7196 |
| PVC-2J Fib Zone 2a | 0.1778 | 39.7271 | 0.0542 | 0.0001 | 0.0001 | 0.7315 |

| Sample I.D. and Zone | Wt % Mg | Wt % Ca | Wt % Mn | Wt % Fe | Wt % Sr | MgCO3 |
|---|---|---|---|---|---|---|
| PVC-2J Fib Zone 2a | 0.1653 | 39.8865 | 0.0650 | 0.0001 | 0.0150 | 0.6779 |
| PVC-2J Fib Zone 2a | 0.1556 | 39.8325 | 0.0387 | 0.0001 | 0.0269 | 0.6391 |
| PVC-2J Fib Zone 2a | 0.1314 | 40.0422 | 0.0573 | 0.0001 | 0.0008 | 0.5374 |
| PVC-2J Fib Zone 2a | 0.2100 | 40.0182 | 0.0387 | 0.0001 | 0.0273 | 0.8569 |
| PVC-2J Fib Zone 2a | 0.1664 | 40.0874 | 0.0356 | 0.0282 | 0.0041 | 0.6793 |
| PVC-2J Fib Zone 2a | 0.2064 | 39.6999 | 0.0001 | 0.0001 | 0.0109 | 0.8504 |
| PVC-2J Fib Zone 2a | 0.1549 | 39.8620 | 0.0077 | 0.0508 | 0.0001 | 0.6363 |
| PVC-2J Fib Zone 2a | 0.1860 | 40.1393 | 0.0001 | 0.0001 | 0.0119 | 0.7585 |
| PVC-2J Fib Zone 2a | 0.1880 | 39.9655 | 0.0108 | 0.0635 | 0.0207 | 0.7688 |
| PVC-2J Fib Zone 2a | 0.1773 | 40.2171 | 0.0139 | 0.0014 | 0.0119 | 0.7219 |
| PVC-2J Fib Zone 2a | 0.1720 | 39.6300 | 0.0015 | 0.0001 | 0.0001 | 0.7104 |
| PVC-2J Fib Zone 2a | 0.7650 | 39.4028 | 0.0449 | 0.0395 | 0.0142 | 3.0970 |
| PVC-2J Fib Zone 2a | 0.1819 | 39.5181 | 0.0573 | 0.0776 | 0.0336 | 0.7517 |
| PVC-2J Fib Zone 2a | 0.1758 | 39.9328 | 0.0001 | 0.0071 | 0.0109 | 0.7201 |
| PVC-2J Fib Zone 2a | 0.1609 | 39.6321 | 0.0062 | 0.0001 | 0.0205 | 0.6652 |
| PVC-2J Fib Zone 2a | 0.1867 | 39.8869 | 0.0356 | 0.0367 | 0.0194 | 0.7645 |
| PVC-2J Fib Zone 2a | 0.1535 | 40.0548 | 0.0000 | 0.0056 | 0.0117 | 0.6279 |
| PVC-2J Fib Zone 2a | 0.1735 | 40.1742 | 0.0403 | 0.0466 | 0.0001 | 0.7056 |
| PVC-2J Fib Zone 2b | 0.1728 | 39.6473 | 0.0155 | 0.0000 | 0.0153 | 0.7133 |
| PVC-2J Fib Zone 2b | 0.1408 | 39.8457 | 0.0325 | 0.0127 | 0.0034 | 0.5790 |
| PVC-2J Fib Zone 2b | 0.1544 | 39.9504 | 0.0542 | 0.0395 | 0.0230 | 0.6320 |
| PVC-2J Fib Zone 2b | 0.1900 | 39.7858 | 0.0155 | 0.0001 | 0.0049 | 0.7815 |
| PVC-2J Fib Zone 2b | 0.1859 | 40.1780 | 0.0001 | 0.0339 | 0.0028 | 0.7562 |
| PVC-2J Fib Zone 2b | 0.3057 | 39.9130 | 0.0341 | 0.0001 | 0.0391 | 1.2455 |
| PVC-2J Fib Zone 2b | 0.1279 | 39.8490 | 0.0139 | 0.0001 | 0.0305 | 0.5261 |
| PVC-2J Fib Zone 3a | 0.1381 | 39.6633 | 0.0650 | 0.0113 | 0.0001 | 0.5695 |
| PVC-2J Fib Zone 3a | 0.1708 | 39.7631 | 0.0356 | 0.0310 | 0.0119 | 0.7024 |
| PVC-2J Fib Zone 3a | 0.1518 | 39.6598 | 0.0046 | 0.0169 | 0.0052 | 0.6269 |
| PVC-2J Fib Zone 3a | 0.1738 | 39.6596 | 0.0108 | 0.0254 | 0.0306 | 0.7162 |
| PVC-2J Fib Zone 3a | 0.2963 | 39.8523 | 0.0263 | 0.0014 | 0.0145 | 1.2107 |
| PVC-2J Fib Zone 3a | 0.1563 | 39.7027 | 0.0155 | 0.0424 | 0.0230 | 0.6445 |
| PVC-2J Fib Zone 3a | 0.1581 | 40.2438 | 0.0031 | 0.1059 | 0.0016 | 0.6425 |
| PVC-2J Fib Zone 3a | 0.1786 | 39.9809 | 0.0031 | 0.0001 | 0.0001 | 0.7311 |
| PVC-2J Fib Zone 3a | 0.1541 | 40.3264 | 0.0001 | 0.0268 | 0.0132 | 0.6258 |
| PVC-2J Fib Zone 3a | 0.2019 | 39.8793 | 0.0155 | 0.0607 | 0.0414 | 0.8264 |
| PVC-2J Fib Zone 3a | 0.1496 | 40.2161 | 0.0001 | 0.0113 | 0.0070 | 0.6090 |

| Sample I.D. and Zone | Wt % Mg | Wt % Ca | Wt % Mn | Wt % Fe | Wt % Sr | MgCO3 |
|---|---|---|---|---|---|---|
| PVC-2J Fib Zone 3a | 0.2049 | 39.8839 | 0.0015 | 0.0001 | 0.0028 | 0.8395 |
| PVC-2J Fib Zone 3a | 0.2122 | 39.4885 | 0.0093 | 0.0438 | 0.0259 | 0.8775 |
| PVC-2J Fib Zone 3a | 0.1287 | 39.9356 | 0.0124 | 0.0001 | 0.0184 | 0.5286 |
| PVC-2J Fib Zone 3a | 0.1623 | 39.3910 | 0.0108 | 0.0113 | 0.0212 | 0.6646 |
| PVC-2J Fib Zone 3a | 0.1880 | 40.0913 | 0.0001 | 0.0212 | 0.0001 | 0.7674 |
| PVC-2J Fib Zone 3a | 0.1622 | 40.3251 | 0.0001 | 0.0056 | 0.0150 | 0.6586 |
| PVC-2J Fib Zone 3a | 0.1048 | 40.3703 | 0.0279 | 0.0085 | 0.0001 | 0.4261 |
| PVC-2J Fib Zone 3a | 0.1932 | 39.6164 | 0.0418 | 0.0409 | 0.0176 | 0.7967 |
| PVC-2J Fib Zone 3a | 0.1725 | 40.0354 | 0.0201 | 0.0226 | 0.0228 | 0.7049 |
| PVC-2J Fib Zone 3a | 0.1626 | 39.9567 | 0.0449 | 0.0226 | 0.0065 | 0.6651 |
| PVC-2J Fib Zone 3a | 0.2288 | 39.6860 | 0.0402 | 0.0212 | 0.0101 | 0.9401 |
| PVC-2J Fib Zone 3a | 0.1442 | 40.3930 | 0.0001 | 0.0099 | 0.0145 | 0.5843 |
| PVC-2J Fib Zone 3a | 0.2101 | 40.0327 | 0.0001 | 0.0169 | 0.0001 | 0.8572 |
| PVC-2J Fib Zone 3b | 0.1907 | 39.7631 | 0.0015 | 0.0001 | 0.0016 | 0.7845 |
| PVC-2J Fib Zone 3b | 0.2230 | 39.3099 | 0.0310 | 0.0324 | 0.0287 | 0.9251 |
| PVC-2J Fib Zone 3b | 0.1993 | 39.9324 | 0.0387 | 0.0001 | 0.0122 | 0.8157 |
| PVC-2J Fib Zone 3b | 0.2677 | 39.8348 | 0.0062 | 0.0212 | 0.0119 | 1.0948 |
| PVC-2J Fib Zone 3b | 0.1409 | 39.6619 | 0.0402 | 0.0042 | 0.0008 | 0.5817 |
| PVC-2J Fib Zone 3b | 0.2115 | 40.2267 | 0.0309 | 0.0001 | 0.0323 | 0.8584 |
| PVC-2J Fib Zone 3b | 0.1404 | 40.1247 | 0.0015 | 0.0010 | 0.0028 | 0.5730 |
| PVC-2J Fib Zone 3b | 0.2008 | 39.5188 | 0.0387 | 0.0001 | 0.0010 | 0.8301 |
| PVC-2J Fib Zone 3b | 0.2034 | 40.0372 | 0.0155 | 0.0268 | 0.0085 | 0.8299 |
| PVC-2J Fib Zone 3b | 0.2511 | 39.6710 | 0.0001 | 0.0001 | 0.0365 | 1.0328 |
| PVC-2J Fib Zone 3b | 0.2496 | 39.8768 | 0.0015 | 0.0001 | 0.0153 | 1.0207 |
| PVC-2J Fib Zone 3b | 0.2273 | 40.0889 | 0.0093 | 0.0001 | 0.0021 | 0.9259 |
| PVC-2J Fib Zone 4a | 0.2128 | 40.0950 | 0.0139 | 0.0127 | 0.0057 | 0.8673 |
| PVC-2J Fib Zone 4a | 0.1897 | 39.9871 | 0.0743 | 0.0028 | 0.0088 | 0.7755 |
| PVC-2J Fib Zone 4a | 0.1902 | 39.6013 | 0.0001 | 0.0522 | 0.0001 | 0.7846 |
| PVC-2J Fib Zone 4a | 0.2178 | 40.0379 | 0.0031 | 0.0001 | 0.0194 | 0.8886 |
| PVC-2J Fib Zone 4a | 0.1842 | 39.8525 | 0.0139 | 0.0169 | 0.0342 | 0.7551 |
| PVC-2J Fib Zone 4a | 0.2185 | 39.6518 | 0.0155 | 0.0001 | 0.0176 | 0.9005 |
| PVC-2J Fib Zone 4a | 0.1629 | 40.1281 | 0.1146 | 0.0226 | 0.0150 | 0.6637 |
| PVC-2J Fib Zone 4a | 0.1742 | 40.2571 | 0.0001 | 0.0001 | 0.0001 | 0.7087 |
| PVC-2J Fib Zone 4a | 0.1857 | 39.8511 | 0.0001 | 0.0071 | 0.0044 | 0.7627 |
| PVC-2J Fib Zone 4a | 0.2224 | 40.2074 | 0.0001 | 0.0198 | 0.0088 | 0.9033 |
| PVC-2J Fib Zone 4a | 0.2151 | 40.0549 | 0.0001 | 0.0001 | 0.0386 | 0.8776 |

| Sample I.D. and Zone | Wt % Mg | Wt % Ca | Wt % Mn | Wt % Fe | Wt % Sr | MgCO3 |
|---|---|---|---|---|---|---|
| PVC-2J Fib Zone 4a | 0.2121 | 39.3700 | 0.0805 | 0.0409 | 0.0132 | 0.8780 |
| PVC-2J Fib Zone 4a | 0.1560 | 40.1048 | 0.0712 | 0.0014 | 0.0083 | 0.6357 |
| PVC-2J Fib Zone 4a | 0.1205 | 39.7125 | 0.0015 | 0.0001 | 0.0001 | 0.4974 |
| PVC-2J Fib Zone 4a | 0.1519 | 40.1012 | 0.0851 | 0.0001 | 0.0001 | 0.6193 |
| PVC-2J Fib Zone 4a | 0.2262 | 39.6253 | 0.0325 | 0.0212 | 0.0261 | 0.9310 |
| PVC-2J Fib Zone 4a | 0.2265 | 39.7419 | 0.0031 | 0.0141 | 0.0355 | 0.9299 |
| PVC-2J Fib Zone 4a | 0.2086 | 39.5484 | 0.0001 | 0.0001 | 0.0160 | 0.8618 |
| PVC-2J Fib Zone 4a | 0.1743 | 40.2247 | 0.0526 | 0.0183 | 0.0001 | 0.7084 |
| PVC-2J Fib Zone 4a | 0.2521 | 39.8202 | 0.0341 | 0.0001 | 0.0168 | 1.0320 |
| PVC-2J Fib Zone 4b | 0.1972 | 40.1597 | 0.0077 | 0.0001 | 0.0001 | 0.8035 |
| PVC-2J Fib Zone 4b | 0.2518 | 39.7945 | 0.0170 | 0.0001 | 0.0005 | 1.0320 |
| PVC-2J Fib Zone 4b | 0.1701 | 39.9371 | 0.0093 | 0.0001 | 0.0001 | 0.6967 |
| PVC-2J Fib Zone 4b | 0.2717 | 40.0597 | 0.0093 | 0.0226 | 0.0001 | 1.1050 |
| PVC-2J Fib Zone 4b | 0.2462 | 39.6680 | 0.0139 | 0.0141 | 0.0150 | 1.0127 |
| PVC-2J Fib Zone 4b | 0.2593 | 40.1593 | 0.0001 | 0.0001 | 0.0153 | 1.0530 |
| PVC-2J Fib Zone 5a | 0.1910 | 39.8028 | 0.0108 | 0.0000 | 0.0300 | 0.7845 |
| PVC-2J Fib Zone 5a | 0.1649 | 39.9409 | 0.0000 | 0.0268 | 0.0001 | 0.6764 |
| PVC-2J Fib Zone 5a | 0.1803 | 40.0074 | 0.0279 | 0.0550 | 0.0223 | 0.7364 |
| PVC-2J Fib Zone 5a | 0.2437 | 39.7483 | 0.0001 | 0.0113 | 0.0028 | 1.0005 |
| PVC-2J Fib Zone 5a | 0.2454 | 39.9807 | 0.0155 | 0.0169 | 0.0001 | 1.0014 |
| PVC-2J Fib Zone 5a | 0.1989 | 39.6753 | 0.0139 | 0.0001 | 0.0179 | 0.8189 |
| PVC-2J Fib Zone 5a | 0.1968 | 39.7365 | 0.1162 | 0.0551 | 0.0075 | 0.8072 |
| PVC-2J Fib Zone 5a | 0.1999 | 40.1684 | 0.0001 | 0.0001 | 0.0017 | 0.8138 |
| PVC-2J Fib Zone 5a | 0.2567 | 39.8593 | 0.0001 | 0.0240 | 0.0104 | 1.0500 |
| PVC-2J Fib Zone 5a | 0.1324 | 39.7856 | 0.1223 | 0.0409 | 0.0062 | 0.5445 |
| PVC-2J Fib Zone 5a | 0.1683 | 39.9071 | 0.0001 | 0.0001 | 0.0001 | 0.6902 |
| PVC-2J Fib Zone 5a | 0.1298 | 39.8863 | 0.0387 | 0.0451 | 0.0140 | 0.5333 |
| PVC-2J Fib Zone 5a | 0.1574 | 39.6481 | 0.0170 | 0.0579 | 0.0104 | 0.6489 |
| PVC-2J Fib Zone 5a | 0.1796 | 39.3465 | 0.0588 | 0.0522 | 0.0085 | 0.7460 |
| PVC-2J Fib Zone 5a | 0.2471 | 39.6556 | 0.0124 | 0.0169 | 0.0083 | 1.0165 |
| PVC-2J Fib Zone 5a | 0.1205 | 39.8490 | 0.0975 | 0.0141 | 0.0001 | 0.4947 |
| PVC-2J Fib Zone 5a | 0.1907 | 39.6102 | 0.0217 | 0.0099 | 0.0001 | 0.7871 |
| PVC-2J Fib Zone 5a | 0.2136 | 39.7354 | 0.0883 | 0.0140 | 0.0287 | 0.8772 |
| PVC-2J Fib Zone 5a | 0.1881 | 40.1402 | 0.0046 | 0.0212 | 0.0163 | 0.7662 |
| PVC-2J Fib Zone 5a | 0.2085 | 40.1535 | 0.0263 | 0.0113 | 0.0001 | 0.8485 |
| PVC-2J Fib Zone 5a | 0.1863 | 39.8202 | 0.0821 | 0.0226 | 0.0001 | 0.7643 |

| Sample I.D. and Zone | Wt % Mg | Wt % Ca | Wt % Mn | Wt % Fe | Wt % Sr | MgCO3 |
|---|---|---|---|---|---|---|
| PVC-2J Fib Zone 5a | 0.1834 | 39.8070 | 0.0789 | 0.0001 | 0.0127 | 0.7531 |
| PVC-2J Fib Zone 5a | 0.1880 | 40.0271 | 0.0743 | 0.0001 | 0.0111 | 0.7677 |
| PVC-2J Fib Zone 5a | 0.2117 | 39.6245 | 0.1548 | 0.0127 | 0.0001 | 0.8706 |
| RHB-2C-B Fib Zone 1a | 0.1405 | 39.4707 | 0.5887 | 0.0127 | 0.0093 | 0.5773 |
| RHB-2C-B Fib Zone 1a | 0.2030 | 39.9017 | 0.4436 | 0.0226 | 0.0001 | 0.8252 |
| RHB-2C-B Fib Zone 1a | 0.1725 | 39.7870 | 0.0232 | 0.0183 | 0.0001 | 0.7094 |
| RHB-2C-B Fib Zone 1a | 0.1899 | 39.8714 | 0.0062 | 0.0001 | 0.0140 | 0.7787 |
| RHB-2C-B Fib Zone 1a | 0.1380 | 40.2425 | 0.1143 | 0.0831 | 0.0000 | 0.5602 |
| RHB-2C-B Fib Zone 1a | 0.1293 | 40.3769 | 0.0294 | 0.0000 | 0.0240 | 0.5250 |
| RHB-2C-B Fib Zone 1a | 0.1890 | 39.8493 | 0.0124 | 0.0578 | 0.0292 | 0.7746 |
| RHB-2C-B Fib Zone 1a | 0.1321 | 39.8845 | 0.0711 | 0.0381 | 0.0222 | 0.5412 |
| RHB-2C-B Fib Zone 1a | 0.1729 | 40.0204 | 0.0387 | 0.0028 | 0.0001 | 0.7065 |
| RHB-2C-B Fib Zone 1a | 0.1492 | 39.7542 | 0.0247 | 0.0239 | 0.0173 | 0.6144 |
| RHB-2C-B Fib Zone 1a | 0.1459 | 39.7782 | 0.0882 | 0.0085 | 0.0135 | 0.6006 |
| RHB-2C-B Fib Zone 1a | 0.2270 | 39.7322 | 0.0001 | 0.0169 | 0.0194 | 0.9327 |
| RHB-2C-B Fib Zone 1a | 0.1603 | 40.2992 | 0.0093 | 0.0381 | 0.0001 | 0.6505 |
| RHB-2C-B Fib Zone 1a | 0.1462 | 39.8172 | 0.0001 | 0.0001 | 0.0088 | 0.6022 |
| RHB-2C-B Fib Zone 1a | 0.2452 | 39.4760 | 0.0000 | 0.0338 | 0.0119 | 1.0034 |
| RHB-2C-B Fib Zone 1a | 0.1566 | 40.3397 | 0.0000 | 0.0296 | 0.0110 | 0.6360 |
| RHB-2C-B Fib Zone 1a | 0.1327 | 39.9760 | 0.0371 | 0.0366 | 0.0000 | 0.5440 |
| RHB-2C-B Fib Zone 1a | 0.1690 | 39.8962 | 0.0015 | 0.0197 | 0.0010 | 0.6937 |
| RHB-2C-B Fib Zone 1a | 1.6697 | 38.0569 | 0.0588 | 0.0212 | 0.0151 | 6.7348 |
| RHB-2C-B Fib Zone 1b | 0.1567 | 39.2530 | 0.6533 | 0.0001 | 0.0036 | 0.6461 |
| RHB-2C-B Fib Zone 1b | 0.1375 | ##### | 0.3494 | 0.0647 | 0.0049 | 0.5686 |
| RHB-2C-B Fib Zone 1b | 0.1773 | 39.3377 | 0.5360 | 0.0099 | 0.0230 | 0.7307 |
| RHB-2C-B Fib Zone 1b | 0.1280 | 39.4345 | 0.3604 | 0.0183 | 0.0109 | 0.5282 |
| RHB-2C-B Fib Zone 1b | 1.3833 | 38.4530 | 0.1422 | 0.0254 | 0.0211 | 5.5799 |
| RHB-2C-B Fib Zone 1b | 0.1723 | 39.9487 | 0.0000 | 0.0014 | 0.0000 | 0.7059 |
| RHB-2C-B Fib Zone 2a | 0.1577 | 39.1254 | 0.8668 | 0.0141 | 0.0001 | 0.6502 |
| RHB-2C-B Fib Zone 2a | 0.1520 | 39.4526 | 0.6966 | 0.0000 | 0.0000 | 0.6236 |
| RHB-2C-B Fib Zone 2a | 0.1618 | 39.2309 | 0.8851 | 0.0028 | 0.0001 | 0.6649 |
| RHB-2C-B Fib Zone 2a | 0.1122 | 38.9849 | 0.5182 | 0.0000 | 0.0000 | 0.4672 |
| RHB-2C-B Fib Zone 2a | 0.1254 | 39.1980 | 0.4640 | 0.0001 | 0.0001 | 0.5199 |
| RHB-2C-B Fib Zone 2a | 0.1201 | 39.4178 | 0.5224 | 0.0620 | 0.0000 | 0.4946 |
| RHB-2C-B Fib Zone 2a | 0.1520 | 38.8371 | 0.9668 | 0.0113 | 0.0179 | 0.6299 |
| RHB-2C-B Fib Zone 2a | 0.1347 | 3.5645 | 0.3353 | 0.0451 | 0.0052 | 0.5536 |

| Sample I.D. and Zone | Wt % Mg | Wt % Ca | Wt % Mn | Wt % Fe | Wt % Sr | MgCO3 |
|---|---|---|---|---|---|---|
| RHB-2C-B Fib Zone 2a | 0.1444 | 39.0417 | 0.5936 | 0.0001 | 0.0001 | 0.5992 |
| RHB-2C-B Fib Zone 2a | 0.1221 | 38.3163 | 0.9782 | 0.0254 | 0.0000 | 0.5131 |
| RHB-2C-B Fib Zone 2a | 0.1285 | 38.8428 | 0.5841 | 0.0001 | 0.0026 | 0.5365 |
| RHB-2C-B Fib Zone 2a | 0.1414 | 38.8505 | 0.5318 | 0.0000 | 0.0000 | 0.5908 |
| RHB-2C-B Fib Zone 2a | 0.1523 | 39.2606 | 0.2845 | 0.0001 | 0.0060 | 0.6325 |
| RHB-2C-B Fib Zone 2a | 0.1646 | 38.8573 | 0.3911 | 0.0000 | 0.0018 | 0.6881 |
| RHB-2C-B Fib Zone 2a | 0.0995 | 38.9243 | 0.6783 | 0.0014 | 0.0001 | 0.4140 |
| RHB-2C-B Fib Zone 2a | 0.1272 | 39.1156 | 0.6232 | 0.0197 | 0.0000 | 0.5275 |
| RHB-2C-B Fib Zone 2a | 0.1188 | 40.1016 | 0.3526 | 0.0310 | 0.0001 | 0.4823 |
| RHB-2C-B Fib Zone 2a | 0.1199 | 39.5064 | 0.1392 | 0.0860 | 0.0000 | 0.4956 |
| RHB-2C-B Fib Zone 2a | 0.1293 | 39.2082 | 0.4991 | 0.0451 | 0.0001 | 0.5356 |
| RHB-2C-B Fib Zone 2a | 0.1376 | 38.7291 | 1.0169 | 0.0141 | 0.0163 | 0.5716 |
| RHB-2C-B Fib Zone 2a | 0.1365 | 38.9488 | 0.5562 | 0.0507 | 0.0001 | 0.5683 |
| RHB-2C-B Fib Zone 2a | 0.1306 | 39.6240 | 0.2256 | 0.0056 | 0.0001 | 0.5378 |
| RHB-2C-B Fib Zone 2b | 0.0899 | 39.2858 | 0.5765 | 0.0296 | 0.0000 | 0.3716 |
| RHB-2C-B Fib Zone 2b | 0.1482 | 39.0372 | 0.5132 | 0.0127 | 0.0000 | 0.6155 |
| RHB-2C-B Fib Zone 2b | 0.1109 | 39.8820 | 0.3368 | 0.0732 | 0.0031 | 0.4530 |
| RHB-2B-C1 Fib Zone 1a | 0.2823 | 39.6392 | 0.0388 | 0.0043 | 0.0000 | 1.1597 |
| RHB-2B-C1 Fib Zone 1a | 0.1494 | 39.9973 | 0.1858 | 0.0216 | 0.0087 | 0.6102 |
| RHB-2B-C1 Fib Zone 1a | 0.2290 | 39.4598 | 0.0000 | 0.0101 | 0.0000 | 0.9476 |
| RHB-2B-C1 Fib Zone 1a | 0.1714 | 39.9804 | 0.0372 | 0.0388 | 0.0145 | 0.7008 |
| RHB-2B-C1 Fib Zone 1a | 0.1524 | 39.9777 | 0.0000 | 0.0461 | 0.0254 | 0.6239 |
| RHB-2B-C1 Fib Zone 1a | 0.2256 | 39.8029 | 0.0001 | 0.0072 | 0.0188 | 0.9254 |
| RHB-2B-C1 Fib Zone 1a | 0.2780 | 39.3585 | 0.0326 | 0.0058 | 0.0045 | 1.1290 |
| RHB-2B-C1 Fib Zone 1a | 0.1734 | 40.2309 | 0.0000 | 0.0000 | 0.0000 | 0.7057 |
| RHB-2B-C1 Fib Zone 1a | 0.2170 | 40.1690 | 0.0403 | 0.0043 | 0.0140 | 0.8816 |
| RHB-2B-C1 Fib Zone 1a | 0.1768 | 39.7180 | 0.0744 | 0.3620 | 0.0193 | 0.7230 |
| RHB-2B-C1 Fib Zone 1a | 0.1671 | 40.0438 | 0.0093 | 0.0115 | 0.0001 | 0.6830 |
| RHB-2B-C1 Fib Zone 1a | 0.1451 | 39.7948 | 0.0031 | 0.0001 | 0.0001 | 0.5979 |
| RHB-2B-C1 Fib Zone 1a | 0.1699 | 39.5031 | 0.1256 | 0.0058 | 0.0034 | 0.7027 |
| RHB-2B-C1 Fib Zone 1a | 0.1405 | 39.5848 | 0.0543 | 0.0014 | 0.0061 | 0.5815 |
| RHB-2B-C1 Fib Zone 1b, 2 | 0.1458 | 39.6817 | 0.0232 | 0.0001 | 0.0016 | 0.6017 |
| RHB-2B-C1 Fib Zone 1b, 2 | 0.1511 | 40.0428 | 0.0001 | 0.0001 | 0.0001 | 0.6189 |
| RHB-2B-C1 Fib Zone 1b, 2 | 0.1634 | 39.8710 | 0.0108 | 0.0201 | 0.0018 | 0.6705 |
| RHB-2B-C1 Fib Zone 1b, 2 | 0.1832 | 40.0349 | 0.0233 | 0.0173 | 0.0001 | 0.7483 |
| RHB-2B-C1 Fib Zone 1b, 2 | 0.1635 | 40.0975 | 0.0217 | 0.0245 | 0.0013 | 0.6673 |

| Sample I.D. and Zone | Wt % Mg | Wt % Ca | Wt % Mn | Wt % Fe | Wt % Sr | MgCO3 |
|---|---|---|---|---|---|---|
| RHB-2B-C1 Fib Zone 1b, 2 | 0.1707 | 40.1871 | 0.0001 | 0.0001 | 0.0172 | 0.6952 |
| RHB-2B-C1 Fib Zone 1b, 2 | 0.1114 | 39.7357 | 0.0636 | 0.0072 | 0.0021 | 0.4598 |
| RHB-2B-C1 Fib Zone 1b, 2 | 0.1371 | 39.6186 | 0.0512 | 0.0144 | 0.0106 | 0.5666 |
| RHB-2B-C1 Fib Zone 3 | 0.1510 | 40.2849 | 0.0031 | 0.0130 | 0.0000 | 0.6138 |
| RHB-2B-C1 Fib Zone 3 | 0.2172 | 39.2636 | 0.0621 | 0.0706 | 0.0151 | 0.9015 |
| RHB-2B-C1 Fib Zone 3 | 0.1765 | 39.7671 | 0.0310 | 0.0317 | 0.0214 | 0.7258 |
| RHB-2B-C1 Fib Zone 3 | 0.1256 | 39.5511 | 0.0620 | 0.0129 | 0.0001 | 0.5201 |
| RHB-2B-C1 Fib Zone 3 | 0.5116 | 39.1930 | 0.0109 | 0.0691 | 0.0001 | 2.1067 |
| RHB-2B-C1 Fib Zone 3 | 0.1716 | 39.7922 | 0.0001 | 0.0490 | 0.0162 | 0.7056 |
| RHB-2B-C1 Fib Zone 3 | 0.1655 | 39.6857 | 0.0001 | 0.0647 | 0.0001 | 0.6827 |
| RHB-2B-C1 Fib Zone 3 | 0.1312 | 39.0859 | 0.0001 | 0.0158 | 0.0001 | 0.5497 |
| RHB-2B-C1 Fib Zone 3 | 0.1878 | 39.6954 | 0.0001 | 0.0532 | 0.0087 | 0.7733 |
| RHB-2B-C1 Fib Zone 3 | 0.1798 | 40.2019 | 0.0001 | 0.0001 | 0.0090 | 0.7317 |
| RHB-2B-C1 Fib Zone 3 | 0.1526 | 39.6032 | 0.0341 | 0.0202 | 0.0146 | 0.6309 |
| RHB-2B-C1 Fib Zone 3 | 0.1879 | 39.9653 | 0.0001 | 0.0302 | 0.0267 | 0.7682 |
| RHB-2B-C1 Fib Zone 3 | 0.1624 | 39.9543 | 0.0031 | 0.0290 | 0.0209 | 0.6658 |
| RHB-2B-C1 Fib Zone 3 | 0.1501 | 39.6224 | 0.0078 | 0.0001 | 0.0214 | 0.6204 |
| RHB-2B-C1 Fib Zone 3 | 0.1451 | 39.5058 | 0.0093 | 0.0001 | 0.0378 | 0.6019 |
| RHB-2B-C1 Fib Zone 3 | 0.1681 | 40.2665 | 0.0001 | 0.0001 | 0.0001 | 0.6841 |
| RHB-2B-C1 Fib Zone 3 | 0.7282 | 39.2854 | 0.0001 | 0.0001 | 0.0001 | 2.9657 |
| RHB-2B-C1 Fib Zone 3 | 0.3189 | 39.5283 | 0.0078 | 0.0144 | 0.0001 | 1.3121 |
| RHB-2B-C1 Fib Zone 3 | 0.3948 | 40.0039 | 0.0109 | 0.0519 | 0.0001 | 1.5987 |
| RHB-2B-C1 Fib Zone 3 | 0.1633 | 39.7197 | 0.0140 | 0.0086 | 0.0106 | 0.6731 |
| RHB-2B-C1 Fib Zone 3 | 0.1291 | 39.6064 | 0.0001 | 0.0001 | 0.0085 | 0.5343 |
| RHB-2H Fib Zone 1 | 0.1761 | 39.7639 | 0.0001 | 0.0551 | 0.0112 | 0.7237 |
| RHB-2H Fib Zone 1 | 0.1954 | 40.0210 | 0.0001 | 0.0247 | 0.0043 | 0.7978 |
| RHB-2H Fib Zone 1 | 0.2304 | 39.9371 | 0.0001 | 0.0001 | 0.0001 | 0.9424 |
| RHB-2H Fib Zone 1 | 0.2278 | 39.7719 | 0.0001 | 0.0464 | 0.0001 | 0.9350 |
| RHB-2H Fib Zone 1 | 0.3457 | 38.9709 | 0.0515 | 0.0493 | 0.0202 | 1.4384 |
| RHB-2H Fib Zone 1 | 0.2446 | 39.2718 | 0.0593 | 0.1145 | 0.0123 | 1.0130 |
| RHB-2H Fib Zone 1 | 0.1973 | 39.8886 | 0.0374 | 0.0001 | 0.0072 | 0.8084 |
| RHB-2H Fib Zone 1 | 0.2338 | 39.9163 | 0.0001 | 0.0087 | 0.0125 | 0.9566 |
| RHB-2H Fib Zone 1 | 0.2089 | 39.9766 | 0.0001 | 0.0001 | 0.0083 | 0.8539 |
| RHB-2H Fib Zone 1 | 0.2632 | 40.0340 | 0.0001 | 0.0001 | 0.0367 | 1.0723 |
| RHB-2H Fib Zone 1 | 0.2339 | 40.0208 | 0.0312 | 0.0261 | 0.0001 | 0.9535 |
| RHB-2H Fib Zone 1 | 0.1696 | 40.2257 | 0.0156 | 0.0217 | 0.0165 | 0.6901 |

| Sample I.D. and Zone | Wt % Mg | Wt % Ca | Wt % Mn | Wt % Fe | Wt % Sr | MgCO3 |
|---|---|---|---|---|---|---|
| RHB-2H Fib Zone 1 | 0.2258 | 39.9793 | 0.0001 | 0.0087 | 0.0035 | 0.9226 |
| RHB-2H Fib Zone 2 | 0.8595 | 8.9938 | 0.0414 | 0.1375 | 0.0304 | 3.4948 |
| RHB-2H Fib Zone 2 | 0.2738 | 39.5152 | 0.0188 | 0.0160 | 0.0208 | 1.1292 |
| RHB-2H Fib Zone 2 | 0.7799 | 39.2114 | 0.0204 | 0.0392 | 0.0252 | 3.1705 |
| RHB-2H Fib Zone 2 | 0.2430 | 39.4180 | 0.0110 | 0.1149 | 0.0134 | 1.0043 |
| RHB-2H Fib Zone 2 | 0.9795 | 38.9754 | 0.0250 | 0.0174 | 0.0238 | 3.9743 |
| RHB-2H Fib Zone 2 | 0.4977 | 39.6906 | 0.0360 | 0.0189 | 0.0088 | 2.0237 |
| RHB-2H Fib Zone 2 | 0.8729 | 39.1082 | 0.0110 | 0.0001 | 0.0364 | 3.5471 |
| RHB-2H Fib Zone 2 | 0.2902 | 39.2189 | 0.0438 | 0.1524 | 0.0208 | 1.2003 |
| RHB-2H Fib Zone 2 | 0.2743 | 39.2712 | 0.0470 | 0.2135 | 0.0177 | 1.1327 |
| RHB-2H Fib Zone 2 | 0.4268 | 39.1954 | 0.0203 | 0.1117 | 0.0141 | 1.7597 |
| RHB-2H Fib Zone 2 | 0.4927 | 39.5960 | 0.0141 | 0.0943 | 0.0193 | 2.0068 |
| RHB-2H Fib Zone 2 | 0.6639 | 38.9961 | 0.0001 | 0.0668 | 0.0179 | 2.7269 |
| RHB-2H Fib Zone 2 | 0.4450 | 39.3186 | 0.0001 | 0.0638 | 0.0112 | 1.8298 |
| RHB-2H Fib Zone 2 | 0.5895 | 39.5092 | 0.0062 | 0.0174 | 0.0195 | 2.4001 |
| PVC-2G-Bill, Fib 1 | 0.1709 | 40.2862 | 0.0001 | 0.0001 | 0.0001 | 0.6943 |
| PVC-2G-Bill, Fib 1 | 0.1250 | 40.0155 | 0.0044 | 0.0001 | 0.0079 | 0.5124 |
| PVC-2G-Bill, Fib 1 | 0.2286 | 39.6992 | 0.0001 | 0.0112 | 0.0001 | 0.9408 |
| PVC-2G-Bill, Fib 1 | 0.1188 | 39.7878 | 0.0573 | 0.0376 | 0.0001 | 0.4886 |
| PVC-2G-Bill, Fib 1 | 0.1687 | 40.2817 | 0.0001 | 0.0001 | 0.0128 | 0.6861 |
| PVC-2G-Bill, Fib 1 | 0.1771 | 40.3149 | 0.0147 | 0.0223 | 0.0074 | 0.7188 |
| PVC-2G-Bill, Fib 1 | 0.2052 | 39.9632 | 0.0001 | 0.0279 | 0.0001 | 0.8398 |
| PVC-2G-Bill, Fib 1 | 0.1734 | 40.1241 | 0.0368 | 0.0796 | 0.0001 | 0.7061 |
| PVC-2G-Bill, Fib 2 | 0.1546 | 39.9075 | 0.0001 | 0.0042 | 0.0131 | 0.6349 |
| PVC-2G-Bill, Fib 2 | 0.2194 | 39.9174 | 0.0001 | 0.0294 | 0.0264 | 0.8978 |
| PVC-2G-Bill, Fib 2 | 0.2301 | 39.8405 | 0.0001 | 0.0266 | 0.0185 | 0.9429 |
| PVC-2G-Bill, Fib 2 | 0.2155 | 39.4522 | 0.0001 | 0.0294 | 0.0001 | 0.8920 |
| PVC-2G-Bill, Fib 2 | 0.2090 | 40.0129 | 0.0118 | 0.0001 | 0.0001 | 0.8414 |
| PVC-2G-Bill, Fib 2 | 0.2757 | 39.7150 | 0.0162 | 0.0001 | 0.0305 | 1.1308 |
| PVC-2G-Bill, Fib 2 | 0.2384 | 39.3987 | 0.0030 | 0.0140 | 0.0085 | 0.9879 |
| PVC-2G-Bill, Fib 2 | 0.1421 | 39.5158 | 0.0384 | 0.0700 | 0.0001 | 0.5879 |
| PVC-2G-Bill, Fib 2 | 0.1315 | 39.5284 | 0.0870 | 0.0112 | 0.0001 | 0.5439 |
| PVC-2G-Bill, Fib 2 | 0.2205 | 39.1624 | 0.0030 | 0.0280 | 0.0149 | 0.9186 |
| RHB-3R-A2, Fib1 | 0.1585 | 39.4447 | 0.0060 | 0.1137 | 0.0552 | 0.6561 |
| RHB-3R-A2, Fib1 | 0.1785 | 39.8568 | 0.0001 | 0.0682 | 0.0195 | 0.7323 |
| RHB-3R-A2, Fib1 | 0.1928 | 39.3786 | 0.0001 | 0.0114 | 0.0828 | 0.7995 |

| Sample I.D. and Zone | Wt % Mg | Wt % Ca | Wt % Mn | Wt % Fe | Wt % Sr | MgCO3 |
|---|---|---|---|---|---|---|
| RHB-3R-A2, Fib1 | 0.2211 | 39.1803 | 0.0001 | 0.0185 | 0.1106 | 0.9197 |
| RHB-3R-A2, Fib1 | 0.1314 | 39.6981 | 0.0225 | 0.0071 | 0.0076 | 0.5423 |
| RHB-3R-A2, Fib1 | 0.1538 | 40.3843 | 0.0001 | 0.0427 | 0.0001 | 0.6236 |
| RHB-3R-A2, Fib1 | 0.2148 | 39.5585 | 0.0255 | 0.0299 | 0.0138 | 0.8867 |
| RHB-3R-A2, Fib1 | 0.1706 | 39.4052 | 0.0001 | 0.0284 | 0.0005 | 0.7081 |
| RHB-3R-A2, Fib1 | 0.1284 | 39.7675 | 0.0001 | 0.0043 | 0.0001 | 0.5298 |
| RHB-3R-A2, Fib1 | 0.1452 | 40.2708 | 0.0001 | 0.0171 | 0.0001 | 0.5907 |
| RHB-3R-A2, Fib1 | 0.1486 | 40.0109 | 0.0105 | 0.0512 | 0.0070 | 0.6081 |
| RHB-3R-A2, Fib1 | 0.2051 | 40.0984 | 0.0001 | 0.0100 | 0.0018 | 0.8361 |
| RHB-3R-A2, Fib1 | 0.1986 | 39.9442 | 0.0225 | 0.0001 | 0.0001 | 0.8134 |
| RHB-3R-A2, Fib1 | 0.2056 | 39.5885 | 0.0510 | 0.0185 | 0.0167 | 0.8481 |
| RHB-3R-A2, Fib1 | 0.1654 | 40.0876 | 0.0419 | 0.0057 | 0.0448 | 0.6746 |
| RHB-3R-A2, Fib1 | 0.1721 | 40.2771 | 0.0001 | 0.0014 | 0.0001 | 0.6990 |
| RHB-3R-A2, Fib1 | 0.1304 | 39.7521 | 0.0001 | 0.0142 | 0.0086 | 0.5381 |
| RHB-3R-A2, Fib1 | 0.1716 | 39.9416 | 0.0225 | 0.0001 | 0.0001 | 0.7034 |
| RHB-3R-A2, Fib1 | 0.1659 | 39.4459 | 0.0015 | 0.0441 | 0.0001 | 0.6882 |
| RHB-3R-A2, Fib1 | 0.1886 | 39.7704 | 0.0001 | 0.0170 | 0.0185 | 0.7758 |

| On-Shelf Fibrous Calcite | | | | | | Mole % |
|---|---|---|---|---|---|---|
| Sample I.D. and Zone | Wt % Mg | Wt % Ca | Wt % Mn | Wt % Fe | Wt % Sr | MgCO3 |
| IS-90-47a Fib Zone 1a, 1b | 0.3080 | 39.6156 | 0.1859 | 0.0001 | 0.0111 | 1.2610 |
| IS-90-47a Fib Zone 1a, 1b | 0.2739 | 39.7056 | 0.0434 | 0.0001 | 0.0215 | 1.1236 |
| IS-90-47a Fib Zone 1a, 1b | 0.2161 | 39.3589 | 0.1533 | 0.0001 | 0.0010 | 0.8944 |
| IS-90-47a Fib Zone 1a, 1b | 0.2814 | 39.5523 | 0.1780 | 0.0028 | 0.0153 | 1.1556 |
| IS-90-47a Fib Zone 1a, 1b | 0.3567 | 39.5722 | 0.1037 | 0.0001 | 0.0132 | 1.4611 |
| IS-90-47a Fib Zone 1a, 1b | 0.4437 | 39.7459 | 0.0077 | 0.0001 | 0.0347 | 1.8060 |
| IS-90-47a Fib Zone 1a, 1b | 0.2584 | 38.7430 | 0.1642 | 0.0169 | 0.0001 | 1.0804 |
| IS-90-47a Fib Zone 1a, 1b | 0.3533 | 35.5341 | 0.1425 | 0.0071 | 0.0135 | 1.4473 |
| IS-90-47a Fib Zone 1a, 1b | 0.2704 | 39.5548 | 0.0527 | 0.0001 | 0.0052 | 1.1138 |
| IS-90-47a Fib Zone 1a, 1b | 0.3100 | 39.6248 | 0.1115 | 0.0001 | 0.0088 | 1.2706 |
| IS-90-47a Fib Zone 1a, 1b | 0.3360 | 38.9085 | 0.2043 | 0.0001 | 0.0210 | 1.3977 |
| IS-90-47a Fib Zone 1a, 1b | 0.3542 | 39.7015 | 0.0557 | 0.0212 | 0.0202 | 1.4478 |
| IS-90-47a Fib Zone 1a, 1b | 0.2154 | 39.8224 | 0.1254 | 0.0056 | 0.0023 | 0.8821 |
| IS-90-47a Fib Zone 1a, 1b | 0.2977 | 39.3089 | 0.1532 | 0.0001 | 0.0135 | 1.2303 |
| IS-90-47a Fib Zone 1a, 1b | 0.2843 | 39.6276 | 0.1424 | 0.0198 | 0.0039 | 1.1656 |
| IS-90-47a Fib Zone 1a, 1b | 0.2791 | 39.4837 | 0.0836 | 0.0001 | 0.0316 | 1.1500 |
| IS-90-47a Fib Zone 1a, 1b | 0.2360 | 39.2978 | 0.1022 | 0.0325 | 0.0148 | 0.9776 |
| IS-90-47a Fib Zone 1a, 1b | 0.2897 | 39.0018 | 0.1393 | 0.0014 | 0.0174 | 1.2069 |
| IS-90-47a Fib Zone 1a, 1b | 0.2740 | 39.6908 | 0.1130 | 0.0001 | 0.0137 | 1.1227 |
| IS-90-47a Fib Zone 1a, 1b | 0.3069 | 39.4259 | 0.1672 | 0.0085 | 0.0376 | 1.2633 |
| IS-90-47a fib Zone 1c, 2a | 0.1781 | 39.7801 | 0.0248 | 0.0001 | 0.0220 | 0.7319 |
| IS-90-47a fib Zone 1c, 2a | 0.2222 | 39.5065 | 0.0387 | 0.0001 | 0.0101 | 0.9176 |
| IS-90-47a fib Zone 1c, 2a | 0.2261 | 39.3022 | 0.1269 | 0.0183 | 0.0093 | 0.9371 |
| IS-90-47a fib Zone 1c, 2a | 0.2100 | 39.6558 | 0.0001 | 0.0001 | 0.0016 | 0.8655 |
| IS-90-47a fib Zone 1c, 2a | 0.2373 | 39.4188 | 0.0294 | 0.0155 | 0.0225 | 0.9820 |
| IS-90-47a fib Zone 1c, 2a | 0.3021 | 39.7824 | 0.0001 | 0.0071 | 0.0158 | 1.2365 |
| IS-90-47a fib Zone 1c, 2a | 0.1979 | 40.1052 | 0.0434 | 0.0226 | 0.0184 | 0.8059 |
| IS-90-47a fib Zone 1c, 2a | 0.2058 | 39.7608 | 0.0201 | 0.0198 | 0.0148 | 0.8449 |
| IS-90-47a fib Zone 1c, 2a | 0.2994 | 40.0504 | 0.0496 | 0.0001 | 0.0231 | 1.2157 |
| IS-90-47a fib Zone 1c, 2a | 0.2068 | 39.6158 | 0.0294 | 0.0381 | 0.0275 | 0.8522 |
| IS-90-47a fib Zone 1c, 2a | 0.2127 | 40.0530 | 0.0139 | 0.0001 | 0.0003 | 0.8673 |
| IS-90-47a fib Zone 1c, 2a | 0.1965 | 39.9516 | 0.0077 | 0.0254 | 0.0091 | 0.8037 |
| IS-90-47a fib Zone 1c, 2a | 0.2265 | 39.9385 | 0.0001 | 0.0001 | 0.0200 | 0.9259 |
| IS-90-47a fib Zone 1c, 2a | 0.1629 | 39.9605 | 0.0217 | 0.0127 | 0.0291 | 0.6664 |
| IS-90-47a Fib Zone 2b, 2c | 0.1451 | 39.5109 | 0.0279 | 0.0170 | 0.0171 | 0.6016 |

| Sample I.D. and Zone | Wt % Mg | Wt % Ca | Wt % Mn | Wt % Fe | Wt % Sr | MgCO3 |
|---|---|---|---|---|---|---|
| IS-90-47a Fib Zone 2b, 2c | 0.2218 | 39.8410 | 0.0001 | 0.0250 | 0.0065 | 0.9091 |
| IS-90-47a Fib Zone 2b, 2c | 0.2050 | 39.5640 | 0.0171 | 0.0282 | 0.0243 | 0.8689 |
| IS-90-47a Fib Zone 2b, 2c | 0.2367 | 39.7799 | 0.0449 | 0.0325 | 0.0150 | 0.9704 |
| IS-90-47a Fib Zone 2b, 2c | 0.2361 | 40.2258 | 0.0325 | 0.0042 | 0.0101 | 0.9582 |
| IS-90-47a Fib Zone 2b, 2c | 0.2474 | 39.5013 | 0.1177 | 0.0001 | 0.0008 | 1.0201 |
| IS-90-47a Fib Zone 2b, 2c | 0.1529 | 39.7748 | 0.0635 | 0.0141 | 0.0044 | 0.6292 |
| IS-90-47a Fib Zone 2b, 2c | 0.2432 | 40.0649 | 0.0155 | 0.0001 | 0.0036 | 0.9903 |
| IS-90-47a Fib Zone 2b, 2c | 0.1882 | 40.0037 | 0.0001 | 0.0127 | 0.0049 | 0.7703 |
| IS-90-47a Fib Zone 2b, 2c | 0.3302 | 39.7530 | 0.0217 | 0.0001 | 0.0132 | 1.3500 |
| IS-90-47a Fib Zone 2b, 2c | 0.1996 | 39.8267 | 0.0001 | 0.0268 | 0.0083 | 0.8192 |
| IS-90-47a Fib Zone 2b, 2c | 0.3604 | 39.3198 | 0.0047 | 0.0000 | 0.0197 | 1.4882 |
| IS-90-47a Fib Zone 2b, 2c | 0.2154 | 39.8680 | 0.0341 | 0.0001 | 0.0001 | 0.8827 |
| IS-90-47a Fib Zone 2b, 2c | 0.2071 | 40.1948 | 0.0387 | 0.0056 | 0.0057 | 0.8417 |
| IS-90-47a Fib Zone 2b, 2c | 0.2668 | 39.8032 | 0.0001 | 0.0001 | 0.0057 | 1.0928 |
| IS-90-47a Fib Zone 2b, 2c | 0.1928 | 39.6360 | 0.0186 | 0.0001 | 0.0001 | 0.7950 |
| IS-90-47a Fib Zone 2b, 2c | 0.2047 | 39.6728 | 0.0170 | 0.0127 | 0.0010 | 0.8435 |
| IS-90-47a Fib Zone 2b, 2c | 0.1926 | 39.9446 | 0.0232 | 0.0466 | 0.0001 | 0.7882 |
| IS-90-47a Fib Zone 2b, 2c | 0.3778 | 39.6291 | 0.0046 | 0.0155 | 0.0236 | 1.5471 |
| IS-90-47a Fib Zone 2b, 2c | 0.2496 | 39.5033 | 0.0232 | 0.0071 | 0.0001 | 1.0299 |
| IS-90-47a Fib Zone 2b, 2c | 0.2374 | 39.9054 | 0.0697 | 0.0113 | 0.0001 | 0.9698 |
| IS-90-46 Zone Fib 1 | 0.2533 | 40.0245 | 0.0292 | 0.0157 | 0.0141 | 0.9593 |
| IS-90-46 Zone Fib 1 | 0.1535 | 39.9209 | 0.0245 | 0.0100 | 0.0001 | 0.6297 |
| IS-90-46 Zone Fib 1 | 0.2281 | 39.7574 | 0.0092 | 0.0313 | 0.0081 | 0.9365 |
| IS-90-46 Zone Fib 1 | 0.1887 | 40.1430 | 0.0215 | 0.0228 | 0.0026 | 0.7684 |
| IS-90-46 Zone Fib 1 | 0.2524 | 40.1558 | 0.0077 | 0.0199 | 0.0001 | 1.0250 |
| IS-90-46 Zone Fib 1 | 0.1967 | 39.8755 | 0.0475 | 0.0824 | 0.0001 | 0.8051 |
| IS-90-46 Zone Fib 1 | 0.2231 | 40.0325 | 0.0475 | 0.0001 | 0.0157 | 0.9102 |
| IS-90-46 Zone Fib 1 | 0.2576 | 40.0487 | 0.0230 | 0.0043 | 0.0261 | 1.0483 |
| IS-90-46 Fib Zone 2 | 0.1708 | 40.0471 | 0.0316 | 0.0000 | 0.0121 | 0.6979 |
| IS-90-46 Fib Zone 2 | 0.1907 | 39.7174 | 0.0362 | 0.0175 | 0.0003 | 0.7847 |
| IS-90-46 Fib Zone 2 | 0.1994 | 40.2299 | 0.0001 | 0.0001 | 0.0219 | 0.8101 |
| IS-90-46 Fib Zone 2 | 0.1976 | 40.0863 | 0.0031 | 0.0305 | 0.0139 | 0.8056 |
| IS-90-46 Fib Zone 2 | 0.2739 | 40.1221 | 0.0001 | 0.0043 | 0.0021 | 1.1131 |
| IS-90-46 Fib Zone 2 | 0.3310 | 39.8531 | 0.0170 | 0.0144 | 0.0169 | 1.3498 |
| IS-90-46 Fib Zone 2 | 0.2409 | 40.0864 | 0.0170 | 0.0072 | 0.0161 | 0.9802 |
| IS-90-46 Fib Zone 2 | 0.2481 | 39.8260 | 0.0001 | 0.0114 | 0.0165 | 1.0160 |

| Sample I.D. and Zone | Wt % Mg | Wt % Ca | Wt % Mn | Wt % Fe | Wt % Sr | MgCO3 |
|---|---|---|---|---|---|---|
| TH-89-95, Fib1 | 0.1975 | 39.3872 | 0.0030 | 0.0238 | 0.0246 | 0.8198 |
| TH-89-95, Fib1 | 0.2302 | 39.9836 | 0.0000 | 0.0084 | 0.0000 | 0.9400 |
| TH-89-95, Fib1 | 0.2172 | 40.1414 | 0.0192 | 0.0168 | 0.0013 | 0.8837 |
| TH-89-95, Fib1 | 0.1724 | 39.0231 | 0.0015 | 0.0911 | 0.0280 | 0.7223 |
| TH-89-95, Fib1 | 0.2490 | 39.2550 | 0.0074 | 0.0001 | 0.0238 | 1.0341 |
| TH-89-95, Fib1 | 0.1707 | 39.2421 | 0.0001 | 0.0714 | 0.0080 | 0.7117 |
| TH-89-95, Fib1 | 0.2741 | 39.8014 | 0.0369 | 0.0028 | 0.0151 | 1.1223 |
| TH-89-95, Fib1 | 0.1686 | 39.9436 | 0.0222 | 0.0001 | 0.0162 | 0.6904 |
| TH-89-95, Fib1 | 0.1773 | 39.6947 | 0.0001 | 0.0028 | 0.0036 | 0.7304 |
| TH-89-95, Fib1 | 0.1772 | 39.5765 | 0.0355 | 0.0001 | 0.0074 | 0.7321 |
| TH-89-95, Fib1 | 0.1873 | 39.2557 | 0.0074 | 0.0840 | 0.0036 | 0.7790 |
| TH-89-95, Fib1 | 0.1675 | 39.8185 | 0.0281 | 0.0098 | 0.0000 | 0.6890 |
| TH-89-95, Fib1 | 0.2362 | 40.0022 | 0.0296 | 0.0477 | 0.0001 | 0.9629 |
| TH-89-95, Fib1 | 0.1547 | 40.0022 | 0.0428 | 0.0000 | 0.0131 | 0.6330 |
| TH-89-95, Fib1 | 0.2141 | 39.2866 | 0.0340 | 0.0112 | 0.0001 | 0.8895 |
| TH-89-95, Fib1 | 0.1982 | 40.1631 | 0.0488 | 0.0000 | 0.0087 | 0.8062 |
| TH-89-95, Fib1 | 0.1701 | 39.5628 | 0.0104 | 0.0000 | 0.0000 | 0.7032 |

| Shelf-Edge Bladed Calcite | | | | | | Mole % |
|---|---|---|---|---|---|---|
| Sample I.D. and Zone | Wt % Mg | Wt % Ca | Wt % Mn | Wt % Fe | Wt % Sr | MgCO3 |
| PVC-2J, Bladed | 0.1794 | 40.0671 | 0.0820 | 0.0071 | 0.0217 | 0.7317 |
| PVC-2J, Bladed | 0.1662 | 39.4184 | 0.0728 | 0.0001 | 0.0001 | 0.6895 |
| PVC-2J, Bladed | 0.1687 | 39.0509 | 0.1115 | 0.0099 | 0.0148 | 0.7060 |
| PVC-2J, Bladed | 0.1255 | 38.9865 | 0.6796 | 0.0268 | 0.0000 | 0.5215 |
| PVC-2J, Bladed | 0.1143 | 39.8019 | 0.1068 | 0.0268 | 0.0031 | 0.4703 |
| PVC-2J, Bladed | 0.2463 | 40.2141 | 0.0496 | 0.0056 | 0.0039 | 0.9987 |
| PVC-2J, Bladed | 0.2196 | 39.8393 | 0.1331 | 0.0056 | 0.0062 | 0.8979 |
| PVC-2J, Bladed | 0.1634 | 39.7816 | 0.1563 | 0.0169 | 0.0215 | 0.6701 |
| PVC-2J, Bladed | 0.1110 | 39.3061 | 0.3142 | 0.0310 | 0.0104 | 0.4601 |
| PVC-2J, Bladed | 0.2056 | 39.0327 | 0.0945 | 0.1581 | 0.0104 | 0.8572 |
| PVC-2J, Bladed | 0.1980 | 39.2861 | 0.1362 | 0.0268 | 0.0003 | 0.8213 |
| PVC-2J, Bladed | 0.1344 | 40.0325 | 0.1178 | 0.0127 | 0.0001 | 0.5497 |
| PVC-2J, Bladed | 0.1752 | 39.7242 | 0.1191 | 0.0001 | 0.0269 | 0.7199 |
| PVC-2J, Bladed | 0.1753 | 39.6830 | 0.1022 | 0.0001 | 0.0264 | 0.7220 |
| PVC-2J, Bladed | 0.2395 | 39.4865 | 0.1053 | 0.0001 | 0.0210 | 0.9875 |
| PVC-2J, Bladed | 0.1494 | 40.1463 | 0.1037 | 0.0508 | 0.0362 | 0.6083 |
| PVC-2J, Bladed | 0.1227 | 39.2286 | 0.1316 | 0.0254 | 0.0244 | 0.5115 |
| PVC-2J, Bladed | 0.1873 | 39.9921 | 0.1549 | 0.0169 | 0.0001 | 0.7637 |
| RHB-2C-B, Bladed | 0.1903 | 39.6591 | 0.1778 | 0.0352 | 0.0000 | 0.7824 |
| RHB-2C-B, Bladed | 0.2188 | 39.6889 | 0.1144 | 0.1099 | 0.0000 | 0.8976 |
| RHB-2C-B, Bladed | 0.2825 | 39.3852 | 0.0340 | 0.0945 | 0.0039 | 1.1664 |
| RHB-2C-B, Bladed | 0.1866 | 39.4095 | 0.2151 | 0.0000 | 0.0000 | 0.7719 |
| RHB-2C-B, Bladed | 0.2534 | 38.9664 | 0.0572 | 0.1790 | 0.0088 | 1.0565 |
| RHB-2C-B, Bladed | 0.2466 | 39.6456 | 0.0665 | 0.0550 | 0.0000 | 1.0129 |
| RHB-2C-B, Bladed | 0.2521 | 39.4768 | 0.0186 | 0.1170 | 0.0016 | 1.0392 |
| RHB-2C-B, Bladed | 0.1780 | 39.7452 | 0.0417 | 0.2494 | 0.0000 | 0.7293 |
| RHB-2C-B, Bladed | 0.1425 | 39.1938 | 0.2350 | 0.0001 | 0.0001 | 0.5937 |
| RHB-2C-B, Bladed | 0.2446 | 39.1148 | 0.0201 | 0.2453 | 0.0000 | 1.0155 |
| RHB-2C-B, Bladed | 0.2557 | 39.7041 | 0.0155 | 0.2805 | 0.0060 | 1.0455 |
| RHB-2C-B, Bladed | 0.2867 | 39.8838 | 0.0000 | 0.0338 | 0.0062 | 1.1702 |
| RHB-2C-B, Bladed | 0.1701 | 39.8448 | 0.0000 | 0.0437 | 0.0135 | 0.6989 |
| RHB-2C-B, Bladed | 0.2426 | 40.0854 | 0.0000 | 0.0169 | 0.0000 | 0.9875 |
| RHB-2C-B, Bladed | 0.0237 | 39.1899 | 0.1159 | 0.1099 | 0.0078 | 0.9834 |
| RHB-2C-B, Bladed | 0.1768 | 39.5370 | 0.1129 | 0.0437 | 0.0000 | 0.7307 |
| RHB-2C-B, Bladed | 0.2678 | 38.9632 | 0.0170 | 0.0973 | 0.0018 | 1.1186 |

| Sample I.D. and Zone | Wt % Mg | Wt % Ca | Wt % Mn | Wt % Fe | Wt % Sr | MgCO3 |
|---|---|---|---|---|---|---|
| RHB-2C-B, Bladed | 0.1780 | 39.4219 | 0.1393 | 0.0564 | 0.0000 | 0.7364 |
| RHB-2C-B, Bladed | 0.1550 | 3.8557 | 0.2304 | 0.0254 | 0.0001 | 0.6341 |
| RHB-2C-B, Bladed | 0.1883 | 39.4692 | 0.0000 | 0.0353 | 0.0109 | 0.7803 |
| PCV-2G-Bill, Blade1 | 0.1541 | 39.8076 | 0.0802 | 0.0000 | 0.0626 | 0.6329 |
| PCV-2G-Bill, Blade1 | 0.1375 | 39.3835 | 0.0570 | 0.0277 | 0.0609 | 0.5707 |
| PCV-2G-Bill, Blade1 | 0.1373 | 39.4768 | 0.0949 | 0.0001 | 0.0388 | 0.5694 |
| PCV-2G-Bill, Blade1 | 0.1622 | 39.7314 | 0.0994 | 0.0319 | 0.0262 | 0.6667 |
| PCV-2G-Bill, Blade1 | 0.1589 | 39.7489 | 0.0938 | 0.0208 | 0.0140 | 0.6538 |
| PCV-2G-Bill, Blade1 | 0.0505 | 39.8407 | 0.0337 | 0.0001 | 0.0232 | 0.2080 |
| PCV-2G-Bill, Blade1 | 0.1551 | 39.6839 | 0.1451 | 0.0001 | 0.0237 | 0.6391 |
| PCV-2G-Bill, Blade1 | 0.1443 | 38.8528 | 0.3975 | 0.0278 | 0.0612 | 0.6035 |
| PCV-2G-Bill, Blade1 | 0.1419 | 39.2720 | 0.2540 | 0.0056 | 0.0171 | 0.5897 |
| PCV-2G-Bill, Blade1 | 0.1818 | 39.1362 | 0.0692 | 0.3251 | 0.0074 | 0.7545 |
| PCV-2G-Bill, Blade1 | 0.1577 | 39.7390 | 0.0809 | 0.0001 | 0.0001 | 0.6486 |
| PCV-2G-Bill, Blade2 | 0.1190 | 38.6590 | 0.5594 | 0.0573 | 0.0182 | 0.4990 |
| PCV-2G-Bill, Blade2 | 0.1640 | 39.2232 | 0.1327 | 0.0001 | 0.0001 | 0.6826 |
| PCV-2G-Bill, Blade2 | 0.1828 | 39.3455 | 0.0811 | 0.0424 | 0.0243 | 0.7588 |
| PCV-2G-Bill, Blade2 | 0.1356 | 39.0069 | 0.0870 | 0.0322 | 0.0361 | 0.5687 |
| PCV-2G-Bill, Blade2 | 0.1251 | 38.8536 | 0.3879 | 0.0182 | 0.0001 | 0.5238 |
| PCV-2G-Bill, Blade2 | 0.1396 | 39.0206 | 0.0870 | 0.0001 | 0.0001 | 0.5859 |
| PCV-2G-Bill, Blade2 | 0.1684 | 39.2540 | 0.1033 | 0.0154 | 0.0001 | 0.7013 |
| PCV-2G-Bill, Blade2 | 0.1490 | 39.1465 | 0.5596 | 0.0001 | 0.0151 | 0.6169 |
| PCV-2G-Bill, Blade2 | 0.1396 | 38.6563 | 0.4814 | 0.0126 | 0.0363 | 0.5867 |
| PCV-2G-Bill, Blade2 | 0.1508 | 39.7568 | 0.0295 | 0.0391 | 0.0223 | 0.6200 |
| PCV-2G-Bill, Blade2 | 0.1313 | 39.7570 | 0.0280 | 0.1357 | 0.0336 | 0.5400 |
| PCV-2G-Bill, Blade2 | 0.1895 | 39.3717 | 0.0796 | 0.0014 | 0.0456 | 0.7859 |
| PCV-2G-Bill, Blade2 | 0.1658 | 39.5631 | 0.0870 | 0.0895 | 0.0038 | 0.6845 |

| On-Shelf Bladed Calcite | | | | | | Mole % |
|---|---|---|---|---|---|---|
| Sample I.D. and Zone | Wt % Mg | Wt % Ca | Wt % Mn | Wt % Fe | Wt % Sr | MgCO3 |
| IS-90-47a, Bladed 1, 2 | 0.1722 | 39.3118 | 0.1703 | 0.0000 | 0.0129 | 0.7149 |
| IS-90-47a, Bladed 1, 2 | 0.4844 | 38.7925 | 0.0852 | 0.0001 | 0.0001 | 2.0135 |
| IS-90-47a, Bladed 1, 2 | 0.3828 | 39.2275 | 0.2230 | 0.0127 | 0.0065 | 1.5767 |
| IS-90-47a, Bladed 1, 2 | 0.2849 | 39.6506 | 0.0155 | 0.0001 | 0.0075 | 1.1704 |
| IS-90-47a, Bladed 1, 2 | 0.4506 | 38.2802 | 0.6884 | 0.0226 | 0.0158 | 1.8783 |
| IS-90-47a, Bladed 1, 2 | 0.2811 | 39.9826 | 0.1037 | 0.0127 | 0.0001 | 1.1437 |
| IS-90-47a, Bladed 1, 2 | 0.2807 | 39.4301 | 0.0155 | 0.0183 | 0.0001 | 1.1589 |
| IS-90-47a, Bladed 1, 2 | 0.1208 | 39.5867 | 0.0805 | 0.0014 | 0.0093 | 0.4994 |
| IS-90-47a, Bladed 1, 2 | 0.1403 | 39.4960 | 0.1316 | 0.0042 | 0.0001 | 0.5808 |
| IS-90-47a, Bladed 1, 2 | 0.1529 | 39.7483 | 0.1053 | 0.0001 | 0.0001 | 0.6293 |
| IS-90-47a, Bladed 1, 2 | 0.1786 | 39.6236 | 0.1192 | 0.0001 | 0.0001 | 0.7361 |
| IS-90-47a, Bladed 1, 2 | 0.2149 | 39.4817 | 0.3145 | 0.0240 | 0.0001 | 0.8840 |
| IS-90-47a, Bladed 1, 2 | 0.4863 | 39.6119 | 0.0666 | 0.0141 | 0.0001 | 1.9809 |
| IS-90-47a, Bladed 1, 2 | 0.2126 | 3.0982 | 0.2850 | 0.0085 | 0.0000 | 0.8837 |
| IS-90-47a, Bladed 1, 2 | 0.1856 | 39.7545 | 0.2338 | 0.0001 | 0.0148 | 0.7602 |
| IS-90-47a, Bladed 1, 2 | 0.1536 | 39.2947 | 0.1440 | 0.0000 | 0.0000 | 0.6384 |
| IS-90-47a, Bladed 1, 2 | 0.1737 | 39.9590 | 0.2167 | 0.0001 | 0.0001 | 0.7088 |
| IS-90-47a, Bladed 1, 2 | 0.1476 | 39.6596 | 0.0913 | 0.0014 | 0.0000 | 0.6084 |
| IS-90-47a, Bladed 1, 2 | 0.1613 | 40.0126 | 0.1301 | 0.0001 | 0.0001 | 0.6588 |
| IS-90-47a, Bladed 1, 2 | 0.1691 | 39.7807 | 0.1812 | 0.0071 | 0.0000 | 0.6936 |
| IS-90-47a, Bladed 1, 2 | 0.1786 | 39.0093 | 0.1193 | 0.0240 | 0.0192 | 0.7471 |
| IS-90-47a, Bladed 1, 2 | 0.1536 | 40.0738 | 0.1286 | 0.0000 | 0.0000 | 0.6263 |
| IS-90-47a, Bladed 1, 2 | 0.1666 | 39.3264 | 0.1501 | 0.0282 | 0.0005 | 0.6921 |
| IS-90-47a, Bladed 1, 2 | 0.1642 | 39.5761 | 0.1672 | 0.0198 | 0.0000 | 0.6771 |
| IS-90-47a, Bladed 1, 2 | 0.1466 | 39.0762 | 0.2861 | 0.0099 | 0.0001 | 0.6115 |
| IS-90-47a, Bladed 1, 2 | 0.1056 | 39.7205 | 0.1100 | 0.0001 | 0.0280 | 0.4359 |
| IS-90-47a, Bladed 1, 2 | 0.1909 | 39.5650 | 0.1580 | 0.0001 | 0.0001 | 0.7873 |
| IS-90-47a, Bladed 1, 2 | 0.0400 | 40.1179 | 0.0975 | 0.0001 | 0.0233 | 0.1640 |
| IS-90-47a, Bladed 1, 2 | 0.2774 | 39.6384 | 0.0279 | 0.0001 | 0.0124 | 1.1400 |
| IS-90-47a, Bladed 1, 2 | 0.3150 | 37.9645 | 1.1316 | 0.0113 | 0.0158 | 1.3213 |
| IS-90-47a, Bladed 1, 2 | 0.2041 | 39.0063 | 0.5092 | 0.0113 | 0.0067 | 0.8465 |
| IS-90-47a, Bladed 1, 2 | 0.4025 | 39.4186 | 0.0031 | 0.0000 | 0.0021 | 1.6553 |
| TH-89-95, Blade1 | 0.1260 | 40.1497 | 0.0502 | 0.0000 | 0.0023 | 0.5150 |
| TH-89-95, Blade1 | 0.2135 | 39.7558 | 0.0044 | 0.1638 | 0.0000 | 0.8749 |
| TH-89-95, Blade1 | 0.1230 | 40.1917 | 0.0546 | 0.0714 | 0.0118 | 0.5009 |

| Sample I.D. and Zone | Wt % Mg | Wt % Ca | Wt % Mn | Wt % Fe | Wt % Sr | Mole % |
|---|---|---|---|---|---|---|
| TH-89-95, Blade1 | 0.1071 | 40.2500 | 0.0192 | 0.1357 | 0.0277 | 0.4357 |
| TH-89-95, Blade1 | 0.2110 | 39.5941 | 0.0001 | 0.2452 | 0.0001 | 0.8678 |
| TH-89-95, Blade1 | 0.1048 | 39.9733 | 0.0502 | 0.0196 | 0.0151 | 0.4300 |
| TH-89-95, Blade1 | 0.1464 | 39.8167 | 0.0192 | 0.0924 | 0.0001 | 0.6011 |
| TH-89-95, Blade1 | 0.1055 | 40.0421 | 0.0251 | 0.1217 | 0.0001 | 0.4311 |
| TH-89-95, Blade1 | 0.1992 | 39.7141 | 0.0192 | 0.1483 | 0.0074 | 0.8183 |
| TH-89-95, Blade1 | 0.0801 | 39.8697 | 0.0177 | 0.1022 | 0.0461 | 0.3292 |
| TH-89-95, Blade1 | 0.2221 | 38.9740 | 0.0311 | 0.1908 | 0.0000 | 0.9271 |
| TH-89-95, Blade1 | 0.1702 | 39.8735 | 0.0546 | 0.1526 | 0.0001 | 0.6965 |
| TH-89-95, Blade1 | 0.1799 | 38.8841 | 0.0310 | 0.1710 | 0.0059 | 0.7536 |

| On-Shelf Blocky Clear Calcite | | | | | | Mole % |
|---|---|---|---|---|---|---|
| Sample I.D. and Zone | Wt % Mg | Wt % Ca | Wt % Mn | Wt %Fe | Wt %Sr | MgCO3 |
| IS-90-47a Blocky-clear 1 | 0.3012 | 39.2965 | 0.0001 | 0.0903 | 0.0001 | 1.2464 |
| IS-90-47a Blocky-clear 1 | 0.2965 | 39.3015 | 0.0526 | 0.1228 | 0.0044 | 1.2243 |
| IS-90-47a Blocky-clear 1 | 0.3011 | 39.3559 | 0.0325 | 0.1044 | 0.0186 | 1.2421 |
| IS-90-47a Blocky-clear 1 | 0.2303 | 39.7062 | 0.0341 | 0.0339 | 0.0091 | 0.9454 |
| IS-90-47a Blocky-clear 1 | 0.1444 | 39.9738 | 0.0418 | 0.0988 | 0.0001 | 0.5903 |
| IS-90-47a Blocky-clear 1 | 0.2411 | 39.9420 | 0.0217 | 0.1454 | 0.0000 | 0.9825 |
| IS-90-47a Blocky-clear 1 | 0.3103 | 40.0463 | 0.0000 | 0.1397 | 0.0000 | 1.2581 |
| IS-90-47a Blocky-clear 1 | 0.2987 | 39.4377 | 0.0279 | 0.1016 | 0.0052 | 1.2305 |
| IS-90-47a Blocky-clear 2 | 0.2569 | 39.5524 | 0.0696 | 0.0861 | 0.0205 | 1.0566 |
| IS-90-47a Blocky-clear 2 | 0.3212 | 39.4120 | 0.0388 | 0.0848 | 0.0265 | 1.3225 |
| IS-90-47a Blocky-clear 2 | 0.3095 | 39.1008 | 0.0263 | 0.0748 | 0.0003 | 1.2864 |
| IS-90-47a Blocky-clear 2 | 0.2981 | 38.9571 | 0.0635 | 0.0452 | 0.0075 | 1.2435 |
| IS-90-47a Blocky-clear 2 | 0.3227 | 39.7345 | 0.0201 | 0.0945 | 0.0383 | 1.3178 |
| IS-90-47a Blocky-clear 2 | 0.2909 | 39.9320 | 0.0001 | 0.1144 | 0.0031 | 1.1846 |
| IS-90-47a Blocky-clear 2 | 0.2990 | 39.6216 | 0.0001 | 0.0861 | 0.0174 | 1.2269 |
| IS-90-47a Blocky-clear 2 | 0.3236 | 39.4283 | 0.0108 | 0.0466 | 0.0091 | 1.3344 |
| IS-90-47a Blocky-clear 2 | 0.3709 | 39.1057 | 0.0573 | 0.0198 | 0.0135 | 1.5366 |
| IS-90-47a Blocky-clear 2 | 0.2827 | 39.2744 | 0.0093 | 0.0480 | 0.0150 | 1.1710 |
| IS-90-47a Blocky-clear 2 | 0.2125 | 39.2450 | 0.0279 | 0.1285 | 0.0192 | 0.8825 |
| IS-90-47a Blocky-clear 2 | 0.2414 | 39.2279 | 0.0666 | 0.1623 | 0.0001 | 1.0003 |
| IS-90-47a Blocky-clear 2 | 0.1828 | 39.2424 | 0.0248 | 0.1185 | 0.0001 | 0.7607 |
| IS-90-47a Blocky-clear 2 | 0.2066 | 39.5656 | 0.0449 | 0.1087 | 0.0001 | 0.8510 |
| IS-90-47a Blocky-clear 2 | 0.1779 | 39.4356 | 0.0790 | 0.1200 | 0.0073 | 0.7361 |
| IS-90-47a Blocky-clear 2 | 0.2141 | 39.3314 | 0.0511 | 0.1679 | 0.0023 | 0.8857 |
| IS-90-47a Blocky-clear 2 | 0.2333 | 39.7628 | 0.0077 | 0.1609 | 0.0001 | 0.9554 |
| IS-90-47a Blocky-clear 2 | 0.2680 | 39.3890 | 0.0495 | 0.0988 | 0.0001 | 1.1060 |
| IS-90-47a Blocky-clear 3 | 0.2095 | 39.8023 | 0.0387 | 0.1256 | 0.0101 | 0.8574 |
| IS-90-47a Blocky-clear 3 | 0.3108 | 39.6490 | 0.0001 | 0.0353 | 0.0001 | 1.2752 |
| IS-90-47a Blocky-clear 3 | 0.2044 | 39.8874 | 0.0279 | 0.0127 | 0.0228 | 0.8375 |
| IS-90-47a Blocky-clear 3 | 0.2573 | 39.7539 | 0.0449 | 0.0001 | 0.0001 | 1.0548 |
| IS-90-47a Blocky-clear 3 | 0.2407 | 39.7505 | 0.0001 | 0.0071 | 0.0010 | 0.9889 |
| IS-90-47a Blocky-clear 3 | 0.1640 | 39.8303 | 0.0248 | 0.0001 | 0.0039 | 0.8063 |
| IS-90-47a Blocky-clear 3 | 0.1293 | 38.1367 | 1.4043 | 0.0846 | 0.0000 | 0.5408 |
| IS-90-47a Blocky-clear 3 | 0.3614 | 39.8356 | 0.0371 | 0.0001 | 0.0001 | 1.4733 |
| IS-90-47a Blocky-clear 3 | 0.1879 | 39.6088 | 0.1440 | 0.0000 | 0.0000 | 0.7737 |

| Sample I.D. and Zone | Wt % Mg | Wt % Ca | Wt % Mn | Wt %Fe | Wt %Sr | MgCO3 |
|---|---|---|---|---|---|---|
| IS-90-47a Blocky-clear 3 | 0.2714 | 38.9866 | 0.0526 | 0.0790 | 0.0093 | 1.1317 |
| IS-90-47a Blocky-clear 3 | 0.3044 | 39.5267 | 0.0310 | 0.1101 | 0.0254 | 1.2506 |
| IS-90-47a Blocky-clear 3 | 0.3236 | 39.6403 | 0.0449 | 0.1651 | 0.0176 | 1.3224 |
| IS-90-47a Blocky-clear 3 | 0.2531 | 39.3095 | 0.0001 | 0.1214 | 0.0001 | 1.0486 |
| TH-89-180, Blocky-clear 1 | 0.4497 | 38.9386 | 0.0109 | 0.0550 | 0.0327 | 1.8655 |
| TH-89-180, Blocky-clear 1 | 0.1503 | 38.9887 | 0.0062 | 0.0318 | 0.0639 | 0.6310 |
| TH-89-180, Blocky-clear 1 | 0.4314 | 38.8461 | 0.0670 | 0.0304 | 0.0016 | 1.7954 |
| TH-89-180, Blocky-clear 1 | 0.4919 | 38.7097 | 0.0312 | 0.0651 | 0.0253 | 2.0484 |
| TH-89-180, Blocky-clear 1 | 0.3363 | 39.2239 | 0.0140 | 0.1244 | 0.0276 | 1.3907 |
| TH-89-180, Blocky-clear 1 | 0.3969 | 39.6052 | 0.0592 | 0.0578 | 0.0000 | 1.6223 |
| TH-89-180, Blocky-clear 1 | 0.3348 | 38.9475 | 0.0109 | 0.0535 | 0.0305 | 1.3951 |
| TH-89-180, Blocky-clear 1 | 0.3753 | 39.1239 | 0.0047 | 0.0318 | 0.0122 | 1.5559 |
| TH-89-180, Blocky-clear 1 | 0.4450 | 38.4937 | 0.0389 | 0.0940 | 0.0183 | 1.8657 |
| TH-89-180, Blocky-clear 1 | 0.2766 | 39.1724 | 0.0359 | 0.0188 | 0.0309 | 1.1490 |
| TH-89-180, Blocky-clear 2 | 0.3653 | 39.4122 | 0.0545 | 0.0723 | 0.0167 | 1.5013 |
| TH-89-180, Blocky-clear 2 | 0.4642 | 39.1012 | 0.0171 | 0.0637 | 0.0001 | 1.9176 |
| TH-89-180, Blocky-clear 2 | 0.1522 | 39.5038 | 0.0062 | 0.0723 | 0.0529 | 0.6295 |
| TH-89-180, Blocky-clear 2 | 0.2468 | 39.6662 | 0.0436 | 0.0607 | 0.0412 | 1.0133 |
| TH-89-180, Blocky-clear 2 | 0.3404 | 39.9456 | 0.0265 | 0.0564 | 0.0178 | 1.3836 |
| TH-89-180, Blocky-clear 2 | 0.4190 | 39.2644 | 0.0592 | 0.0911 | 0.0001 | 1.7237 |
| TH-89-180, Blocky-clear 2 | 0.4167 | 39.1078 | 0.0856 | 0.0809 | 0.0231 | 1.7213 |
| TH-89-180, Blocky-clear 2 | 0.3302 | 39.4536 | 0.0561 | 0.0419 | 0.0205 | 1.3581 |
| TH-89-180, Blocky-clear 2 | 0.2054 | 39.5679 | 0.0001 | 0.0679 | 0.0380 | 0.8472 |
| TH-89-180, Blocky-clear 2 | 0.1817 | 39.9905 | 0.0078 | 0.0592 | 0.0396 | 0.7426 |
| TH-89-180, Blocky-clear 2 | 0.2128 | 39.5827 | 0.0171 | 0.0564 | 0.0489 | 0.8773 |
| TH-89-180, Blocky-clear 2 | 0.4514 | 39.0725 | 0.0545 | 0.1258 | 0.0001 | 1.8631 |
| TH-89-180, Blocky-clear 2 | 0.2399 | 39.2643 | 0.0001 | 0.0737 | 0.0531 | 0.9956 |
| TH-89-180, Blocky-clear 2 | 0.2417 | 39.2364 | 0.0156 | 0.0665 | 0.0375 | 1.0035 |
| TH-89-180, Blocky-clear 2 | 0.2086 | 39.6710 | 0.0342 | 0.0535 | 0.0419 | 0.8576 |
| TH-89-180, Blocky-clear 2 | 0.3765 | 39.1207 | 0.0592 | 0.0795 | 0.0001 | 1.5581 |
| TH-89-180, Blocky-clear 2 | 0.1593 | 39.9758 | 0.0140 | 0.0217 | 0.0433 | 0.6520 |
| TH-89-180, Blocky-clear 2 | 0.4017 | 39.5309 | 0.0327 | 0.0665 | 0.0037 | 1.6454 |
| TH-89-180, Blocky-clear 2 | 0.2669 | 38.9725 | 0.0062 | 0.0361 | 0.0473 | 1.1156 |
| TH-89-180, Blocky-clear 2 | 0.4561 | 39.6109 | 0.0343 | 0.0405 | 0.0069 | 1.8601 |
| IS-90-46, Blocky-clear 1 | 0.0626 | 40.2497 | 0.0001 | 0.0255 | 0.0396 | 0.2552 |
| IS-90-46, Blocky-clear 1 | 0.1369 | 39.9270 | 0.0734 | 0.1036 | 0.0149 | 0.5600 |

| Sample I.D. and Zone | Wt % Mg | Wt % Ca | Wt % Mn | Wt %Fe | Wt %Sr | MgCO3 |
|---|---|---|---|---|---|---|
| IS-90-46, Blocky-clear 1 | 0.0913 | 40.3503 | 0.0001 | 0.0397 | 0.0154 | 0.3714 |
| IS-90-46, Blocky-clear 2 | 0.1174 | 39.8622 | 0.1024 | 0.0001 | 0.0094 | 0.4828 |
| IS-90-46, Blocky-clear 2 | 0.1045 | 39.9089 | 0.0183 | 0.0440 | 0.0227 | 0.4296 |
| IS-90-46, Blocky-clear 2 | 0.2457 | 39.4779 | 0.0413 | 0.0341 | 0.0368 | 1.0140 |
| IS-90-46, Blocky-clear 3 | 0.1609 | 40.1649 | 0.1253 | 0.0001 | 0.0120 | 0.6540 |
| IS-90-46, Blocky-clear 3 | 0.3111 | 39.1646 | 0.0550 | 0.1021 | 0.0182 | 1.2888 |
| IS-90-46, Blocky-clear 3 | 0.1949 | 40.1885 | 0.0001 | 0.0978 | 0.0846 | 0.7916 |
| IS-90-46, Blocky-clear 4 | 0.1812 | 39.7850 | 0.0810 | 0.0199 | 0.0001 | 0.7439 |
| IS-90-46, Blocky-clear 4 | 0.1818 | 40.1413 | 0.2261 | 0.0156 | 0.0001 | 0.7379 |
| IS-90-46, Blocky-clear 4 | 0.3046 | 40.0156 | 0.0397 | 0.1305 | 0.0001 | 1.2364 |

| Shelf-Edge Overgrowth Calcite | | | | | | Mole % |
|---|---|---|---|---|---|---|
| Sample I.D. and Zone | Wt % Mg | Wt % Ca | Wt % Mn | Wt % Fe | Wt % Sr | MgCO3 |
| RHB-6B-T FeOvg 1,2,3 | 0.3556 | 39.8935 | 0.0001 | 0.1278 | 0.0073 | 1.4449 |
| RHB-6B-T FeOvg 1,2,3 | 0.2157 | 39.9215 | 0.0135 | 0.1392 | 0.0377 | 0.8802 |
| RHB-6B-T FeOvg 1,2,3 | 0.3862 | 38.8439 | 0.0015 | 0.2213 | 0.0073 | 1.6062 |
| RHB-6B-T FeOvg 1,2,3 | 0.3823 | 39.5160 | 0.0314 | 0.1533 | 0.0000 | 1.5647 |
| RHB-6B-T FeOvg 1,2,3 | 0.1616 | 39.7967 | 0.0209 | 0.1036 | 0.0411 | 0.6635 |
| RHB-6B-T FeOvg 1,2,3 | 0.2382 | 39.9549 | 0.0105 | 0.1178 | 0.0338 | 0.9708 |
| RHB-6B-T FeOvg 1,2,3 | 0.3384 | 39.3807 | 0.0389 | 0.1520 | 0.0096 | 1.3922 |
| RHB-6B-T FeOvg 1,2,3 | 0.2803 | 39.6523 | 0.0045 | 0.0965 | 0.0001 | 1.1499 |
| RHB-6B-T FeOvg 1,2,3 | 0.3001 | 40.0086 | 0.0135 | 0.1534 | 0.0001 | 1.2179 |
| RHB-6B-T FeOvg 1,2,3 | 0.3138 | 39.8845 | 0.0001 | 0.1477 | 0.0001 | 1.2773 |
| RHB-6B-T FeOvg 1,2,3 | 0.3426 | 39.6702 | 0.0464 | 0.1107 | 0.0104 | 1.3998 |
| RHB-6B-T FeOvg 1,2,3 | 0.1119 | 39.7840 | 0.0195 | 0.1534 | 0.0000 | 0.4608 |
| RHB-6B-T FeOvg 1,2,3 | 0.1482 | 39.5209 | 0.0390 | 0.1791 | 0.0000 | 0.6127 |
| RHB-6B-T FeOvg 1,2,3 | 0.1321 | 39.3153 | 0.0345 | 0.1678 | 0.0044 | 0.5482 |
| RHB-6B-T FeOvg 1,2,3 | 0.1375 | 39.7568 | 0.0000 | 0.0284 | 0.0060 | 0.5663 |
| RHB-6B-T FeOvg 1,2,3 | 0.1072 | 40.0229 | 0.0180 | 0.1504 | 0.0444 | 0.4380 |
| RHB-6B-T FeOvg 1,2,3 | 0.1983 | 39.4874 | 0.0255 | 0.0000 | 0.0331 | 0.8212 |
| RHB-6B-T FeOvg 1,2,3 | 0.0852 | 40.0049 | 0.0000 | 0.0441 | 0.0000 | 0.3499 |
| RHB-6B-T FeOvg 1.1 | 1.8972 | 36.6803 | 0.0389 | 0.5513 | 0.0139 | 7.7742 |
| RHB-6B-T FeOvg 1.1 | 1.5751 | 37.4382 | 0.0568 | 0.7078 | 0.0194 | 6.3979 |
| RHB-3RA2 FeOvg 1 | 0.1371 | 39.7399 | 0.0224 | 0.1077 | 0.0106 | 0.5644 |
| RHB-3RA2 FeOvg 1 | 0.1543 | 39.8539 | 0.0359 | 0.0822 | 0.0057 | 0.6331 |
| RHB-3RA2 FeOvg 1 | 0.1960 | 39.0154 | 0.0478 | 0.1489 | 0.0001 | 0.8185 |
| RHB-3RA2 FeOvg 1 | 0.1861 | 39.7116 | 0.0404 | 0.3076 | 0.0104 | 0.7621 |
| RHB-3RA2 FeOvg 1 | 0.1036 | 39.5900 | 0.0463 | 0.2168 | 0.0001 | 0.4275 |
| RHB-3RA2 FeOvg 1 | 0.1328 | 39.9938 | 0.0478 | 0.1730 | 0.0145 | 0.5424 |
| RHB-3RA2 FeOvg 1 | 0.3727 | 38.8460 | 0.0449 | 0.2387 | 0.0000 | 1.5495 |
| RHB-3RA2 FeOvg 1 | 0.1190 | 39.1232 | 0.0449 | 0.2885 | 0.0000 | 0.4959 |
| RHB-3RA2 FeOvg 1 | 0.1522 | 39.4016 | 0.0509 | 0.1761 | 0.0039 | 0.6310 |
| RHB-3RA2 FeOvg 1 | 0.1930 | 39.7204 | 0.0479 | 0.1676 | 0.0000 | 0.7917 |
| RHB-3RA2 FeOvg 1 | 0.2313 | 39.6532 | 0.0435 | 0.2189 | 0.0102 | 0.9481 |
| RHB-3RA2 FeOvg 1 | 0.1350 | 39.7495 | 0.0420 | 0.1691 | 0.0107 | 0.5551 |
| RHB-3RA2 FeOvg 1 | 0.2213 | 39.9545 | 0.0734 | 0.2883 | 0.0349 | 0.8985 |
| RHB-3RA2 FeOvg 1 | 0.1739 | 39.2464 | 0.0719 | 0.2045 | 0.0001 | 0.7220 |
| RHB-3RA2 FeOvg 1 | 0.2336 | 38.7317 | 0.0434 | 0.2132 | 0.0359 | 0.9797 |

| Shelf-Edge Ferroan Blocky White Calcite | | | | | | Mole % |
|---|---|---|---|---|---|---|
| Sample I.D. and Zone | Wt % Mg | Wt % Ca | Wt % Mn | Wt % Fe | Wt % Sr | MgCO3 |
| PVC-2J, Blocky-white to Csc, Fe | 0.2755 | 39.3264 | 0.0464 | 0.0423 | 0.0001 | 1.1396 |
| PVC-2J, Blocky-white to Csc, Fe | 0.2681 | 39.8277 | 0.0387 | 0.1284 | 0.0238 | 1.0945 |
| PVC-2J, Blocky-white to Csc, Fe | 0.1199 | 39.8550 | 0.0712 | 0.0607 | 0.0028 | 0.4921 |
| PVC-2J, Blocky-white to Csc, Fe | 0.3208 | 39.4019 | 0.0372 | 0.0353 | 0.0001 | 1.3233 |
| PVC-2J, Blocky-white to Csc, Fe | 0.3717 | 39.4358 | 0.0341 | 0.0212 | 0.0001 | 1.5283 |
| PVC-2J, Blocky-white to Csc, Fe | 0.2184 | 39.2923 | 0.0124 | 0.1072 | 0.0001 | 0.9060 |
| PVC-2J, Blocky-white to Csc, Fe | 0.1787 | 39.4621 | 0.0836 | 0.1594 | 0.0083 | 0.7385 |
| PVC-2J, Blocky-white to Csc, Fe | 0.2718 | 39.4425 | 0.0387 | 0.0536 | 0.0003 | 1.1221 |
| PVC-2J, Blocky-white to Csc, Fe | 0.3112 | 39.4583 | 0.0651 | 0.0367 | 0.0001 | 1.2809 |
| PVC-2J, Blocky-white to Csc, Fe | 0.3467 | 38.9136 | 0.0000 | 0.0396 | 0.0000 | 1.4460 |
| PVC-2J, Blocky-white to Csc, Fe | 0.1972 | 39.4320 | 0.0325 | 0.0451 | 0.0001 | 0.8172 |
| PVC-2J, Blocky-white to Csc, Fe | 0.2785 | 39.0927 | 0.0403 | 0.0551 | 0.0000 | 1.1592 |
| PVC-2J, Blocky-white to Csc, Fe | 0.3206 | 39.9171 | 0.0263 | 0.0480 | 0.0001 | 1.3053 |
| PVC-2J, Blocky-white to Csc, Fe | 0.3155 | 39.9243 | 0.0093 | 0.0000 | 0.0080 | 1.2856 |
| PVC-2J, Blocky-white to Csc, Fe | 0.2449 | 40.1156 | 0.0001 | 0.0522 | 0.0001 | 0.9954 |
| PVC-2J, Blocky-white to Csc, Fe | 0.1219 | 39.8747 | 0.0263 | 0.0254 | 0.0001 | 0.5008 |
| PVC-2J, Blocky-white to Csc, Fe | 0.3156 | 39.4280 | 0.0480 | 0.0325 | 0.0000 | 1.3011 |
| PVC-2J, Blocky-white to Csc, Fe | 0.3002 | 39.3374 | 0.0217 | 0.0494 | 0.0001 | 1.2409 |
| PVC-2J, Blocky-white to Csc, Fe | 0.3040 | 39.2099 | 0.0589 | 0.0325 | 0.0192 | 1.2594 |
| PVC-2J, Blocky-white to Csc, Fe | 0.3040 | 39.5854 | 0.0263 | 0.0551 | 0.0001 | 1.2482 |
| PVC-2J, Blocky-white to Csc, Fe | 0.2942 | 39.6000 | 0.0201 | 0.0762 | 0.0000 | 1.2077 |
| PVC-2J, Blocky-white to Csc, Fe | 0.2983 | 39.5549 | 0.0062 | 0.0085 | 0.0001 | 1.2284 |
| PVC-2J, Blocky-white to Csc, Fe | 0.2832 | 39.4035 | 0.0341 | 0.0396 | 0.0000 | 1.1694 |
| PVC-2J, Blocky-white to Csc, Fe | 0.2803 | 39.5441 | 0.0201 | 0.0932 | 0.0280 | 1.1524 |
| PVC-2J, Blocky-white to Csc, Fe | 0.2755 | 39.2528 | 0.0000 | 0.0607 | 0.0034 | 1.1434 |
| PVC-2J, Blocky-white to Csc, Fe | 0.3013 | 39.6299 | 0.0357 | 0.0325 | 0.0106 | 1.2364 |
| PVC-2J, Blocky-white to Csc, Fe | 0.2659 | 39.9372 | 0.0077 | 0.0254 | 0.0000 | 1.0851 |
| PVC-2J, Blocky-white to Csc, Fe | 0.2626 | 39.5969 | 0.0263 | 0.0466 | 0.0044 | 1.0806 |
| PVC-2J, Blocky-white to Csc, Fe | 0.2619 | 39.8477 | 0.0093 | 0.0000 | 0.0062 | 1.0716 |
| PVC-2J, Blocky-white to Csc, Fe | 0.2516 | 39.8828 | 0.0248 | 0.0141 | 0.0329 | 1.0278 |
| PVC-2J, Blocky-white to Csc, Fe | 0.2679 | 39.6011 | 0.0139 | 0.0409 | 0.0000 | 1.1020 |
| PVC-2J, Blocky-white to Csc, Fe | 0.3104 | 39.5714 | 0.0093 | 0.0508 | 0.0001 | 1.2760 |
| PVC-2J, Blocky-white to Csc, Fe | 0.2671 | 39.5851 | 0.0263 | 0.0000 | 0.0000 | 1.0995 |
| PVC-2J, Blocky-white to Csc, Fe | 0.2597 | 39.6027 | 0.0001 | 0.0297 | 0.0001 | 1.0696 |
| PVC-2J, Blocky-white to Csc, Fe | 0.3540 | 39.3177 | 0.0310 | 0.1342 | 0.0000 | 1.4585 |

| Sample I.D. and Zone | Wt % Mg | Wt % Ca | Wt % Mn | Wt % Fe | Wt % Sr | MgCO3 |
|---|---|---|---|---|---|---|
| PVC-2J, Blocky-white to Csc, Fe | 0.1949 | 39.8489 | 0.1162 | 0.1652 | 0.0005 | 0.7964 |
| PVC-2J, Blocky-white to Csc, Fe | 0.2279 | 39.0643 | 0.0666 | 0.1243 | 0.0001 | 0.9492 |
| RHB-2B-C, Blocky-white, Fe 1, 2 | 0.1466 | 39.4282 | 0.0869 | 0.0288 | 0.0180 | 0.6080 |
| RHB-2B-C, Blocky-white, Fe 1, 2 | 0.2384 | 39.2185 | 0.0326 | 0.0922 | 0.0063 | 0.9905 |
| RHB-2B-C, Blocky-white, Fe 1, 2 | 0.2273 | 39.8729 | 0.0543 | 0.1481 | 0.0095 | 0.9276 |
| RHB-2B-C, Blocky-white, Fe 1, 2 | 0.1645 | 39.0571 | 0.1195 | 0.0144 | 0.0093 | 0.6878 |
| RHB-2B-C, Blocky-white, Fe 1, 2 | 0.2141 | 38.9145 | 0.0202 | 0.3066 | 0.0164 | 0.8932 |
| RHB-2B-C, Blocky-white, Fe 1, 2 | 0.4147 | 38.6410 | 0.0450 | 0.2232 | 0.0127 | 1.7304 |
| RHB-2B-C, Blocky-white, Fe 1, 2 | 0.1738 | 39.1015 | 0.1132 | 0.0144 | 0.0001 | 0.7254 |
| RHB-2B-C, Blocky-white, Fe 1, 2 | 0.1243 | 39.6663 | 0.0527 | 0.0001 | 0.0064 | 0.5141 |
| RHB-2B-C, Blocky-white, Fe 1, 2 | 0.2264 | 39.2405 | 0.1210 | 0.1239 | 0.0001 | 0.9382 |
| RHB-2B-C, Blocky-white, Fe 1, 2 | 0.2079 | 39.0031 | 0.1490 | 0.0259 | 0.0146 | 0.8686 |
| RHB-2B-C, Blocky-white, Fe 1, 2 | 0.1772 | 39.7191 | 0.0465 | 0.0158 | 0.0154 | 0.7291 |
| RHB-2B-C, Blocky-white, Fe 1, 2 | 0.1911 | 39.2304 | 0.0853 | 0.0360 | 0.0001 | 0.7957 |
| RHB-2B-C, Blocky-white, Fe 1, 2 | 0.1822 | 39.1437 | 0.0001 | 0.1440 | 0.0101 | 0.7601 |
| RHB-2B-C, Blocky-white, Fe 1, 2 | 0.1807 | 39.7048 | 0.0001 | 0.0144 | 0.0001 | 0.7442 |
| RHB-2B-C, Blocky-white, Fe 1, 2 | 0.1583 | 39.8291 | 0.1752 | 0.0259 | 0.0019 | 0.6485 |
| RHB-2B-C, Blocky-white, Fe 1, 2 | 0.2616 | 39.0690 | 0.0388 | 0.1670 | 0.0106 | 1.0876 |
| RHB-2B-C, Blocky-white, Fe 1, 2 | 0.2283 | 39.3078 | 0.0496 | 0.1296 | 0.0148 | 0.9447 |
| RHB-2B-C, Blocky-white, Fe 1, 2 | 0.1548 | 39.5657 | 0.1473 | 0.0201 | 0.0127 | 0.6384 |
| RHB-2B-C, Blocky-white, Fe 1, 2 | 0.2392 | 39.3517 | 0.0155 | 0.0000 | 0.0159 | 0.9914 |

| On-Shelf Ferroan Blocky White Calcite | | | | | | Mole % |
|---|---|---|---|---|---|---|
| Sample I.D. and Zone | Wt % Mg | Wt % Ca | Wt % Mn | Wt % Fe | Wt % Sr | MgCO3 |
| TH-89-212A, Blocky-white, Fe 1 | 0.2121 | 38.9363 | 0.0605 | 0.1123 | 0.0511 | 0.8865 |
| TH-89-212A, Blocky-white, Fe 1 | 0.1696 | 39.0370 | 0.0465 | 0.0763 | 0.0595 | 0.7094 |
| TH-89-212A, Blocky-white, Fe 1 | 0.2527 | 38.9159 | 0.0450 | 0.1268 | 0.0001 | 1.0557 |
| TH-89-212A, Blocky-white, Fe 1 | 0.3255 | 38.6359 | 0.0311 | 0.1729 | 0.0001 | 1.3650 |
| TH-89-212A, Blocky-white, Fe 1 | 0.3289 | 38.8969 | 0.0001 | 0.1874 | 0.0193 | 1.3703 |
| TH-89-212A, Blocky-white, Fe 1 | 0.1278 | 39.0248 | 0.0001 | 0.0691 | 0.9310 | 0.5362 |
| TH-89-212A, Blocky-white, Fe 1 | 0.3321 | 39.1030 | 0.0435 | 0.1311 | 0.0074 | 1.3766 |
| TH-89-212A, Blocky-white, Fe 1 | 0.3373 | 38.6159 | 0.0714 | 0.1454 | 0.0183 | 1.4139 |
| TH-89-212A, Blocky-white, Fe 1 | 0.3326 | 38.7699 | 0.0419 | 0.1196 | 0.0146 | 1.3647 |
| TH-89-212A, Blocky-white, Fe 1 | 0.3638 | 39.1246 | 0.0217 | 0.1931 | 0.0077 | 1.5041 |
| TH-89-212A, Blocky-white, Fe 1 | 0.2499 | 38.7719 | 0.0109 | 0.1210 | 0.0230 | 1.0493 |
| TH-89-212A, Blocky-white, Fe 1 | 0.2612 | 39.0608 | 0.0481 | 0.1296 | 0.0001 | 1.0873 |
| TH-89-212A, Blocky-white, Fe 1 | 0.3000 | 38.9736 | 0.0279 | 0.1585 | 0.0148 | 1.2483 |
| TH-89-212A, Blocky-white, Fe 2 | 0.3752 | 39.2530 | 0.0450 | 0.1686 | 0.0001 | 1.5450 |
| TH-89-212A, Blocky-white, Fe 2 | 0.3253 | 38.6766 | 0.0031 | 0.1470 | 0.0164 | 1.3634 |
| TH-89-212A, Blocky-white, Fe 2 | 0.3323 | 38.6762 | 0.0574 | 0.1627 | 0.0273 | 1.3913 |
| TH-89-212A, Blocky-white, Fe 2 | 0.3081 | 38.7593 | 0.0388 | 0.2004 | 0.0379 | 1.2868 |
| TH-89-212A, Blocky-white, Fe 2 | 0.3340 | 39.1465 | 0.0512 | 0.1845 | 0.0050 | 1.3807 |
| TH-89-212A, Blocky-white, Fe 2 | 0.3392 | 38.9515 | 0.0419 | 0.1917 | 0.0001 | 1.4089 |
| TH-89-212A, Blocky-white, Fe 2 | 0.3521 | 38.7852 | 0.0047 | 0.1931 | 0.0034 | 1.4690 |
| TH-89-212A, Blocky-white, Fe 2 | 0.1604 | 39.1414 | 0.0466 | 0.1355 | 0.0302 | 0.6689 |
| TH-89-212A, Blocky-white, Fe 2 | 0.3325 | 39.3442 | 0.0466 | 0.0981 | 0.0162 | 1.3701 |
| TH-89-212A, Blocky-white, Fe 2 | 0.3285 | 39.0342 | 0.0496 | 0.1368 | 0.0294 | 1.3642 |
| TH-89-212A, Blocky-white, Fe 2 | 0.3251 | 39.1651 | 0.0233 | 0.1627 | 0.0177 | 1.3458 |
| TH-89-212A, Blocky-white, Fe 2 | 0.3211 | 39.1044 | 0.0450 | 0.1729 | 0.0159 | 1.3306 |
| TH-89-212A, Blocky-white, Fe 2 | 0.3504 | 39.1779 | 0.0310 | 0.1412 | 0.0223 | 1.4479 |
| TH-89-212A, Blocky-white, Fe 2 | 0.3435 | 38.8962 | 0.0031 | 0.1932 | 0.0188 | 1.4292 |
| TH-89-212A, Blocky-white, Fe 2 | 0.3516 | 38.5894 | 0.0248 | 0.2159 | 0.0167 | 1.4737 |
| TH-89-212A, Blocky-white, Fe 2 | 0.3343 | 39.1171 | 0.0062 | 0.1629 | 0.0024 | 1.3846 |
| TH-89-212A, Blocky-white, Fe 2 | 0.3042 | 39.5137 | 0.0481 | 0.1800 | 0.0058 | 1.2482 |
| TH-89-212A, Blocky-white, Fe 2 | 0.3049 | 38.9256 | 0.0606 | 0.1269 | 0.0109 | 1.2711 |

| Shelf-Edge Vein Calcite | | | | | | Mole % |
|---|---|---|---|---|---|---|
| Sample I.D. and Zone | Wt % Mg | Wt % Ca | Wt % Mn | Wt % Fe | Wt % Sr | MgCO3 |
| RHB-2H vein edge | 0.3382 | 38.5951 | 0.0670 | 0.3860 | 0.0093 | 1.4122 |
| RHB-2H vein edge | 0.1800 | 39.4966 | 0.0732 | 0.3240 | 0.0157 | 0.7405 |
| RHB-2H vein edge | 0.2981 | 39.2446 | 0.0499 | 0.3211 | 0.0077 | 1.2287 |
| RHB-2H vein edge | 0.1390 | 39.3740 | 0.0421 | 0.2025 | 0.0157 | 0.5754 |
| RHB-2H vein edge | 0.2115 | 39.4918 | 0.0638 | 0.3686 | 0.0000 | 0.8682 |
| RHB-2H vein edge | 0.1334 | 39.2225 | 0.0733 | 0.1606 | 0.0165 | 0.5551 |
| RHB-2H vein edge | 0.2486 | 39.0643 | 0.0343 | 0.3497 | 0.0001 | 1.0311 |
| RHB-2H vein edge | 0.2787 | 39.0502 | 0.0560 | 0.3799 | 0.0058 | 1.1544 |
| RHB-2H Vein center | 0.1367 | 39.5823 | 0.0093 | 0.2225 | 0.0106 | 0.5643 |
| RHB-2H Vein center | 0.1716 | 39.2497 | 0.0249 | 0.1344 | 0.0001 | 0.7140 |
| RHB-2H Vein center | 0.1568 | 39.3040 | 0.0312 | 0.2588 | 0.0061 | 0.6496 |
| RHB-2H Vein center | 0.1807 | 38.9045 | 0.0203 | 0.2877 | 0.0322 | 0.7551 |
| RHB-2H Vein center | 0.2016 | 39.1583 | 0.0389 | 0.2891 | 0.0260 | 0.8366 |
| RHB-2H Vein center | 0.1876 | 39.2166 | 0.0421 | 0.2921 | 0.0001 | 0.7775 |

| On-Shelf Ferroan Coarse Sparry Calcite | | | | | | Mole % |
|---|---|---|---|---|---|---|
| Sample I.D. and Zone | Wt % Mg | Wt % Ca | Wt % Mn | Wt %Fe | Wt %Sr | MgCO3 |
| TH-89-95B, Csc-Spar 1 | 0.1509 | 39.4079 | 0.0222 | 0.0996 | 0.0223 | 0.6260 |
| TH-89-95B, Csc-Spar 1 | 0.1357 | 39.5725 | 0.0222 | 0.0729 | 0.0272 | 0.5610 |
| TH-89-95B, Csc-Spar 1 | 0.1132 | 39.4393 | 0.0281 | 0.1024 | 0.0308 | 0.4698 |
| TH-89-95B, Csc-Spar 1 | 0.1350 | 39.7589 | 0.0163 | 0.0940 | 0.0003 | 0.5560 |
| TH-89-95B, Csc-Spar 1 | 0.1552 | 39.3375 | 0.0001 | 0.0954 | 0.0001 | 0.6455 |
| TH-89-95B, Csc-Spar 1 | 0.0725 | 39.7828 | 0.0340 | 0.0421 | 0.0001 | 0.2995 |
| TH-89-95B, Csc-Spar 1 | 0.1296 | 39.7462 | 0.0178 | 0.0295 | 0.0001 | 0.5344 |
| TH-89-95B, Csc-Spar 1 | 0.1913 | 39.5428 | 0.0059 | 0.1178 | 0.0001 | 0.7895 |
| TH-89-95B, Csc-Spar 1 | 0.1757 | 39.4240 | 0.0222 | 0.0842 | 0.0001 | 0.7281 |
| TH-89-95B, Csc-Spar 1 | 0.2420 | 39.2850 | 0.0001 | 0.1741 | 0.0001 | 1.0022 |
| TH-89-95B, Csc-Spar 1 | 0.1514 | 39.8792 | 0.0843 | 0.0828 | 0.0001 | 0.6207 |
| TH-89-95B, Csc-Spar 1 | 0.1803 | 39.4661 | 0.0030 | 0.0744 | 0.0275 | 0.7464 |
| TH-89-95B, Csc-Spar 1 | 0.2354 | 39.1040 | 0.0163 | 0.1362 | 0.0001 | 0.9798 |
| TH-89-95B, Csc-Spar 1 | 0.3252 | 36.1670 | 0.0237 | 0.4334 | 0.0000 | 1.4480 |
| TH-89-95B, Csc-Spar 1 | 0.2107 | .38.9161 | 0.0118 | 0.0842 | 0.0001 | 0.8839 |
| TH-89-95B, Csc-Spar 1 | 0.1462 | 39.1176 | 0.0178 | 0.0632 | 0.0000 | 0.6121 |
| TH-89-95B, Csc-Spar 1 | 0.1617 | 39.2671 | 0.0266 | 0.1052 | 0.0001 | 0.6724 |
| TH-89-95B, Csc-Spar 1 | 0.1450 | 39.7363 | 0.0370 | 0.0983 | 0.0149 | 0.5961 |
| TH-89-95B, Csc-Spar 1 | 0.1415 | 39.1778 | 0.0001 | 0.0926 | 0.0001 | 0.5907 |
| TH-89-95B, Csc-Spar 1 | 0.1103 | 39.4625 | 0.0001 | 0.1081 | 0.0139 | 0.4579 |
| TH-89-95B, Csc-Spar 1 | 0.1331 | 39.4380 | 0.0311 | 0.0098 | 0.0001 | 0.5529 |
| TH-89-95B, Csc-Spar 1 | 0.0942 | 39.7630 | 0.0370 | 0.1221 | 0.0023 | 0.3888 |
| TH-89-95B, Csc-Spar 1 | 0.0998 | 39.4284 | 0.0252 | 0.0786 | 0.0087 | 0.4142 |
| TH-89-95B, Csc-Spar 1 | 0.1548 | 39.4182 | 0.2337 | 0.0954 | 0.0121 | 0.6414 |
| TH-89-95B, Csc-Spar 1 | 0.0735 | 39.3305 | 0.0399 | 0.0575 | 0.0001 | 0.3064 |
| TH-89-95B, Csc-Spar 1 | 0.1617 | 39.1346 | 0.0001 | 0.0589 | 0.0001 | 0.6755 |
| TH-89-95B, Csc-Spar 1 | 0.1537 | 39.2102 | 0.0207 | 0.1080 | 0.0049 | 0.6411 |
| IS-90-0A, Csc-Spar 1,2 | 0.1215 | 39.7160 | 0.0207 | 0.0576 | 0.0648 | 0.5010 |
| IS-90-0A, Csc-Spar 1,2 | 0.1090 | 39.6542 | 0.0044 | 0.0463 | 0.0358 | 0.4513 |
| IS-90-0A, Csc-Spar 1,2 | 0.1267 | 39.9087 | 0.0385 | 0.0632 | 0.0702 | 0.5195 |
| IS-90-0A, Csc-Spar 1,2 | 0.1110 | 39.6669 | 0.0473 | 0.0870 | 0.0681 | 0.4574 |
| IS-90-0A, Csc-Spar 1,2 | 0.1268 | 39.8149 | 0.0296 | 0.0956 | 0.0762 | 0.5205 |
| IS-90-0A, Csc-Spar 1,2 | 0.1297 | 39.7412 | 0.0400 | 0.1123 | 0.0764 | 0.5330 |
| IS-90-0A, Csc-Spar 1,2 | 0.1225 | 39.2388 | 0.0001 | 0.0745 | 0.0877 | 0.5106 |
| IS-90-0A, Csc-Spar 1,2 | 0.1089 | 40.0281 | 0.0001 | 0.0884 | 0.0779 | 0.4454 |

| Sample I.D. and Zone | Wt % Mg | Wt % Ca | Wt % Mn | Wt %Fe | Wt %Sr | MgCO3 |
|---|---|---|---|---|---|---|
| IS-90-0A, Csc-Spar 1,2 | 0.1187 | 39.6087 | 0.0089 | 0.0365 | 0.0864 | 0.4907 |
| IS-90-0A, Csc-Spar 1,2 | 0.1160 | 39.8678 | 0.0222 | 0.0702 | 0.0969 | 0.4765 |
| IS-90-0A, Csc-Spar 1,2 | 0.1115 | 39.5745 | 0.0001 | 0.0351 | 0.1065 | 0.4615 |
| IS-90-0A, Csc-Spar 1,2 | 0.0766 | 39.4247 | 0.0592 | 0.1010 | 0.0001 | 0.3185 |
| IS-90-0A, Csc-Spar 1,2 | 0.0940 | 36.0695 | 0.0282 | 0.1664 | 0.0000 | 0.4258 |
| IS-90-0A, Csc-Spar 1,2 | 0.2297 | 39.2405 | 0.0001 | 0.1011 | 0.0013 | 0.9537 |
| IS-90-0A, Csc-Spar 1,2 | 0.7664 | 38.4268 | 0.0400 | 0.1151 | 0.0001 | 3.1753 |
| IS-90-0A, Csc-Spar 1,2 | 0.2315 | 38.9793 | 0.0178 | 0.0997 | 0.0103 | 0.9680 |
| IS-90-0A, Csc-Spar 1,2 | 0.1967 | 39.6441 | 0.0001 | 0.1263 | 0.0347 | 0.8095 |
| IS-90-0A, Csc-Spar 1,2 | 0.2321 | 39.1702 | 0.0607 | 0.0955 | 0.0239 | 0.9648 |
| IS-90-0A, Csc-Spar 1,2 | 0.2264 | 39.2348 | 0.0400 | 0.0534 | 0.0028 | 0.9409 |
| IS-90-0A, Csc-Spar 1,2 | 0.2354 | 39.3489 | 0.0296 | 0.0436 | 0.0001 | 0.9752 |
| IS-90-0A, Csc-Spar 1,2 | 0.2373 | 39.0135 | 0.0355 | 0.0590 | 0.0177 | 0.9913 |
| IS-90-0A, Csc-Spar 1,2 | 0.2490 | 39.1192 | 0.0400 | 0.0618 | 0.0095 | 1.0373 |
| IS-90-0A, Csc-Spar 1,2 | 0.2585 | 39.2311 | 0.0400 | 0.1011 | 0.0280 | 1.0712 |
| IS-90-0A, Csc-Spar 1,2 | 0.2561 | 39.0554 | 0.0148 | 0.0716 | 0.0134 | 1.0677 |
| IS-90-0A, Csc-Spar 1,2 | 0.1162 | 38.0566 | 0.0000 | 0.0478 | 0.0216 | 0.4999 |
| IS-90-0A, Csc-Spar 1,2 | 0.2737 | 39.2164 | 0.0518 | 0.1588 | 0.0000 | 1.1331 |
| IS-90-0A, Csc-Spar 1,2 | 0.0776 | 39.2241 | 0.0089 | 0.0885 | 0.0001 | 0.3241 |
| IS-90-0A, Csc-Spar 1,2 | 0.2661 | 39.2071 | 0.0504 | 0.1110 | 0.0001 | 1.1037 |
| IS-90-0A, Csc-Spar 1,2 | 0.4581 | 39.3345 | 0.0311 | 0.1320 | 0.0001 | 1.8782 |
| IS-90-0A, Csc-Spar 1,2 | 0.1493 | 39.0138 | 0.0459 | 0.0745 | 0.0842 | 0.6247 |
| IS-90-0A, Csc-Spar 1,2 | 0.5038 | 38.6820 | 0.0104 | 0.1250 | 0.0304 | 2.0964 |
| IS-90-0A, Csc-Spar 1,2 | 0.2063 | 39.2246 | 0.0207 | 0.1026 | 0.0080 | 0.8575 |
| IS-90-0A, Csc-Spar 1,2 | 0.2183 | 39.5744 | 0.0074 | 0.1335 | 0.0049 | 0.8992 |
| IS-90-0A, Csc-Spar 1,2 | 0.2242 | 39.2804 | 0.0785 | 0.1265 | 0.0031 | 0.9289 |
| IS-90-0A, Csc-Spar 1,2 | 0.2069 | 39.4941 | 0.0237 | 0.0773 | 0.0001 | 0.8545 |
| IS-90-0A, Csc-Spar 1,2 | 0.1429 | 38.9755 | 0.0489 | 0.0717 | 0.0345 | 0.5992 |
| IS-90-0A, Csc-Spar 1,2 | 0.2260 | 39.5651 | 0.0563 | 0.1026 | 0.0219 | 0.9306 |
| IS-90-0A, Csc-Spar 1,2 | 0.1588 | 39.4954 | 0.0222 | 0.0927 | 0.0229 | 0.6567 |
| IS-90-0A, Csc-Spar 1,2 | 0.2076 | 39.8015 | 0.0504 | 0.1110 | 0.0129 | 0.8504 |
| IS-90-0A, Csc-Spar 1,2 | 0.1596 | 39.5037 | 0.0089 | 0.1265 | 0.0286 | 0.6598 |
| IS-90-0A, Csc-Spar 1,2 | 0.1227 | 39.9849 | 0.0637 | 0.0646 | 0.0111 | 0.5022 |
| IS-90-0A, Csc-Spar 1,2 | 0.1315 | 40.2712 | 0.0370 | 0.0814 | 0.0051 | 0.5338 |
| IS-90-0A, Csc-Spar 1,2 | 0.2371 | 39.5174 | 0.0341 | 0.1236 | 0.0139 | 0.9765 |
| IS-90-0A, Csc-Spar 1,2 | 0.2428 | 38.6793 | 0.0667 | 0.0703 | 0.0046 | 1.0219 |

| Sample I.D. and Zone | Wt % Mg | Wt % Ca | Wt % Mn | Wt %Fe | Wt %Sr | MgCO3 |
|---|---|---|---|---|---|---|
| IS-90-0A, Csc-Spar 1,2 | 0.1886 | 39.0970 | 0.0163 | 0.1165 | 0.0001 | 0.7875 |
| IS-90-0A, Csc-Spar 1,2 | 0.2303 | 39.0424 | 0.0400 | 0.0675 | 0.0160 | 0.9617 |
| IS-90-0A, Csc-Spar 1,2 | 0.2376 | 39.4274 | 0.0415 | 0.0970 | 0.0131 | 0.9814 |

| Shelf-Edge Ferroan Coarse Pink Sparry Calcite | | | | | | Mole % |
|---|---|---|---|---|---|---|
| Sample I.D. and Zone | Wt % Mg | Wt % Ca | Wt % Mn | Wt % Fe | Wt % Sr | MgCO3 |
| PVC-2J Pink Csc-Spar 1 | 0.1822 | 38.7813 | 0.1116 | 0.1979 | 0.0001 | 0.7649 |
| PVC-2J Pink Csc-Spar 1 | 0.2248 | 38.6838 | 0.1131 | 0.2429 | 0.0001 | 0.9436 |
| PVC-2J Pink Csc-Spar 1 | 0.2636 | 38.8479 | 0.1457 | 0.2373 | 0.0145 | 1.0984 |
| PVC-2J Pink Csc-Spar 1 | 0.2691 | 39.0330 | 0.1038 | 0.2456 | 0.0001 | 1.1166 |
| PVC-2J Pink Csc-Spar 2,3 | 0.2296 | 39.1211 | 0.0774 | 0.2625 | 0.0001 | 0.9524 |
| PVC-2J Pink Csc-Spar 2,3 | 0.2693 | 9.0654 | 0.2184 | 0.2387 | 0.0001 | 1.1147 |
| PVC-2J Pink Csc-Spar 2,3 | 0.2844 | 38.8738 | 0.1378 | 0.2385 | 0.0001 | 1.1834 |
| PVC-2J Pink Csc-Spar 2,3 | 0.1847 | 38.9046 | 0.0883 | 0.1484 | 0.0001 | 0.7731 |
| PVC-2J Pink Csc-Spar 2,3 | 0.3135 | 38.6344 | 0.0666 | 0.2470 | 0.0001 | 1.3123 |
| PVC-2J Pink Csc-Spar 2,3 | 0.2298 | 38.8443 | 0.0682 | 0.2316 | 0.0161 | 0.9608 |
| PVC-2J Pink Csc-Spar 2,3 | 0.2663 | 38.8980 | 0.1348 | 0.2584 | 0.0124 | 1.1087 |
| PVC-2J Pink Csc-Spar 2,3 | 0.2238 | 38.8541 | 0.0869 | 0.2362 | 0.0001 | 0.9353 |
| PVC-2J Pink Csc-Spar 2,3 | 0.2565 | 38.8416 | 0.1952 | 0.2598 | 0.0001 | 1.0688 |
| PVC-2J Pink Csc-Spar 2,3 | 0.2598 | 38.5259 | 0.1116 | 0.3461 | 0.0001 | 1.0905 |
| PVC-2J Pink Csc-Spar 2,3 | 0.3113 | 38.8360 | 0.0186 | 0.0522 | 0.0001 | 1.3031 |
| PVC-2J Pink Csc-Spar 2,3 | 0.2492 | 38.7827 | 0.1781 | 0.2641 | 0.0088 | 1.0396 |
| PVC-2J Pink Csc-Spar 2,3 | 0.1944 | 39.2719 | 0.0883 | 0.1849 | 0.0174 | 0.8056 |
| PVC-2G-Bill, Pink Csc-Spar 1 | 0.1868 | 39.7157 | 0.0456 | 0.0978 | 0.0432 | 0.7678 |
| PVC-2G-Bill, Pink Csc-Spar 1 | 0.2453 | 39.6017 | 0.0692 | 0.2484 | 0.0146 | 1.0044 |
| PVC-2G-Bill, Pink Csc-Spar 1 | 0.2646 | 39.5846 | 0.0001 | 0.2292 | 0.0001 | 1.0862 |
| PVC-2G-Bill, Pink Csc-Spar 1 | 0.2581 | 39.7423 | 0.0456 | 0.0642 | 0.0072 | 1.0573 |
| PVC-2G-Bill, Pink Csc-Spar 1 | 0.2347 | 39.3476 | 0.0781 | 0.2794 | 0.0001 | 0.9679 |
| PVC-2G-Bill, Pink Csc-Spar 1 | 0.2813 | 39.1561 | 0.0604 | 0.2557 | 0.0001 | 1.1633 |
| PVC-2G-Bill, Pink Csc-Spar 1 | 0.1993 | 39.4664 | 0.0280 | 0.1732 | 0.0001 | 0.8229 |
| PVC-2G-Bill, Pink Csc-Spar 1 | 0.2144 | 39.4237 | 0.0589 | 0.2289 | 0.0087 | 0.8837 |

| Shelf-Edge Ferroan Coarse Pink to White Sparry Calcite (intermediate) | | | | | | Mole % |
|---|---|---|---|---|---|---|
| Sample I.D. and Zone | Wt % Mg | Wt % Ca | Wt % Mn | Wt % Fe | Wt % Sr | MgCO3 |
| PVC-2J Csc-pink to white 1 | 0.2770 | 38.5764 | 0.1410 | 0.2331 | 0.0001 | 1.1625 |
| PVC-2J Csc-pink to white 1 | 0.2719 | 38.8556 | 0.1038 | 0.3627 | 0.0166 | 1.1309 |
| PVC-2J Csc-pink to white 1 | 0.2359 | 38.7012 | 0.0929 | 0.2838 | 0.0001 | 0.9882 |
| PVC-2J Csc-pink to white 1 | 0.1306 | 39.0043 | 0.0992 | 0.1441 | 0.0001 | 0.5461 |
| PVC-2J Csc-pink to white 1 | 0.2770 | 38.5635 | 0.1333 | 0.3150 | 0.0005 | 1.1613 |
| PVC-2J Csc-pink to white 1 | 0.2220 | 38.6116 | 0.1564 | 0.5194 | 0.0001 | 0.9279 |
| PVC-2J Csc-pink to white 1 | 0.2503 | 39.0259 | 0.0977 | 0.2262 | 0.0001 | 1.0403 |
| PVC-2J Csc-pink to white 1 | 0.2711 | 38.7077 | 0.1007 | 0.3121 | 0.0001 | 1.1328 |
| PVC-2J Csc-pink to white 1 | 0.2610 | 39.0606 | 0.1038 | 0.2232 | 0.0001 | 1.0832 |
| PVC-2J Csc-pink to white 1 | 0.1654 | 39.3218 | 0.1038 | 0.2359 | 0.0001 | 0.6843 |
| PVC-2J Csc-pink to white 1 | 0.1796 | 38.9846 | 0.0899 | 0.2909 | 0.0070 | 0.7480 |
| PVC-2J Csc-pink to white 1 | 0.2612 | 39.0942 | 0.1254 | 0.2851 | 0.0086 | 1.0817 |

| Shelf-Edge Ferroan Sparry Calcite (Co-precipitated with ferraon baroque dolomite) | | | | | | Mole % |
|---|---|---|---|---|---|---|
| Sample I.D. and Zone | Wt % Mg | Wt % Ca | Wt % Mn | Wt % Fe | Wt % Sr | MgCO3 |
| RHB-2C-B Csc-Fe (Co-ppt), 1a, 1b | 0.1237 | 40.1359 | 0.0000 | 0.0423 | 0.0000 | 0.5047 |
| RHB-2C-B Csc-Fe (Co-ppt), 1a, 1b | 0.2087 | 40.1560 | 0.0278 | 0.0225 | 0.0000 | 0.8483 |
| RHB-2C-B Csc-Fe (Co-ppt), 1a, 1b | 0.7160 | 39.3365 | 0.0495 | 0.0817 | 0.0270 | 2.9065 |
| RHB-2C-B Csc-Fe (Co-ppt), 1a, 1b | 0.1232 | 40.2423 | 0.0001 | 0.0536 | 0.0001 | 0.5021 |
| RHB-2C-B Csc-Fe (Co-ppt), 1a, 1b | 0.1096 | 39.8570 | 0.0001 | 0.0493 | 0.0008 | 0.4504 |
| RHB-2C-B Csc-Fe (Co-ppt), 1a, 1b | 0.1324 | 39.9641 | 0.0062 | 0.0169 | 0.0001 | 0.5435 |
| RHB-2C-B Csc-Fe (Co-ppt), 1a, 1b | 0.2325 | 40.1581 | 0.0480 | 0.0001 | 0.0091 | 0.9445 |
| RHB-2C-B Csc-Fe (Co-ppt), 1a, 1b | 0.3956 | 39.9493 | 0.0309 | 0.0479 | 0.0057 | 1.6038 |
| RHB-2C-B Csc-Fe (Co-ppt), 1a, 1b | 0.2356 | 40.1983 | 0.0077 | 0.0226 | 0.0008 | 0.9567 |
| RHB-2C-B Csc-Fe (Co-ppt), 1a, 1b | 0.2348 | 39.9015 | 0.0155 | 0.0042 | 0.0001 | 0.9604 |
| RHB-2C-B Csc-Fe (Co-ppt), 1a, 1b | 0.2119 | 40.0735 | 0.0124 | 0.0690 | 0.0001 | 0.8624 |
| RHB-2C-B Csc-Fe (Co-ppt), 1a, 1b | 0.2099 | 39.6000 | 0.0309 | 0.0380 | 0.0001 | 0.8657 |
| RHB-2C-B Csc-Fe (Co-ppt), 1a, 1b | 0.6134 | 39.3410 | 0.0155 | 0.0282 | 0.0000 | 2.5051 |
| RHB-2C-B Csc-Fe (Co-ppt), 1a, 1b | 0.0480 | 40.4575 | 0.0000 | 0.0324 | 0.0000 | 0.1956 |
| RHB-2C-B Csc-Fe (Co-ppt), 1a, 1b | 0.0861 | 40.3031 | 0.0510 | 0.0352 | 0.0000 | 0.3506 |
| RHB-2C-B Csc-Fe (Co-ppt), 1a, 1b | 0.1452 | 39.9876 | 0.0201 | 0.0493 | 0.0080 | 0.5943 |
| RHB-2C-B Csc-Fe (Co-ppt), 1a, 1b | 0.3580 | 39.8517 | 0.0309 | 0.0381 | 0.0001 | 1.4580 |
| RHB-2C-B Csc-Fe (Co-ppt), 1a, 1b | 0.1712 | 39.7220 | 0.0356 | 0.0169 | 0.0098 | 0.7045 |
| RHB-2C-B Csc-Fe (Co-ppt), 1a, 1b | 0.1836 | 40.0089 | 0.0433 | 0.0465 | 0.0036 | 0.7504 |
| RHB-2C-B Csc-Fe (Co-ppt), 2 | 0.1732 | 38.9544 | 0.0232 | 0.2451 | 0.0013 | 0.7239 |
| RHB-2C-B Csc-Fe (Co-ppt), 2 | 0.0871 | 39.1674 | 0.0974 | 0.2157 | 0.0000 | 0.3628 |
| RHB-2C-B Csc-Fe (Co-ppt), 2 | 0.1521 | 39.4766 | 0.0402 | 0.3670 | 0.0000 | 0.6281 |
| RHB-2C-B Csc-Fe (Co-ppt), 2 | 0.3058 | 39.7904 | 0.0000 | 0.0296 | 0.0000 | 1.2511 |
| RHB-2C-B Csc-Fe (Co-ppt), 2 | 0.7688 | 39.3657 | 0.0046 | 0.0973 | 0.0000 | 3.1141 |

| Shelf-Edge Ferroan Baroque Dolomite | | | | | | Mole % |
|---|---|---|---|---|---|---|
| Sample I.D. and Zone | Wt % Mg | Wt % Ca | Wt % Mn | Wt % Fe | Wt % Sr | MgCO3 |
| RHB-2C-B Fedol 1,2 | 11.4573 | 22.2854 | 0.1097 | 2.2262 | 0.0000 | 44.0823 |
| RHB-2C-B Fedol 1,2 | 11.1967 | 22.5141 | 0.1172 | 2.6611 | 0.0000 | 42.9640 |
| RHB-2C-B Fedol 1,2 | 10.7565 | 22.6253 | 0.1541 | 3.0293 | 0.0088 | 41.5835 |
| RHB-2C-B Fedol 1,2 | 11.1854 | 23.1267 | 0.0711 | 1.8880 | 0.0000 | 42.9151 |
| RHB-2C-B Fedol 1,2 | 11.7924 | 22.2902 | 0.0617 | 1.8036 | 0.0001 | 45.1417 |
| RHB-2C-B Fedol 1,2 | 10.6334 | 23.7226 | 0.0710 | 2.0783 | 0.0000 | 40.9656 |
| RHB-2C-B Fedol 1,2 | 10.6300 | 22.6758 | 0.2160 | 2.8059 | 0.0220 | 41.3535 |
| RHB-2C-B Fedol 1,2 | 10.7836 | 23.1139 | 0.1204 | 2.2871 | 0.0000 | 41.7160 |
| RHB-2C-B Fedol 1,2 | 10.8863 | 22.7555 | 0.1065 | 1.7974 | 0.0196 | 42.6547 |
| RHB-2C-B Fedol 1,2 | 10.3030 | 22.8204 | 0.1833 | 3.2997 | 0.0258 | 40.1401 |
| RHB-2C-B Fedol 1,2 | 10.6981 | 22.7066 | 0.0617 | 3.2442 | 0.0001 | 41.2924 |
| RHB-2C-B Fedol 1,2 | 10.5781 | 22.5589 | 0.1109 | 3.2252 | 0.0001 | 41.1405 |
| RHB-2C-B Fedol 1,2 | 10.0773 | 22.2839 | 0.1260 | 4.4547 | 0.0950 | 39.3764 |
| RHB-2C-B Fedol 1,2 | 9.8685 | 22.5617 | 0.1152 | 4.7619 | 0.0001 | 38.4364 |
| RHB-2C-B Fedol 1,2 | 11.1718 | 22.4967 | 0.1205 | 2.3463 | 0.0000 | 43.1508 |
| RHB-2C-B Fedol 1,2 | 11.9877 | 21.8533 | 0.0201 | 1.8270 | 0.0000 | 46.0264 |
| RHB-2C-B Fedol 1,2 | 11.4829 | 22.9215 | 0.0495 | 1.3819 | 0.0000 | 44.1514 |
| RHB-2C-B Fedol 1,2 | 11.7753 | 21.9838 | 0.0495 | 1.8502 | 0.0000 | 45.4025 |
| RHB-2C-B Fedol 1,2 | 11.5773 | 22.4462 | 0.0603 | 1.7610 | 0.0036 | 44.5544 |
| RHB-2C-B Fedol 1,2 | 10.8105 | 22.8238 | 0.1684 | 2.7098 | 0.0001 | 41.7288 |
| RHB-2C-B Fedol 1,2 | 10.7258 | 22.4959 | 0.1047 | 3.2085 | 0.0000 | 41.5539 |
| RHB-2C-B Fedol 1,2 | 10.4773 | 22.5686 | 0.0847 | 3.5649 | 0.0209 | 40.6734 |
| RHB-2C-B Fedol 1,2 | 9.8322 | 22.8308 | 0.1351 | 4.6226 | 0.0000 | 38.1833 |
| RHB-2C-B Fedol 1,2 | 10.4563 | 22.2950 | 0.0740 | 4.0707 | 0.0001 | 40.5560 |
| RHB-2C-B Fedol 1,2 | 10.9476 | 22.0600 | 0.1402 | 3.2334 | 0.0130 | 42.4334 |
| RHB-2C-B Fedol 1,2 | 11.1487 | 22.7742 | 0.1016 | 2.7108 | 0.0104 | 42.5709 |
| RHB-2C-B Fedol 1,2 | 10.3299 | 22.8083 | 0.0126 | 4.0120 | 0.0001 | 39.7839 |
| RHB-2C-B Fedol 1,2 | 10.4010 | 22.4035 | 0.0986 | 4.1162 | 0.0001 | 40.2776 |
| RHB-2C-B Fedol 1,2 | 11.2224 | 22.8158 | 0.0464 | 1.5059 | 0.0146 | 43.5998 |
| RHB-2C-B Fedol 1,2 | 11.3665 | 22.6491 | 0.0448 | 1.8412 | 0.0000 | 43.8455 |
| RHB-2C-B Fedol 1,2 | 11.3799 | 22.3058 | 0.0356 | 1.6475 | 0.0001 | 44.3822 |
| RHB-2B-C1 Fedol 1a, 1b, 2c, 2e | 10.4960 | 22.3369 | 0.0772 | 3.5935 | 0.0000 | 40.9345 |
| RHB-2B-C1 Fedol 1a, 1b, 2c, 2e | 11.0937 | 22.4077 | 0.0557 | 2.4849 | 0.0008 | 43.0161 |
| RHB-2B-C1 Fedol 1a, 1b, 2c, 2e | 11.2821 | 22.4448 | 0.1363 | 1.9622 | 0.0000 | 43.7143 |
| RHB-2B-C1 Fedol 1a, 1b, 2c, 2e | 11.4294 | 22.4896 | 0.0727 | 1.8097 | 0.0001 | 44.1481 |

| Sample I.D. and Zone | Wt % Mg | Wt % Ca | Wt % Mn | Wt % Fe | Wt % Sr | MgCO3 |
|---|---|---|---|---|---|---|
| RHB-2B-C1 Fedol 1a, 1b, 2c, 2e | 11.2239 | 22.5110 | 0.0372 | 1.8247 | 0.0000 | 43.6947 |
| RHB-2B-C1 Fedol 1a, 1b, 2c, 2e | 11.4951 | 22.6308 | 0.0743 | 1.4399 | 0.0118 | 44.4118 |
| RHB-2B-C1 Fedol 1a, 1b, 2c, 2e | 11.7077 | 22.4599 | 0.0040 | 1.4088 | 0.0001 | 45.0989 |
| RHB-2B-C1 Fedol 1a, 1b, 2c, 2e | 11.1406 | 22.9542 | 0.1379 | 1.7739 | 0.0113 | 43.0173 |
| RHB-2B-C1 Fedol 1a, 1b, 2c, 2e | 11.1325 | 23.1999 | 0.1022 | 1.9386 | 0.0003 | 42.6668 |
| RHB-2B-C1 Fedol 1a, 1b, 2c, 2e | 10.4533 | 21.8237 | 0.1202 | 4.4715 | 0.0071 | 40.6898 |
| RHB-2B-C1 Fedol 1a, 1b, 2c, 2e | 10.7532 | 21.8334 | 0.1158 | 3.5425 | 0.0079 | 42.0213 |
| RHB-2B-C1 Fedol 1a, 1b, 2c, 2e | 12.5071 | 21.8135 | 0.0202 | 0.8700 | 0.0000 | 47.8760 |
| RHB-2B-C1 Fedol 1a, 1b, 2c, 2e | 12.0537 | 22.7980 | 0.0358 | 0.5225 | 0.0085 | 46.1371 |
| RHB-2B-C1 Fedol 1a, 1b, 2c, 2e | 11.7352 | 22.3151 | 0.0513 | 1.1768 | 0.0093 | 45.4741 |
| RHB-2B-C1 Fedol 1a, 1b, 2c, 2e | 11.1875 | 22.7164 | 0.0294 | 2.2832 | 0.0000 | 43.0765 |
| RHB-2B-C1 Fedol 1a, 1b, 2c, 2e | 11.5235 | 22.4367 | 0.0481 | 1.4824 | 0.0028 | 44.6678 |
| RHB-2B-C1 Fedol 1a, 1b, 2c, 2e | 11.4022 | 22.3212 | 0.0465 | 1.9755 | 0.0039 | 44.1588 |
| RHB-2B-C1 Fedol 1a, 1b, 2c, 2e | 11.5951 | 22.3770 | 0.0280 | 1.2537 | 0.0001 | 45.0742 |
| RHB-2B-C1 Fedol 1a, 1b, 2c, 2e | 11.4647 | 22.7776 | 0.0093 | 1.5905 | 0.0020 | 44.1363 |
| RHB-2B-C1 Fedol 1a, 1b, 2c, 2e | 11.4766 | 22.7368 | 0.0544 | 1.4854 | 0.0051 | 44.2458 |
| RHB-2B-C1 Fedol 1a, 1b, 2c, 2e | 10.6703 | 22.3472 | 0.0957 | 3.4717 | 0.0076 | 41.3919 |
| RHB-2B-C1 Fedol 1a, 1b, 2c, 2e | 10.0123 | 22.4638 | 0.0816 | 4.8089 | 0.0000 | 38.8599 |
| RHB-2B-C1 Fedol 1a, 1b, 2c, 2e | 10.0577 | 22.2953 | 0.1420 | 4.3990 | 0.0001 | 39.3549 |
| RHB-2B-C1 Fedol 1a, 1b, 2c, 2e | 9.9935 | 22.2031 | 0.0816 | 4.8424 | 0.0000 | 39.0330 |
| RHB-2B-C1 Fedol 1a, 1b, 2c, 2e | 11.0643 | 22.4666 | 0.0990 | 2.8337 | 0.0001 | 42.6091 |
| RHB-2B-C1 Fedol 1a, 1b, 2c, 2e | 10.7341 | 22.2543 | 0.0913 | 3.0585 | 0.0000 | 41.9266 |
| RHB-2B-C1 Fedol 1a, 1b, 2c, 2e | 11.1469 | 21.9530 | 0.0943 | 2.9098 | 0.0071 | 43.2535 |
| RHB-2B-C1 Fedol 1a, 1b, 2c, 2e | 11.4320 | 22.2442 | 0.0668 | 2.0868 | 0.0001 | 44.2068 |
| RHB-2B-C1 Fedol 1a, 1b, 2c, 2e | 10.9413 | 22.2296 | 0.1101 | 2.5894 | 0.0062 | 42.7389 |
| RHB-2B-C1 Fedol 1a, 1b, 2c, 2e | 11.4699 | 22.6493 | 0.0435 | 1.2295 | 0.0000 | 44.5252 |
| RHB-2B-C1 Fedol 1a, 1b, 2c, 2e | 11.5517 | 22.6382 | 0.0373 | 1.2193 | 0.0025 | 44.7238 |
| RHB-2B-C1 Fedol 1a, 1b, 2c, 2e | 11.4387 | 22.8620 | 0.0589 | 1.3310 | 0.0000 | 44.1491 |
| RHB-2B-C1 Fedol 1a, 1b, 2c, 2e | 11.1227 | 22.4239 | 0.0652 | 2.3586 | 0.0226 | 43.1382 |
| RHB-2B-C1 Fedol 1a, 1b, 2c, 2e | 11.6238 | 22.3070 | 0.0466 | 1.4791 | 0.0000 | 45.0237 |
| RHB-2B-C1 Fedol 1a, 1b, 2c, 2e | 11.0661 | 23.4692 | 0.0388 | 1.3381 | 0.0001 | 42.7275 |
| RHB-2B-C1 Fedol 1a, 1b, 2c, 2e | 10.9965 | 22.0876 | 0.0959 | 2.8273 | 0.0056 | 42.8435 |
| RHB-2B-C1 Fedol 1a, 1b, 2c, 2e | 11.3075 | 22.2268 | 0.0975 | 2.2813 | 0.0001 | 43.7874 |
| RHB-3R-A2, Fedol1 | 11.3353 | 22.4634 | 0.0898 | 2.2932 | 0.0000 | 43.6027 |
| RHB-3R-A2, Fedol1 | 10.7079 | 22.8412 | 0.1062 | 2.4790 | 0.0000 | 41.6872 |
| RHB-3R-A2, Fedol1 | 11.3707 | 22.1582 | 0.1153 | 2.0587 | 0.0000 | 44.1476 |

| Sample I.D. and Zone | Wt % Mg | Wt % Ca | Wt % Mn | Wt % Fe | Wt % Sr | MgCO3 |
|---|---|---|---|---|---|---|
| RHB-3R-A2, Fedol1 | 11.7517 | 22.0949 | 0.0809 | 1.8707 | 0.0000 | 45.1954 |
| RHB-3R-A2, Fedol1 | 11.8357 | 21.8921 | 0.0450 | 1.6049 | 0.0000 | 45.8193 |
| RHB-3R-A2, Fedol1 | 11.5918 | 22.0471 | 0.0554 | 1.9043 | 0.0000 | 44.9012 |
| RHB-3R-A2, Fedol1 | 10.7717 | 22.5580 | 0.1360 | 2.8843 | 0.0019 | 41.8013 |
| RHB-3R-A2, Fedol1 | 11.3498 | 22.5164 | 0.0793 | 2.1326 | 0.0150 | 43.6987 |
| RHB-3R-A2, Fedol1 | 11.0778 | 22.0285 | 0.0807 | 2.8766 | 0.0001 | 43.0618 |
| RHB-3R-A2, Fedol1 | 9.9694 | 23.1010 | 0.1033 | 3.0441 | 0.0001 | 39.3270 |
| RHB-3R-A2, Fedol1 | 10.7836 | 22.6604 | 0.1047 | 2.9040 | 0.0001 | 41.7375 |
| RHB-3R-A2, Fedol1 | 10.8417 | 22.6148 | 0.1107 | 2.6133 | 0.0044 | 42.1124 |
| RHB-3R-A2, Fedol1 | 10.9520 | 22.7446 | 0.0718 | 2.6402 | 0.0008 | 42.2413 |
| RHB-6B-T, Fedol 1, 2 | 10.4340 | 22.9502 | 0.0090 | 2.8144 | 0.0000 | 40.7872 |
| RHB-6B-T, Fedol 1, 2 | 9.6772 | 22.5606 | 0.0727 | 5.1712 | 0.0000 | 37.7389 |
| RHB-6B-T, Fedol 1, 2 | 10.0452 | 22.4650 | 0.0803 | 4.1656 | 0.0066 | 39.3619 |
| RHB-6B-T, Fedol 1, 2 | 10.2803 | 22.2849 | 0.0893 | 4.0457 | 0.0000 | 40.1640 |
| RHB-6B-T, Fedol 1, 2 | 10.2256 | 22.6345 | 0.0417 | 4.0836 | 0.0001 | 39.7132 |
| RHB-6B-T, Fedol 1, 2 | 10.1543 | 22.4956 | 0.0447 | 4.0317 | 0.0025 | 39.7079 |
| RHB-6B-T, Fedol 1, 2 | 8.1326 | 25.3005 | 0.0698 | 4.3914 | 0.0000 | 31.9944 |
| RHB-6B-T, Fedol 1, 2 | 9.5586 | 22.4172 | 0.1128 | 5.2038 | 0.0030 | 37.5295 |
| RHB-6B-T, Fedol 1, 2 | 10.2271 | 22.1755 | 0.0715 | 3.8604 | 0.0000 | 40.2837 |
| RHB-6B-T, Fedol 1, 2 | 9.7656 | 22.1826 | 0.0935 | 5.3948 | 0.0002 | 38.1304 |
| RHB-6B-T, Fedol 1, 2 | 10.4424 | 22.7639 | 0.0403 | 3.1034 | 0.0000 | 40.8307 |
| RHB-6B-T, Fedol 1, 2 | 10.0938 | 22.8903 | 0.0193 | 4.3227 | 0.0069 | 39.0203 |
| RHB-6B-T, Fedol 1, 2 | 10.5709 | 22.6332 | 0.5520 | 3.2243 | 0.0000 | 41.0913 |
| RHB-6B-T, Fedol 1, 2 | 10.8843 | 22.7214 | 0.0613 | 2.4690 | 0.0003 | 42.2425 |
| RHB-6B-T, Fedol 1, 2 | 10.2363 | 22.6030 | 0.0744 | 3.9311 | 0.0125 | 40.0524 |
| RHB-6B-T, Fedol 1, 2 | 10.6481 | 22.5847 | 0.0433 | 2.9558 | 0.0001 | 41.5115 |
| RHB-6B-T, Fedol 1, 2 | 10.3210 | 22.6086 | 0.0521 | 3.5706 | 0.0086 | 40.2975 |
| RHB-6B-T, Fedol 1, 2 | 9.8668 | 22.7038 | 0.0372 | 4.2929 | 0.0105 | 38.6570 |
| RHB-6B-T, Fedol 1, 2 | 10.5526 | 23.1823 | 0.0209 | 3.0140 | 0.0000 | 40.6912 |
| RHB-6B-T, Fedol 1, 2 | 10.1251 | 22.9534 | 0.0045 | 3.9714 | 0.0042 | 39.2794 |
| RHB-6B-T, Fedol 1, 2 | 10.9263 | 23.0800 | 0.0494 | 1.9980 | 0.0094 | 42.3206 |
| RHB-6B-T, Fedol 1, 2 | 10.1227 | 22.5859 | 0.0611 | 3.6171 | 0.0042 | 39.8169 |
| RHB-6B-T, Fedol 1, 2 | 11.1635 | 23.0124 | 0.0494 | 1.3961 | 0.0001 | 43.3547 |
| RHB-6B-T, Fedol 1, 2 | 10.8542 | 22.8720 | 0.0299 | 2.0486 | 0.0000 | 42.3489 |
| RHB-6B-T, Fedol 1, 2 | 11.0097 | 22.8361 | 0.0569 | 1.7081 | 0.0152 | 42.9531 |

| On-Shelf Ferroan Baroque Dolomite | | | | | | Mole % |
|---|---|---|---|---|---|---|
| Sample I.D. and Zone | Wt % Mg | Wt % Ca | Wt % Mn | Wt %Fe | Wt %Sr | MgCO3 |
| IS-90-0A, Fedol1 | 11.0632 | 23.0164 | 0.0578 | 1.2177 | 0.0000 | 43.2530 |
| IS-90-0A, Fedol1 | 11.1480 | 22.0843 | 0.0754 | 2.3260 | 0.0000 | 43.5686 |
| IS-90-0A, Fedol1 | 11.0445 | 22.4383 | 0.1527 | 1.6097 | 0.0000 | 43.4459 |
| IS-90-0A, Fedol1 | 11.2266 | 22.3209 | 0.0933 | 1.8626 | 0.0000 | 43.8272 |
| IS-90-0A, Fedol1 | 11.2980 | 22.2737 | 0.1672 | 1.9328 | 0.0000 | 43.9238 |
| IS-90-0A, Fedol1 | 10.5373 | 22.9939 | 0.1153 | 2.4651 | 0.0208 | 41.1414 |
| IS-90-0A, Fedol1 | 11.3831 | 22.2462 | 0.1332 | 1.8969 | 0.0000 | 44.1900 |
| IS-90-0A, Fedol1 | 11.2185 | 22.9051 | 0.0650 | 1.8390 | 0.0205 | 43.2393 |
| IS-90-0A, Fedol1 | 11.1734 | 22.9154 | 0.0754 | 2.0140 | 0.0000 | 43.0062 |
| IS-90-0A, Fedol1 | 11.1703 | 22.6774 | 0.1713 | 1.8030 | 0.0001 | 43.3224 |
| IS-90-0A, Fedol1 | 10.7586 | 22.1384 | 0.1123 | 2.8930 | 0.0000 | 42.2011 |
| IS-90-0A, Fedol1 | 11.2680 | 22.0066 | 0.0237 | 2.1191 | 0.0001 | 44.1062 |
| IS-90-0A, Fedol1 | 11.5884 | 22.5369 | 0.2044 | 1.3128 | 0.0000 | 44.7111 |
| IS-90-0A, Fedol1 | 11.5713 | 22.6293 | 0.0711 | 1.8573 | 0.0000 | 44.2745 |
| IS-90-0A, Fedol1 | 11.7206 | 22.4748 | 0.3790 | 0.9665 | 0.0033 | 45.2148 |
| IS-90-0A, Fedol1 | 11.2125 | 22.6049 | 0.0770 | 1.9511 | 0.0000 | 43.4507 |
| IS-90-0A, Fedol1 | 10.9870 | 22.6284 | 0.1049 | 2.8080 | 0.0025 | 42.2907 |
| IS-90-0A, Fedol1 | 10.9378 | 22.3425 | 0.1199 | 2.6190 | 0.0001 | 42.5914 |
| IS-90-0A, Fedol1 | 11.2831 | 22.2329 | 0.1640 | 1.8918 | 0.0019 | 43.9656 |
| IS-90-0A, Fedol1 | 11.1003 | 22.6348 | 0.1095 | 1.7789 | 0.0033 | 43.2736 |
| IS-90-0A, Fedol1 | 11.3360 | 22.6228 | 0.1137 | 1.7776 | 0.0001 | 43.8017 |
| IS-90-0A, Fedol1 | 10.9720 | 23.0728 | 0.0459 | 1.9634 | 0.0282 | 42.4485 |
| IS-90-0A, Fedol1 | 11.1547 | 22.5240 | 0.0915 | 1.7692 | 0.0001 | 43.5296 |
| IS-90-0A, Fedol1 | 11.2080 | 22.5390 | 0.0649 | 1.6242 | 0.0014 | 43.7582 |
| IS-90-0A, Fedol1 | 11.3306 | 22.7971 | 0.0948 | 1.7182 | 0.0258 | 43.6572 |
| IS-90-0A, Fedol1 | 11.2323 | 23.0108 | 0.0785 | 1.5416 | 0.0033 | 43.3771 |
| IS-90-0A, Fedol1 | 11.3181 | 23.0157 | 0.1423 | 1.5285 | 0.0107 | 43.5180 |

# APPENDIX F

## RADIOGENIC STRONTIUM ANALYSES

## ($^{87}Sr/^{86}Sr$ With MATCHING $\delta^{13}C$ and $\delta^{18}O$)

## PROCEDURES FOR Sr ISOTOPIC ANALYSIS OF CARBONATE

Milligram quantities of powdered carbonate were dissolved in 15 ml Savellex PAF vials using 250 $\mu$l of doubly distilled 5N $HNO_3$. Strontium was separated from the matrix using EiChrom SrSpec resin, a crown-ether Sr-selective resin (50-100 $\mu$m diameter) loaded into the tip of a 10 ml BioRad polypropylene column refitted with 2 mm polyethylene frit. The total resin volume was approximately 50 $\mu$l. The resin was cleaned with repeated washes of deionized water and conditioned with 5N $HNO_3$. Strontium was loaded and washed into 1 ml of 5N $HNO_3$ and then collected with 1 ml of deionized water. Procedural strontium blanks were about 50 picograms (pg) and the strontium loaded blanks were less than 3 pg. The SrSpec resin was presoaked and flushed with water to remove any strontium present from the resin in the manufacturing process. Strontium was ionized on a tungsten filament ribbon and $Ta_2O_5$ emitter solution (Brick, 1986). Isotopic data were collected on a VG Sector54 in a quintuple-collector dynamic mode, using the internal ratio $^{86}Sr/^{88}Sr = 0.1194$ to correct for mass fractionation and normalization to the SRM 987 Sr carbonate standard, which yields a value of $0.71025 \pm 0.000016$ (2s, n=112). Typical internal precision for most strontium carbonate runs using this procedure was 0.0006 to 0.0009% standard error.

| Radiogenic Strontium Analyses With Matching Stable Carbon And Oxygen Isotope Data | | | | | | |
|---|---|---|---|---|---|---|
| Mass Spec Number and Sample I.D. (matching stable carbon and oxygen isotope data) | Position Meters | D O18 (PDB) | D C13 (PDB) | Wt. mg. Sr Sample | 87Sr/86Sr | 2Sigma |
| 1452 C1-136 RVC TH-89-77b Blocky-white, Fe 1 | 168.8 | -8.2 | 0.6 | 0.025 | 0.708158 | 0.000008 |
| 1461 C1-137 IS-90-43b Fe-Csc-Spar 1R | 232.9 | -8.5 | 0.4 | 0.033 | 0.708325 | 0.000008 |
| 1470 C1-139 RV10 TH-89-95b Csc-Fe 1 | 184.9 | -8.6 | 0.5 | 0.017 | 0.708278 | 0.000012 |
| 1471 C1-139 RV16 TH-89-126 Blocky-clear | 212.8 | -7.7 | 0.3 | 0.019 | No Run | No Run |
| 1570, 1606, 1610 TH-89-95 (slab) Fib. 2,3,4 | 184.9 | -4.7 | 0.6 | 0.017 | 0.708269 | 0.000012 |
| 1618 C1-155 RV1 PVC-2G (Bill) Csc-pink | 26.6 | -11.0 | 0.8 | 0.023 | 0.708548 | 0.000014 |
| 1622 C1-156 RV3 PVC-2A-1a Csc-Fe | 24.60 | -8.6 | 0.9 | 1.009 | 0.709423 | 0.000008 |
| 1650, 1651, 1802 PVC-2G(Bill) Fib 1,2,8 | 26.6 | -5.0 | 0.9 | 0.018 | 0.708453 | 0.000008 |
| 1683 & 4804 C2-38-S17 PVC-2J Csc-pink 2, 4 | 32.5 | -10.1 | 0.7 | 0.118 | 0.708588 | 0.00001 |
| 1747 C1-164 RVA OTH-90-2A Bardol 1(dolo. split) | 74.1 | -8.7 | -0.1 | 0.182 | 0.709244 | 0.00001 |
| 1751 C1-164 RV1 PVC-1A-T Bardol 1(dolo. split) | 11.6 | -7.8 | 1.7 | 0.107 | 0.709444 | 0.000008 |
| 1754 C1-165 RV9 RHB-2C-B Bardol 1(dolo. split) | 41.5 | -5.7 | 1.7 | 0.086 | 0.709758 | 0.000012 |
| 1755 C1-165 RV16 IS-90-0A Bardol 1(dolo. split) | 28.1 | -7.7 | 0.5 | 0.061 | 0.709111 | 0.000008 |
| 1757 C1-166 RHB-6B-T Bardol 1(dolo. split) | 183.4 | -7.9 | 1.9 | 0.049 | 0.709031 | 0.000008 |
| 1759 C1-165 RV13 RHB-3R-a2 Bardol 1(dolo.split) | 99.5 | -7.6 | 1.6 | 0.084 | 0.709299 | 0.000012 |
| 1850 C1-174 RV12 TH-89-26B Blocky-white, Fe 1 | 125.40 | -8.2 | -0.5 | 0.068 | 0.708349 | 0.00001 |
| 1984 C1-188 RV10 IS-90-47b2 (slab) Fib 3 | 234.7 | -4.5 | 0.5 | 0.012 | 0.708253 | 0.00001 |
| 2002 BL1-11 Boat 15 TH-90-212 Blocky-white Fe | 298.8 | -7.5 | 0.0 | 0.063 | 0.708409 | 0.000008 |
| 4791 C2-375-S16 RHB-2C-B Csc-Fe (Co-ppt) 3 | 41.5 | -11.0 | -0.3 | 0.106 | 0.709092 | 0.00001 |

# APPENDIX G

## ATOMIC ABSORPTION ANALYSES

## (WHOLE ROCK)

## EXPLANATION

Trace element data for the 68 whole rock samples from third-order sequences 2 and 3 are given by Johnson (1988). Sample names used by Johnson are consistent with Appendix A of this report. Fourteen Middle Ordovician whole rock limestone samples were obtained from Sequence 4 of the Middle Ordovician Chickamauga Group at Thorn Hill, Tennessee. These samples (starting with "TH") are representative of the Lincolnshire, Rockdell, and Benbolt Formations. Additional analyses are presented for comparative purposes. Middle Ordovician Ottosee oolite, ooid grainstone samples from the Alcoa Highway section start with the prefix "AL." The Alcoa Highly section is discussed by Cantrell (1982) and Cantrell and Walker (1985). Upper Cambrian ooid grainstone samples from the Nolichucky Shale at Interstate 75 start with the prefix "IOA." The Interstate 75 section is discussed by Weber (1988).

These limestone samples and an additional limestone standard (NBS-20) were crushed and about 5 grams of the sample was dissolved in 250 ml of 25% glacial acetic acid for about 24 hour. The solution was then brought to 500 ml with distilled water and the insoluble reside (ISR) was filtered following the method of Johnson (1988). Note that the limestone standard consisted of 2.5 grams in 125 ml of 25% glacial acetic acid brought to a final volume of 250 ml.

| Atomic Absorption Analyses of Bulk Rock Samples | | | | | | |
|---|---|---|---|---|---|---|
| Sample | Sample Wt. | Dissolved | Sr | Mn | Fe | Mg |
| | grams | Wt. (grams) | ppm | ppm | ppm | ppm |
| TH-88-1 | 5.08 | 4.76 | 127 | 302 | 590 | 177 |
| TH-88-2 | 5.07 | 4.78 | 234 | 194 | 684 | 1172 |
| TH-88-3 | 5.08 | 4.61 | 398 | 258 | 3761 | 1271 |
| TH-88-4 | 5.15 | 4.66 | 156 | 302 | 623 | 198 |
| TH-88-6 | 5.39 | 4.52 | 147 | 307 | 514 | 527 |
| TH-88-7 | 5.13 | 4.40 | 133 | 457 | 536 | 507 |
| TH-88-9 | 5.07 | 4.72 | 118 | 428 | 412 | 198 |
| TH-88-10 | 5.32 | 4.87 | 120 | 296 | 283 | 386 |
| TH-88-11 | 5.09 | 4.84 | 113 | 280 | 438 | 2361 |
| TH-88-12 | 5.19 | 4.81 | 126 | 301 | 375 | 369 |
| TH-88-1a | 0.02 | 0.02 | 305 | 499 | 121 | 3072 |
| TH-88-9a | 0.05 | 0.05 | 226 | 341 | 311 | 3435 |
| TH-88-9b | 0.02 | 0.02 | 279 | 454 | 23 | 3739 |
| TH-88-11a | 0.02 | 0.02 | 289 | 407 | 2688 | 2346 |
| AL-89-1 | 1.09 | 1.04 | 473 | 577 | 5400 | 4501 |
| AL-89-2 | 1.09 | 1.06 | 439 | 653 | 6153 | 5966 |
| AL-89-3 | 1.09 | 1.05 | 452 | 630 | 10603 | 6536 |
| AL-89-4 | 1.09 | 1.05 | 459 | 636 | 5524 | 5655 |
| AL-89-5 | 1.12 | 1.00 | 371 | 1025 | 4628 | 21699 |
| IOA-0.5m | 1.10 | 1.02 | 327 | 675 | 4631 | 12425 |
| IOA-1.8m | 1.12 | 0.89 | 310 | 660 | 4382 | 24845 |
| IOA-3.9m | 1.04 | 0.93 | 297 | 641 | 2952 | 7346 |
| IOA-4.1 | 1.15 | 0.94 | 302 | 656 | 4522 | 23757 |
| IOA-5.4 | 1.11 | 1.02 | 352 | 553 | 3555 | 11018 |
| NBS 20 | 2.54 | 2.28 | 201 | | | |
| NBS 20 | 2.54 | 2.28 | | | | 2769 |
| NBS 20 | 2.54 | 2.28 | | | | 3748 |
| NBS 20 | 2.54 | 2.28 | | | | 3408 |
| NBS 20 | 2.54 | 2.28 | | | | 4063 |
| NBS 20 | 2.54 | 2.28 | | 220 | | |
| NBS 20 | 2.54 | 2.28 | | 222 | | |
| NBS 20 | 2.54 | 2.28 | | 218 | | |
| NBS 20 | 2.54 | 2.28 | | 196 | | |
| NBS 20 | 2.54 | 2.28 | | | 1572 | |

| Sample | Sample Wt. | Dissolved | Sr | Mn | Fe | Mg |
|---|---|---|---|---|---|---|
| | grams | Wt. (grams) | ppm | ppm | ppm | ppm |
| NBS 20 | 2.54 | 2.28 | | | 1619 | |
| NBS 20 | 2.54 | 2.28 | | | 1524 | |
| NBS 20 | 2.54 | 2.28 | | | 1538 | |

# VITA

David Mark Steinhauff was born in Bakersfield, California, May 20, 1958 and grew up in the East San Francisco Bay Area were he attended elementary and high school. He graduated from Dublin High School in June, 1976; with highest honors from Chabot College in June, 1978 (A.A., General Education); with honors from the University of California, Davis, June 1981 (B.S., Anthropology); from California State University, Sacramento, in August, 1983 (B.S., Geology); and from The Ohio State University, Columbus, in December, 1985 (M.S., Geology). He entered the PhD program in Geology at the University of Tennessee, Knoxville, in the Fall of 1986 and was Center of Excellence Fellow during the 1986/1987 academic year. Mr. Steinhauff has been affiliated with the Geological Society of America since 1983 and was elected to full membership in 1991. He has been a junior member of the American Association of Petroleum Geologists since 1984, and has been affiliated with SEPM (Society for Sedimentary Geology) and Sigma Gama Epsilon since 1987. He was elected an associate member of Sigma Xi in 1989.

His professional experience includes an internship with the California Division of Mines and Geology in 1983; a research associateship with the Institute of Polar Studies at Ohio State, 1983 through 1985; and summer positions with Shell U.S.A. and Exxon U.S.A, in 1985 and 1987, respectively. He has also held teaching assistantships at Ohio State and Tennessee. He has been employed as an environmental consultant and hydrogeologist since July, 1991. He is presently under contract to Martin Marietta Energy Systems at the Health and Safety Research Division of the Oak Ridge National Laboratory.